WATER TREATMENT USING GRAPHITE ADSORBENTS WITH ELECTROCHEMICAL REGENERATION

A thesis submitted to The University of Manchester for the Degree of Doctor of Philosophy in the Faculty of Engineering and Physical Science

January 2012

Syed Nadir Hussain

School of Chemical Engineering and Analytical Sciences

The University of Manchester

Contents

List of Figures

List of Tables

Abstract

Increased public awareness, stricter legislation standards, and environmental and health effects associated with water pollution are driving the development of improved wastewater treatment techniques. In order to meet these challenges, a novel and cost effective process has been developed at the University of Manchester to treat water contaminated with dissolved organics by exploiting a combination of adsorption and electrochemical regeneration. Adsorption of organics takes place on the surface of a non-porous and highly electrically conductive graphite adsorbent, followed by anodic electrochemical regeneration leading to oxidation of the adsorbed organic contaminants. The mechanism of degradation of adsorbed organics during electrochemical regeneration is particularly important from the point of view of the breakdown products. Ideally, complete oxidation of the adsorbed organics to CO_2 and H_2O should occur, but it is also possible that intermediate by-products may be formed. These breakdown products could be released into the water, be released as gases during the regeneration process or may remain adsorbed on the surface of the adsorbent. Information about the breakdown products is an important requirement for the commercial application of the process. This PhD project focused on an investigation of the formation of intermediate oxidation products released into the water (liquid phase) and with the regeneration gases. Phenol was chosen as a model pollutant and a graphite intercalation compound (GIC) adsorbent, Nyex®1000 (Arvia® Technology Ltd) was used. The main oxidation products formed during both batch and continuous adsorption with electrochemical regeneration were 1,4-benzoquinone, maleic acid, oxalic acid, 4-chlorophenol and 2,4-dichlorphenol. These compounds were detected in small concentrations compared to the overall concentration of the phenol removed. Two mechanisms of organic oxidation during electrochemical regeneration of the GIC adsorbents were identified. The first was the complete oxidation of the adsorbed species on the surface of the adsorbent and the second involved the indirect electrochemical oxidation of organics in solution. Breakdown products were found to be formed due the indirect oxidation of organics in solution.

The formation of (chlorinated and non-chlorinated) breakdown products was found to be dependant on current density, pH, initial concentration, chloride content and the electrolyte used in the cathode compartment. The concentrations of chlorinated breakdown products can be minimized by using low current density, low initial concentrations, a chloride-free environment and/or treating the water over a number of adsorptions and regeneration cycles. On the other hand, non-chlorinated breakdown products can be minimized by applying higher current density and treating the solution over several cycles of adsorption and regeneration. Therefore, selection of optimum conditions is important to reduce the formation of undesirable breakdown products. The formation of free chlorine during batch electrochemical regeneration was also investigated under a range of operating conditions including the initial concentration of chloride ions, current density and pH. The outcomes of

this study have important implications in optimising the conditions for the formation of chlorinated breakdown products and in exploring the role of electrochlorination for water disinfection.

Analysis of the regeneration gases has revealed that the main components of the gases generated during the electrochemical regeneration of GIC adsorbents were CO_2 and H_2O. A preliminary mass balance has suggested that about 60% of the adsorbed phenol was oxidised completely to CO_2. However, further work is needed to determine the fate of the remaining phenol.

The surface characterization of the GIC adsorbent during adsorption and electrochemical regeneration was carried out using surface techniques including Fourier transform infrared spectroscopy (FTIR), Raman spectroscopy, Energy dispersive X-ray spectroscopy (EDS) and Boehm titration. FTIR and Raman spectroscopy were found to be unsuitable for determining the concentration changes at the surface of the adsorbent during adsorption and regeneration. However, Boehm titration has shown that the GIC adsorbent has phenolic, carboxylic and lactonic groups. The concentrations of phenolic groups were found to be higher after phenol adsorption and to decrease during electrochemical regeneration. The results of EDS analysis gave results which were consistent with these observations.

Another important aspect of this PhD project was to explore the potential application of adsorption and electrochemical regeneration using GIC adsorbents to water disinfection. A model microorganism *E. coli* was selected for adsorption and electrochemical regeneration studies under a range of experimental conditions. This study has provided evidence that the process of adsorption and electrochemical regeneration using GIC adsorbents can be used for disinfection of water. Disinfection of water was found to be a combination of two processes: the adsorption of microorganisms followed by their deactivation on the surface; and electrochemical disinfection in solution due to indirect oxidation. The possible disinfection mechanisms involved in these processes include electrochlorination, pH changes and deactivation by direct oxidation of microorganisms. Scanning electron microscopy was found to be a useful tool for investigating changes in surface morphology of microorganisms during adsorption and electrochemical regeneration.

The disinfection of a variety of bacteria, fungi and yeasts was tested and evaluated. However, disinfection of protozoa including *C. parvum* was not demonstrated successfully. It was also demonstrated that the process of adsorption with electrochemical regeneration using GIC adsorbents can be used to simultaneously remove organics and to disinfect microorganisms.

Declaration

No portion of the research work presented in this thesis has been submitted in support of an application for another degree or qualification of this or any other university or other institute of learning.

Copyright Statement

i. The author of this thesis (including any appendices and/or schedules to this thesis) owns any copyright in it (the "Copyright") and s/he has given The University of Manchester the right to use such Copyright for any administrative, promotional, educational and/or teaching purposes.

ii. Copies of this thesis, either in full or in extracts, may be made only in accordance with the regulations of the John Rylands University Library of Manchester. Details of these regulations may be obtained from the Librarian. This page must form part of any such copies made.

iii. The ownership of any patents, designs, trade marks and any and all other intellectual property rights except for the Copyright (the "Intellectual Property Rights") and any reproductions of copyright works, for example graphs and tables ("Reproductions"), which may be described in this thesis, may not be owned by the author and may be owned by third parties. Such Intellectual Property Rights and Reproductions cannot and must not be made available for use without the prior written permission of the owner(s) of the relevant Intellectual Property Rights and/or Reproductions.

iv. Further information on the conditions under which disclosure, publication and exploitation of this thesis, the Copyright and any Intellectual Property Rights and/or Reproductions described in it may take place is available from the Head of School of (School of Chemical Engineering and Analytical Sciences) (or the Vice-President) and the Dean of the Faculty of Life Sciences, for Faculty of Life Sciences' candidates.

Confidentiality

The results obtained in this PhD project may be useful in terms of commercial applications for the Arvia® Process. Due to intellectual property rights and commercial confidentiality of the project, this thesis is restricted for general access in the library for 5 years.

Acknowledgements

First and foremost, I would like to express my deepest gratitude to my supervisor, Dr. E.P.L Roberts for his support, motivation and guidance. He has always been very helpful in providing me the right direction for my research work and thesis preparation. He is a very kind and polite person and has provided me with a high level of appreciation and encouragement in achieving the objectives of this project. I really enjoyed his intellectual contribution to my work. I have no words to express my gratitude for the help, motivation and support of Dr. Andrew K. Campen, Process Chemist at Arvia Technology Ltd, who has been so kind and friendly in providing me with guidance and assistance for this project. I am grateful to the co-investigators Dr. Hafiz Anwaar Asghar, Dr. Nigel Willis Brown and David Sanderson for providing me their valuable suggestions.

I would like to thank Elizabeth Davenport, Patrick Hill and Eric Warburton for providing me with assistance in developing analytical techniques including HPLC, GC/MS, SEM and EDS. Special thanks go to Thomas Szpitter and John Riley for their cooperation in providing me with technical assistance while working in the laboratories.

I would like to acknowledge the expertise of Geoffrey Dent for providing me with knowledgeable suggestions and guidance regarding surface characterization of GIC adsorbents. I would also like to extend my thanks to Vicky Fawcett, Konrad Dorling and Amina Belghabon for assisting me in my work on Raman spectroscopy and FTIR for surface characterization. Special thanks go to Raja Ibrahim, Zaenab Abd Allah and Adam Higginson for helping me in my work on FTIR for gas analysis. I also acknowledge Ernesto Hernandez for giving me useful suggestions in the design of gas flow measuring apparatus.

I would also like to acknowledge the help and contribution of Dr. Nuria De las heras, Dr. Antoine Trzcinski and Dr. Ian Cooper in my disinfection work. Many thanks to Dr. Ruohang Wang for providing me all the facilities in my disinfection work. I am also grateful to Khalid Luti and Marie Goldrick for providing me with guidance in developing disinfection performance techniques.

I owe my deepest gratitude to my friend Hamed Sattar for his help regarding my thesis. I am indeed indebted to Hamed Sattar who has been so kind in spending a lot of his valuable time in making my thesis presentable. It is with great pleasure that I thank, The University of the Punjab, Lahore, Pakistan for giving me the scholarship to carry out this study at the University of Manchester, UK.

At last but not least, I feel great honour to pay special gratitude to all the members of my family for their support and prayers. I dedicate the credit from this work to my grandmother (late), my mother and my father. I would like to acknowledge the support and encouragement of my wife who managed my absence with courage and fortitude, and finally, I acknowledge the love of my daughters Laiba and Maham, and my nephews Umar, Hasnain and Hamza.

Abbreviations

Abbreviation	Description
ACF	Activated Carbon Fibre
ATR	Attenuated Total Reflection
AV-17	Acid Violet
BDD	Boron Doped Diamond
BET	Branauer Emmett Teller
BFA	Body Fluid Analog
BOD	Biochemical Oxygen Demand
BQ	Benzoquinone
C. parvum	Cryptosporodium parvum
CAT	Catechol
CFU	Colony Forming Unit
COD	Chemical Oxygen Demand
DC	Direct Current
DCP	Dichlorophenol
DNA	Deoxyribonucleic Acid
DPD	Diethyl-p-phenylenediamine
DRIFTS	Diffuse Reflectance Infrared Fourier Transform Spectroscopy
DSA	Dimensionally Stable Anode
DTGS	Deuterated Triglycine Sulphate
E. coli	Escherichia coli
EDS	Energy Dispersive X-Ray Spectroscopy
EPA	Environmental Protection Agency
EQCM	Electrochemical Quartz Crystal Microbalance
GAC	Granular Activated Carbon
GC	Gas Chromatography
GIC	Graphite Intercalation Compound
GPC	Gel Permeation Chromatography
HPLC	High Performance Liquid Chromatography
HQ	Hydroquinone
IC	Inorganic Carbon
ICE	Instantaneous Current Efficiency
L. pneumophila	Legionella pneumophila
M	Molar
MCP	Monochlorophenol
MS	Mass Spectrometry
NHE	Normal Hydrogen Electrode
NIST	National Institute of Standards and Technology
NMR	Nuclear Magnetic Resonance
P. aeruginosa	Pseudomonas aeruginosa
PAC	Powdered Activated Carbon
PAS	Photoacoustic Spectroscopy

Continued

Abbreviation	Description
R. turoloides	Rhodosporidium turoloides
RNA	Ribonucleic Acid
S. aureus	Staphylococcus aureus
S. cerevisiae	Saccharomyces cerevisiae
SBR	Sequential Batch Reactor
SCE	Saturated Calomel Electrode
SHE	Standard Hydrogen Electrode
TC	Total Carbon
TC	Theoretical Charge
TCP	Trichlorophenol
TOC	Total Organic Carbon
TPD	Temperature Programmed Desorption
UV	Ultraviolet
XPS	X-ray Photoelectron Spectroscopy

Nomenclature

Symbol	Description	Unit
[B]	Concentration of base solution	M
[HCl]	Concentration of HCl used for titration	M
C_e	Equilibrium concentration of adsorbate in the solution	mg L^{-1}
C_f	Final concentration of adsorbate in solution	mg L^{-1}
C_i	Initial concentration of adsorbate in solution	mg L^{-1}
F	Faraday's constant	96485.34 C mol^{-1}
I	Electric current	A
K_a	Langmuir constant	L mg^{-1}
K_a	Dissociation constant of HOCl	M
K_F	Freundlich constant	mg g^{-1}(L mg^{-1})$^{1/n}_F$
K_H	Equilibrium constant for the hydrolysis reaction of Cl_2	$(mol\ L^{-1})^2$
m	Mass of adsorbent	g
N	Staging index	
n_F	Freundlich intensity parameter	
N_{GSF}	Moles of graphite surface functionalities	Mole
P	Pressure	Atm
q_e	Amount of adsorbate adsorbed on the surface per unit mass of adsorbent at equilibrium	mg g^{-1}
q_i	Adsorptive capacity of fresh adsorbent	mg g^{-1}
q_m	Langmuir monolayer capacity	mg g^{-1}
q_r	Adsorptive capacity of regenerated adsorbent	mg g^{-1}
R	Universal gas constant	8.314 J $K^{-1}mol^{-1}$
R^2	Correlation coefficient	
T	Time	S
T	Temperature	K
V	Volume of solution	L
V_a	Volume of the aliquot taken from the filtrate	mL
V_B	Volume of base mixed with graphite sample	mL
V_{CO2}	Volumetric flow rate of gas	L sec^{-1}
V_{HCl}	Volume of HCl solution required for neutralization	mL
Z	Average number of bacteria	
γ	Regeneration efficiency	%
Φ	Fractional charge yield	

Chapter 1

Introduction and Background

This introductory chapter sets up the significance of treating low concentrations of organics from wastewaters with a brief discussion on various methods used for removing non-biodegradable species from waste effluents. In addition, the importance of removing pathogenic microorganism has also been highlighted. Various techniques which can be used for regenerating activated carbons are described and their relative merits and disadvantages are discussed. An innovative and state of the art process of adsorption with electrochemical regeneration using a highly conducting non-porous graphite based adsorbent is introduced. The background to this project is briefly outlined and the detailed research objectives related to this project has been identified. A brief outline of the research methodology which will be used to meet these objectives is provided. In addition, the potential benefits associated with the outcomes of this research have also been presented and the structure of the thesis is explained at the end of the chapter.

1.1 Introduction

Water is an indispensable commodity for all living creatures on the planet. Naturally occurring water contains inorganic ions, dissolved gases and organics, solid matter such as colloids, silts and suspended solids and biological material such as bacteria and viruses *(Crittenden et al. 2005)*. Contamination of water caused by organic constituents originates from natural organic matter, compounds generating from human activities and compounds formed during treatment and disinfection of water. Industries that consume large quantities of chemicals in various manufacturing processes are a significant source of organic pollution of water. Rapid industrialisation and urbanization, as a consequence, is intensively depleting the basic characteristics of the environment due to the release of hazardous and toxic substances into water. The organic impurities present in water could cause serious threat to the quality of water for a number of reasons. They are broken down by the microorganisms present in water which results in a decrease in the oxygen content of

the water thereby affecting the aerobic activity within the water source *(Misra et al. 2006)*. This issue has been of great importance because the input of dissolved oxygen in a water body is mainly due to atmospheric diffusion through the surface and is limited by the low solubility of oxygen in water (12.8 mg O_2 L^{-1} at 5 ^oC to 7.7 mg O_2 L^{-1} at 30 ^oC) *(Horan, 1990)*. The other adverse environmental impacts caused by organic contaminants include acute toxicity (*Halling-Sorensen et al. 1998)*, resistant development in bacteria *(Kummerer, 2004)*, genotoxicity and endocrine disruption *(Arcand-Hoy et al. 1998)*. Hence, water pollution due to the discharge of coloured, toxic and non-biodegradable organic contaminants from the industrial, municipal and agricultural sectors has become a serious concern for the world today. This is mainly due to public consciousness about the importance of the protection of the environment, as well as the health effects of pollution. In addition, advanced analytical and instrumental techniques are becoming available to detect and measure trace quantities of toxic organic pollutants in wastewater. The presence of these chemical hazards deteriorate the quality of water and make it unfit for its intended uses. Keeping in view the overall aspects of water pollution, microbiological contamination is the most important issue concerning public health. A variety of pathogenic microorganisms is found in wastewater including bacteria, fungi and viruses *(See Chapter 7)*. These micro-species can occur in a very large number, for example in the case of bacteria the total counts have been measured in the range of $1-38 \times 10^6$ mL^{-1} *(Horan, 1990)*. They may be excreted by human beings and animals that are infected with these pathogenic microorganisms. The pathogenic bacteria of the human origin cause many diseases of gastrointestinal tract such as typhoid, dysentry, diarrrhea, paratyphoid and cholera *(Metcalf and Eddy, 2003)*. Furthermore, water borne contaminations caused by the presence of pathogens in water could spread diseases of epidemic proportions particularly in the non-developing countries. According to world health organization, nearly half of the population in these countries suffers from health problems associated with the lack of safe drinking water or due to the presence of microbiologically contaminated water *(WHO, 1992)*. The scarcity of water free of undesirable species has made water reclamation an important issue.

The organic content of wastewater is traditionally measured by using parameters such as BOD, COD or TOC. Biochemical oxygen demand (BOD) is the most widely

used parameter for determining the organic pollution of wastewater which involves the measurement of dissolved oxygen consumed by microorganisms in the biochemical degradation of organic constituents. This measure gives an indication of the readily available biodegradable organic matter of an effluent. However, it is associated with certain disadvantages such as longer incubation periods (5 days), poor reproducibility of the results (±15%) and its limitation to biodegradable organics *(Horan, 1990)*. COD (chemical oxygen demand) is the amount of oxygen required for the chemical oxidation of organic material present in water and it gives a better indication of the total organic load of water with good reproducibility of results *(±5−10%)*. In addition, it is comparatively a rapid test producing data within 3 hours *(Horan, 1990)*. The TOC (total organic carbon) test is used to determine the total organic carbon in an aqueous sample and usually it gives a measure of the pollution characteristics of a wastewater *(Metcalf and Eddy, 2003)*. It is the most rapid test (5−10 minutes) compared to BOD and COD which makes it important in wastewater monitoring applications.

There are different processes for the removal of low concentrations of organic pollutants from wastewater such as chemical *(Levec and Pintar, 1995)* and electrochemical oxidation *(Martinez-Huitle and Ferro, 2006) (See Chapter 4)*, coagulation and flocculation *(Bratby, 2006)*, membrane separation *(Strathmann, 1976)*, biological treatment *(Kuritz and Wolk, 1995)* and adsorption *(Bansal and Goyal, 2005)*. Biodegradation is the most widely used and low cost alternative to many physical and chemical means used for the removal of organic pollutants from water. However, it is only associated with the removal of those organics which are capable of undergoing biological decomposition. Coagulation/flocculation and chlorination processes have been extensively used for the treatment of water containing natural organic matters and trace organic contaminants. These processes are not completely successful in removing the pollutants from wastewater and often generate sludge which requires further treatment and disposal *(Semerjian and Ayoub, 2003)*. Natural organic matters have been found to react with disinfectants such as chlorine, ozone, chlorine dioxide and chloramines. They produce other disinfection products such as trihalomethanes, haloacetic acids, bromoform, dibromoacetic acid etc which are toxic compounds *(Technology Review, 2007; Richardson et al. 2003)*. A range of membrane processes have been used in wastewater treatment for

producing high quality water. However, the deposition of natural organic matter as well as trace organic contaminants can foul the membrane materials which can significantly affect the operating cost and performance of membrane technology for wastewater treatment *(Technology Review, 2007)*. Membranes are expensive to purchase and due to their fouling the cleaning and/or replacement of membranes can be frequently required which increases the operating cost *(Owen et al. 1995)*. In addition, a concentrate stream is produced which will require further treatment. Pollutants which are not amenable to biological treatment are usually chemically stable species and are not easily mineralized. It is therefore necessary to adopt reactive systems such as chemical oxidation and advanced chemical oxidation. Advanced oxidation processes are characterized by the production of hydroxyl radicals. They make use of expensive reactants such as H_2O_2 and/or O_3 and therefore their application is usually limited to contaminants that are not readily treated by more economical treatment processes *(Andreozzi et al. 1999)*.

Adsorption has become increasingly important in recent years due to its high efficiency in the removal of non-biodegradable contaminants. Activated carbon is considered to be the most effective material for the removal of low concentrations of organics from wastewaters *(Halhouli et al. 1995)*. The economics and feasibility of the adsorption process on a large scale employed for the treatment of wastewater depends upon the regeneration and reuse of the activated carbon. However, problems associated with the regeneration of activated carbon remain a key issue. Thermal regeneration techniques are widely used but these are characterized by 5–10% material losses, high energy costs and off-site regeneration which results in high transportation cost *(Miguel et al. 2001)*. One solution is to eliminate the regeneration process by exploiting low cost adsorbents which are natural materials and wastes and by-products generated from many industries. These indigenous materials are used as such or after a minor treatment *(Gupta et al. 2009)*. They are based on carbonaceous waste products such as fly ash *(Wang and Jiang, 2007; Rastogi et al. 2008)*, peat *(Couillard, 1994)*, straw *(Streat et al. 1995)*, used rubber tyres *(Streat et al. 1995)*, lignite *(Allen and Koumanova, 2005)*, bagasse pith *(McKay et al. 1987)*, dried activated sludge *(Aksu and Yener, 2001)*, saw dust *(Malik, 2004)*, fertilizer plant waste slurry *(Bhatnagar and Jain, 2005)* and many others that can be used on a once through basis. However, this approach will only change the physical state of the

pollutant from liquid to solid phase, and the contaminated solid phase will require careful disposal. The second approach is to investigate economically viable and environmentally friendly regeneration techniques such as chemical/solvent regeneration *(Sutikno and Himmeistein, 1983)*, microbial regeneration *(Hutchinson and Robinson, 1990)*, wet air oxidation *(Shende and Mahajani, 2002)*, ultrasonic *(Lim and Okada, 2004; Schueller and Yang, 2001)* and electrochemical regeneration *(Minghua et al. 2005) (See Chapter 4)*. Regeneration of activated carbon by bacteria is a feasible and economical method for biologically degradable adsorbates whereby the added bacteria is immobilized on the porous surface of activated carbon. This interaction between the bacteria and the adsorbate degrades the adsorbed species with the evolution of metabolism by-products. The common disadvantages of biological method includes longer regeneration times (20–50 days), partial clogging of the pores by the products of bacteria metabolism and the need to separate the adsorbent from biomass after the completion of regeneration which is a difficult process *(Bandosz, 2006)*. In addition, this approach is limited to contaminants which are biodegradable. Chemical/solvent regeneration is a technique that involves desorption or extraction of the adsorbed species by means of an organic solvent or inorganic chemicals. It is a simple and inexpensive method but is associated with regeneration efficiencies below 70% and about 10−15% of the pores of activated carbon become blocked by the solvent *(Berenguer et al. 2010)*. Moreover, reuse of the solvent requires expensive regeneration techniques such as distillation or liquid-liquid extraction. Wet air oxidation of the spent activated carbon is another alternative to thermal regeneration, in which a slurry of adsorbent is directly regenerated without dewatering and is therefore associated with no particulate emissions and carbon losses are less than 7% *(Mishra et al. 1995)*. However, it utilises high temperatures (125–300^{o}C) and pressures (0.5–20 Mpa) *(Kolaczkowski et al. 1999)* with associated high costs, which is the main drawback of this process. The application of an acoustic field in the form of ultrasound appears to be promising for the regeneration of adsorbents; however it needs extensive work in optimizing frequency and intensity of ultrasound and developing adsorbents with greater mechanical strength so that they can withstand the acoustic effects *(Rege and Yang, 1998)*. Electrochemical regeneration of activated carbons has been developed as a feasible alternative to thermal regeneration *(Narbaitz and Cen, 1994)*. It has a number of potential advantages compared to the thermal regeneration, including in

situ regeneration, minimal adsorbent losses, high regeneration efficiencies and suitability for use in small and medium sized treatment units *(Narbaitz and Karimi-Jashni, 2009) (See Chapter 4)*. Nevertheless, the high porosity of activated carbon and its low electrical conductivity lead to long regeneration times and high energy consumption *(Brown et al. 2004a&b)*.

In order to address these problems associated with the regeneration of activated carbon, a non-porous graphite based adsorbent material called Nyex®, has been developed to remove low concentrations of coloured, toxic and non-biodegradable organic pollutants from wastewaters *(Brown, 2009)*. This material is a graphite intercalation compound (GIC) *(Eccleston et al. 2009)*. Graphite is a naturally occurring form of crystalline carbon. It has a layered structure with the carbon atoms in the layers arranged in a network of regular hexagons. Intercalation is the insertion of ions, atoms or molecules into the interplanar voids of a lamellar structure without destruction of the host's layered bonding network *(Ebert, 1976) (See Chapter 2)*. These adsorbent materials have low adsorptive capacity due to their non-porous character. The intra-particle diffusion which is the rate determining step for non-porous solids is eliminated. This in turn increases the adsorption rate at the expense of a much reduced adsorption capacity *(Brown et al. 2004a&b)*. However, the Nyex® has been characterized by its high electrical conductivity, which is about 5 to 10 times greater than that of activated carbon and allows its simple, cheap and quick electrochemical regeneration *(Eccleston et al. 2009)*. In addition, the non-porous character of Nyex® facilitates electrochemical regeneration because the electrochemical effects are confined to the external surface of carbon as suggested by *Narbaitz and Cen (1994)*. These GIC adsorbents have been effective in removing a wide range of organic contaminants from wastewater such as natural organic matter, pesticides (atrazine and metaldehyde), chlorinated species (chlorinated phenols, dichloromethane, trichloroethylene), oils and solvents, hard COD and organic dyes *(Brown, 2009; Brown et al. 2004a&b; Brown and Roberts, 2007)*. Besides their applications in the removal of trace organic impurities from water, these materials have also the capability of treating highly contaminated wastes where other process options are limited such as colour removal from highly saline waste streams *(Brown, 2009)*.

1.2 The Arvia® Process

An innovative and state-of-the art process for water treatment was developed at the University of Manchester, UK *(Brown, 2005)*. This project is based on the adsorption of non-biodegradable organics present as trace impurities in water onto a graphite intercalation compound (GIC) adsorbent (Nyex®). The process of exploiting such an adsorbent for adsorption and electrochemical regeneration in treating water contaminated with organics is being commercialized by the University of Manchester's spin-out company Arvia Technology Ltd. This technology has a number of potential benefits compared to other traditional reclamation processes. It not only removes the contaminant from the water by adsorption, it also completely destroys the contaminant though anodic oxidation. Consequently, the process does not generate any secondary sludge or waste streams other than the gaseous products which are safely discharged into the atmosphere. In addition, electrochemical regeneration is carried out at room temperature and pressure with low cost, no or minimal use of chemicals. A simple process design has been developed with no moving parts and with the potential for simple scale up *(Lab News, 2008)*.

The process can be operated in batch as well as in continuous mode.

1.2.1 Batch Process

Electrochemical regeneration can be carried out in a simple batch electrochemical cell *(Brown et al. 2004a)*, shown in Figure. 1.1. Batch adsorption is followed by solid/liquid separation and batch electrochemical regeneration. The batch electrochemical regeneration cell is typically composed of an anode, such as a graphite or coated titanium plate, a perforated stainless steel cathode, and the electrodes are separated by a micro-porous polyethylene membrane. A bed of adsorbent to be regenerated is located between the anode and the membrane and a DC current is applied across the bed, resulting in the electrochemical regeneration of the adsorbent through anodic oxidation.

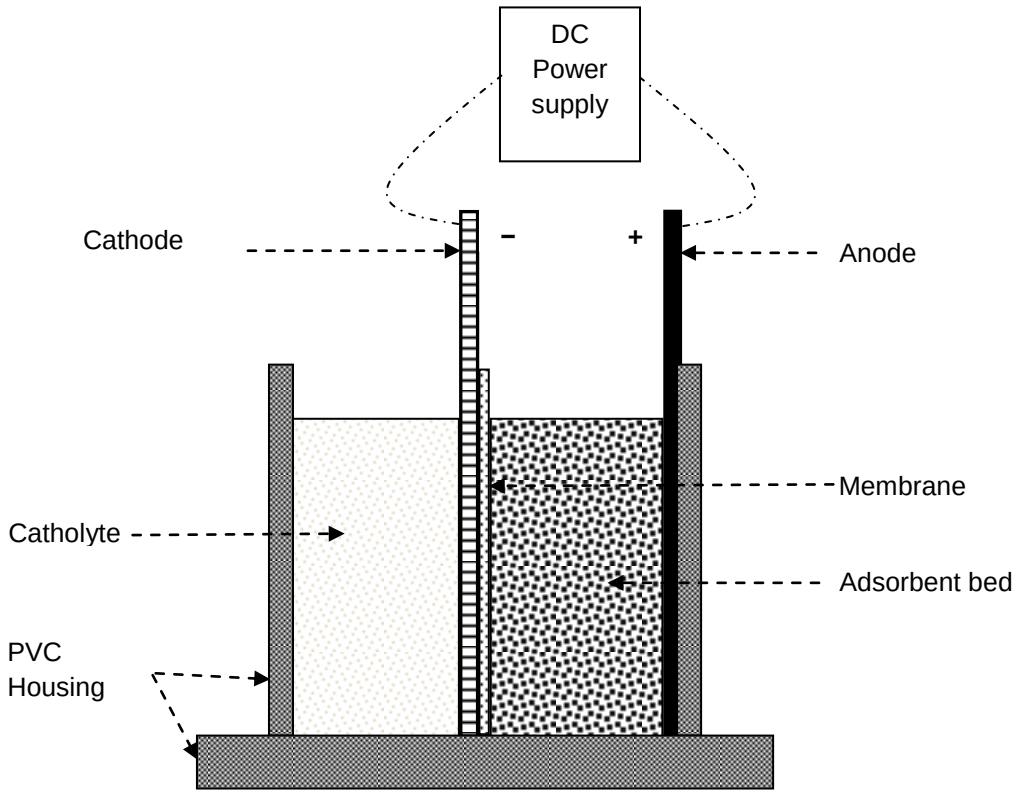

Figure 1.1: *Schematic diagram of a batch electrochemical cell for regeneration, Brown et al. (2004a)*

1.2.2 Continuous Process

A continuous and simultaneous adsorption and electrochemical regeneration unit was developed which would be applicable to a wide range of wastewater treatment applications such as tertiary treatment of sludge, effluent polishing, groundwater treatment, colour removal, industrial effluent treatment and removal of pesticides etc *(Eccleston et al. 2010).*

This unit consists of a reservoir having an inlet and outlet for the water to be treated, with a regeneration chamber within the reservoir, as shown in figure 1.2. The design has no internal moving parts and continuous adsorption and regeneration are achieved by fluidising adsorbent particles with air within the adsorption zone (see figure 1.2), which drives the hydrodynamic control of the whole unit. The incoming effluent enters at the bottom on both sides of the reservoir. The effluent flows

upwards in the risers through the adsorption zones, until it overflows out of the unit at the top of the reservoir. The base of each riser is equipped with a set of nozzles through which air is sparged which causes entrainment of regenerated particles from the bottom of the regeneration zone so that they are mixed with the incoming effluent. The flow of air is adjusted in such a way that the solids are thoroughly mixed and a suspension of adsorbent particles is maintained. During this process the adsorption of unwanted pollutants take place onto the surface of the adsorbent. At the top of the adsorption zones, air bubbles disengage and the water flows into a settlement zone, in which the loaded solid particles are separated out from the upward flowing treated effluent. As the high density solid particles settle in the centre of the unit, they form a moving bed between the anode and the membrane in the regeneration chamber. A dimensionally stable anode (DSA) current feeder is in contact with the moving adsorbent bed forming the anode. A perforated stainless steel cathode is typically used, as before. An acidic NaCl catholyte solution is continuously pumped through the cathode compartment. It is separated from the anode by a micro-porous polyethylene membrane. A direct current is passed between the anode and cathode plates in order to electrochemically regenerate the adsorbent bed. Adsorbed organics on the surface of adsorbent are oxidized into simple molecules. At the cathode, reduction of water takes place producing hydrogen gas. A number of reactions occur at the Nyex® surface which acts as the anode. These reactions include oxidation of the adsorbed organics (by direct and/or indirect oxidation) to carbon dioxide and/or other breakdown products, the oxidation of chloride ions to chlorine; and the oxidation of water *(Brown et al. 2004a)*.

Any gases produced in the regeneration zone rise in the form of small bubbles that escape from the top of the cell into the atmosphere. In this way, the Nyex® particles are continuously circulated within the reservoir through the adsorption zone, then move downwards as a bed in the regeneration zone, and then re-enter the adsorption zone. Thus adsorption and electrochemical regeneration take place continuously and simultaneously within the process operation. Further details of the continuous process are described elsewhere *(Eccleston et al. 2010; Mohammed et al. 2011)* and in chapter 4 (see section 4.4.1)

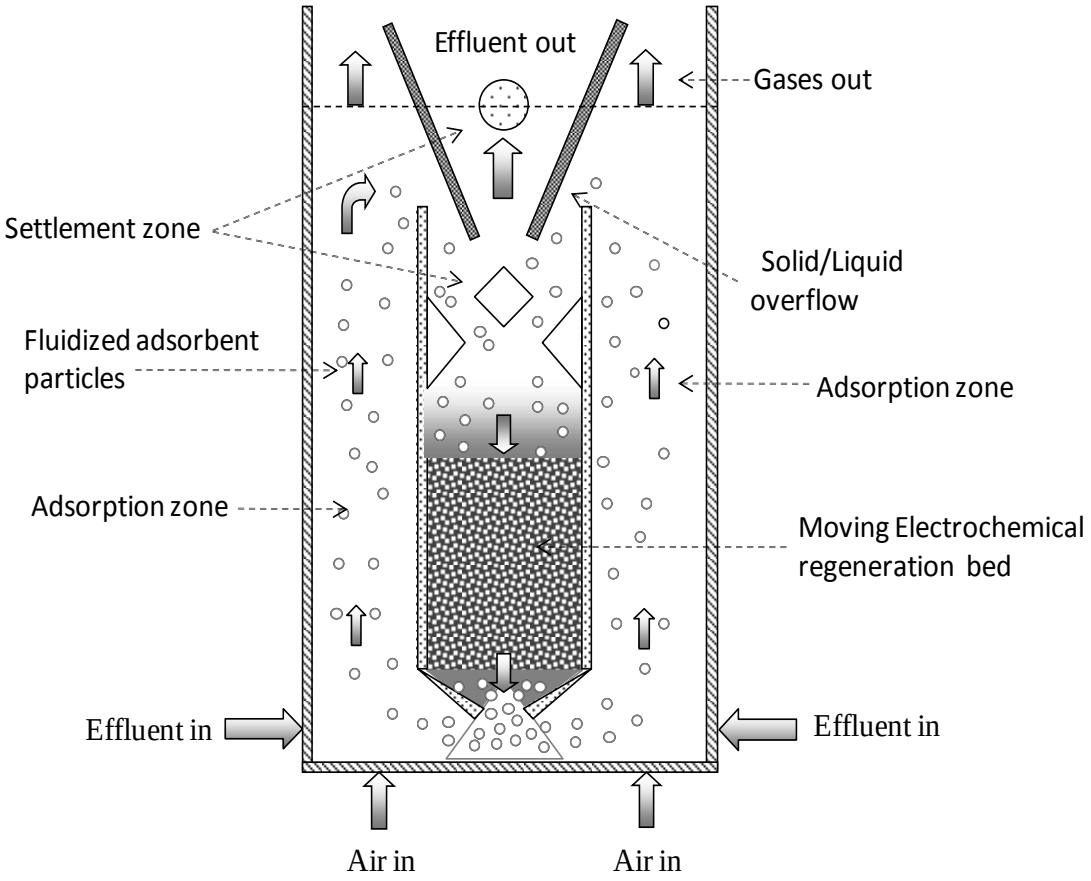

Figure 1.2: *Continuous adsorption and electrochemical regeneration unit*

The Arvia® process is an effective method for removing a variety of organic pollutants from wastewaters because it removes the contaminants by adsorption with rapid electrochemical regeneration of the adsorbent. However, there is a need for further information about the mechanism of the electrochemical regeneration for successful application and commercialization of this technology. It has been suggested that all adsorbed species are mineralized completely during electrochemical regeneration *(Brown and Roberts, 2007)* leaving no intermediate breakdown products in the treated water. In order to elucidate the processes occurring during the electrochemical regeneration of the GIC adsorbent, a thorough and detailed investigation is required to evaluate the presence of breakdown products in solution and in the gaseous phase. The aim of this PhD research is firstly to investigate the electrochemical regeneration of a non-porous graphite based adsorbent (GIC) regarding the formation of intermediate breakdown products and the

fate of the adsorbed species. Secondly, this project also aims to investigate the application of the Arvia® process to water disinfection which would be a novel application since previous studies have focussed on dissolved contaminants. The background to this project and the detailed objectives are further discussed in the proceeding sections.

1.3 Nature of Problem

Electrochemical oxidation has significant potential for application to water and wastewater treatment because of its ability to remove a wide variety of organic impurities. However, the process also has some disadvantages such as high cell potentials due to the low electrical conductivity of water and the associated increased electrical power requirements *(Anglada et al. 2009)*. Mass transfer limitations can also be an important factor when removing low concentration of organics. On the other hand, removal of organics by activated carbon adsorption is an effective and widely used process *(Jiuhui, 2008; Halhouli et al. 1995)*. However, while adsorption is effective at removing contaminants, the process transfers the contaminant onto the solid phase adsorbent which will become saturated and must be disposed of or regenerated, as discussed before. In addition, the intra-particle diffusion usually controls the rate of adsorption and desorption of organics from activated carbons which require long adsorption and regeneration times *(Narbaitz and Cen, 1994)*. These issues have been addressed by research at the University of Manchester which has led to the development of a process (the Arvia® process) in which the organic substances from water are adsorbed onto the surface of a GIC adsorbent prior to its electrochemical oxidation in a simple electrochemical cell with low cell potentials associated to high electrical conductivity of the adsorbent *(Eccleston et al. 2009)*. An ideal electrochemical regeneration process should mineralize the adsorbed pollutants completely into CO_2 and H_2O thereby converting the pollutants into less harmful products. However, depending upon the mechanism of the regeneration process, the contaminants may not be mineralized completely and therefore some of the adsorbed organics might be converted into undesirable breakdown products *(Vlyssides et al. 2004)*. In the Arvia® process, electrochemical regeneration of GIC adsorbents is achieved through the anodic oxidation of the adsorbed species in which each particle of adsorbent behaves as an anode within the electrochemical cell. The regenerated

adsorbent, including any water trapped in the bed of adsorbent, is transferred without additional treatment to the next adsorption cycle. This means that no secondary waste is being generated in the process. However, partially oxidized organics could be released into the treated water causing contamination with potentially more toxic compounds. The nature and concentrations of the breakdown products generated during electrochemical oxidation could play an important role in determining the toxicity of the treated effluent.

1.4 Project Objectives

The main goal of this research project is to investigate the formation of breakdown products during the electrochemical oxidation of adsorbed organics on the surface of GIC adsorbents. The determination of the oxidation products will help in determining the possible pathway or mechanism of the electrochemical degradation of adsorbed organics. Keeping in view the oxidation mechanism, the process conditions will be optimised in order to minimise the presence of breakdown products in the treated water, particularly organo-chlorinated compounds which can occur during electrochemical oxidation and can be toxic than the original organic contaminants *(Henschler, 1994)*. The fate of the adsorbed organics and the mechanism of regeneration are clearly of great significance in achieving the potential benefits of the process of adsorption with electrochemical regeneration. This project also aims to determine the nature, rate of formation and concentration of the any gases generated during the electrochemical regeneration process. The reason for looking at the gases is to assist in understanding the mechanism of breakdown since some breakdown products will appear as gases. The evaluation of these gases is particularly important for large scale applications of the process of adsorption with electrochemical regeneration because the evolution of toxic breakdown products released as regeneration gases could pollute the surrounding atmosphere. This determination would permit safe operation of the process of adsorption with electrochemical regeneration with appropriate handling of the gases generated during large scale operation. During electrochemical regeneration of GIC adsorbents, the fingerprints of the adsorbed organics will also determine the nature of species formed to the surface. This work also aims in attempting a preliminary investigation of the surface of these adsorbents during the adsorption and electrochemical

regeneration process. Any changes in the species present on the surface would be helpful in determining the mechanism of electrochemical regeneration.

Another important aspect of this PhD project is the evaluation of the performance of the process of adsorption with electrochemical regeneration for water disinfection. The adsorption of microorganisms on the surface of GIC adsorbent materials and their behaviour during electrochemical regeneration needs thorough investigation. The evaluation of in-situ free chlorine generation is also important to investigate the role of electrochlorination in the process of adsorption with electrochemical regeneration. The outcomes of this study will determine whether the process of adsorption with electrochemical regeneration is potentially applicable to water disinfection, an application which has not been previously studied. The project will also investigate whether the process can remove the organic pollutants and disinfect water simultaneously. This approach is focused on addressing water treatment problems where a variety of pollutants along with pathogenic microorganisms may be present such as swimming pool water.

1.5 Research Tasks

This PhD project covers the following research tasks:

- Investigation of the breakdown products which occur in the liquid phase during electrochemical regeneration of GIC adsorbents loaded with a model contaminant.
- Elucidation of a probable mechanism of electrochemical regeneration of GIC adsorbents loaded with a model contaminant.
- Determination of the adsorption behaviour of GIC adsorbents for possible breakdown products.
- Investigation of the formation of free chlorine during electrochemical regeneration of GIC adsorbents.
- Evaluation of the formation of chlorinated breakdown products in the liquid phase during batch and continuous water treatment by adsorption with electrochemical regeneration.

- Determination of operating conditions for water treatment by adsorption with electrochemical regeneration that minimize the formation of chlorinated breakdown products.
- Evaluation of gases formed during electrochemical regeneration of GIC adsorbents loaded with a model contaminant.
- Investigation of the composition of adsorbed species and how these change during regeneration of GIC adsorbents.
- Investigation of the suitability and applicability of adsorption and electrochemical regeneration for the disinfection of water, including the treatment of different species of bacteria and fungi.
- Evaluation of the simultaneous treatment of dissolved organics and microorganisms by adsorption with electrochemical regeneration.

1.6 Research Methodology

A model pollutant has been selected for detailed study of its oxidation mechanism during electrochemical regeneration of a GIC adsorbent loaded with the selected pollutant. The selection of this pollutant was based on the availability of detailed information about the electrochemical oxidation products of this pollutant in the literature. Batch adsorption and electrochemical regeneration studies have been carried out using a GIC adsorbent and the selected model pollutant. Analysis of the liquid samples during adsorption and regeneration cycles has been carried out using GC-MS which made possible the identification of the compounds generated during the electrochemical process. After the species were identified, their concentrations were determined using high pressure liquid chromatography. The formation of breakdown products has been investigated under a range of experimental conditions. The formation of breakdown products has also been investigated for continuous water treatment by adsorption with electrochemical regeneration.

In addition to breakdown products, the concentration of free chlorine has been determined under a range of operating conditions by using a standard method for chlorine measurement.

For the investigation of breakdown products in the regeneration gases, a closed cell has been constructed which enables gases formed during regeneration to be collected and analysed. The rate of formation of gases has been determined under controlled conditions in an attempt to complete a mass balance for the treated contaminant.

Surface characterization and the determination of the changes in the species on the adsorbent surface have been evaluated by a range of surface techniques including Fourier transform infrared spectroscopy (FTIR), Raman spectroscopy, energy dispersive X-ray spectroscopy (EDS) and Boehm titration.

In order to evaluate the performance of the process of adsorption with electrochemical regeneration for water disinfection, a model microorganism has been selected. The process of adsorption with electrochemical regeneration was evaluated for disinfection performance under a range of experimental conditions. Scanning electron microscopy was used in order to get information about changes in the morphology of microorganisms during adsorption and electrochemical regeneration. Different types of bacteria and other microorganisms such as fungal spores were tested for treatment by the process of adsorption with electrochemical regeneration. In addition, the treatment of swimming pool water has been evaluated.

1.7 Potential Benefits

This project provides new data on breakdown products and intermediates formed during electrochemical regeneration of GIC adsorbents used in the process of water treatment by adsorption with electrochemical regeneration developed at the University of Manchester. The identification of these breakdown products will play an important role in determining the performance of the electrochemical process and in understanding the mechanism of electrochemical regeneration. In addition, in depth information about the mechanism of regeneration and formation of undesirable compounds may enable identification of operating conditions which minimise or eliminate the presence of such compounds in the treated water. On the other hand, successful application of the process of adsorption with electrochemical regeneration to water disinfection will not only provide the advantages associated with

electrochemical disinfection but also simultaneous removal of microorganisms and dissolved organics may be possible.

1.8 Structure of Thesis

In order to present comprehensibly the investigations and outcomes of this research project, the thesis has been structured and divided into the following chapters.

Chapter 1 Introduction and Background

This chapter describes the importance of water and wastewater treatment. Different methods employed for treating organic pollutants present in wastewater are discussed. The removal of low concentrations of organics from wastewater by the combined process of adsorption and electrochemical regeneration employing GIC adsorbents in the Arvia® process is introduced. The detailed project objectives are considered, along with the research methodology and the tasks that have been formulated to achieve the objectives.

Chapter 2 Adsorption and Graphite Intercalation Compounds

A brief description of the adsorption process including both physical and chemical adsorption is provided. In order to illustrate the mathematical understanding of the adsorption equilibrium, theoretical adsorption isotherms such as the Freundlich and Langmuir isotherms are described. Activated carbon and its use as a potential adsorbent for removing organic pollutants from wastewater have also been discussed. This chapter presents a brief introduction to graphite intercalation compounds, considering their structure, properties and applications. Graphite bisulphate intercalation compound, which is used throughout this study, has also been discussed.

Chapter 3 Water Treatment by Electrochemical Oxidation

This chapter introduces various electrochemical processes used for water treatment by giving particular attention to electrochemical oxidation. A literature review regarding the mechanism of electrochemical oxidation of organic pollutants present

in water has been discussed. The concept of combined adsorption with electrochemical regeneration has been highlighted. This chapter also contains a detailed literature review regarding the mechanism of electrochemical regeneration of activated carbon. This is followed by the information on breakdown products formed during the electrochemical oxidation of phenol in solution and electrochemical regeneration of the activated carbon. Finally, the surface chemistry of activated carbon and various graphite intercalation compounds after electrochemical treatment have been illustrated briefly.

Chapter 4 Formation of Breakdown Products in Liquid Phase during Electrochemical Regeneration of GIC Adsorbents

This chapter presents the details of the materials and methods along with findings during the investigation of the formation of non-chlorinated break down products released in liquid phase in the batch and continuous Arvia® process under different experimental conditions. The theoretical aspects of free chlorine formation during an electrochemical process are presented. Experimental details with their results about the formation of free chlorine under different anolyte and catholyte conditions have been given. A detailed investigation of the formation of the chlorinated break down products in the batch and continuous Arvia® process under different experimental conditions has also been presented by giving special attention to the conditions that minimize the formation of chlorinated species during the electrochemical regeneration of Nyex® materials.

Chapter 5 Evaluation of Gases during Electrochemical Regeneration of GIC adsorbents

The significance of evaluating the regeneration gases and thus the formation of any breakdown products formed in the gaseous form during electrochemical process in the Arvia® technology is presented. The materials and methods used for the identification and quantification of the off gases have been described. This chapter also narrates the attempt which has been made to perform a mass balance of the pollutant in the batch Arvia® process. Finally, the limitations regarding the evaluation of the off gases and the mass balance has been described.

Chapter 6 Surface Investigation of GIC Adsorbents during Adsorption and Electrochemical regeneration

This chapter introduces different techniques used for investigating the fingerprints of the pollutant on the surface of Nyex® materials during adsorption and particularly during electrochemical regeneration in the batch Arvia® process. The materials and methods along with their findings and limitations are presented.

Chapter 7 Electrochemical Disinfection of Water

This chapter provides some basic concepts of electrochemical disinfection of water by giving special emphasis to the mechanism of disinfection. A brief review of the literature regarding electrochemical disinfection of water has been presented. It also describes the disinfection of the bacteria adsorbed on the surface of granular activated carbon. Various microorganisms and the techniques used for evaluating the disinfection performance have been explained in this chapter.

Chapter 8 Disinfection of Water by Adsorption with Electrochemical Regeneration

This chapter investigates the application of the Arvia® process to disinfect microorganisms in water. The materials and methods and the results of this investigation at different experimental conditions have been laid out. Detailed scanning electron microscopy of microorganisms during adsorption and electrochemical regeneration has been presented. The capability of the Arvia® process in the removal of organics and disinfecting bacteria simultaneously has also been given by treating artificial swimming pool water. Finally, water contaminated with different types of bacteria and fungus have been tested by the batch Arvia® process in order to strongly support the application of the Arvia® process to water disinfection.

Chapter 9 Conclusions and Recommendations

The conclusions of the work undertaken in this project with some future recommendations are presented in this chapter.

Chapter 2

Adsorption and Graphite Intercalation Compounds

This chapter provides a brief description of the fundamentals of adsorption. In order to illustrate the physical significance of the adsorption isotherm, the classification of the shapes of adsorption isotherms and the mathematical models such as the Freundlich and Langmuir models have been described. Activated carbon and its use as a potential adsorbent for removing organic pollutants from wastewater have also been discussed. This chapter also presents a brief introduction to graphite intercalation compounds (GICs) including their structure, properties and applications. A brief literature review regarding the use of GICs for water treatment has also been presented.

2.1 Adsorption

Adsorption is a surface phenomenon in which molecules of a solute (adsorbate) distributes themselves between two phases one of which is a solid phase (adsorbent) whilst the other may be a liquid or a gas. The distribution of the adsorbate between the phases depends upon the nature of the forces which exist between the molecules of adsorbate and solvent and the adsorbent which in turn depends upon the nature of the adsorbent and the physiochemical features of the adsorbate *(Site, 2001)*. Thus, the adsorption may be physical or chemical based on the nature of interaction of a particular species between the two phases involved. In physical adsorption the molecules of an adsorbate in the liquid or gas phase interact with the surface of a solid adsorbent by weak van der Waals forces, similar to vapour condensation or liquid precipitation. Physical adsorption is a reversible phenomenon in that the adsorbed species are again released in solution on the decrease in solution concentration, whereas in chemisorption the molecules are strongly bonded to the surface by the exchange or sharing of electrons. Chemical adsorption is not easily reversed due to the involvement of chemical bonds and therefore regeneration of the

adsorbent could be a potential problem. Chemisorption is restricted to one layer of adsorbed species; however it may be followed by additional physically adsorbed layers. In water treatment, the impurities are most commonly removed by mechanism of physical adsorption.

Besides numerous applications in industry and environmental protection *(Dabrowski, 1999)*, adsorption has extensive applications in water treatment because it is relatively a fast, inexpensive and widely applicable method for the removal of soluble and insoluble impurities and biological contaminants with removal efficiency of 90–99% *(Ali and Gupta, 2006)*. Activated carbon, synthetic polymeric, and silica based materials are the principal adsorbents for the removal of impurities from water. However, because of the high cost of synthetic polymers and silica based adsorbents, they are rarely used in water treatment applications *(Metcalf and Eddy, 2003)*. Adsorption of organic compounds in the liquid phase on activated carbon depends upon a number of factors *(Haghseresht et al. 2002)* including:

- The physical nature of the adsorbent, including the surface area *(Zhang et al. 2005)*, pore structure *(Li et al. 2002)*, ash content *(Leng and Pinto, 1997)*, and surface functional groups *(Coghlin and Ezra, 1968; Dabrowski et al. 2005)*
- The nature of the adsorbate, including the functional groups *(Franz et al. 2000)*, molecular weight, size, hydrophobicity, solubility and polarity *(Moreno-Catilla, 2004; Lin and Hsu, 1995)*
- The solution conditions, including the adsorbate concentration *(Tan and Teo, 1987)*, pH *(Halhouli et al. 1995)*, ionic strength *(Al-Degs et al. 2008)*, temperature *(Schreiber et al. 2005)* and presence of competitive adsorbate *(Knettig et al. 1986)*

2.2 Activated Carbon

Activated carbon is the most widely used adsorbent in water treatment for the removal of taste and odour causing compounds, colour forming chemicals, disinfection by-products, synthetic organic chemicals such as pesticides, herbicides, detergents, polycyclic aromatic hydrocarbons, phenolic compounds and some inorganic species such as perchlorate, arsenic, heavy metals etc. *(Crittenden et al.*

2005; Dabrowski, 2001). On the other hand, natural organic matter is a complex mixture of decomposition compounds of animal and plant materials and is found in varying concentrations in all natural waters. Natural organic matter is typically composed of a range of organic compounds such as proteins, amino-acids, humic and fulvic acids *(Dabrowski, 2001)*. These compounds may react with disinfectants such as chlorine and form toxic disinfection by-products which are effectively removed by adsorption with granular activated carbons.

Activated carbon constitutes the porous structure with a large internal surface area (500−1500 $m^2 g^{-1}$) *(Noyes, 1991)*. The overall porous structure of activated carbon is formed by a wide range of pore sizes. They may be divided into three basic classes namely micropores (<1 nm), mesopores (>1 nm and <25 nm) and macropores (>25 nm) *(Metcalf and Eddy, 2003)*. Commercially, activated carbons are classified on the basis of their particle size and shape into powdered and granular activated carbons. Powdered activated carbons (PAC) have a particle size usually less than 100 μm. Due to their small particle size, high adsorption rates are possible which is basically due to the lower diffusional resistance to adsorption. Granular activated carbons (GAC) have a relatively large particle size compared to PAC. They are more desirable for continuous adsorption processes. GAC has a relatively high adsorptive capacity, selectivity, stability, ability to withstand thermal regeneration and resistance to attrition losses during transport and handling. These characteristics of GAC are important for applications in water treatment *(Dabrowski, 2001)*. In addition, the hydrophobic and organophillic nature of activated carbon is also significant for their use in water treatment *(Ruthven, 1984)*. However, the economic feasibility of water treatment by adsorption employing activated carbon depends upon the availability of an efficient means of regenerating and recycling the activated carbon after its adsorptive capacity has been exhausted *(Muranaka et al. 2010)*. Although thermal regeneration is the most widely used technique for regenerating activated carbon, it has certain disadvantages including high operating costs and loss of surface area by destruction of micropores of the adsorbent *(Muranaka et al. 2010)*. Moreover, the organo chloro compounds adsorbed on the activated carbons are not efficiently destroyed and elimination of toxic gaseous by-products may pollute the surrounding environment *(Toledo et al. 2003; Okawa et al. 2007)*. Other regeneration techniques and their relative merits and disadvantages

have been briefly discussed in Chapter 1. Electrochemical regeneration of GIC adsorbents, used in this research project, is described in Chapter 3.

2.3 Adsorption Isotherm

An adsorption isotherm is a graphical representation of the equilibrium between the concentrations of an adsorbate in the liquid phase to its concentration adsorbed on the surface of an adsorbent at a given temperature. This is normally developed by exposing a given amount of adsorbate in a fixed volume of liquid to varying amounts of the adsorbent. The shape of the adsorption isotherm is mainly determined by the adsorption mechanism and therefore the classification of the shapes of adsorption isotherms is important. These shapes can be used to investigate the nature of adsorption and the physical nature of the adsorbate and the adsorbent surface. *Giles et al. (1960)* have proposed four different classes of the adsorption isotherms for the adsorption of organic adsorbates from dilute solutions, namely the 'S', L (Langmuir type), H (high affinity), and C (constant partition) as shown in Figure 2.1. This classification is based on the slope of the initial portion of the isotherm curve which depends upon the rate of change of site availability with increasing adsorbate loading *(Patakioutas and Albanis, 2002)*. The variations in each class are further divided into sub-groups depending upon the shapes of the upper portions of the curves that show the behaviour at higher concentrations.

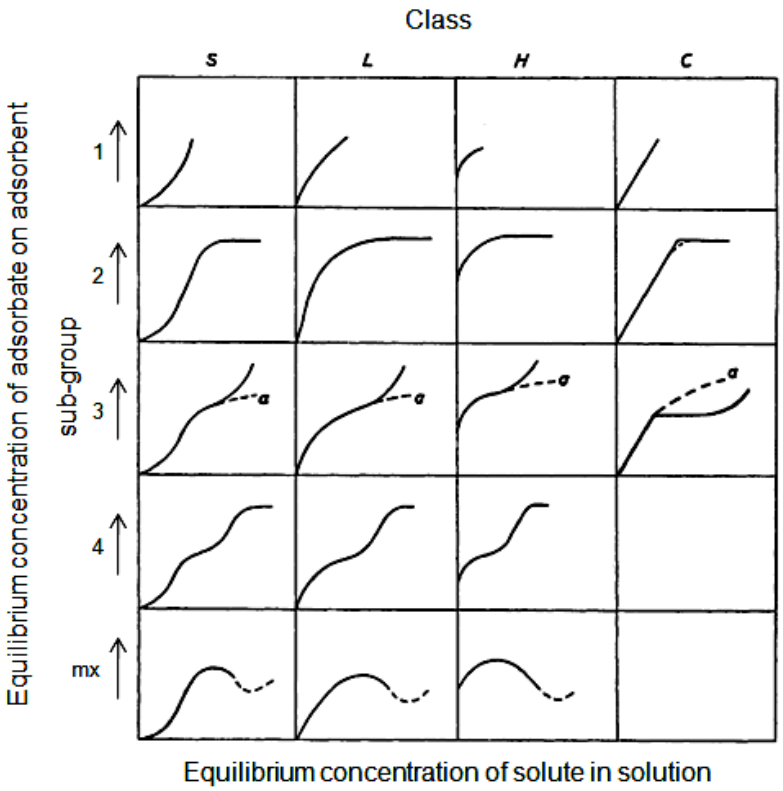

Figure 2.1: *Classification of adsorption isotherm shapes; Giles et al. (1960)*

The 'L' Isotherm

The shape of the L-type isotherm is concave to the liquid phase equilibrium concentration axis, showing the progressive saturation of the adsorbent surface. In addition, the slope of the isotherm steadily falls with concentration due to the coverage of the adsorption sites. According to *Giles et al. (1960)*, if the adsorbate molecules in the adsorbed monolayer are oriented in such a way that the new surface formed has less attraction for the adsorbate molecules; the curve has a long plateau (L−2). Further adsorption above the plateau in the L−2 sub-class leads to L−3 group and if that leads to a second plateau then it becomes L−4 *(Rao, 2004)*. These 'L' shape adsorption isotherms are the best known types and the L−2 shape with a plateau occurs for the majority of the adsorption cases from dilute solutions *(Giles et al. 1960)*. Examples of the systems showing this type of adsorption isotherms include high polar adsorbates and adsorbents, and mono-functional ionic adsorbates with strong intermolecular interactions *(Calvet, 1989)*.

The ‘S’ Isotherm

These S-shaped curves are characterized by the initial increase in the slope with an increase in the adsorbate concentration in the solution. This shows that the adsorption is readily increased as the concentration of the adsorbate is increased. The new surface offers a stronger attraction to more adsorbate molecules than the adsorbent surface and therefore, the adsorption curve rises steadily without any plateau. However, at low concentrations, the adsorbent has higher affinity for the solvent compared to the adsorbate *(Patakioutas and Albanis, 2002)*. According to *Giles et al. (1960)*, for this type of isotherm to take place, the adsorbate molecules with moderate interactions are vertically packed in a regular array in the adsorbed layer with strong competition from the solvent or other adsorbed species.

The ‘H’ Isotherm

The ‘H’ isotherm curve is basically a special case of the ‘L’ isotherm that appears for the dilute solutions in which the adsorbate has high affinity for the adsorbent. For this type of isotherm, the initial slope is almost vertical which shows that the adsorbate has a very high affinity for the adsorbent.

The ‘C’ Isotherm

This type of adsorption isotherm shows a straight line with zero origin up to a point of maximum adsorption followed by an abrupt horizontal plateau. This means that the ratio between the concentration of adsorbate in solution and the adsorbed amount is constant at any concentration before the horizontal part of the curve. This ratio is usually called the ‘distribution coefficient’ which corresponds to the partitioning of an adsorbate between the two phases. The linear relationship indicates that the number of sites available for adsorption remains constant throughout the whole range of adsorbate concentration up to the saturation of the adsorbent. A porous solid surface and an adsorbate with higher affinity for the solid than the solvent are the basic conditions to be fulfilled by this type of adsorption isotherm. In addition, the adsorbate should have the capability to penetrate readily into the adsorbent more easily than the solvent *(Giles et al. 1960)*.

2.4 Mathematical Modelling of the Adsorption Isotherms

Various models are available to describe experimentally measured adsorption isotherms, and this can provide information about the sorption mechanism, the surface properties and affinity of the sorbent *(Kumar and Sivanesan, 2005)*. In addition, the mathematical analysis of the adsorption isotherm data can be useful in order to develop design models for adsorption processes. The Freundlich and the Langmuir models are the most commonly used adsorption isotherms for liquid/solid systems *(Ho, 2004)*. A wide variety of adsorption data can be easily and simply fitted to these adsorption isotherms *(Kinnlburgh, 1986)*.

2.4.1 Freundlich Adsorption Isotherm

The Freundlich adsorption isotherm is an empirical relationship used to describe the equilibrium conditions for a sorption system involving a heterogeneous surface *(Freundlich, 1906)*. The Freundlich isotherm is defined by the following equation:

$$q_e = K_F C_e^{\frac{1}{n_F}} \qquad (2.1)$$

where C_e (mg L^{-1}) is the equilibrium concentration of adsorbate in the solution for the liquid solid systems, q_e (mg g^{-1}) is the amount of adsorbate adsorbed on the surface per unit mass of adsorbent at equilibrium, K_F [mg g^{-1} (L $mg^{-1})^{1/n}{}_F$] and n_F are empirical constants. K_F indicates the adsorption capacity of the adsorbent and ($1/n_F$) gives an indication of the effect of concentration on the adsorption capacity *(Ozer et al. 1999)*. In addition, the magnitude of n_F also gives an indication of the favourability of the adsorbent/adsorbate system. Values of $n_F > 1$ represent favourable adsorption conditions *(McKay, 1982)*. This equation is applicable to non-ideal sorption on heterogeneous surfaces as well as multilayer sorption *(Ho et al. 2002)*. Since the Freundlich isotherm is a power law expression, the amount of adsorbate on the surface of adsorbent increases as the concentration of the adsorbate in solution increases and therefore theoretically, an infinite adsorbent laoding (q_e) can occur on the adsorbent (assuming a positive value of n_F).

The non-linear expression for the Freundlich isotherm, equation (2.1) can be linearized to give equation (2.2).

$$log(q_e) = log(K_F) + \frac{1}{n_F} log(C_F) \quad (2.2)$$

The values of K_F and n_F can be determined from the intercept, *log* (K_F), and the slope, $(1/n_F)$ respectively, obtained after plotting *log* (q_e) against *log* (C_F). These constants can also be evaluated using Solver in Excel Microsoft® 2007.

2.4.2 Langmuir Adsorption Isotherm

The Langmuir isotherm is a theoretical expression obtained by assuming that the adsorption does not proceed beyond the formation of a monolayer on a homogenous adsorbent surface *(Langmuir, 1916).* At equilibrium a saturation point is reached at high concentration where no further adsorption can take place. Adsorption is assumed to occur on specific homogenous sites available on the surface of the adsorbent *(Allen et al. 2003).* Once a molecule occupies a site, no further adsorption can take place at that site. It is further based on the assumption that there is no interaction between adjacent adsorbed molecules. The Langmuir adsorption isotherm is only applicable to monolayer adsorption whereas the Freundlich adsorption isotherm is applicable to monolayer as well as multilayer adsorption. The Langmuir isotherm equation can be defined as:

$$q_e = \frac{q_m \ K_a \ C_e}{1 + K_a \ C_e} \quad (2.3)$$

where q_m $(mg\ g^{-1})$ is the Langmuir monolayer adsorption capacity, and K_a $(L\ mg^{-1})$ is a constant which represents quantitatively the affinity between the adsorbent and adsorbate.

The linear form of Langmuir equation is:

$$\frac{C_e}{q_e} = \frac{1}{q_m} C_e + \frac{1}{K_a q_m} \quad (2.4)$$

The values of Langmuir constants, q_m and K_a can thus be evaluated by plotting (C_e/q_e) versus C_e and from the slope, $(1/K_a q_m)$ and intercept, $(1/q_m)$, respectively. These constants can also be evaluated using Solver in Excel Microsoft® 2007.

2.5 Graphite

Carbon exits in two allotropic forms namely amorphous and crystalline. The crystalline forms of carbon include diamond, fullerenes and graphite. Graphite is a naturally occurring substance and is composed of a series of stacked parallel planar layers. The carbon atoms in each layer are arranged in regular hexagons in such a way that each carbon atom is surrounded by three other atoms. The distance between two adjacent layers of graphite is 3.3538 Å and the carbon to carbon distance in the hexagonal array is 1.42 Å *(Charlier et al. 1989; Emeleus and Sharpe, 1959)*. The intraplanar binding forces in each layer provided by covalent and metallic bonding are large in comparison to the interplanar van der Waals binding forces. This accounts for the anisotropic behaviour of graphite. Graphite is a good electrical conductor due to in-plane metallic bonding and a poor thermal conductor due to weak van der Waals forces between the layers. In addition, owing to the anisotropic character of graphite, the carbon layers in graphite can slide over each other and it is therefore a good lubricant material *(Chung, 2002)*. Graphite reacts with many chemical species to form compounds which can be divided into three categories namely surface, substitution and intercalation compounds. Of all the known compounds of graphite, intercalation compounds are the most significant *(Chung, 2002)*.

2.6 Graphite Intercalation Compounds

GICs are formed by the insertion of atoms, ions or molecules of a different chemical species, called intercalating agents or intercalates, between the layers of a graphite host material (Figure 2.2). They are introduced in the interplanar interstitial sites of

the graphite crystal in such a way that the layer structure of the graphite is retained *(Fischer, 1980; Chung, 2002)*. The high degree of structural ordering of graphite gives significant physical features to the intercalation compounds. Staging is the most important and characteristic ordering property of GICs *(Charlier et al. 1989)*. It is characterised by the intercalate layers which are periodically arranged in a matrix of graphite layers. GICs are thus recognized by the staging index *(n)* which determines the number of graphite layers between the adjacent intercalate layers. Hence a GIC with stage 1 has the highest concentration of intercalate compared to compounds with stages 2 and 4 as shown in the Figure 2.3.

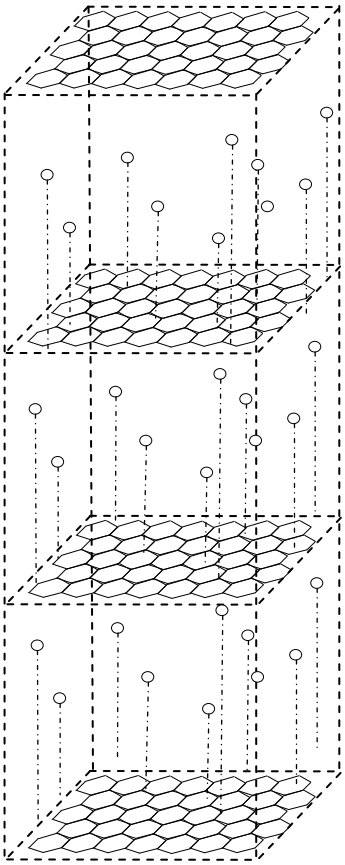

Figure 2.2: *Schematic diagram illustrating the arrangement of graphite and intercalating agent in a GIC. The stacking of the graphite layers are shown as a network of hexagons connected with each other, whereas the intercalant species are indicated by small hollow balls bonded between the graphite layers.*

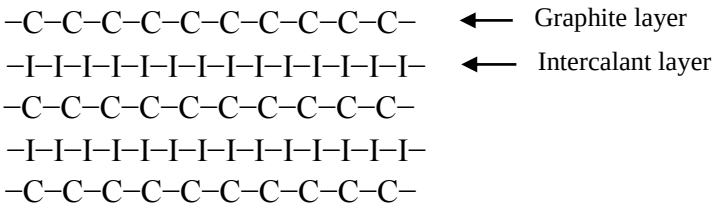

(a) Stage 1

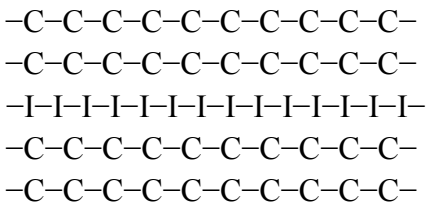

(b) Stage 2

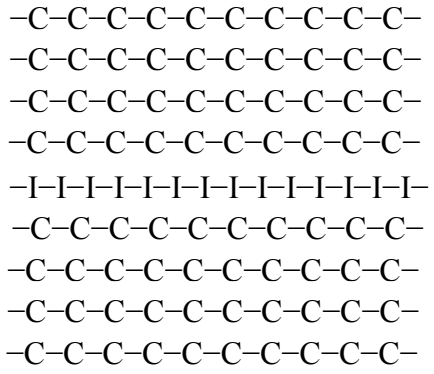

(c) Stage 4

Figure 2.3: *Schematic diagram showing staging phenomenon in GICs. The graphite layers are indicated by –C−C− and the intercalant layers by –I−I−.*

2.6.1 Properties of Graphite Intercalation Compounds

GICs have received considerable scientific and technical interest during the last two decades because of the structural flexibility associated with the host graphite materials *(McKelvy and Glaunsinger, 1990)*. These materials possess a wide spectrum of physical properties, including electrical conductivity, superconductivity, phase transitions etc. Since the concentration of free carriers in a host graphite is very low (approximately 10^{-4} free carriers per atom at room temperature),

intercalation with different chemical species at different concentrations allows wide variations of the free carrier concentration leading to a control on the electrical, thermal and magnetic properties of the original graphite *(Dresselhaus and Dresselhaus, 1981).* In this aspect, the effect of intercalation on the basal plane electrical conductivity of graphite is of great significance due to the manufacturing of intercalation compounds with metal intercalants which give basal plane electrical conductivity thirteen times that of the host graphite and one half of the conductivity of copper *(Fischer, 1980).* The remarkable increase of the in-plane electrical conductivity is due to the electronic interactions of the carbon sheets of the graphite host structure with intercalate *(Ebert, 1976).* This electronic interaction causes the transfer of charge from the intercalate layer, where free carriers have low mobility, to the graphite layer where the mobility is high *(Dresselhaus and Dresselhaus, 1981).* However, the conductivity may be affected by the presence of defects in the original graphite material or formed during the intercalation process *(Boehm et al. 1994).*

2.6.2 Classification of Graphite Intercalation Compounds

A wide range of GICs can be made by the insertion of different species into the host graphite. The weak host interactions between the layers of carbon are replaced by stronger guest-host interactions upon the formation of GICs *(McKelvy and Glaunsinger, 1990).* In addition, the intercalants expand the interplanar spacing between the layers of graphite without disturbing the graphite layers. The intercalating agents are commonly classified according to their bonding mechanism with the host graphite material. Some of the species that donate an electron to the π electronic network of graphite form donor compounds. Conversely, an electronegative species accepts an electron and forms an ionic bond with the π electronic network of graphite resulting in the formation of acceptor GICs *(Noel and Santhanam, 1997; Boehm et al. 1994).* Donor intercalation compounds are the compounds of graphite with alkali and alkaline earth metals. The most widely used intercalation compounds of this category are the compounds of *K, Rb, Cs* and *Li*. A large number of acceptor compounds are based on Lewis acid intercalates for example metal chlorides, bromides and fluorides and strong Bronsted acids such as H_2SO_4 and HNO_3 *(Chung, 2002).*

GICs that are intercalated with one chemical species into the host graphite are called as binary intercalation compounds *(Charlier et al. 1989)* for example graphite bisulphate. On the other hand, in ternary intercalation compounds, two chemical species are intercalated in host graphite either by co-intercalation *(Monyakina et al. 2004; Sorokina et al. 2004)* or by consecutive intercalation *(Maksimova et al. 2004).*

Of all the intercalation compounds of graphite, the acid compounds are of special interest because of their unique electronic properties. The high basal plane conductivity of the acid intercalation compounds is related to the strength of the acid used for intercalation. The stronger the acid the greater is the density of delocalised holes on the graphite layers which increases the conductivity. Moreover, the electrical conductivity is also thought to be dependent upon the anisotropy of graphite *(Fischer, 1980)*. Graphite reacts with sulphuric acid, nitric acid, perchloric acid or triflouroacetic acids to form graphite acid intercalation compounds *(Dresselhaus and Dresselhaus, 1981)*. These intercalates act as acceptors, transforming into negatively charged species in the crystal structure of graphite such as HSO_4^- and NO_3^- ions. Of the total acid present in the interplanar layers of graphite a fraction is ionized to negatively charged species and the rest of the acid remains in an undissociated form. Graphite bisulphate and graphite nitrate are the most significant compounds of this category for practical applications *(Maksimova et al. 2004)*. The GIC compound which has been used in this PhD project is the graphite bi-sulphate intercalation compound. It can be prepared by chemically treating flake graphite with concentrated sulphuric acid in the presence of a strong oxidising medium such as nitric acid, potassium permanaganate, ammonium persulpahte, manganese dioxide, iodic acid etc or by the electrochemical method through anodic oxidation of graphite in H_2SO_4 solution *(Leshin et al. 2003; Brown, 1995)*. The electrochemical method of intercalation is preferred because it gives more information, requires no additional oxidants and is easier to control with a wide range of process parameters *(Shornikova et al. 2005; Leshin et al. 2003)*. Graphite bisulphate is composed of graphite layers and HSO_4^- and H_2SO_4 molecules within the interplanar layers of the graphite. It has chemical formula, $C_{24}HSO_4.yH_2SO_4$ where y can vary between 2 and 2.5 *(Excell et al. 1989)*. The first GICs which were extensively used in industrial applications were graphite bisulphate intercalation compounds *(Savoskin, 2003)*. The uses of GICs have exploited their improved

electrical, electronic and catalytic properties leading to applications in the electrical, electrochemical and chemical industries *(Noel and Santhanam, 1997)*.

2.6.3 Applications of Graphite Intercalation Compounds

Exfoliation

Upon heating to high temperatures (ca. 1000^{o}C), GICs tend to expand or exfoliate along the c-axis (normal to the basal plane) and form worm like structures. The intercalates have a tendency to vaporize or decompose to gaseous products leading to a large expansion along the c-axis, typically about hundreds times the original length due to the process of exfoliation *(Chung, 1987)*. Intercalation compounds formed by using flake graphite are most commonly used for exfoliation. During electrochemical intercalation of graphite, oxygen-containing functional groups are accumulated on the surface; the composition and concentration of these groups are mainly dependent upon the treatment method *(Yakovlev et al. 2004)*. The high temperature during exfoliation causes partial or total volatilization of these surface functional groups, thereby the surface properties of thermally expanded graphite approaches that of the original graphite, but with a substantial increase in surface area. The industrial applications of GICs have been developed over the past ten years due to the exfoliation process, delivering significant features to these materials *(Furdin, 1998)*. One of the main uses of GIC is in intumescent strips on fire doors which expand and seal the door in the event of a fire. Exfoliated graphite can be mechanically compressed or interlocked without a binder into a flexible graphite material. This product has unique properties including resilience, impermeability, chemical and thermal resistance which makes it a good sealing and gasket material for use at high temperatures and in harsh chemical environments *(Chung, 2000; Chung, 2002)*. In addition, exfoliated graphite materials have been reported to have significant applications including electromagnetic interference shielding, oil spill remediation and sorption of biomedical liquids *(Prud'Homme et al. 2009)*.

Use of Exfoliated GIC as Absorbents

Accidental spillage of crude and heavy oils in sea not only causes serious environmental problems but also a large amount of oil is wasted. Exfoliated graphite has promising applications for the sorption and recovery of heavy oils spilled on the

sea surfaces. These materials possess large sorption capacities for heavy oils *(Toyoda, 1998; Toyeda et al. 2002)*. The recovery of the oil after sorption is made simply through compression or by filtration under mild suction *(Inagaki et al. 2000)* or by solvent extraction *(Maryasin et al. 1994)* with a recovery ratio of 60−80% *(Toyoda and Inagaki, 2000)*. In addition, these materials have low density and good chemical stability *(Wang et al. 2010)*. Different heavy oils are absorbed in great amounts (60−80 g of heavy oil per 1 g of exfoliated graphite) on exfoliated graphite with a bulk density of 6 kg m^{-3} in a short time *(Inagaki et al. 2000)*. The high sorption capacity depends upon the porous structure of the exfoliated graphite which is characterised by parameters such as exfoliation volume, pore volume *(Zheng, 2004)* and on the bulk density of the exfoliated graphite *(Toyoda and Inagaki, 2000)*. Furthermore, the time required to achieve absorption equilibrium is related to the grade of the oil recovered in terms of its viscosity. Long equilibrium times have been reported for viscous oils (35 kg m^{-1} s^{-1}) and shorter times (1−2 minutes) were observed for the relatively less viscous oils (0.4 kg m^{-1} s^{-1}) *(Toyoda and Inagaki, 2000)*. There are three types of pores associated with exfoliated graphite structures, namely inter-particle pores with large spaces, crevice like pores on the surface of worm like particles and intra-particle pores inside the particles *(Inagaki et al. 2004)*. The inter-particle pores are developed due to the entangling of worm-like structure of exfoliated graphite and play an important role particularly in the sorption of heavy oil. For heavy oils with relatively low viscosity (0.004 kg m^{-1} s^{-1}), the large adsorption capacity comes from the capillary condensation within the large inter particle spaces (200−600 μm), assisted by crevice like and intra-particle pores *(Toyeda et al. 2002; Tryba et al. 2002)*. The sorption capacity can be increased by increasing the pore volume. About 60% of the oil is sorbed in spaces in the worm like particles *(Zheng et al. 2004)*. Whilst for light oils such as kerosene most of the oil is sorbed in the crevice like pores on the surface of the worm structures of exfoliated graphite. Thermally exfoliated graphite is also an effective sorbent for hydrocarbons such as kerosene (42 g g^{-1}), gasoline (32 g g^{-1}), spindle oil (46 g g^{-1}), acetone (54 g g^{-1}) and isobutanol (44 g g^{-1}) *(Dedov, 2001)*.

Exfoliated graphite/ZnO composites have also been prepared and used for the removal of oil from water *(Yue et al. 2009)*. These composite materials are effective in retaining the ability of exfoliated graphite to re-absorb oil from the water because

the compression and filtration techniques to recover the absorbed oil adversely affects the pore structure of graphite, thereby reducing the sorption capacity of the exfoliate graphite when it is reused *(Yue et al. 2009)*.

Use of Exfoliated GIC as Adsorbents

The high porosity, light weight, hydrophobic nature and high sorption capacity has made exfoliated graphite not only as a potentially inexpensive absorbent for the removal of oils but also for adsorbing large organic compounds such as DDT and dyes from water *(Goshadrou and Moheb, 2011)*. The adsorption of methylene blue from aqueous solutions on exfoliated graphite was observed to be a fast process with equilibrium attained in 5 minutes *(Zhao and Liu, 2009)*. However, *Pang and Gong, (2008)* observed longer equilibrium times (2.4–24 hours) at temperatures in the range 5 to 45^{o}C for the adsorption of acid red 3B on the exfoliated graphite. The adsorption process on a porous carbon material such as exfoliated graphite having different types of pores as described above, involves three phenomena namely external mass transfer, internal diffusion and adsorption. The shorter equilibrium times suggest that the adsorption of organic molecules is a fast process compared to the internal and external diffusion of organics on the porous carbon. The internal diffusion likely dominates the overall adsorption kinetics leading to longer equilibrium adsorption times. The monolayer adsorption of polyethylene glycol with molecular weights (4000, 10000 and 20000) from wastewater on exfoliated graphite has been studied *(Pang, 2010a)*. However, the adsorptive capacity of exfoliated graphite for polyethylene glycol was less than 50 mg g^{-1} in all cases compared to sorption capacities of 131.3 g g^{-1} (SD 300 oil) and 127.8 g g^{-1} (salad oil). Similar results were obtained by *Zhou and Gu, (1989)* for the adsorption of polyethylene glycol from water on active carbon and the isotherms obtained were of Langmuir type, suggesting monolayer adsorption.

Furthermore, a number of studies have been carried out, based on the exploitation of sonication and exfoliated graphite for the decolourization of different dyes *(Li et al. 2007; Song et al. 2008; Li et al. 2009)*. The effect of ultrasound can be explained chemically by the formation of cavitations bubbles on the exposure of ultrasonic waves into aqueous solution which results in hot spots formed due to the violent collapse of bubbles. These are ultimately responsible for generating hydroxyl

radicals which cause the oxidative degradation of the coloured species present into water *(Li et al. 2008)*. Though exfoliated graphite has high surface area relative to the original graphite, ultrasonic waves physically reduce the particle size thereby increasing the surface area available for adsorption on exfoliated graphite. *Li et al. (2009)* has reported the removal of the dye C.I Direct blue 78 from water by the combination of ultrasound and exfoliated graphite. They achieved 98% removal of dye within 20 minutes using 1.0 g L^{-1} exfoliated graphite for a dye concentration of 50 mg L^{-1}. The maximum adsorption capacity for exfoliated graphite was found to be 153 mg g^{-1}. Direct scarlet 4BS was also removed from water with an efficiency of 94% by using ultrasound in combination with exfoliated graphite *(Li et al. 2007)*. Efficient removal of MTBE from aqueous solution (97%) was achieved by implementing ultrasound facilitated adsorption using exfoliated graphite *(Soltani and Moheb, 2010)*.

Exfoliated graphite nanoplatelets are effective adsorbents for the removal of organic pollutants from water due to their high specific area (600−900 m^2 g^{-1}) and hydrophobic nature *(Ion et al. 2011)*. The authors have reported the adsorption of phenol from aqueous solutions using these materials and have found that phenol adsorption increased with increases in adsorbent loading, contact time and phenol concentration. They determined an adsorptive capacity of 214 mg g^{-1} for phenol based on the Langmuir isotherm model. Exfoliated graphite was also used as a support material for depositing different kind of species at its rough surface, for example nano-scale zero valent iron was deposited onto the hydrophobic surface of exfoliated graphite for the removal of nitrate from water. This treatment provides high surface area to the adsorbents so that high activity and greater flexibility could be possible for environmental remediation applications *(Huan et al. 2006)*. TiO_2 loaded exfoliated graphite was used to remove different dyes so that the advantages of adsorption on exfoliated graphite and photocatalysis by titania could be achieved. However, the adsorption on the exfoliated graphite was observed to be more significant than photodegradation by the titanium dioxide *(Pang, 2010b)*.

Although exfoliated graphite is considered a cheap material compared to activated carbon for water remediation applications with its unique adsorption properties, no attempt has been made to regenerate exfoliated graphite loaded with simple organic molecules. Expanding GIC undoubtedly increases the surface area available,

although not as much as could be expected because there are significant closed areas within the structure. On the other hand, its separation from water is excellent because it floats. However, the loss of graphite structure means that the material may not be a good conductor of electricity and therefore it is necessary to compact it to achieve good conductivity. In addition, these materials also need to be wet to get electrochemical regeneration. Consequently, these materials are not suitable for electrochemical regeneration.

The use of unexpanded intercalation compounds as adsorbents for water treatment which can be electrochemically regenerated and recycled has not been studied in detail, with the exception of previous work at the University of Manchester discussed below.

Use of Unexpanded GIC as Adsorbents

In water treatment by adsorption for the removal of organic contaminates, the conventional approach is to use a highly porous material such as activated carbon which gives excellent sorption capacity but also require costly regeneration techniques. In addition, the regeneration of these materials affects the morphology of the complex pore structure thereby reducing their adsorptive capacities after repeated usage. The application of unexpanded intercalated graphite in the form of particulates, flakes and powder as adsorbents followed by their electrochemical regeneration has been patented for the removal of low concentrations of organic pollutants *(Eccleston et al. 2009)*. Due to the absence of internal pores these adsorbents give high adsorption rates at the expense of reduced adsorption capacity for organic compounds. However, the non-porous character of these materials also facilitates electrochemical regeneration. Research to investigate adsorbents possessing high adsorption capacity with good electrochemical regeneration characteristics is being carried out at the University of the Manchester, UK. The removal of coloured substances *(Brown et al. 2004a)*, pesticides *(Brown et al. 2004b)* and phenols *(Brown and Roberts, 2007)* from water using un-expanded GICs as adsorbents with subsequent electrochemical regeneration of the adsorbent has been demonstrated. A review of the previous studies of electrochemical regeneration of GIC carried out at the University of Manchester can be found in chapter 3.

A few studies of adsorption using graphite oxide, which is a highly oxidised form of a GIC, have also been reported in the literature. Graphite oxide can be manufactured by using strong oxidising agents such as potassium permanganate in concentrated sulphuric acid in the liquid state to give a highly oxidised compound which is rich in oxygen containing functional groups such as epoxy, hydroxyl and carboxylic groups *(Hamwi and Marchand, 1996).* Due to the highly hygroscopic nature of graphite oxide, water is always present between the graphite layers which explains that why the interlayer spacing may vary from 6.4 Å to 11.3 Å depending upon the amount of water present between the layers of graphite. Graphite oxide has attained considerable importance in recent years for applications in the manufacture of intercalated composites with unique properties *(Matsuo et al. 2002; Szabo et al. 2005). Bradder et al. (2011)* has reported the removal of methylene blue and malachite green from aqueous solutions by graphite oxide. According to the authors, the adsorption capacity based on Langmuir isotherm was 351 and 248 mg g^{-1} respectively, much higher than that of activated carbon for these dyes. Graphite oxides hydrophobized by n-hexadecylamine were used to adsorb pyrene from water−ethanol solution (1:2) containing 2 mM of pyrene (28.5 mg g^{-1}) *(Matsuo et al. 2003).* According to the authors, pyrene not only adsorbed on the external surfaces but also within the interlayer spacing, as confirmed by X-ray diffraction measurements of the pyrene containing graphite oxide. This was due to the greater interlayer spacing of the graphite oxide as explained above. *Hartono et al. (2009)* used graphite oxide for the adsorption of humic acid from aqueous solutions. The maximum adsorption of graphite oxide from adsorption isotherm was 190 mg g^{-1}, much higher than activated carbon *(Daifullah et al. 2004).* Graphite oxide exhibits a graphene structure with oxidised functional groups, and these features give higher adsorption capacities in comparison to graphite for the removal of organics from water. On the other hand, the layers of carbon in host graphite loose planarity and are converted to a buckling structure during its formation. Consequently, the disruption of π electron system leads to drastic decrease of the high electrical conductivity of graphite *(Boehm et al. 1994).*

2.7 Conclusions

This chapter presented the fundamentals of adsorption by giving a brief insight into the physical and chemical adsorption processes. The classification of adsorption isotherms is important in understanding and predicting the useful parameters and characteristics of the adsorbent/adsorbate system. Activated carbon has been widely used as an adsorbent for applications in water treatment due to its high specific surface area associated with its porous structure. This chapter has also provided an introduction to GICs, the adsorbent material used in this project. Due to their unique physical and chemical properties, these materials have important electrical, electrochemical and chemical applications. A brief literature review on the use of these materials as sorbents is presented which has demonstrated that GICs are promising adsorbents for removing organic pollutants from water and can be considered for electrochemical regeneration due to the high electrical conductivity of GICs.

Chapter 3

Water Treatment by Electrochemical Oxidation

This chapter introduces the environmental applications of electrochemistry and highlights various electrochemical processes used for water treatment by giving particular attention to electrochemical oxidation of organics. The literature regarding the processes occurring at the electrode during the oxidation of organics in water has been reviewed. In particular, the oxidation of phenol which has been widely used as a model pollutant in studies of wastewater treatment, has been considered in detail. This is followed by a discussion of the breakdown products formed during the electrochemical oxidation of phenol in solution. This chapter also contains a brief review of the literature regarding the use of carbon based electrodes in electrochemical cells, and the mechanisms of electrochemical regeneration of activated carbon and GICs. The effect of electrochemical treatment on the surface chemistry of GAC and GICs has also been briefly discussed. The conclusions of the chapter are given in the final section.

3.1 Electrochemistry and Environmental Pollution

There are increasing economic, legal and environmental demands to employ the best existing technology not involving excessive cost and offering pollution free performance. Electrochemistry continues to make many contributions to environmental treatment, recycling of wastes, process control using electrochemical sensors and can play a significant role in clean technology and pollution control, as illustrated by the examples given in table 3.1 *(Walsh, 2001).*

Electrochemical technology is environmentally compatible due to the use of a clean reagent, the electron. In addition, electrochemistry presents promising solutions for the abatement of some of the pollution issues of the process industry. The advantages of electrochemistry for environmental applications include *(Juttner et al. 2000; Rajeshwar and Ibanez, 1997)*:

Versatility

Electrochemical processes involving direct or indirect oxidation and reduction have the capability to treat a variety of pollutants present in the liquid, gas and solid phase and convert them into environmentally friendly or useful products with little or no waste production. In addition, a great number of reactor configurations and shapes employing a variety of electrodes can be used. With minor changes the same reactor can also be used for different electrochemical reactions. In addition, the volumes of fluid which can be treated can be from micro litres to millions of litres.

Selectivity

The ability to control the applied potential can in many cases enable selective treatment, targeting a specific pollutant. Therefore, the by–products of other electrochemically active species can be avoided.

Energy Efficiency

Electrochemical processes are generally operated at low temperatures and pressures and therefore have low energy requirements compared to the non–electrochemical alternatives such as thermal incineration. The electrodes and cells can be designed to minimise power losses caused by poor current distribution, voltage drops and side reactions.

Amenability to automation

The electrical variables, including the electrode potential and cell current are readily compatible with process automation, data acquisition and control systems.

Cost effectiveness

The electrochemical cells and auxiliary equipments used for electrochemical processes are usually simple. In addition, the proper design of cell configurations often makes the process relatively inexpensive.

Safety

Electrochemical processes are relatively safe because they are normally operated under mild conditions employing small quantities of harmless chemicals.

However, there are some disadvantages of electrochemical processes used for environmental treatment due to high capital cost, in some cases high operating costs for electrical power and/or addition of electrolyte, the potential for the formation of toxic products, and the risk of electrode corrosion leading to operational problems and potential contamination *(Anglada et al. 2009).*

Table 3.1: *The scope for electrochemical technology in environmental treatment, (Walsh, 2001)*

Scope	**Examples**
Removal of contaminants	Metal ions, organic, and inorganic removal from water and process liquors
Disinfection of water	Chlorination, peroxy species, or ozone
Avoidance of pollution	Clean electrosynthesis
Remediation of polluted sites	Soil remediation by electrodialysis
Efficient energy conversion	Fuel cells
Monitoring and sensors	In the gas and liquid phase
Recycling of valuable materials	Precious metal deposition
Avoidance of corrosion	Choice of materials/protective coating

3.2 Electrochemical Technologies for Wastewater Treatment

Electrochemical technologies are finding extensive application in water treatment due to the salient features of electrochemistry. These technologies have developed to such a stage that they are not only comparable with other alternatives in terms of cost

but are also more efficient and compact *(Martinez-Huitle and Ferro, 2006)*. They are employed for the removal of metal ions *(Hatfield et al. 1996; Rana et al. 2004)*, and for treating various wastewaters resulting from tannery *(Costa et al. 2008; Szpyrkowicz et al. 1995)*, electroplating *(Bolger and Sziag, 2002; Adhoum et al. 2004)* and textile processing etc *(Chen, 2004; Korbahti et al. 2011)*. In addition, electrochemical technologies have applications in disinfection *(See chapter 7)*, electrodialysis *(Ergun et al. 2008; Marder et al. 2003)*, electrodeionisation *(Guan and Wang, 2008; Yeon et al. 2004)* and the electrochemical oxidation of organics *(See section 3.2.5)*. A number of other electrochemical techniques have also been applied for the removal of impurities from water, including:

3.2.1 Electrocoagulation

Electrocoagulation has been applied on a large scale in treating effluents containing suspended solids, oil and grease, textile dyes, heavy metals and other organic or inorganic contaminants that have a tendency to coagulate *(Canizares et al. 2006; Biswas and Lazarescu, 1991; Merzouk et al. 2009; Do and Chen, 1994; Chen, 2004)*. This process uses some consumable electrodes such as aluminium or iron to provide ions into the water to be treated *(Mollah et al. 2004)*. The metal ions being generated from the corresponding electrodes hydrolyse to form *in-situ* coagulating agents. These coagulants interact with the charged particles of impurities in water; bring about their coagulation and the resulting solid mass is removed by electroflotation *(See section 3.2.2)* or sedimentation and filtration.

3.2.2 Electroflotation

Electroflotation is a process of removing suspended particles from water using finely dispersed electrogenerated gas bubbles. The gas bubbles formed on the surface of an electrode interact with particulate matter and the gas-particulate combinations float to the surface of water, where they are removed by skimming. The process has been widely applied in the mining industry and, to remove oils and other low density suspended particles from wastewater *(Ho and Chen, 1986; Bande et al. 2008; Chen, 2004)*.

3.2.3 Electrolytic Wet Oxidation

In this process, wet air oxidation of organics in aqueous solution is performed in the presence of electric current at high temperature and pressure (250℃ and 7 MPa) *(Serikawa et al. 2000)*. However, relatively mild conditions (120℃ and 0.8 MPa) have also been reported for the removal of dye from water by electrolytic wet oxidation *(Dai et al. 2006)*.

3.2.4 Electrochemical Reduction

Electrochemical reduction is another approach for reducing pollutants in wastewaters. However, it has not been studied as extensively as electrochemical oxidation. Some of the examples of treating wastewaters using this technique include electrochemical reduction of nitrate in water *(Li et al. 2009b)*, treatment of dinitrotoluene and trinitrotolune in munitions wastewater *(Doppalapudi et al. 2003; Palaniswamy et al. 2004)* and electrochemical reduction of chromium etc *(Lugo-Lugo et al. 2010)*.

3.2.5 Electrochemical Oxidation

Electrochemical oxidation is the most widely studied electrolytic technique for eliminating organic pollutants from wastewater. It involves the oxidation of organics at the anode of an electrochemical cell by the action of strong oxidants, similar to chemical oxidation. However, the availability of in-situ electrochemically generated oxidants makes the process more viable and efficient for mineralizing organics in water. Electrochemical oxidation has been successfully applied to a large number of synthetic solutions containing different organic compounds. A few recent examples of electrochemical oxidation of organics in water include oxalic acid *(Scialdone et al. 2009)*, benzene *(Oliveira et al. 2007)*, bisphenol A *(Murugananthan et al. 2008)*, salicylic acid *(Guinea et al. 2008)*, acid orange 7 *(Hammami et al. 2008)*, naphthalene sulphonates *(Panizza et al. 2006)*, benzoic acid *(Velgraki et al. 2010)*, benzoquinone *(Yoon et al. 2007)*, and 2-naphthol, 2-6-dimethyl-pyridine, thiophene, 2-propanol, ethanol and butyric acid *(Canizares et al. 2007; Canizares et al. 2008)*. Electrochemical oxidation of phenol is discussed in detail in section 3.5. There has been a growing interest in the treatment of industrial effluents by electrochemical

oxidation, particularly for effluents possessing high electrical conductivities such as dyehouse wastes *(Chatzisymeon et al. 2006)*, tannery wastewaters *(Rao et al. 2001; Costa et al. 2010)*, municipal wastes *(Tennakoon et al. 1996)*, landfill leachates *(Deng and Englehardt, 2007)* and other saline industrial wastewaters *(Anglada et al. 2010)*. Additional electrolytes are required to be added for the treatment of low conductivity effluents, for example, distillery effluents *(Manisankar et al. 2003)* and cigarette industry wastewater *(Benankiwar, 2002).*

Although the low conductivity of these effluents can be increased by adding an electrolyte, such as NaCl, this also increases the dissolved solid and inorganic content of the water and therefore its reuse becomes problematic. Furthermore, when NaCl is used as an additional electrolyte to enhance the electrical conductivity of the water to be treated, the formation of toxic chlorinated compounds can also occur. On the other hand, the low conductivity of many wastewaters also results in high voltages *(Murphy et al. 1992)* and hence increased energy consumption. In order to operate the electrochemical cells with low voltages, the gap between the electrodes must be minimized.

Low concentrations of organic contaminants in water are difficult to treat electrochemically due to the mass transfer limitation of reactants to the electrode surface. The rate of mass transfer limits the current that can be used as higher currents than the mass transfer limiting current can cause side reactions such as oxygen evolution thereby reducing process efficiency *(Steele et al. 1990; Gherardini et al. 2001). Brown, (2005)* has suggested that adsorption can be used to concentrate the organic contaminant at the surface of electrode prior to electrochemical oxidation, and thus reduce the problems associated with the mass transport limitations. Nevertheless, when the concentration of organic in the water to be treated is high, large amount of charge is required to achieve the complete oxidation of organics to CO_2 and H_2O *(Canizares et al. 2003)*. It has also been suggested that partial degradation of organics to wastes that can be treated by biological means requires less energy. Partial degradation, on the other hand, can produce toxic intermediates and therefore they must be completely removed from water to make it safe *(Canizares et al. 1999)*. The mechanism of electrochemical oxidation reported in the literature is discussed in the following section.

3.3 Mechanism of Electrochemical Oxidation

Electrochemical oxidation of organic pollutants in water can take place according to two pathways, namely direct and in-direct oxidation as shown in Figure 3.1 and 3.2. The pollutants are oxidized at the surface of the anode or in the immediate surrounding of anode in direct oxidation whereas the in-direct oxidation involves intermediate species, produced electrochemically at the surface of the anode that bring about the oxidation of the pollutants in the bulk of solution. Each of these processes are further discussed in the following sections.

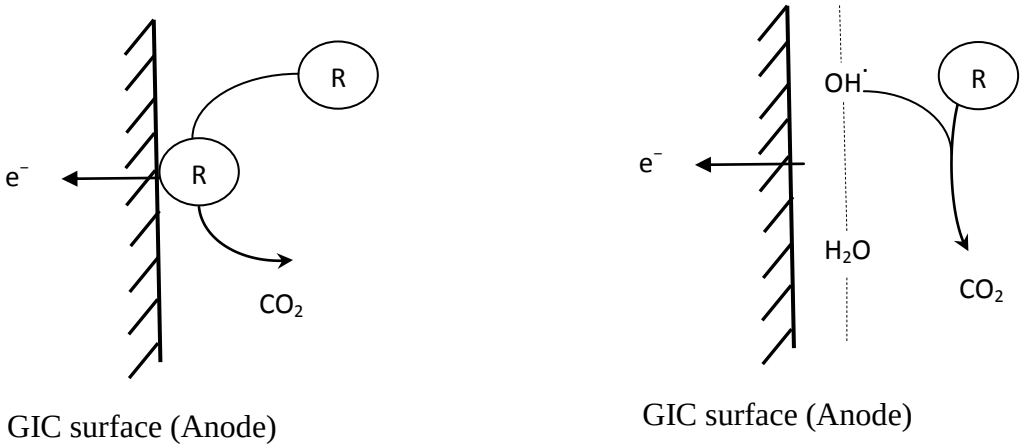

Figure 3.1: *Schematic illustration of (a) oxidation of organics through direct electron transfer; and (b) direct oxidation through the action of hydroxyl radicals produced by water discharge*

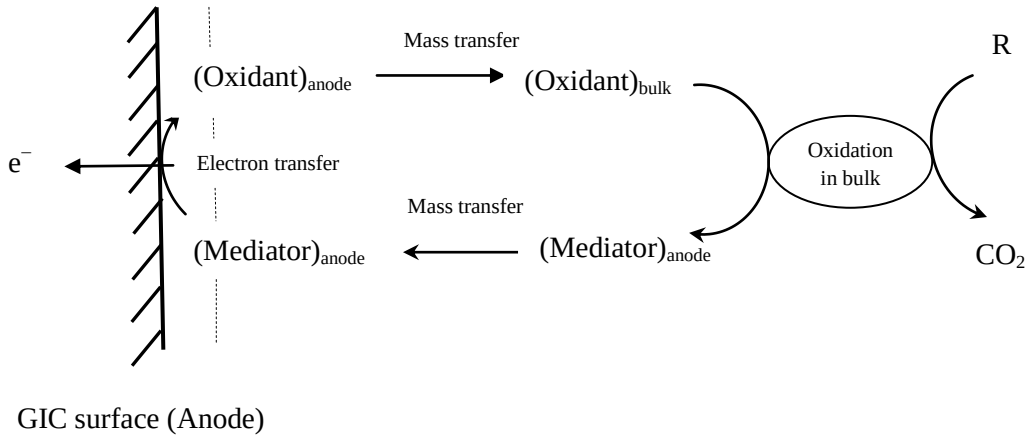

Figure 3.2: *Schematic illustration of indirect oxidation of organics through inorganic mediators*

3.3.1 Direct Electrochemical Oxidation

As mentioned above in direct electrochemical oxidation, the organics are oxidised after adsorbing on the surface of the anode either through direct electron transfer or through the action of hydroxyl radicals without involving any other substances. Two possible pathways have been suggested by *Comninellis, (1994)* for the direct electrochemical oxidation of pollutants, which he has described as electrochemical conversion and electrochemical combustion. In electrochemical conversion, the refractory pollutants are partially oxidised into biodegradable substances, which require further treatment whereas electrochemical combustion does not involve any additional treatment and leads to complete mineralization of the non-biodegradable substances to water and CO_2. *Comninellis, (1994)* has proposed a model for the oxidation of organics at a metal oxide electrode (Figure 3.3). The hydroxyl radicals are generated at the surface of the anode either from the decomposition of water in acidic solutions (equation 3.1) or from the direct conversion of hydroxyl ions in alkaline media (equation 3.2).

$$2H_2O \xrightarrow{\text{acidic}} 2OH^{\cdot} + 2H^{+} + 2e^{-} \quad (3.1)$$

$$OH^{-} \xrightarrow{\text{alkaline}} OH^{\cdot} + e^{-} \quad (3.2)$$

These radicals can be physically or chemically adsorbed on the surface of the anode depending upon the nature of the anode used *(Martinez-Huitle, 2006)*. Two types of electrodes have been recognized, known as active and non-active electrodes *(Canizares et al. 2004; Iniesta et al. 2001)*. On active electrodes, a strong interaction exists between the electrodes and the hydroxyl radicals. Therefore, chemisorption takes place at active electrodes with the hydroxyl radicals reacting at active sites of electrode *(MO)* to give more oxidised sites *(MO_{x+1})* (equation 3.4). On the contrary, weak interactions exists between the hydroxyl radicals and the electrode surface for non-active electrodes due to which hydroxyl radicals remains physically adsorbed on the surface of electrode (equation 3.3).

$$MO_x + OH^{\cdot} \rightarrow MO_x(OH^{\cdot}) \quad (3.3)$$

$$MO_x + OH^{\cdot} \rightarrow MO_{x+1} + H^+ + e^- \quad (3.4)$$

Higher oxidation states are available at the surface of the active electrodes which enables the adsorbed hydroxyl radicals to be chemically interacted with the anode. In addition, the surface redox couple, MO_{x+1}/MO_x, called as chemisorbed active oxygen acts as mediator for the selective conversion of organics on these electrodes (equation 3.5).

$$MO_{x+1} + R \rightarrow MO_x + RO \quad (3.5)$$

As stated above, in electrochemical conversion, the organics *(R)* are not completely oxidised and thereby are converted into products *(RO)* requiring further oxidation. On the other hand, the chemisorbed hydroxyl radicals can combine to evolve oxygen as a side reaction due to the chemical decomposition of higher metal oxide (equation 3.6).

$$2MO_{x+1} \rightarrow 2MO_x + O_2 \quad (3.6)$$

At non-active electrodes, the hydroxyl radicals, also called physi-sorbed active oxygen assists the non-selective oxidation leading to complete mineralization of adsorbed organics into CO_2 and H_2O (equation 3.7).

$$mMO_x(OH^{\cdot}) + R \rightarrow mMO_x + nCO_2 + yH_2O + mH^+ + me^- \quad (3.7)$$

However, because of a similar side reaction for active electrodes, oxygen can also be evolved for the non-active electrodes due to the electrochemical oxidation of hydroxyl radicals (equation 3.8).

$$2MO_x(OH^{\cdot}) \rightarrow 2MO_x + O_2 + 2H^+ + 2e^- \quad (3.8)$$

A non-active anode does not present catalytically active sites necessary for the adsorption of the reactants and the products from the aqueous solution. Therefore these anodes do not take part in the anodic reactions and only act as a sink for the removal of electrons. The electrochemical activity and the chemical reactivity of the

adsorbed hydroxyl radicals strongly depend upon the strength of $MO_x(OH^{\cdot})$ interaction. Further, *Marselli et al. (2003)* suggested that the electrochemical activity and the chemical reactivity are related to the overpotential of oxygen evolution and the rate of organics oxidation with electrogenerated hydroxyl radicals, respectively. Generally, weak $MO_x(OH^{\cdot})$ interaction offers low anode activity towards oxygen evolution (high overvoltage anodes) and high chemical reactivity for the oxidation of organics. This explains why complete mineralization is possible with the non-active anodes. All of these processes (equations, 3.1, 3.3–3.8) for direct anodic oxidation are illustrated in Figure 3.3.

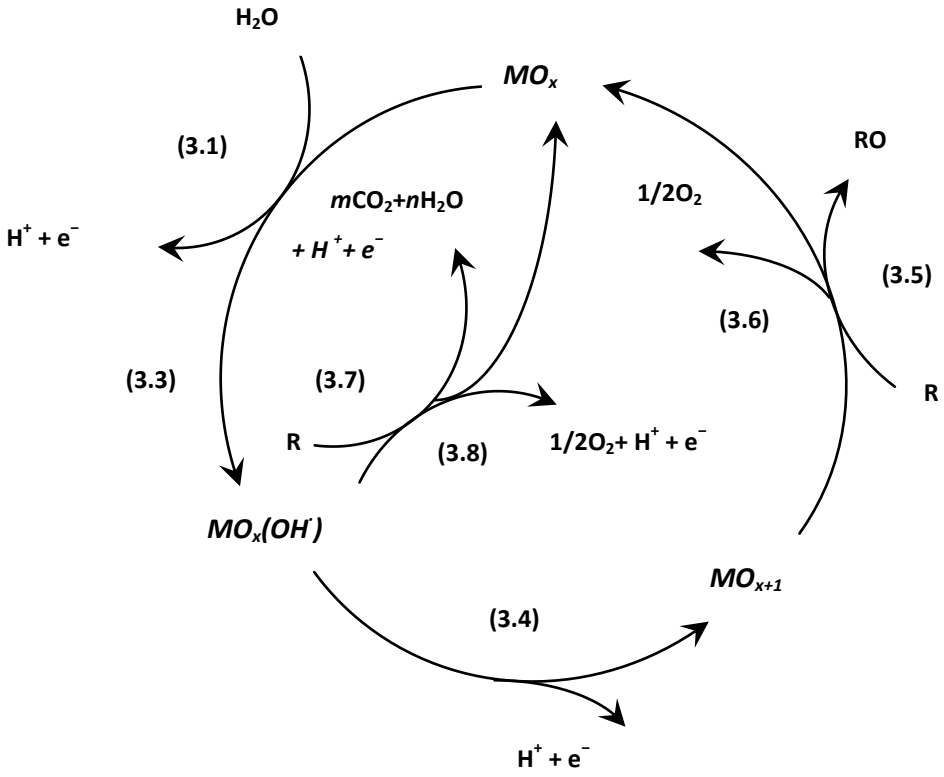

Figure 3.3: *Mechanism of hydroxyl radical formation and destruction during combustion and conversion of organic compounds with simultaneous evolution of oxygen at non–active (reactions 3.1, 3.3, 3.7, 3.8) and active (reactions 3.1, 3.3, 3.4, 3.5, 3.6) anodes respectively, Comninellis (1994)*

3.3.2 Indirect Electrochemical Oxidation

In indirect electrochemical oxidation, an electrochemically oxidised species generated at the anode act as a mediator for the oxidation of organic pollutants in

water. Such reactive species include chlorine, hypochlorite, peroxide, ozone, Fenton's reagent and peroxodisulphate *(Juttner et al. 2000)*. Chlorine and hypochlorite are widely used as electrochemical oxidants due to their effective character and therefore indirect oxidation involving chlorine species have been frequently studied *(Pyo and Moon, 2005)*. The electrochemical oxidation of water usually takes place in the presence of NaCl as supporting electrolyte *(Park et al. 2009)*. The addition of NaCl increases the rate of electrochemical oxidation of the organic pollutants and can lead to complete mineralization due to the participation of active chlorine, in the form of chlorine *(E^o=1.358V)*, hypochlorous acid *(E^o=1.63V)*, and hypochlorite ion *(E^o=0.9V) (Martinez-Huitle and Ferro, 2006)*. *Bonfatti et al. (2000)* extended the reaction scheme proposed by *Comninellis, (1994)* for electrochemical oxidation of organics mediated by active chlorine in alkaline media (Figure 3.4). Besides the formation of adsorbed hydroxyl radicals through the anodic discharge of water, the formation of the chlorohydroxyl radicals adsorbed on the active sites of electrode through the anodic discharge of chlorides takes place simultaneously according to equation 3.9 *(Israilides et al. 1997; Ramalho et al. 2010)*.

$$MO_x + H_2O + Cl^- \rightarrow MO_x(ClOH^{\cdot}) + H^+ + 2e^- \quad (3.9)$$

These radicals can then react with organic contaminates *(R)* to oxidise them *(RO)* or chloride ions to produce free chlorine according to the following equations (3.10 and 3.11) *(Korbahti and Artut, 2010; Chatzisymeon et al. 2010)*.

$$R + MO_x(ClOH^{\cdot}) \rightarrow MO_x + RO + H^+ + Cl^- \quad (3.10)$$

$$H_2O + MO_x(ClOH^{\cdot}) + Cl^- \rightarrow MO_x + Cl_2 + O_2 + 3H^+ + 4e^- \quad (3.11)$$

In the case of complete oxidation, (*R*) will be oxidised to CO_2 and H_2O (Figure 3.4). In addition, the free chlorine generated through reaction (equation 3.11) can react with hydroxide ions to produce hypochlorite under alkaline conditions (equation 3.12).

$$Cl_2 + 2OH^- \rightarrow H_2O + OCl^- + Cl^- \quad (3.12)$$

As shown in equations 3.11 and 3.12, the primary oxidants such as chlorine, oxygen and hypochlorite are formed through direct electrochemical oxidation. Of these oxidants, free chlorine and oxygen can further react at the anode to generate secondary oxidants such as chlorine dioxide and ozone. The chlorohydroxyl radicals created initially have a very short life due to their high oxidation potential. They are, therefore either decomposed to primary (Cl_2, O_2, OCl^-) and secondary oxidants (ClO_2, O_3, H_2O_2) or directly oxidise organic matter adsorbed on the anode surface. However, primary and secondary oxidants have a relatively long life and are able to diffuse away from the electrode surface and bring about the oxidation of organics in solution indirectly *(Chatzisymeon et al. 2006)*. The rate of indirect electrochemical oxidation depends upon the rate of diffusion of these oxidants into the solution, the pH and temperature *(Israilides et al 1997)*. Direct electrochemical oxidation on a non-active anode is considered the most effective pollutant degradation process because primary and secondary oxidants may not be able to completely oxidise organic pollutants to CO_2 and H_2O. In addition, some of the organic compounds can be chlorinated during indirect electrochemical oxidation which can increase the toxicity of the treated water. However, *Zhan et al. (2001)* compared the direct and indirect electrochemical oxidation for the removal of dyestuffs from wastewaters containing NaCl. They obtained 87% COD and 100% colour removal by indirect electrochemical oxidation in 50 minutes. This compares to 47% COD and 50% colour removal in 5 hours by the direct oxidation process. The current efficiency for the two processes was 99 and 16%, respectively. According to the authors, the formation of hypochlorite has increased the degradation rate considerably. The chloride concentration in the water undergoing treatment directly influences the indirect electrochemical oxidation. *Lin et al. (1998)* observed that direct oxidation is the key process for waters associated with low salinities and the indirect oxidation becomes prominent with increasing salinity. They found an increase in the removal of both phenol (71% to 94.2%) and COD (31.2% to 74%) with an increase in NaCl concentration from 0.5 to 3.5%. This suggests that the increased level of treatment observed was due to the increased rate of indirect oxidation. In contrast, *Rajkumar et al. (2005)* observed no significant variation in the COD after treatment when the chloride concentration was increased from 500 to 4500 mg L^{-1} for the removal of

phenol from water. This suggests that direct electrochemical oxidation is the key process for the electrochemical oxidation of phenol. In general, if the water to be treated contains low concentration of chloride, a large amount of salt should be added to increase the process efficiency of indirect electrochemical oxidation.

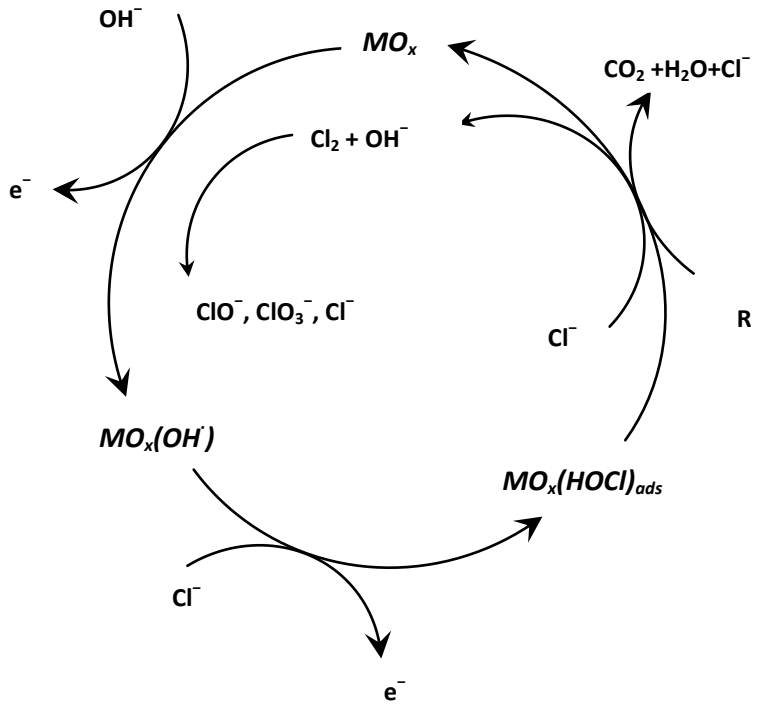

Figure 3.4: *Extension of the reaction mechanism, initially proposed by Comninellis (1994) for the direct electrochemical oxidation of organics (Figure 3.3), for the indirect oxidation mediated by active chlorine (Bonfatti et al. 2000)*

The indirect oxidation of organics can also be achieved using metal ions as mediators where they can be electrochemically oxidized to species with high oxidation potential. This process is frequently called mediated electrochemical oxidation. In this process, a metal ion in acidic medium is oxidised to a higher oxidation state (e.g. equation 3.13, showing the oxidation of silver ions) which then oxidises the organic matter, ideally to CO_2 and H_2O, and the metal ion is reduced to its original oxidation state. Thus, the metal ion is not consumed during the course of the process and acts as a mediator. In addition, the metal ion may react with water to produce hydroxyl radicals useful for the oxidation of organic matter (e.g. equation 3.14). These metal ions are commonly transition metals with high redox potential such as silver, cobalt, cerium and ruthenium, and they act as powerful oxidants for

the degradation of organic contaminants *(Bringmann et al. 1995; Balaji et al. 2007; Davidson et al. 1998).*

$$Ag^{+} \rightarrow Ag^{2+} + e^{-} \quad (3.13)$$

$$Ag^{2+} + H_2O \rightarrow Ag^{+} + H^{+} + OH^{\cdot} \quad (3.14)$$

Irrespective of the oxidation mechanism at the anode, reduction of water takes place at the cathode and hydrogen is produced both in acidic and alkaline conditions *(Vylssides et al. 1999; Israilides et al. 1997).* In acidic solutions, hydroxonium ions are discharged at the cathode to form hydrogen gas (equation 3.15). In alkaline solutions it is supposed that water molecules are directly reduced to produce hydrogen and hydroxyl ions according to equation 3.16.

$$2H_3O^{+} + 2e^{-} \rightarrow H_2 + 2H_2O \quad (3.15)$$

$$2H_2O + 2e^{-} \rightarrow H_2 + 2OH^{-} \quad (3.16)$$

3.4 Role of Anode Materials

The electrode materials used for the electrochemical oxidation of organics should be cheap and stable in the electrolyte conditions. In addition, they should exhibit high activity towards the degradation of organics and low activity towards side reactions such as the evolution of oxygen. The nature of the electrode material influences the selectivity and the efficiency of the electrochemical oxidation of organic compounds *(Comninellis and Chen, 2010)*. The oxidation of organics at active and non–active electrodes has been widely studied in the literature. As a general rule, active anodes with low oxygen evolution overpotential are good electrocatalysts for the oxygen evolution reaction and only allow the partial oxidation of the organics, whereas non–active anodes possessing high oxygen evolution overpotential are poor catalysts for the oxygen evolution reaction and favour the complete oxidation of organics to CO_2 and H_2O. Some of the examples of active anodes include Pt *(Comninellis and Pulgarin, 1991; Comninellis, 1994; Rodgers et al. 1999)* IrO_2 *(Simond and Comninellis, 1997),* Ti/IrO_2 *(Pulgarin et al. 1994; Comninellis and Nerini, 1995)*

and Ti/RuO_2 *(Li et al. 2009a)*. Antimony-doped tin oxide *(Pulgarin et al. 1994)*, lead dioxide *(Tahar and Savall, 1998; Zhou et al. 2005)* and boron doped diamond (BDD) *(Canizares et al. 2002)* have been studied as non-active anodes. Metal oxide coated titanium electrodes such as Ti/IrO_2 and Ti/RuO_2 are often called 'dimensionally stable anodes' (DSA) because the thin conducting layer of metal oxide (IrO_2, RuO_2) is stable and the titanium substrate is corrosion resistant which allows the structure to maintain its dimensional stability. *Pulgarin et al. (1994)* investigated the electrochemical oxidation of an aqueous solution of 1,4-benzoquinone at IrO_2 and SnO_2 anodes. At IrO_2, the rupturing of the benzene ring occurred and carboxylic acids were formed which accumulated as the final oxidation products, indicating that they were poorly degraded. In contrast, CO_2 was the only final oxidation product during the electrochemical degradation of 1,4– benzoquinone at SnO_2 anode, indicating that complete mineralization was achieved. The difference in the oxidation mechanisms was due to the active and non–active behaviour of the IrO_2 and SnO_2, respectively. However, the doped–SnO_2 electrode material has a major drawback of short service life due its deactivation by the formation of a non-conducting layer on the surface *(Montilla et al. 2005; Comninellis and Chen, 2010)*. On the other hand, the BDD anodes are characterised by their inert surface, low adsorption properties, corrosion stability and high oxygen overpotential *(Marselli et al. 2003; Comninellis and Chen, 2010)*. During the process of water discharge, a BDD anode generates large quantities of hydroxyl radicals that are weakly adsorbed on its surface. These radicals have high reactivity for organic oxidation and thus complete mineralization of organic contaminants is possible using these anodes. They have also been reported to offer the largest overpotentials for oxygen evolution from water ever found from an electrode material *(Kraft et al. 2003)*, as shown in table 3.1*(Panizza and Cerisola, 2006)*.

Table 3.2: *Oxygen evolution potential at different anode materials in H_2SO_4 solution, The standard potential for oxygen evolution is 1.23 V vs. NHE (Panizza and Cerisola, 2006). The current density for determination of the onset potential was not specified by Panizza and Cerisola (2006), but based on the data for PbO_2 and BDD presented in their earlier paper (Cerisola and Panizza, 2003) the current density was around 1 mA cm^{-2}*

Anode	**O_2 evolution potential V vs. SHE**	**Conditions**
RuO_2	1.47	0.5 M H_2SO_4
IrO_2	1.52	As above
Pt	1.6	As above
Oriented pyrolytic graphite	1.7	As above
SnO_2	1.9	0.05 M H_2SO_4
PbO_2	1.9	1 M H_2SO_4
BDD	2.3	0.5 M H_2SO_4

Carbon and graphite electrodes have been widely used for the electrochemical oxidation of organics employing three dimensional electrodes such as packed bed, fluidized bed, carbon particles and other types of porous electrode *(Comninellis and Chen, 2010). Canizarres et al. (1999)* has assumed that GAC particles behave as non–active anodes for the electrochemical oxidation of phenol. No information was found in the literature on the behaviour of GIC particles as active or non–active anode other than the work of *Brown and Roberts, (2007)* who carried out the adsorption of phenol on a GIC adsorbent *(Eccleston et al. 2009)* followed by electrochemical regeneration. Their results suggest that the GIC adsorbent acts as non–active anode due to the lack of breakdown products in the aqueous samples. A more recent paper by *Rueffer et al. (2011)* has reported that graphite acts as an active anode for the oxidation of species in the potential range of oxygen evolution and direct electron transfer takes place for those substances that can be oxidized in the range of water stability.

However, using carbon and graphite materials, electrochemical oxidation has also been reported to be accompanied by a decrease in the electrode activity, specifically at high current densities. In addition, although carbon and graphite anodes have a relatively high overpotential for oxygen evolution, at the same time they should be strong enough to withstand the effect of a large quantity of hydroxyl radicals. These

materials are gradually oxidised to CO_2 under anodic conditions, resulting into the continuous corrosion of the electrode material *(Kraft et al. 2003)*. *Awad and Abuzaid, (1999)* observed that the rate of oxidation of phenol and the rate of formation of CO_2 increased while increasing current when phenol was oxidised using a packed bed of graphite particles. The maximum conversion of phenol was 50% and the current efficiency was 70%. The authors claimed that no deterioration of the graphite bed took place, even after operating the bed for 5 months, suggesting that all the CO_2 was formed by phenol oxidation rather than the oxidation of graphite particles. *Gattrel and Kirk, (1990)* observed a rapid decrease in the reaction rate during the oxidation of phenol in a flow cell using reticulated glassy carbon anodes. This was due to the blockage of electrode surface with insoluble polymeric materials. Still, they attained complete phenol oxidation at high temperatures and high applied potentials but at the expense of reduced current efficiency and faster electrode corrosion. *Polcaro et al. (2000)* has demonstrated that a fixed bed of carbon pellets used as three dimensional electrodes was effective not only for the removal of chlorophenols but also the intermediate reaction products. Under current densities of 5mA cm^{-2}, they observed low corrosion effects of the electrodes after they had been in operation for several hours.

3.5 Electrochemical Oxidation of Phenol as a Model Pollutant

Phenol has been the most extensively studied organic compound as a model pollutant for wastewater treatment by electrochemical oxidation since 1950 *(Boudenne et al. 1998)*. It represents a large family of compounds that can cause serious water pollution problems *(Maluleke and Linkov, 2003)*. Phenols are listed as priority pollutants by the US Environmental Protection Agency (EPA) *(Wise and Kuske, 2000)* as well as by European Union *(Zemann and Volgger, 1997)*. This is because of its high toxicity, high oxygen demand (theoretically, 2.4 mg O_2 mg^{-1} phenol) and low biodegradability *(Korbahti and Tanyolac, 2003)*. Phenol concentrations above 2 mg L^{-1} are toxic to fish and concentrations between 10 and 100 mg L^{-1} result in death of aquatic life within 96 hr (*Korbahti and Tanyolac, 2003)*. The wastewater of many industries contains a high concentration of phenol including petroleum refineries, pulp and paper mills, fertilizers, chemical plants, iron

and steel plants, explosive producers and phenolic resin manufacturers *(Canizares et al. 1999; Korbahti et al. 2002)*. Normally, the phenol concentration in industrial wastewaters may range from 200 to 2000 mg L^{-1}, considerably higher than the environmental standards established for release, which are typically below 0.5 mg L^{-1} *(Ahmaruzzaman and Sharma, 2005)*. Phenol can be economically recovered from wastewaters at concentrations above 2000–4000 mg L^{-1} by adsorption onto activated carbon and solvent extraction. However, for relatively low concentrations, biological treatment and destruction by oxidation have been preferred.

Biological treatment is suitable for treating wastewaters containing phenol up to a maximum concentration of 40 mg L^{-1} *(Seker et al. 1997)*. However, phenol is not readily biodegradable and is very toxic to many microorganisms at high concentrations. Among the alternative oxidation processes, photochemical degradation, chemical oxidation, wet oxidation and electrochemical oxidation are of particular interest *(Canizarres et al. 2002)*. Electrochemical oxidation has emerged as an alternative to the traditional phenol destruction processes because many industrial processes produce toxic wastewaters which are not easily biodegradable. They also require costly physical or physico-chemical pretreatments *(Korbahi et al. 2002)*.

Phenol was selected as a model contaminant for the study of adsorption and electrochemical regeneration of GIC adsorbent carried out in this project. Although a general mechanism of direct and indirect electrochemical oxidation of organics have been described in section 3.3, the different processes occurring and the breakdown products formed during electrochemical oxidation of phenol in water are discussed in the following sections.

3.5.1 Mechanism of Electrochemical Oxidation of Phenol

In the literature three processes have been reported, namely partial oxidation, total mineralization and polymerization which lead to removal of phenol from solution during electrochemical treatment. As discussed above, the electrochemical oxidation of organics is largely dependant upon the type of anode used (Section 3.4). *Comninellis and Pulgarin (1993)* conducted a comparative study between

electrochemical oxidation of phenol using Pt and SnO_2 anodes, and chemical oxidation with H_2O_2 in the presence of Fe^{2+} as a catalyst (Fenton's reagent). In the case of chemical oxidation, two techniques were used:

1. Reaction between phenol and H_2O_2 in the presence of Fe^{2+}at room temperature (25^oC)
2. Reaction between phenol and H_2O_2 in the presence of Fe^{2+} at elevated temperature (140^oC)

The results of these experiments indicated that during oxidation with Fenton's reagent at room temperature, hydroxyl radicals were generated from H_2O_2 (equation 3.17) and these were responsible for the oxidation of phenol and/or its intermediate products by electrophilic attack (equation 3.18).

$$Fe^{2+} + H_2O_2 \rightarrow Fe^{3+} + OH^- + OH^{\cdot} \qquad (3.17)$$

$$\{Phenol\} \xrightarrow{OH^{\cdot}/k_1} \begin{Bmatrix} Aromatic \\ Intermediates \end{Bmatrix} \xrightarrow{OH^{\cdot}/k_2} \begin{Bmatrix} Aliphatic \\ Acids \end{Bmatrix} \xrightarrow{OH^{\cdot}/k_3} CO_2 \qquad (3.18)$$

A large amounts of aromatic intermediates were formed which were further oxidised to aliphatic acids (See section 3.5.2 for the breakdown products). The aliphatic intermediates were found to be slow towards further oxidation. Phenol hydroxylation into aromatic intermediates took place instantaneously due to its high rate constant, even at room temperature. However, the rate of subsequent reactions (equation 3.18) was relatively low at room temperature. Similar types of reaction intermediates were observed with electrochemical oxidation using platinum anode. However, using electrochemical oxidation with a Pt anode a higher total organic carbon (TOC) reduction (60%) was observed compared to chemical oxidation with Fenton's reagent at room temperature, where a TOC reduction of only 30% was obtained *(Comninellis and Pulgarin, 1991)*.

During chemical oxidation with Fenton's reagent at high temperature, only a small amount of intermediates was observed. At high temperature all the three steps of equation 3.18 were fast. The main intermediate products were aliphatic acids, but

most of these were further oxidised to carbon dioxide. Electrochemical oxidation with a SnO_2 anode followed a similar reaction pathway to the high temperature chemical oxidation with Fenton's reagent. In this electrochemical process, hydroxyl radicals were produced by the electrochemical oxidation of water at the non-active electrode, as explained in section 3.3, and these oxidised the phenol at the surface of electrode (equation 3.19).

$$C_6H_5OH + 28(OH^{\cdot}_{ads}) \rightarrow 6CO_2 + 17H_2O \quad (3.19)$$

The complete degradation of phenol requires an exchange of 28 electrons by direct and indirect transfer (equation 3.20) *(Tahar and Savall, 1998).*

$$C_6H_5OH + 11H_2O \rightarrow 6CO_2 + 28H^+ + 28e^- \quad (3.20)$$

The decrease in the rate of oxygen evolution and hence an increase in the rate of phenol oxidation was achieved by pretreatment of SnO_2 electrode by anodic polarization that caused an increase in the overpotential for oxygen evolution. For both chemical oxidation at high temperature and electrochemical oxidation on SnO_2, TOC reduction was higher than 90%. According to *Comminellis and Pulgarin, (1993)*, the high temperature oxidation with Fenton's reagent behaved in a similar manner to electrochemical oxidation at the non–active anode (SnO_2) and low temperature chemical oxidation was similar to electrochemical oxidation at the active anode (Pt). However, the relatively higher TOC reduction at the active anode compared to Fenton's reagent at low temperature suggests that direct oxidation also takes place at the anode. Therefore, the electrodes may not behave merely either by active or non–active mechanisms.

Phenol also has the ability to foul electrodes due to the deposition of tarry products during its oxidation. These products are formed due to polymerization of the phenol molecules *(Zareie et al. 2001).* The oxidation of phenols at electrodes produces phenoxy radicals due to an electrophilic attack by hydroxyl radicals on the phenol molecules (equation 3.21). These radicals are responsible for the formation of polymeric materials *(Gattrel and Kirk, 1993b).*

$$C_6H_5OH + OH^{\cdot} \rightarrow C_6H_5O^{\cdot} + H_2O \rightarrow \text{Polymers} \quad (3.21)$$

The polymers formed have a lower oxidation potential than phenol. They can be easily oxidized to radicals that can undergo further polymerization resulting in polymers of higher molecular weights. These polymers adhere to the surface of the electrode leading to the formation a passivating film *(Boudenne et al. 1998).* Electrode fouling is problematic leading to slow reaction rates due to the interference of the polymeric film with the supply of reactant and the removal of products from the reaction zone *(Gattrel and Kirk, 1993b).*

During the anodic oxidation of phenol many researchers have observed the formation of polymeric films on the anode. *Comninellis and Pulgarin, (1991)* found a yellow brown polymeric product during the oxidation of phenol on a platinum anode. They observed that the formation of the polymeric film on platinum was favoured by alkaline media (pH>9), low current density (<30 mA cm^{-2}), high temperature (>50ºC) and high phenol concentration (50 mmol dm^{-3}). This film possessed good electrical conductivity in neutral and alkaline conditions. However, these passivating films can be further oxidised by applying high potential and long oxidation time *(Ferreira et al. 2006)*. Conversely, *Canizzares et al. (1999)* and *Zareie et al. (2001)* observed that polymeric materials were produced at high current density. A number of authors have reported that indirect oxidation due to the electrogenerated hydroxyl radicals did not result in electrode fouling due to the formation of polymeric films *(Iniesta et al. 2001; Zareie et al. 2001).*

Despite of the fact that the formation of polymer films have adverse effects on the performance of electrochemical oxidation of phenol, these can also be converted into insoluble and non-passivating polymeric products *(Tahar and Savall, 1998; Korbahti et al. 2002)*. *Tahar and Savall, (1998)* have found that during electrochemical oxidation of phenol in acidic conditions insoluble polymers were formed which precipitate in the form of solid black particles. They further observed that few polymers were formed at initial phenol concentrations of less than 42 mM. No polymer film was observed below a concentration of 5 mM phenol *(Zareie et al. 2001).*

3.5.2 Breakdown Products Formed during Electrochemical Oxidation of Phenol

The anodic oxidation of phenol has also been studied as a means of producing hydroquinone or benzoquinone *(Sharifan and Kirk, 1986). Smith et al. (1981)* has reported that phenol in aqueous solutions is readily oxidized but the oxidation of by–products is difficult. The information regarding the formation of breakdown products is an important consideration for investigating the mechanism of electrochemical oxidation. A variety of by–products has been reported in the literature formed during the electrochemical oxidation of phenol *(Sharifan and Kirk, 1986)*. Initially, phenol has been observed to be oxidized to hydroquinone which is further oxidized to 1,4–benzoquinone parallel with the formation of hydroquinone and catechol in small quantities (Figure 3.5). Then, oxidation of 1,4–benzoquinone leads, after opening of the aromatic ring, to the formation of carboxylic acids such as maleic and fumaric acids. These are finally converted to carbon dioxide and water.

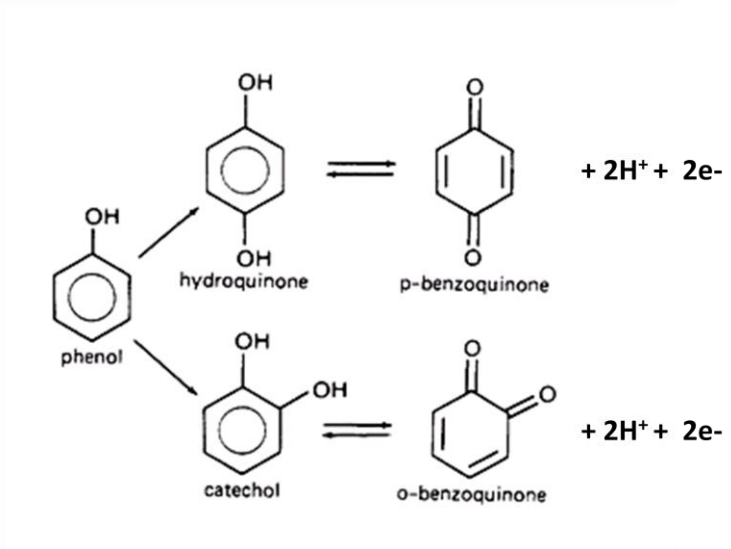

Figure 3.5: *Phenol oxidation to aromatic intermediates with simultaneous formation of hydroquinone and catechol*

In general the electrochemical oxidation of phenol in an aqueous solution is a complex transformation and is not well understood *(Sharifian and Kirk, 1986; Tahar and Savall, 1998). Comninellis, (1991)* analysed the oxidation products generated during electrochemical oxidation of phenol at a platinum anode. Their analysis also revealed that oxidation occurred in two steps:

(a) Formation of aromatic intermediates such as hydroquinone, benzoquinone, and catechol
(b) Rupture of aromatic rings leading to the formation of muconic acid which was further oxidized to C_4 and C_2 aliphatic acids such as maleic, fumaric and oxalic acid. These acids were stable towards further oxidation.

Li et al. (2005) has carried out the electrochemical oxidation of phenol at three different anodes, namely, Ti/SnO_2−Sb, Ti/RuO_2 and Pt. Although phenol was oxidised at a current density of 20 mA cm^{-2} in all the three cases, there was a significant difference in the intermediate breakdown products observed. Higher concentrations of hydroquinone and benzoquinone were observed at Ti/RuO_2 and Pt anodes, and their further degradation took a much longer time compared to the concentration and accumulation of these intermediates electrolysed using a Ti/SnO_2−Sb anode. In addition, relatively large quantities of maleic, succinic and oxalic acid were observed at Ti/RuO_2 and Pt anodes. However, smaller concentrations of maleic and oxalic acids were observed at the Ti/SnO_2−Sb anode. The overall degradation of the carboxylic acids was much slower at Ti/RuO_2 and Pt anodes compared to oxidation using the Ti/SnO_2−Sb anode. In addition, a dark yellow to brown colour was observed to build up in the solutions that were oxidised at Ti/RuO_2 and Pt anodes. This was thought to be due the formation of polymeric materials at these anodes.

Tahar and Savall (1998) studied the electrochemical oxidation of phenol on a Ta/PbO_2 anode in acidic conditions and observed 1, 4–benzoquinone, maleic acid and carbon dioxide as the main products. Hydroquinone, catechol, glyoxal and fumaric, glyoxalic and formic acids were formed in very low concentrations (<0.5 mmol dm^{-3}). The very low concentrations of hydroquinone indicate that its oxidation was rapid. According to the authors the simultaneous generation of carbon dioxide from the beginning of the electrochemical oxidation along with other products was clear from an instantaneous drop in the TOC value. The formation rate of 1, 4–benzoquinone was faster than its degradation rate, so that the oxidation of 1, 4–benzoquinone could be considered to be the limiting step in the degradation of phenol.

It can be concluded from the work reported in the literature that it is possible to oxidise phenol either to aromatic compounds or completely to carbon dioxide by electrochemical oxidation, depending on the experimental conditions. In this context, electrochemical oxidation of phenol at boron- doped diamond electrode (BDD) has shown that at low current density (5 mA cm^{-2}) and high phenol concentration (20 mM) the phenol was oxidised to benzoquinone, hydroquinone and catechol with a low phenol conversion (<20%) *(Iniesta et al. 2001)*. Around 80% of the phenol was converted to aromatic intermediates (benzoquinone, hydroquinone and catechol) with only 5-10% converted to CO_2. According to the authors this was due to a low concentration of electrogenerated hydroxyl radicals on the anode surface relative to phenol. In contrast, at high current density (60 mA cm^{-2}) and low phenol concentration (5 mM), phenol was completely oxidised to CO_2 due to a high local concentration of electrogenerated hydroxyl radicals on the surface of the anode relative to phenol. The percentage of phenol converted into aromatic intermediates was less than 5% whereas the percentage of phenol converted into CO_2 was close to 95%.

Comninellis and Chen, (2010) have further elaborated that the nature and the concentration of breakdown products formed during the electrochemical oxidation of organics depends strongly on the operating regime. In the case of oxidation under current control, a number of intermediates are formed, wheras when oxidation is carried out under mass transport controlled conditions no intermediates occur and CO_2 is the final product.

The pH of the solution strongly influences the nature of the breakdown products formed during electrochemical oxidation of phenol *(Comninellis, 1991)*. In alkaline conditions, hydroquinone and benzoquinone are not detected. The formation of a polymeric film is favourable in alkaline conditions. On the contrary, hydroquinone and benzoquinone are the main intermediate products during electrolysis of phenol in acidic media. However, the formation of polymeric films is inhibited in acidic conditions *(Awad and Abuzaid, 1999)*. For acidic environments, the carbon dioxide formed during oxidation escapes from the electrolyte whereas in alkaline conditions carbon dioxide reacts with alkali forming CO_3^{2-} and/or HCO_3^- *(Comninellis, 1991)*.

The aromatic and aliphatic breakdown products of phenol discussed so far are formed due to the direct oxidation of phenol. On the other hand, chlorinated breakdown products of phenol due to indirect oxidation have also been reported in the literature. Sodium chloride is often present in many industrial wastewaters and it is also a low cost, readily available electrolyte which can be added to reduce the cell potentials. Phenol can be chlorinated during electrochemical oxidation in the presence of chloride, leading to an increase in the toxicity and the environmental hazard associated with wastewaters. *Rajkumar et al. (2005)* investigated the electrochemical oxidation of phenol on a Ti supported TiO_2–RuO_2–IrO_2 anode in the presence of chloride as the supporting electrolyte. The phenol was completely oxidised but with a pronounced formation of chlorinated organic compounds at the start of electrolysis, which was then reduced to low levels during the course of electrolysis. However, the complete elimination of chlorinated organic compounds was not achieved.

During electrochemical oxidation of phenolic wastewater at carbon electrodes in the presence of NaCl, mono–, di–, and tri–substituted chlorophenols have been observed (*Zareie et al. 2001; Korbahti et al. 2002).* These species were observed to be either completely oxidised or contributed towards to the formation of non–passivating polymeric materials on the carbon electrodes. However, no benzoquinone, hydroquinone or catechol was observed in the electrolysis solution. *Comninellis and Nerini, (1995)* did not find chlorinated phenols during electrochemical oxidation of phenol in the presence of NaCl. They suggested that the reaction between ClO^- and phenol occured close to the electrode surface and was very fast. The chlorinated phenols formed are then further degraded to aliphatic acids with ClO^- and/or at the anode. However, they found chlorinated species in both the electrolyte and the evolved gases. Chloroform was the main compound in the evolved gases. The concentration of chlorinated products in the electrolyte reached a maximum and then decreased to low levels. Conversely, the volatile chlorinated compounds increased rapidly. They suggested that the phenol is first oxidised to non–volatile organo-chlorinated compounds which are further degraded to volatile chlorinated compounds.

3.5.3 Quantitative Evaluation of Oxidation

Various methods have been used to quantify the electrochemical oxidation process:

1. The percentage of phenol converted into aromatic intermediates, relative to the amount of degraded phenol, has been defined by *Iniesta et al. (2001)* as:

$$\%\text{Aromatics} = \frac{(\text{Aromatics})}{(\text{Phenol})_o - (\text{Phenol})_t} \times 100 \qquad (3.22)$$

where (Aromatics) is the concentration of aromatic intermediates in mmol dm^{-3}. $(Phenol)_o$ and $(Phenol)_t$ are the concentrations of phenol at start and after a time *t* of electrolysis, respectively in mmol dm^{-3}.

2. Similarly, the percentage of phenol converted into acid intermediates such as fumaric, maleic and oxalic acids, relative to the amount of phenol degraded has been defined as:

$$\%\text{Acids} = \frac{(\text{Acids})}{(\text{Phenol})_o - (\text{Phenol})_t} \times 100 \qquad (3.23)$$

where (Acids) is the concentration of acid intermediates in mmol dm^{-3}.

3. The percentage of phenol converted into carbon dioxide, relative to the amount of phenol, can be calculated from the TOC as *(Tahar and Savall, 1998)*:

$$\%CO_2 = \frac{\frac{[(\text{TOC})_o - (\text{TOC})_t]}{6}}{(\text{Phenol})_o - (\text{Phenol})_t} \times 100 \qquad (3.24)$$

where $(TOC)_o$ and $(TOC)_t$ are the total organic carbon at start and after a time t of electrolysis, respectively in mmol dm^{-3}

4. The current efficiency is defined as the ratio of the charge consumed by the electrode reaction of practical importance divided by the total charge passed

through the circuit. Thus it is the ratio of the the actual charge passed to the theoretical charge required for the desired electrode reaction. The instantaneous current efficiency (ICE) for chemical oxygen demand (COD) removal is determined from the rate of change of COD *(Comninellis, 1991)* during electrolysis as fellows (equation 3.25):

$$\mathrm{ICE} = \frac{[(\mathrm{COD})_t - (\mathrm{COD})_{t+\Delta t}]}{8I\Delta t} F \cdot V \qquad (3.25)$$

where $(COD)_t$ and $(COD)_{t+\Delta t}$ are the chemical oxygen demands at times t and $t+\Delta t$ (in g O_2 dm^{-3}), respectively, I is the current (A), F is the Faraday constant (96485.34 C moL^{-1}), and V is the volume of electrolyte (dm^3) and 8 is a dimensional factor for unit consistence.

3.6 Electrochemical Cells Containing Carbon Based Materials as Electrodes

Although the behaviour of carbon electrode materials as active and non–active anode has already been discussed in section 3.4, this section considers the electrochemical cells which use carbon based materials for the removal of phenol and other organic compounds from water.

Electrochemical cells using carbon electrode materials for the removal of organic pollutants have been reported by a number of authors *(Boudenne et al. 1996; Polcaro et al. 2000; Chen et al. 2010). Boudenne et al. (1996)* used carbon black as a catalytic slurry electrode in combination with Ti/Pt electrodes. Carbon black was used to accelerate the rate of phenol oxidation. In addition, it has high electrical conductivity and good adsorption properties. In the absence of carbon black, phenol was completely converted into hydroquinone in 105 minutes and no conversion into CO_2 was observed even after 8 hours of electrolysis. On the other hand, the phenol was completely oxidised in 30 minutes using carbon black with any breakdown products remaining on the surface of carbon black. They further suggested that the amount of the intermediate products can be decreased by increasing the amount of carbon black. Similar results were obtained by *Polcaro et al. (2000)* who observed

that the ratio between the aromatic and aliphatic intermediates can be decreased by increasing the amount of carbon, suggesting that higher amounts of carbon enhance oxidation. According to *Boudenne et al. (1996),* for a molecule of phenol to be oxidised, it should first be adsorbed on carbon black because most of the oxidation reactions take place at the interface between carbon black and the Ti/Pt electrodes. During contact of the carbon black with Ti/Pt electrodes, oxidation occurs due to the transference of the electrons.

The removal of phenol from water has also been carried out using carbon felt electrodes *(Hernandez et al. 2003).* Carbon felt is a textile material which is consisted of randomly oriented and intertwined carbon fibres. The authors confirmed that the use of carbon felt electrodes provides a phenol oxidation whose products do not inhibit the electrode surface thus allowing effective removal of phenol from water. *Maleki et al. (2006)* used an ionic liquid, n-octyl pyridinum hexaflouro-phosphate (OPFP) as a binder to fabricate a graphite composite electrode with attractive electrochemical properties, which they called as carbon ionic liquid electrode. *Safavi et al. (2007)* used carbon ionic liquid as the working electrode for investigating the electrochemical oxidation of phenolic compounds. They suggested that the oxidation of phenolic compounds on carbon ionic liquid electrode was stable and therefore did not cause electrode fouling.

In order to address the problems of metal based electrodes which are associated with electrode fouling and the need for high concentrations of electrolytes, *Chen et al. (2010)* used granular graphite as the working electrode in the form of a packed bed for the removal of 4-chlorophenol from water. They observed 99% removal of 4-chlorophenol was achieved after 24 h of treatment of a batch of 17.5 L contaminated water for current densities in the range 1–6 mA cm^{-2} with a 2 cm deep bed. They suggested that using granular graphite as an electrode without a supporting electrolyte can reduce the amount of raw material required and thus the cost of treating wastewater containing 4-chlorophenol.

A number of studies have been carried out using GAC within an electrochemical cell. *Xiong et al. (2003)* used a GAC in the form of a packed bed as the working electrode in a three phase three dimensional electrochemical cell to remove formic

acid from water. They used an undivided cell with stainless steel electrodes (anode and cathode), 11 cm apart, and a GAC bed in between the two electrodes. Air was sparged into the GAC bed from the bottom of the electrochemical cell in order to increase the mass transfer within the bed and to provide oxygen to the electrode for some electrochemical reactions such as the formation of H_2O_2 on the electrode. They confirmed that sparging an inert gas into the bed resulted in an increase of COD removal due to the increase in mass transfer and using air resulted in a much larger increase suggesting that electrochemical generation of H_2O_2 or other oxidising species also takes place. However, the COD removal was only increased from 37.9 to 73.4% with a large increase in the voltage applied across the cell (30 V). The authors also suggested that a number of phenomena, including direct and indirect electrochemical oxidation, adsorption, and air stripping etc. may be playing their role in the elimination of formic acid.

3.7 Electrochemical Regeneration of Adsorbents

The electrochemical regeneration of adsorbents involves the removal of species adsorbed onto the surface of an adsorbent by employing electric current in an electrochemical cell so that the adsorptive capacity of the adsorbent is restored. This has been defined in terms of regeneration efficiency (γ) by *Narbaitz and Cen*, (1994) as follows:

$$\gamma = 100\frac{q_r}{q_i} \tag{3.26}$$

Where q_r *(mg* g^{-1}*)* and q_i *(mg* g^{-1}*)* are the adsorptive capacities of regenerated and fresh adsorbent measured under identical conditions.

An ideal electrochemical regeneration should regenerate the adsorbent and completely oxidise the adsorbed species so that they are not transferred to the liquid or gaseous phases. The phenomena involved could be either direct oxidation of the pollutants on the surface of the adsorbent or desorption followed by their oxidation in solution.

3.7.1 Mechanisms of Electrochemical Regeneration of Activated Carbon

In comparison to the numerous studies on electrochemical oxidation of wastewater available in the literature, electrochemical regeneration of adsorbents has not been widely investigated. This section deals with the adsorption of a particular pollutant onto GAC and its subsequent electrochemical regeneration in an electrolytic cell. *Doniat et al. (1980)* used GAC in a divided electrolytic cell to treat a primary domestic effluent. The cell was divided into anode and cathode compartments by a membrane which only allowed the electrolyte to pass between the electrodes. The GAC–electrolyte mixture was circulated through the anodic compartment of the cell in such a way that particles of GAC were in contact with anode during their flow through the cell. The oxidation of the adsorbed impurities on the surface of GAC took place by the oxygen liberated at the anode. They achieved a regeneration efficiency of 75-85%. However, the regeneration time was 4–16 hours. A similar regeneration mechanism has been reported by *Slavinski et al. (1984)* for the electrochemical regeneration of p–nitrotoluene saturated activated carbon in a divided cell. They also suggested that direct anodic oxidation is the phenomena occurring on the surface of GAC. The overall regeneration efficiencies were up to 98% in their experiments.

Narbaitz and Cen, (1994) have demonstrated the electrochemical regeneration of phenol loaded activated carbon, both cathodically and anodically. They used an undivided electrochemical cell, consisted of a single layer of GAC particles on a platinum electrode with 1% NaCl as the electrolyte. The anodic and cathodic regenerations were carried out by polarising the GAC as a anode and cathode, respectively. Their results revealed that cathodic regeneration was 5–10% more efficient than anodic regeneration. However, a small amount of phenol was left in the electrolyte when GAC was regenerated at the cathode. The anolyte was free of the phenol residual for anodic regeneration. In cathodic regeneration, initially phenol was desorbed and then oxidised in the solution, suggesting that phenol desorption and its subsequent destruction is the most likely mechanism of regeneration. Cathode is a reducing electrode and therefore during electrolysis there will be an increase in the local pH. This increase in pH leads a reduction in the absorbability of the phenol

and promotes desorption. At the anode the pH decreased, and the authors suggested that phenol did not desorb at low pH but once the phenol was desorbed it was more efficiently destroyed. The high capacity of activated carbon is due to the adsorption of phenol on the internal surface and the amount of adsorption on the external surface is negligible. However, the electrochemical effects are confined to the external surface which suggests that desorption must occur prior to electrochemical regeneration.

Narbaitz and Cen, (1994) achieved higher regeneration efficiencies (95%) during the first regeneration. A 2% reduction in the efficiency with no apparent carbon loss was observed in subsequent cycles. These results were a significant improvement on those of *Doniat et al. (1980)* who reported a 65% reduction in the adsorptive capacity of activated carbon after 8 cycles of operation during adsorption and electrochemical regeneration of phenol. However, they used anodic oxidation rather than cathodic desorption of phenol. *Narbaitz and Cen, (1994)* concluded that anodic regeneration was relatively efficient in oxidising the residual phenol in the electrolyte compared to cathodic regeneration where higher currents and/or longer regeneration times were required to destroy the residual phenol in the electrolyte. The regeneration efficiency was also found to be dependent upon the nature and concentration of the electrolyte, and the particle size of the GAC. Similar results were obtained by *Zhang et al. (2002)* and *Zhang, (2002)* who observed that cathodic regeneration efficiencies are higher than anodic regeneration efficiencies. Desorption and subsequent oxidation of phenol was found to be responsible for regenerating the activated carbon. In addition, they further confirmed that the regeneration efficiency of activated carbon increased with the electrolyte concentration, regeneration current intensity and treatment time. However, no change of regeneration efficiency was observed after 5 h of regeneration *(Zhang, 2002).*

For GAC electrochemical regeneration discussed so far, the only mixing was due to the generation of the gas bubbles at the electrodes. The effect of electrolyte velocity on the regeneration efficiency has been reported by *Karimi-Jashni and Narbaitz, (2005)*. The cathodic regeneration efficiencies were decreased by increasing the electrolyte mixing, suggesting that a higher degree of mixing decreased the local pH at the cathode which reduced desorption of the phenol. However, no significant

change in the anodic regeneration efficiencies was observed with increasing electrolyte mixing.

Several further studies have also reported higher efficiencies of cathodic versus anodic electrochemical regeneration, including, *Garcia–oton et al. (2005)* who electrochemically regenerated toluene saturated activated carbon in the presence of a supporting electrolyte. A number of adsorption and electrochemical desorption cycles were carried out without a significant loss of the adsorption capacity of the activated carbon. The relatively lower regeneration efficiencies observed during anodic regeneration compared to cathodic treatment, specifically for the adsorption and regeneration of phenol on GAC, may be in part due to pore blocking by polymeric phenol oxidation products *(Berenguer et al. 2009; Doniat et al. 1980)*. In addition the surface groups formed during anodic electrochemical regeneration can also participate to the pore blocking (See section 3.8.3).

In spite of the higher rates of electrochemical regeneration reported using the cathodic processes, electrochemical cells based on anodic oxidation of the adsorbed species are important because of the following reasons *(Brown, 2005)*:

- The anodic oxidation is destructive
- Desorption is a slow process *(Narbaitz and Karimi-Jashni, 2009)*
- Post treatment of desorbed contaminants may be necessary

Canizares et al. (2004) have studied the combined adsorption and electrochemical regeneration of GAC in batch mode, using phenol as a model pollutant. The organic pollutant is initially adsorbed onto the GAC and then it is converted into CO_2 and electrocoagulated solids through anodic oxidation. Electrochemical regeneration of the loaded activated carbon was performed in an electrolytic cell which consisted of two carbon steel concentric cylinders. A polyurethane layer was fixed around the inner solidly made cylinder and the space between this layer and the outer void cylinder was filled with a layer of the GAC. The outer cylinder and the GAC were used as the anode whereas the inner cylinder was the cathode of the electrochemical cell. A regeneration efficiency of 80% was attained during the first regeneration

cycle. A linear decrease in regeneration efficiency was observed for the next three cycles with almost 5% loss in adsorptive capacity per cycle. During the regeneration process, hydroquinone was the only intermediate formed with no carboxylic acids observed. However, yellow insoluble compounds were also observed during the regeneration. The authors explained that these insoluble solids were formed due to the electrochemically assisted coagulation involving the phenol and its oxidation products upon interaction with anodically generated Fe^{3+} ions from the steel anode. It has been stated that the phenol and organic acids can chemically interact with trivalent cations to form insoluble compounds, which explains that why no carboxylic acid was detected during the regeneration of GAC. However, higher current densities favoured CO_2 formation over electrochemically assisted coagulation. For the range of current densities used, the cell potential remained constant during each assay which reveals that passivation of the electrodes did not occur. In their work, they also compared the performance of the system with and without the bed of the GAC. In both cases, similar rates of CO_2 and anodic oxidation of carbon steel indicated that most of the electrochemical processes were occurring on the steel surface suggesting that the GAC bed mainly acts as an adsorbent rather than as an electrode. Thus, desorption of the phenol from the adsorbent prior to electrochemical oxidation is the likely mechanism for regenerating the GAC.

The behaviour of activated carbon as an adsorbent and/or its participation in electrochemical processes was investigated in a three phase electrochemical reactor involving the treatment of p–nitrophenol *(Zhou and Lei, 2006)*. Their system was composed of a cylindrical reactor with a PbO_2 anode and the stainless steel cathode. The cathode was placed surrounding the inner wall of the cell and the anode was located in the centre in contact with which the particles of GAC were packed. The wastewater containing p–nitrophenol and the supporting electrolyte was allowed to pass through the inlet chamber at the bottom, then through the electrochemical cell and finally out of the system through the outlet chamber at the top. In addition, a gas (N_2 or O_2) was sparged from the bottom of the electrochemical cell such that the fluidization of the GAC particles could take place.

In order to evaluate the contribution of the GAC in the process of adsorption and electrochemical oxidation, experiments were carried out with no GAC in the reactor,

using GAC adsorption with no current was applied and electrochemical oxidation with GAC, while keeping all other operating parameters constant. Similar types of breakdown products including, phenol, hydroquinone, benzoquinone, p–nitrocatechol, hydroxyquinol, fumaric acid and oxalic acids were observed in both cases where electrochemical oxidation was applied. However, the concentration trends of hydroquinone, benzoquinone and fumaric acid were not similar. During electrochemical oxidation in the absence of GAC, both hydroquinone and benzoquinone increased during the initial 60 min while the formation of fumaric acid lagged behind. On the other hand, for electrochemical oxidation with GAC, the concentrations of benzoquinone and hydroquinone initially increased during the first 30 min and then decreased with time with significantly lower concentrations of fumaric acid observed in this case. In addition, the concentrations of hydroquinone and benzoquinone were relatively high during the first 30 min of electrochemical oxidation with GAC.

The authors suggested that if GAC had been only acting as adsorbent, the concentration trends of hydroquinone and benzoquinone should be similar to those which occur during electrochemical oxidation in the absence of GAC, and in addition these concentrations should also be lower due to the adsorption onto the activated carbon. They also observed that fumaric acid had the lowest adsorptive capacity compared to benzoquinone and hydroquinone in a separate adsorption experiment, suggesting that its concentration should be similar in the presence and absence of GAC. These results indicated that adsorption was not the only process occurring on the GAC.

The authors believed that electrochemical regeneration of GAC by hydroxyl radical attack of the adsorbed contaminant was the main mechanism of GAC regeneration. The main active species responsible for the electrochemical oxidation of organic impurities was considered to be hydroxyl radicals *(Zhou et al. 2005)*. The oxidation of organic acids has been found to be difficult due to the competitive reaction of hydroxyl radicals with these acids and the phenolic compounds, since the rate of reaction of hydroxyl radicals with organic acids is relatively slow compared to the rate of reaction of hydroxyl acids with phenolic compounds *(Zhou et al. 2005)*.

Due to the relative high adsorptive capacities of p–nitrophenol and benzoquinone, these contaminants remained adsorbed on the GAC leaving behind fumaric acid because of its low adsorption capacity. Thus low concentrations of fumaric acids were observed for the GAC electrochemical oxidation process compared to that in the absence of GAC. In the presence of GAC, it is proposed that p–nitrophenol remained adsorbed and decomposed by electrochemical oxidation. The authors concluded that activated carbon contributed to the treatment of p-nitrophenol in this process by three mechanisms namely, adsorption, electrodesorption and electrochemical regeneration.

The rate of adsorption and desorption of organic compounds from activated carbons is usually controlled by intra-particle diffusion which leads to longer adsorption and regeneration times. *Narbaitz and Cen, (1994)* reported that 6 days were required to achieve equilibrium for adsorption of phenol onto activated carbon (Filtrasorb F–400) and 5 hours were needed to achieve 95% regeneration efficiency during electrochemical regeneration. The following section describes the use of non-porous graphite based materials for the adsorption of organics and their subsequent electrochemical regeneration in order to address the issues associated with electrochemical regeneration of GAC. Thus using graphite adsorbents leads to lower cell voltages and thus lower cost, as well a shorter regeneration times.

3.7.2 Electrochemical Regeneration of GIC adsorbents

As discussed in Chapter 2, activated carbon possesses high adsorption capacities for dissolved organics because of its microporous structure and high internal surface area. Electrochemical regeneration of GAC requires long regeneration times, and the electrical conductivity is relatively low leading to high energy usage during the electrochemical regeneration of GAC. As a general rule, the higher the electrical conductivity of the adsorbent materials, the lower will be the voltages required for electrochemical regeneration and therefore lower will be the energy consumption.

Brown and Roberts, (2007) have been working over the last few years on water treatment by employing the technique of adsorption and electrochemical regeneration of carbon based materials which were later on declared as GIC

adsorbents in a patent *(Eccleston et al. 2009)*. These adsorbents are non-porous in character and have electrical conductivities considerably greater than activated carbon. The use of such materials significantly reduces the time required to achieve both adsorption equilibrium and regeneration but at the expense of reduced adsorbent capacity because of the lack of internal pores in the adsorbent materials. However, the authors have found that in the treatment process in which the adsorbent is recycled after regeneration, the ease of regeneration more than compensates for the low surface area (and hence low adsorption capacity) in comparison to the use of thermal regeneration of activated carbons *(Eccleston et al. 2009)*. This can be explained by considering that although the capacity of GICs on each use is low, this capacity is rapidly available again after regeneration, so that with multiple regeneration cycles high capacities can be achieved with small amounts of adsorbent.

Brown et al. (2004a) carried out the electrochemical regeneration of GIC material (Nyex–100) loaded with crystal violet dye in a divided electrolytic cell. Their system operated in batch mode with the adsorbent being initially loaded with pollutant. The electrochemical cell consisted of an anode and cathode compartments separated by a polymer membrane. The anode was a mixed metal oxide coated titanium and the cathode was stainless steel. The loaded adsorbent with 1% NaCl as an electrolyte was pressed into the anode compartment to form a particulate bed that was regenerated by applying a current in the range 125−1000 mA (corresponding to current densities in the range 5.5–44.5 mA cm^{-2}) and the regeneration time was (1.5–30 min). They found that the regeneration efficiency increased with increasing charge passed with a maximum efficiency of 100%, attained after passing a charge of 25 C g^{-1} (achieved with a current density of 20 mA cm^{-2} passed for 10 min). This suggests that the amount of charge passed for regenerating the adsorbent was significantly lower than that required to regenerate phenol loaded GAC by *Narbaitz and Cen, (1994)*. However, the GAC had a much higher adsorbate loading (107 mg g^{-1} phenol) compared to Nyex–100 (≈1 mg g^{-1} phenol) *(Brown, 2005)*. The authors have also reported a fall in the regeneration efficiency as the current density was increased. The possible cause of this reduction could be an increase in the side reactions that occurred at high current densities. In addition, the increase in cell potentials observed with an increase in current density also increased the power consumption.

Brown and Roberts, (2007) also studied the removal of phenol from water by adsorption and electrochemical regeneration using GIC in the electrochemical cell described above. High regeneration efficiencies were achieved by passing a charge of 25 C g^{-1} over a number of cycles through a bed of adsorbent loaded with phenol, using a current density of 20 mA cm^{-2} for 10 min. Though not significant, there was a 1.3% reduction in the regeneration efficiency per cycle during the five adsorption and regeneration cycles *(Brown, 2005)*. They also treated an industrial effluent containing high organic contents (COD, 11070 mg L^{-1}) and 137 mg L^{-1} dichloromethane. Their results indicated that the treatment with GIC adsorbent led to a linear removal of COD for each adsorption and regeneration cycle. This linear removal indicated that 100% regeneration efficiency was achieved on each cycle at 20 mA cm^{-2} current density in 10 minutes. However, it was also shown that 99% of the dichlormethane was removed after the first cycle. The process of adsorption and electrochemical regeneration using GIC has also been shown to be effective for the removal of low concentrations of atrazine from water *(Brown et al. 2004b)*. In this context, the removal of atrazine to below 1.0µg L^{-1} was demonstrated.

Based on their previous batch studies *(Brown et al. 2004a, 2004b; Brown and Roberts, 2007)*, *Eccleston et al. (2010)* have patented a continuous process for adsorption with electrochemical regeneration in the same unit (See Chapter 1 for a description of the continuous device). A recent paper on the continuous process has shown the removal of an organic dye, acid violet 17 (AV–17), from water for a range of AV–17 inlet concentrations and solution flow rates *(Mohammad et al. 2011)*. Removals of the dye of 98% or higher for inlet concentrations of up to 250 mg L^{-1} were obtained in a single pass treatment. Even with an inlet concentration of 500 mg L^{-1}, 95% removal was achieved. However, when the solution flow rate was increased at an inlet concentration of 500 mg L^{-1}, the percentage removal decreased, presumably due to the decreased residence time and the higher loading of AV–17 on the adsorbent. No attempt was made to determine the possible breakdown products released in solution during the continuous treatment of AV–17. However, the authors have determined the TOC of the effluent and observed that its removal was only 20–30% even when the percent removal of AV–17 was more than 90%. This indicates the presence of intermediate breakdown products in solution.

On the other hand, during electrochemical regeneration of phenol loaded adsorbent (Nyex–100) in the batch electrochemical cell, very few breakdown products were formed even when regeneration charge was insufficient for 100% regeneration *(Brown and Roberts, 2007)*. After regeneration the authors did not believe that break down products were present on the surface of adsorbent since the adsorptive capacity of the regenerated adsorbent was similar to fresh adsorbent. They suggested that phenol was fully oxidized (mineralised) during the electrochemical regeneration. However, they also believe that any desorption of adsorbed species or intermediate oxidation products (which could be more toxic than the starting contaminants) could contaminate the treated water after subsequent cycles. Therefore, a detailed investigation is required to determine the fate of the adsorbed species for the process of adsorption and electrochemical regeneration using GIC adsorbents.

3.7.3 Changes in Surface Chemistry of Adsorbents Due To Electrochemical Oxidation

The electrochemical regeneration of GAC at the anode or cathode of an electrochemical cell promotes oxidation and reduction of the carbon surface respectively. As a result, the surface chemistry and thus the adsorption characteristics of the GAC are altered. The surface effects of GAC associated with electrochemical treatment have been studied by *Mehta and Flora, (1997)*, using phenol as the adsorbate. They observed that under oxic conditions (when oxygen was present), a decrease in adsorptive capacity resulted from both anodic and cathodic treatment. On the other hand, for anoxic conditions (no oxygen), a decrease in the adsorptive capacity was noted only for the anodic treatment, with no change in the adsorptive capacity observed during cathodic treatment.

The adsorptive capacity of carbon based adsorbent is strongly influenced by the chemical nature of the surface *(Nevskaia et al. 1999)*. Extensive studies have been carried out in the literature to investigate the surface functional groups of activated carbon. The tendency of carbon to chemisorb oxygen is greater than its affinity to adsorb other species *(Dabrowski et al. 2005)*. Oxygen chemisorbs at the surface of

activated carbon to form carbon-oxygen surface functional groups such as carboxyl, phenols, lactones, aldehydes, ketones, quinones, hydroquinones and ethereal structures. These groups may be acidic, basic or neutral and give the carbon surface an acidic or basic character which in turn depends upon the preparation and treatment conditions of activated carbon.

After anodic treatment, an increase in phenolic, strongly and weakly acidic carboxyl groups, suggesting that the carbon surface became more acidic upon oxidation *(Mehta and Flora, 1997)*. These acidic surface groups are responsible for the decrease in adsorptive capacity of activated carbon for phenol adsorption. During anodic oxidation, surface oxides are formed as the GAC surface donates electrons (equations 3.27 and 3.28).

$$C + H_2O \rightarrow C - O + 2H^+ + 2e^- \quad (3.27)$$

$$C + OH^- \rightarrow C - OH + e^- \quad (3.28)$$

On further reaction, these oxides may convert to form CO_2 as follows:

$$C - O + H_2O \rightarrow CO_2 + 2H^+ + 2e^- \quad (3.29)$$

$$C - OH + OH^- \rightarrow CO_2 + 2H^+ + 3e^- \quad (3.30)$$

The decrease in adsorptive capacity of GAC for phenol has been further explained by the following two reasons:

1. The decrease in surface carbonyl groups by oxidation to carboxylic groups during anodic treatment of GAC may decrease its adsorptive capacity for phenol

2. The change in specific surface area of the GAC due to its oxidation to CO_2 may also be responsible for a decrease in adsorptive capacity of GAC (equations 3.29 and 3.30)

In contrast to the decrease in adsorptive capacity of activated carbon after anodic treatment, *Brown et al. (2004b)* observed that modification of the surface of a GIC adsorbent (Nyex−100) on electrochemical regeneration can result in adsorptive capacities up to three times greater than the adsorption capacity of the GIC before regeneration (for a pesticide adsorbate). The authors suggested that the untreated GIC has a strong graphitic structure and on electrochemical regeneration the surface roughness increased due to the breakage of flat graphene layers. Oxygen containing functional groups are primarily found at the edges of broken graphite planes with basal planes consisting of large fused aromatic structures *(Mattson et al. 1969).* Consequently, the relative contribution of the edges with oxygen containing functional groups will increase which should decrease the adsorptive capacity as discussed before for activated carbon. However, an increase in the adsorbate uptake suggests that the conversion of carbonyl oxygen to carboxylic groups is less significant than the increase in edge/plane effects due to the electrochemical oxidation. The observed increase in adsorptive capacity may also be attributed to an increase in the specific surface area by surface roughening.

3.8 Conclusions

This chapter has discussed the importance of electrochemical techniques for the treatment of organics, with particular emphasis on electrochemical oxidation of organics. A detailed review of the direct and indirect electrochemical oxidation of organics has revealed that it involves a number of different reactions occurring at the surface of anode and in the bulk solution. Even the use of a model pollutant resulted in a complex oxidation mechanism. Phenol has been used as a model compound for investigating electrochemical oxidation due to its high toxicity, high oxygen demand and low biodegradability. There is extensive literature available on the electrochemical oxidation of this compound. The nature and concentration of intermediate breakdown products formed during the electrochemical oxidation of phenol has been found to be dependent on the experimental conditions including current density, pH, and concentration. This chapter has also briefly evaluated the performance of different electrode materials for the electrochemical oxidation of organic pollutants. It has been concluded that anodes with low oxygen evolution overpotential (such as Pt, IrO_2 etc) only allow the partial oxidation of organics due to

the accumulation of intermediate oxidation products. However, complete mineralization of the organics can be achieved by employing anodes with high oxygen overpotential (such as SnO_2, BDD etc). The use of carbon based materials in electrochemical cells as electrodes which assist the removal of organics from water has been reviewed. Carbon based materials can be effectively used in electrochemical cells as electrodes for the removal of organics from water.

In contrast to the electrochemical oxidation of organics in water, electrochemical regeneration of adsorbents has not been widely studied. The anodic regeneration and cathodic desorption of the adsorbed organics are the two main mechanisms of electrochemical regeneration of GAC. It has been shown that in spite of the higher rates of electrochemical regeneration reported using a cathodic process, electrochemical cells based on anodic oxidation of the adsorbed species are important. However, a literature review on electrochemical regeneration of GAC has revealed that it involves longer adsorption and regeneration times thus affecting the process cost. The removal of low concentrations of organics by adsorption and electrochemical regeneration using GIC materials has emerged as an alternative not only to the available technologies for water treatment but it also presents practical solutions to the problems associated with the use of GAC. Recent studies have shown that GIC materials can be effectively regenerated due to their non-porous character and high electrical conductivity. However, the investigation of the possible breakdown products formed during the electrochemical regeneration of GIC adsorbents are an important consideration keeping in view the practical application of this technique for water treatment. In addition, the nature and concentration of the intermediate products can help to determine the mechanism of electrochemical regeneration of GIC adsorbents. Finally, previous work has shown that electrochemical treatment affects the surface chemistry of adsorbents which can further alter the adsorption characteristics of the adsorbents.

Chapter 4

Formation of Breakdown Products in the Liquid Phase during Electrochemical Regeneration of GIC Adsorbents

This chapter describes an experimental investigation of the formation of non-chlorinated breakdown products released in the liquid phase during the batch process of adsorption with electrochemical regeneration. A detailed investigation of the formation of chlorinated breakdown products in the batch process is also given. In addition, the conditions that minimize the formation of chlorinated breakdown products during the electrochemical regeneration of GIC adsorbents are evaluated. The generation of free chlorine was investigated under different process conditions. The fate of the breakdown products during the continuous process of adsorption and electrochemical regeneration has also been investigated. Finally, the conclusions of the study are presented.

4.1 Investigation of Non-Chlorinated Breakdown Products in Batch Studies

In this section an investigation of the formation of non-chlorinated breakdown products released in solution during batch adsorption and electrochemical regeneration of GIC adsorbents under different experimental conditions is described. The formation and fate of chlorinated by–products during batch adsorption with electrochemical regeneration is considered in section 4.2.

4.1.1 Materials

Phenol was chosen as a model pollutant for adsorption with electrochemical regeneration of GIC adsorbents as explained in section 3.5. Analytical grade phenol was supplied as a white crystalline powder by Sigma-Aldrich®. Analytical grades of other organic chemicals including 1,4–benzoquinone, hydroquinone, catechol, fumaric, maleic and oxalic acids, and inorganic chemicals such as phosphate buffers, NaCl, Na_2SO_4, HCl, H_2SO_4 etc. were also supplied by Sigma-Aldrich®. All solutions

were made up using ultrapure water obtained from a laboratory purification unit (Millipore™ Elix 5). The conductivity of the water was < 0.2 μS cm^{-1} at 25℃ and the total organic carbon content was <30 ppb. The adsorbent used in this project was a hydrogen sulphate intercalated GIC known as Nyex®1000 supplied by Arvia Technology Ltd in the form of graphitic flakes. The flakes were observed to be flat with a smooth morphology as shown in figure 4.1. The specification for Nyex®1000 provided by Arvia® shows that it has 98 % carbon content. Mercury porosimetry showed that there are no pores and therefore no internal surface area. The mean particle diameter as determined by Mastersizer-2000 (Malvern Instruments, UK) was 484 μm (range 50–850μm). Some batches of Nyex®1000 provided by Arvia Technology Ltd contained a significant quantity of fine particles with diameters < 150 μm. To minimise the variability of the Nyex®, the same batch of Nyex®1000 (which contained relatively small quantities of fine particles) was used throughout this study. The Brunauer Emmett Teller (BET) surface area of Nyex®1000 was determined by nitrogen adsorption and found to be around 1.0 $m^2 g^{-1}$.

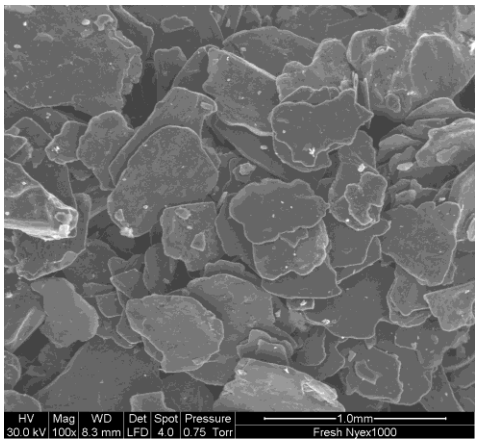

Figure 4.1: *SEM image of GIC particles showing smooth and flat morphology at 100x magnification*

4.1.2 Equipment and Methodology

Electrochemical regeneration using the batch electrochemical cell

For preliminary investigations of the formation of breakdown products, batch adsorption was followed by adsorbent/liquid separation and electrochemical regeneration in a simple batch cell, as briefly explained in Chapter 1, Fig 1.1. Further

details of the cell are given in Figure 4.2. The anode current feeder of the cell was composed of iridium/ruthenium mixed metal oxide coated titanium plate (supplied by Electrode Products Technology Ltd). The cathode was a perforated stainless steel plate, with 1 mm thickness and 3mm diameter perforations giving an open area of 33%. The anodic and cathodic compartments were separated by a microporous Daramic 350 membrane, a high molecular weight polyethylene ribbed sheet containing amorphous silica. The active area of each electrode was 25 cm^2, with anode and cathode compartments being 10 mm wide. The cell was constructed from grey PVC using solvent adhesive construction. The DC power source was supplied by Thurlby Thandar Instruments (PL 320QMD).

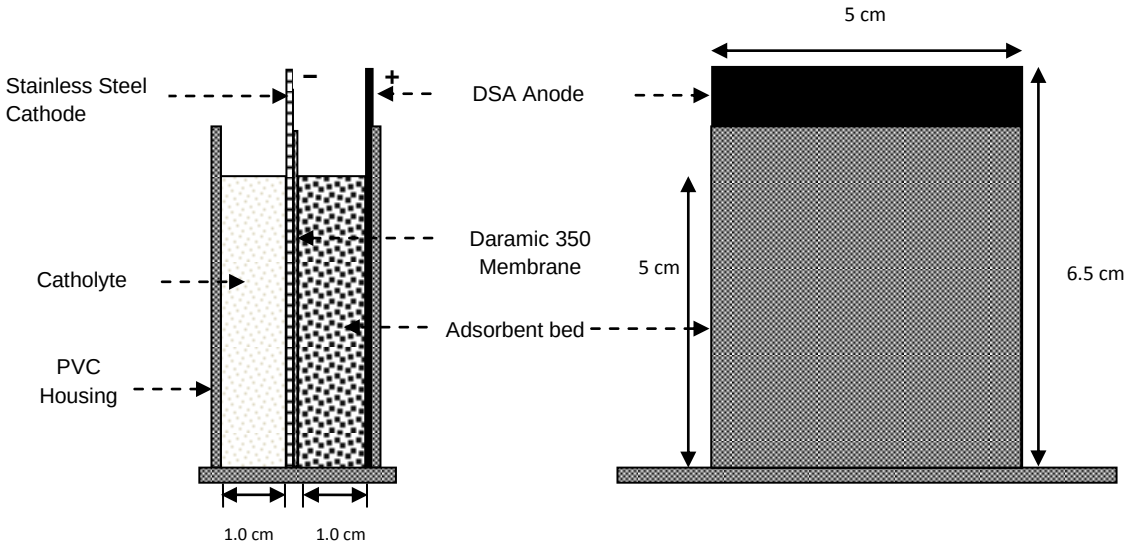

(a) Front View (b) Side View

Figure 4.2: *Schematic diagram of a batch electrochemical cell used for regeneration showing front and side views.*

(a) Initial Adsorption

A specified quantity of adsorbent (Nyex®1000) was added to 100 mL of 100 mg L^{-1} phenol solution in a 250 mL volumetric flask and mixed for 30 minutes (a time necessary to achieve equilibrium; *Brown and Roberts, 2007*) on a UNIMAX 1010 shaker (Heidolph, UK) at 400 rpm. After adsorption the contents of the flask were vacuum filtered using a VWR–413 grade filter paper and the concentration of phenol in the filtrate was determined (See section 4.1.3 for the analytical method).

(b) Electrochemical Regeneration

The phenol loaded filtered adsorbent was pressed into the anode compartment of the cell to make an adsorbent bed 10 mm thick. No electrolyte was added to the anode compartment because of the associated cost and the contamination of the treated water. On the other hand, it was not necessary to add electrolyte to the anode compartment because of the high electrical conductivity of the GIC adsorbent. A bed of GIC particles has an electrical conductivity of 0.32 Ω^{-1} cm^{-1} which is almost 12 times higher than the electrical conductivity of a bed of GAC *(Eccleston, et al. 2010)*. On the cathode side, 0.3% NaCl solution acidified with 5M HCl (to pH, 2±1) was added to the same level as the adsorbent bed on other side of the membrane (as shown in Figure 4.2). The pH of the catholyte was maintained acidic because under alkaline conditions plasticizers are leached out from Daramic 350 membrane making the membrane brittle. The reduction of the water on the cathode produces alkali that necessitates pH adjustment to maintain acid conditions in the cathode compartment in order to avoid membrane deterioration. The power supply was connected to the anode and cathode of the cell and a DC current of 500 mA (current density 20 mA cm^{-2}; optimised by *Brown et al. 2004a*) was applied across the cell for regeneration times in the range of 2–15 minutes. This gave a charge passed in the range of 4–30 C g^{-1} (calculated on the basis of 15 g of the adsorbent) at a current density of 20 mA cm^{-2}. There was no flow in the cell and the only mixing was caused by the gas bubbles generated at the electrodes.

(c) Re-adsorption

After regeneration, the catholyte was gently poured from the cell and all the contents of anode compartment, without any additional treatment, were transferred to a 250 mL flask containing a fresh 100 mL batch of 100 mg L^{-1} phenol solution. Re–adsorption was carried out under identical conditions to the initial adsorption stage.

(d) Sample collection for analysis

After re–adsorption, the flasks contents were vacuum filtered, and the filtrate was analysed to determine its phenol content and break down products using HPLC as described in section 4.1.3. Initially, these samples were run on a GC/MS to identify

the nature of the breakdown products as explained in section 4.1.3. The steps (b), (c) and (d) were repeated for adsorption and electrochemical regeneration over a number of cycles for regeneration times in the range of 2–15 minutes.

Adsorption Studies

(a) Kinetics of adsorption

A kinetic study of phenol adsorption onto GIC was carried out to determine the time required to achieve equilibrium at different initial concentrations. It was conducted by mixing 100 g of adsorbent with 1 L phenol solution of initial concentrations of 30 and 100 mg L^{-1} in a 1 L volumetric flask on a magnetic stirrer (Gallenkamp) at a speed of 700 rpm. Samples (10 mL) were taken every 5 min for the first 30 min and subsequently every 10 and 20 min, and the experimental duration was up to 2 hours. These samples were filtered through a 0.45 μm syringe filter (Phenomenex Ltd) and analysed for phenol concentration (using the method described in section 4.1.3).

(b) Adsorption isotherms

Adsorption isotherms were determined for phenol and its intermediate oxidation products by mixing a range of known concentrations of 100 mL of adsorbate solution with 20 g of adsorbent in 250 mL volumetric flasks. Mixing was carried out using a magnetic stirrer (ER LAUDA, Germany) at 700 min^{-1} for 30 min at room temperature. This was observed to be the time required to attain equilibrium during the kinetic study of phenol adsorption. The same equilibrium time (30 min) was assumed to be applicable for the study of the adsorption isotherms of the breakdown products. Initial and final samples were taken during each experiment and these were analysed as specified in section 4.1.3. The adsorbent loading, q (mg g^{-1}), was determined from the initial and final concentrations as:

$$q = \frac{(C_i - C_f)}{m} V \tag{4.1}$$

where C_i and C_f are the initial and final concentrations (mg L^{-1}) of adsorbate, V is the volume (L) of solution and m is the mass (g) of adsorbent used.

(c) Competitive adsorption

Competitive adsorption of phenol with its aromatic breakdown products was investigated by mixing a range of known masses of adsorbent with 100 mL of a mixed solution containing known concentrations of phenol, benzoquinone, hydroquinone and catechol using a magnetic stirrer (ER LAUDA, Germany) at 700 min^{-1} for 30 min at room temperature. In another experiment, the competitive adsorption of phenol with benzoquinone only was determined by the same procedure. Initial and final (after adsorption) samples were filtered through a 0.45 μm syringe filter and analysed as specified in section 4.1.3.

Electrochemical regeneration studies using the mini-sequential batch reactor

The mini-sequential batch reactor (SBR) is a Y–shaped electrochemical cell (Figure 4.3) designed by Arvia® Technology Ltd with a number of improved features over the simple batch electrochemical cell namely:

- Both adsorption and electrochemical regeneration are carried out in the same unit
- Mixing of the adsorbent with solution during adsorption is achieved by sparging air in a similar manner to the continuous process of adsorption and electrochemical regeneration (Figure 1.2)
- The separation of solid particles from the liquid is achieved by gravity sedimentation rather than filtration, so that loss of the adsorbent is minimized

The mini-SBR was constructed with identical materials of construction to the batch electrochemical cell. However, the anode current feeder was a graphite plate 5 mm thick. The cathode was constructed from perforated 316 stainless steel material with a thickness of 1 mm and 3 mm diameter perforations. The area of each electrode was 50 cm^2. The electrode compartments were separated by a microporous Daramic 350 membrane. During adsorption, air was supplied from an air compressor (Airmaster Tiger 8/25 Turbo) through an array of orifices at the base of the cell to bring about the mixing of the adsorbent with the water. The flow rate of air was maintained at 10–12 L min^{-1} (measured using a rotameter). A mini-SBR with increased electrode area of 70 cm^2 was also used for these experiments.

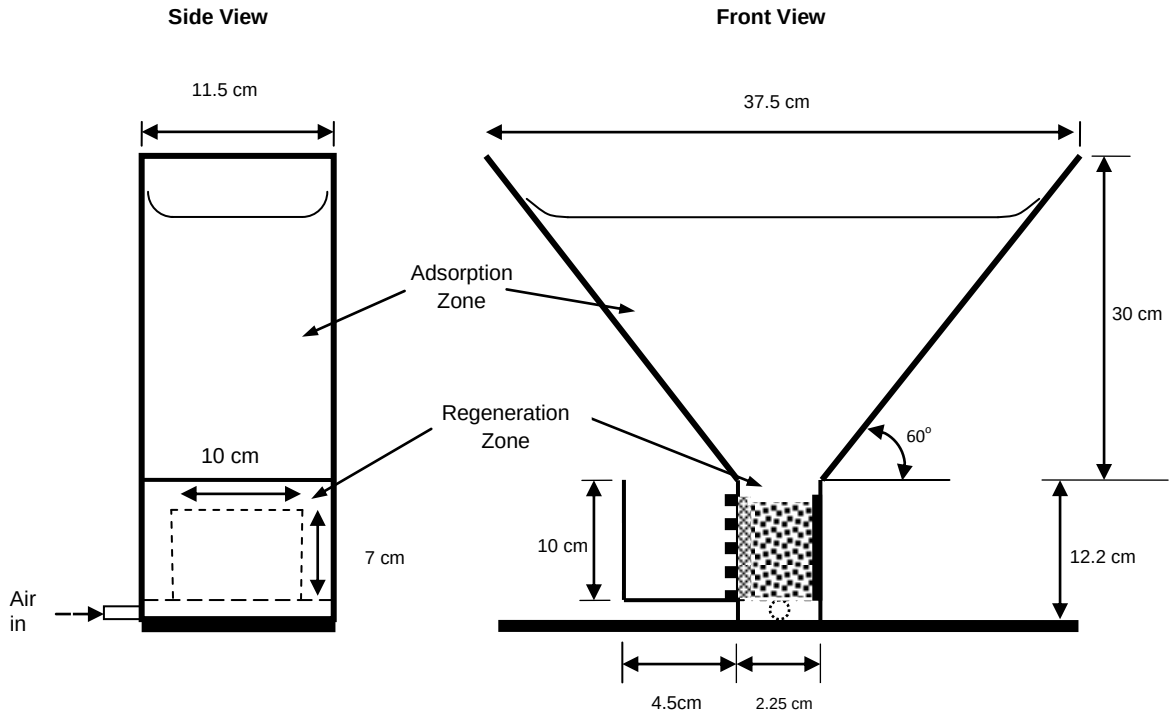

(a)

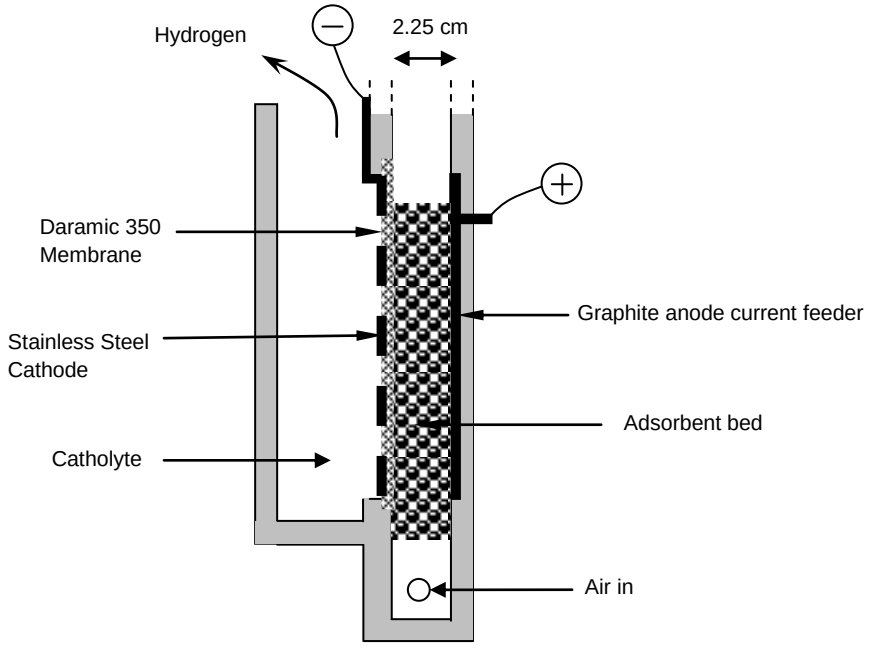

(b)

Figure 4.3: *Schematic diagram of the mini-sequential batch reactor (SBR) used for adsorption and electrochemical regeneration studies. (a) Schematic diagram showing side and front views of the mini-SBR, and (b) Schematic diagram showing a cross section of the electrochemical regeneration zone*

(a) Batch adsorption and electrochemical regeneration

For batch adsorption and electrochemical regeneration, a known mass of adsorbent was added to a measured volume of phenol solution of known concentration in the mini-SBR and mixed for 30 minutes using air. After the completion of adsorption, the air supply was turned off and the adsorbent particles were allowed to settle for 2 min. The adsorbent settled into the anode compartment of the electrochemical cell at the base of the mini-SBR to form a uniform bed of particles as shown in Figure 4.3. Following settling of the adsorbent in the mini-SBR, a sample of the supernatant water was collected and analysed as described in section 4.1.3. No additional electrolyte was used in the anode compartment. However, on the cathode side, 400 mL of 0.3% NaCl solution (w/v) acidified with 5 M HCl (to pH, 2±1) (unless otherwise stated) was added as an electrolyte so that the catholyte was at the same level as the bed of settled adsorbent. After connecting the power supply to the anode and cathode of the electrochemical cell, a specified DC current was supplied for a fixed regeneration time so that the electrochemical regeneration of the adsorbent could take place. Current densities in the range of 10–40 mA cm^{-2} were used corresponding to an applied current of 0.5–2.0 A. The applied current was held constant for the duration of the regeneration time and the voltage across the electrochemical cell was monitored. During electrochemical regeneration, the only mixing occurring was due to the gas bubbles generated at the electrodes. After the completion of regeneration, the current was turned off and a sample of water was again taken from the supernatant liquid for analysis (using the method described in section 4.1.3). Subsequently, the solution present above the regenerated bed and the catholyte were siphoned off separately. Care was taken to minimise the removal of adsorbent during siphoning, and any adsorbent removed was allowed to settle and returned to the cell. A measured volume of phenol solution of known concentration was added to the mini-SBR and re–adsorption was carried out under identical conditions to the initial adsorption stage. For adsorption and electrochemical regeneration over a number of cycles, the adsorption and regeneration procedure was repeated several times. The pH of the treated solution was also monitored during adsorption and regeneration cycles using a Cyber Scan pH 1500 meter (Eutech Instruments, Singapore).

The effect of various parameters including pH, additional electrolyte and recycling of treated solution on the adsorption and electrochemical regeneration of GIC adsorbent, and electrochemical oxidation of phenol without adsorbent was investigated in the mini-SBR as follows:

Effect of electrolyte type in anode compartment

The effect of additional electrolyte on adsorption and electrochemical regeneration was investigated by preparing phenol solution in water containing a specified concentration of electrolytes such as sodium chloride or sodium sulphate. In all other respects the procedure was as described above for batch adsorption and electrochemical regeneration. The effect of the nature of the catholyte on the adsorption and electrochemical regeneration has been discussed in section 4.2.3

Effect of pH

During electrochemical regeneration of the GIC adsorbent, acidic conditions prevailed due to the generation of acid at the anode and diffusion of acid through the membrane from the cathode of the electrochemical cell. Thus, the effect of neutral and alkaline pH on the formation of the breakdown products during adsorption and electrochemical regeneration was also investigated. In this context, phenol solutions of known concentrations were prepared using phosphate buffers to maintain a pH of 7 and 9 throughout the course of the experiments. In all other respects, the procedure was as described above for batch adsorption and electrochemical regeneration.

Effect of recycling of treated solution

Normally, the solution in the mini-SBR after each cycle of regeneration was replaced with a fresh phenol solution of same volume and concentration for the next adsorption cycle. The behaviour when the same solution of phenol was treated over several cycles was investigated by not siphoning off the treated solution at the end of each regeneration. By this method a number of adsorption and regeneration cycles were carried out as described above.

Electrochemical oxidation of phenol without adsorbent

In order to compare the behaviour of electrochemical oxidation of phenol in the mini-SBR without adsorbent under differential experimental conditions, a measured volume of known concentration of phenol solution containing a specified amount of a particular electrolyte (NaCl or Na_2SO_4) was transferred into the mini-SBR. Samples of solution were taken at regular intervals during electrochemical treatment, but in all other respects the electrochemical regeneration procedure described above.

4.1.3 Analysis

Phenol and its oxidation products were analysed using high performance liquid chromatography (HPLC, Varian Prostar). This was carried out by comparing the retention times of the standard compounds of phenol and its oxidation products. All aqueous samples were filtered through a 0.45 μm filter (Phenomenex Ltd) prior to their injection into the respective column.

Separation of the aromatic compounds such as phenol, 1,4-benzoquinone, hydroquinone and catechol was performed using a C18 column (Phenomenex, Macclesfield, UK). The mobile phase was 50% methanol (HPLC grade) in ultrapure water at a flow rate of 0.75 mL min^{-1} through the column. The oven temperature was maintained at 25°C. A UV detector was used at wavelengths of 210 and 254 nm *(Wu et al. 2001).*

Separation of the organic acids such as fumaric, maleic and oxalic acid was carried out using a Hi–Plex–H column *(Canizares et al. 2004).* The mobile phase was 0.1 % trifluoroacetic acid in ultrapure water at a flow rate of 0.6 mL min^{-1} and the oven temperature was maintained at 60°C. UV detection was carried out at 210 nm.

A GC/MS was used to identify the compounds present, with a HP–5MS column with a stationary phase of 5% phenyl–95% methyl polysiloxane, supplied by Agilent Technologies. Compounds such as 1,4-benzoquinone, hydroquinone and catechol were identified by a library match, provided by Agilent and also confirmed by running standard samples of these compounds. All aqueous samples were filtered using 0.45 μm filter (Phenomenex, Ltd) prior to their injection in GC/MS.

Total organic carbon (TOC) of samples was determined using a TOC analyzer, $V_{CSH/CSN}$, made by Shimadzu Corporation. This system determines total organic carbon by removing the inorganic carbon (IC) and then measuring the total carbon (TC) of the sample to obtain the TOC directly. The total organic carbon corresponds to the carbon which is chemically bonded to hydrogen and oxygen to form organic compounds. The inorganic carbon corresponds to gaseous carbonates and carbonate ions. The acidified sample (to pH 2–3) is sparged with air to convert the IC in the sample to carbon dioxide. The carbon dioxide was then detected by the infrared analyser. The remaining carbon measured to determine total organic carbon directly. For this, a sample was introduced into the TC combustion tube, which filled with an oxidation catalyst and heated to 953 K. The sample burned in the combustion tube and, as a result, the TC components in the sample were converted to CO_2. Carrier gas flows to the combustion tube and carries the sample combustion products from the combustion tube to an electronic dehumidifier, where the gas cooled and dehydrated. The gas then carried the combustion products through a halogen scrubber to remove chlorine and other halogens. Finally, the carrier gas delivered the combustion products to the cell of an infrared gas analyser, where the CO_2 was detected. The peak area is proportional to the TC concentration of the sample.

4.1.4 Results and Discussion

(a) Preliminary investigation of the formation of breakdown products in the batch electrochemical cell

In continuation of the preliminary investigation about the formation of the breakdown products by *Brown and Roberts, (2007)*, electrochemical regeneration of phenol loaded adsorbent (Nyex®1000) was performed in the batch electrochemical cell (Figure 4.2) at different regeneration times, according to the procedure explained in section 4.1.2. Analysis of aqueous samples taken during the electrochemical regeneration at different charge passed per gram (4–30 C g^{-1}) using GC/MS, showed that the main aromatic break down product was 1,4-benzoquinone (See appendix A). However, hydroquinone and catechol were also detected using HPLC. The concentrations of these compounds were quantified using HPLC as described in section 4.1.3. The aliphatic intermediate oxidation products including oxalic and

maleic acids were identified and quantified by HPLC as described in section 4.1.3. These aliphatic compounds were present in relatively low concentrations (Figure 4.4). Among the aromatic intermediates, the concentration of hydroquinone formed was lower compared to the concentrations of catechol and benzoquinone in all the cases (the maximum concentration of hydroquinone was less than 2 mg L^{-1}) (Figure 4.4). Previous studies have indicated that hydroquinone is the first product formed by the electrochemical oxidation of phenol and that it can be further oxidized rapidly by the transfer of two electrons *(Tahar & Savall, 1998).*

Although a fresh batch of phenol solution is used on each cycle, the concentrations of benzoquinone and catechol were observed to decrease with each regeneration cycle whereas the concentration of hydroquinone remained relatively constant as shown in Figure 4.4. These observations suggest that small concentrations of benzoquinone and catechol were adsorbing onto GIC adsorbent during the subsequent adsorption cycles. However, the adsorptive capacities of these aromatic intermediates at low concentrations are relatively low compared to the adsorptive capacity of phenol at 100 mg L^{-1} (see adsorption studies). Thus phenol would be preferentially adsorbed during adsorption cycles leaving behind small concentrations of intermediates in the solution. On the other hand, the surface renewal of Nyex®1000 during the electrochemical regeneration appeared to induce additional adsorptive capacity possibly leading to increased adsorption of these species. The concentration of benzoquinone and catechol were slightly higher for the longer regeneration times as shown in Figure 4.4. Although the concentration of these intermediates is relatively small compared to the initial concentration of phenol to be treated, they are significant when compared with the phenol which was concentrated onto the surface of Nyex®1000 after adsorption.

Brown & Roberts (2007) studied the batch electrochemical regeneration of Nyex®100 loaded with phenol (1 mg g^{-1}) using a regeneration time of 2 min. The only difference in the experimental conditions was the use of a different adsorbent: Nyex®100 in place of Nyex®1000. Nyex®100 is similar to Nyex®1000 but with a smaller particle size (ca. 130μm) and a greater specific surface area (2.75 m^2 g^{-1}). Their results also revealed that the principle break down products were

hydroquinone, benzoquinone, maleic and oxalic acids in very low concentrations. However, no catechol was detected in their experiment. According to the authors the break down products might have been adsorbed onto the surface of Nyex® or phenol has been fully mineralized and therefore few breakdown products were released into solution after regeneration. Although Nyex®100 has a slightly higher adsorptive capacity than that of Nyex®1000, in order to achieve effective solid/liquid separation by sedimentation; Nyex®100 was replaced by Nyex®1000 due to its better settling characteristics. During the electrochemical regeneration of Nyex®1000, the breakdown products were observed even when the charge was sufficient to attain ca. 100% regeneration of the adsorbent (corresponding to a regeneration time of 15 min) (Figure 4.4). There was observed to be an increase in regeneration efficiency with an increase in the regeneration time as shown in figure 4.5. The actual charge passed for 100% adsorbent regeneration was about 520% of the theoretical charge required for complete phenol oxidation and thus the current efficiency (based on mineralisation of phenol) was about 20%. In addition, the results suggested that increased amounts of the breakdown products were observed with an increase of charge passed per gram of Nyex®1000 (Figure 4.4). The observed intermediates are consistent with the most likely reaction route for the electrochemical oxidation of phenol given by *Canizares, et al. (2004)* as:

$$PhOH \rightarrow HQ \Leftrightarrow BQ \rightarrow C_4 acid \rightarrow C_2 acid \rightarrow CO_2 \qquad (4.2)$$

The breakdown products observed may also be present on the adsorbent surface, and in order to provide further information on the processes occurring the adsorption characteristics of phenol and these compounds has been studied and is discussed in the following section.

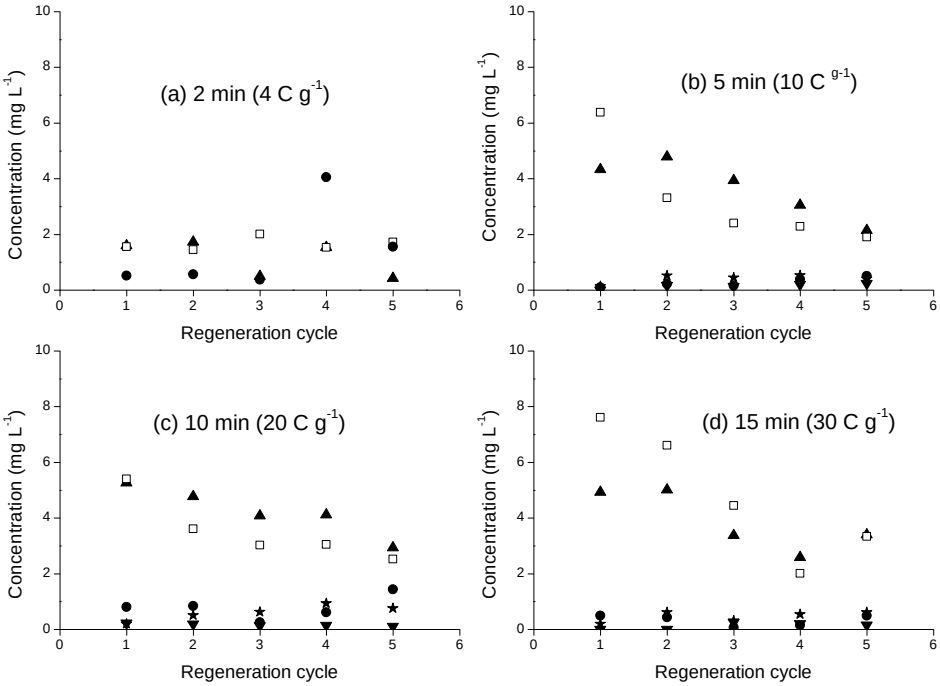

Figure 4.4: *Electrochemical breakdown products of phenol in the filtrate after a series of adsorption/regeneration cycles at a current of 0.5 A (current density: 10 mA cm^{-2}) with a regeneration time of 2–15 min (charge passed 4–30 C g^{-1}). Nyex® dose: 15 g (100 mL)$^{-1}$; Phenol: 100 mg L^{-1} (▲) Benzoquinone; (□) Catechol; (●) Hydroquinone; (▼) Oxalic acid; (★) Maleic acid*

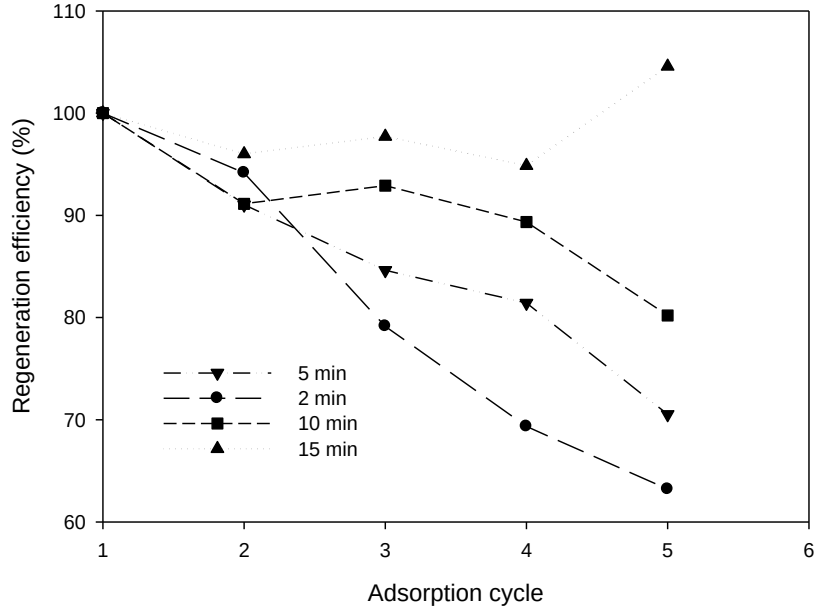

Figure 4.5: *Effect of number of adsorption/regeneration cycles of phenol loaded adsorbent (Nyex®1000) on percent regeneration efficiency for a range of regeneration times (2–15 min) and charge passed (4–30 C g^{-1}). Cycle 1 was for fresh Nyex®1000. Regeneration efficiency was calculated using equation 3.26*

Adsorption Studies

(i) Adsorption kinetics

The adsorption of phenol onto GIC adsorbent was studied at different initial concentrations as a function of contact time in order to determine the equilibrium time. Adsorption of phenol onto Nyex®1000 was observed to be a fast process with 75% and 57% of the equilibrium concentration achieved within 10 min for 30 and 100 mg L^{-1} phenol, respectively (Figure 4.6). Thus, the curves in figure 4.6 fall sharply in the initial stages, indicating that there are sufficient accessible sites on the adsorbent. Ultimately, a plateau was reached in both the curves which showed that the solution and adsorbent are in equilibrium. However, after 30 min a gradual and slight decrease in the solution concentration could be due to the formation of some fines of Nyex®1000 by attrition. The time required to achieve equilibrium was therefore assumed to be 30 minutes for 30 and 100 mg L^{-1} phenol concentrations. The initial concentrations of phenol used in this study did not appear to have a significant effect on equilibrium time. However, an increase in phenol concentration resulted in an increase in phenol uptake due to the greater mass transfer driving effect which permits more phenol to pass from the bulk phase boundary to the GIC surface. The adsorption capacity at equilibrium increased from 6 mg to 15.5 mg, per 100 g, with an increase in initial phenol concentration from 30 to 100 mg L^{-1}. These results are consistent with those obtained by *Brown and Roberts (2007)* for the adsorption of phenol onto Nyex®100. They achieved 90% of the equilibrium adsorption capacity within 4 min using an initial phenol concentration of 250 mg L^{-1}. The complete equilibrium was achieved after approximately 30 min. The high rate of adsorption for these adsorbents can be explained by the non-porous nature of the GIC. The surface area available for adsorption is very low (1 $m^2 g^{-1}$) compared to porous adsorbents, for example activated carbons (500−1500 $m^2 g^{-1}$) *(Noyes, 1991).* Thus, most of the adsorption takes place on the external surface area of GIC due to the absence of internal pores. In contrast, phenol adsorption onto activated carbons requires much longer adsorption times to achieve equilibrium *(Narbaitz and Cen, 1994; Hameed and Rehman, 2008)*. For adsorption on activated carbons, the adsorbate must diffuse into the porous structure of activated carbons leading to a requirement for longer contact times and intra-particle diffusion is often the rate

limiting step. Due to the absence of internal pores in GIC adsorbents, the rate of adsorption only depends upon the diffusion across the liquid film surrounding the adsorbent particles to the exterior of the adsorbent, and the rate of adsorption of the adsorbate at active sites on the adsorbent. Since sufficient turbulence was provided in the mini-SBR, the adsorption process at the active sites on the adsorbent may be considered to be the rate limiting step for adsorption on GIC adsorbents.

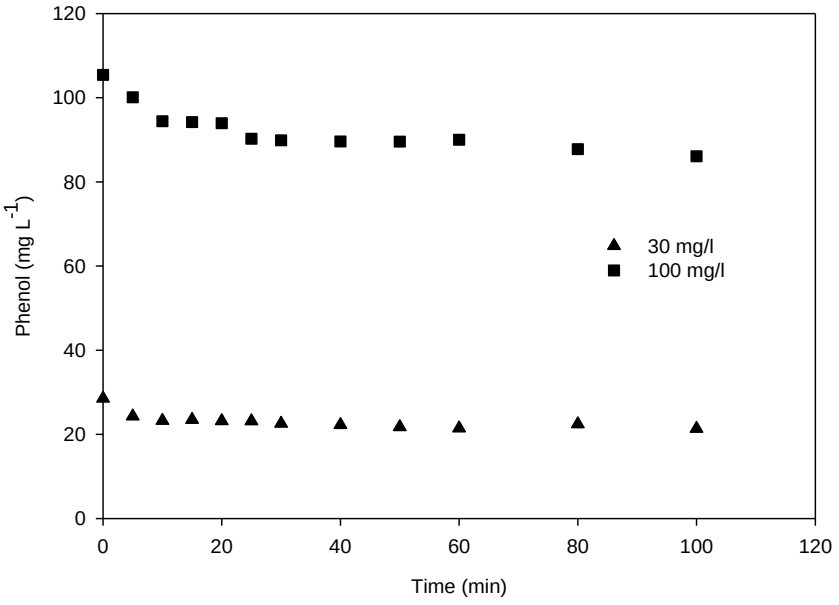

Figure 4.6: *Adsorption kinetics of phenol onto Nyex®1000 in the mini-SBR using 100 g of Nyex®1000 and 1 L phenol solution with initial concentrations of about 30 and 100 mg L^{-1}*

(ii) Adsorption isotherms

The objective of developing adsorption isotherms for phenol and its possible breakdown products was to evaluate the adsorptive capacities of these species onto GIC adsorbent. The results reveal that two different types of adsorption isotherms were observed for aromatic compounds and carboxylic acids (Figure 4.7–4.8). The adsorption of phenol and its aromatic intermediates (benzoquinone, hydroquinone and catechol) were described by the L–shaped (type I) isotherms (See chapter 2). These isotherms increased sharply at low concentrations due to the availability of readily accessible sites at the beginning of adsorption under these conditions. At high

concentrations, the GIC adsorbent became saturated and thus a plateau was reached indicating that no more sites were available for adsorption. The adsorptive capacities of phenol, hydroquinone, benzoquinone and catechol onto GIC adsorbent closely match each other (Figure 4.7). In contrast, isotherms for carboxylic acids can be illustrated with the S–shaped (type III) curves (See chapter 2) and thus shows that adsorption of these compounds on GIC only takes place at high concentration. It also indicates that the GIC adsorbent has higher affinity for the water than for the carboxylic acids at low concentrations. This explains why the carboxylic acids barely adsorbed at concentrations below 30 mg L^{-1} (Figure 4.8). *Canizares et al. (2004)* found similar results for the adsorption of phenol and its oxidation products on granular activated carbon. According to them, a typical type I adsorption isotherm was observed for the aromatic compounds (phenol and hydroquinone) and type III adsorption isotherm was found for the carboxylic acids (maleic and oxalic acids).

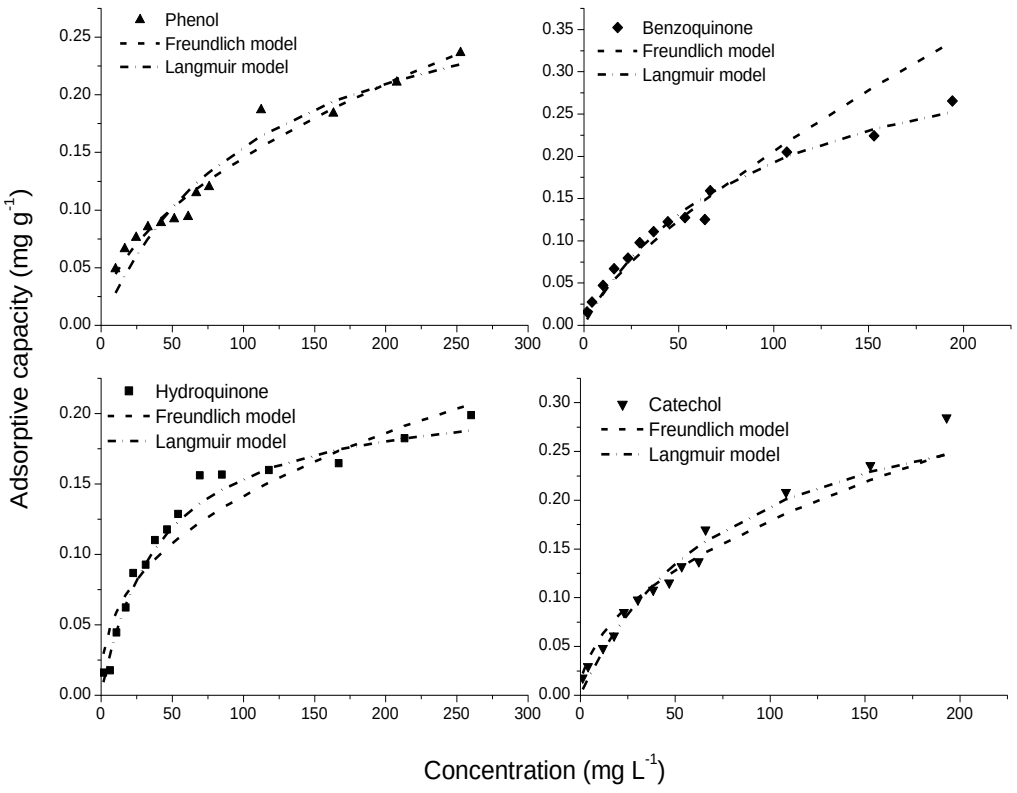

Figure 4.7: *Adsorption isotherms of phenol and its aromatic intermediate products onto Nyex®1000 in a 250 mL volumetric flask using 20 g of Nyex®1000 mixed with 100 mL of solution of various initial concentrations*

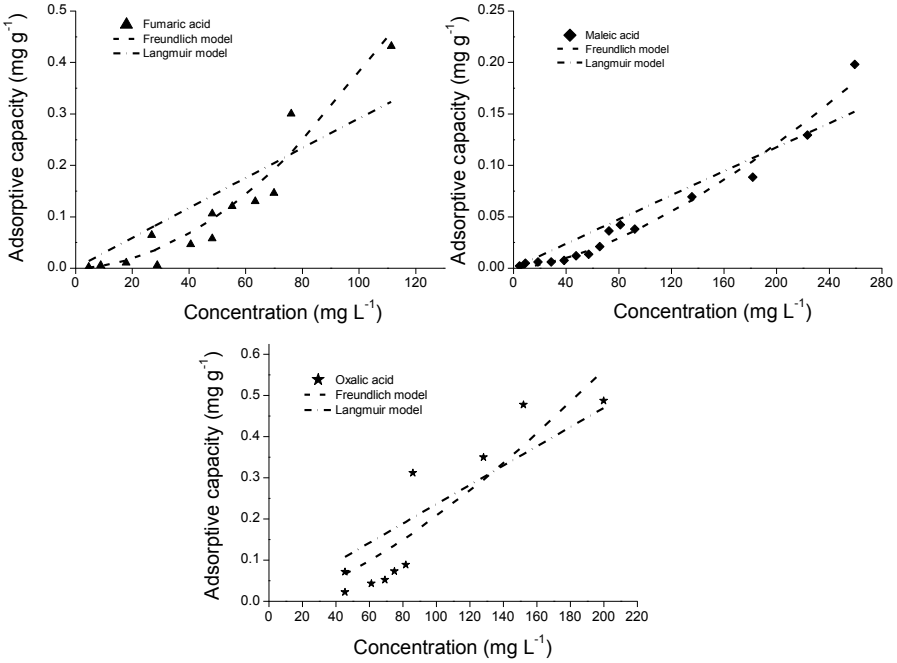

Figure 4.8: *Adsorption isotherms of aliphatic carboxylic acids onto Nyex®1000 in a 250 mL volumetric flask using 20 g of Nyex®1000 mixed with 100 mL of solution of various initial concentrations*

The Freundlich and Langmuir isotherm models were fitted to the experimental data using the Solver function in Microsoft® Excel 2007 by varying the parameters of these isotherms to reach a minimum value of the sum of the errors squared or a maximum value of the correlation coefficient (R^2) between the data (C_e and q_e) and each adsorption model.

The results in table 4.1 show that both models give fairly good fits to the experimental data according to the values of correlation coefficient (R^2) with a few exceptions. The Langmuir equation yields a better fit for benzoquinone, hydroquinone and catechol indicating monolayer adsorption. Phenol data fitted well to both the adsorption models. It can also be seen that the values of ($1/n_F$) are less than unity for phenol and aromatic intermediates and thus the curves are characterized by a concave Freundlich isotherm, indicating that significant adsorption takes place at low concentrations. However, the increase in the amount

adsorbed with concentration becomes less significant at higher concentrations. On the other hand, K_F can serve as a measure of the relative adsorptive capacities of different compounds on GIC adsorbent. Based on this, although benzoquinone was observed to have the same shape of adsorption isotherm, the values of K_F suggest that the adsorptive capacity of benzoquinone is lower than that of phenol, hydroquinone and catechol.

Considering the small surface area of GIC adsorbent (1 m^2 g^{-1}), the Langmuir monolayer converge of maleic, fumaric and oxalic acids are much above the actual adsorption capacities (Table 4.1). Thus, these carboxylic acids are not well described by the Langmuir isotherms, as shown from the values of R^2 in table 4.1. The maleic and fumaric acid fit better to the Freundlich isotherm. However, oxalic acid does not even show a good fit to the Freundlich equation, as can be seen from the value of R^2.

Table 4.1: *Freundlich and Langmuir parameters for the adsorption of phenol and its breakdown products on GIC adsorbent*

	Freundlich model			***Langmuir model***		
Compound	**$K_F \times 10^4$ [$mg \cdot g^{-1}(L \cdot mg^{-1})^{1/n_F}$]**	**$1/n_F$**	**(R^2)**	**q_m ($mg \cdot g^{-1}$)**	**$K_a \times 10^4$ ($L \cdot mg^{-1}$)**	**(R^2)**
Phenol	131	0.522	0.993	0.324	91.20	0.988
Benzoquinone	70	0.734	0.86	0.371	109	0.976
Hydroquinone	229.5	0.395	0.914	0.218	238.4	0.977
Catechol	187.6	0.490	0.923	0.35	124.7	0.958
Maleic acid	0.32	1.555	0.975	17.43	0.34	0.902
Fumaric acid	0.508	1.923	0.933	72	1.08	0.752
Oxalic acid	2.6	1.450	0.816	26	0.33	0.741

(iii) Catalytic behaviour of GIC adsorbent

During the adsorption studies of hydroquinone, some formation of benzoquinone was also observed for each concentration of hydroquinone (Figure 4.9). It is most likely that the Nyex®1000 particles, which are basically graphite particles with hydrogen sulphate intercalation, might have catalysed the aromatic oxidation in

aqueous conditions. In order to confirm the catalytic behaviour of GIC particles, an experiment was performed in such a way that 100 mL of 200 mg L^{-1} hydroquinone solution in water was stirred for 30 min with (20 g) and without Nyex®1000 particles in two separate volumetric flasks. Afterwards, the samples from both the flasks were analysed for hydroquinone and any other oxidation product. For the flask which was simply agitated without adding Nyex®1000, the initial and final samples were exactly the same and there was not observed to be any formation of other species. For the latter case, 14 mg L^{-1} of benzoquinone was also detected in solution after the adsorption of hydroquinone onto Nyex®1000. This demonstrated clearly that graphite particles catalysed the oxidation of hydroquinone to benzoquinone. The rate of oxidation of hydroquinone in terms of the rate of formation of benzoquinone appears to increase with the concentration of hydroquinone (Figure 4.9). It is also important to mention here that the experimental solutions used were not deoxygenated. Under these circumstances, graphite might have catalysed oxygen reduction coupled to oxidation. However, this needs further investigation.

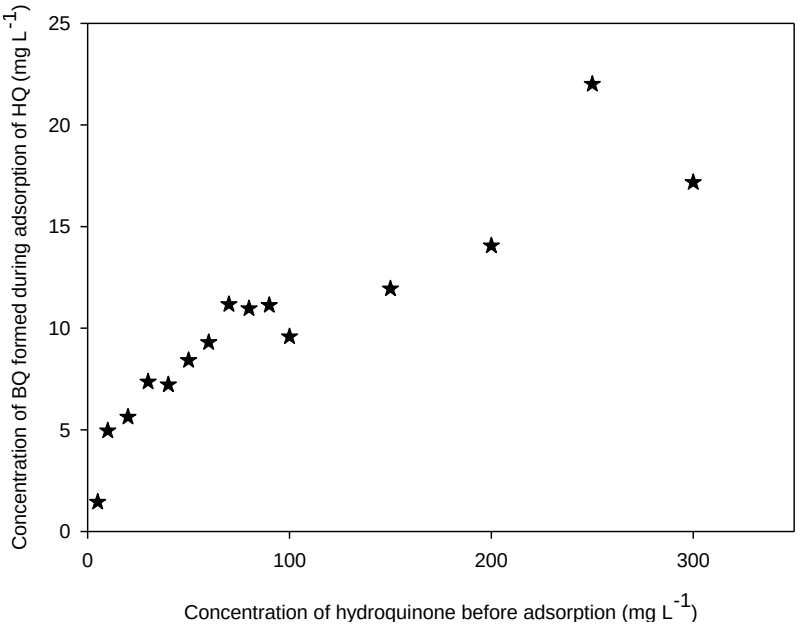

Figure 4.9: *Formation of benzoquinone (BQ) during adsorption of hydroquinone (HQ) on GIC adsorbent at different initial concentrations of HQ*

Keeping in view the fact that some of the hydroquinone has been oxidised rather than adsorbed due to the formation of benzoquinone, the actual loading of hydroquinone on the GIC adsorbent will be lower than that calculated from the concentration of hydroquinone. Thus, the adsorption isotherm of hydroquinone has been corrected by adjusting the value of *q* to account for the oxidation of hydroquinone to benzoquinone (Figure 4.10). This assumes that the adsorption of hydroquinone was not significantly affected by the presence of the benzoquninone.

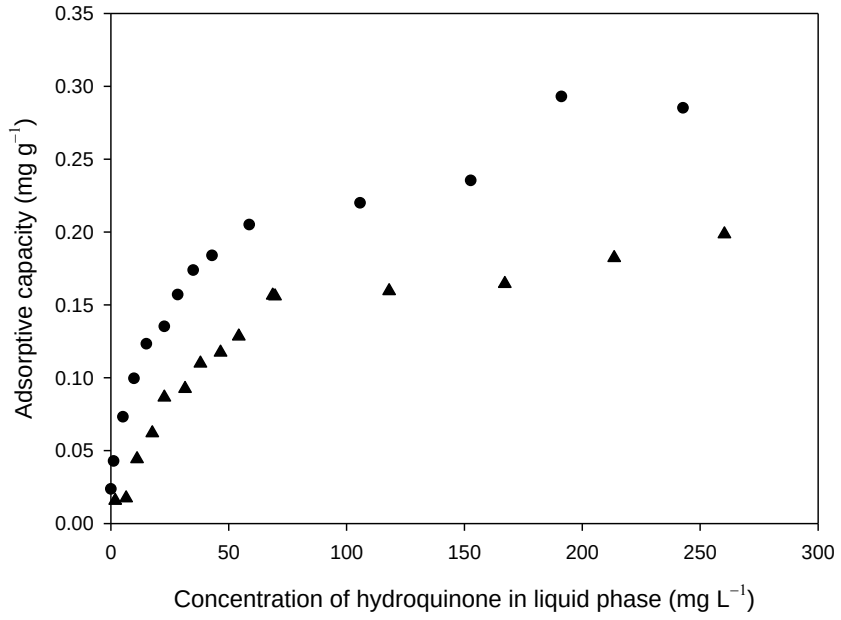

Figure 4.10: *Adsorption isotherms of hydroquinone with (▲) and (•) without corrected concentration of hydroquinone in solution after adsorption on GIC adsorbent due to the formation of benzoquinone*

It could not be stated here with confidence that the graphite is actually playing an important role in this oxidative reaction as a catalyst because in the graphite bisulphate intercalation compound (Nyex®1000) the chemical behaviour of molecules (intercalant) could also contribute to the oxidation reaction. *Bertin et al. (1974)* studied esterification reactions in the presence of graphite bisulphate and they explained that the esterifying capacity of graphite bisulphate could be estimated as 5.5×10^{-2} mole of acid and alcohol per gram. According to them, the graphite bisulphate served the purpose of an acid catalyst. This is an area where further investigation is required. The catalytic behaviour of GIC particles could also be

somehow related with the wet air oxidation of aqueous phenol catalysed by active carbon observed in a trickle bed reactor at mild conditions of temperature (140°C) and pressure (4.7 Mpa) *by Fortuny et al. (1998)*.

(iv) Competitive adsorption (preferential adsorption)

As benzoquinone, hydroquinone and catechol were observed to be the main intermediate products during studies in the batch electrochemical cell, their adsorption behaviour on GIC adsorbent is also important when all of them are present in solution with phenol. Thus, the competitive adsorption of these species with phenol was also investigated. The results revealed that the decrease in concentration of phenol and catechol in solution with an increase of the adsorbent dose was similar up to a dose of 100 g L^{-1} (Figure 4.11, a). At higher doses, the concentration of catechol decreased below that of phenol as shown in figure 4.11 (a). In contrast, the concentration of benzoquinone increased with an increase of adsorbent dose which explained that hydroquinone whose concentration was drastically decreased as it appeared to be converted into benzoquinone (Figure 4.11, a). The GIC particles catalysed the oxidation of hydroquinone into benzoquinone, as explained above. Therefore, in another experiment the competitive adsorption of phenol with benzoquinone only was studied. Both of these compounds appeared to show a similar decrease in concentration with an increase of adsorbent dose (Figure 4.11, b). It can be further concluded from these results that all of these species in their mixture exhibit similar adsorption characteristics on the GIC adsorbent. It has been reported that in the adsorption of phenols on activated carbons, the role of the donor–acceptor mechanism involving carbonyl oxygen groups of the activated carbon acting as an electron donor and the aromatic ring of the phenols as an acceptor is important *(Mattson et al. 1969)*. Based on the similar adsorption behaviour of phenol and its aromatic intermediates, it may be speculated that the adsorption of these compounds on the GIC adsorbent occurs through the donor−acceptor mechanism. This mechanism has been further explained in section 4.2.3.

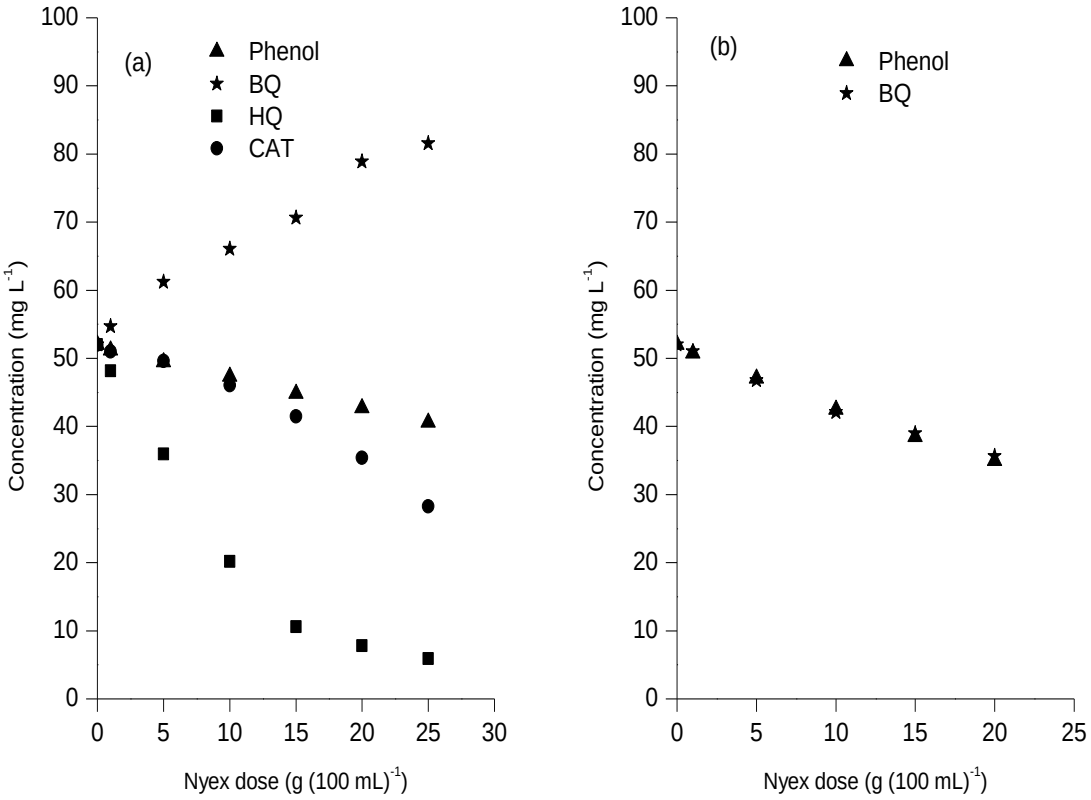

Figure 4.11: *Filtrate phenol and aromatic intermediates concentrations after adsorption on Nyex®1000 with a range of doses; (a): Initial concentration of 52 mg L^{-1} of phenol, benzoquinone (BQ), hydroquinone (HQ) and catechol (CAT); (b) Initial concentration of 52 mg L^{-1} of phenol and benzoquinone*

Adsorption and electrochemical regeneration studies in the mini-SBR

(a) Mechanism of electrochemical regeneration of GIC adsorbents

The preliminary investigation on the formation of breakdown products in the batch electrochemical cell using 100 mg L^{-1} phenol solution at 20 mA cm^{-2} with different amounts of charge passed showed that the principle oxidation products were benzoquinone, hydroquinone and catechol (Figure 4.4). It was speculated that relatively high concentrations (100 mg L^{-1}) of phenol might have led to the formation of breakdown products. *Rajkumar et al. (2005)* observed that during the electrochemical oxidation of phenol the percentage removal of COD decreased by

increasing the phenol concentration for the same amount of charge passed due to the formation of greater amounts of intermediate products. Similarly, *Zhou et al. (2001)* observed that during the electrochemical oxidation of phenol at 7.5 mA cm^{-2} in an undivided electrochemical cell using a PbO_2 anode, the concentration of benzoquinone formed increased by about eight times with an increase in phenol concentration from 100 to 400 mg L^{-1}. The higher the initial concentration of phenol during adsorption on GIC adsorbent, the higher will be the adsorbent loading (see adsorption studies) and thus more quantities of the breakdown products can be formed for the same amount of charge passed. Thus a low concentration of phenol during adsorption and electrochemical regeneration of GIC adsorbent will either result in complete phenol oxidation or will give only small amounts of breakdown products in solution. In other words, the electrochemical regeneration of GIC adsorbent was thought to be concentration dependent as far as the formation of intermediate breakdown products is concerned. Thus, in order to investigate the behaviour of relatively low initial concentrations of phenol, a series of adsorption and electrochemical regeneration were performed with 10 and 20 mg L^{-1} phenol in the mini-SBR. Prior to these experiments for low concentrations, the actual charge required for complete regeneration of phenol loaded GIC adsorbent was determined. In this context, a number of regeneration cycles of the phenol loaded adsorbent were carried out with 20 mg L^{-1} phenol at 10 mA cm^{-2}, and at different regeneration times (10 and 20 min) to give different charge passed. The results indicated that 4.28 C g^{-1} was required for the complete regeneration of phenol loaded GIC (0.05 mg g^{-1}) for which the regeneration time was 20 min at the applied current of 0.5 A (Figure 4.12).

The fractional charge yield was calculated, based on the assumption that phenol was oxidised completely to CO_2 using:

$$\Phi^{e}_{C_6H_5OH} = \frac{28(C_i - C_f)VF}{94It} \tag{4.3}$$

where C_i and C_f are the phenol concentrations before and after adsorption (g L^{-1}), V is the volume (L), F is the Faraday Constant (96,485.34 C mol^{-1}), I is the current (A) and t is the time passed (s).

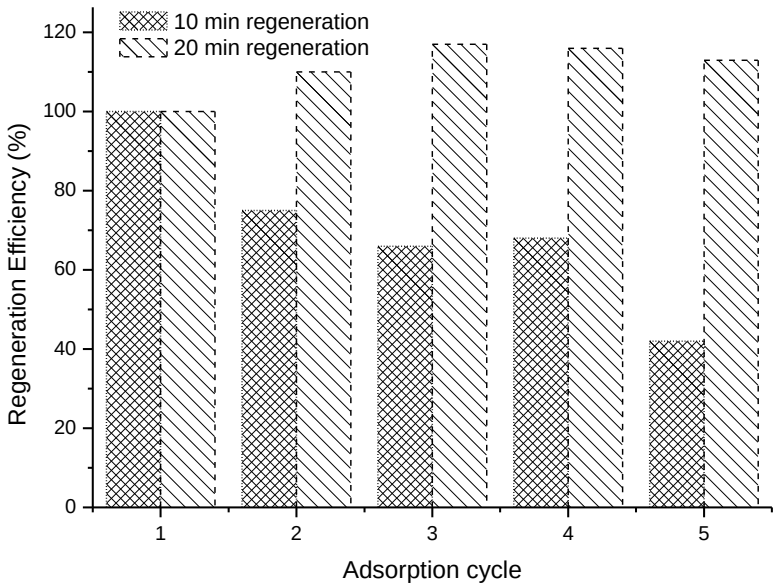

Figure 4.12: *Effect of number of adsorption/regeneration cycles on the regeneration efficiency of phenol loaded Nyex®1000 for regeneration times of 10 and 20 min at 0.5 A.*

The actual charge passed (4.28 C g^{-1}) was about three times the theoretical charge (1.35 C g^{-1}) required for the complete oxidation of adsorbed phenol (0.05 mg g^{-1}), giving a fractional charge yield of 31.5%. The percent regeneration efficiency was above 100 for all the adsorption cycles (Figure 4.12). An increase in the regenerated adsorptive capacity above 100% (in excess of the original adsorptive capacity) could be due to the following possibilities *(Brown et al. 2004b)*:

- The transfer of oxidising species from the regenerated bed to the phenol solution resulting in the removal of phenol by chemical oxidation rather than adsorption.
- The formation of internal pores increasing the surface area available for adsorption.
- Modification of the surface chemistry of GIC adsorbent during electrochemical regeneration.

On the other hand, a drop in percent regeneration efficiency was observed when only 2.14 C g^{-1} (0.5 A was supplied for 10 min) was used to regenerate the loaded adsorbent (0.05 mg g^{-1}) (Figure 4.12). However, the fractional charge yield for these conditions was about 63%. Thus, a series of adsorption and electrochemical regeneration were performed with 10 and 20 mg L^{-1} phenol at a current of 0.5 A (10 mA cm^{-2}) for 20 min. The results revealed that for both concentrations there was the same formation of principle oxidation products including benzoquinone and hydroquinone (Figure 4.13). However, no catechol and carboxylic acids were detected. The concentration of hydroquinone remained below 1 mg L^{-1} during adsorption as well as during regeneration cycles (Figure 4.13). The concentrations of the hydroquninone and benzoquinone shown in figures 4.13 b & d are similar to the concentrations obtained in the small batch cell with a significantly higher (100 mg L^{-1}) initial phenol concentration (see figure 4.4 a). This suggests that the initial concentration of phenol does not significantly affect the formation of these breakdown products during electrochemical regeneration of GIC adsorbent. The formation of benzoquinone and hydroquinone during the first adsorption (before regeneration) could be due to the oxidation of phenol catalysed by GIC particles by air in the mini-SBR (Figure 4.13 a & c).

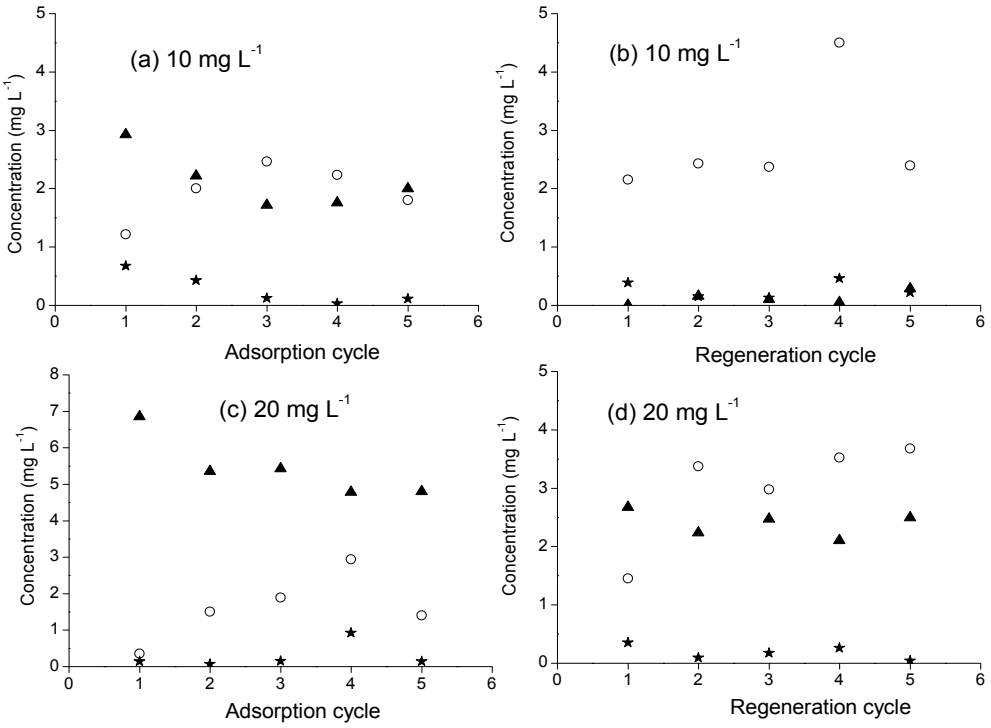

Figure 4.13: *Breakdown products during adsorption and regeneration cycles in the mini-SBR when 500 mL phenol of 10 and 20 mg L^{-1} was mixed with 140 g Nyex®1000 for 30 min. Regeneration was carried out at 0.5 A for 20 min and charge passed was 4.28 C g^{-1}. (▲) Phenol, (○) Benzoquinone,* (★) *Hydroquinone*

It is interesting to observe from figure 4.13 that some phenol which was left in the solution after each adsorption was degraded during its respective regeneration cycle. However, the process of adsorption with electrochemical regeneration (Arvia®) aims to oxidise the adsorbed organics present on the surface of GIC adsorbents. The results suggest that along with the degradation of adsorbed species on the surface of GIC, indirect electrochemical oxidation of organic species which was not adsorbed but was in contact with the surface of GIC particles was also taking place. Thus, the observed breakdown products may have resulted from the electrochemical oxidation of organics present in the liquid bulk rather than due to oxidation of adsorbed species. *Brown and Roberts, (2007)* suggested that during the electrochemical regeneration of GIC adsorbent, the surface of GIC particles may be behaving as a non–active electrode. In the present investigation on the formation of breakdown

products, the results have suggested a new hypothesis of electrochemical regeneration of GIC adsorbent which is based on the following assumptions:

- The adsorbed organics on the surface of GIC particles get completely oxidised either due to the transfer of electrons or by hydroxyl radicals (Figure 4.14). Thus, they are not converted into intermediate oxidation products in solution.

- The electrochemically produced hydroxyl radicals (through direct oxidation) and other oxidants (through indirect oxidation) are responsible for the degradation of organics present in the liquid phase which have not been adsorbed on the surface of the GIC adsorbent (Figure 4.14)

- Due to an insufficient amount of hydroxyl radicals generated in the electrochemical process the formation of some breakdown products could not be avoided.

- Mass transfer limitation is another important factor which could be the actual cause of incomplete oxidation especially when dealing with low concentration of organics.

This suggests that the electrochemical oxidation of organics present in water and in contact with the GIC particles is responsible for the formation of breakdown products.

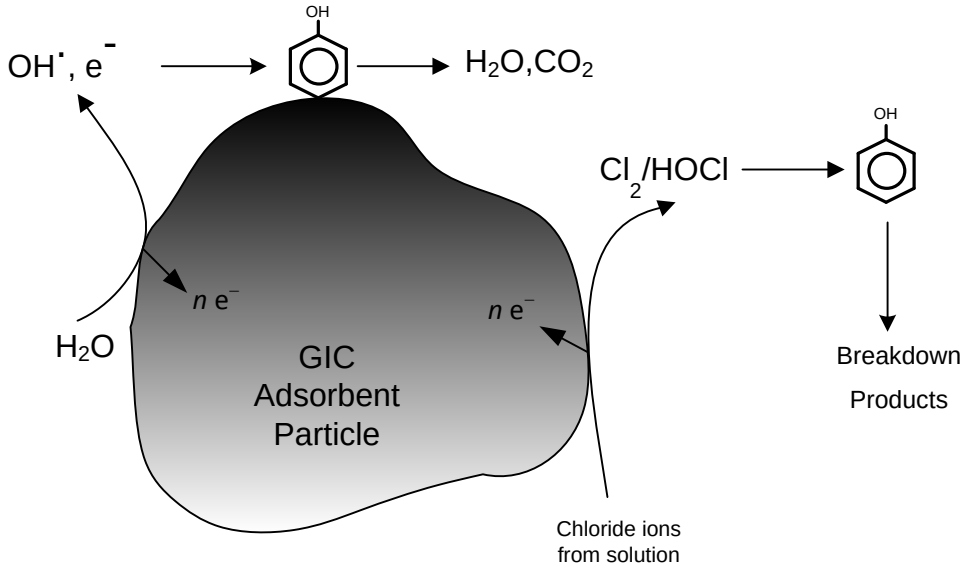

Figure 4.14: *Schematic illustration of the complete degradation of adsorbed phenol and the formation of breakdown products due to indirect oxidation of dissolved phenol*

To provide supporting evidence for this hypothesis, ideally there should not be any phenol present in the bulk of solution in contact with the GIC adsorbent during its electrochemical regeneration. In this situation anything released into solution during regeneration will definitely be coming off the GIC surface. Regardless of the concentration of phenol, some quantity of it will always be in equilibrium with the adsorbent. In an attempt to remove any non–adsorbed species, phenol was adsorbed onto GIC adsorbent in the mini-SBR for 30 min. After adsorption the liquid was completely removed from the cell and was replaced with 500 mL deionised water followed by mixing with GIC particles for five minutes. The cell was then drained and filled again with 500 mL of fresh deionised water. Thus a number of washings of phenol loaded GIC adsorbent were carried out to remove any non–adsorbed phenol in the mini-SBR. Since phenol is weakly adsorbed onto GIC, to minimize the loss of adsorbed phenol from the surface, a batch of phenol loaded GIC was also gently washed with 500 mL deionised water in a volumetric flask for a number of times in a separate experiment. Electrochemical regeneration of phenol loaded GIC adsorbent after the fifth wash from both the experiments was carried out in the mini-SBR for 20 min at a current of 0.5A (10 mA cm^{-2}). The results indicated that the

concentration of phenol in solution decreased with the number of washes in both experiments (Figure 4.15). It could not be neglected here that along with the phenol which was present in the bulk of liquid, some of it might be coming off the GIC surface due to the weak van der Waal's adsorption forces. In the present circumstances, it is difficult to differentiate quantitatively between these two sources of phenol. It appears from figure 4.15 that a comparatively smaller quantity of phenol was removed during gentle washing compared to washing achieved in the mini-SBR. Thus, the quantity of phenol which was still remained on the surface of adsorbent was found 1.3 times more (0.055 mg g^{-1}) with gentle washing compared to its loading (0.042 mg g^{-1}) after washed in the mini-SBR. During electrochemical regeneration of these phenol loaded GIC adsorbents, there was more formation of benzoquinone for the former case (washing in the mini-SBR) even though the loading of phenol was lower, as shown in figure 4.16. In the latter case (washing in a flask), less benzoquinone was formed although the loading of phenol on the adsorbent was 1.3 times of its loading in the former case. In contrast, the concentration of phenol present in solution was greater in the former case. The error in the analysis was estimated to be ±10% for concentrations of <50 mg L^{-1} from the calibration curves of phenol and benzoquinone. These results suggest that the electrochemical oxidation on the surface of GIC adsorbent was not responsible for generating intermediate breakdown products. These findings suggest that the breakdown products were formed due to incomplete electro-oxidation of the organics present in the liquid bulk. As mentioned earlier, it is impossible to remove all the organics from the solution due to equilibrium between the concentration of organic in solution and on the surface of adsorbent. However, high capacity adsorbents might be useful in the further investigation of this phenomenon, which will be the subject of future work.

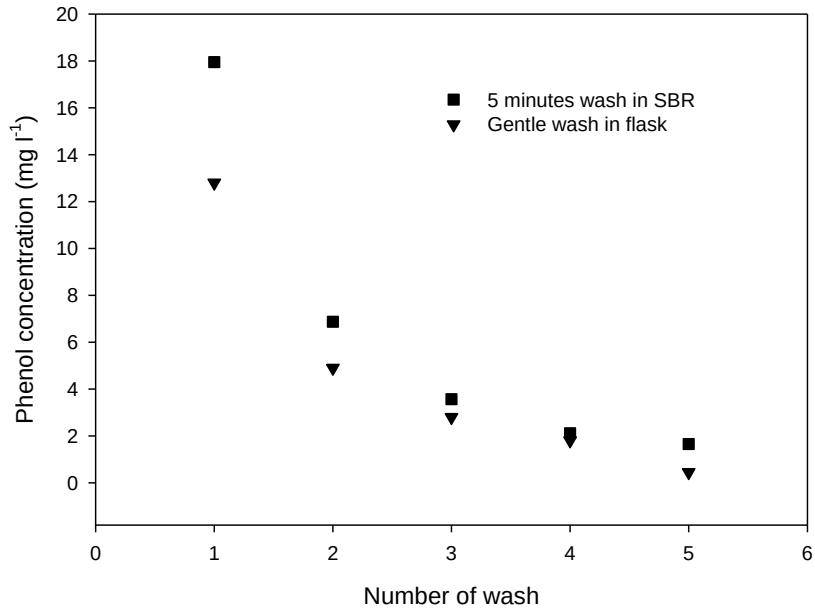

Figure 4.15: *Washing of phenol loaded Nyex®1000 in the mini-SBR and a volumetric flask*

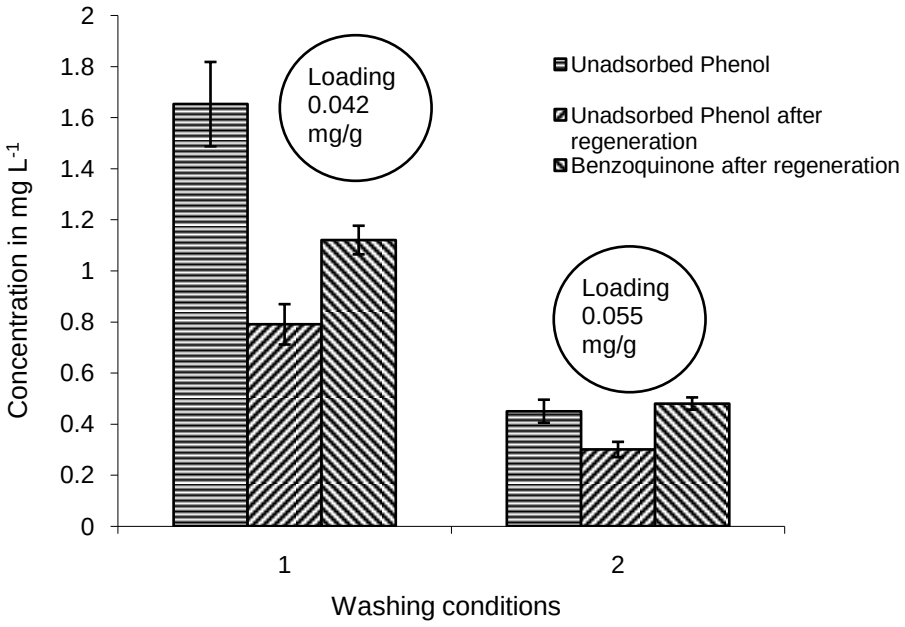

Figure 4.16: *Electrochemical regeneration of washed Nyex®1000, (1) washing in the mini-SBR, (2) gentle washing in a volumetric flask*

(b) Effect of operating parameters on the formation of breakdown products

The following section will investigate the effect of operating parameters including current density, electrolyte and pH on the formation of breakdown products in the process of adsorption with electrochemical regeneration.

(i) Effect of current density

The electrochemical regeneration of an adsorbent requires the passage of current (electrons) through the adsorbent bed. The charge passed can be changed by changing the current or the regeneration time. Current density can be expressed in terms of the current per unit area of electrode (current feeder) or per unit area of adsorbent surface (mA cm^{-2}). In this project it is based on the unit area of electrode. The electrochemical regeneration of phenol loaded GIC adsorbent was carried out at a range of current densities 10–40 mA cm^{-2} in the mini-SBR. Current densities higher than 40 mA cm^{-2} were not used because of the deterioration of the graphite anode current feeder at high current densities and long treatment times. Scanning electron micrographs of the fresh and used graphite plate current feeder are shown in figure 4.17, which indicates that the graphite plate was oxidised at high current density. In addition, very fine particles of carbon were observed in solution, during operation at high current density which makes the filtration of the samples extremely difficult. On the other hand, the GIC adsorbent was not observed to lose fine particles like the graphite plate shown in figure 4.17. However, the maximum current density used was upto 40 mA cm^{-2} for a number of electrochemical regeneration cycles with a treatment time of 20 min. Therefore, relatively high current densities amd several cycles of regeneration are required to evaluate the electrochemical stability of GIC adsorbent.

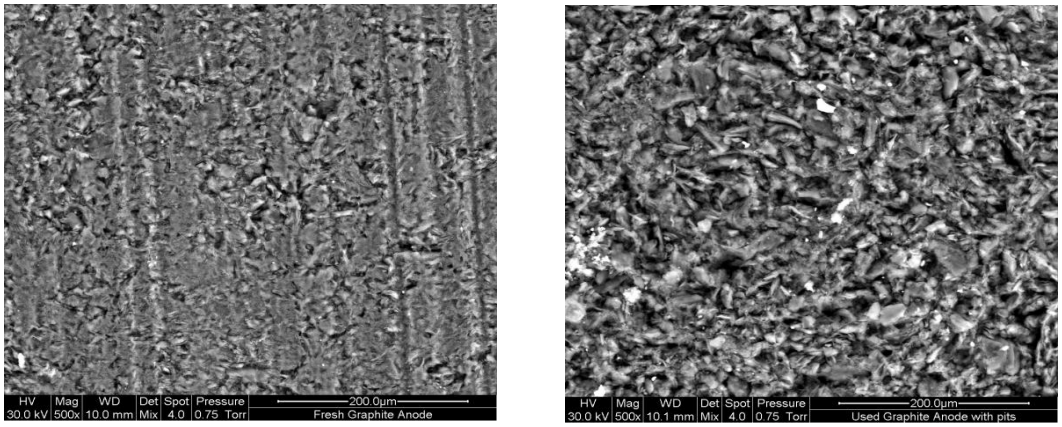

Figure 4.17: *Scanning electron micrographs (SEM) of a fresh and used graphite anode at 500x magnification. Electrochemical regeneration conditions for the used graphite anode current feeder were 50 mA cm^{-2} for about 2 hr*

The results show that p–benzoquinone, maleic and oxalic acid were the main breakdown products observed during adsorption and regeneration cycles carried out under all current densities (10–40 mA cm^{-2}) (Figures 4.19, 4.22). Very low concentrations of hydroquinone were detected during experiments at 10 and 20 mA cm^{-2} which is consistent with the previous studies carried out in batch electrochemical cell (data not shown). The small concentrations of hydroquinone can be explained by its transformation to p-benzoquinone owing to its relatively high oxidation rate constant compared to benzoquinone *(Pimentel et al. 2008)*. On the other hand, data for 30 and 40 mA cm^{-2} indicated no formation of hydroquinone. Catechol was only observed for adsorption and regeneration cycles at 20 and 30 mA cm^{-2} (data only shown for 20 mA cm^{-2}). Catechol can be formed by the electrochemical oxidation of phenol according to the reaction pathway given in equation 4.4 *(Gattrel & Kirk, 1993b)* (See also chapter 3). No ortho-benzoquinone was found among the reaction intermediates.

$$Phenol \xrightarrow{-2e^-,-2H^+,+H_2O} \begin{cases} HQ \xleftrightarrow{-2e^-,-2H^+} p-BQ \\ CAT \xleftrightarrow{-2e^-,-2H^+} o-BQ \end{cases} \quad (4.4)$$

For 10 mA cm^{-2}, there was an average drop of ca. 30% in phenol concentration during the regeneration cycles which was higher than the average decrease in concentration (ca. 20%) during adsorption cycles (Figure 4.18). This observation suggests that the electrochemical process was significantly affecting the electrochemical oxidation of phenol in solution. There was a greater decrease of 40, 50 and 60% in the phenol concentration during regeneration cycles at 20, 30 and 40 mA cm^{-2}, respectively, for about the same decrease in phenol concentration during the subsequent adsorption cycles (Figure 4.18). The approximate decrease in phenol concentration during adsorption cycles was 23, 21 and 22% at 20, 30 and 40 mA cm^{-2}, respectively. The faster phenol degradation at higher current density indicates that the rate of electrochemical oxidation of phenol in solution was affected strongly by the current density.

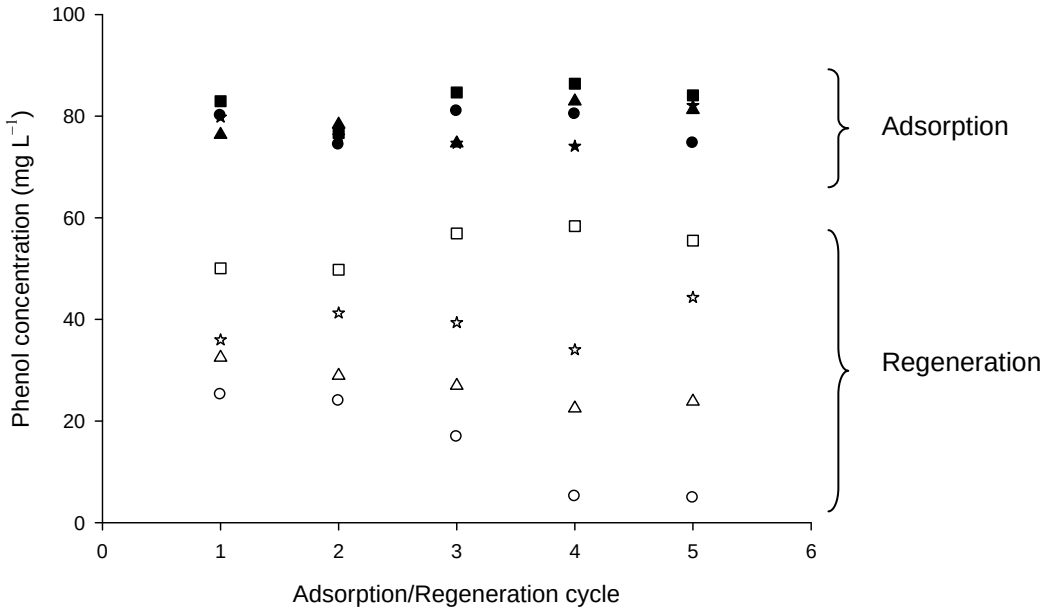

Figure 4.18: *Phenol concentration during multiple adsorption and regeneration cycles at various current densities, treating 500 mL solution containing 100 mg L^{-1} of phenol at the start of each cycle. The Nyex®1000 dose was 150 g. A current of 0.5, 1.0, 1.5 and 2.0 A was applied to give current density of 10, 20, 30 and 40 mA cm^{-2}, respectively (50 cm^2 electrode area) for 20 min regeneration time. Adsorption cycles: (■) 10 mA cm^{-2};(★)20 mA cm^{-2}; (▲)30 mA cm^{-2}; (●) 40 mA cm^{-2}, Regeneration cycles: (□)10 mA cm^{-2};(☆) 20 mA cm^{-2}; (△) 30 mA cm^{-2}; (o) 40 mA cm^{-2}*

Iniesta et al. (2001) suggested that high concentrations of electrochemically generated hydroxyl radicals can be achieved at higher current densities with a BDD electrode which can oxidise phenol completely without the formation of significant amount of breakdown products. The increase in current density did not significantly affect the concentration of breakdown products formed during the electrochemical regeneration of phenol loaded GIC adsorbent. Even for comparatively high current densities of 30 and 40 mA cm^{-2}, the concentration of benzoquinone formed was only slightly lower than its concentration at current densities of 10 and 20 mA cm^{-2} (Figure 4.19). However, an increase in current density increases the rate of degradation of benzoquinone as shown in figure 4.19.

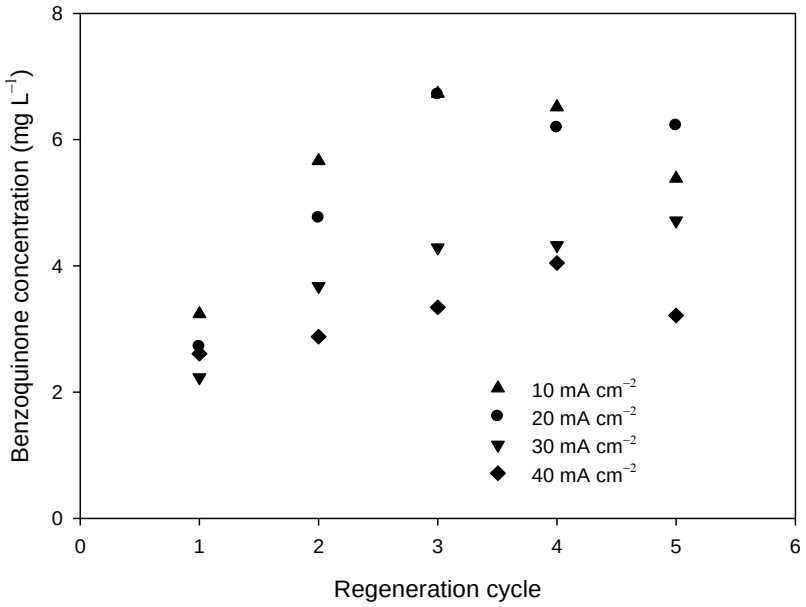

Figure 4.19: *Formation of benzoquinone in solution after a series of regeneration cycles at different current densities: (▲)10 mA cm^{-2}; (●) 20 mA cm^{-2}; (▼) 30 mA cm^{-2}; (♦) 40 mA cm^{-2}*

The present investigation also reveals that along with the oxidation of the adsorbed phenol onto the surface of GIC adsorbent, small concentrations of breakdown products are also adsorbed onto GIC surfaces during the subsequent adsorption cycles. Figure 4.20 shows the concentration of benzoquinone and catechol during adsorption and regeneration cycles at 20 mA cm^{-2}. The relatively higher concentrations of benzoquinone and catechol formed during the regeneration cycles appear to be adsorbed during the adsorption cycles. However, if there are oxidising

species present in the bed, these could react with the benzoquinone and catechol, reducing their concentrations. There may also be radical species adsorbed on the surface of the adsorbent which could react with benzoquinone and catechol. For the range of current density studied, there was not a pronounced effect on the percent regeneration efficiency, suggesting that the increase in current density was not affecting the regeneration of adsorbed phenol onto GIC adsorbent and thus the adsorbent can be regenerated even by applying low current densities. More than 80% regeneration efficiency was attainable in almost all the cases (Figure 4.21). The actual charge passed was in the range of 4–16 C g^{-1} for current densities of 10–40 mA cm^{-2}. However, the theoretical charge required for complete mineralization of the adsorbed phenol was around 2 C g^{-1}.

In addition, the regeneration efficiencies of phenol loaded GIC adsorbent under various current densities also indicated that the adsorbed breakdown products were also oxidised along with the phenol. In contrast, the effect of current density was significant in the electrochemical oxidation of phenol in solution.

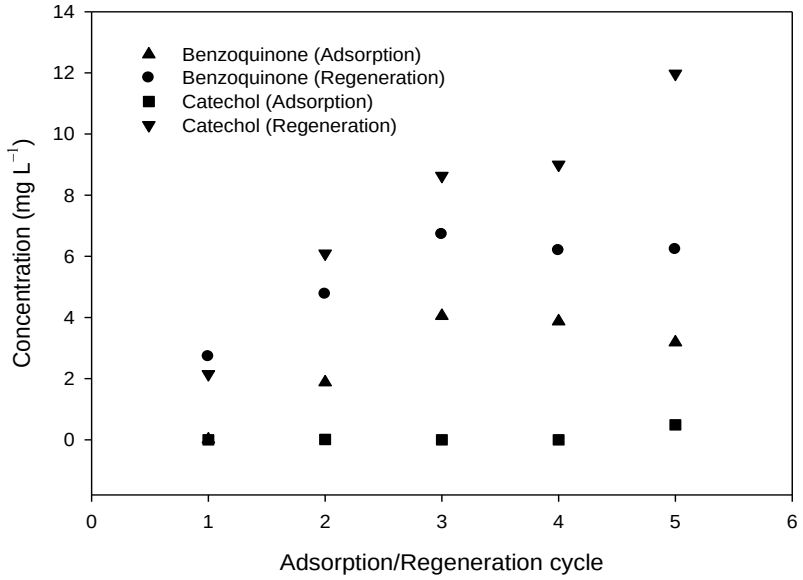

Figure 4.20: *Concentrations of benzoquinone and catechol in solution after a series of adsorption and regeneration cycles at 20 mA cm^{-2}, Benzoquinone: (▲) adsorption; (●) regeneration, Catechol: (■) adsorption; (▼) regeneration*

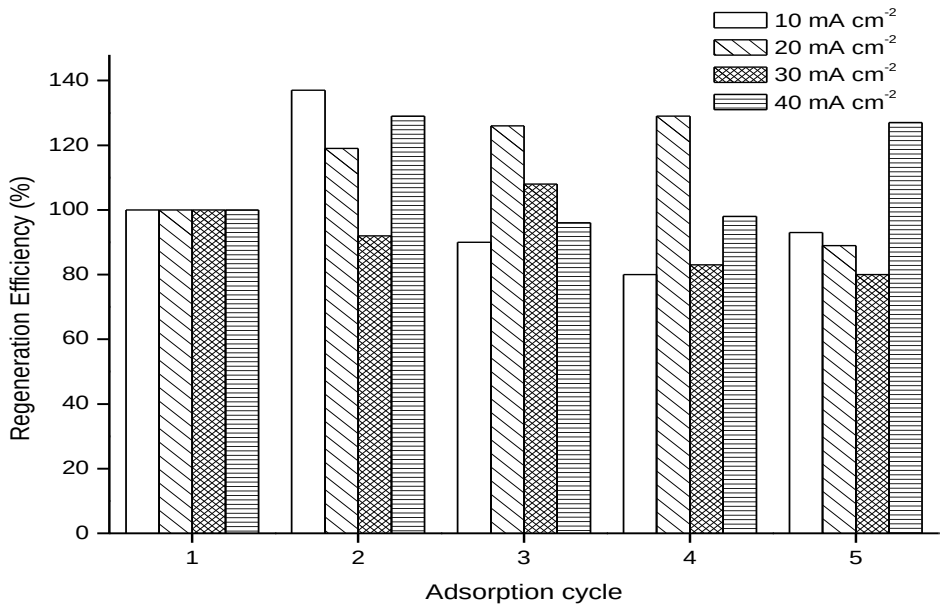

Figure 4.21: *Effect of current density on percent regeneration efficiency of phenol loaded Nyex®1000 with an initial concentration of 100 mg L^{-1} of 500 mL phenol solution, Nyex®1000 dose 150 g. A current of 0.5–2.0 A was applied to give current density in the range of 10–40 mA cm^{-2}, respectively for 20 min. Cycle 1 is for fresh adsorbent*

As far as the formation of organic acids is concerned, higher concentrations of oxalic acids were observed for current densities of 30 and 40 mA cm^{-2}, indicating increased phenol oxidation (Figure 4.22). The concentration of maleic acid was also found to increase with an increase in current density. However, the amount of oxalic acid was found to be larger than that of maleic acid. Phenol is first oxidised to quinonic species (cyclic intermediates) followed by the ring opening reaction forming organic acids which are ultimately converted into CO_2 and H_2O (See chapter 3). According to *Tahar and Savall, (1998)* the degradation of p–benzoquinone can be considered as a rate limiting step in the electrochemical oxidation of phenol into aliphatic carboxylic acids. If this is true then at higher current density the comparatively high concentration of oxalic acid suggest that the degradation of phenol could be through the direct oxidation of phenol into carboxylic acids. It shows that phenol removal was more likely to be degraded to carboxylic acids at higher current density. *Wu and Zhou (2001)* observed similar findings for the partial electrolytic degradation of phenol to organic acids. The decrease in phenol concentration in solution during all the regeneration cycles of phenol loaded GIC adsorbent does not appear to be

proportionally converted into these intermediate by-products. Thus, an investigation of the chlorinated breakdown products is required (See section 4.2).

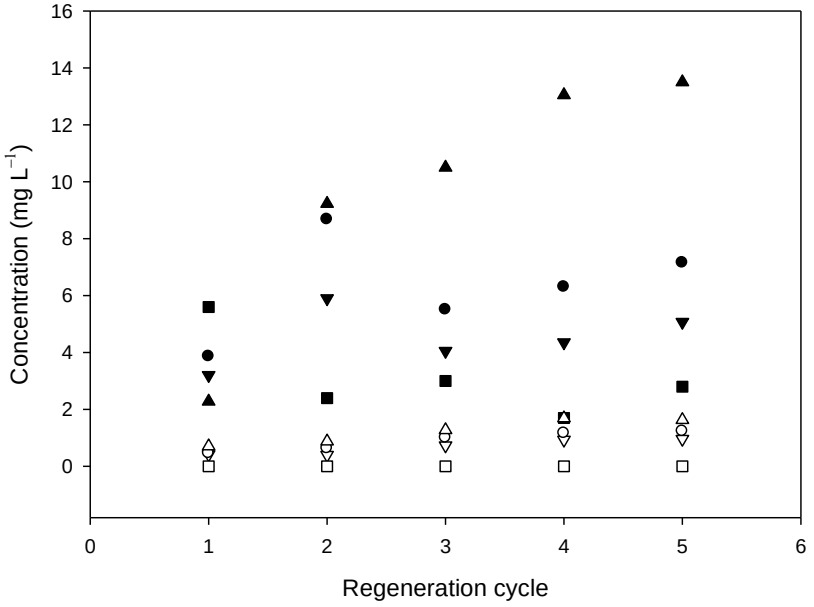

Figure 4.22: *Formation of carboxylic acids in solution after a series of electrochemical regeneration cycles at a range of current densities in the mini–SBR, Oxalic acid: (■)10 mA cm^{-2} ; (▼) 20 mA cm^{-2} (●) 30 mA cm^{-2}; (▲)40 mA cm^{-2}, Maleic acid: (□) 10 mA cm^{-2}; (▽) 20 mA cm^{-2}; (○) 30 mA cm^{-2}; (△)40 mA cm^{-2}*

The removal of TOC is an important parameter for wastewater containing organic pollutants because it determines the extent of degradation or mineralisation (See chapter 1). The oxidation of phenol in solution during the regeneration cycles at different current densities was further confirmed by a drop in the TOC as shown in figure 4.23 (b) which was achieved after their subsequent adsorptions, figure 4.23 (a). The results also reveal that though the phenol removal in solution was significant at higher current densities, the phenol does not appear to be completely oxidised into CO_2 and thus the drop in the TOC during regeneration cycles was not proportional to the decrease in phenol concentrations. In contrast, it may also be possible that some of the phenol is polymerized on the surface of the adsorbent and thus the TOC in solution could decrease without the formation of CO_2. Moreover, the decrease in phenol concentration due to electrochemical oxidation in solution was not completely converted into the cyclic intermediates such as quinones and aliphatic carboxylic acids. It seems likely that other breakdown products such as

chlorophenols were being generated (See section 4.2). On the other hand, the removal of TOC on each adsorption cycle almost corresponds to the proportional decrease in phenol concentration at various current densities; supporting the hypothesis that complete oxidation of adsorbed phenol on the surface of GIC adsorbent was taking place.

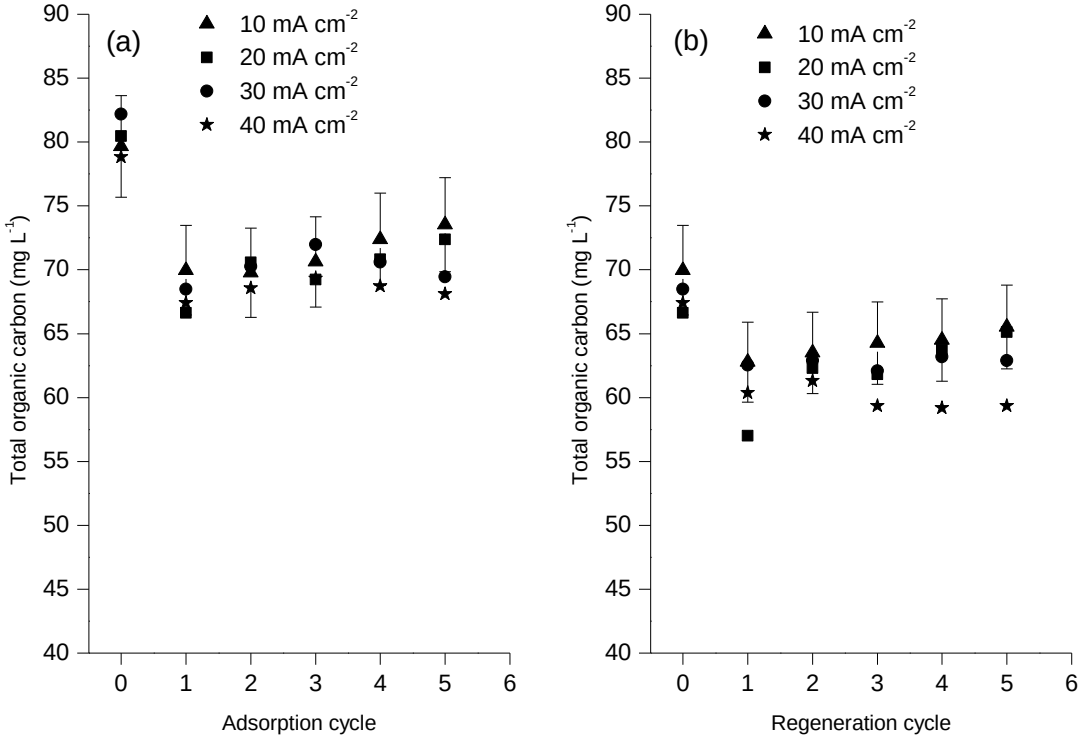

Figure 4.23: *Total organic carbon contents during adsorption (a) and regeneration (b) cycles at current density in the range of 10–40 mA cm^{-2}, The error in the analysis was estimated to be ±5% based on the variation of TOC for the same initial solution of phenol (100 mg L^{-1}) for all of the four experiments*

In order to further elaborate that the oxidation of adsorbed species was not the same as the indirect oxidation of species in solution, electrochemical oxidation of phenol solution was carried out without the use of GIC adsorbent in the mini-SBR at current densities in the range of 10–40 mA cm^{-2}. This was achieved by adding a supporting electrolyte, sodium sulphate with the phenol solution. The concentration profile of phenol as a function of electrolysis time is shown in figure 4.24. The results suggest that the removal of phenol in solution increases with an increase in current density. This is due to an increase of ionic transport which increases the rate of electrode reactions responsible for phenol oxidation. Similar findings have been reported by

Awad and Abuzaid, (1999) for the oxidation of phenol on a graphite anode at different current densities. The results also show that in the first 20 min of electrochemical process, the phenol removal was 14, 24, 36 and 66% for 10, 20, 30 and 40 mA cm^{-2} (Figure 4.24) Comparison with figure 4.18 suggests that higher rates of phenol removal in solution were observed in the presence of GIC adsorbent which acts as a high surface area packed bed electrode.

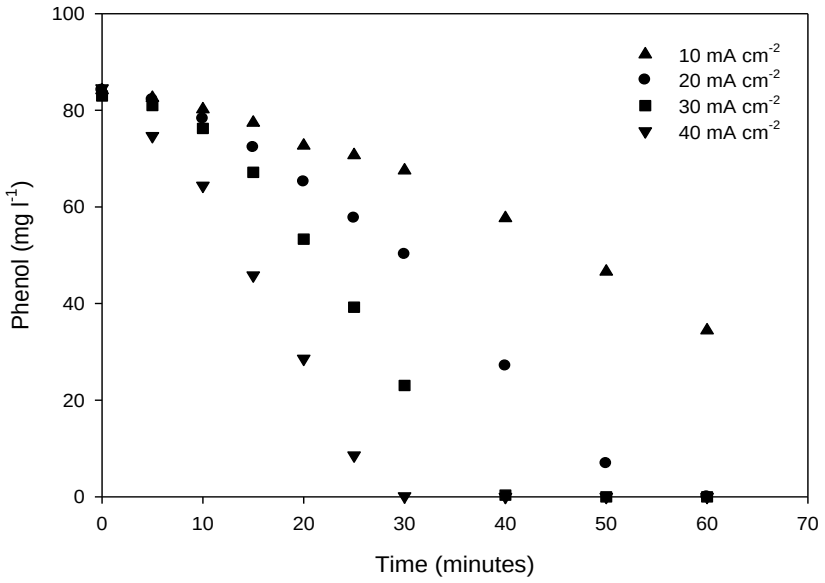

Figure 4.24: *Electrochemical oxidation of 500 mL of 85 mg L^{-1} phenol solution without Nyex® 1000 adsorbent using 0.3% (w/v) sodium sulphate at different current densities in the mini–SBR: A current of 0.7, 1.4, 2.1 and 2.8 A was applied for 20 min to give current density of 10, 20, 30 and 40 mA cm^{-2}, respectively (70 cm^2 electrode area), (▲)10 mA cm^{-2}; (●) 20 mA cm^{-2}; (■) 30 mA cm^{-2} (▼) 40 mA cm^{-2}*

The formation of benzoquinone during electrochemical oxidation without GIC adsorbent also showed similar trends to its formation in the presence of GIC adsorbent at various current densities (Figure 4.25). Less quantities of benzoquinone were observed at relatively high current densities which suggest that the rate of degradation of benzoquinone increased with an increase in the current density. The concentrations of benzoquinone in the first 20 min at various current densities closely match its formation in the presence of GIC adsorbent. This further indicates that electrochemical oxidation of adsorbed phenol on the surface of GIC adsorbent was not responsible for the formation of intermediate breakdown products and it

seems likely that the adsorbed phenol was completely mineralized. The results of electrochemical oxidation of phenol in solution also reveal that the rate of degradation of benzoquinone in the initial stages of electrochemical oxidation appears to be slower than its rate of formation at the later stages of oxidation (figure 4.25).

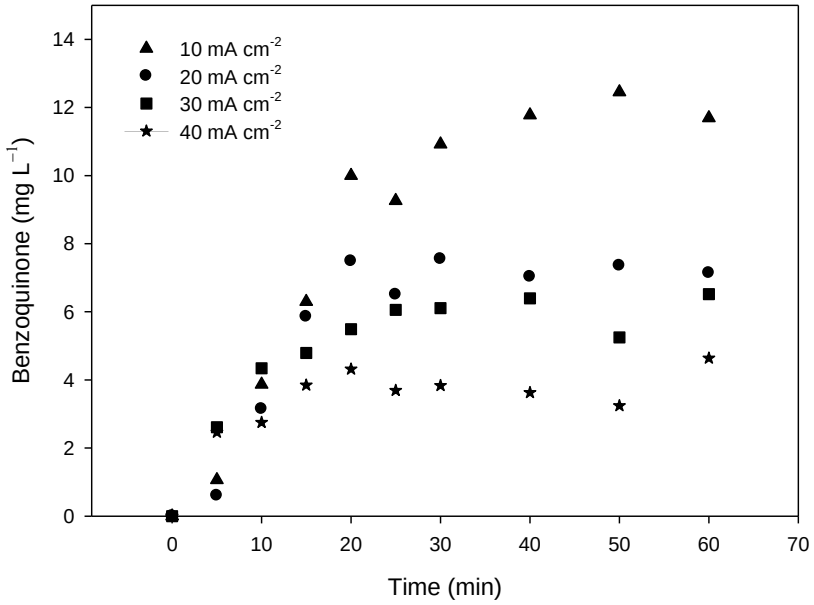

Figure 4.25: *Formation of benzoquinone during electrochemical oxidation of phenol solution without GIC adsorbent at different current densities in the mini–SBR: (▲)10 mA cm^{-2}; (●) 20 mA cm^{-2}; (■) 30 mA cm^{-2}; (★) 40 mA cm^{-2}*

An increase in concentration of oxalic acid was observed with an increase in current density during electrochemical oxidation of phenol without GIC adsorbent as shown in figure 4.26. The higher concentrations of oxalic acid suggest not only increased phenol oxidation but also slower oxidation of oxalic acid into CO_2, particularly for the electrochemical oxidation at 40 mA cm^{-2}. These results are consistent with studies of electrochemical oxidation of phenol reported in the literature *(Comninellis, 1994; Canizares et al. 2005).* It was observed that the amount of maleic acid formed was far less than that of oxalic acid.

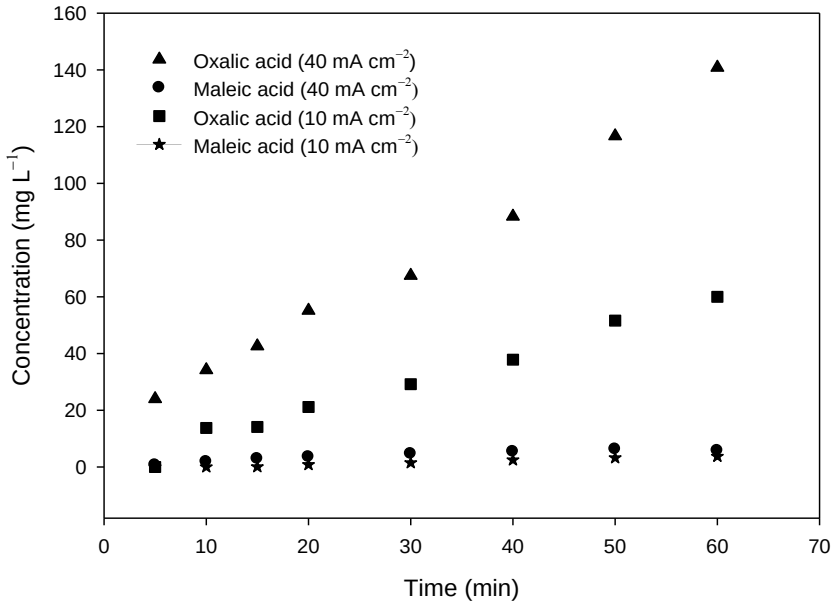

Figure 4.26: *Formation of carboxylic acids during electrochemical oxidation of phenol solution without GIC adsorbent at different current densities in the mini–SBR*

Based on the data obtained for electrochemical regeneration of GIC adsorbent and for electrochemical oxidation of phenol in solution without GIC adsorbent at 10 and 40 mA cm^{-2}, it can be concluded that the process of adsorption with electrochemical regeneration using GIC adsorbents generates breakdown products largely due to oxidation of phenol in solution, by the same mechanism of indirect electrochemical oxidation (observed without the adsorbent).

(ii) Effect of supporting electrolytes with phenol solution

The addition of a supporting electrolyte can increase the electrochemical treatability of waters containing organic compounds *(Palma-Goyes et al. 2010; Yavuz and Koparal, 2006).* The electrochemical oxidation of phenol solution has been extensively studied using higher concentrations of supporting electrolytes *(Rajkumar et al. 2005).* From the practical point of view low concentration of electrolytes is important. Thus, in the present investigation low concentrations of supporting electrolytes were used with phenol to evaluate their effect on the formation of breakdown products. This was carried out by treating 100 mg L^{-1} phenol solution

containing 1% (w/v) sodium sulphate or sodium chloride. The catholyte was the same 0.3% (w/v) NaCl solution acidified with HCl. The use of supporting electrolytes has also been reported to increase the regeneration efficiencies of GAC *(Narbaitz and Cen, 1994; Zhang et al. 2002)*. In the presence of sodium chloride high regeneration efficiencies have been observed compared to other electrolytes. *Brown et al. (2004b)* also observed that increasing the electrolyte concentration results in an increase in the regeneration efficiencies of GIC adsorbent (Nyex®100) loaded with crystal violet. They found no additional benefit for NaCl concentration above 4% for Nyex®100 This can be compared with GAC for which *Narbaitz and Cen, (1994)* observed no increase in regeneration efficiency for addition of more than 1% NaCl for GAC loaded with phenol.

In this study, no work was carried out to determine the effect of electrolyte concentration on the regeneration efficiencies of GIC adsorbent. However, the effect of low concentrations of electrolytes including sodium chloride and sodium sulphate on the formation of breakdown products has been investigated. The results indicate that similar low concentrations of benzoquinone, hydroquinone and catechol were formed when NaCl or Na_2SO_4 was added, as shown in figure 4.27. As expected greater regeneration efficiencies were observed in the case of NaCl compared to the Na_2SO_4 electrolyte (Figure 4.28). In addition, the electrochemical oxidation rate of phenol when Na_2SO_4 was the electrolyte was significantly lower than that in a NaCl electrolyte system. This was due to the increased indirect oxidation as a result of the formation of active chlorine species such as free chlorine, hypochlorous acid and hypochlorite, which thus affected the degradation of organics in solution (see section 4.2). The relatively low rate of phenol removal in solution for Na_2SO_4 was due to the fact that sulphate is an inert electrolyte which does not normally produce any reactive species during electrolysis. It may generate persulphate under special conditions but this effect is unlikely to be significant under the conditions studied *(Rajkumar et al. 2005).*

The decrease in the concentration of phenol in solution during regeneration cycles when sodium sulphate was added as an electrolyte can be compared to the electrochemical oxidation of phenol in solution during regeneration cycles when no electrolyte was used with GIC adsorbent (see figure 4.18). These findings suggest

that the addition of sodium chloride and sodium sulphate with phenol studied did not affect the process mechanism as far as the formation of breakdown products is concerned.

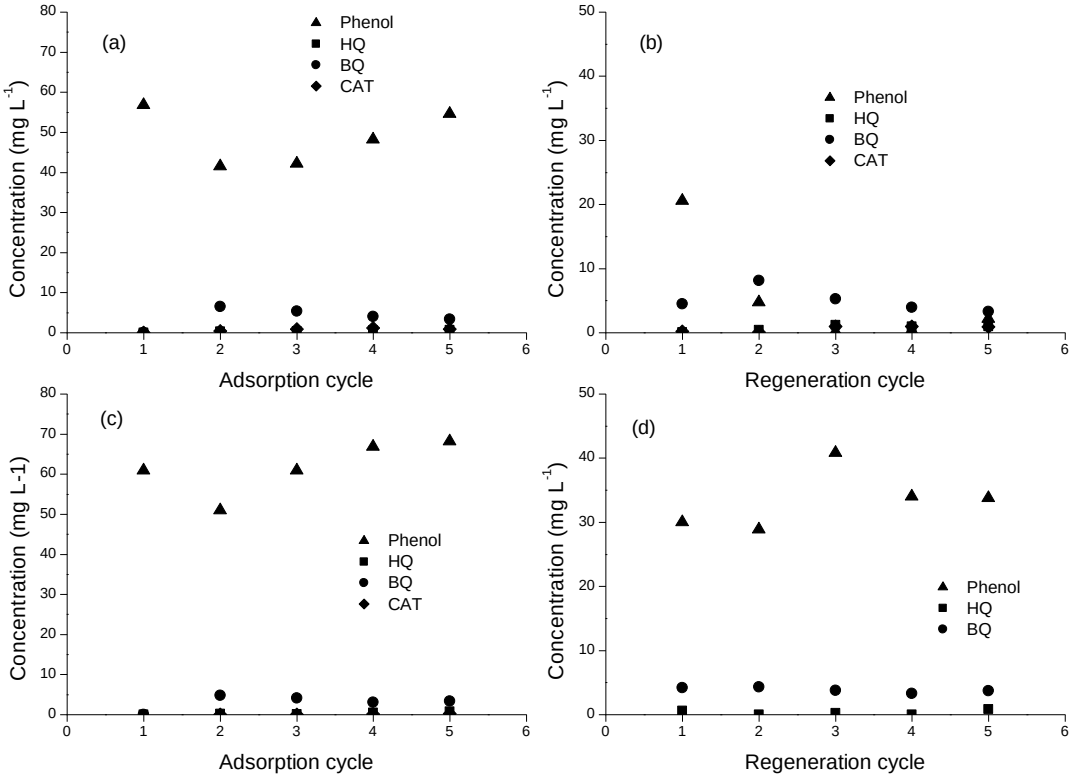

Figure 4.27: *Breakdown products during adsorption and regeneration cycles in the mini-SBR when 500 mL phenol of 100 mg* L^{-1} *containing* 1% NaCl (a&b) and 1% Na_2SO_4 (c&d) *was mixed with 140 g Nyex®1000 for 30 min. Regeneration was carried out at 0.7 A for 20 min and current density was 10 mA* cm^{-2}

Comparison of the adsorption cycles for the two electrolytes with that of figure 4.18 reveal that the adsorption capacity of GIC adsorbent for phenol has increased by using additional electrolytes with the phenol solution compared to the situation when no electrolyte was used with Nyex®/phenol system. A comparison of the adsorption capacity in the presence of NaCl and Na_2SO_4; and when no electrolyte was used is shown in figure 4.29 which suggests that the adsorptive capacity of GIC adsorbent over a number of adsorption cycles remained highest when 1% NaCl was used. *Zhang et al. (2002)* has observed similar findings for the adsorption of phenol on activated carbon with and without 2% NaCl. It is well known that the dissolved salts in aqueous media influence the adsorption capacity of many organics on activated

carbon. In general increasing the salt concentration increases the adsorption capacity *(Arafat et al. 1999)*. The salts may be involved in a variety of mechanisms including interactions with adsorbates in solution or on the carbon surface and altering the charge on carbon surfaces. Sodium ions have been found to increase the adsorption capacity of many organic compounds including aniline and benzoic acids under specific pH conditions. In this context, the positive salt cations may neutralize the negative charge of the carbon surface and thus enabling the surface to adsorb more adsorbate molecules. *Halhouli et al. (1995)* also found that sodium chloride increases the adsorption of phenol on activated charcoal, particularly with higher concentrations of NaCl (pH 7). According to them, the increase in adsorption capacity was attributed to partially nullifying the repulsive forces between the adjacent adsorbed $C_6H_5O^-$ ions. The actual mechanism which enhances the adsorption capacity of GIC adsorbents by the use of electrolytes needs further investigation.

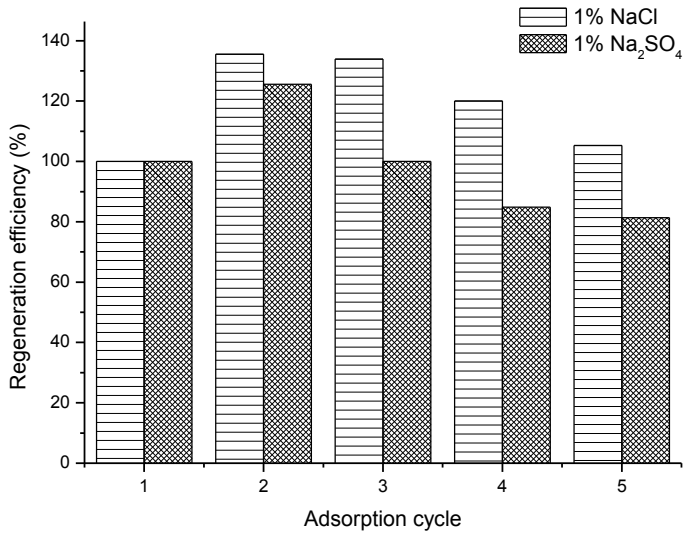

Figure 4.28: *Effect of additional electrolytes (Na_2SO_4 and NaCl) on percent regeneration efficiency of phenol loaded Nyex®1000 with an initial concentration of 100 mg L^{-1} of 500 mL phenol solution, Nyex®1000 dose 150 g. Cycle 1 is for fresh adsorbent and current density was 10 mA cm^{-2}* in each case.

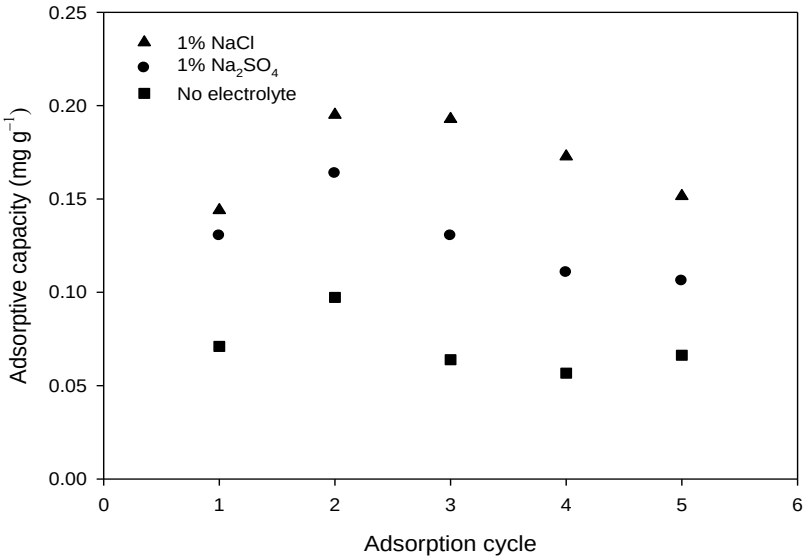

Figure 4.29: *Comparison of the adsorption capacity of GIC adsorbent over a number of adsorption cycles with (NaCl and Na_2SO_4) and without additional electrolyte, when 500 mL of 100 mg L^{-1} of phenol (containing 1% NaCl or 1% Na_2SO_4) was mixed with 150 g of the adsorbent and regeneration was carried out at 10 mA cm^{-2} for 20 min.*

(iii) Effect of pH

During electrochemical regeneration of GIC adsorbents, the pH of the solution decreased due to the formation of hydrogen ions from water oxidation. Thus, irrespective of the starting pH, the pH decreases during the electrochemical oxidation. In addition, a decrease in pH was also observed during the first adsorption indicating the release of some acidic functional groups from the surface of GIC adsorbent. However, during continuous operation of adsorption with electrochemical regeneration, the drop in pH is only localized and thus does not decrease the pH of the treated water significantly (see chapter 8). Thus, the nature of the breakdown products formed during electrochemical regeneration of GIC was investigated at neutral and alkaline pH. The pH of the water was adjusted using phosphate buffers as described in section 4.1.2. However, in the cathode compartment, 0.3% NaCl solution acidified with HCl was used as usual. It has been reported in the literature that the pH of the solution strongly influences the nature of the breakdown products formed during electrochemical oxidation of phenol *(Comninellis, 1991).*

The results indicate that only extremely low concentrations (< 60 µg L^{-1}) of benzoquinone were detected during adsorption and regeneration cycles at neutral and

alkaline pH (Figure 4.30). These results are consistent with the studies reported in the literature about the electrochemical oxidation of phenol at alkaline pH. The removal of phenol in solution during electrochemical regeneration cycles at neutral and alkaline pH show that the removal rate is almost doubled under alkaline conditions. This might be due to the conversion of phenol into polymeric materials at alkaline conditions because phenol has the tendency to foul electrodes due to the deposition of tarry deposits. These materials have been considered as phenolic polymerization products formed during the electrochemical oxidation of phenol, particularly under alkaline conditions *(Zareie et al. 2001)*. The oxidation of phenol at solid electrodes generates phenoxy radicals which due to coupling forms a passivating polymeric film on the electrodes. During electrochemical regeneration of the GIC adsorbent at neutral and alkaline pH, there was observed a constant voltage drop across the mini-SBR during all the regeneration cycles indicating that phenol was not deactivating the adsorbent due to the conversion of phenol into polymeric materials (data not shown). This could simply be because the bed has a very high surface area the amount of polymer formed is too small to affect the cell voltage.

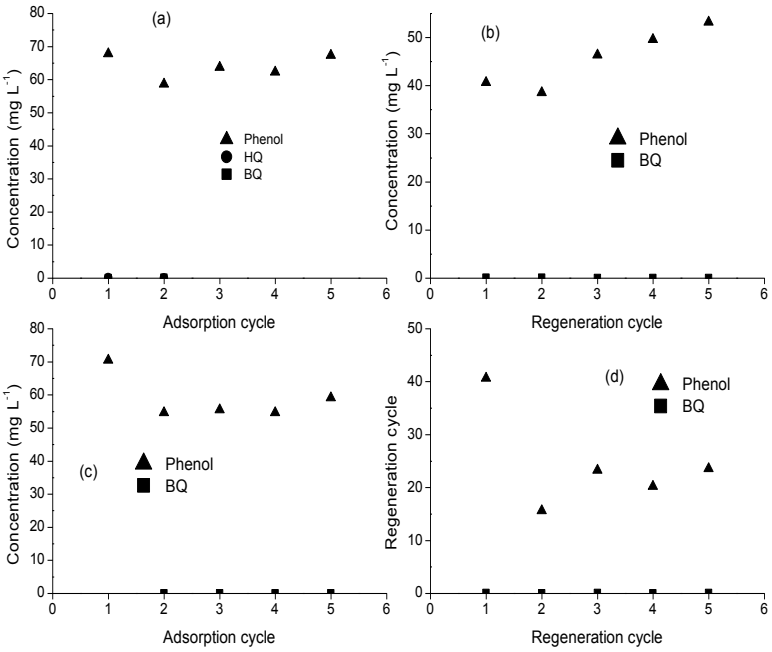

Figure 4.30: *Breakdown products during adsorption and regeneration cycles in the mini-SBR when 500 mL of 100 mg L^{-1} phenol at pH 7 (a&b) and pH 9 (c&d) was mixed with 140 g Nyex®1000 for 30 min. Regeneration was carried out at 0.7 A for 20 min and current density was 10 mA cm^{-2}*

If some of the phenol was converting into polymeric materials, these species might be removed from the surface of GIC particles during mixing of the adsorbent with water in the subsequent adsorption cycles and thus reactivating the adsorbent for regeneration cycles. Therefore in order to further confirm that whether the polymeric species were formed and removed due to mixing, electrochemical oxidation of phenol solution at neutral and alkaline pH was performed in the mini-SBR without the addition of GIC adsorbent for a relatively longer time. The voltage of the electrochemical cell was monitored during the electrolysis of the phenol solution. The results indicate that voltage drop across the electrochemical cell was fairly constant at neutral and alkaline pH showing that there was no formation of polymers on the surface of the graphite anode, even for a longer electrochemical oxidation times (Figure 4.31). However, the voltage drop is dominated by the cathode and membrane, so changes at the anode may be too small to see. As far as the formation of breakdown products is concerned, low concentrations of benzoquinone were observed during electrochemical oxidation at alkaline pH with concentrations similar to those observed in the presence of the GIC adsorbent. The formation of low concentrations of hydroquinone, benzoquinone and catechol has also been shown in figure 4.31. These results are not consistent with the literature which suggests that alkaline conditions are favourable for the formation of polymeric materials. *(Comninellis, 1991).* It has also been reported that the fraction of phenol converted into polymeric materials is a function of the initial concentration of phenol, the current density, temperature and pH of the solution *(Tahar et al., 2009)*. The findings of current study suggest that relatively low concentrations of phenol and current density may dominate over the effect of alkaline conditions for polymer formation. The process of treating water using GIC adsorbents with electrochemical regeneration involves low organic concentrations, low current densities, ambient temperatures and slightly acidic conditions. Thus, it is most likely that under these conditions phenol was not converted into polymeric products. On the other hand, the GIC particles have a high surface area compared to the flat anode plate, the coating coverage may be so small that a large number of regeneration cycles would be required to observe the formation of polymers on the GIC adsorbent. In addition, polymeric particles may have been produced and these have accumulated within the adsorbent bed. The relatively high removal rate of phenol at alkaline pH may be due

to its conversion into other breakdown products. However, this is an area which requires further investigation.

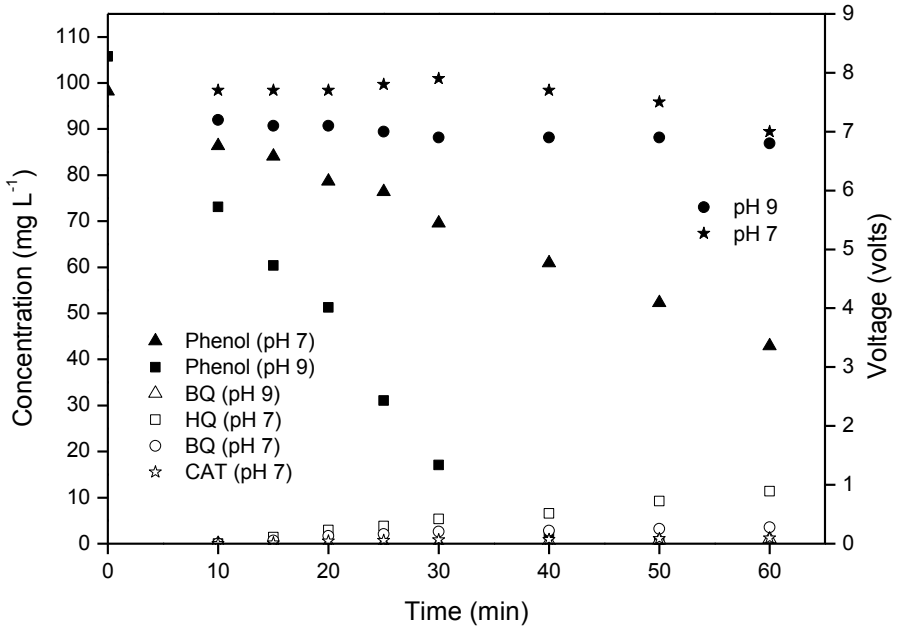

Figure 4.31: *Electrochemical oxidation of 500 mL of 100 mg L^{-1} phenol solution in the mini-SBR (without GIC adsorbent) where the pH was maintained at 7 and 9 using phosphate buffers. A current of 0.7 A (10 mA cm^{-2}) was allowed to pass through the cell for 60 min.*

(iv) Effect of recycling of treated solution

In order to investigate the effect of recycling of the same solution, a series of adsorption and regeneration cycles were performed with 500 mL of 50 mg L^{-1} phenol solution in the mini-SBR at 20 and 40 mA cm^{-2} in such a way that after each regeneration cycle the solution was not replaced. The figure 4.32 shows the removal of phenol and formation of benzoquinone at 20 and 40 mA cm^{-2} during adsorption and regeneration cycles. These results indicate that the concentration of phenol decreased with adsorption and regeneration cycles leading to an almost negligible concentration of phenol after the 3rd adsorption cycle. On the other hand, the concentration of benzoquinone increased up to 3rd adsorption cycle and afterwards it appeared to decrease in subsequent cycles. These results suggest that the rate of formation of benzoquinone was faster than its rate of degradation for the current

densities studied. However, not only were lower concentrations of benzoquinone observed at higher current density but they also degraded at a faster rate (Figure 4.32). This could be associated with a higher rate of formation of hydroxyl radicals at increased current density. It is clear from these results that by recycling the treated solution over a number of adsorption and regeneration cycles, the phenol can be completely eliminated. Furthermore it seems likely that after a few more cycles at 40 mA cm^{-2} the benzoquinone would also be eliminated.

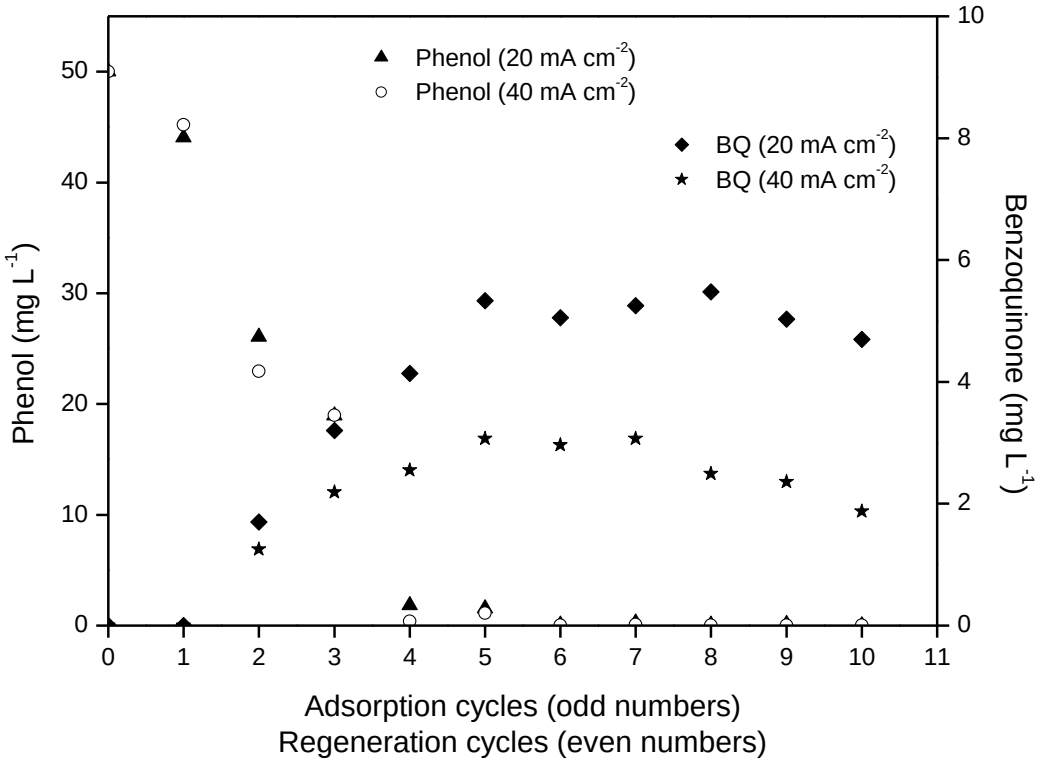

Figure 4.32: *Multiple adsorption and regeneration cycles with the same initial 500 mL of 50 mg L^{-1} phenol with 140 g of Nyex®1000 in the mini-SBR at 20 and 40 mA cm^{-2}, A current of 1.4 and 2.8 A was applied for 20 min (20 and 40 mA cm^{-2}, respectively)*

4.1.5 Conclusions

This section has given important information about the formation of breakdown products during electrochemical regeneration of the GIC adsorbent using phenol as a model pollutant. The preliminary investigation in a simple batch electrochemical cell

has revealed that the main breakdown products include benzoquinone, hydroquinone, catechol, maleic and oxalic acids. However, these species were observed in low concentrations compared to the initial concentration of the phenol.

The adsorption studies of phenol and its aromatic intermediates including benzoquinone, catechol and hydroquinone showed that all of these species have almost the same adsorption characteristics for the GIC adsorbents and these are described by L–shaped adsorption isotherms (see chapter 2). On the other hand, carboxylic acids including maleic and oxalic acids were observed to follow the S–shaped adsorption isotherms and thus they are poorly adsorbed onto GIC adsorbent at low concentrations. It has also been shown that GIC particles in addition to their adsorption capability have the ability to catalyse the oxidation of hydroquinone into benzoquinone in solution at ambient conditions.

This study has revealed that the formation of intermediate oxidation products was not due to the relatively high concentrations of phenol (100 mg L^{-1}) since the same set of breakdown products were observed when treating lower concentrations of phenol (10 & 20 mg L^{-1}) in the mini-sequential batch reactor. It was interesting to note that during the electrochemical regeneration of GIC adsorbent, some of the phenol present in solution was also oxidised. It was concluded that the mechanism of electrochemical regeneration of GIC adsorbents involved the oxidation of the species adsorbed onto GIC particles and the indirect electrochemical oxidation of species present in solution. The results suggest that the breakdown products observed were forming due to the indirect electrochemical oxidation of phenol present in solution.

The effect of operating parameters including current density, pH of the solution, addition of electrolytes with phenol solution on the electrochemical regeneration of GIC adsorbent with special reference to the formation of intermediate oxidation products has further revealed that:

- Electrochemical oxidation was found to be more effective in decreasing the concentration of phenol in solution during electrochemical regeneration of the GIC adsorbent in comparison to the removal of phenol by adsorption onto the GIC adsorbent.
- The effect of current density on regeneration efficiencies was not significant; more than 80% regeneration efficiency was attained for all the cases studied.
- The concentration of benzoquinone was found to decrease with an increase in the current density. However, greater concentrations of maleic and oxalic acids were formed during electrochemical regeneration at higher current densities.
- The effect of current density on the formation of breakdown products during electrochemical regeneration of GIC adsorbent was shown to have similarities with the formation of intermediate oxidation products during the electrochemical oxidation of phenol in solution (without the GIC adsorbent).
- The same pattern of breakdown products was observed during adsorption and electrochemical regeneration of GIC adsorbents using sodium chloride or sodium sulphate as additional electrolyte. However, the adsorption capacity of GIC adsorbent for phenol was found to increase with the addition of electrolytes. The highest regeneration efficiencies were observed when NaCl was added to the solution.
- During adsorption and electrochemical regeneration of GIC adsorbent at neutral and alkaline pH, very low concentrations of benzoquinone were observed, similar to studies of the electrochemical oxidation of phenol at alkaline pH reported in the literature. Based on the fairly constant values of voltage drop during the electrochemical oxidation of phenol at neutral and alkaline pH, it was concluded that there was no was no significant formation of polymeric materials under these conditions.
- A number of adsorption and electrochemical regeneration cycles with the same batch of phenol solution at different current densities has shown that this technique is quite effective in completely oxidising the phenol, as well as eliminating the breakdown products formed in solution. However, higher current densities were found to lead to lower concentrations of breakdown products after several cycles.

4.2 Investigation of chlorinated breakdown products in batch studies

The following section deals with the formation and the fate of chlorinated breakdown products released in solution during the batch process of adsorption and electrochemical regeneration of GIC adsorbent under a range of experimental conditions.

4.2.1 Materials and Methods

The liquid samples which were collected during adsorption and electrochemical regeneration using the batch electrochemical cell, as described in section 4.1.2, were analysed using GC/MS for the identification of any chlorinated breakdown products (see section 4.1.3 for analysis). The chromatograms with their relevant (m/z) spectra for some of the samples have been provided in appendix A which shows that mono-, di- and tri-substituted chlorinated phenols were observed during these studies.

The adsorption isotherms of various mono-, di- and tri-chlorinated phenol were determined using the methodology as described in section 4.1.2 (adsorption studies) and following the analysis as described in section 4.2.2. In addition, competitive adsorption was also investigated for the chlorinated breakdown products by mixing a range of known masses of adsorbent with 100 mL of a solution containing a mixture of 2-chlorophenol, 4-chlorophenol, 2-4-dichlorophenol and 2,4-6-trichlorphenol (each at a concentration of 50 mg L^{-1}) for 30 minutes on a magnetic stirrer (ER LAUDA, Germany) at 700 min^{-1} for 30 min at room temperature. Initial and final samples after adsorption were filtered using a 0.45 μm syringe filter and analysed as described in section 4.2.2.

In addition, for the experiments described in section 4.1.2 (adsorption and electrochemical regeneration studies using the mini-sequential batch reactor), the liquid samples were analysed for the chlorinated oxidation products as specified in section 4.2.2. The results of a number of these experiments for chlorinated breakdown products are discussed in section 4.2.3 below.

4.2.2 Analysis

The mono- (CP), di- (DCP) and tri-chlorophenols (TCP) were analysed using high performance liquid chromatography (HPLC, Varian ProStar) with a C18 Phenomenex (Macclesfield, UK) column. Analysis was carried out by comparing the retention times of the standard compounds of various chlorophenols. The mobile phase was composed of acetonitrile and ultrapure water containing 0.01 M H_3PO_4 (HPLC grade). The oven temperature was maintained at 35°C, and a UV detector was used at 230 nm. The gradient of the mobile phase used was as follows:

Table 4.2: *Gradient used for mobile phase in determining the chlorophenols onto HPLC.*

Time (min)	% Water	% Acetonitrile
0	80	20
20	55	45
15	20	80

4.2.3 Results and Discussion

(a) Adsorption Isotherms

Since chlorinated breakdown products of phenol were identified by GC/MS in the samples collected during adsorption and electrochemical regeneration, their adsorption isotherms were investigated for the GIC adsorbent. The results revealed that the GIC offered varying adsorption capacities for mono-, di-, and tri-chlorinated phenols in the order TCP>DCP>MCP, suggesting that increasing the degree of chlorination strongly influenced the adsorptive capacity of the GIC adsorbents (Figure 4.33). However, the adsorptive capacities of even mono-chlorophenols are still higher than that of phenol and its non-chlorinated aromatic intermediates including benzoquinone, hydroquinone and catechol (Figures 4.7 & 4.33). The adsorption isotherms of the different isomeric forms of mono-, di-, and tri-chlorphenols exhibited similar adsorption capacity (Figure 4.33). In addition, each of these isotherms can be described by the L-shaped isotherm similar to that of phenol,

suggesting that there is no strong competition between water and chlorphenols to occupy the adsorption sites. A similar effect of increased capacity with increased chlorination of chlorinated phenols on both Nyex®100, a powdered GIC adsorbent, (*Brown and Roberts, (2007))*, and GAC have been reported *(Streat et al. 1995)*. A possible explanation for the adsorption behaviour of these aromatics on carbon involves the donor-acceptor mechanism *(Mattson et al. 1969)*. Carbonyl oxygen on the carbon surface acts as an electron donor while the aromatic ring acts as an electron acceptor. The chloro groups are electron withdrawing leading to a decrease in the electron density within the π system of the aromatic ring in phenol molecules. Thus, the electron density in the aromatic ring decreases as the number of chlorine atoms increases in the phenol molecule leading to greater adsorption on GAC. The same mechanism is likely to occur for the adsorption of chlorophenols on GIC adsorbents.

The adsorption data was further analyzed by applying the Freundlich and the Langmuir isotherm models. The parameters of these models including corresponding values of coefficient of correlation (R^2) for all the chlorophenols are given in table 4.3.

Table 4.3: *Freundlich and Langmuir parameters for the adsorption of chlorophenols on GIC adsorbent.*

	Freundlich model			***Langmuir model***		
Compound	**$K_F \times 10^4$ $[mg \cdot g^{-1}(L \cdot mg^{-1})^{1/n}_F]$**	**$1/n_F$**	**(R^2)**	**q_m $(mg \cdot g^{-1})$**	**$K_a \times 10^4$ $(L \cdot mg^{-1})$**	**(R^2)**
2-CP	785.28	0.328	0.787	0.324	1305	0.987
3-CP	495.19	0.4525	0.974	0.404	513	0.957
4-CP	848.63	0.357	0.959	0.548	354.5	0.911
2,4-DCP	1609.8	0.37	0.890	0.543	3262	0.878
2,5-DCP	1240.5	0.383	0.924	0.447	3211	0.916
2,6-DCP	936	0.383	0.562	0.447	3211	0.916
3,5-DCP	50	3.93	0.325	0.397	4206	0.895
2,4,6-TCP	143.6	0.545	0.960	1.520	517.7	0.913

The coefficients of correlation are high (>0.91) for both models for some of the compounds including 4-CP, 3-CP, 2,5-DCP and 2,4,6-TCP showing a good agreement between the experimental and predicted values. For all compounds the Langmuir model gave a good fit to the data with R^2>0.85. However for the Freundlich model a poor fit was obtained in some cases (Table 4.3). A comparison of these models with the experimental adsorption data for all of these compounds have been provided in appendix C.

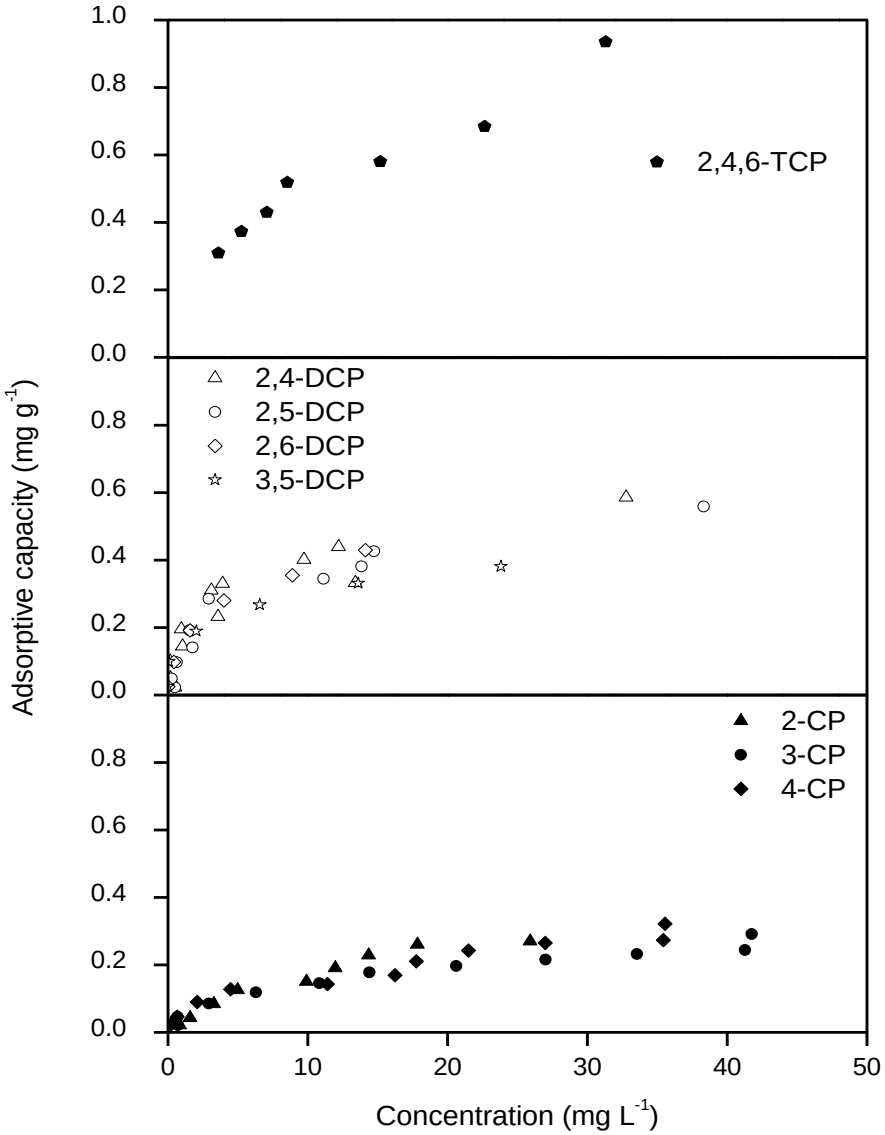

Figure 4.33: *Adsorption isotherms of mono-, di-, and tri-chlorphenols onto Nyex®1000 in a 250 mL volumetric flask using 20 g of Nyex®1000 mixed with 100 mL of solution of various initial concentrations.*

Although it was evident from the adsorption isotherms that 2,4,6-TCP has higher adsorption capacity on the GIC adsorbent than the mono-, and di-chlorphenols, the adsorption behaviour of a solution containing 2-CP, 4-CP, 2,4-DCP and 2,4,6-TCP on the GIC adsorbent was further investigated. The results revealed that with an increase in the dose of GIC adsorbent, there was observed to be a decrease in the concentration of these compounds (Figure 4.34). For the same initial concentration of each species in the solution and with the same dose of adsorbent, the decrease in the concentration of each category was in the order of TCP>DCP>CP suggesting that TCP is preferentially adsorbed than DCP which in turn has more affinity for the adsorbent than MCP.

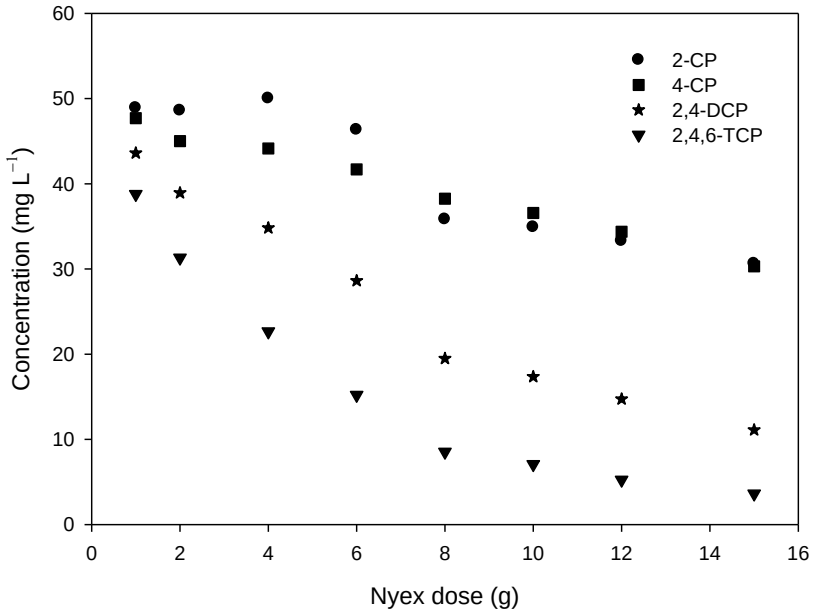

Figure 4.34: *Filtrate concentrations of 2-CP, 4-CP, 2,4-DCP and 2,4,6-TCP after adsorption on Nyex®1000 with a range of doses; Initial concentration: 52 mg L^{-1} of 2-CP, 4-CP, 2,4-DCP and 2,4,6-TCP.*

(b) Effect of current density on the formation of chlorinated intermediates

The concentrations of chlorinated phenols detected during electrochemical regeneration of GIC adsorbent loaded with phenol at 10 and 40 mA cm^{-2} (see section 4.1.2) has been given in figure 4.35 (a) and (b). The main chlorinated breakdown

products observed were 2-CP, 4-CP and 2,4-DCP with lower concentrations of 2,4-DCP than 2-CP and 4-CP. The results indicate that the concentration of chlorinated phenols increased with an increase in current density. In addition, an increase in current density increased the degree of chlorination leading to the formation of various di- and tri-chlorinated phenols. However, the concentrations of di- and tri-chlorinated phenols remained lower than that of mono-chlorinated phenols (Figure 4.35). The effect of current density on the formation of chlorinated species can be explained by the greater free chlorine concentrations at higher current density and vice versa (see section 4.3). Consequently, there was an increase in the rate of indirect electrochemical oxidation of phenol with an increase in current density leading to increased amounts of chlorinated phenols. These results can be compared to the formation of chlorophenols during electrochemical oxidation of phenol solution containing 0.5% sodium sulphate without GIC adsorbent as shown in figure 4.35 (c) and (d). At 10 mA cm^{-2} lower concentrations of chlorinated species were observed in this case due to the low concentration of free chlorine generated during electrochemical oxidation in the absence of the adsorbent (see section 4.3). This was not true for electrochemical oxidation of phenol solution at 40 mA cm^{-2} where higher concentrations of the various chlorinated phenols were observed, suggesting that an increase in current density also increases the concentrations of chlorinated phenols in the absence of the adsorbent. These results suggest that the mechanism of formation of chlorinated breakdown products during electrochemical regeneration of the GIC adsorbent was associated with the indirect oxidation of phenol present in solution. It is concluded that the phenol adsorbed onto the surface of GIC adsorbent does not contribute to the chlorinated by-products detected in solution. Figure 4.35 (c) shows that 2-CP, 4-CP and 2,4-DCP were formed during electrolysis (in the absence of the adsorbent) at 10 mA cm^{-2} and oxidised afterwards with the passage of time. Electrochemical oxidation of phenol solution at 40 mA cm^{-2} generated 2-CP, 4-CP, 2,4-DCP, 2,6-DCP, 3,5-DCP and 2,4,6-TCP. Initially the concentration of mono- and di-substituted chlorinated phenols increased until after 30 min the concentrations started to decrease, as shown in figure 4.35 (d). The 2,4,6-TCP appeared after 10 min, increased to its maximum concentration after 40 min and then decreased with time.

As discussed above, chlorinated breakdown products were formed due to indirect oxidation of phenol in solution during the electrochemical regeneration of the GIC adsorbent. The results obtained in the absence of the adsorbent suggest that higher current density for longer regeneration times can completely oxidise the chlorophenols formed in solution due to indirect oxidation

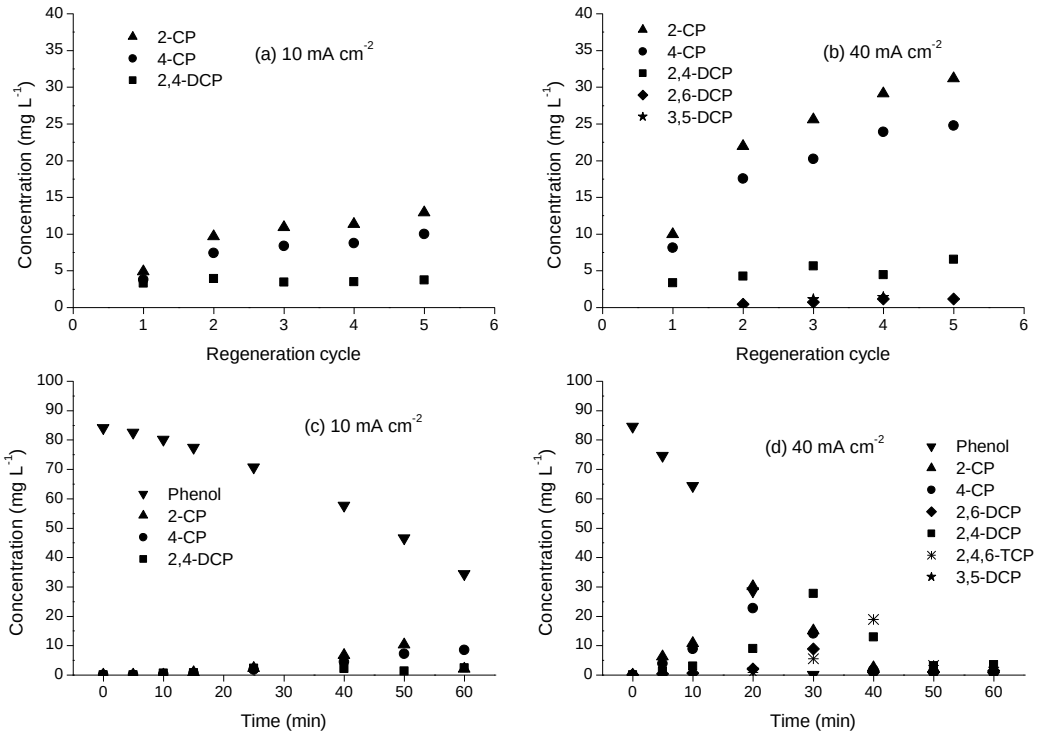

Figure 4.35: *(a–b)Formation of chlorophenols during regeneration cycles at (a) 10 and (b) 40 mA cm^{-2} with an initial phenol concentration of 100 mg L^{-1} of 500 mL phenol solution, Nyex®1000 dose 150 g. A current of 0.5 and 2.0 A was applied for 10 and 40 mA cm^{-2} respectively (50 cm^2 electrode area);(c–d) Formation of chlorphenols during electrochemical oxidation of 500 mL of 85 mg L^{-1} phenol solution without Nyex® 1000 adsorbent using 0.3% (w/v) sodium sulphate at (c)10 and (d) 40 mA cm^{-2} in the mini–SBR: A current of 0.7 and 2.8 A was applied for 20 min to give current density of 10 and 40 mA cm^{-2}, respectively (70 cm^2 electrode area).*

(c) Conditions that minimize the formation of the chlorinated breakdown products

In order to minimize the formation of chlorinated phenols during electrochemical regeneration of the GIC adsorbents, a number of suggested conditions were considered.

(i) Batch recycle mode

The phenol solution may be treated over a number of adsorption and regeneration cycles so that the chlorinated phenols are completely oxidised. The results show that the chlorphenols which were formed due to indirect oxidation of phenol in solution during the electrochemical regeneration of GIC adsorbent were adsorbed onto the adsorbent during the subsequent adsorption cycles as shown in figure 4.36. In this way along with the adsorbed phenol, these species are also oxidised at the surface of the adsorbent leading to treated water which is almost completely free of toxic chlorinated by-products.

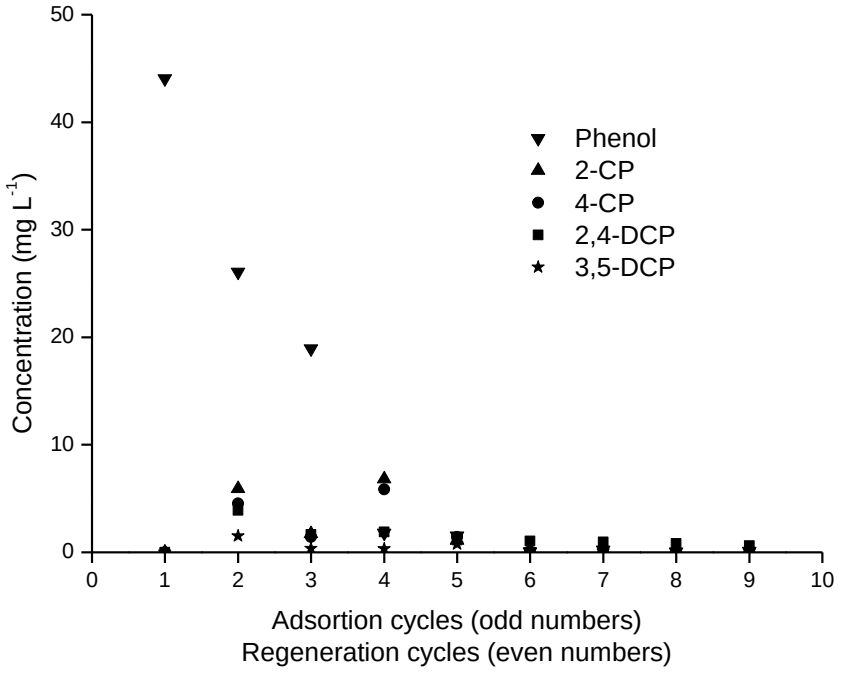

Figure 4.36: *Multiple adsorption and regeneration cycles with the same initial 500 mL of 50 mg L^{-1} phenol with 140 g of Nyex®1000 in the mini-SBR at 20 mA cm^{-2} showing the formation and elimination of chlorphenols, A current of 1.4 A was applied for 20 min.*

(ii) Using low current density

As discussed before that an increase in current density increases the concentration of chlorinated breakdown products and thus using low current densities may minimize the formation of the chlorinated species due to the small concentrations of free chlorine generated (see section 4.3). In this context, multiple adsorption and regeneration cycles were performed for 100 ppm phenol solution at 5 mA cm^{-2} in the mini-SBR according to the procedure specified in section 4.1.2. The regeneration time was increased from 20 to 40 min (so that the charge passed per g of adsorbent was the same as that at 10 mA cm^{-2}) with the aim of obtaining 100% regeneration of the adsorbent. The results indicated the formation of 2-CP, 4-CP and 2,4-DCP at relatively low concentrations during the regeneration cycles (figure 4.37) compared to the formation of same species at 10 mA cm^{-2} (figure 4.35, a). On the other hand, the adsorption cycles at 5 mA cm^{-2} showed only a few µg L^{-1} of 4-CP (figure 4.37), with no other chlorinated phenols detected. The low concentrations of chlorinated phenols can be explained by the relatively low concentrations of free chlorine formed at 5 mA cm^{-2} during the electrochemical regeneration of the GIC adsorbent. Electrochemical regeneration of fresh adsorbent without phenol solution was performed at 5 and 10 mA cm^{-2} according to the procedure described in section 4.3. The concentration of free chlorine at 10 mA cm^{-2} after 20 minutes was approx 12 mg L^{-1} whereas for 5 mA cm^{-2} it was approximately 7 mg L^{-1} even after 40 min of electrochemical regeneration (Figure 4.37)

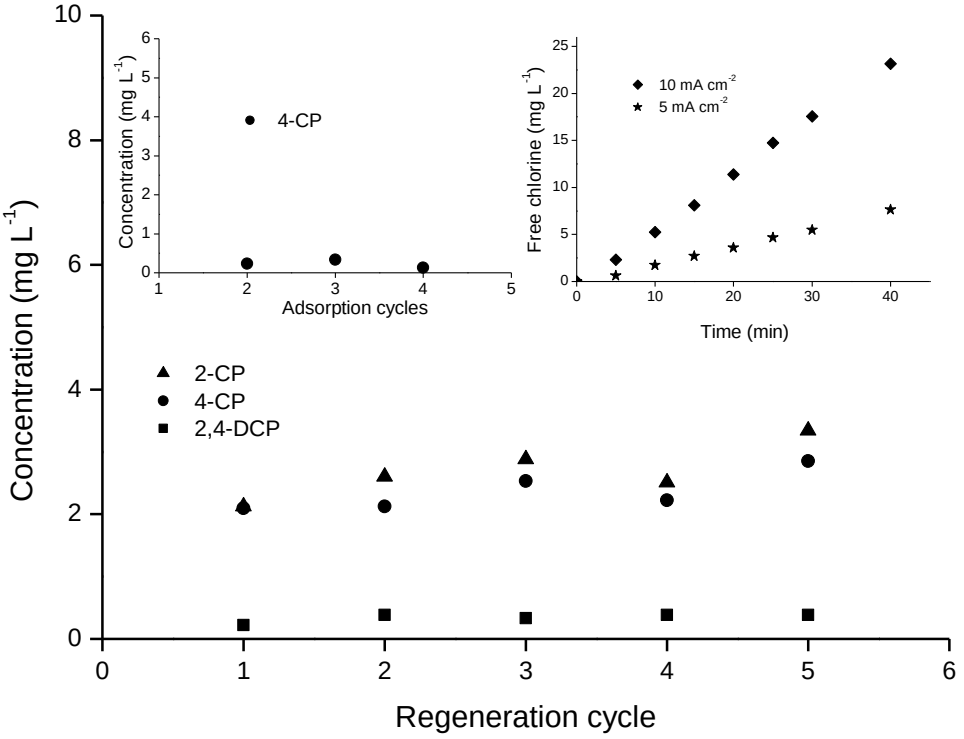

Figure 4.37: *Formation of chlorophenols during adsorption and regeneration cycles at 5 mA cm^{-2} with an initial phenol concentration of 100 mg L^{-1} of 500 mL phenol solution, Nyex®1000 dose 150 g. A current of 0.35A (5 mA cm^{-2}) was applied for 40 min (70 cm^2 electrode area). This figure also shows the formation of free chlorine detected.*

(iii) Using low phenol concentration

With a low initial concentration of phenol (10 mg L^{-1}), very low concentrations of 4-CP and 2,4-DCP were observed after the regeneration cycles at 10 mA cm^{-2} compared to the formation of these species with an initial concentration of 100 mg L^{-1} phenol solution (Figures 4.38 and 4.35,a). This suggests that an increase in initial phenol concentrations leads to an increase in the amounts of the chlorinated species, presumably due to the increased phenol concentration in solution. The Arvia® process has been designed to treat low concentrations of organics by adsorption with electrochemical regeneration of GIC adsorbent and under these conditions the concentration of chlorinated breakdown products generated will be very low.

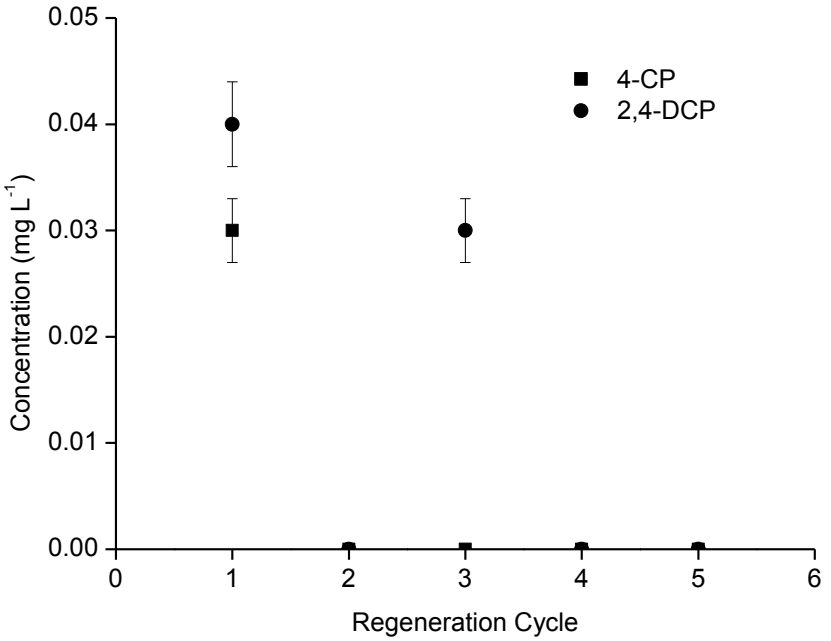

Figure 4.38: *Formation of chlorinated breakdown products during regeneration cycles in the mini-SBR when 500 mL phenol of 10 mg L^{-1} was mixed with 140 g Nyex®1000 for 30 min. Regeneration was carried out at 0.5 A for 20 min; (50 cm^2 electrode area). The detection limit of the analysis is about 0.02 mg L^{-1}*

(iv) Using sodium sulphate as catholyte in place of sodium chloride

If chloride ions are not present in the water to be treated then the only source of free chlorine formation is the chloride ions from the catholyte of the mini-SBR. In order to completely avoid the formation of chlorinated intermediate oxidation products, the catholyte solution can be changed from sodium chloride to sodium sulphate. Thus, to evaluate the performance of sodium sulphate as the catholyte, multiple adsorption and regeneration cycles were performed for an initial concentration of 100 mg L^{-1} of phenol solution using 0.3% Na_2SO_4 solution acidified with H_2SO_4 as catholyte at 10 and 20 mA cm^{-2} according to the procedure specified in section 4.1.2. The results revealed that phenol loaded GIC adsorbent using sodium sulphate can be as effectively regenerated, as was observed in the case of sodium chloride catholyte (Figure 4.39). Above 80% regeneration efficiency was observed at both current densities. Benzoquinone, hydroquinone, maleic and oxalic acids were found as the main breakdown products and no chlorinated breakdown products were observed (data not shown). Thus, sodium sulphate can be used effectively as the catholyte in

the process of adsorption with electrochemical regeneration of GIC adsorbent and there is no issue of the formation of chlorinated intermediate oxidation products.

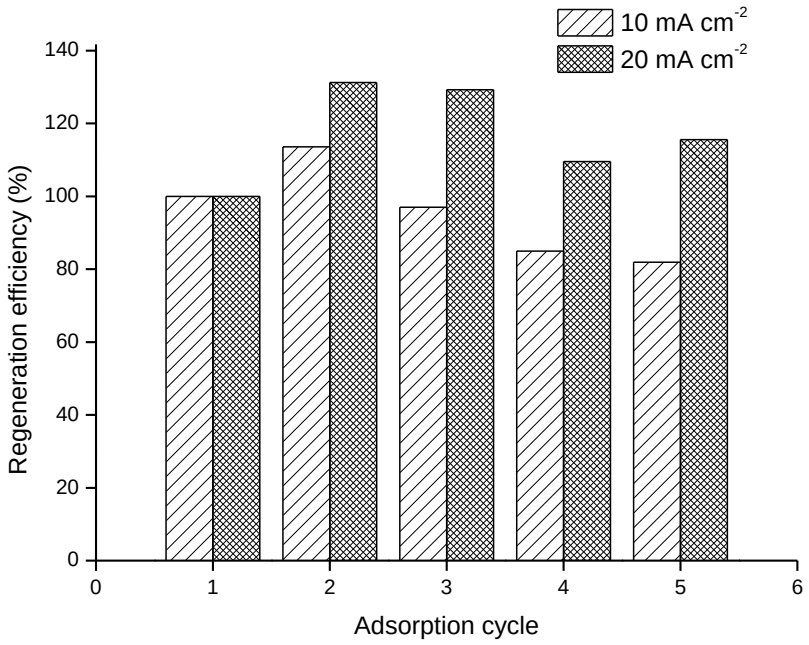

Figure 4.39: *Effect of number of adsorption/regeneration cycles on the regeneration efficiency of 100 mg L^{-1} phenol; Nyex®1000 dose 150g for 500 mL of phenol solution in the mini–SBR. Regeneration was carried out at 10 and 20 mA cm^{-2}, for 20 min, (70 cm^2 electrode area). The catholyte was 0.3% Na_2SO_4 (w/v) acidified using H_2SO_4*

4.2.4 Conclusions

The formation of chlorinated by–products of phenol during electrochemical regeneration of the GIC adsorbent has been investigated. Various mono-, di- and tri-chlorophenols were observed during the regeneration process. Their adsorption isotherms revealed similar adsorption behaviour on the GIC adsorbent. However, the adsorptive capacity of chlorinated phenols for GIC adsorbent was found to be related to the degree of chlorination, in the order of TCP>DCP>MCP.

Current density has a significant effect on the formation of chlorinated breakdown products during the electrochemical regeneration of GIC adsorbents. There was an increase in the concentration of chlorinated phenols with an increase in current

density. In addition, an increase in current density was also found to enhance the degree of chlorination leading to the formation of a variety of di- and tri-chlorinated phenols. The formation of chlorinated by-products was found to be a function of the availability of free chlorine. In addition, higher initial phenol concentrations also increased the concentration of chlorinated by–products. The results suggest that chlorinated phenols are formed by reactions between free chlorine and species in solution, rather than by oxidation of adsorbed species.

Conditions that minimize the formation of chlorinated breakdown products during electrochemical regeneration of GIC adsorbent have been suggested and evaluated. These include low current density, low initial phenol concentration, recycle batch mode and using a chloride free catholyte.

4.3 Investigation of free chlorine in batch studies

During electrochemical regeneration of the GIC adsorbent, the oxidation of the adsorbed organics to carbon dioxide and/or other breakdown products takes place (see section 4.1 and 4.2). The analysis of the gases formed during electrochemical regeneration of the GIC adsorbent has been discussed in chapter 5. In addition, a number of other reactions also occur on the surface of GIC particles including oxidation of chloride ions to chlorine. Since an aqueous solution of sodium chloride is used as an electrolyte in the cathode compartment during electrochemical regeneration of the GIC adsorbent, a detailed investigation of the formation of free chorine has been carried out and is discussed in this section. Prior to discussing the experimental investigation of chlorine formation, the chemistry of free chlorine in water is discussed which will be helpful in understanding the mechanism of free chlorine formation.

Chlorine is added to water as a disinfectant and when elemental liquid chlorine (Cl_2) is added into water, it may exist in the form of dissolved gas (Cl_2), hypochlorous acid (HOCl) and/or the hypochlorite ion (OCl^-) *(White, 2010)*. The residual concentration of these species in water is collectively known as free chlorine. The dissolved chlorine in water will form hypochlorous and hydrochloric acid according to equation (4.5):

$$Cl_2 + H_2O \leftrightarrow HOCl + H^+ + Cl^- \quad (4.5)$$

The equilibrium for this reaction can be expressed as follows:

$$K_H = \frac{[HOCl][H^+][Cl^-]}{Cl_2} \quad (4.6)$$

where K_H is the equilibrium constant (mol L^{-1})^2, and the square brackets indicate the concentrations expressed in mol L^{-1}. The value of K_H is 4.5×10^{-4} (mol L^{-1})^2 at 25℃ *(Metcalf and Eddy, 2003).*

Since HOCl is a weak acid, it further dissociates into hypochlorite and hydrogen ions depending upon the pH of the solution as:

$$HOCl \leftrightarrow H^+ + OCl^- \quad (4.7)$$

Hypochlorous acid is one of the most powerful oxidising agents and an effective chlorinating agent *(Smith et al. 1991).* In addition, it is more effective as a disinfectant than the hypochlorite ions *(White, 2010).* The extent to which hypochlorous acid dissociates depends upon the pH and temperature of the water. At higher pH, the HOCl will react to form hypochlorite ions (equation 4.7). The hydrochlorous acid predominates at 3.3<pH<7.5 while the main species of free chlorine is hypochlorite ions at pH>7.5 *(Zanoni et al. 2004).* The extent of the dissociation can be calculated as:

$$K_a = \frac{[H^+]\,[OCl^-]}{[HOCl]} \quad (4.8)$$

where K_a is the dissociation constant that varies with temperature and the square brackets indicate molar concentrations. The value of K_a is 3×10^{-8} M at 25℃ *(Metcalf and Eddy, 2003).*

In addition, to the major chlorine species [Cl_2(aq), HOCl and OCl^-], other chlorine intermediates including trichloride ion (Cl_3^-), chlorine hemi-oxide (Cl_2O) and H_2OCl^+ can also be formed at pH<4 *(Deborde and Gunten, 2008)*. The (Cl_2O) and H_2OCl^+ are formed in low concentrations and they are likely to be of little

significance in dilute solutions. The trichloride ion is a complex formed by molecular chlorine and chloride ions:

$$Cl_2 + Cl^- \leftrightarrow Cl_3^- \quad (4.9)$$

The equilibrium for this reaction can be expressed as follows:

$$K_3 = \frac{[Cl_3^-]}{[Cl_2][Cl^-]} \quad (4.10)$$

where K_3 is the equilibrium constant, and the square brackets indicate the concentrations expressed in mol L^{-1}. The value of K_3 is 0.191 (L mol^{-1}) at 25℃ *(Deborde and Gunten, 2008).*

The relative distribution of these species at a fixed concentration of chloride ions can be expressed as follows:

$$\%Cl_2 = \frac{[Cl_2]}{[Cl_2] + [HOCl] + [OCl^-] + [Cl_3^-]} \times 100 \quad (4.11)$$

$$\%HOCl = \frac{[HOCl]}{[Cl_2] + [HOCl] + [OCl^-] + [Cl_3^-]} \times 100 \quad (4.12)$$

$$\%OCl^- = \frac{[OCl^-]}{[Cl_2] + [HOCl] + [OCl^-] + [Cl_3^-]} \times 100 \quad (4.13)$$

$$\%Cl_3^- = \frac{[Cl_3^-]}{[Cl_2] + [HOCl] + [OCl^-] + [Cl_3^-]} \times 100 \quad (4.14)$$

Using the expressions for K_H (equation 4.6), k_a (equation 4.8) and K_3 (equation 4.10), and the well know relationship that pH is equivalent to the negative logarithm of the hydrogen ion concentration, the equations can be re-written to give relative distribution of free chlorine species from the equilibrium constants of the respective reactions as follows:

$$\%Cl_2 = \frac{1}{1 + \frac{K_H}{[Cl^-]}10^{pH} + \frac{K_H k_a}{[Cl^-]}10^{2pH} + K_3[Cl^-]} \times 100 \quad (4.15)$$

$$\%HOCl = \frac{1}{1 + \frac{[Cl^-]}{K_H 10^{pH}} + k_a 10^{pH} + \frac{K_3[Cl^-]^2}{K_H 10^{pH}}} \times 100 \quad (4.16)$$

$$\%OCl^- = \frac{1}{1 + \frac{[Cl^-]}{K_H k_a 10^{2pH}} + \frac{1}{k_a 10^{pH}} + \frac{K_3[Cl^-]^2}{K_a K_H 10^{2pH}}} \times 100 \quad (4.17)$$

$$\%Cl_3^- = \frac{1}{1 + \frac{1}{K_3[Cl^-]} + \frac{K_H 10^{pH}}{K_3[Cl^-]^2} + \frac{K_a K_H 10^{2pH}}{K_3[Cl^-]^2}} \times 100 \quad (4.18)$$

These equations (4.15–4.18) can now be directly used to evaluate the percentages of molecular chlorine, hypochlorous acid, hypochlorite ion and trichloride ion as a function of pH in a solution of free chlorine at a specific chloride concentration and temperature. It is clear from equation 4.5 that low pH and high chloride concentration favours the formation of Cl_2 (aq). Therefore, in concentrated chlorine solution, the total free chlorine concentration consists of molecular chlorine, hypochlorous acid and hypochlorte ion. Although, trichloride contains active chlorine, but its concentration relative to Cl_2 (aq) and HOCl is expected to be significantly small in chlorine solutions, unless a high concentration of chloride ion is present *(White, 2001)*. The relative distribution of main chlorine species [Cl_2 (aq), HOCl andOCl^-], ignoring the low concentrations of trichloride ions, at 20℃ as a function of pH is given in figure 4.40.

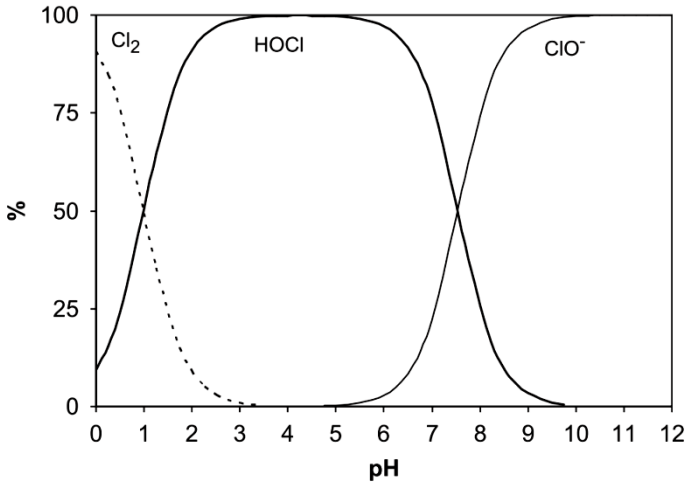

Figure 4.40: *Relative distribution of free chlorine species as a function of pH at 25^{o}C and for a chloride concentration of 177.5 mg L^{-1}, (Deborde and Gunten, 2008)*

Industrially chlorine is produced electrochemically which is one of the most important electrochemical processes *(Oliveira et al. 2007)*. Chlorine is produced by the oxidation of chloride ions as:

$$2Cl^- \rightarrow Cl_2 + 2e^- \qquad (4.19)$$

Free chlorine is a well know by-product during the electrolysis of water containing chloride ions. In the process of adsorption with electrochemical regeneration of GIC adsorbents (Arvia®), an aqueous solution of sodium chloride is used as the catholyte and thus chloride ions migrate from the cathode side of electrochemical cell to the anode through the membrane. At the anode these ions may be oxidised to chlorine gas (or hypochlorite or hypochlorous acid depending on the pH) according to equation (4.19). As in other electrochemical processes, a possible side reaction at the anode is the evolution of oxygen which often cannot be fully avoided. Oxygen evolution takes place according to one of the following reactions:

$$2H_2O \rightarrow O_2 + 4H^+ + 4e^- \qquad (4.20)$$

Or

$$4OH^- \rightarrow O_2 + 2H_2O + 4e^- \qquad (4.21)$$

Hydrogen evolution also takes place simultaneously at the cathode as:

$$2H^+ + 2e^- \rightarrow H_2 \quad (4.22)$$

The graphite plate in the mini-SBR actually serves as current feeder because the surface of GIC particles is acting as the anode. This section aims to investigate the formation of free chlorine during the electrochemical regeneration of GIC materials in the mini-SBR at different experimental conditions.

4.3.1 Materials and Methods

Phenol was used as a model pollutant and Nyex®1000 was used as the adsorbent. All chemicals either used in the experiments or used in the analysis were supplied as analytical grade by Sigma-Aldrich®.

Electrochemical regeneration of fresh GIC adsorbent

The electrochemical regeneration of fresh GIC adsorbent (the material as supplied before it has been used for adsorption) was studied in order to investigate the effect of different parameters on the formation of free chlorine:

(i) Effect of catholyte composition

The effect of catholyte composition was studied either by changing the concentration of NaCl (0.1–2% w/v) for the same concentration of HCl (0.05 M) or by changing the concentration of HCl (0.05–0.5 M) for the same concentration of NaCl (0.3%). A sample of 120 g of Nyex®1000 was transferred into the mini-SBR, 500 mL of deionised water was added and mixed with Nyex®1000 by air sparging for 30 min. This was done to give similar mixing time as applied for adsorption of phenol onto the GIC adsorbent and also to fully wet the GIC particles. After mixing, the air supply was turned off and Nyex®1000 particles were allowed to settle on the anode side of the mini-SBR to form a uniform bed of particles as shown in Figure 4.3. In the cathode compartment, a specified concentration of NaCl and HCl was added as an electrolyte. A DC current of 0.7 A (10 mA cm^{-2}) was supplied for 140 min. 10

mL samples were taken after every five minutes for first 30 min and then every 10 min for remaining duration of the experiment. During sampling, the current was stopped momentarily and air was supplied for a few seconds to get a more uniform sample. The samples were filtered through a 0.45μm syringe filter and were immediately analysed for free chlorine (see below). The pH of water above the Nyex®1000 was also monitored using a Cyber Scan pH meter *(Eutech Instruments, Singapore)* when each sample was taken.

(ii) Effect of neutral pH

Initially, no attempt was made to keep the pH constant because acidic conditions exist during the electrochemical regeneration of GIC adsorbent due to the generation of hydrogen ions (eq 3.4). However during the continuous process of adsorption with electrochemical regeneration there is not a significant drop in pH and almost neutral pH can be achieved. In order to see the effect of neutral pH on the formation of free chlorine, 120 g of Nyex®1000 was transferred into the mini-SBR along with 500 mL of deionised water buffered with sodium phosphate (pH 7.0) and mixing was performed with the help of air sparging for 30 min. After mixing, the air supply was turned off and the particles of adsorbent were allowed to settle into the anode compartment of the electrochemical cell in the mini-SBR. In the cathode compartment, 0.3% NaCl solution (w/v) acidified with 5M HCl (to pH 1–2) was added as an electrolyte. A DC current of 0.7 A (10 mA cm^{-2}) was applied to regenerate the GIC bed. Samples (10 mL) were taken after every five min for first 30 min and after every 10 min till the duration of experiment. During sampling, as before the current was stopped momentarily and air was supplied for a few seconds. The samples were filtered through a 0.45μm syringe filter and were immediately analysed for free chlorine (see below). The pH of the water above the Nyex®1000 was also determined when each sample was taken.

(iii) Effect of current density

The electrochemical regeneration of fresh GIC adsorbent was carried out at different currents (0.7–2.1 A) to give current densities in the range of 10–30 mA cm^{-2} and

thus to explore the effect on the formation of free chlorine. For these experiments, the same methodology as outlined above in (ii) was adopted.

(iv) Effect of NaCl added to the water on the anode side

The formation of free chlorine was expected to be dependent on the concentration of chloride ions present in catholyte and/or their transfer from the catholyte to the anode under the influence of the applied cell voltage. The effect of the presence of chloride ions in the anode compartment was also studied by adding a specific amount of sodium chloride to the water on the anode side. In this context, 120 g of Nyex®1000 was transferred with 500 mL of 0.9% NaCl (w/v) in deionised water into the mini-SBR. The same procedure as outlined above in (ii) was adopted.

(v) Electrochemical oxidation of deionised water with sodium sulphate electrolyte

Electrochemical oxidation of deionised water was carried out with the help of an electrolyte to understand the role of GIC particles on the formation of free chlorine. For this 500 mL of 0.5% Na_2SO_4 (w/v) in deionised water was added into the mini-SBR without any Nyex®1000 adsorbent. In the cathode compartment, 0.3% NaCl solution (w/v) acidified with 5M HCl (to pH 1–2) was added as an electrolyte. A DC current of 0.7 A was supplied for 65 min. Samples (10 mL) were taken from the anode compartment every five minutes for first 30 min and every 10 min until 60 min had elapsed. The last sample was taken at 65 min. During sampling, the current was stopped momentarily and the water was slightly stirred with a glass rod for few seconds to obtain a representative sample. The samples filtered through a 0.45 μm syringe filter and were immediately analysed for free chlorine (see below). The pH of the water was also determined when each sample was taken.

Electrochemical Regeneration of phenol loaded GIC adsorbent

In order to study the formation of free chlorine in the actual (Arvia®) process which consists of adsorption of pollutant onto the surface of GIC adsorbent and then its subsequent electrochemical regeneration, 120 g of Nyex®1000 was transferred along with 500 mL of phenol solution having different initial concentrations in the range of

20–100 mg L^{-1} into the mini-SBR. Afterwards, the same methodology of adsorption and electrochemical regeneration as applied in (ii) above was adopted. A sample of solution was taken after adsorption and analysed for the phenol concentration. In addition to analysing the samples for free chlorine as mentioned in (ii), these samples were also analysed for phenol and its oxidation products (see section 4.1.3). The pH of the water above the Nyex®1000 was also determined when each sample was taken.

4.3.2 Analysis

The concentration of free chlorine was determined by a DPD colorimetric method. This method is applicable to natural and treated waters at concentrations from 0.2 to 4 mg L^{-1} of chlorine *(Clesceri, 1998)*. For higher concentrations appropriate dilutions were made prior to the analysis. The method uses an indicator, N,N-diethyl-p-phenylenediamine (DPD), which instantly reacts with free chlorine and produces a red colour. The intensity of this colour is spectroscopically measured at 515 nm and compared with a series of standards. The results are calculated as mg L^{-1} Cl. For the determination of phenol and its non-chlorinated oxidation products, please see section (4.1.2)

4.3.3 Results and Discussion

(i) Effect of catholyte composition

The results show that the rate of formation of free chlorine increased with an increase in the initial concentration of NaCl in the catholyte (Figure 4.41). This was presumably due to an increased concentration of chloride ions in solution in the anode compartment. The results also show that the free chlorine formation was relatively fast during the initial stage of the electrochemical process at all NaCl concentrations and then it appeared to decrease in the later stage of experiments for catholyte concentration of 1% NaCl or less (Figure 4.41). However, for 2% catholyte the rate of formation of free chlorine was observed to increase in the later stages of the process (Figure 4.41). *Oliveira et al. (2007)* observed a similar trend during their study on the influence of the anode material ($Ti/Sn_{(1-x)}$ Ir_xO_2 with different

compositions of Iridium, and graphite) on the generation of free chlorine by the electrochemical oxidation of 0.05 mol L^{-1} NaCl. However, they found that the production of active chlorine was much higher for DSA electrodes compared to a graphite electrode (<4mg L^{-1} even after 40 min at 25 mA/cm^2), indicating that DSA electrodes exhibited enhanced eletrocatalytic activity in comparison to graphite. During the electrochemical regeneration of the GIC adsorbent, 17, 20, 29 and 36 mg L^{-1} of free chlorine was formed for 0.1, 0.3, 1 and 2% NaCl in the catholyte, suggesting that the GIC particles performed better than the graphite electrode used by *Oliveira et al. (2007)*.

A low initial pH of 2.7 was observed was due to the washing of Nyex®1000 with water resulting in the release of acidic species from its surface. The pH decreased from 2.7 to around 1.9 during the course of the electrochemical process (data not shown). It can be seen from figure 4.40 that at pH less than 3 some of the free chlorine will be present as dissolved aqueous chlorine. Since the mini-SBR was an open system, the escape of some of the dissolved chlorine, especially during the time when air was blown through the cell, could not be avoided. This could be a contributing factor causing the reduction in the rate of formation of free chlorine after 20 min (Figure 4.41).

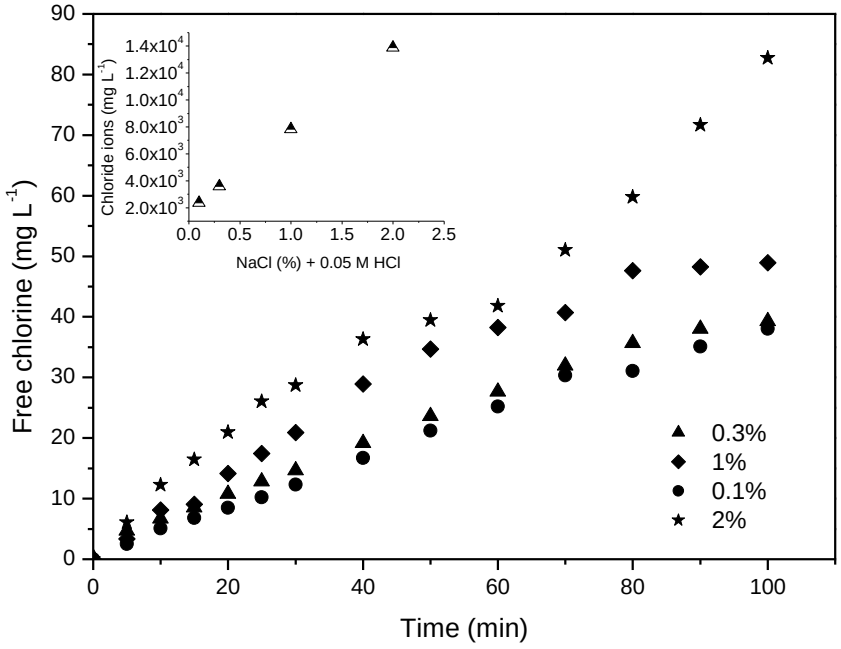

Figure 4.41: *Effect of time on formation of free chlorine at different concentrations of NaCl in the catholyte in the range of 0.1–2% (w/v) containing 0.05M HCl when 140 g of Nyex®1000 was mixed with 500 mL water for 30 min and then regenerated at 0.7 A (10 mA cm^{-2}) current for 100 min*

Similar trends were observed during electrochemical regeneration of GIC adsorbent at different concentrations of HCl in the range of 0.05–0.5M and 0.3% (w/v) NaCl in the catholyte (Figure 4.42). This suggests that the rate of formation of free chlorine is in fact dependent upon the concentration of the chloride ions in catholyte which can be increased either by increasing the amount of salt or by increasing the concentration of HCl. For economical reasons, it is likely to be more appropriate to increase the concentration of the salt in order to produce more free chlorine.

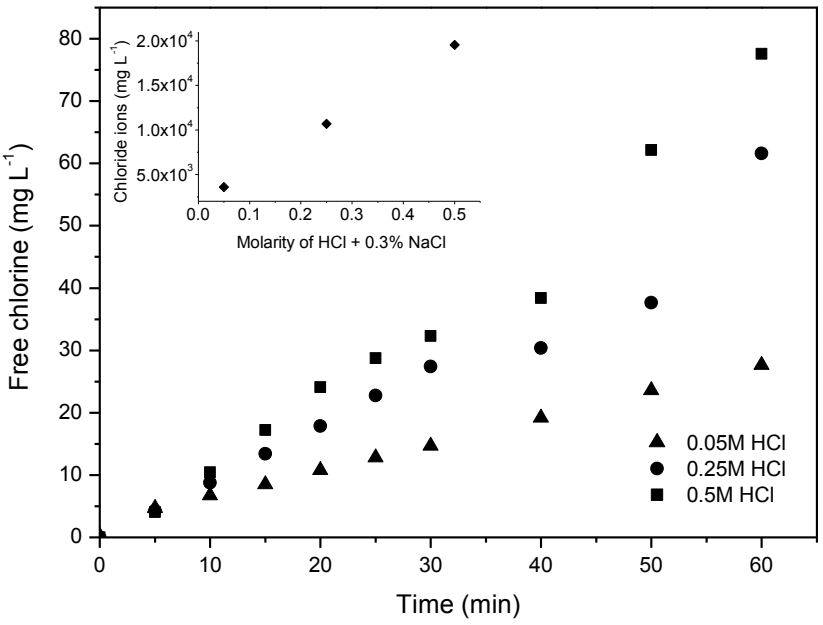

Figure 4.42: *Formation of free chlorine at different HCl concentrations of catholyte in the range of 0.05–0.5M for 0.3% NaCl (w/v) when 140 g of Nyex®1000 was mixed with 500 mL of water for 30 min and then regenerated at 0.7 A (10 mA cm^{-2}) current for 100 min*

Current efficiency can be defined as the ratio of the theoretical charge requirement for a desired reaction to the actual charge consumed. The percentage charge yield (current efficiency) for the generation of free chlorine can be calculated from:

$$\Phi^{e}_{Cl_2} = \frac{2F[Cl_2]V}{It} \times 100 \qquad (4.23)$$

where F is Faraday's constant (96485.35 C mol^{-1}), V is the volume (L), I is the current (A) and t is the time in seconds.

The maximum values of current efficiency were observed after five minutes of electrochemical treatment, for all the concentrations of sodium chloride in the catholyte, as shown in Figure 4.43. The current efficiency subsequently decreased in all cases, with a faster decrease during the initial stages. The decrease in current

efficiency was presumably due to oxygen evolution caused by the discharge of water according to equation 4.20 *(Abdel et al. 1993; Scialdone et al. 2009)*. The low values of current efficiency associated with the production of free chlorine in this study could be associated with the concentrations of chloride ions present and the type of electrode used *(Kraft, 2008)*. The observed current efficiencies (for 0.1% NaCl) can be compared with the values of less than 2% obtained for free chlorine formation when platinum and boron-doped diamond electrodes were used with a chloride concentration of 180 mg L^{-1} *(Kraft, 2008)*. The concentration of chloride ions used by *Kraft, (2008)* was much less than the initial chloride concentration used in the cathode compartment of the mini-SBR. The results show that at the start of the electrochemical process, higher current efficiencies were obtained with higher concentrations of chloride ions. This observation suggests that, under these conditions, the rate of formation of free chlorine was influenced by the rate of mass transfer of chloride from the catholyte. The average chloride ion flux was estimated to be around 0.004 mg min^{-1} cm^{-2} (based on membrane area) for free chlorine formation when 0.3% NaCl was used as catholyte.

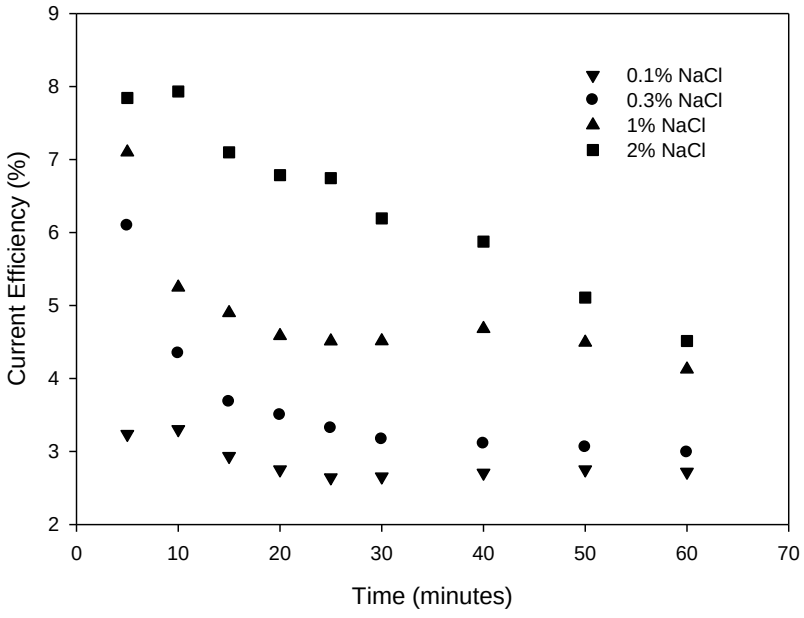

Figure 4.43: *Current efficiency during the formation of free chlorine at different NaCl concentrations of catholyte in the range of 0.1–2% (w/v) containing 0.05M HCl when 140 g of Nyex®1000 was mixed with water for 30 min and then regenerated at 0.7 A (10 mA cm^{-2}) current for 100 min*

(ii) Effect of current density

Figure 4.44 shows the effect of current density on the formation of free chlorine in solution, when the current was varied from 0.7 to 2.1 A to give current densities in the range of 10–30 mA cm^{-2}. The results reveal that the higher the current applied, the higher the chlorine concentration that could be formed. The results also indicate that even a comparatively low current density of 10 mA cm^{-2} promotes the oxidation of chloride ions into chlorine. In addition, the effect of increasing the current density on the formation of free chlorine is more significant than that achieved by increasing the chloride concentration of the catholyte under the experimental conditions studied. However, the maximum current efficiency remained below 4% for 20 and 30 mA cm^{-2} as shown in figure 4.45. A higher current density was found to improve the rate of free chlorine formation but not the current efficiency. When the process is under the influence of mass transfer, lower current density is expected to give rise to higher current efficiency *(Scialdone et al. 2009)*.

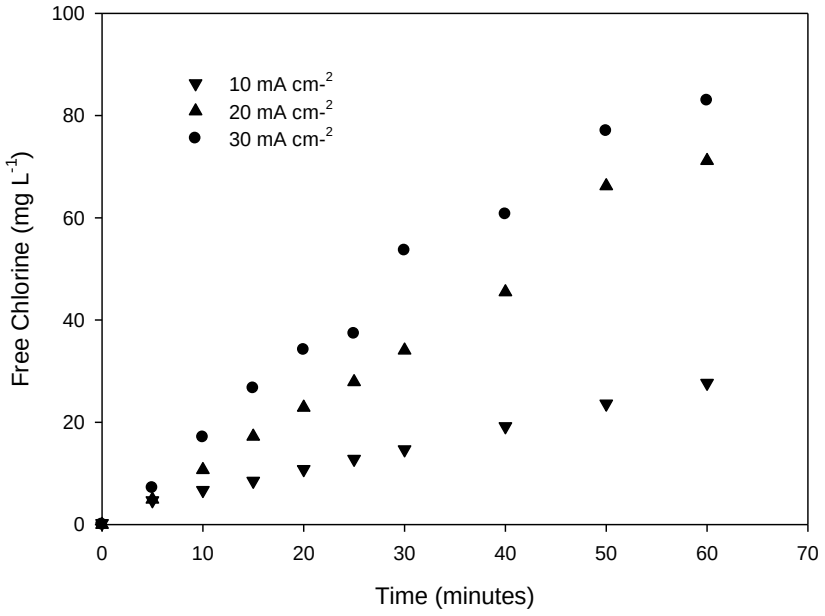

Figure 4.44: *Effect of current density on the formation of free chlorine when 140 g of Nyex®1000 was mixed with 500 mL of water and then regeneration was carried out at 0.7, 1.4 and 2.1 A for 60 min. Catholyte was 0.3% (w/v) NaCl solution containing 0.05M HCl*

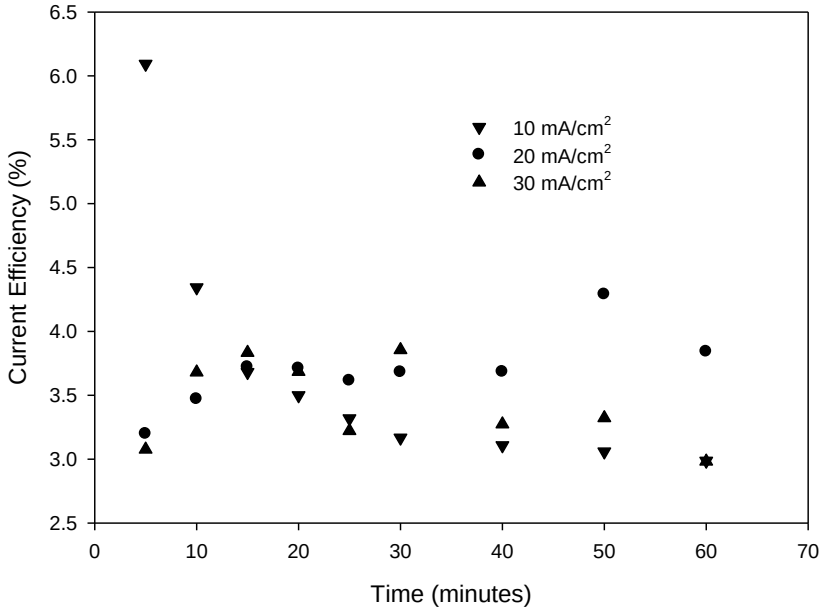

Figure 4.45: *Current efficiency during the formation of free chlorine at current density in the range of 10–30 mA cm^{-2} when 140 g of Nyex®1000 was mixed with water for 30 min and then regenerated at 0.7 A current for 60 min, Catholyte used was 0.3% (w/v) NaCl solution containing 0.05M HCl*

(iii) Effect of neutral pH on free chlorine formation

During the course of an electrochemical process which has not been buffered to keep constant pH conditions, the evolution of both oxygen and chlorine result in a decrease in the pH of the water adjacent to the anode surface. In the case of oxygen evolution, hydrogen ions are being produced according to equation 4.20. When chlorine is being generated at the anode, it immediately undergoes hydrolysis and therefore also produces hydrogen ions according to equation 4.5. Due to both of these processes, acidic conditions exist during electrochemical regeneration of GIC adsorbent. Therefore in order to evaluate the formation of free chlorine at neutral pH in the batch electrochemical process, the pH of the water was adjusted at 7.0 using a phosphate buffer. The results show that the concentration of free chlorine increased with time but appeared to approach a maximum concentration of around 6 mg L^{-1} after 140 min (Figure 4.46). This concentration was only about 30% of the free chlorine concentration obtained when no buffer was added at the same catholyte composition (acidified 0.3% NaCl) (Figure 4.41). These results suggest that either the formation of chlorine is pH dependent or some side reaction is taking place

which inhibits the anodic evolution of chlorine, ultimately reducing the concentration of free chlorine. *Abdel et al. (1993)* explained that when the anode becomes more acidic, the thermodynamic voltage for oxygen evolution becomes more anodic. This situation favours the evolution of chlorine which is independent of pH. At a neutral pH, the oxygen evolution is likely to be competing with chlorine evolution and therefore affecting the rate of free chlorine generation. The trend of current efficiency versus time was similar to the previous case where the pH was not controlled, although the current efficiency was significantly lower, with a maximum value of around 2% (Figure 4.47).

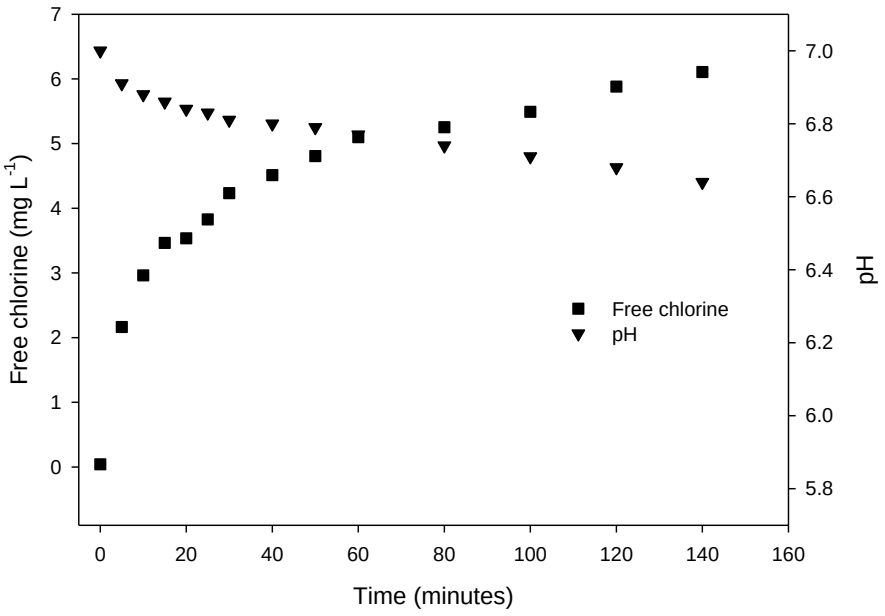

Figure 4.46: *Formation of free chlorine during electrochemical regeneration of fresh Nyex®1000 using phosphate buffer to maintain neutral pH at 0.7A (10 mA cm^{-2}) with a cell voltage of 3.7 V. Catholyte used was 0.3% (w/v) NaCl solution containing 0.05M HCl*

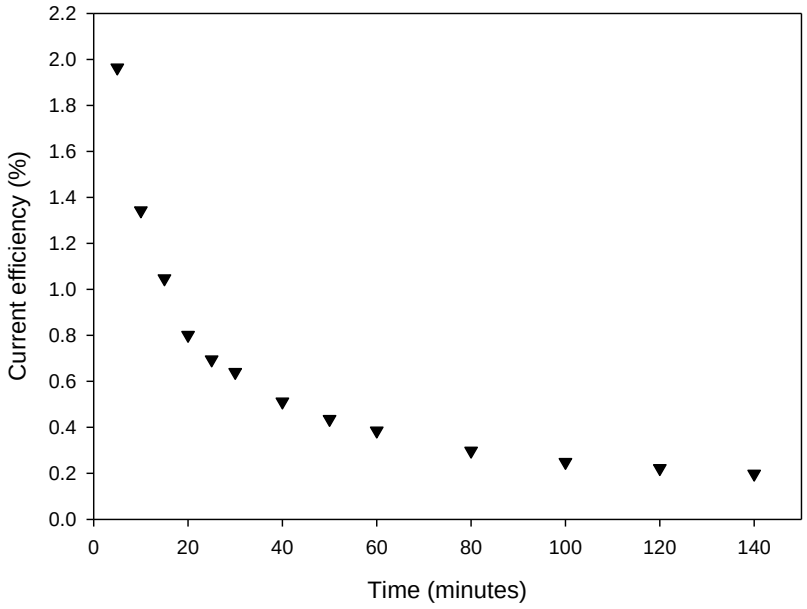

Figure 4.47: *Current efficiency versus time during electrochemical regeneration of fresh Nyex®1000 using phosphate buffer to maintain neutral pH at 0.7 A (10 mA cm^{-2}) with a cell voltage of 3.7 V.*

(iv) Effect of NaCl as anolyte on the formation of free chlorine

The current efficiency associated with the formation of free chlorine in the electrochemical regeneration of GIC adsorbent could be limited due to:

- The low initial concentration of chloride ions
- Mass transfer limitations
- Poor kinetics due to the electrode material

In an attempt to study the effect of an increase in chloride concentration on the formation of free chlorine in the Arvia® process, normal saline [9 g L^{-1} NaCl (w/v)] was used in the anode compartment with the Nyex®1000. This is equivalent to 5450 mg L^{-1} of chloride concentration in the anode compartment. The results show that free chlorine concentration increased to 87 mg L^{-1} in 110 min (Figure 4.48) which was approximately 2.5 times greater than the free chlorine produced when no chloride was added to the anode compartment (Figure 4.41) for the same catholyte composition (acidified 0.3% NaCl). After 110 min, the drop in the concentration of free chlorine was probably due to the loss of chlorine by stripping during air sparging.

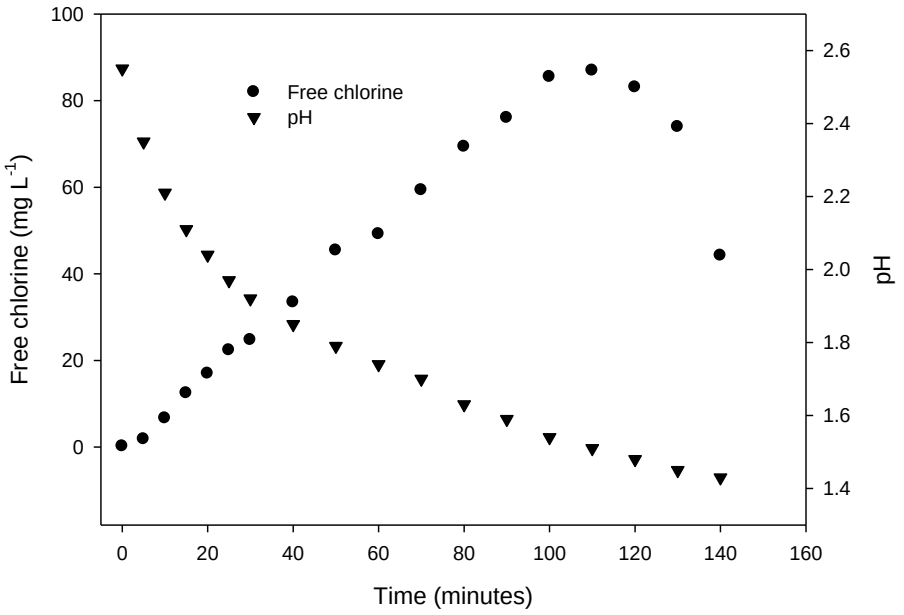

Figure 4.48: *Free chlorine formation during electrochemical regeneration of fresh Nyex®1000 using deionised saline water at 0.7 A (10 mA cm^{-2}) with a cell voltage of 4.1-5.6 V. Catholyte used was 0.3% (w/v) NaCl solution containing 0.05M HCl*

In this case the current efficiency followed a somewhat different trend, initially increasing to a maximum of around ca. 4% after 25 min, remained almost constant until 110 min of treatment, then decreasing due to the decreasing free chlorine concentration (Figure 4.49). The current efficiencies obtained can be compared to the current efficiency (4.6%) reported for iridium oxide coated titanium anode at a low chloride concentration of 60 mg L^{-1} *(Kraft et al. 1999)*. The constant current efficiency observed after 20 min suggests that the supply of chloride ions onto the surface of GIC particles was not mass transfer limited, compared to the previous cases where the chloride ions were required to transfer from the cathode to the anode compartments by diffusion and ionic migration through the membrane.

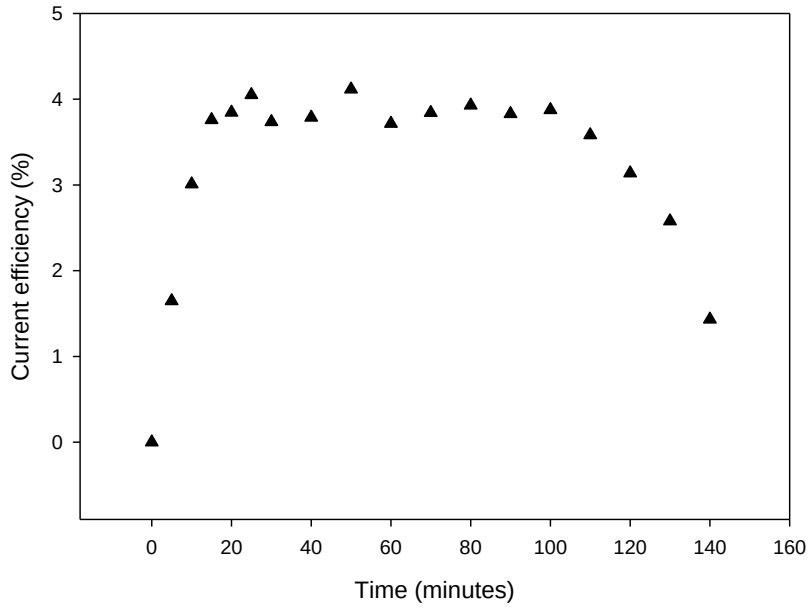

Figure 4.49: *Effect of time on current efficiency during electrochemical regeneration of fresh Nyex®1000 using deionised saline water at 0.7 A (10 mA cm^{-2}) with a cell voltage of 4.1-5.6 V.*

(v) Free chlorine formation during electrochemical oxidation of deionised water using sodium sulphate in the mini-SBR

In order to compare the formation of free chlorine at the graphite anode of the mini-SBR without the addition of GIC particles, the electrochemical oxidation of water using 0.5% Na_2SO_4 as an electrolyte was carried out. The results show that the presence of sodium sulphate with deionised water as an electrolyte suppressed the formation of free chlorine and only approximately 4 mg L^{-1} of free chlorine was formed in 30 min (Figure 4.50). A significant amount of free chlorine was formed in the presence of GIC particles compared to the case when no GIC was used in the mini-SBR. In addition, very low values of current efficiency were associated with the formation of free chlorine during electrochemical oxidation of water using sodium sulphate in the absence of GIC adsorbent (Figure 4.50). The current efficiency first increased to a value of 0.68 and then appeared to decrease as shown in figure 4.50.

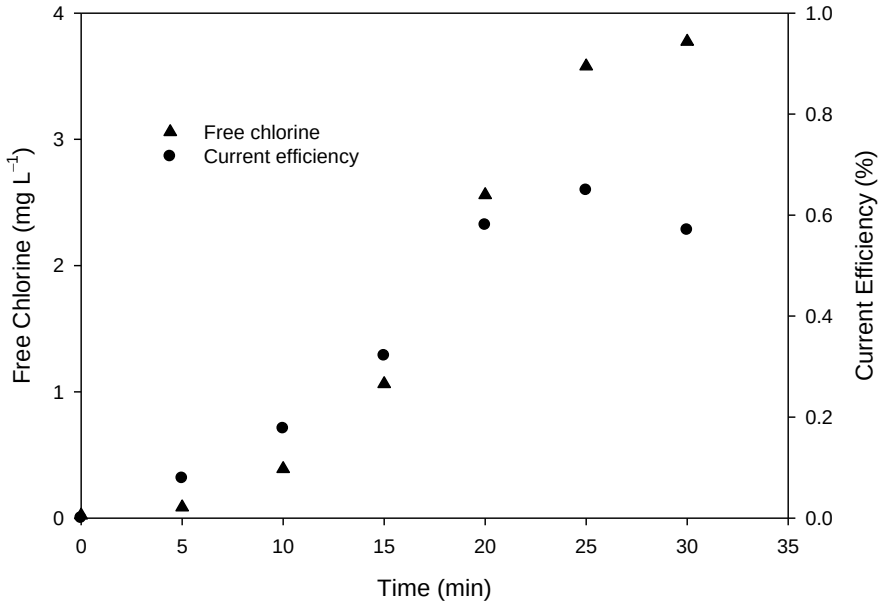

Figure 4.50: *Free chlorine formation and current efficiency during electrochemical oxidation of deionised water containing 0.5% sodium sulphate as anolyte at 0.7 A (10 mA cm^{-2}) with a cell voltage of 7.1-5.7 V.*

(vi) Free chlorine generation during electrochemical regeneration of phenol loaded GIC adsorbent

In all the situations discussed above, the objective was to quantify the free chlorine formed under a range of experimental conditions. In the actual process of adsorption with electrochemical regeneration using GIC adsorbents the role of free chlorine could be more crucial as it could react with the adsorbed or dissolved organics and convert them into chlorinated compounds which could be more toxic than the original organic contaminant. These species would be a problem only if they were released into solution. In order to investigate this process, different initial concentrations of phenol (20, 50 and 100 mg L^{-1}) were adsorbed onto Nyex®1000 and their subsequent electrochemical regeneration was carried out in the mini-sequential batch reactor. The results show that during the course of electrochemical regeneration of phenol loaded Nyex®1000 at different initial concentrations, the amount of free chlorine increased to a moderate level during the period of phenol oxidation and then increased to a comparatively higher concentration upon the complete removal of phenol (Figure 4.51 – 4.53). The first section in all cases might be representing the balance of free chlorine available after a portion of it has been

reacted with phenol and the second part showed the free chlorine available after the phenol had been depleted. These results are in good agreement with work on electrolytic destruction of urea in dilute chloride solution using DSA electrodes operated in batch recycle mode *(Hernlem, 2005)*. The reaction of free chlorine with phenols could bring about the chlorination of the aromatic ring firstly and successive chlorination will lead to the formation of mono-, di- and tri-chlorophenols *(Gallard, 2002)*. While the concentration of phenol diminishes during the course of electrochemical regeneration of Nyex®1000, the concentration of the intermediate product, benzoquinone, initially increased and then remained almost constant. This suggests that the benzoquinone did not react with the free chlorine to form chloro-benzoquinone. The rate of decrease of phenol concentration was relatively fast compared to the case when there was no formation of free chlorine (data not shown). The decrease in pH during electrochemical regeneration was from 2.2 to 1.5 (not shown). At pH below 2 the major component of free chlorine is molecular chlorine and this was thought to be a stronger oxidant than HOCl which could explain the higher rates of phenol oxidation *(Rule et al. 2005)*.

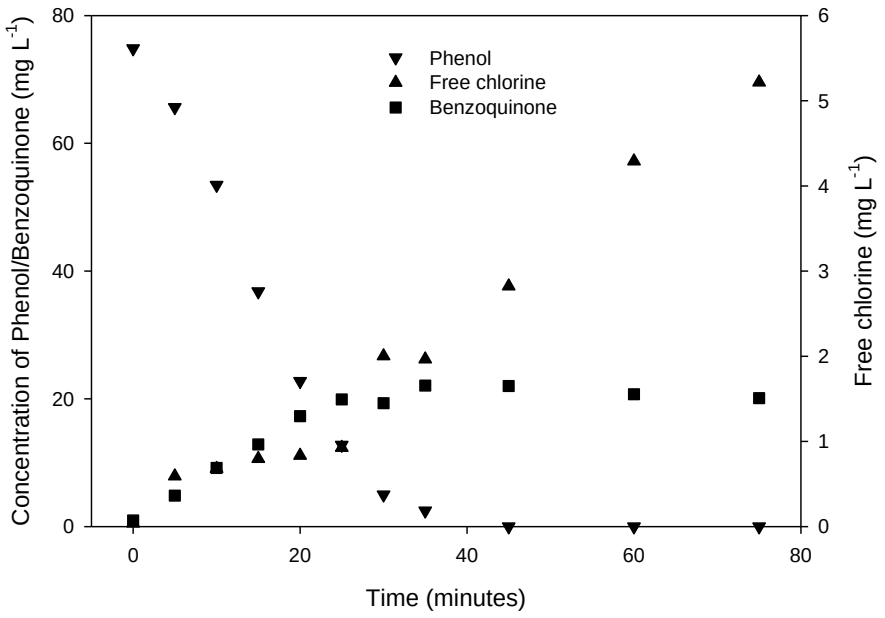

Figure 4.51: *Free chlorine formation and breakdown products generated during electrochemical regeneration of phenol loaded Nyex®1000 at an initial concentration of 100 mg L^{-1}, 0.7 A (10 mA cm^{-2}) with a cell voltage of 6.0-8.1. Catholyte used was 0.3% (w/v) NaCl solution containing 0.05M HCl*

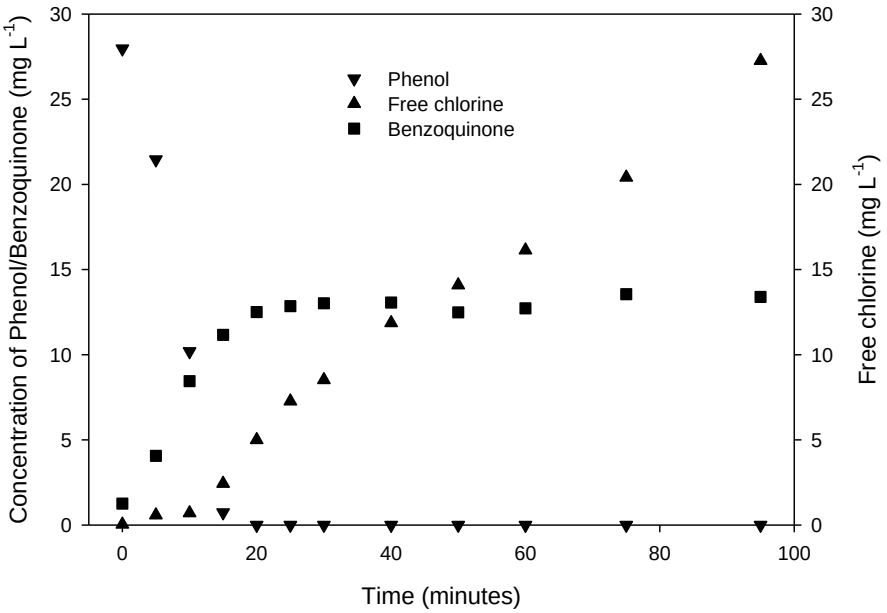

Figure 4.52: *Free chlorine formation and breakdown products generated during electrochemical regeneration of phenol loaded Nyex®1000 at an initial concentration of 50 mg L^{-1}, 0.7 A (10 mA cm^{-2}) with a cell voltage of 5.4-6.1, pH varies from 2.35 to 1.68.*

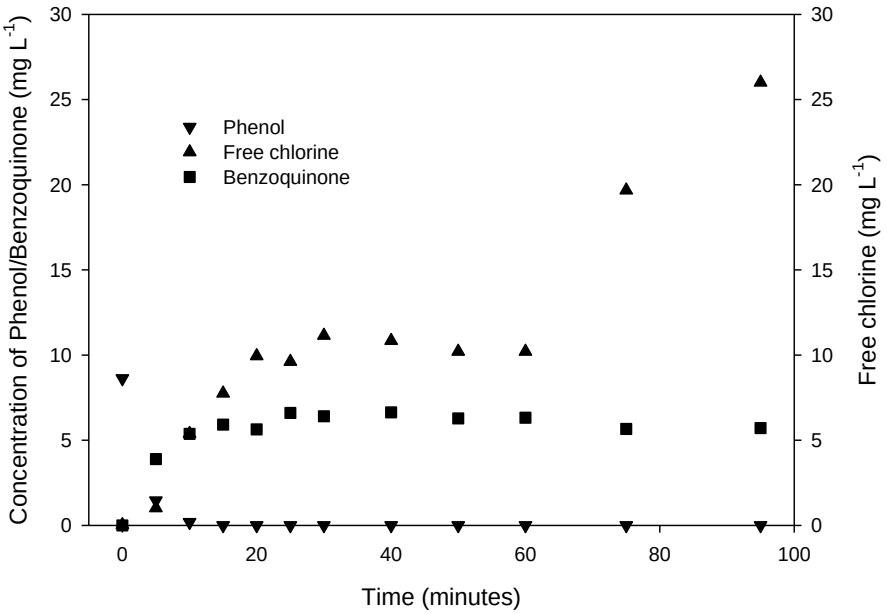

Figure 4.53: *Free chlorine formation and breakdown products generated during electrochemical regeneration of phenol loaded Nyex®1000 at an initial concentration of 20 mg L^{-1}, 0.7 A (10 mA cm^{-2}) with a cell voltage of 5.1-6.3, pH varies from 2.26 to 1.66.*

4.3.4 Conclusions

This section has demonstrated that the formation of free chlorine during electrochemical regeneration of the GIC adsorbent is a function of various parameters including the initial concentration of chloride ions, current density, and pH. The rate of formation of free chlorine increases with an increase in the concentration of chloride ions in the catholyte, which can be increased either by increasing the concentration of sodium chloride or HCl. The current efficiency associated with the generation of free chlorine was also found to increase with an increase in the chloride concentration in the catholyte with the highest value of around 8% obtained when 14 g L^{-1} (2% w/v NaCl and 0.05M HCl) of chloride ions were present in the catholyte. However, the current efficiency decreased with the passage of time during the electrochemical regeneration of GIC adsorbent. These findings suggest that the generation of free chlorine was occurring under the influence of mass transfer. It has also been shown in this section that the effect of increasing the current density on the rate of formation of free chlorine was larger than that achieved by increasing the chloride contents of catholyte. However, the current efficiency was not found to be improved with an increase of current density. The concentration of free chlorine was reduced by 30% during electrochemical oxidation of fresh GIC adsorbent at neutral pH in comparison to the concentration formed under acidic conditions. An experiment carried out in the absence of the adsorbent highlighted the importance of GIC particles in enhancing the rate of formation of free chlorine during the electrochemical regeneration of the adsorbent. The concentration of free chlorine formed during electrochemical oxidation of water with sodium sulphate as catholyte was significantly lower than that obtained during electrochemical regeneration in the presence of the GIC adsorbent.

The rate of formation of free chlorine was reduced when phenol was present in solution, indicating that the reaction of free chlorine with phenol was occurring. Benzoquinone formed during the electrochemical regeneration at different initial concentrations of phenol was not found to react with the free chlorine.

These findings regarding the formation of free chlorine during electrochemical regeneration of GIC adsorbent at different experimental conditions has important

implications for optimising the conditions to minimize the formation of chlorinated breakdown products (see section 4.2) and for electrochemical disinfection (see chapter 8).

4.4 Investigation of breakdown products during continuous adsorption with electrochemical regeneration

4.4.1 Materials and Methods

The continuous adsorption and electrochemical regeneration unit was introduced in chapter 1 (see section 1.2.2). The reactor shown schematically in figure 1.2 was designed to perform continuous adsorption and electrochemical regeneration in separate zones in the same unit. The reactor used in this study was constructed from clear polycarbonate and the internal dimensions of the unit were 35 cm wide, 2.2 cm deep and 147 cm tall. The adsorption zone consisted of two symmetrical side zones, each with a rectangular cross section of 10 cm by 2.2 cm. The regeneration section was composed of an anode and cathode separated by a membrane and with a bed of GIC particles flowing downward in the anode compartment. The anode current feeder used was a mixed metal oxide coated titanium (Electrode Products Technology Ltd, UK) and the cathode was a perforated stainless steel plate. The area of each electrode was 12 cm wide by 60 cm in height. A microporous polyethylene membrane (Daramic GmbH, Germany) separated the GIC adsorbent from the cathode. In order to generate mixing and to circulate the adsorbent continuously, air was injected at the bottom of both adsorption zones through 14 injection nozzles. The total flow rate of air was adjusted to ca. 5 L min^{-1} so that the injected air entrained the adsorbent from the bottom of the regeneration zone into the adsorption zones and a uniform bed movement is attained. The effluent to be treated was injected close to the bottom of the adsorption zones. At the top of the adsorption zones, the air bubbles disengaged and the water flowed into a settlement zone, in which the loaded solid particles were separated out from the upward flowing treated effluent. As the high density solid particles settled in the centre of the unit, they formed a moving bed between the anode and the membrane in the regeneration chamber.

To start up the continuous unit, it was necessary to develop a bed of GIC adsorbent in the regeneration zone. The reactor was filled with clean water from a feed tank using a perilistaltic pump (figure 4.54). A solution of sodium chloride (0.3% w/v) at pH 1(adjusted using HCl) from a separate tank was circulated through the cathode compartment as shown in figure 4.54. A mass of 2.5 kg of GIC adsorbent (2.5 kg) was present in the cell. It was set initially in motion by injecting a moderate air flow to the outer nozzles located near the walls of the reactor in order to have adsorbent circulation in the two adsorption zones. At this stage, no air was injected at the injection points close to the regeneration bed. After the build up of the bed in the regeneration zone, air was supplied to the injection nozzles close to the bed so that the bed also started to move. These conditions were then maintained to have steady state bed movement.

The adsorbent was cleaned for 3 hours by running tap water at a current density of 7 mA cm^{-2}. The flow rate of water was adjusted at 200 mL min^{-1}. After the adsorbent had been cleaned, the water supply was turned off and the feed was switched to second tank which was filled with 25 L of 500 mg L^{-1} of phenol solution. It was allowed to flow through the reactor in a recirculation mode i.e. the outlet from the reactor was returned to the feed tank, under the following operating conditions:

- Solution flow rate = 380 mL min^{-1}
- Solution concentration = 500 mg L^{-1}
- Current = 7 mA cm^{-2}
- Run time = 21 h
- Air flow rate = 4.8 L min^{-1}
- Mode = Recirculation

Samples were taken from the feed tank and the reactor outlet every 30 minutes. The flow rate of the pump was checked every hour by collecting solution into a measuring cylinder for five minutes. The pH of the catholyte was checked using pH paper and was maintained at around 1–2.

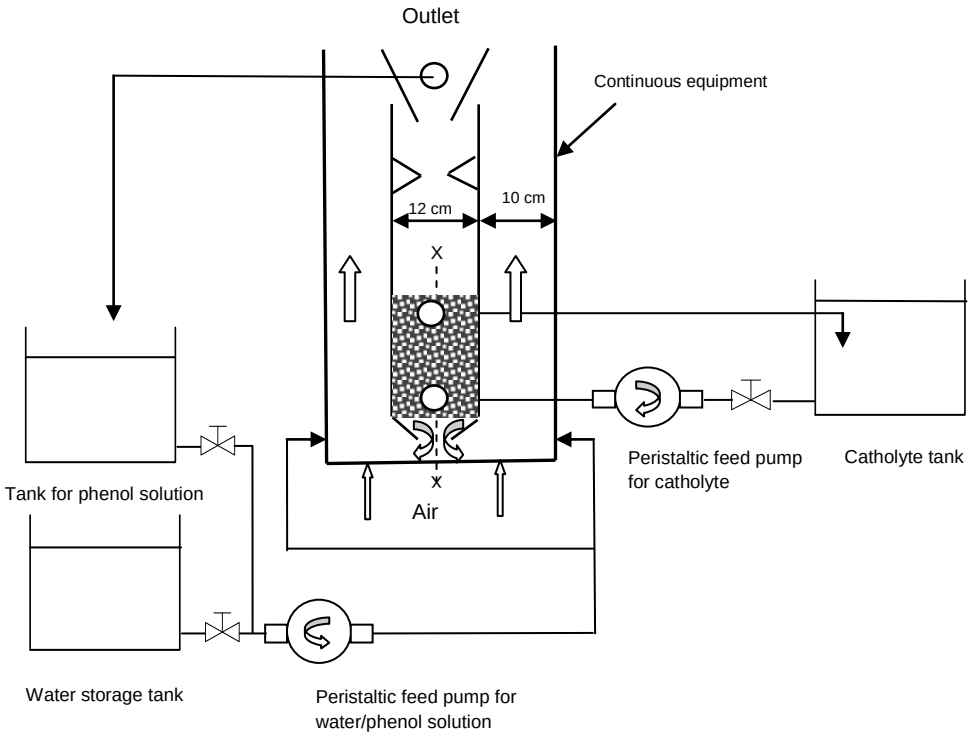

(a)

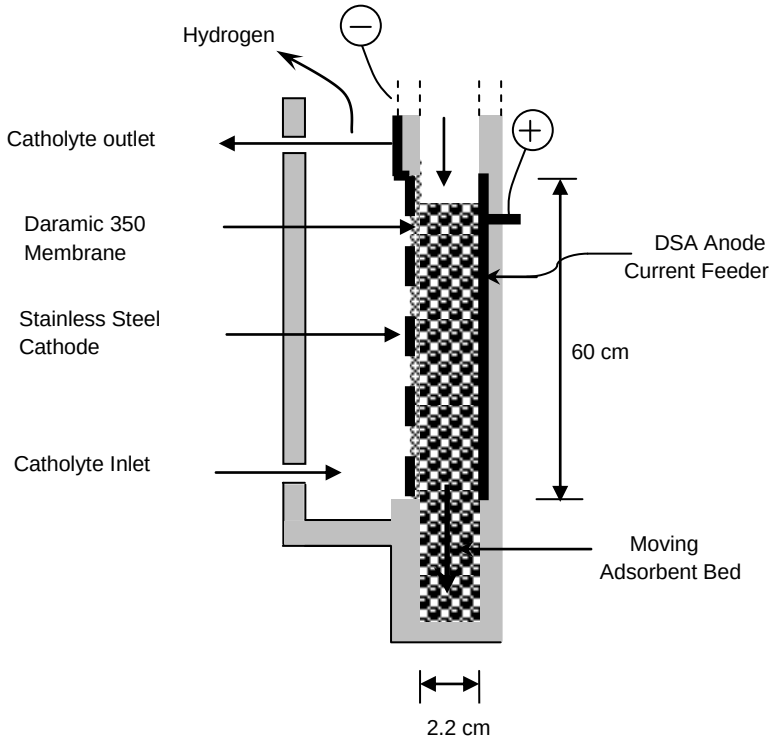

(b)

Figure 4.54: *Schematic diagram of the equipment used for continuous adsorption and electrochemical regeneration. (a) Schematic diagram of the continuous unit with auxiallry equipments, and (b) Schematic diagram of the electrochemical regeneration zone illustrating a cross section through line X-X in (a)*

4.4.2 Results and Discussions

The electrochemical regeneration of GIC adsorbent loaded with phenol in the continuous electrochemical reactor has similarities with the studies carried out in batch electrochemical cells. In this context, the principle aromatic breakdown product was 1,4-benzoquinone, formed during the continuous electrochemical regeneration of GIC adsorbent at a current density of 7 mA cm^{-2}. Benzoquinone was detected in the feed tank as well as in outlet stream (Figure 4.55). The concentration of benzoquinone was slightly higher in the outlet compared to its concentration in the feed tank as shown in figure 4.55. This suggests that benzoquinone was being generated in the reactor throughout the experiment. Conversely, the concentration of phenol in the tank was higher than its concentration in the outlet, indicating that phenol removal / oxidation was occurring in the reactor. The concentration of phenol was eliminated completely from the water outlet stream after 15 hours of operation (Figure 4.53). The concentration of benzoquinone increased over this time interval and the maximum concentration of benzoquinone generated was 56 mg L^{-1} after 21 hours. This accumulation of benzoquinone indicated that the formation rate was greater than the rate of degradation. This suggests that the oxidation of benzoquinone can be considered as the rate limiting step for the oxidation of phenol into carboxylic acids. The other non-chlorinated aromatic intermediate identified was hydroquinone, present in very low concentrations (data not shown). As has already been discussed, hydroquinone is the first product formed directly by the oxidation of phenol. The presence of very low concentrations of hydroquinone suggests that its oxidation into benzoquinone is relatively fast.

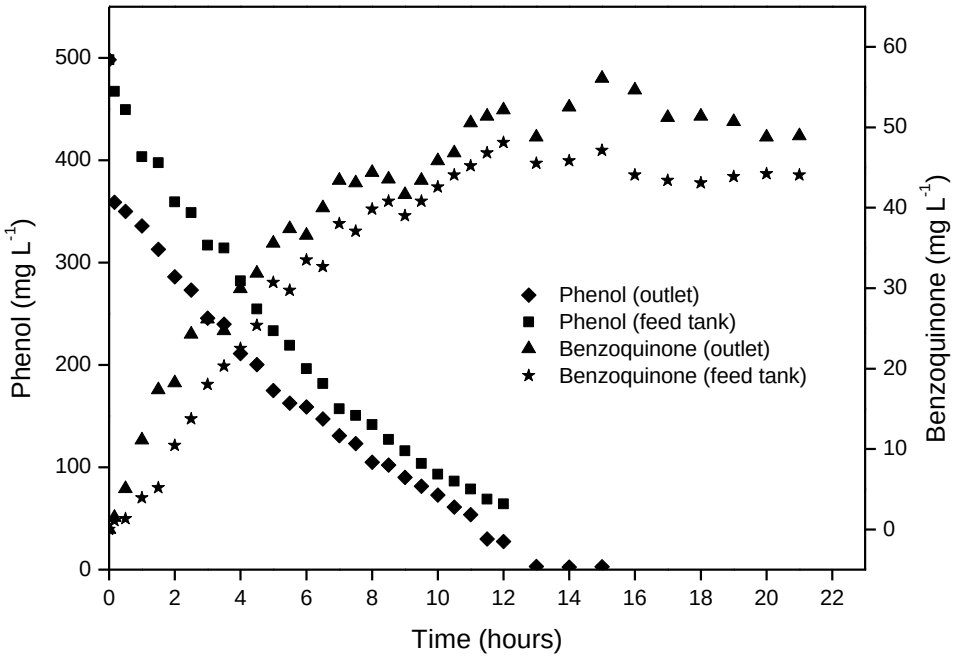

Figure 4.55: *Concentration of phenol and benzoquinone during continuous adsorption and electrochemical regeneration for 500 mg L^{-1} phenol solution at 7 mA cm^{-2}*

As far as the formation of chlorinated breakdown products was concerned, small concentrations of 2-chlorophenol (2-CP) and 4-chlorophenol (4-CP) were formed during the initial period of operation, but these gradually disappeared at long operating times as shown in figure 4.56. In addition, extremely small concentrations of 2,4-dichlorophenol (2,4-DCP) were also detected during the continuous process. The concentrations of the mono-chlorphenols increased in the initial 8–9 h both in the tank and reactor outlet. After around 10 h of operation the concentrations of mono-chlorophenols started to decrease with almost negligible concentrations detected after 20 h. The relatively low concentrations of chlorinated breakdown products during the continuous electrochemical regeneration could be due to the low current density used. The data compares with the formation of chlorophenols during the batch electrochemical regeneration of GIC adsorbent for 100 mg L^{-1} phenol solution at 10 mA cm^{-2}. As discussed in section 4.2, high concentrations of phenol in solution results in relatively high concentrations of chlorophenols. However, the low

current density is more important in minimizing the formation of chlorinated species even for higher concentrations of phenol in the starting solution.

On the other hand, the low current density was not effective for decreasing the concentration of benzoquinone during the time period when the concentrations of mono-chlorphenols started to decrease. In addition, chlorophenols are known to have a higher adsorptive capacity than phenol and benzoquinone and thus they are likely to be preferentially adsorbed on the GIC adsorbent. Adsorption may be followed by the oxidation of these species on the surface of adsorbent during electrochemical regeneration leading to a solution with relatively high concentrations of benzoquinone.

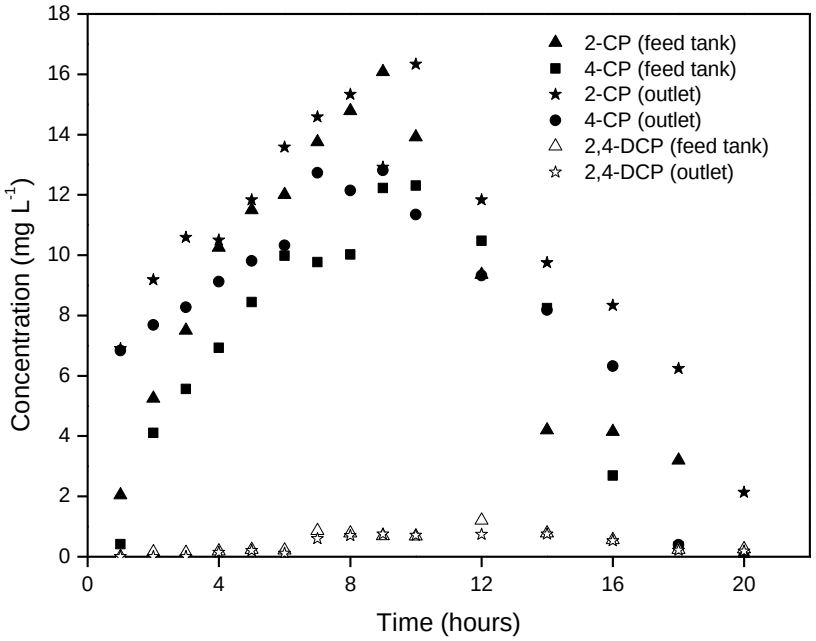

Figure 4.56: *Concentrations of chlorphenols during continuous adsorption and electrochemical regeneration for 500 mg L^{-1} phenol solution at 7 mA cm^{-2}*

In addition to the formation of these aromatic intermediates, maleic and oxalic acid were also observed during the continuous process as shown in figure 4.57. Relatively low concentrations of maleic acid were found in comparison to the oxalic acid whose concentration increased with time. The trends of the formation of carboxylic acids closely match with the formation of these acids during the batch regeneration studies (see section 4.1.4).

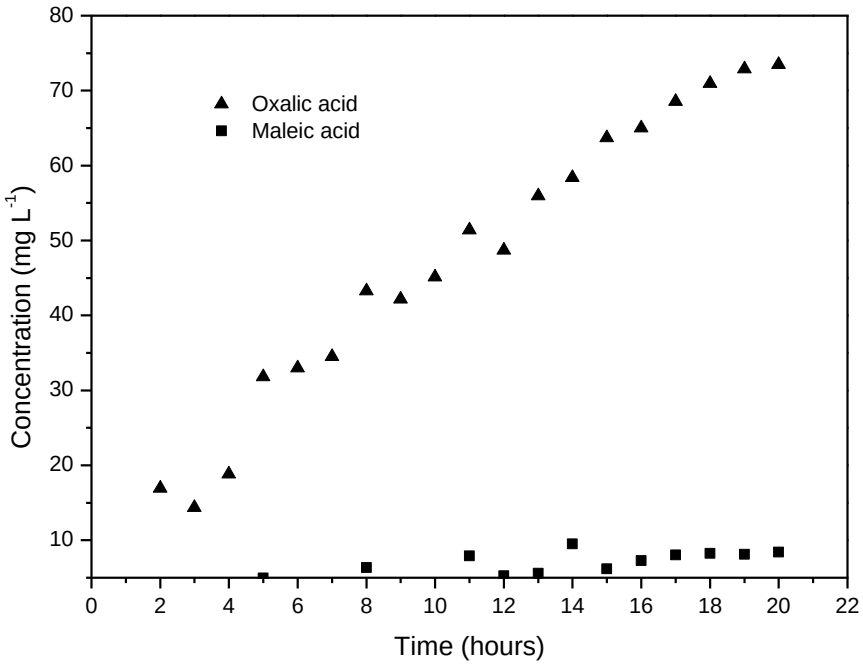

Figure 4.57: *Concentrations of maleic and oxalic acids in the water outlet during continuous adsorption and electrochemical regeneration for 500 mg L^{-1} phenol solution at 7 mA cm^{-2}*

In order to further analyse the continuous process of adsorption with electrochemical regeneration, it was assumed that the benzoquinone was the main aromatic intermediate generated during the continuous electrochemical regeneration for the phenol solution. The percentage of phenol degraded and the percentage of aromatics formed relative to the amount of phenol removed during the continuous process were calculated as *(Iniesta et al. 2001)*:

$$\%\,\text{Phenol Converted} = \frac{(\text{Phenol})_o - (\text{Phenol})_t}{(\text{Phenol})_0} \times 100 \tag{4.24}$$

$$\%\text{Aromatics} = \frac{[\text{Aromatics}]}{(\text{Phenol})_o - (\text{Phenol})_t} \times 100 \tag{4.25}$$

where [Aromatics] is the concentration of aromatic intermediates (benzoquinone) in mmol dm^{-3}. $(Phenol)_o$ and $(Phenol)_t$ are the concentrations of phenol at the start of the process and at any time *t* in mmol dm^{-3}.

The figure 4.58 showed that around 10% of the phenol was converted to aromatics after 12 hour. It is also clear from the data shown in figure 4.55, that 50% of the total benzoquinone formed was produced in the first 3 hours suggesting that the rate of formation of benzoquinone was high in the first 3-4 hours. Similarly the rate of removal of phenol was higher in the first few hours as shown in figure 4.55. In the first 12 hours, the phenol concentration in the outlet stream has been reduced by 95%. The data in figure 4.58 also shows that approximately 4% of the phenol was converted to chlorophenols during the first 10 h, but after this the percentage converted to chlorophenols fell close to zero after 20 h of treatment. This suggests that less phenol is converted to chlorinated breakdown products compared to the formation of non-chlorinated products.

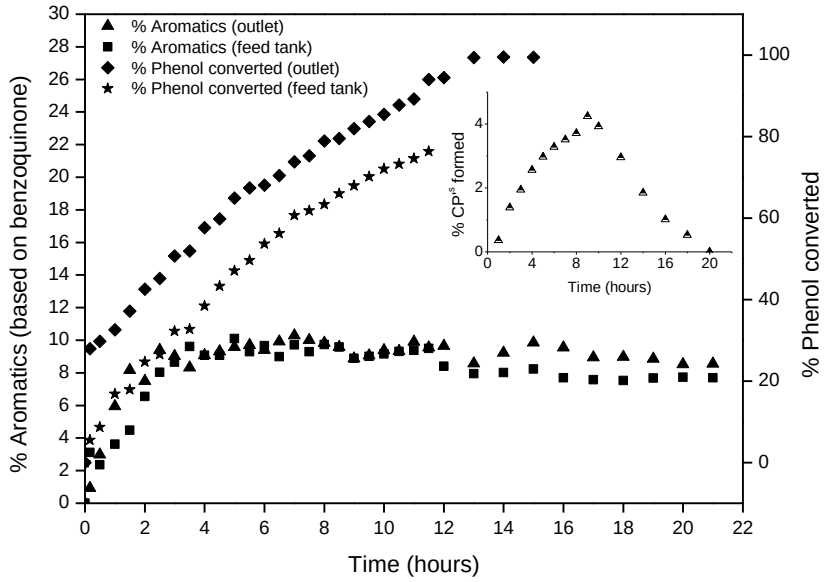

Figure 4.58: *Trend of the percentage of aromatics formed relative to the percentage of phenol removed. This figure also shows the percentage of chlorophenols formed during the continuous electrochemical regeneration*

In addition to the breakdown products for the continuous process, the observed decrease in TOC of the water both in feed tank and the outlet stream, as shown in figure 4.59, suggests that the organic contaminants and breakdown products have been removed and destroyed.

However, it may also be possible that the phenol ends up in another form such as a polymer which needs further investigation (see chapter 9). The results show that the

removal of organic carbon was rapid at the beginning of the electrochemical regeneration. At long times, the concentration of organic carbon (TOC) reached a steady state, with only 64% removal achieved after 21 h of treatment. Of the total TOC removal achieved after 21 hours, 95% of this was achieved in the first 12 hours. Based on the amounts of known breakdown products in solution after 21h, the corresponding value of TOC may be estimated around 40% of the TOC actually present in solution after 21 h. The remaining TOC may be due to the formation of polymers that needs further investigation.

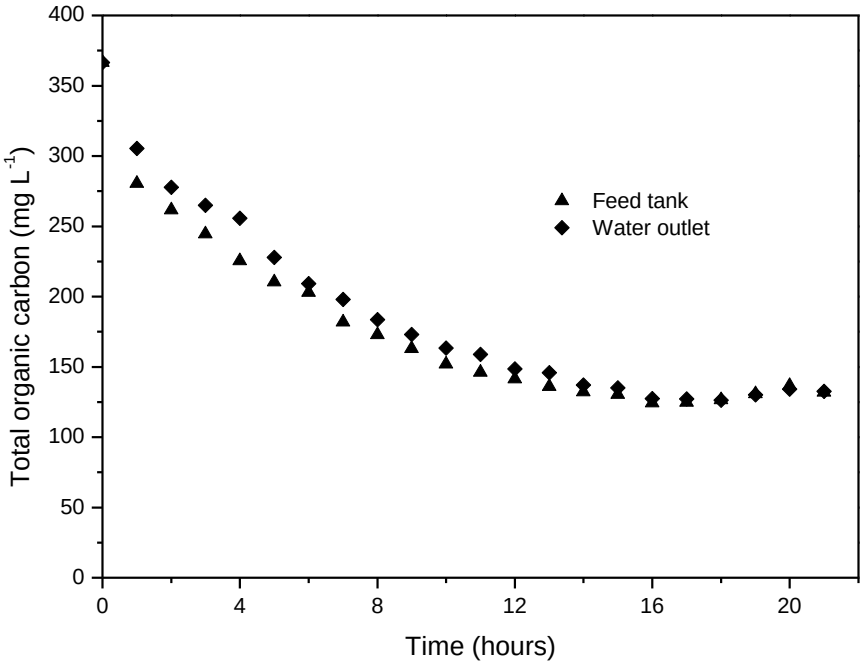

Figure 4.59: *Total organic carbon during the treatment of 500 mg L^{-1} phenol solution in the continuous adsorption and electrochemical regeneration unit at 7 mA cm^{-2}*

4.4.3 Conclusions

The continuous process of adsorption with electrochemical regeneration of GIC adsorbent has similarities with the studies carried out in the batch mode. Benzoquinone was found to be the main intermediate product. The rate of formation of benzoquinone was found to be higher than its rate of degradation, especially during the first 12 h of treatment. Maleic acid was found in low concentration

whereas the concentration of oxalic acid was found to increase with time showing the oxidation of aromatic intermediates such as benzoquinone. Among the chlorinated breakdown products, 2-CP, 4-CP and 2,4-DCP were observed at low concentrations. The relatively low concentrations of chlorophenols observed were probably due to the relatively low current density of 7 mA cm^{-2} used during the continuous operation. Only 64% TOC removal was possible in 21 h of treatment of 500 mg L^{-1} phenol solution in a batch-recirculation mode using the continuous electrochemical regeneration cell. Based on these findings, it can be anticipated that lower phenol concentrations and relatively higher current density can improve the percentage TOC removal.

4.5 Overall conclusions

The results presented in this chapter have demonstrated that intermediate oxidation products are formed during the electrochemical regeneration of the GIC adsorbent in the batch as well as continuous process. This chapter has introduced two mechanisms involved during electrochemical regeneration of the GIC adsorbent. The first is the complete oxidation of the adsorbed species on the surface of the adsorbent and the second involves the indirect electrochemical oxidation of organics present in solution. The results indicate that the breakdown products are largely formed due to the indirect electrochemical oxidation of organics in solution.

The concentrations of the breakdown products are significantly lower than the initial concentration of the organics. The work on the formation of chlorinated breakdown products has shown that their concentrations depends upon a range of variables including current density, initial concentration, chloride contents and electrolyte type. In this context, the concentrations of chlorinated intermediates can be minimized by using low current density, low initial concentrations, chloride free environment and treating water over a number of adsorption and regeneration cycles. The formation of non-chlorinated species was found largely dependent on current density and pH. However, the formation of these species can be minimised by applying higher current densities and treating solution over several cycles of adsorption and regeneration. It has also been shown that the GIC adsorbents have the capability of adsorbing a variety of intermediate oxidation products even in low

concentrations. It can be anticipated that the GIC adsorbents with increased adsorption capacity could further reduce the potential formation of breakdown products.

Whilst the conclusions from the work presented in this chapter are promising, a number of areas have been highlighted which requires further work.

Chapter No. 5
Evaluation of gases during electrochemical regeneration of GIC adsorbents

The gases evolved during electrochemical regeneration of GIC adsorbents and thus the formation of any breakdown products released in gaseous state are investigated. The materials and methods used for the identification and quantification of the off gases have been described. A preliminary attempt to perform a mass balance for removal and oxidation of a pollutant during adsorption and electrochemical regeneration is also presented. Finally, the limitations regarding the evaluation of the off gases and the mass balance has been discussed.

5.1 Background

The principle breakdown products formed during electrochemical regeneration of the GIC adsorbent in treating the aqueous solution of phenol were discussed in chapter 4. A variety of oxidation intermediates including aromatics, aliphatic acids and chlorinated species have been investigated. As far as full mineralization of phenol is concerned the final oxidation products should be simply carbon dioxide and water. However, some toxic gases may also be evolved during the electrochemical regeneration of GIC adsorbent such as chlorinated organic species. The amounts and concentrations of such gases should be determined for the large scale applications of water treatment by adsorption using GIC adsorbents with electrochemical regeneration. This chapter focuses on a preliminary investigation of the gases generated during the electrochemical regeneration of the GIC adsorbents.

A number of reactions may take place at the surface of GIC particles including the oxidation of adsorbed organics and organics present in solution to carbon dioxide and/or other breakdown products (by direct and/or indirect oxidation), the oxidation of chloride ions to chlorine; and the oxidation of water. At the cathode reduction of water takes place producing hydrogen. The electrode reactions can thus be summarised as follows.

Anode (Oxidation):

- Oxidation of organics to CO_2 and/or break down products
- $2Cl^- \rightarrow Cl_2 + 2e^-$
- $H_2O \rightarrow \frac{1}{2}O_2 + 2H^+ + 2e^-$

Cathode (Reduction):

- $H_2O + e^- \rightarrow \frac{1}{2}H_2 + HO^-$

The quantitative determination of evolved gases is particularly important in order to establish the mass balance for the adsorbed organics on the surface of the GIC adsorbent. In addition, the evolution of gases (especially carbon dioxide) during electrochemical regeneration gives important information regarding the mechanism of electrochemical oxidation. *Comninellis and Pulgarin, (1991)* has suggested direct oxidation of phenol and/or its aromatic intermediates to CO_2 during electrochemical oxidation of phenol on a platinum electrode based on the trend of formation of CO_2.

It may also be possible that the GIC itself may be oxidised to CO_2 during electrochemical regeneration. In such circumstances it is difficult to quantify the amount of gases being generated from the oxidation of the adsorbed species. However, an attempt has been made to address this issue in the following sections.

5.2 Equipment and Methodology

5.2.1 Materials

In order to investigate the breakdown products in the gas phase, phenol was used as a model pollutant in order to complement the investigation of breakdown products in the liquid phase (See chapter 4). Nyex®1000 was used as the GIC adsorbent (see chapter 4, section 4.1). All the chemicals used in these experiments were of analytical grade, supplied by Sigma Aldrich®.

5.2.2 Electrochemical Cell Design

The mini-SBR shown in figure 4.3 (see chapter 4) is an air sparged electrochemical cell that is open from the top side. Thus, the gases being generated during electrochemical regeneration of the GIC adsorbent are simply vented out of the cell. It is not possible to collect these gases for analysis in this configuration. In addition, the gases generated during electrochemical regeneration are mixed with the sparge gas (air) and so will be at low concentrations and therefore difficult to detect. Furthermore, the adsorption and electrochemical regeneration of volatile pollutants in water such as mercaptans are problematic because the data will be confused by losses of the contaminant by air stripping. In order to address these issues associated with the mini-SBR, it was modified by a fellow research student, Michael Conti-Ramsden, working on the removal of mercaptans from water. The new design is a liquid agitated cell as shown in figure 5.1. The top of the cell was fitted with a flanged seal, so that it could be removed. During adsorption, mixing was achieved when water was pumped to the bottom of the cell using a peristaltic pump as shown in figure 5.1. Water flows up through the cell and exits at the outlet, and is re-circulated. The flow of water was adjusted to around 1.2 L min^{-1} in order to maintain a uniform suspension of solid particles so that the adsorbent was thoroughly mixed with the flowing water. During this process the adsorption of unwanted pollutants took place on the surface of the adsorbent. The cell used a 10 mm thick graphite anode and the cathode was a perforated 316 stainless steel sheet with a thickness of 1 mm and 3 mm diameter perforations giving an open area of 33%. The electrodes were separated by a microporous Daramic 350 membrane, a high molecular weight microporous polyethylene ribbed sheet containing amorphous silica. The area of each electrode was 50 cm^2. The total height of the cell (39 cm) was selected in such a way that there should be a minimum entrainment of adsorbent along with the re-circulated water. The other dimensions of the electrochemical cell are given in figure 5.1. After the completion of adsorption, the pump was stopped and the solid particles were allowed to settle to form a bed of particles as shown in Figure 5.1. During the regeneration process any gases generated rose to the top of the cell and were collected in an attached sample bag.

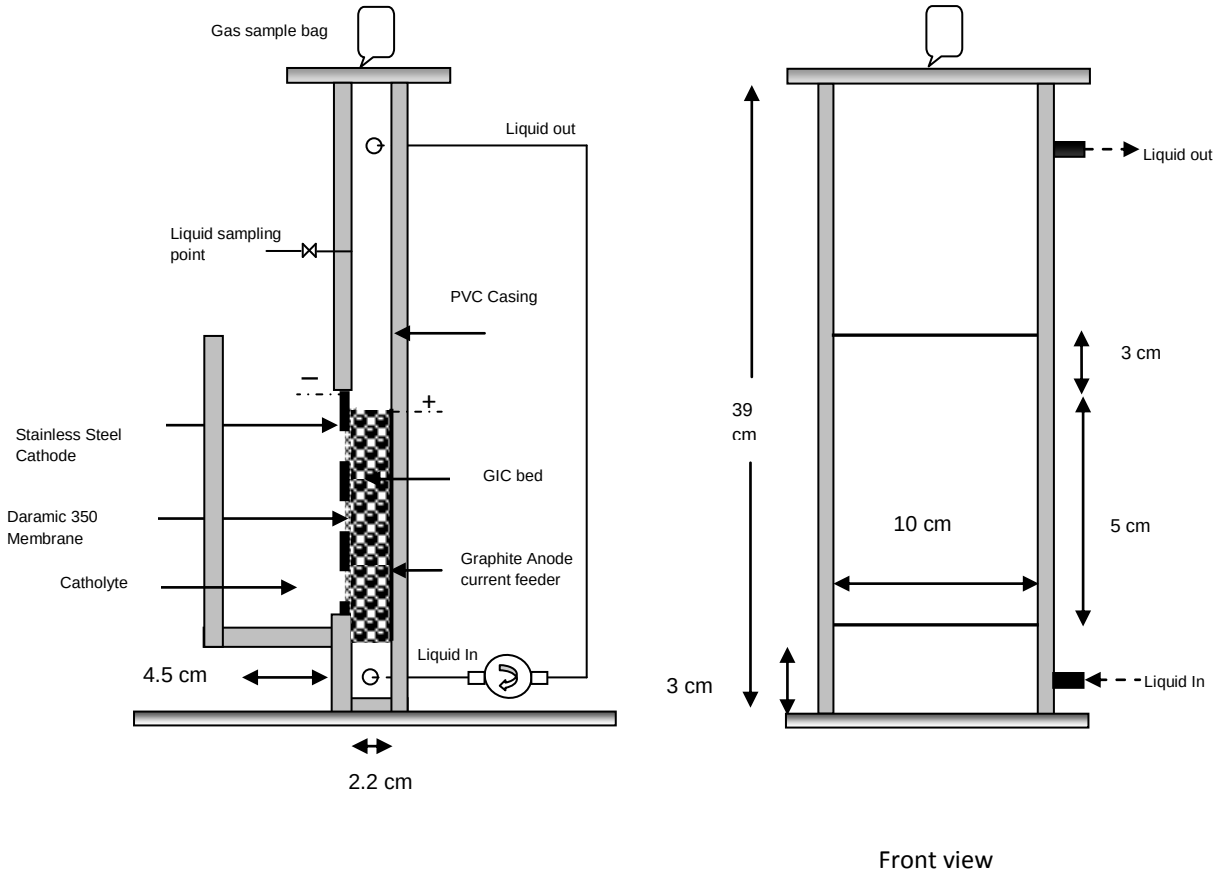

Figure 5.1: *Schematic diagram of the liquid agitated mini-SBR used for the purpose of collecting gases during the process of adsorption and electrochemical regeneration studies (the side view shows the adsorbent bed settled in the electrochemical cell when the peristaltic pump has been switched off).*

5.2.3 Flow Measurement of Gases Generated During Electrochemical Regeneration

To measure the small volumes of gases being generated during electrochemical regeneration of the GIC adsorbent was a challenging task. Preliminary trials were performed using a soap bubble flow meter. However, the small volume of gas formed during regeneration was not measured by this flow meter. A number of gas bubblers were also tested, but these were not able to provide accurate data. A gas measuring system was designed using a graduated cylinder which was similar to an equipment used to measure biogases from an anaerobic reactor *(Hernandez and Edyvean, 2011).* A schematic diagram of this arrangement is shown in figure 5.2.

The open end of an inverted graduated cylinder filled with water was submerged in a shallow tank. One end of a U-shaped tube was placed inside the inverted cylinder. This tube was connected to a syringe in order to draw gas out of the inverted cylinder so that it could be filled with water. Initially the cylinder was filled with water so that the volume of gas generated would be indicated on the scale of the graduated cylinder. A tube was connected to the top of the liquid agitated mini-SBR and its open end was inserted into the base of the inverted cylinder. During electrochemical regeneration of the adsorbent in the liquid agitated mini-SBR, the gases generated would thus flow through the tube into the inverted cylinder. The gases occupy the upper part of the inverted cylinder and consequently, the water level falls down in the cylinder. The volumetric flow rate of gases produced during electrochemical regeneration can be determined from the decrease in the level of water in the inverted cylinder (knowing the area of cylinder) in a given period of time. The gases collected in the graduated cylinder could be taken out in the syringe by the same procedure as described above for raising water level in the cylinder. The gas sample from the syringe was transferred to a multipass Fourier transform infrared (FTIR) gas cell for analysis (see section 5.3).

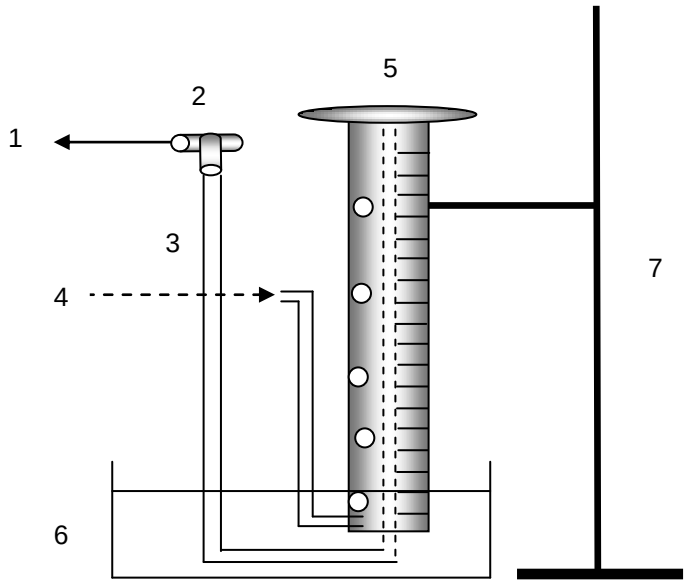

Figure 5.2: *Schematic diagram of the arrangement for gas measurement; (1) Bi-functional outlet attached to syringe: this can be used either to raise the level of liquid in the cylinder or to collect a gas sample, (2) pinch valve, (3) U-shaped tube, (4) inlet for the gas produced during the experiment in the liquid agitated mini-SBR, (5) graduated cylinder, (6) water tank and (7) burette stand.*

5.2.4 Experimental Methodology

A volume of 1 L of phenol solution of 100 mg L^{-1} concentration was added to the liquid agitated mini-SBR which filled the cell to just above the sample point (Figure 5.1). A known mass of the GIC adsorbent was added to the solution and the top of the cell was sealed in place. In order to carry out adsorption, the pump was started to recirculate the solution for 30 min at a flow rate of 1.2 L min^{-1}. After the completion of adsorption, the pump was stopped and the GIC particles were allowed to settle for five min. In the cathode compartment, 400 mL of 0.3% NaCl solution (w/v) acidified with 5 M HCl (to pH, 2±1) was added as an electrolyte so that the catholyte was at the same level as the bed of settled adsorbent. A DC current was supplied for a fixed regeneration time so that the electrochemical regeneration of the adsorbent could take place. Current densities in the range of 10–20 mA cm^{-2} were used corresponding to an applied current of 0.5–1.0 A. During the regeneration process, gases were released from the adsorbent bed and were either collected in a gas sample bag fixed at the top of the electrochemical cell or were fed to the inverted graduated cylinder (Figures 5.1 and 5.2). Some of the entrapped gases within the bed were allowed to move out of the bed by gently tapping the cell wall adjacent to the bed. After the completion of regeneration the gas bag was carefully closed and analysed using FTIR as described in section 5.3. Afterwards, the solution present above the regenerated bed was siphoned off. Care was taken to minimise the removal of adsorbent during siphoning, and any adsorbent removed was allowed to settle out and returned to the cell. A sample of solution was taken for analysis of phenol and breakdown products.

A measured volume of fresh phenol solution of known concentration was added to the liquid agitated mini-SBR and re–adsorption was carried out under identical conditions to the initial adsorption stage. For adsorption and electrochemical regeneration over a number of cycles, the adsorption and regeneration procedure was repeated several times and the gases generated during each cycle were collected for analysis. The concentrations of phenol and its breakdown products after adsorption and regeneration cycles were determined using HPLC as described in chapter 4 (see section 4.1.2).

As mentioned above, along with the oxidation of adsorbed species on the surface of the GIC adsorbent, water, other species in solution and the adsorbent itself may also be oxidised. Thus the gases collected during electrochemical regeneration of phenol loaded GIC adsorbent will not be purely representative of the gases produced due to the oxidation of the adsorbed phenol. Electrochemical regeneration of phenol loaded GIC adsorbent was normally carried out under constant current conditions. In order to evaluate the gas produced from the oxidation of water, other dissolved species and the adsorbent, regeneration was also carried out in the absence of phenol. This control experiment was carried out at the same potential as that used during electrochemical regeneration of the phenol loaded adsorbent. Thus the rate and composition of the gases generated could be compared to get a better indication of the gases associated with the phenol oxidation. To perform the electrochemical regeneration at constant potential, a three electrode system (working, counter and reference electrode) was used. The arrangement used is illustrated in Figure 5.3; an AgCl/Ag reference electrode was used in a separate compartment, filled with saturated NaCl, and connected to the solution via a Luggin capillary. A constant current was applied during electrochemical regeneration of the phenol loaded GIC adsorbent using a PC controlled EG & G263A potentiostat. The potential of the phenol loaded GIC adsorbent relative to the solution during regeneration at the applied current density was determined using the setup shown in figure 5.3. Regeneration of a fresh adsorbent (i.e. with no phenol loaded on the surface) was carried out by controlling the electrode potential, while collecting and analysing the gases produced during this control experiment.

A measured mass of GIC adsorbent was mixed with a known volume of phenol solution for 30 minutes in the liquid agitated mini-SBR. On completion of adsorption, about half of the supernatant liquid was drained from the mini-SBR. Afterwards, the reference electrode (AgCl/Ag) was placed just above the adsorbent bed and the top cover of the liquid agitated mini-SBR was closed. Electrochemical regeneration of phenol loaded adsorbent was carried out as stated above. The flow rate of the gases generated was measured as described above in section 5.2.3. The analysis of the gases for CO_2 and CO was carried out using FTIR as described in section 5.3. The regeneration was repeated using the same setup but with a fresh adsorbent (i.e. with no phenol loading), and the potential was controlled using the

potentiostat to the same potential as that measured for the bed of GIC adsorbent loaded with phenol. The rate of gas generation was determined as before and gas samples were taken for analysis. Comparison of the flow rates and composition of the gases generated provides further information about the products of the oxidation of phenol.

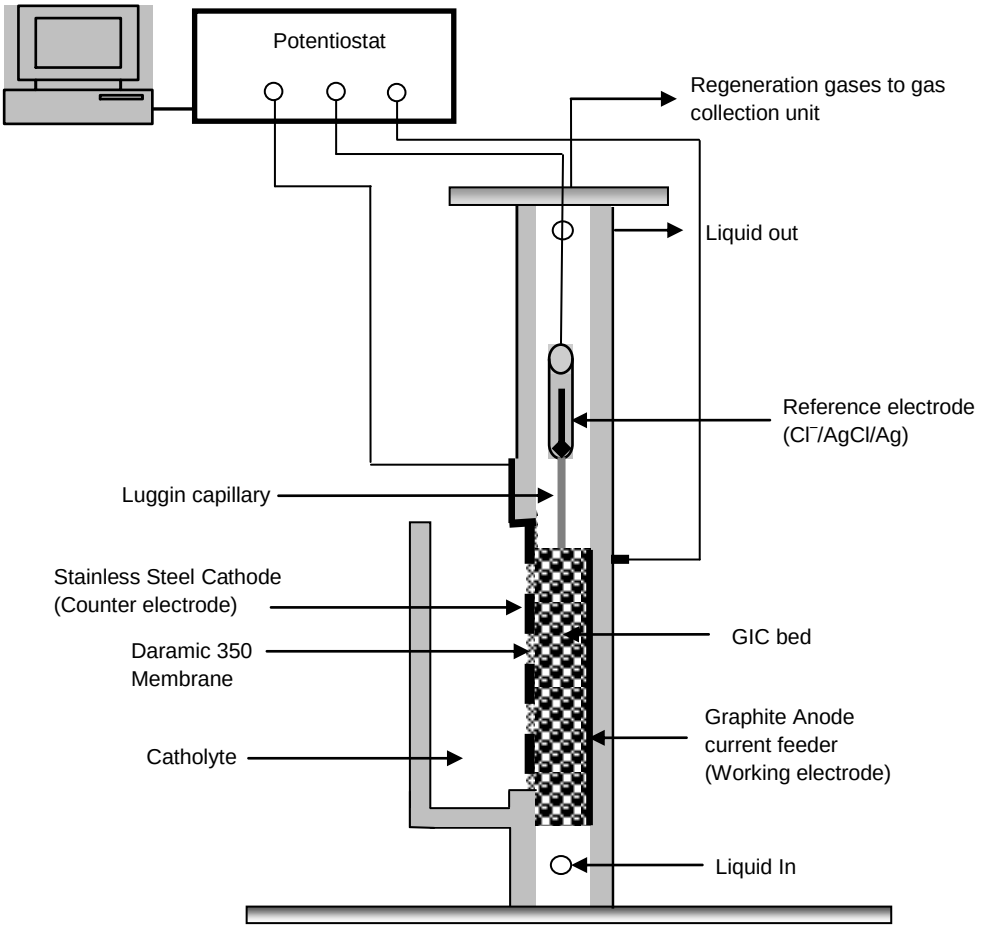

Figure 5.3: *Three electrodes arrangement with Luggin capillary and potentiostat used to measure or control the potential of the GIC adsorbent during regeneration.*

5.3 Analysis

In the preliminary experiments, samples from a gas bag were transferred to a multi-pass FTIR cell *(Specac Tornado E10)* (Shown in figure 5.1). Since the volume of gas collected during the regeneration cycles was quite small, the gases were forced to

flow from the bag into multi-pass cell by applying a vacuum in the multi-pass cell. Similarly, the syringe containing a gas sample was attached to the multipass cell through which the sample was transferred due to vacuum. The Fourier transform infrared (FTIR) spectrum was measured using a Bruker Equinox 55 spectrometer with the settings shown in Table 5.1. Before running each sample, the background spectrum was measured in order to produce a relative scale for the absorption intensity.

Table 5.1: *Scan parameters for FTIR*

Parameter	***Setting***
Number of Scans	50
Gain	62
Resolution	1 cm^{-1}
Slit width	0.65 mm
Detector	Princeton Gamma–Tech (PGT)

5.4 Results and Discussion

5.4.1 Identification of Gaseous By-products during Electrochemical Regeneration in the Liquid Agitated mini-SBR

Preliminary experiments were performed with 100 mg L^{-1} phenol solution for a number of adsorption and regeneration cycles at 10 mA cm^{-2} in the liquid agitated mini-SBR according to the procedure described in section 5.2.4. The gas samples were collected using a sample bag as shown in figure 5.1. The FTIR spectrum obtained for the gas sample collected during the first regeneration contained numerous H_2O and CO_2 bands as shown in Figure 5.4. In addition to this, some fine structure was observed between 960 and 1080 cm^{-1}. This could be due to C–O or C–H stretches.

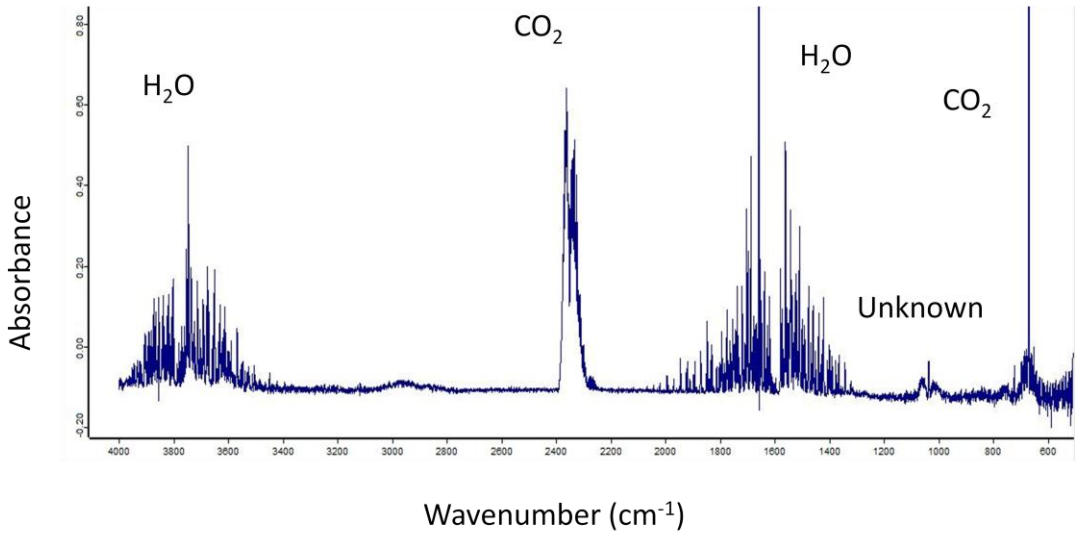

Figure 5.4: *FTIR spectrum of gas collected during the first electrochemical regeneration of phenol loaded GIC adsorbent (0.115 mg g^{-1}) showing the presence of CO_2 at 10 mA cm^{-2} (0.5 A for 20 min), GIC adsorbent dose 130 g in 1 L of 100 mg L^{-1} phenol solution*

For the second regeneration, the FTIR spectrum of the gas generated was similar to that for the first regeneration with numerous water and CO_2 bands. A fine structure was also observed between 2000 and 2250 cm^{-1} which indicates the presence of very small amounts of CO (Figure 5.5). The presence of CO_2 and CO was confirmed by comparing the actual spectrum with the reference spectra (NIST database) of CO_2 and CO (Figure 5.6).

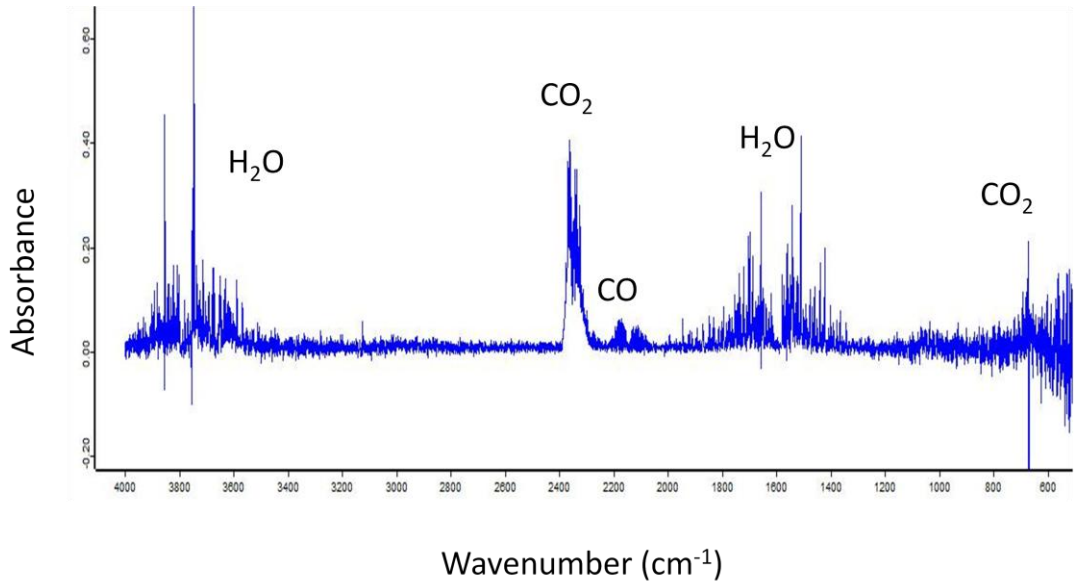

Figure 5.5: *FTIR spectrum of gas collected during second electrochemical regeneration cycle of the phenol loaded (0.121 mg g^{-1}) GIC adsorbent showing the formation of CO_2 and CO at 10 mA cm^{-2} (0.5 A for 20 min), GIC adsorbent dose 130 g in 1 L of 100 mg L^{-1} phenol solution*

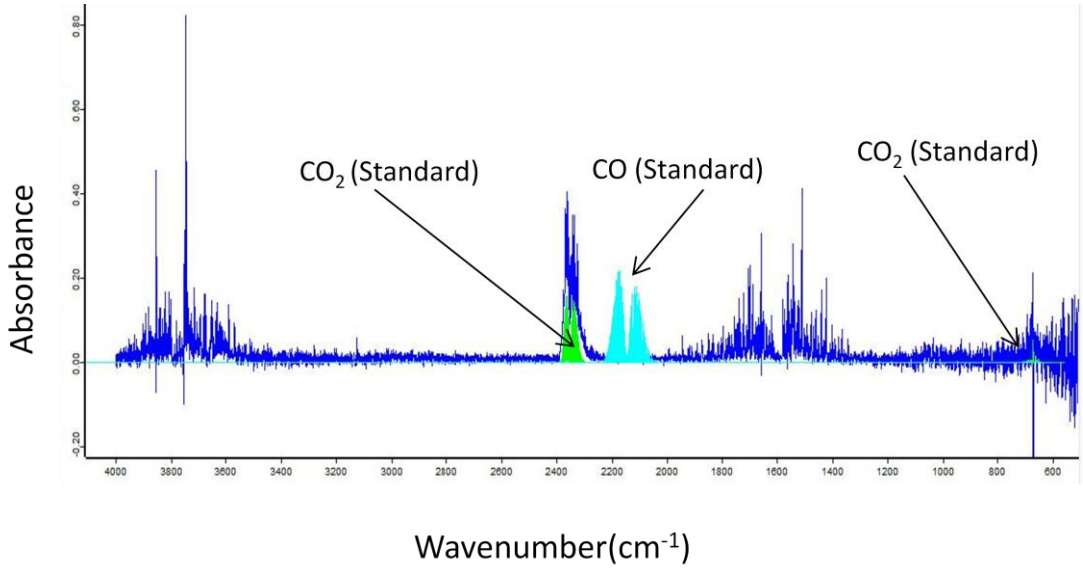

Figure 5.6: *Comparison of the spectrum obtained during second electrochemical regeneration of phenol loaded (0.121 mg g^{-1}) GIC adsorbent with standard spectra of CO_2 and CO*

These results suggest that CO_2 and CO were the main breakdown products observed in the gaseous phase during electrochemical regeneration of a phenol loaded GIC adsorbent in the liquid agitated mini-SBR.

A control experiment was performed for which the phenol solution was replaced with deionised water. In all other respects, the procedure was as described for multiple adsorptions and regenerations in section 5.2.4. The results for the second electrochemical regeneration without any phenol adsorbed, however with the same regeneration conditions, indicate the presence of CO_2 and H_2O in smaller concentrations (Figure 5.7). These results suggest that at least part of the carbon dioxide generated was associated with oxidation of adsorbed phenol on the surface of the GIC adsorbent. In addition, no carbon monoxide was detected in the absence of phenol. This issue has been further investigated in the preceding section.

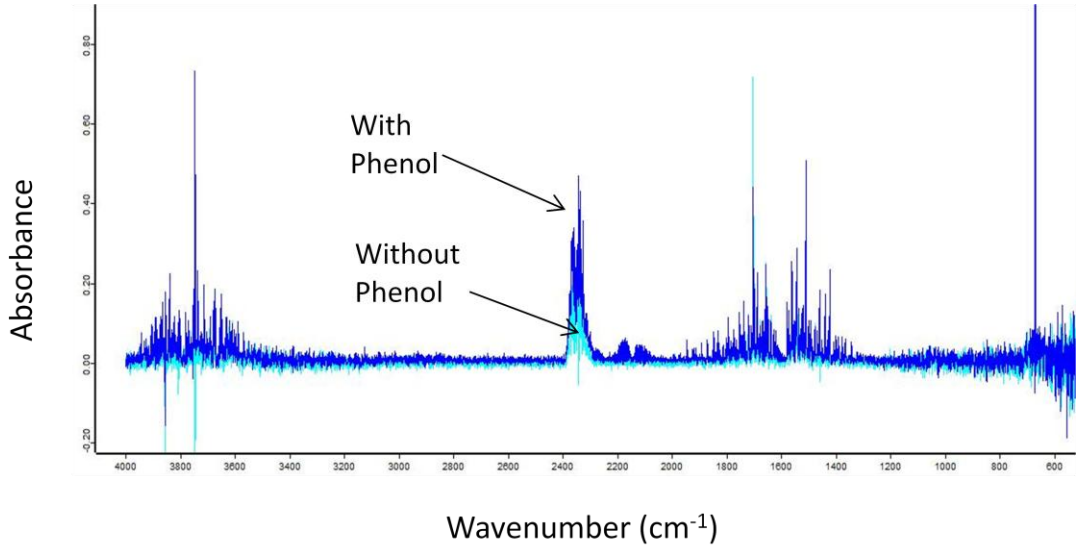

Figure 5.7: *Comparison of FTIR spectrum of a sample of gas obtained during the second electrochemical regeneration of phenol loaded (0.121 mg g^{-1}) GIC adsorbent with that obtained from a sample of gas generated when only deionised water was used in place of phenol solution, for the same regeneration conditions (10 mA cm^{-2}; 20 min regeneration).*

5.4.2 Flow Measurement of Gases during Electrochemical Regeneration of the GIC adsorbent

The flow rate of the gases generated during regenerations at current densities of 10 and 20 mA cm^{-2} was measured using the apparatus as described in section 5.2.3. The results show that about 16 mL of gas was collected in 20 min during various regeneration cycles at 10 mA cm^{-2} (corresponding to a rate of 0.0332 mmol min^{-1}) (Figure 5.8). As expected, there was observed to be an increase in the volume of gases generated with an increase in the current density, with almost double the volume of gas generated at 20 mA cm^{-2} (1.5 mL min^{-1}) compared to the volume of gas produced at 10 mA cm^{-2} (Figure 5.8). These results suggest that the amount of gas evolved during electrochemical regeneration of the GIC adsorbent is proportional to current density under the conditions studied.

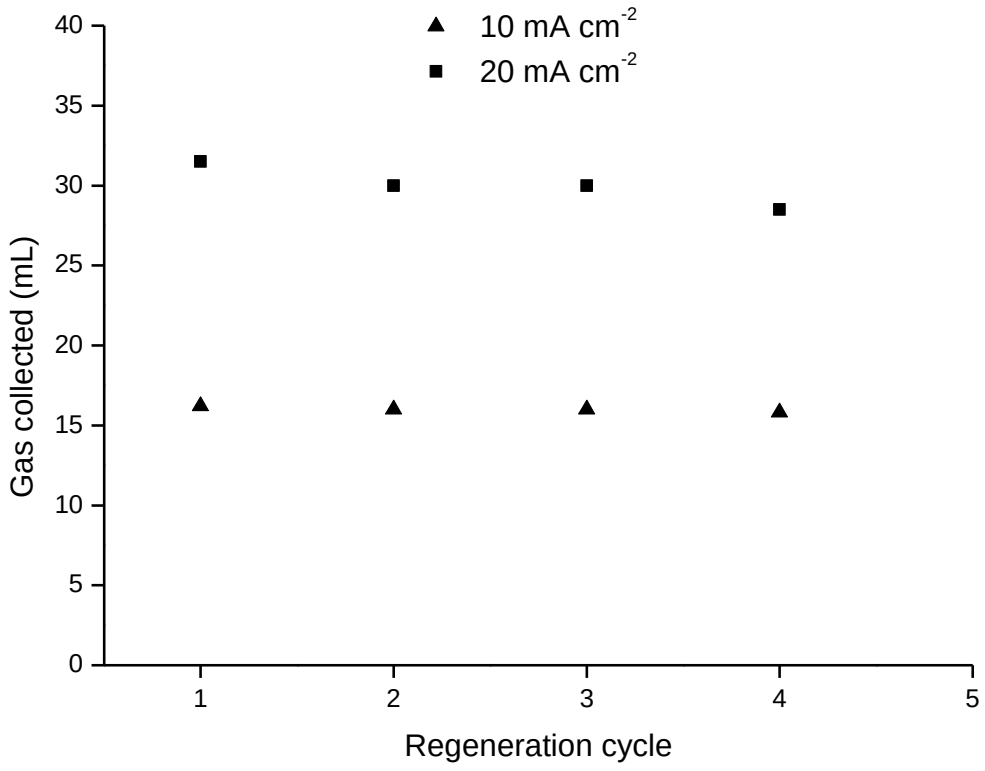

Figure 5.8: *The volume of gas generated during each electrochemical regeneration cycle of phenol loaded (0.115 mg g^{-1}) GIC adsorbent. Regeneration was carried out at 0.5 and 1.0 A corresponding to current densities of 10 and 20 mA cm^{-2} for a duration of 20 min. A GIC adsorbent dose of 130 g in 1 L of 100 mg L^{-1} phenol solution was used.*

Several factors could contribute to the amount of gases generated during electrochemical regeneration of the GIC adsorbents:

- Electrochemical oxidation of adsorbed phenol at the surface of GIC adsorbent
- Electrochemical oxidation of water or other species in solution
- Electrochemical oxidation of GIC particles themselves
- Indirect electrochemical oxidation of phenol in solution

In order to investigate the role of these phenomena, three experiments were carried out:

- After the first adsorption of phenol on the GIC adsorbent according to the procedure described in section 5.2.4, electrochemical regeneration was carried out at 10 mA cm^{-2} and the volume of gases evolved was measured at different intervals of time using the apparatus described in section 5.2.3.

- In place of phenol adsorption on the GIC adsorbent, mixing of the adsorbent was carried out with deionised water in the liquid agitated mini-SBR and then electrochemical regeneration was carried out at 10 mA cm^{-2} according to the procedure described in section 5.2.4. The volume of gases generated was measured as described in section 5.2.3.

- For electrochemical oxidation of phenol without GIC adsorbent, 1L of phenol solution (100 mg L^{-1}) containing 0.5% Na_2SO_4 as electrolyte was treated in the liquid agitated mini-SBR at 10 mA cm^{-2} and the volume of gases evolved were measured at different intervals of time using the apparatus described in section 5.2.3

Figure 5.9 shows that flow rate of gases generated at the start of the electrochemical regeneration of phenol loaded adsorbent increased from zero to an almost constant value in 20 mL min^{-1}. The relatively low values of measured flow rate at the start of the process could be due to the entrapment of gases in the adsorbent bed or due to

the gases generated dissolving into solution. On gentle tapping at different locations of the anode plate, the quantity and velocity of the gas bubbles rising in the liquid present above the adsorbent bed were always observed to increase. Without any phenol adsorbed; comparatively less gas was evolved under the same regeneration conditions. These results suggest that relatively increased gas flow rates were observed presumably due to the oxidation of phenol at the surface of the GIC adsorbent. This phenomenon is discussed below. On the other hand, the volume of the gases evolved during electrochemical oxidation of phenol in solution without GIC adsorbent was significantly lower compared to the gases generated during electrochemical regeneration of GIC adsorbent with and without phenol adsorbed. These results also suggest that each GIC particle behaves as an anode on which the oxidation of water takes place.

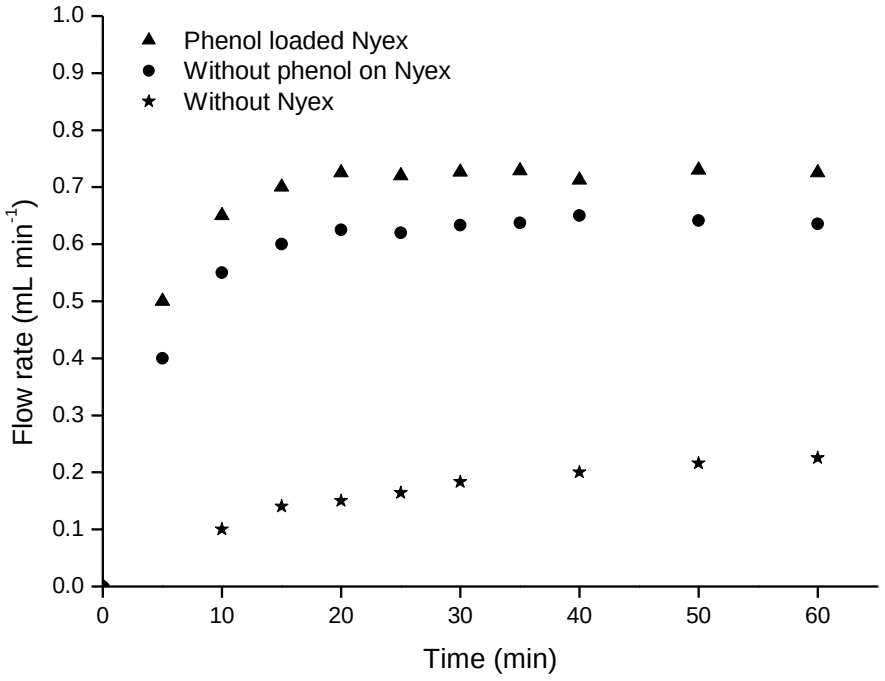

Figure 5.9: *Flow rate of gas generated during electrochemical regeneration of the GIC adsorbent with (0.115 mg g^{-1}) and without phenol adsorption, and during indirect electrochemical oxidation of phenol in solution (i.e. in the absence of adsorbent) in the liquid agitated mini-SBR. Operating conditions: GIC adsorbent dose 130 g in 1 L solution; Phenol concentration: 100 mg L^{-1}; Regeneration current: 0.5 A (10 mA cm^{-2}). During electrochemical oxidation of phenol in solution, 0.5% Na_2SO_4 was used as an electrolyte.*

During electrochemical regeneration of GIC adsorbents, a number of gas forming reactions (5.1–5.5) including oxidation of adsorbed phenol to CO_2 and CO, oxidation of water to O_2, oxidation of graphite to CO_2 and CO may take place according to the following equations:

$$C_6H_5OH + 11H_2O \rightarrow 6CO_2 + 28H^+ + 28e^- \quad (5.1)$$

$$C_6H_5OH + 5H_2O \rightarrow 6CO + 16H^+ + 16e^- \quad (5.2)$$

$$2H_2O \rightarrow O_2 + 4H^+ + 4e^- \quad (5.3)$$

$$C + 2H_2O \rightarrow CO_2 + 4H^+ + 4e^- \quad (5.4)$$

$$C + H_2O \rightarrow CO + 2H^+ + 2e^- \quad (5.5)$$

Using above equations and ideal gas law (PV=nRT), the volumetric flow rate (L sec^{-1}) of CO_2, CO and O_2 evolved from various reactions can be calculated as:

$$(Vco_2)_{phenol} = \frac{IRT}{P\left(\frac{28}{6}\right)F} \quad (5.6)$$

$$(Vco)_{phenol} = \frac{IRT}{P\left(\frac{16}{6}\right)F} \quad (5.7)$$

$$V_{O_2} = \frac{IRT}{4PF} \quad (5.8)$$

$$(Vco_2)_{graphite} = \frac{IRT}{4PF} \quad (5.9)$$

$$(Vco)_{graphite} = \frac{IRT}{2PF} \quad (5.10)$$

where *P* is the pressure in atmosphere, *T* is the temperature in Kelvin, *R* is the universal gas constant (8.314 J K^{-1} mol^{-1}), *I* is the current passed (A) and *F* is the Faraday's constant 96485.34 C mol^{-1}.

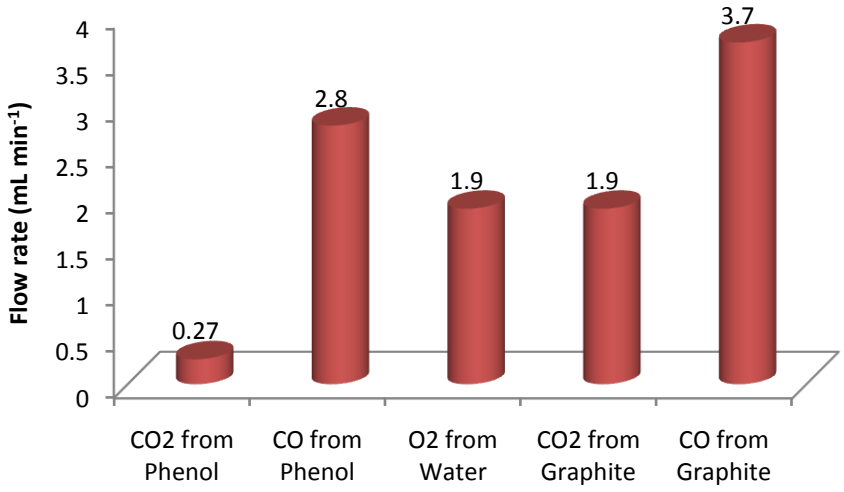

Figure 5.10: *Comparison of predicted gas flow rate (calculated from Faraday's law and the ideal gas equation) assuming various reactions during electrochemical regeneration of GIC adsorbents. The volume flow rates were calculated using equations 5.6–5.10 for a current of 0.5 A, T = 298 K and P = 1 atm. The fractional charge yield for each reaction is unity.*

The predicted rate of gas generation assuming all of the current is used for each of the possible reactions is shown in figure 5.10. The measured rate of gas generation (figure 5.9) was significantly lower than the values shown in figure 5.10, possibly due to dissolution of the gases generated in the water. It has been demonstrated that CO was also evolved during electrochemical regeneration of GIC adsorbents (see section 5.4.1). Oxidation of phenol to CO would be expected to generate gas at a higher rate than reactions that might occur in the absence of phenol (Figure 5.10). In practice, the oxidation of phenol takes place through the formation of both CO_2 and CO. Therefore, if we neglect the effect of gases dissolving in solution, it is possible that the sum of CO_2 and CO evolved due to the oxidation of phenol may exceed the volume of O_2 produced during electrochemical regeneration of GIC adsorbent without phenol as observed in figure 5.9. However, further work is needed to investigate the effects of gas dissolution so that the Faradaic gas generation rates can be fully explained.

The liquid agitated mini-SBR shown in figure 5.1 was used for the electrochemical regeneration of GIC adsorbents under constant current conditions. The electrode potential was however, not kept constant in this method and therefore reaction

selectivity cannot be achieved. For carrying out electrochemical regeneration at constant potential, a cell equipped with three electrodes is required. In this method, the electrode potential was kept constant against a reference electrode in order to produce the same electrochemical conditions for the water/GIC oxidation as occurred in the presence of phenol. The aim of this experiment was to investigate how much O_2/CO_2 was generated from water electrolysis and oxidation of the adsorbent under these conditions. By comparing the amount of gases generated during electrochemical regeneration with and without phenol loaded on the GIC adsorbent at the same potential, information about the phenol oxidation products can be obtained (see section 5.4.3).

5.4.3 Concentration of Gaseous Breakdown Products

The main gaseous breakdown products observed during the electrochemical regeneration of GIC adsorbent were CO_2 and CO as described in section 5.4.1. No chlorinated breakdown product was identified in the regeneration gases analysed. For FTIR spectra, the concentrations of evolved gases (CO_2 and CO) were calculated by comparing with standard spectra from National Institute of Standards and Technology (NIST). The standard spectral files correspond to absorbance for a sample concentration of one part-per-million (ppm) over an optical path length of one meter (m) and at a temperature of 296 Kelvin (K). Concentrations of each species were determined by integrating the area under a peak using Brukers OPUS software and then comparing with standard spectrum produced by NIST for 1 ppm, and using the following equation:

$$\text{Concentration} = \frac{\text{Concentration of standard} \times \text{Integrated area of peak} \times \text{Optical length}}{\text{Integrated area of standard} \times \text{Experimental path length}}$$

where the optical and experimental path lengths were 1 and 5.3 m respectively. The volume of the multi-pass cell was 1L. It is also important to mention here that once a gas sample was transferred to the multi-pass cell, the volume of the sample becomes equal to the volume of the multipass cell which was operated under vacuum.

The results show that during electrochemical regeneration of phenol loaded GIC adsorbent at 10 mA cm^{-2}, the concentration of CO_2 and CO increased with the passage of time, suggesting that they might be dissolving in the water and then the concentration was increasing as the water was saturated. However, the concentration of CO remains below that of CO_2 (Figure 5.11). The amount of inorganic carbon in the water before and after treatment should be determined in order to investigate the dissolution of CO_2 into water during these experiments in future.

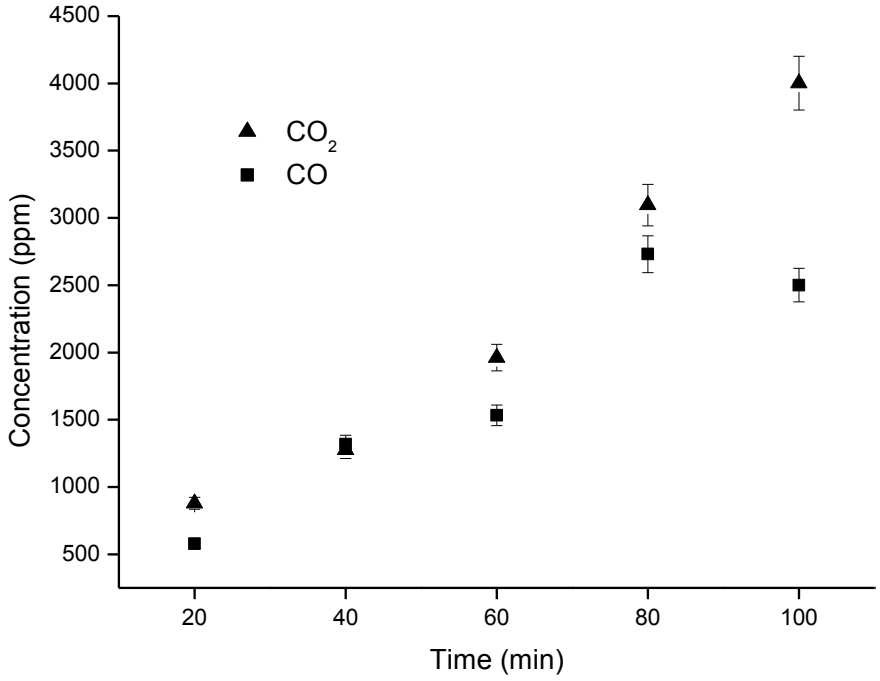

Figure 5.11: *Measured concentrations of CO_2 and CO during electrochemical regeneration of phenol loaded GIC adsorbent at 10 mA cm^{-2}. The same volume of sample was taken in each time interval. The concentrations plotted were obtained from the average of three experiments and error bars show standard deviation of these values.*

Complete oxidation of phenol can be described according to the equation:

$$C_6H_5OH + 11H_2O \rightarrow 6CO_2 + 28H^+ + 28e^- \quad (5.11)$$

The theoretical amount of CO_2 produced due to the complete oxidation of a specific amount of adsorbed phenol can be calculated from equation 5.11. The measured amount of CO_2 may be generated from the oxidation of phenol in solution or from the oxidation of GIC particles as discussed in sections 5.2.4 and 5.4.2. It is therefore difficult to determine the amount of carbon dioxide generated from the electrochemical oxidation of phenol on the GIC adsorbent. In order to investigate this, the amount of CO_2 generated during electrochemical regeneration of GIC adsorbent was carried out with and without phenol operating at the same potential, using a potentiostat as described in section 5.2.4. In this context, the electrochemical regeneration of phenol loaded GIC adsorbent was carried out at 0.5 A (10 mA cm^{-2}) and the corresponding potential of the GIC adsorbent bed increased gradually from 0.98 to 1.12 Vs AgCl/Ag reference electrode during the whole duration of the experiment (Figure 5.12). In order to perform the electrochemical regeneration of the GIC adsorbent without phenol, the potential was increased gradually from 0.98 to 1.12 V vs AgCl/Ag reference electrode. The corresponding current remained below 0.32 A during the whole duration of the experiment (Figure 5.12).

The results show that during the electrochemical regeneration of phenol loaded GIC adsorbent the volume of the gases evolved (15.5 mL) was significantly higher than the volume evolved during the electrochemical regeneration of the GIC adsorbent without phenol (2 mL) in the control experiment. Thus, the difference of the two volumes (13.5 mL) can be considered to be an indication of the amount of gas evolved due to the electrochemical oxidation of the adsorbed phenol. The volumes of gases and concentrations of CO_2 in the gases obtained are given in table 5.2.

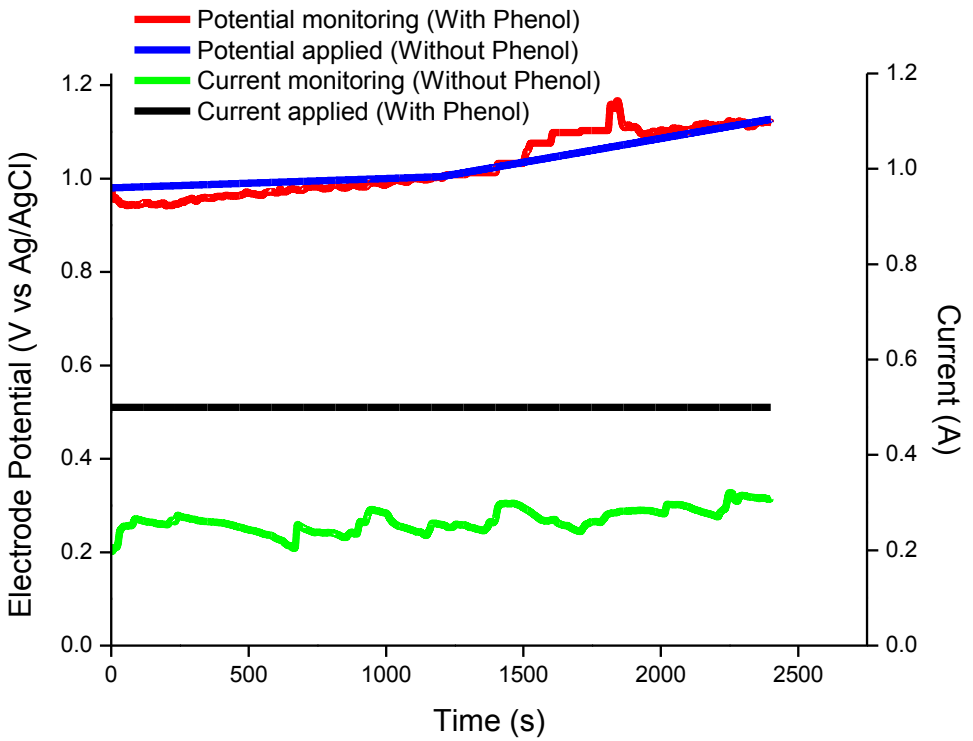

Figure 5.12: *Electrochemical regeneration of GIC adsorbent with (0.115 mg g^{-1}) and without phenol using potentiostat. A current of 0.5 A was applied during regeneration of phenol loaded adsorbent and the potential increased gradually from 0.98 to 1.12 V vs Ag/AgCl. During electrochemical regeneration of GIC adsorbent without phenol, the potential was increased from 0.98 to 1.12 V vs Ag/AgCl and the corresponding current was monitored.*

The results show that during electrochemical regeneration of phenol loaded GIC adsorbent, the volume of gases evolved during first and subsequent 20 min do not differ significantly. However, in the absence of phenol the volume of gases generated in first and subsequent 20 min intervals varied considerably and also suggests that the oxidation of water and/or the oxidation of graphite adsorbent occur at a lower rate. This is due to the lower current involved than the current for the case with phenol (Figure 5.12). However, the increase in the volume of gases in the subsequent 20 min without phenol can be explained that after 20 min it is assumed that that all of the phenol initially adsorbed on the surface of GIC adsorbent gets oxidised and thus the oxidation of GIC surface takes place afterwards at the same regeneration conditions.

Table 5.2: *Concentrations of CO_2 and the volume of gas generated during electrochemical regeneration of GIC adsorbent with (0.115 mg g^{-1}) and without phenol. A current of 0.5 A was applied using a potentiostat and potential was measured. The same potential was applied during the regeneration of the adsorbent without phenol.*

Time (min)	**Volume of gases with phenol (mL)**	**Volume of gases without phenol (mL)**	**CO_2 concentration with phenol (ppm)**	**CO_2 concentration without phenol (ppm)**
20	15.5	2.0	1440	420
40	16.5	11.5	3420	720

The standard electrode potentials for some of the reactions (5.1–5.5) occurring during electrochemical regeneration of GIC adsorbents are given in table 5.3. It is clear from the data given in table 5.3, that the standard electrode potential of phenol oxidation is significantly lower than the respective potentials of oxygen and chlorine evolution. Thus, it is likely to be expected that these reactions do not take place under the experimental conditions given in figure 5.12. However, the standard electrode potential for carbon oxidation is comparable with phenol oxidation, suggesting that phenol can be oxidised at low potentials (<0.4V vs. Ag/AgCl) in the potential region of carbon oxidation stability. In addition, the lower potential of phenol oxidation compared to the potential for GIC oxidation can be considered to explain that significantly lower volume of gases was generated (in 20 min) in the absence of phenol (table 5.2). However, after 20 minutes, the increase in the volume of gases was due to the increase of potential as shown in figure 5.12. This suggested that the rate of GIC oxidation is dependent upon the potential.

Table 5.3: *Standard Electrode Potentails for the reactions taking place during electrochemical regeneration of GIC adsorbents. Potential of Ag/AgCl (KCl, saturated at 25 ^{o}C) reference electrode is +0.199 V against SHE (Janata, 2009).*

Reaction	**E^{o} (V vs. SHE)**	**E^{o} (V vs. Ag/AgCl)**	**Reference**
Phenol mineralization: $C_6H_5OH + 11H_2 \rightarrow 6CO_2 + 28H^+ + 28e^-$	0.108	0.307	*Comninellis & Chen, (2010)*
Oxygen evolution: $2H_2O \rightarrow O_2 + 4H^+ + 4e^-$	1.230	1.429	*Pletcher, 1991*
Chlorine evolution: $2Cl^- \rightarrow Cl_2 + 2e^-$	1.358	1.557	*Pletcher, 1991*
Carbon oxidation to CO_2: $C + 2H_2O \rightarrow CO_2 + 4H^+ + 4e^-$	0.207	0.406	*Kinoshita, (1988)*
Carbon oxidation to CO: $C + H_2O \rightarrow CO + 2H^+ + 2e^-$	0.518	0.717	*Kinoshita, (1988)*

Theoretically, the complete oxidation of one mole of phenol produces six moles of CO_2 (equation 5.11). Thus, a total decrease of 15 mg L^{-1} phenol concentration from 100 mg L^{-1} due to adsorption on the GIC adsorbent (corresponding to 0.16 mmol of phenol) should ideally generate 0.95 mmol of CO_2 during electrochemical regeneration of the loaded adsorbent (corresponding to ca. 21 mL of CO_2 at 20^{o}C and 1 atm). The data presented in table 5.2 shows that during the first 20 minutes of regeneration, 15.5 mL of gas was evolved (corresponding to 0.644 mmol of gas, calculated at 20^{o}C and 1 atm). In addition, 2 mL of gas (corresponding to 0.083 mmol of gas) was produced during the electrochemical regeneration of the GIC adsorbent without any phenol adsorbed, but at the same potential. Thus, assuming that the difference between these two gas evolutions corresponds to the amount of CO_2 generated due to oxidation of phenol, it can be inferred that around 0.561 mmol of CO_2 was generated, indicating that ca. 60% of the adsorbed phenol was oxidised to CO_2. On the other hand, the high values of regeneration efficiency (ca. 90%, see chapter 4) of phenol loaded GIC adsorbent suggests that more CO_2 should be produced from these experiments. The fact that the amount of CO_2 produced during

electrochemical regeneration of phenol loaded GIC adsorbent was less than that expected from complete oxidation of the phenol could be due the fact that some CO_2 may have dissolved in solution. In addition, the other possible explanations could be that some of the phenol is oxidised to non-gaseous products e. g polymers that then get knocked off the graphite or even carbonisation of the phenol.

This is an indirect calculation of the percentage of phenol oxidised to CO_2 because the mass of CO_2 formed during electrochemical regeneration could not be evaluated from the concentrations given in table 5.2 since the pressure in the multipass cell was not measured. Although this was a preliminary investigation of the mass balance of the adsorbed phenol, a detailed study should be carried out in future by trying different adsorbent loadings particularly using high capacity GIC adsorbents. In addition, the amount of CO_2 actually produced from the oxidation of the adsorbed phenol could be evaluated using isotope labelling techniques (see chapter 9).

5.5 Conclusions

CO_2 and CO were detected as the main breakdown products in the gaseous form during the electrochemical regeneration of GIC adsorbent with and without phenol adsorption. However, relatively small amounts of CO_2 and CO were detected when regeneration was carried out without phenol. The concentrations of CO_2 and CO also increased with time.

A gas measuring apparatus using a graduated cylinder enabled the measurement of the small volumes of gases evolved during the electrochemical regeneration of GIC adsorbents in the liquid agitated mini-SBR. The volume of gases generated increased with an increase in the current density. A comparison of the amount of regeneration gases revealed that less gas was evolved during the electrochemical regeneration of GIC adsorbent when no phenol was adsorbed, suggesting that relatively increased gas flow rates were presumably due to the oxidation of phenol at the surface of the GIC adsorbent. Furthermore, the volume of the gases evolved during electrochemical oxidation of phenol in solution without GIC adsorbent was significantly lower

compared to the gases generated during electrochemical regeneration of GIC adsorbent with and without phenol adsorption.

Electrochemical regeneration at constant potential has shown that both the volume and CO_2 concentration of the gas evolved during regeneration of phenol loaded adsorbent were significantly higher than the volume and CO_2 concentration of the gas obtained when no phenol was present. The difference between the CO_2 concentrations and volumes of these gases can be considered to be associated with the oxidation of adsorbed phenol at the adsorbent surface. A preliminary mass balance has revealed that about 60% of the total amount of the adsorbed phenol is accounted for by the measured carbon dioxide in the evolved gas. Further work is needed to complete the mass balance for the adsorbed pollutant.

Chapter 6
Surface Investigation of GIC adsorbents during adsorption and electrochemical regeneration

This chapter discusses the results from a range of surface analysis techniques used to investigate the characteristics of the pollutant and any breakdown products adsorbed on the surface of GIC materials. The materials and methods along with the findings and limitations are presented.

6.1 Introduction

The physical structure of graphitic materials is composed of carbon atoms grouped into planar layers of fused aromatic rings (called graphene layers) *(Bandoscz and Ania, 2006).* The graphene layers are stacked on top of each other by van der Waal's forces, whether in an ordered structure for example graphite (see chapter 2) or with a disordered stack of the layers for example in activated carbon and carbon black *(Bandoscz and Ania, 2006).* The physiochemical characteristics of carbons are determined mainly by the presence of atoms in the carbon structure that are not carbon, called heteroatoms, such as oxygen, nitrogen, hydrogen, sulphur and phosphorous. The functional groups present on the carbon surfaces are formed from these heteroatoms. The type and concentration of the surface functional groups present on the carbon depends upon the carbon type and pretreatment *(Bandoscz and Ania, 2006).* The surface groups and the delocalized electrons of the graphitic structure determine the acidic or basic character of the carbon surface *(Laszlo and Szucs, 2001).* In general, when the carbon surface is exposed to air or oxidising agents, oxygen is chemisorbed and exists in the form of oxides. Oxygen is a dominant heteratom in the carbon matrix. Oxygen containing surface functional groups can be divided into three classes according to their chemical properties, namely acidic, basic and neutral *(Shafeeyan et al. 2010).* The acidic functional groups include carbonyl, carboxyl, lactonic and phenolic whereas pyrones, chromes, ketones and quinones are considered to be basic surface functional groups. These groups are mainly present on the outer surface or edges of the basal plane and have a

critical influence on the chemical nature of the carbon. In carbon materials, the outer sites constitute the majority of the adsorption surface on which these groups are present. Consequently, the concentration of these groups has a strong impact on the adsorption characteristics of the carbon *(Karanfil, 1999)*.

The oxidation of carbon surfaces may be carried out by gases, aqueous oxidants *(Mangun et al. 1999)* or by electrochemical oxidation *(Jannakoudakis et al. 1990)*. Gaseous oxidation with oxygen, air, steam or carbon dioxide at low temperature leads to the formation of strong acidic surface groups such as carboxylic groups. Weak oxidants including phenolic groups are created during oxidation at high temperature *(Shafeeyan et al. 2010)*. Liquid phase oxidation with nitric and/or sulphuric acid may lead to the formation of carboxylic, lactonic and / or phenolic hydroxyl groups on the carbon surfaces. The anodic electrochemical oxidation of graphitic materials in aqueous solutions creates surface oxides including carboxylic and phenolic groups *(Besenhard and Fritz, 1983)*. The composition of the oxides formed during anodic oxidation depends upon the pH, electrolyte composition and current density *(Jannakoudakis et al. 1990)*.

In addition to the functional groups mentioned above it has been shown that the π electron system of the basal planes of carbon attracts the protons from aqueous solutions of acids due to their basic character *(Boehm, 1994)*. Basic groups are difficult to determine because acidic groups are relatively abundant and therefore they diminish the reactivity of basic groups *(Tessmer et al. 1997)*. Various chemical and physical characterization techniques have been employed to detect and verify the presence of these functional groups on carbon surfaces.

In this study it has been shown that the breakdown products formed during the electrochemical regeneration of phenol loaded GIC adsorbent resulted from the indirect homogeneous oxidation of phenol in solution (See chapter 4). These species have also been observed to be adsorbed onto the surface of GIC adsorbent. The regeneration efficiencies of phenol loaded GIC adsorbent under various current densities indicate that the adsorbed breakdown products are also oxidised along with the phenol (see chapter 4). Thus, it is required to investigate the surface of GIC

adsorbents after adsorption and electrochemical regeneration for the surface functional groups.

6.2 Techniques for Surface Characterization of Adsorbents

In an attempt to investigate any adsorbed breakdown products present during the course of electrochemical regeneration of GIC adsorbent, various surface analytical techniques including Fourier transform infrared spectroscopy (FTIR), Raman spectroscopy, energy dispersive X-ray spectroscopy (EDS) and Boehm titration were applied for surface characterization of the GIC adsorbents.

6.2.1 Fourier Transform Infrared Spectroscopy

Infrared (IR) spectroscopy is a technique that deals with the infrared region of the electromagnetic spectrum and it can be applied to identify the functional groups present on carbon surfaces such as on activated carbons. It has contributed a great deal to the understanding of the surface functional groups associated with activated carbons *(Ishizaki and Marti, 1981)*. However, it can be difficult to interpret the IR spectra because the peaks obtained usually indicate combined interactions of different functional groups. In addition, IR does not provide quantitative determination of the individual functional groups present on the carbon surface *(Shafeeyan et al. 2010).* Fourier transform infrared spectroscopy (FTIR) can be effectively used to study the groups present on carbon *surfaces (Meldrum et al. 1985)*. FTIR is one of the most powerful analysis techniques and has been used for the evaluation of the chemical structure of carbon materials. It has also been employed to investigate the oxygen containing functional groups on graphite oxides *(Hontoria-Lucas et al. 1995; Han and Lu, 2007)*. The FTIR spectrum is a plot of the measured infrared intensity versus wavenumber (mid infrared, 4000–400 cm^{-1}) of light. Thus, by measuring the spectra of fresh, adsorbed and regenerated GIC, the surface functional groups present can be investigated.

There are various sampling techniques that are used in combination with FTIR which allow for direct measurement of the spectrum of solids in their original state. These techniques include:

Attenuated Total Reflection

Attenuated total reflection (ATR) is one of the sampling techniques used to obtain IR spectra of difficult samples that cannot be readily examined by the normal IR technique. ATR is suitable for studying highly absorbing solid materials, including films, coatings, powders and threads *(Settle, 1997)*. In addition, ATR requires little or no sample preparation and thus, is one of the most versatile sampling techniques.

With an ATR accessory, the detector measures the changes that occur in a totally internally reflected IR beam when it comes in contact with a sample. A beam of infrared light is directed onto an optically dense crystal with a high refractive index at an angle greater than the critical incident angle *(Burgi, 2006)*. The resulting internal reflection generates an evanescent wave that extends into the sample held in contact with the ATR crystal (Figure 6.1). The beam penetrates a very short distance beyond the interface, typically at a depth of few micrometers. When the sample absorbs energy in the IR region, the evanescent wave is attenuated and then directed at the detector in the IR spectrometer.

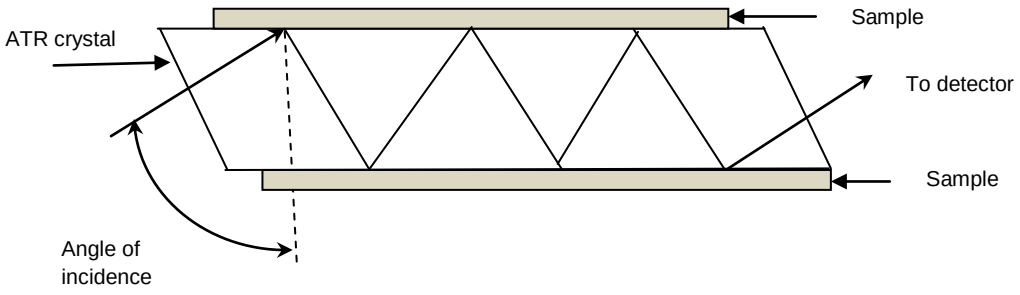

Figure 6.1: *An ATR cell (Stuart, 1997)*

Diffuse Reflectance Infrared Fourier Transform Spectroscopy

Diffuse reflectance infrared Fourier transform spectroscopy (DRIFTS) is mainly used for obtaining IR spectra of powders and rough surfaces including coal, paper and cloth *(Settle, 1997)*. In this technique IR radiation is focused onto the surface of a sample placed in a cup and consequently two types of reflections are observed namely specular and diffuse reflectance. In specular reflectance, the IR radiation directly reflects off the surface whereas in diffuse reflectance IR radiation penetrates into the sample and then scatters in all directions. Special reflections accessories are used to collect and refocus the resulting diffusely scattered light, while minimizing the specular reflectance which otherwise complicates the IR spectra. The sample can be analysed either directly or as dispersions in IR-transparent medium such as KBr. Dilution of a sample in a non-absorbing medium increases the proportion of diffuse reflectance in all the light reflected. Normally, the sample is diluted to 5–10% by weight in KBr.

Infrared Microspectroscopy

Infrared microspectroscopy is an important technique for analysing difficult or small samples including trace contaminants in semiconductor processing, multilayer laminates and forensic samples. Samples can be examined with IR microscopes, with a resolution limit of about 10 μm, using a mercury cadmium telluride (MCT) detector *(Settle, 1997).*

6.2.2 Raman Spectroscopy

When a beam of monochromatic light is incident on a sample, some of the light is transmitted, absorbed and scattered. Mainly the scattered light has the same wavelength as the incident light. However, a small fraction (1 in 10^4 photons) of the scattered light is shifted in wavelength by molecular vibrations and rotations of the molecules in the sample. The spectrum of this wavelength shifted scattered light is called a Raman spectrum *(Pelletier, 1999)*. Raman spectrum typically contains many sharp bands that are characteristic of the specific molecules in the sample. The intensity of a Raman spectrum is proportional to the concentration of the specific molecule in a sample and therefore can be used for quantitative determination.

Raman spectroscopy has been used to investigate the structural and electronic characteristics of graphite materials, providing useful information on the defects and stacking order *(Ferrari, 2007; Ni et al. 2008)*. In addition, the Raman spectra of samples in aqueous solutions can be obtained without major interference from water vibrations because water is a weak Raman scatterer *(Ferraro and Nakamoto, 2003)*. This feature of Raman spectroscopy was useful in this study for the analysis of wet samples of the GIC adsorbent after adsorption and electrochemical regeneration.

6.2.3 Energy Dispersive X-ray Spectroscopy (EDS)

EDS is an analytical technique used to identify the elemental composition or chemical characterization of a sample. It depends on the interaction between electromagnetic radiation and matter. The electromagnetic radiation excites the atoms in a sample that subsequently produce X-rays to discharge the excess energy. Some of the X-rays energies are characteristic of the atoms present, allowing atomic identification. These appear as peaks in the spectrum and the relative peak intensities can be related to relative atomic concentrations *(Holloway and Vaidyanathan, 2010)*.

6.2.4 Boehm Titration

Boehm proposed acid/base titration to determine the acidic and basic functional groups of a carbon surface *(Boehm, 1994; Boehm, 2002)*. In this technique, the acidic or basic functional groups of carbon material are contacted with specific bases or acids in aqueous solutions. The quantity of acids or bases that has reacted with their respective functional groups is determined through titration. The amount of various oxygen containing functional groups can be determined by assuming that NaOH neutralizes carboxylic, phenolic and lactonic groups; Na_2CO_3 neutralizes carboxylic and lactonic groups and $NaHCO_3$ neutralizes only carboxylic groups. On the other hand, the basic groups can be calculated from the amount of HCl that is consumed by the basic functional groups on carbon surfaces.

6.3 Materials and Methods

In order to investigate the surface chemistry of GIC adsorbent during adsorption and electrochemical regeneration, phenol was used as a model pollutant in order to complement the investigation of breakdown products in the liquid and gaseous phases (See chapters 4 and 5). Nyex®1000 was used as the GIC adsorbent (see chapter 4, section 4.1). All the chemicals used in these experiments were of analytical grade, supplied by Sigma Aldrich® (unless otherwise stated).

FTIR and ATR

A Thermo scientific Nicolet™ Is™10 FTIR equipped with DTGS (deuterated triglycine sulphate) detector was used for measuring the spectra of fresh, adsorbed and regenerated GIC adsorbents. Each spectrum represents 100 co-added scans at a spectral resolution of 4 cm^{-1} in the range of 4000–400 cm^{-1}. An ATR single reflection diamond crystal was used in conjunction with FTIR.

Pressed discs containing 2 wt% adsorbent were prepared by mixing a sample with powdered KBr *(FT-IR grade, Sigma-Aldrich®)* in an agate mortar. The resulting mixture was then transferred to a 13 mm diameter pellet die *(Specac, UK)* and was pressed by applying a load of 10 tonnes (ca. 7.5 tonnes cm^{-2}) for 1 min using a manual hydraulic press *(Specac, UK)*. A clear and delicate disk was formed containing some black dots of GIC adsorbent. The FTIR spectrum of the sample was determined using the Nicolet™ Is™ FTIR instrument.

Infrared Microscope

Infrared microspectroscopy of the samples was carried out using a Varian 620-IR FTIR imaging microscope available in the Manchester Interdisciplinary Biocentre (MIB), University of Manchester, UK. A sample of adsorbent was placed on a microscopic slide and viewed under the IR microscope. The IR was used in reflection mode at a spectral resolution of 4 cm^{-1} and 128 scans were obtained in the range of 4000–400 cm^{-1}.

DRIFTS

A Nicolet Magna–IR 560 equipped with DTGS detector *(Nicolet Instrument Inc., Madison, USA)* available in the School of Chemistry, University of Manchester, UK was used in conjunction with a diffuse reflectance attachment to analyse the samples. Prior to analysis, the samples were air dried for 24 h and then ground down to <300 μm in an agate mortar. Samples were analysed as a mixture of powdered KBr and 5 wt% adsorbent.

Raman Spectroscopy

Raman analysis of the Nyex® 1000 adsorbent was carried out using a LabRAM HR (HORIBA JOBIN YVON). The laser excitation wavelength was at 632.82 nm and no sample preparation was required.

Boehm Titration

Three samples of known mass of GIC adsorbent (5 g) were added to 50 mL of an aqueous solution containing 0.05 M NaOH (prepared from 98% analytical reagent grade, Sigma-Aldrich®, UK), Na_2CO_3 (prepared from 99.9% analytical reagent grade, Fison Scientific equipment, UK) and $NaHCO_3$ (prepared from 99% analytical reagent grade, BDH laboratory supplies, UK), respectively. The samples were mixed for 24 h using a magnetic stirrer (ER LAUDA, Germany) at 700 min^{-1} at room temperature and then filtered to remove the adsorbent particles. A 10 mL aliquot was taken from each of the filtrates. These were titrated against 0.05 M HCl solution (prepared from 37% HCl, sigma-Aldrich®, UK) using phenolphthalein and methyl orange indicators for strong acid–strong base and strong acid–weak base, respectively. The volume of HCl required to neutralize the filtrate in each case was determined. A blank sample of 0.05 M NaOH, Na_2CO_3 and $NaHCO_3$ solution was agitated filtered and titrated in parallel for reference.

The amounts of surface functional groups were determined as *(Goertzen et al. 2010)*:

$$N_{GSF} = [B]V_B - [HCl]V_{HCl}\frac{V_B}{V_a}$$

where N_{GSF} is the number of moles of graphite surface functionalities on 5 g sample; [B] is the concentration of base used (0.05 M); V_B denotes the volume of base mixed

with the graphite sample (50 mL); V_a is the volume of the aliquot taken from the filtrate (10 mL); [HCl] denotes the concentration of HCl solution used for titration (0.05 M); and V_{HCl} is the volume of HCl solution required for neutralisation of the filtrate.

The amount of phenolic, carboxylic and lactonic functional groups present on the adsorbent were determined from the differences in the calculated amounts of N_{GSF} with each of the bases used *(Goertzen et al. 2010)*. As described in section 6.2.4, NaOH reacts with all these groups and therefore N_{GSF} obtained from NaOH will indicate the amount of total functional groups (phenolic, carboxylic and lactonic). Na_2CO_3 reacts only with carboxylic and lactonic groups and therefore the difference between the N_{GSF} values obtained using NaOH and Na_2CO_3 will give the amount of phenolic groups present. Similarly, $NaHCO_3$ reacts only with carboxylic groups and therefore the difference between the N_{GSF} values obtained using Na_2CO_3 and $NaHCO_3$ will give the amount of lactonic groups present. The amount of carboxylic groups can be directly determined from the amount of $NaHCO_3$ reacted.

General Procedure for Batch Adsorption and Electrochemical Regeneration

For batch adsorption and electrochemical regeneration, a mass of adsorbent was added to a measured volume of phenol solution of known concentration in the mini-SBR (see chapter 4) and mixed for 30 minutes using air sparging. After the completion of adsorption, the air supply was turned off and the adsorbent particles were allowed to settle for 2 min. Following settling of the adsorbent in the mini-SBR, a sample of the supernatant water was collected and analysed for phenol (see chapter 4). Afterwards, the solution present above the settled adsorbent was siphoned off and the sample of settled adsorbent was taken for analysis using the techniques described above. In the cathode compartment, 400 mL of 0.3% NaCl solution (w/v) acidified with 5 M HCl (to pH, 2±1) was added as an electrolyte. After connecting the power supply to the anode and cathode of the electrochemical cell, a DC current was supplied for a fixed regeneration time so that the electrochemical regeneration of the adsorbent took place. Samples of the adsorbent during regeneration were removed at different intervals of time and analysed using the techniques described above. For re-adsorption, a volume of phenol solution of known concentration was

added to the mini-SBR and was mixed under identical conditions to the initial adsorption stage.

6.4 Results and Discussion

6.4.1 Surface Analysis Using Various FTIR Techniques

Using FTIR with various combinations including ATR, DRIFTS and IR microscope, no useful data was obtained regarding the surface characteristics of the GIC adsorbents during adsorption and electrochemical regeneration. This was probably due to the both the small concentrations of surface groups and adsorbates on the GIC surface, and the black colour of the GIC adsorbents. The details of these results are provided in appendix B.

6.4.2 Surface Analysis by Raman Spectroscopy

Infrared spectroscopy has been used to characterise the surface functional groups in coals *(Iglesias et al. 1998)*, carbon blacks *(Rositani et al. 1987)* and activated carbons *(Biniak et al. 1997)*. However, IR spectra of carbon based materials are difficult to obtain because of the problems associated with sample preparation, poor transmission and uneven light scattering *(Fuente et al. 2003)*. In addition, the electronic structure of carbon materials results in a strong IR absorption. Some of these problems can be overcome by using most recently developed techniques such as DRIFTS *(Fanning and Vannice, 1993)*. Nevertheless, no spectral information was obtained for GIC adsorbents using FTIR with a range of techniques as described above.

Raman spectroscopy has been successful in studies of diamond, fullerenes, carbon nanotubes and graphite *(Yasuda et al. 2003)*. Thus, Raman spectroscopy of GIC adsorbent was performed for the samples collected after adsorption and during regeneration. The results indicated the presence of three peaks at Raman shifts of 1341, 1590 and 2680 cm^{-1} for a sample of fresh GIC adsorbent (Figure 6.2). A single crystal of graphite produces only one peak at 1575 cm^{-1} (the G peak of crystalline graphite) *(Filik, 2005)*. For materials such as activated charcoal and carbon black a

second peak also appears at 1355 cm^{-1} (D peak from disordered graphite). When the amount of disorder increases in graphite, the intensity of the 'D' peak also increases relative to the intensity of the 'G' peak. The peak at around 1355 cm^{-1} is due to imperfections such as defects, discontinuities in the crystallites stacking and disorder in the crystal structure of graphite *(Pan, et al. 2002)*. Graphene has a characteristic Raman peak at around 2680 cm^{-1} (2D). This is the second order or overtone of the 'D' peak. The Raman spectrum observed for GIC adsorbent is thus consistent with what would be expected for a graphitic material. The slight shift in the observed peaks, and the presence of the graphene peak at 2680 cm^{-1}, may be because Nyex®1000 is a graphite intercalation compound (GIC) rather than a pure graphite.

The Raman spectra of phenol loaded GIC adsorbent (0.12 mg g^{-1}) and the same sample after it has been regenerated at 0.5 A for 10 min (2.14 C g^{-1}, 10 mA cm^{-2}) were very similar to that of the fresh GIC adsorbent (Figures 6.3–6.6). No peak was observed in the spectrum which would correspond to phenol or any other aromatic group present on the surface of GIC adsorbent. For regeneration times of 20 and 30 min, the spectra showed the presence of relatively larger 'D' peaks compared to the respective peaks present in the spectra of fresh and phenol adsorbed adsorbent (Figures 6.5–6.6). This suggests that during the course of electrochemical regeneration some disorder was being created in the GIC adsorbent sample. *Brown et al. (2004)* observed that during electrochemical regeneration of phenol loaded GIC adsorbent, the surface roughness was increased due to the break-up of flat graphene layers. This roughness may be responsible for inducing disorder into the GIC adsorbent and ultimately increasing the relative intensity of the 'D' peak. After regeneration time of 10 min the 'D' peak was similar to that of the fresh and phenol loaded adsorbent sample, suggesting that longer regeneration times were needed to induce disorder in the GIC (Figure 6.4). Further work is needed to investigate this behaviour and to determine the reproducibility of the findings.

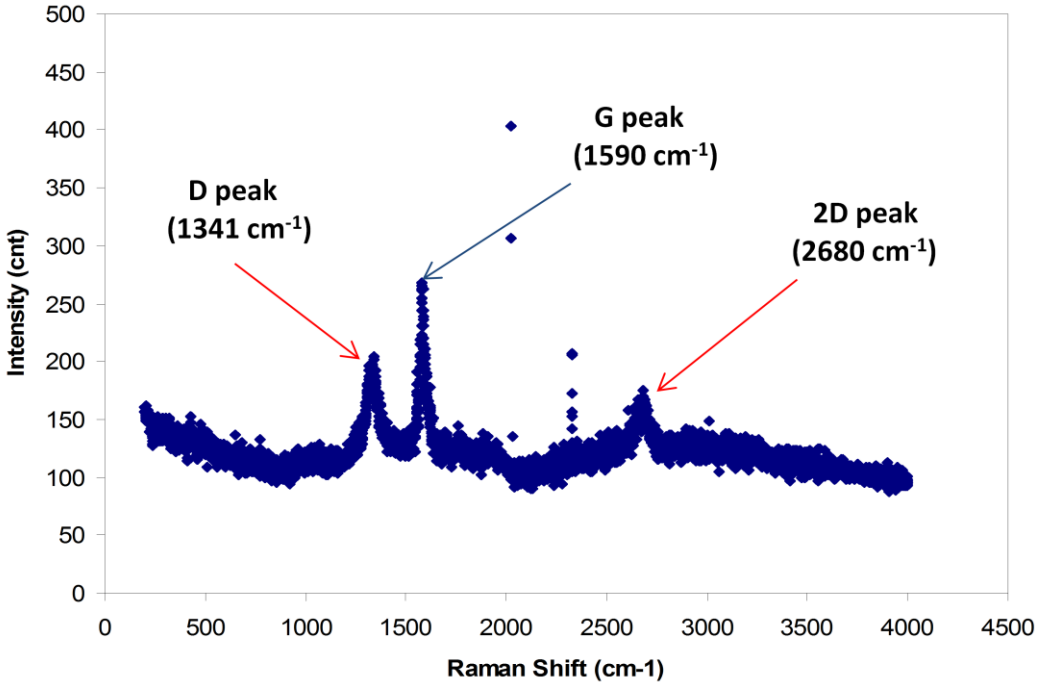

Figure 6.2: *Raman spectrum of fresh GIC adsorbent (Nyex® 1000).*

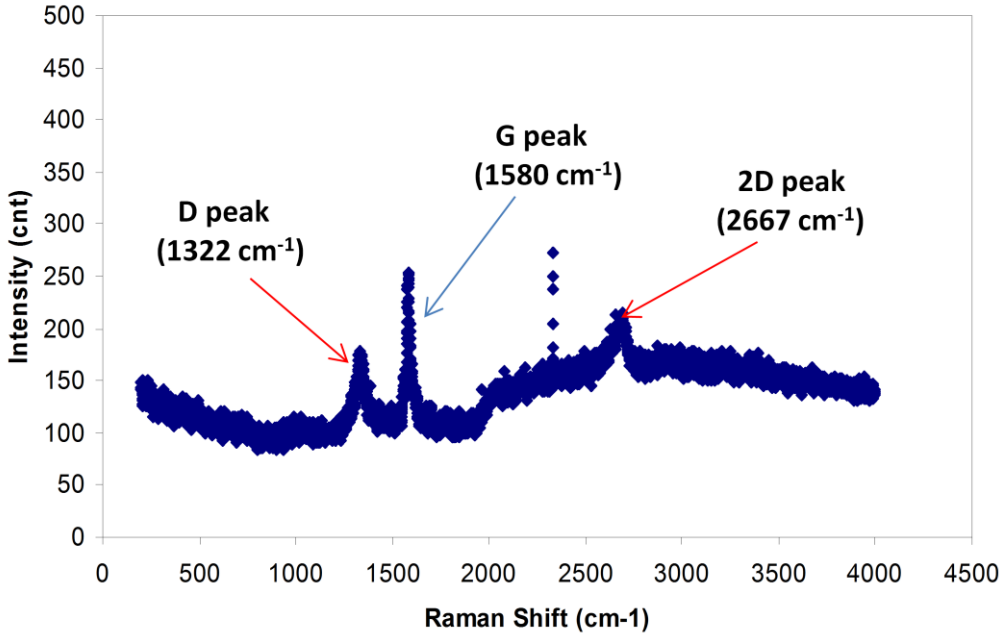

Figure 6.3: *Raman spectrum of phenol loaded GIC adsorbent (0.12 mg g^{-1}). Adsorption conditions: 100 mg L^{-1} of 500 mL phenol solution was mixed with 130 g of GIC adsorbent for 30 min in the mini-SBR*

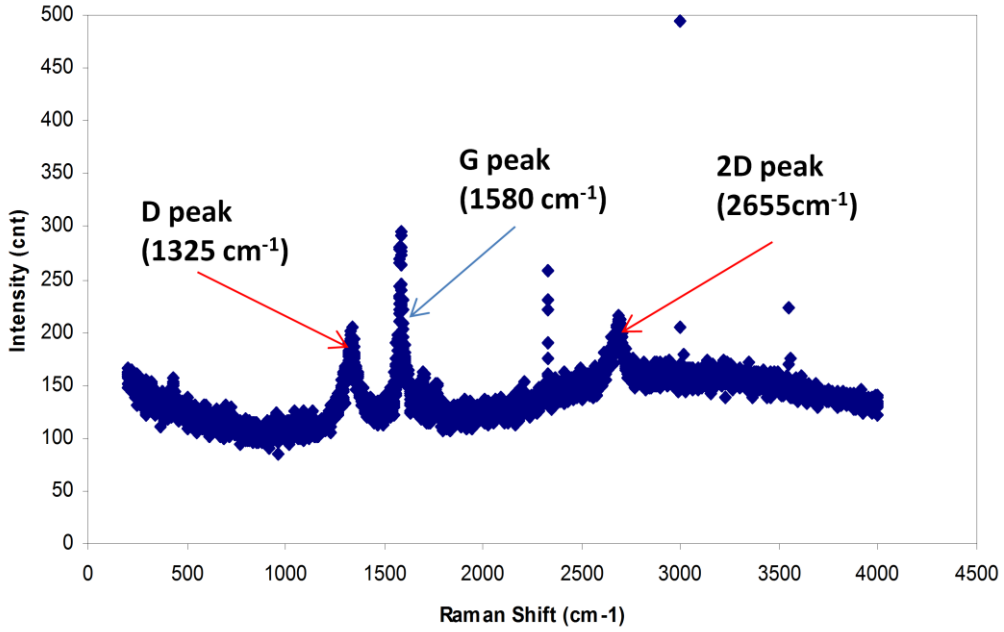

Figure 6.4: *Raman spectrum of regenerated (adsorption conditions as for figure 6.3) GIC adsorbent after 10 min at 0.5 A (2.14 C g^{-1}) corresponding to a current density of 10 mA cm^{-2}.*

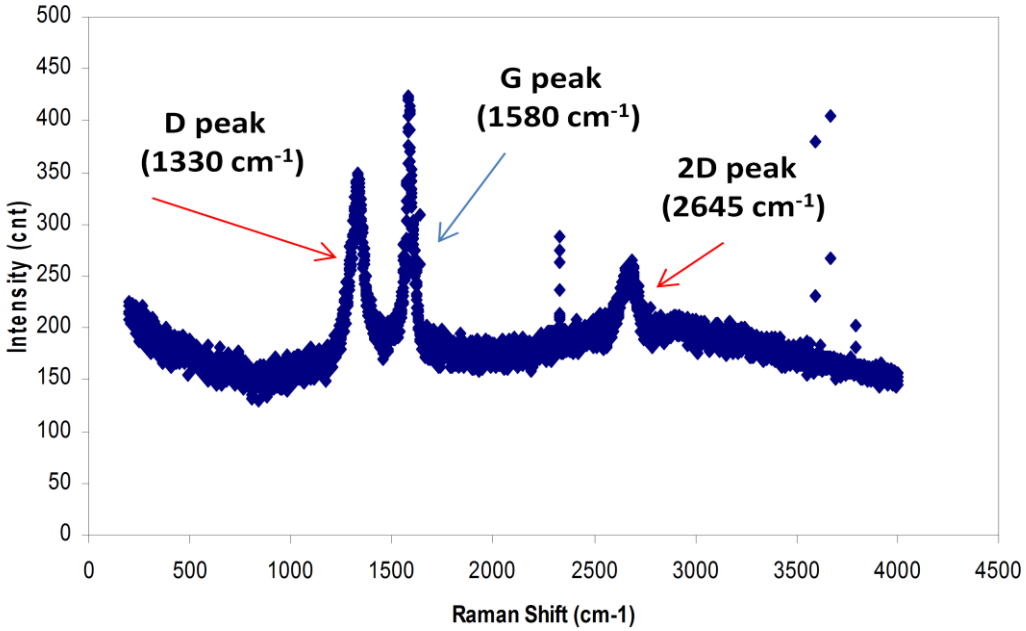

Figure 6.5: *Raman spectrum of regenerated (adsorption conditions as for figure 6.3) GIC adsorbent after 20 min at 0.5 A (4.28 C g^{-1}) corresponding to a current density of 10 mA cm^{-2}.*

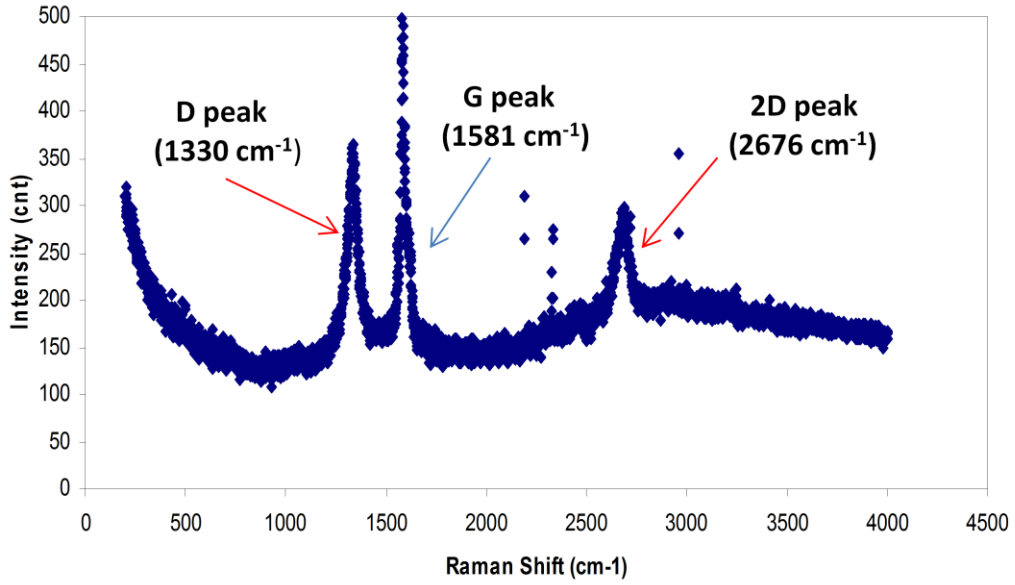

Figure 6.6: *Raman spectrum of regenerated (adsorption conditions as for figure 6.3) GIC adsorbent after 30 min at 0.5 A (6.42 C g^{-1}) corresponding to a current density of 10 mA cm^{-2}.*

6.4.3 Boehm Titration

The Boehm titration results presented in figure 6.7 show that fresh, adsorbed and regenerated GIC adsorbent samples had oxygen containing functional groups including phenolic, carboxylic and lactonic groups which are considered strongly acidic by nature. The presence of these groups on the surface of fresh GIC adsorbent is due to the oxidation of graphite by sulphuric acid during the manufacture of graphite hydrogen sulphate intercalation compound. The data shown in figure 6.7 indicates that the concentration of total surface functionality increased slightly for the GIC sample simply mixed with water using air in the mini-SBR. This could be due air oxidation of GIC particles in the mini-SBR leading to an enhanced surface functionality. The total surface functionalities were observed to increase during electrochemical regeneration of GIC adsorbent without phenol. This further indicates that there is an increase in surface functionalities with an increase in the regeneration time. It is important to note that this increase was largely due to an increase in phenolic and carboxylic functional groups. This was expected because electrochemical oxidation of graphitic materials in aqueous solutions creates surface oxides which are mainly composed of phenolic and carboxylic groups *(Besenhard and Fritz, 1983).*

The results also indicate that the concentration of phenolic groups is high in phenol loaded GIC adsorbent (1st adsorption) compared to fresh GIC adsorbent, suggesting the adsorption of phenol onto GIC adsorbent. However, these were found to be decreased during the electrochemical regeneration at 10 and 20 min (figure 6.7). In contrast, the concentration of carboxylic groups appeared to increase slightly during electrochemical regeneration of phenol loaded GIC adsorbent, possibly suggesting the oxidation of the adsorbed phenol to carboxylic species. This also illustrates nicely that anodic oxidation leads to an increase in carboxylic groups, consistent with oxygen transfer and oxidation to CO_2**.** It is important to note that regenerated samples after phenol adsorption did not show a considerable increase in the amount of total surface functionalities. Re-adsorption of phenol onto GIC adsorbent (2nd adsorption) subsequent to electrochemical regeneration leads to an increase in the amount of phenolic groups as in the first adsorption cycle. For a phenol loading of 0.1 mg g^{-1}, the concentration of phenol in mol g^{-1} is 1.06×10^{-6}, which is obviously a very small value compared to the phenolic groups concentrations calculated using Boehm titration (Figure 6.7). This suggests that the increase of phenolic groups on adsorption cannot be explained simply by the adsorption of phenol as the concentration of functional groups is much higher than the number of moles of phenol adsorbed per gram. However, this needs further investigation.

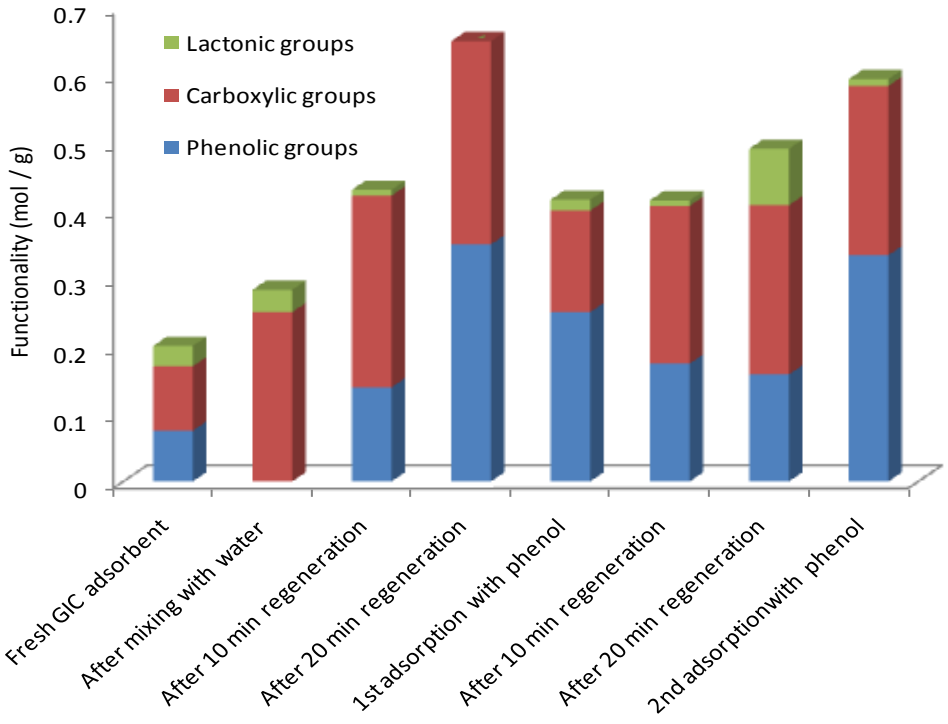

Figure 6.7: *Concentration and distribution of surface functional groups obtained from fresh, adsorbed and electrochemically regenerated GIC adsorbents using Boehm titration. Operating conditions with phenol: 130 g of GIC adsorbent was mixed with 500 mL of phenol solution of 100 mg L^{-1} in the mini-SBR for 30 min, giving a phenol loading of around 0.12 mg g^{-1}. Regeneration of settled adsorbent was carried out at 0.5 A (10 mA cm^{-2}); re-adsorption was carried out under the same conditions as maintained for the first cycle. Operating conditions without phenol: 130 g of GIC adsorbent was mixed with 500 mL of deionised water in the mini-SBR; regeneration of settled adsorbent was carried out at 0.5 A (10 mA cm^{-2}).*

6.4.4 Energy Dispersive X-ray Spectroscopy (EDS)

EDS was used in order to investigate the elemental analysis of the surface of the GIC adsorbent. This technique cannot be used to find out the type and concentration of functional groups present on adsorbents. An increase in the concentration of surface oxygen could be treated as an indication of the increase in oxygen containing functional groups. Samples of fresh, phenol adsorbed, and electrochemically regenerated GIC adsorbent were analysed using EDS. The results obtained from EDS are presented in figure 6.8. A slight increase in the oxygen concentration was observed for the phenol loaded GIC adsorbent (within the resolution of the beam and excited flat areas from which the X-rays are generated) compared to the fresh

sample. However, a significant increase in the oxygen concentration was found for the phenol adsorbed sample when the analysis was carried out on an edge of a GIC particle (figure 6.8). This was expected because rough surfaces and edges contain relatively high concentrations of functional groups attached compared to flat surfaces. As explained in section 6.1, in graphitic materials the graphene layers are piled up on top of each other by van der Waal's forces. Two distinct sites can be differentiated in the graphene layers: basal and edges carbon atoms *(Bandoscz and Ania, 2006)*. The disordered fraction of carbon materials such as activated carbons contains a large number of imperfections and defects. These sites along with the edges of carbon layers are associated with higher densities of unpaired electrons and therefore show greater tendency to chemisorb heteroatoms including oxygen, hydrogen, nitrogen and sulphur etc leading to the formation of stable surface compounds. It is well know that the edges of graphene layers have higher reactivity towards heteroatoms compared to the basal planes *(Bandoscz and Ania, 2006)*. This suggests that phenol adsorption takes place preferentially on the edges of the GIC particles due to the presence of relatively increased percentage of oxygen containing functional groups (figure 6.8). *Mattson et al. (1969)* proposed that phenol adsorbs on activated carbons by a donor-acceptor complex mechanism involving carbonyl oxygen in functional groups attached to the carbon surface acting as the electron donor and the aromatic ring of the phenol acting as the electron acceptor.

The data presented in figure 6.8 also shows that the percentage of oxygen increases with an increase in the electrochemical regeneration time. This could be due to the electrochemical oxidation of graphite particles leading to the formation of surface oxides *(Besenhard and Fritz, 1983).* Another contributing factor could be the formation of some defects and imperfections with greater concentrations of oxygen containing functional groups *(Bandoscz and Ania, 2006)*. These results are consistent with the data obtained with Boehm titration as shown in figure 6.7. *Brown et al. (2004)* explained that the similar surface area of fresh (2.75 m^2 g^{-1}) and electrochemically regenerated Nyex®100 (2.8 m^2 g^{-1}), the creation of internal pores on GIC adsorbents was unlikely. However, surface roughening was observed by SEM images after electrochemical treatment. They suggested that this surface roughness could be due to exfoliation of some of the graphene layers from the GIC surface.

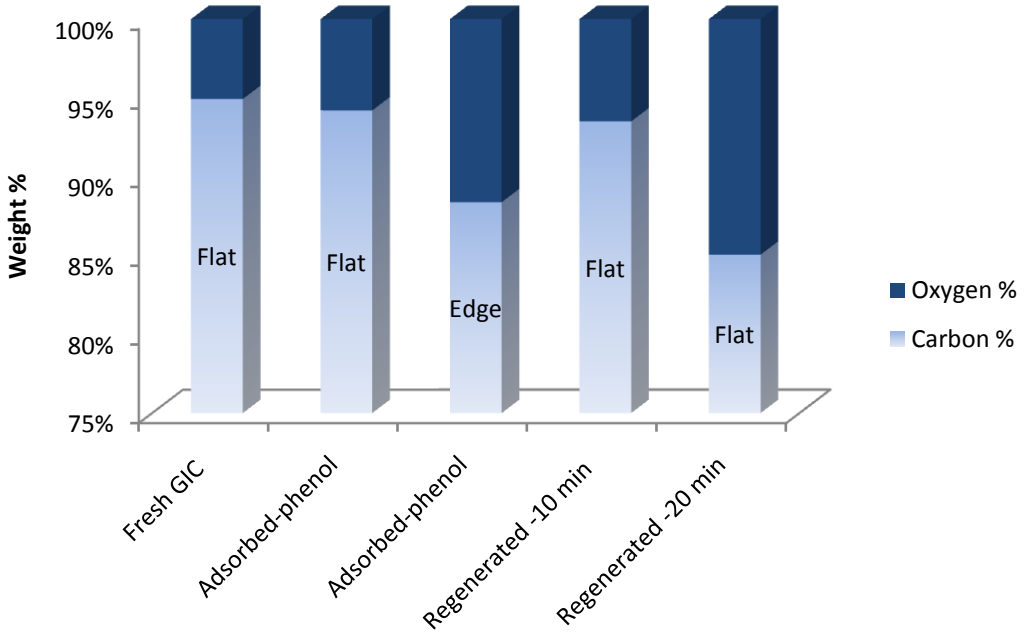

Figure 6.8: *Elemental analysis of fresh, adsorbed and electrochemically regenerated GIC adsorbent (Nyex®1000) samples using EDS. Operating conditions: 130 g of GIC adsorbent was mixed with 500 mL of 100 mg L^{-1} phenol solution in the mini-SBR (giving a phenol loading of around 0.12 mg g^{-1}); regeneration of settled adsorbent was carried out at 0.5 A (10 mA cm^{-2}).*

6.5 Conclusions

No spectral information could be obtained for GIC adsorbents during adsorption and electrochemical regeneration using FTIR technique in combination with ATR and KBr discs. This was probably because the GIC samples were not ground up, and the low concentrations of the adsorbates on the adsorbent surface. Similarly no useful spectrum was obtained for fresh, adsorbed and regenerated GIC adsorbents using DRIFTS, even though a relatively high concentration of phenol was used for this investigation. This disappointing result could be due to the dark nature of the GIC samples leading to a poor signal. Alternatively the dilution of the samples with KBr which further diluted the adsorbate could also have limited the signal associated with adsorbed species. Infrared microscopy could not detect any surface groups present on the GIC adsorbent during adsorption and electrochemical regeneration. Again this could be due to the low concentrations at the adsorbent surface.

Raman spectroscopy was successful in determining the graphite peaks for the GIC adsorbent but no surface groups were detected during adsorption and electrochemical regeneration. The increase in surface roughness during electrochemical regeneration was evident from the Raman spectra.

The Boehm titration was successful in showing that fresh, adsorbed and regenerated GIC adsorbent samples had oxygen containing functional groups including phenolic, carboxylic and lactonic groups which are considered strongly acidic by nature. The titration results also indicate that the concentration of phenolic groups was higher on phenol loaded samples compared to the fresh GIC adsorbent, confirming the adsorption of phenol onto the adsorbent. These groups were also found to decrease during electrochemical regeneration suggesting the oxidation of the phenol at the surface of the adsorbent.

EDS can be used to derive indirect information about the changes in the surface functionalities during adsorption and electrochemical regeneration of GIC adsorbents. An increase in the percentage of oxygen on the surface of the GIC was observed for the phenol loaded GIC adsorbent compared to the fresh GIC. The concentration of oxygen was significantly higher on the edges compared to the flat surface of the GIC particles, suggesting that the concentration of functional groups, and hence adsorption sites, was higher on the edges. The results obtained with EDS were approximately consistent with the results of the Boehm titration.

Future work is required to investigate the surface of GIC adsorbents during adsorption and electrochemical regeneration using techniques such as photoacoustic spectroscopy (PAS) and temperature programmed desorption (TPD) (see chapter 9). In addition, high capacity GIC adsorbents should be used to investigate the surface changes during adsorption and electrochemical regeneration.

Chapter 7
Electrochemical disinfection of water

This chapter discusses the importance of disinfection of water by considering the variety of microorganisms present in water. A comparison of different methods used to determine the concentrations of bacteria is reported. Various disinfection techniques are briefly discussed along with their relative advantages and disadvantages. The fundamentals of electrochemical disinfection of water and the mechanism of disinfection during electrochemical processes have also been explained. This chapter also describes the adsorption and electrochemical destruction of bacteria adsorbed on carbon surfaces. The use of GIC materials in disinfection of water employing adsorption with electrochemical regeneration is evaluated. The conclusions drawn from this study are provided at the end of this chapter.

7.1 Introduction

Disinfection of water is the removal, inactivation or killing of pathogenic microorganisms including bacteria, viruses and fungi which are harmful to human health, in order to prevent their growth and re-production. Disinfection is usually achieved by damage to the cell wall of microorganisms. Disinfection can also occur due to changes in cell permeability, alteration of the colloidal nature of protoplasm, alteration of organism DNA or RNA and inhibition of enzyme activity. These disturbances ultimately become the cause of the death of microorganisms *(Metcalf and Eddy, 2003)*. There are two types of disinfection, primary and secondary. In primary disinfection, a required level of microorganism inactivation is achieved whereas in secondary disinfection a disinfectant residual is maintained in the finished water which prevents the re-growth of microorganisms *(Boyce, 1996)*.

Microbiological contamination of water has long been a serious concern regarding public health. Drinking water is normally obtained from rivers, streams and lakes. These natural water sources often contain harmful microorganisms and may polluted

with domestic (grey and black water) and industrial wastewater. This wastewater consists of the following wastes *(Pelczar et al, 1993)*:

- Domestic waterborne wastes such as grey water (wastewater generated from domestic processes such as dish washing, laundry and bathing) and black waters (water from toilets or sewage). Grey water is distinct from black water in the amount and composition of its chemical and biological contaminants (faeces or toxic chemicals)
- Industrial waterborne wastes such as acids, oil, greases and animal and vegetable matter discharged by factories
- Ground, surface and atmospheric waters that enter the sewerage system.

7.2 Types of Microorganisms Present in Wastewater

There are different types and numbers of microorganisms in wastewaters due to variations in their composition. Microorganisms are those species that are too small to be seen without a microscope. Some of these organisms are bacteria while others are fungi, algae, protozoa and viruses *(Metcalf and Eddy, 2003)*. They can vary in size from <20 nm (some viruses) to several micrometers in the case of protozoal parasites.

7.2.1 Coliform & Other Bacteria

Coliform are a grouping of bacteria, the classical species in this group are *Escherichia coli (E .coli)* and *Enterobacter-aerogenes*. Some coliforms are harmless while others are of pathogenic nature. The pathogenic bacteria are responsible for many diseases including typhoid fever, cholera, diarrhoea and dysentery *(Mara and Horan, 2003)*. These microorganisms enter into bodies of water via intestinal discharges of humans and animals. Some coliform species particularly *E. coli, Streptococcus faecalis* and *Clostridium perfringens* are normal inhabitants of the large intestine of humans and other animals and are consequently present in faeces. For example, most strains of *(E. coli)* are harmless and live in the intestines of healthy humans and animals, however some of the strains are powerful toxins such as E. *coli O157:H7* that can cause sever illness leading to bloody diarrhoea and

abdominal cramps *(Cheremisinoff, 2002)*. Therefore the presence of these bacterial species in water is evidence of faecal pollution of human or animal origin. Furthermore, E. *coli* is universally used as an indicator microorganism *(Delaedt et al. 2008)*. Among the bacterial pathogens *Legionella*, *Pseudomonas aeroginosa* and *Staphyllococous aureus* are important microorganisms present in wastewater (see chapter 8).

7.2.2 Algae

The term algae are used for microorganisms that photosynthesize. When water is exposed to sunlight, algal growth occurs. The occurrence of algae in water is much like the growth of weeds in a garden. Algae are present in all natural aquatic environments. They become the cause of turbidity, discoloration, odour and taste in water. Microorganisms of this class include diatoms, yellow and green algae. These algae are capable of producing substances toxic to humans and animals *(Gilroy et al. 2000)*.

7.2.3 Protozoa

Protozoa are microorganisms that are classified as unicellular eukaryotes. Species that have a cell nucleus are called as eukaryotes. Protozoa usually range from 10–50 μm, but can grow up to 1 mm, and so are easily seen under a microscope. Gardia Lamblia is a flagellated protozoan that is parasitic in the intestines of humans and animals. The lifecycle of these species has two stages, one of which is a cyst form that can be ingested from contaminated water. Once the cyst enters the stomach, the organism is released into the gastrointestinal tract where it will adhere to the intestinal wall. Eventually the protozoa will move into the large intestine where they encyst again and are excreted in the faeces and back into the environment. In the body, the giardia causes giardiasis, a disease characterized by symptoms such as diarrhoea, abdominal cramps, nausea, weight loss, and general gastrointestinal distress. Cryptosporidium parvum is another protozoan parasite that causes cryptosporidiosis, a disease which includes symptoms of diarrhoea, headache, abdominal cramps, nausea, vomiting, and a low fever. However, most protozoa are non-pathogenic in nature *(Metcalf and Eddy, 2003)*.

7.2.4 Viruses

Many viruses are known to be excreted from humans through the intestinal tract. From sewage they may enter into sources of drinking water. The enteroviruses are most commonly found in sewage. They include the polio, coxsacki and echo viruses. Rotaviruses are also of major importance. Hepatitis A is an enteric virus that is very small. It can be transferred through contaminated water. Symptoms such as an inflamed liver, accompanied by lassitude, anorexia, weakness, nausea, fever and jaundice are common *(Metcalf and Eddy, 2003).*

7.3 Quantitative Measurement of Bacterial Population

There is a range of methods used for measuring the total population of bacteria in a suspension. These are based on the following types of measurement *(Pelczar et al. 1993).*

Cell Count

The number of bacteria present in a sample can be measured directly using a microscope or an electronic particle counter. Alternatively, the cells may be measured by a colony counting technique.

Cell Mass

The amount of bacteria present can be measured directly by weighing, by a measurement of cell nitrogen, or indirectly by turbidity.

The determination of dry weight involves cell separation by membrane filtration or centrifugation, washing steps and drying to constant weight. This method can only be used with dense cell suspensions and the cells must be free of all any other suspended solids *(Richmond, 2004).*

The major constituent of a microorganism is protein and since nitrogen is a characteristic part of proteins, one can measure a bacterial population in terms of bacterial nitrogen. This is usually performed by a quantitative chemical analysis for

nitrogen. Bacterial nitrogen determinations are rather laborious and can only be applied for cell suspensions free of all other sources of nitrogen *(Pelczar et al. 1993).*

The main methods used are discussed below.

7.3.1 Direct Microscopic Count using a Counting Chamber

Bacteria can be counted directly with a counting chamber. This is a device used to determine the number of cells per unit volume in a cell suspension. The most widely used type is Petroff-Hausser counting chamber as shown in figure 7.1 *(Pelczar et al. 1993).* This is a special slide accurately ruled into squares that are 1/400 mm^2 in area. A glass cover slip rests 1/50 mm above the slide so that the volume in a square is 1/20,000 mm^3. A suspension of unstained bacteria can be counted with the help of a microscope. Very dense suspensions can be counted after proper dilution of the suspension. However, suspensions having low numbers of bacteria can not be counted accurately. If an average of *Z* bacteria is present in each ruled square then there are $Z \times 2 \times 10^7$ bacteria per millilitre.

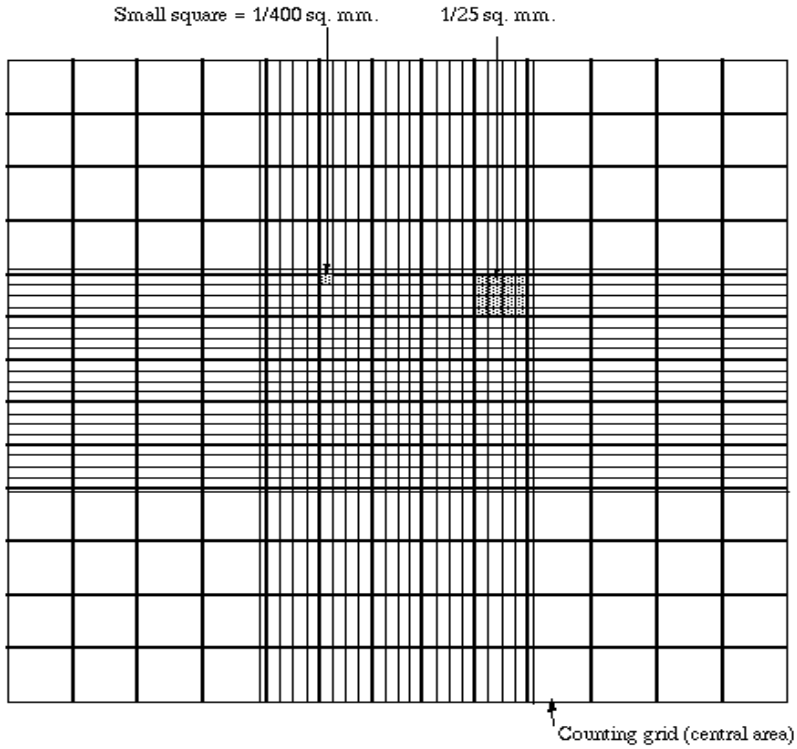

Figure 7.1: *A diagram of a counting chamber used to count the total number of bacteria*

A major advantage of direct counts is the speed with which results can be obtained. However, it is not possible to distinguish between living and dead cells by this method. Therefore, the direct microscopic count is not useful for determining the number of viable cells in a culture.

7.3.2 Electronic Enumeration of Cell Numbers

The bacterial suspension is placed inside an electronic particle counter which consists of a tiny orifice 10 to 30 μm in diameter. The bacteria are passed through this orifice which connects the two compartments of the counter containing an electrically conductive solution. As each bacterial particle passes through the orifice, the electrical resistance between the two compartments increases momentarily. This generates an electrical signal which is automatically counted. Although this method is rapid, it requires sophisticated electronic equipment. Also the orifice tends to become clogged *(Pelczar et al. 1993).*

7.3.3 Turbidimetric Method

Bacteria in a suspension absorb and scatter light passing though them so that a culture of more than 10^7–10^8 cells per millilitre appears turbid to the naked eye. A spectrophotometer or colorimeter can be used for turbidimetric measurements of cell mass. Though turbidimetry is a simple and rapid method used to enumerate bacterial growth, it is not possible to measure cultures grown in deeply coloured media or cultures that contain suspended material other than bacteria. The dead as well as living cells both contribute to turbidity of the suspension and thus the number of living cells can not be counted.

7.3.4 Measurement of Viable Cells

In determining the total number of cells using the methods discussed above there is no way to know the proportion of viable cells. Therefore techniques that allow cells to grow or multiply may be used to determine the concentration of viable cells.

There are two techniques to achieve this function *(Pelczar et al. 1993)*:

- The plate count method
- Membrane filter count

The plate count method

This method allows determination of the cell population which will grow under certain defined conditions. Serial dilutions of bacterial suspension are made, prior to their plating onto a suitable growth medium such as agar, in such a way that 100 µL of a given sample is transferred into an eppendorf tube containing 900 µL of normal saline to give 10^{-1} dilution (Figure 7.2). After thorough mixing, 100 µL of this 10^{-1} dilution sample is transferred to another eppendorf tube which also contains 900 µL of normal saline to give 10^{-2} dilution. Thus, a number of 10- fold dilutions are made in this way (Figure 7.2). This is usually done to achieve a number of colonies to be counted in the range of 30 to 300 per mL.

Within this range the count can be accurate, and the possibility of interference of the growth of one organism with that of another is minimized. A measured volume of suspension is either spread over the surface of the growth medium. Alternatively the suspension may be mixed with the medium prior to its solidification and poured into the plate. The plates are incubated so that colonies are formed.

Multiplication of a bacterium on solid media results in the formation of a macroscopic colony visible to naked eye. Colonies are usually counted by illuminating them from below so that they are easily visible. A large magnifying lens is often used to count the number of colonies. Various electronic techniques have also been developed for the counting of colonies formed by this method. It is likely to be assumed that each colony arises from an individual viable cell. Hence, a colony count performed on a plate reveals the viable microbial population of the inoculums. Total number of colonies is counted and this number multiplied by dilution factor provides concentration of cells in the original sample.

One important limitation of the plate count technique is that each viable microorganism which is capable of growing under specified conditions may not give rise to one colony. The method is thus only applicable when the bacterial suspension is homogenous and there is no formation of aggregates of cells. On the other hand, if the cells have the tendency to aggregate the resulting counts will be lower than the number of individual cells. For this reason the counts are often reported as colony-forming units per millilitre rather than number of bacteria per millilitre. However this technique is useful in determining the number of live bacteria in milk, water, foods and many other materials. It has the advantage of sensitivity since very small numbers of microorganisms can be counted.

The number of colony forming units (CFU) per mL can be calculated as:

$$\text{CFU mL}^{-1} = \frac{\text{Number of colonies formed}}{\text{Volume of sample (mL)} \times \text{Total dilution used}} \qquad (7.1)$$

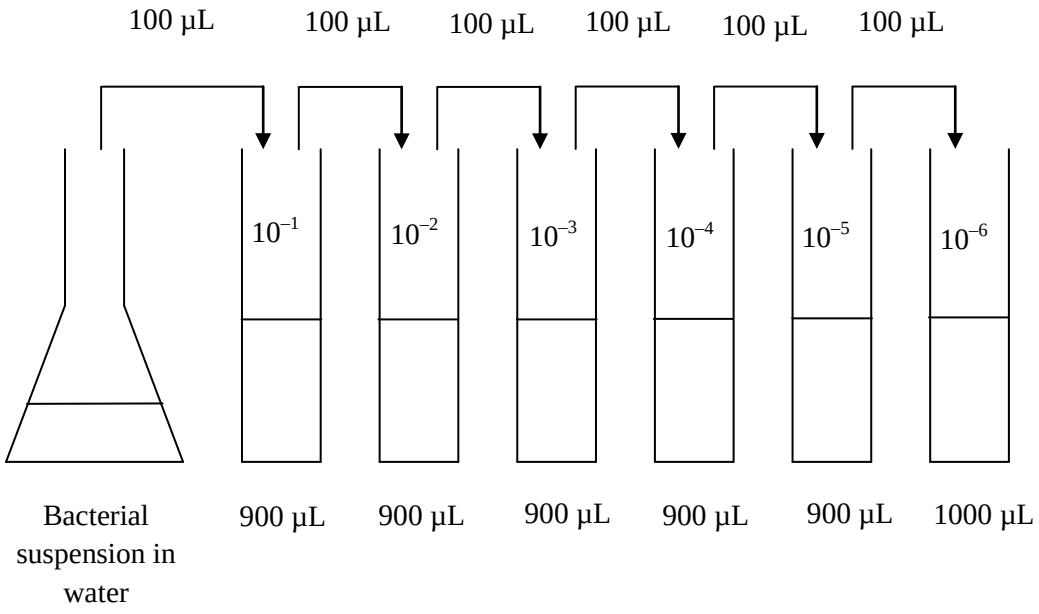

Figure 7.2: *Schematic representation of serial dilutions of bacterial suspension. The numbers 10^{-1}, 10^{-2} etc indicate the total dilution used and 900 µL is the volume of normal saline added to each tube.*

Membrane Filter Count

This technique is a useful variation of the plate count method and is based on the use of molecular or membrane filters to trap microorganisms prior to their incubation. The membrane filters have a known porosity and pore size sufficiently small to trap microorganisms. The filter with its trapped bacteria is placed in a special plate containing a pad saturated with an appropriate growth medium. During incubation, the microorganisms grow into colonies which appear on the membrane surface. Special media and dyes can be used to detect certain types of organisms more easily than with the conventional plate count. This method is particularly valuable for samples containing very low concentrations of viable cells, as a very large sample can be filtered *(Metcalf and Eddy, 2003; Pelczar et al. 1993).*

7.4 Disinfection Techniques

The purpose of disinfection is the elimination of pathogens that are responsible for waterborne diseases. The transmission of diseases including typhoid, paratyphoid fevers, diarrhoea and cholera etc can be controlled with treatments that substantially reduce the concentrations of viable microorganisms in water. Chlorination is the most commonly used chemical method of water disinfection which is very effective for removing almost all microbial pathogens. It is used for both primary and secondary disinfection *(White, 2010).* However, the use of chlorine as a disinfectant is also associated with the following disadvantages:

- Unfavourable taste and odour associated with the use of chlorine in drinking water.
- Chlorine has been identified as a source of potentially toxic disinfection by-products. It reacts with a variety of organic impurities in water and converts them into trihalomethanes and other halogenated hydrocarbons *(Boorman et al. 1999)*
- It is ineffective when used alone against some microorganisms such as cryptosporidium parvum *(Venezel et al. 1997).*
- There are significant hazards associated with the transport and storage of chlorine.

Because of these factors, alternative technologies for water disinfection have been developed. These alternatives include chemical and physical processes. Chemical methods employ disinfectants such as ozone *(Cho et al. 2003; Camel and Bermond, 1998)*, chlorine dioxide *(Junli et al. 1997)*, hypochlorite *(Bolyard and Fair, 1992)*, bromine *(Moore et al. 1992)*, iodine *(Chang, 1958)*, bromine chloride *(Taylor and Butler, 1982)*, ferrate *(Jiang and Panagoulopoulos, 2006)*, copper *(Kim et al. 2004)*, silver *(Kim et al. 2004)*, potassium permanganate *(Chen and Yeh, 2005)* and hydrogen peroxide *(Drogui et al. 2001)*. Physical methods include thermal treatment, ultraviolet irradiation *(Bergmann et al. 2002; Campbell et al. 1995)*, ultrasonication *(Hua and Thompson, 2000; Jyoti and Pandit, 2001)*, pulsed electric fields irradiation *(Anpilov et al. 2002; Narsetti et al. 2006)*, filters capable of retaining bacteria and reverse osmosis *(Kerwick et al.2005; Madaeni, 1999)*.

A comparison of the relative advantages and disadvantages of a number of these disinfection methods is discussed below.

Among chemical alternatives, chlorine dioxide can effectively destroy pathogenic microorganisms. It is a stronger oxidant than chlorine and also provides longer residual as a secondary disinfectant. In addition, in the absence of chlorine, ClO_2 does not produce trihalomethanes *(Anderson et al. 1982)*. On the other hand the disadvantages of ClO_2 are its relatively high cost and production problems. When bromine chloride is used as a disinfectant, it provides more disinfection than chlorine because of its higher reactivity towards microorganisms. However, in the presence of organics during disinfection, brominated compounds are formed which are generally more toxic than the chlorinated organics *(Richardson et al. 1999)*. Silver and copper are powerful inorganic disinfectants for water. Their respective ions are electrochemically produced from electrodes made of silver and copper contained within a flow cell. They are effective in relatively low concentrations compared to the amount of chlorine required in chlorination processes. They do not produce disinfection by-products in the treated water. However, the disinfection process using silver and copper ionization system have scaling problems of the electrodes and the installation and maintenance costs are high *(Block, 2001; Kim et al. 2004)*. In ozonation, ozone is widely used to disinfect water due to its strong biocidal and oxidising properties *(Cho et al. 2003)*. This technique is widely used for primary

disinfection in many parts of the world *(Block, 2001)*. Ozone as an unstable gas is normally generated onsite. However, ozone dose not provide a residual effect and a secondary disinfectant, normally chlorine is required when disinfection is carried out with ozone.

A combination of coagulation, filtration, settling and disinfection makes water potable. In fact, insoluble oxides are formed when chlorine, chlorine dioxide or ozone is added to raw water containing iron and manganese. Filtration becomes necessary because ozonation and chlorination may cause flocculation of dissolved organics in raw water which increases turbidity *(Smith et al. 1991).*

In physical disinfection methods, ultraviolet irradiation effectively destroys microorganisms and no residual toxicity is produced. In addition, it is more effective than chlorine in disinfecting most viruses, spores and cysts *(Metcalf and Eddy, 2003)*. However, it does not provide any residual effect and thus a secondary disinfectant is required with ultraviolet irradiation. It is also an energy intensive technique. Ultrasonic irradiation is an important alternative to chemical disinfectants. It can effectively inactivate a variety of microorganisms including bacteria and yeasts *(Anderson et al. 1982)*. In addition to disinfection, this technique also contributes to hardness removal by precipitating calcium and magnesium oxides. However, thick films of water attenuate the sound waves and reduce the effectiveness of the process. It is also a relatively expensive method of disinfection *(Anderson et al. 1982).*

Other physio-chemical systems such as photocatalysis using titanium dioxide *(Butterfield et al. 1997; Watts et al. 1995)* and photodynamic disinfection *(Bonnett et al. 2006)* have become increasingly important *(Kerwick et al. 2005)*. However, these methods do not generate a disinfectant residual in the finished water, similar to high intensity pulsed electric fields and ultraviolet light etc. Hence these methods are suitable only for primary disinfection where a residual of disinfection is not required. In contrast, electrochemical disinfection of water has emerged as a promising alternative to chlorine providing both primary and secondary disinfection *(Kerwick et al. 2005).*

7.5 Electrochemical Disinfection

The prospective use of electrochemical disinfection of water by electrolysis has been studied since the 1950s; however, systems other than those generating chlorine by electrochlorination has not yet gained widespread acceptance within the water industry *(Bergmann et al. 2002)*. Electrochemical disinfection has the potential to be developed as a robust, cost effective and environmentally friendly alternative for the disinfection of water and wastewater *(Patermarakis and Fountonkidis, 1990)*. It has the ability to destroy a large variety of microorganisms from viruses through bacteria and algae to relatively large species such as Euglena *(Stoner and Cahen, 1982)*. During electrochemical disinfection water is passed through a disinfector, an electrolytic cell, which is equipped with a set of electrodes. The effectiveness of electrochemical disinfection is mainly dependent upon cell configuration, electrode material, electrolyte composition, microorganism, water flow rate and current density *(Kerwick et al. 2005)*. One of the main advantages of electrochemical disinfection is the on-site production of disinfectants in the same device, for example: the production of chlorine by electrolysing a mixture of sewage with sea water. In this way, the common drawbacks of chlorination including transportation and storage of hazardous chemicals can be avoided *(Patermarakis and Fountoukidis, 1990)*. Thus, electrochlorination is the most popular method of water disinfection. The devices used for electrochemical processes can be divided into two categories: direct electrolysers and mixed oxidant generators. In direct electrolysers, the oxidants are directly produced from the water to be treated which then interfere with the microorganisms present in contaminated water whereas mixed oxidant generators use a concentrated brine solution to produce a mixture of strong oxidising species including free chlorine, hydrogen peroxide and other short lived radicals *(Venczel et al. 1997)*.

7.5.1 Mechanism of Electrochemical Disinfection

While electrochemical disinfection has been studied extensively, the mechanisms of disinfection have not been fully understood. Several mechanisms have been proposed for electrochemical inactivation or killing of microorganisms including oxidative stress, cell death due to electrochemically generated oxidants, irreversible

permeabilization of cell membranes by the applied electric field and electrochemical oxidation of vital cellular constituents during exposure to electric current *(Weaver and Chizmadzhev, 1996)*. *Weaver and Chizmadzhev (1996)* performed experiments on artificial bilayer lipid membranes and observed that on exposure to electric field the membrane stores charge just like a capacitor. As a result, transient pores are formed in the membrane. The reversibility of this electropermeabilization depends upon the magnitude of induced transmembrane potential and the duration of exposure to the electric field. Longer exposure times and transmembrane potential above one volt lead to irreversible permeabilization and ultimately causes the cell to die. Deactivation or death of cells occurs due to the formation of permanent pores, destabilization of cell membranes and loss of cell components.

Electrochlorination is considered to be the most effective method of disinfection for waters containing chloride ions. These ions are oxidized at the anode producing free chlorine species including Cl_2, HOCl and OCl^- (See chapter4, section 4.3). The disinfective action is due to the active chlorine compounds, Cl_2, HOCl and OCl^- which takes place in the bulk of the water. In addition, the active chlorine species can also provide residual disinfection capacity *(Stoner and Cahen, 1982)*. However, the enhanced inactivation of microorganisms associated with electrochemical disinfection cannot be fully described by the formation of free chlorine species *(Jeong et al. 2006)*.

Many studies in the literature have indicated that the disinfecting efficiency of electrochlorination is much higher than that of chlorination because of the generation of other oxidants during the electrochemical process *(Martinez-Huitle and Brillas, 2008)*. *Son et al. (2004)* evaluated the disinfection efficiency of a mixed oxidant solution representing electrochemically generated oxidants, and compared it to that of a free chlorine solution on the basis of equal concentration of oxidant. They observed that the mixed oxidant solution was 20–50% more efficient in inactivating E. *coli* and *Bacillus subtilis* at certain pH conditions (pH 8.2). Similar findings have been observed by *Diao et al. (2004)* during the inactivation of E. *coli* by various disinfection techniques including electrochemical disinfection, chlorination, ozonation and by Fenton reaction. They used scanning electron microscopy (SEM), a powerful technique used to investigate the detailed morphology of microorganisms.

Their results demonstrated that the electrochemical process is highly effective for wastewater disinfection. Surface deformations of E. *coli* were observed after chlorination and ozonation which were in contrast to intracellular leakage observed after electrochemical disinfection and Fenton reaction. The similarity between SEM results for electrochemical disinfection and Fenton reaction supported the hypothesis that predominant killing of microrganisms by electrochemical method is provided by high energy intermediate products such as free radicals and not by chlorine generated electrochemically. The electrochemically generated oxidants move freely to the interior of the cell and help in the deactivation process.

Furthermore, the higher disinfecting power of electrochlorination can be explained by the oxidant role of the reactive oxygen species including hydroxyl radicals ($OH^{\cdot}$), atomic oxygen ($O^{\cdot}$), hydrogen peroxide (H_2O_2) and ozone (O_3) *(Martinez-Huitle and Brillas, 2008)*. These species are produced by water discharge at the anode (equations 7.1–7.5) and are responsible for the inactivation of microorganisms due to indirect oxidation. The standard formation potential of a number of oxidants is given in Appendix-G.

$$H_2O \rightarrow OH^{\cdot} + H^+ + e^- \quad (7.1)$$

$$OH^{\cdot} \rightarrow O^{\cdot} + H^+ + e^- \quad (7.2)$$

$$2O^{\cdot} \rightarrow O_2 \quad (7.3)$$

$$2OH^{\cdot} \rightarrow H_2O_2 \quad (7.4)$$

$$O_2 + O^{\cdot} \rightarrow O_3 \quad (7.5)$$

Due to the high reactivity of $OH^{\cdot}$ and $O^{\cdot}$, once desorbed these radicals remain confined near the electrode in a thin layer of solution *(Polcaro et al. 2007)*. These species are unstable, rapidly forming oxygen (eq 7.3) or other reactive oxygen species such as ozone and hydrogen peroxide (eq 7.4–7.5). The higher oxidation potential of the reactive oxygen species makes them more efficient disinfectants than chlorine for all kinds of microorganisms *(Jeong et al. 2006)*. However, because of

the very short life of these radicals this kind of disinfective action must take place in the vicinity of the electrode surface and not in the bulk of water leading to a small residual disinfection capacity.

In addition, to the reactive oxygen species, relatively weak oxidants such as peroxodisulphate, peroxodicarbonate and peroxodiphosphate can also be formed due to the oxidation of sulphate or bisulphate, bicarbonate and phosphate ions present in water at the surface of anode (equations 7.6–7.8) *(Martinez-Huitle and Brillas, 2008)*. However, peroxodicarbonate and peroxodisulphate are also considered strong oxidising agents for bacteria *(Patermarakis and Fountoukidis, 1990)*. This type of action is expected to take place in the bulk of the water.

$$2HSO_4^- \rightarrow S_2O_8^{2-} + 2H^+ + 2e^- \quad (7.6)$$

$$2HCO_3^- \rightarrow C_2O_6^{2-} + 2H^+ + 2e^- \quad (7.7)$$

$$2PO_4^{3-} \rightarrow P_2O_8^{4-} + 2e^- \quad (7.8)$$

Patermarakis and Fountoukidis, (1990) has also indicated similar processes (equation 7.1–7.8) occur during the disinfection of natural water contaminated with coliforms and faecal streptococci using electrochemical treatment with titanium electrodes. They also verified the residual disinfection capacity by mixing electrochemically treated disinfected natural water with contaminated water.

On the other hand, the electrical field might also directly cause the death of bacteria by electrochemical reaction taking place inside them and/or by the charge transferred from the microorganisms to the anode at a potential insufficient to cause the electrolysis of water *(Porta and Kulhanek, 1986)*. In addition, electric fields are also capable of destroying cells without rupturing the cell membranes, for example by electrochemical oxidation of intracellular coenzyme A *(Matsunaga et al. 1985)*. *Matsunaga et al. (1985)* found that electrochemical disinfection can occur due to direct transfer of electrons between a bacterial cell and an electrode rather than the production of oxidising species. The authors attached cells of saccharomyces

cerevisiae to the surface of a graphite electrode and the respiratory activity and viability of the microbial cells were monitored when a constant potential was applied to the graphite electrode. In order to elucidate the disinfection mechanism, they first covered the electrode surface with a dialysis membrane which stopped the direct contact between microbial cells and the electrode. No killing of microorganisms was observed in this case. When no membrane was used to cover the cells, a decreased respiratory activity and subsequent microbial cell death was observed by applying a potential of 0.74 volt versus saturated calomel electrode. Disinfection was found to be due to the electrochemical oxidation of intracellular coenzyme A (CoA) and different from methods which generate toxic substances such as chlorine and H_2O_2 which attack microorganisms suspended in the water. The electron transfer was mediated by CoA in the cell wall of saccharomyces which were attached to the surface of the graphite electrode. This study thus suggested that for microorganisms attached to an electrode the disinfection mechanism is direct intracellular oxidation. This method is useful for the clean disinfection of water because toxic substances are not produced. *Kitajma et al. (1988)* have also shown that electrochemical disinfection can occur by direct electron transfer between a microorganism and an electrode rather than the generation of disinfectants by electrochemical oxidation. They studied electrochemical sterilization using a carbon fibre micro electrode. However, this mechanism can only take place at the time of electrolysis and therefore no residual disinfection capacity is expected. In this mechanism, the microorganisms must be attached to the electrode surface on which their oxidation takes place. This mechanism may take place during the disinfection of microorganisms using the Arvia® process since an adsorption step is used prior to electrochemical regeneration.

7.5.2 Electrodes used for Electrochemical Disinfection

The mechanism of electrochemical disinfection depends upon the nature of the electrode, the quality of water and the type of current used. Since the most reactive oxidising species generated during the electrochemical process have a very short life time, thus their role in solution is only important when using direct current (DC) *(Martinez-Huitle and Brillas, 2008)*. In addition, alternating current has been reported to be less effective than DC *(Porta and Hulnek, 1986)*. A variety of

electrodes have been utilized including metals *(Guillou and Murr, 2002; Kerwick et al. 2005; Tiesler, 1985),* mixed metal oxides *(Li et al. 2004)*, carbon (*Grainer et al. 1975; Stoner and Cahen, 1982; Matsunga et al. 1992)* and boron-doped diamond *(Dittmar and Worch, 2009; Palmas et al. 2007).*

Graphite electrodes have been used for electrochemical disinfection because of their low cost and relatively high electrochemical stability particularly in chloride containing solutions *(Stoner and Cahen, 1982).* Composite electrodes consisting of graphite fibres in an epoxy matrix have shown better performance than graphite plate *(Stoner and Cahen, 1982).* However, graphite electrodes were unable to disinfect a large number of microorganisms because of their small surface area *(Matsunga et al. 1992a).* A carbon-cloth electrode consisting of carbon fibers woven into a 0.4 mm thick material was used to enhance the surface area *(Matsunaga et al. 1992a)*. These electrodes were effective in killing *E. coli* cells, 10^2 per cm^3 at 0.7 V versus saturated calomel electrode (SCE). The authors claimed that disinfected bacteria were not adsorbed onto the electrode surface allowing continuous disinfection of water. The use of other carbon based materials in electrochemical disinfection of water is discussed in the following section.

7.5.3 Electrochemical Disinfection of Bacteria Adsorbed on Granular Activated Carbon

Granular activated carbon (GAC) has been used for the removal of organic compounds causing unpleasant tastes, odours and coloured substances from drinking water *(Stuffet, 1980).* In addition, GAC is also effective in adsorbing trihalomethanes and other carcinogenic disinfection by–products *(Gopal et al. 2007; Technology Review, 2007).* However, this treatment can result in bacterial growth on activated carbon *(Wilcox, 1983)*. The bacterial growth on activated carbon is considered to be due to the following factors:

- The adsorptive properties of GAC lead to adsorption of some compounds which serve as nutrients for bacterial growth.
- Bacteria are protected from the fluid shear forces due to the porous surface of the GAC particles.
- The presence of different functional groups on the carbon surface promotes microbial attachment.

Therefore, bacteria attached to GAC are extremely resistant to many disinfectants *(Wilcox, 1983, Berman, 1988).* Bacterial colonization on activated carbon stops further attachment of bacteria. Electrochemical disinfection of bacteria adsorbed onto the surface of activated carbon has been evaluated by *Matsunaga et al. (1992b, 1994). Matsunaga et al. (1992b)* studied electrochemical disinfection of bacteria adsorbed on GAC in a 10 mL beaker containing 2 g of GAC connected by carbon fibres and separated from a reference and counter electrode in another 10 mL beaker by a salt bridge. They incubated an *E. coli* suspension with GAC for about 5 h at room temperature. The GAC was then washed with water to remove un-adsorbed *E. coli* cells and then resuspended in water and a constant potential was applied from a potentiostat. The authors believed that *E. coli* cells attached to GAC were killed electrochemically due to the electrochemical oxidation of the bacterial cells. They also tested other bacteria with the same procedure and demonstrated that the survival ratio of E. *coli*, *Staphylococuus aureus*, *Bacillus subtilis* and *Saccharomyces cerevisiae* was below 1% at applied potentials of 0.75, 0.80, 1.0 and 0.65 V versus SCE respectively. The survival ratio was defined as follows:

$$\text{Survival ratio (\%)} = \frac{\text{Viable cell number after treatment}}{\text{Viable cell number before treatment}} \times 100$$

The number of viable microorganisms in the water sample was determined by plating the sample on an agar medium plate after incubation.

In order to have complete sterilization of the adsorbed bacteria, electrical contact is essential for each GAC particle. Moreover, the electrical conductivity of GAC depends on the electrical contact of each GAC particle. However, after the adsorption of bacteria onto the surface of GAC, the electrical contact can be

disrupted by the formation of a bacterial film on the GAC surface. The authors suggested that the survival ratio can be further lowered by utilizing more electrically conductive materials such as activated carbon fibre felt (ACF) cloth in order to obtain greater disinfection efficiency. ACF has been used as an adsorbent because of its large surface area to weight ratio. In addition, it is more electrically conductive than GAC because of its fibrous structure *(Matsunga et al. 1994)*. *Matsunaga et al. (1994)* designed a reactor in which ACF tubes were used as electrodes. A smaller tube was used as the working electrode (diameter 18 mm, length 100 mm, thickness 5 mm) and a larger one (diameter 38 mm, length 100 mm, thickness 5 mm) served as counter electrode. The smaller tube was placed inside the larger tube with a 5mm space in between the tubes and an SCE reference electrode was used. The *E. coli* cells were adsorbed onto the surface of ACF and the viable concentration of the water was reduced from 22 cells mL^{-1} to <10 cells mL^{-1} when a potential of 0.8V vs SCE was applied across the reactor. The authors have also shown that ACF presented better adsorption capacity for *E. coli* than activated carbon and carbon cloth. They concluded that an electrochemical reactor employing ACF could be used to generate clean and safe drinking water; however additional separation systems would be required for non-bacterial pathogens including viruses and parasites.

The rate of disinfection may be further enhanced by increasing the contact between the microorganism and electrode, for example by improving the mixing dynamics in the reactor *(Okachi, 1997)*. On this basis the ACF reactor developed by *Matsunaga et al. (1994)* was modified by *Okachi, (1997)*. The improved reactor enabled more bacteria adsorption on the ACF surface and prevented bacterial attachment to the inner surface of the resin reactor case. However, the effectiveness of disinfection was also observed to decrease with time when a potential of 1.0 volt versus SCE was applied. The dead bacteria adsorbed onto the ACF surface and stopped further electrical contact between ACF and the viable bacteria. The dead bacterial cells were removed by applying negative potentials. Effective disinfection of drinking water for 840 h at a flow rate of 300 mL min^{-1} was achieved by the use of an alternating potential of 1 and – 0.8 V versus SCE for disinfecting and desorbing bacterial cells. It was also observed that the accumulation of bacteria on the ACF reactor caused an increase in current which enabled the self detection of microbial fouling. Although carbon fibre *(Matsunga et al. 1994)* and activated carbon *(Matsunaga et al. 1992 b)*

have been shown to be effective for electrochemical disinfection of attached bacteria at relatively low potentials, the attachment of the dead bacteria on the solid surfaces can interfere with continuous operation.

It is anticipated that GIC materials will be effective for electrochemical disinfection as the GIC adsorbent may adsorb a variety of microorganisms including bacteria present in water. The conductivity of the adsorbent bed within the anodic compartment of the batch electrochemical cell (Figure 4.2) has been shown to be over 13 times greater with the GIC materials (Nyex®100) compared with powdered activated carbon in the same electrochemical cell *(Brown, 2005)*. Thus, it is expected that the high electrical conductivity of the GIC will allow for the electrochemical destruction of the adsorbed microorganisms and a greater disinfection capacity will be achieved. In addition to the disinfection of water by adsorption and electrochemical regeneration process, trace organics present in water could also be removed simultaneously (See chapter 8).

Other carbon based materials used for electrochemical disinfection include carbon nano-tube based micro-filters that have been shown to be effective for the removal of bacteria and viruses *(Vecitis et al. 2011)*. *Vecitis et al. (2011)* demonstrated the efficiency of an anodic multiwalled carbon nanotube for the removal and inactivation of bacteria (E. *coli*) and viruses (MS2). At applied cell potentials of 2–3 V, the electrochemical multi-walled nano-tube filter significantly reduced the number of bacteria and viruses in the effluent. However, the main limitation of the process is scale-up which will require the production of larger carbon nanotube filters.

7.6 Conclusions

Disinfection of drinking water is essential for public health. A variety of microorganisms is present in water including bacteria, viruses and fungi. Chlorine is the most commonly used and effective disinfectant. However, concern due to the formation of undesirable chlorinated compounds has increased interest in the use of alternative treatment processes including UV and ultrasonic irradiation, ozonation and electrochemical disinfection. A brief comparison of the relative merits and de-

merits of many physical and chemical methods has illustrated that electrochemical disinfection has become an increasingly important and promising alternative to chlorine. Electrochemical disinfection can provide both the primary and residual disinfection. Despite its great potential and efficacy, the mechanisms of inactivation of organisms are not fully understood. A number of theories have been proposed to elucidate the mechanism which includes electro-chlorination, electrochemically generated oxidants, production of high energy intermediate products such as free radicals, and destruction caused by the electric field. The adsorption of bacteria onto GAC and activated carbon fibres has also been demonstrated. Microorganisms attached to the surface of GAC were killed electrochemically. This technique has been reported to be clean and safe for the treatment of drinking water. It is also believed that graphite intercalation compounds (GIC) may adsorb bacteria and other microorganisms that are harmful to human health. As the GIC materials are more electrically conductive than GAC, it is speculated that a greater electrochemical disinfection capacity may be achieved.

Chapter 8
Disinfection of water by adsorption with electrochemical regeneration

This chapter presents an experimental investigation of the application of adsorption with electrochemical regeneration using GIC adsorbents to disinfect microorganisms in water. The materials and methods used and the results obtained under a range of experimental conditions are described. In order to explore the disinfection mechanism, scanning electron microscope images of microorganisms observed on samples obtained during adsorption and electrochemical regeneration are presented. The potential of the process for the simultaneous removal of organics and disinfection of bacteria has also been evaluated by treating artificial swimming pool water. Finally, water contaminated with different types of bacteria, fungus and yeast have been treated by adsorption and electrochemical regeneration in order to investigate the application of the Arvia® process to water disinfection.

8.1 Adsorption and electrochemical regeneration using a model microorganism (*Escherichia coli)*

In this section, an investigation of the adsorption of an enteropathogenic bacterium, *Escherichia coli*, onto Nyex®1000 particles and the subsequent electrochemical regeneration of the adsorbent using the mini-SBR under a range of experimental conditions is described. The aim of this study was to explore the effect of various operating parameters on the disinfection performance.

8.1.1 Materials

Escherichia coli (*E. coli*) was chosen as a test microorganism for disinfection experiments. *E. coli* is currently the most specific indicator for faecal contamination of a water source and therefore it is considered as a model organism in laboratory research. The cells are about 2 μm long and 0.5 μm in diameter, with a cell volume of 0.6 – 0.7 μm^3 *(Kubitschek, 1990)*. Optimal growth of *E. coli* occurs at 37ºC. Under a microscope, *E. coli* is a rod-shaped prokaryotic cell (Figure 8.1), which has a long,

rapidly rotating flagellum (tail) used for movement. A strain of *E. coli* is a sub-group within the species that has unique characteristics that distinguish it from other *E. coli* strains. These differences are often detectable on the molecular level and may result in changes to the physiology or life cycle of the bacterium. For example, a strain may gain pathogenic capacity or the ability to resist antimicrobial agents. Different strains of *E. coli* are often host-specific, making it possible to determine the source of faecal contamination in environmental samples.

Initial disinfection trials were made using *E. coli* C600 obtained from Dr. Ruohang Wang, Laboratory Manager, School of Chemical Engineering & Analytical Science, at the University of the Manchester. However, this strain of *E. coli* showed contamination on nutrient agar plates after the samples were incubated to determine a viable cell count. Therefore another *E. coli* strain MS101 was obtained from the School of Biological Sciences, University of the Manchester. This strain of *E. coli* is non-pathogenic and has antibiotic resistance against nalidixic acid and streptomycin sulphate *(Stehling et al. 2008)*.

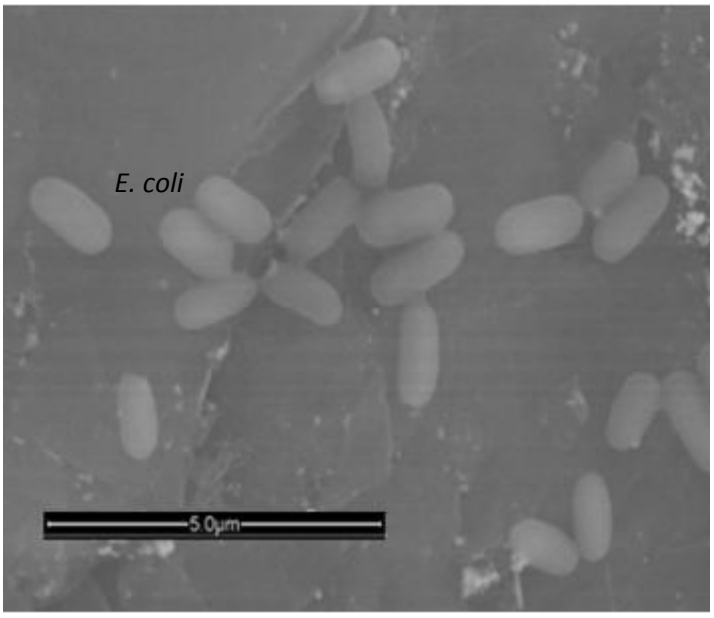

Figure 8.1: *Scanning electron micrograph of Escherichia coli* C600 *at 24000x magnification showing the rod shaped cells.*

Nutrient agar is a microbiological growth solid medium used for the cultivation of bacteria and for the enumeration of organisms in water, sewage, faeces and other materials. The composition of nutrient agar as supplied by Lab M (UK) contains beef extract, peptone, sodium chloride and agar no.2 at concentrations of 3, 5, 8 and 12 g L^{-1}, respectively.

Nutrient broth is a general purpose broth for the culture of non-fastidious microorganisms in liquid medium. This was supplied by Lab M (UK) and consisted of beef extract, peptone no.1 and sodium chloride with concentrations of 10, 10 and 5 g L^{-1} respectively.

All other chemicals including phosphate buffers, sodium chloride and sodium phosphate were supplied as analytical grade by Sigma Aldrich®. The ultra-pure water used for preparing bacterial suspensions and all other solutions was obtained from a laboratory Autostill™ 4000x (Jencons Scientific Ltd). The Nyex®1000 was used as a GIC adsorbent, supplied by Arvia Technology Ltd (see chapter 4 for specifications).

8.1.2 Viable count

The number of viable cells was evaluated using the plate count method *(Pelczar et al. 1997).* In this context, a number of serial dilutions of *E. coli* MS101suspension were made in such a way that 100 µL of a given sample was transferred into an eppendorf tube containing 900 µL of normal saline to give 10^1 dilution. The contents of the tube were thoroughly mixed on a spinmix vortex (Gallenkamp, UK) for a few seconds. From 10^1 dilution, 100 µL was transferred to another eppendorf tube which also contained 900 µL of normal saline to give 10^2 dilution. Thus, a number of dilutions up to 10^9 were made in this way (see chapter 7 for details). However, the actual number of dilutions depends upon the concentration of a given sample with the requirement of a greater number of dilutions for concentrated samples and vice versa. The solid cultivation medium was prepared by adding 28 g of nutrient agar to 1 L of ultra-pure water, as specified by the supplier (Lab M, UK). It was then allowed to soak for 10 min, swirled to mix and sterilized for 15 min at 121℃. After sterilization, the agar medium was cooled down to ca. 50℃ in a laminar flow cabinet

(Microflow, Intermed) to keep it in liquid form. At this stage, streptomycin sulphate was added to the agar at a concentration of 50 μg per mL of agar solution. Afterwards, the agar medium was gently added into petri dishes. Normally, 20–25 mL of agar is required to prepare a petri dish. These were then allowed to cool down in the laminar flow cabinet so that the agar gel solidified. A petri dish was then marked out into four equal quarters for the incubation of various dilutions of a given sample. For one sample, five drops of each dilution with a total volume of 50 μL (each drop is around 10 μL) were gently dropped onto each quarter of the petri dish, with different dilutions in each quarter. The petri dish with the inoculated sample was then placed in an incubator (Gallenkamp, UK) at 37°C for 24 h for incubation. The colonies that appeared on the petri dish after 24 h were counted as shown in figure 8.2 and the number of colony forming units per mL (CFU mL^{-1}) can be calculated using equation 7.1 (see chapter 7).

This method is by far the most sensitive method for determining the bacterial number, since even a single viable cell in a suspension can be detected *(Doelle 1994; Pelczar et al. 1993).* For this method, the plates should be inoculated with a sample dilution giving between 30 and 300 colonies for greatest accuracy. Error can arise with this method due to sampling and dilution errors, errors in pipetting volumes of diluted samples, microbial distribution errors and errors in counting colonies etc *(Jarvis, 2008).* The dilution error is assumed to be about 5–6% *(Doelle, 1994).* The distribution error is dependent on the number of colonies and is relatively small with high counts. The precision of the colony counts with different range of counts is given in table 8.1 *(Jarvis, 1989).* For the viable count method used in this project, a count of one colony in a 50 μL sample of dilution (10^0) gives a detection limit of around 20 CFU mL^{-1}.

Table 8.1: *The precision of colony counts with number of colonies (Jarvis, 1989)*

No. of colonies counted	Limited precision (closest to %)	Approximate 95% confidence limits of the colony count
500	±9	455–545
400	±10	360–440
320	±11	284–356
200	±14	172–228
100	±20	80–120
80	±22	62–98
50	±28	36–64
30	±37	19–41
20	±47	11–19
16	±50	8–24
10	±60	4–16
6	±83	1–11

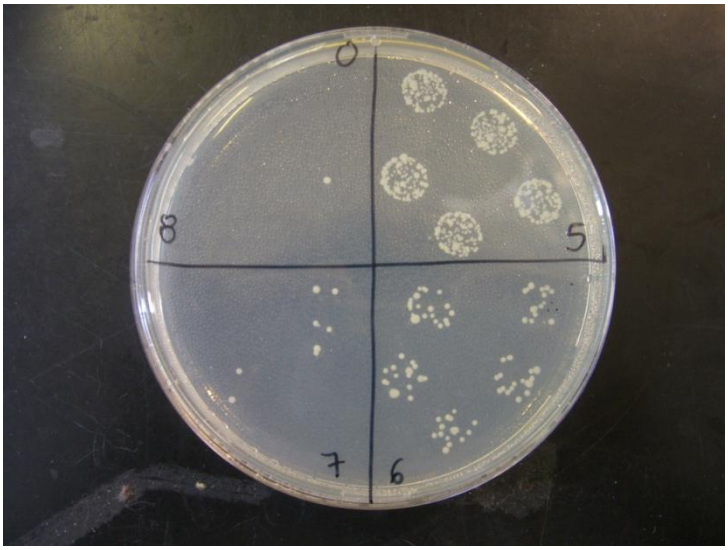

Figure 8.2: *Clear and distinct colonies of* E. coli MS101 *grown on a nutrient agar plate. The numbers 5, 6, 7 and 8 indicate the level of dilution (i.e* 10^5*,* 10^6*,* 10^7 *and* 10^8*, respectively) used for the samples in each quarter of the plate.*

8.1.3 Methods

Preparation of *E. coli* suspension in water

Two 250 mL volumetric flasks each with 5 g of Nutrient broth No.2 was allowed to soak with 200 mL of ultra-pure water for 10 min and then swirled to mix. This was prepared according to the concentration (25 g L^{-1}) as specified by the supplier (Lab M, UK). The mouths of flasks were covered with an aluminium foil and were placed in an autoclave at 121ºC for 15 min. After sterilization, the flasks were cooled down to room temperature in a laminar flow cabinet. Streptomycin sulphate was added to the broth at a concentration of 50 μg per mL of broth solution. The *E. coli* frozen stock culture was removed from a −70°C freezer and brought to the laminar flow cabinet. The 250 mL shaker flasks containing 200 mL of nutrient broth were inoculated each with five loopful of frozen stock culture of *E. coli*. The frozen stock culture was returned to the −70°C freezer, the volumetric flasks were placed on an orbital incubator shaker (Gallenkamp) set at 100 rpm and 37°C for 24 h. After incubation, the contents of flasks developed turbidity indicating the growth of *E. coli* in the nutrient broth. Afterwards, the flask contents were divided into eight 50 mL Nalgene^{R} centrifuge tubes (Oak Ridge style 3119) with a volume of 25 mL of *E. coli* suspension in each tube. They were centrifuged at 8000 rpm for 10 min at 25ºC in a high speed centrifuge (Beckmann). Centrifugation of the culture media containing suspensions of *E. coli* resulted in a tight pellet at the bottom of each centrifuge tube. The supernatant liquid from each centrifuge tube was poured off and the pellet was gently cleaned with sterile normal saline to remove any traces of broth. These pellets were finally re-suspended in a known volume of sterile normal saline (unless otherwise stated) to give a concentration of ca. 10^{7}–10^{8} CFU mL^{-1} of *E. coli*. The water containing suspension of *E. coli* was then used for the subsequent experiments. All processes were carried out using aseptic technique. The workspace and hands were sterilized by using 70 % ethanol. All glassware, test water and growth media were sterilized by autoclaving at 121ºC for 15 min.

Kinetics of *E. coli* adsorption onto GIC adsorbent

Volumes of 200 and 120 mL of cell suspension with initial concentrations of 1.58×10^9 and 1.0×10^9 CFU mL^{-1} (determined by carrying out a viable cell count on a sample of the suspension) were added to 500 mL volumetric flasks containing 20 and 5 g of GIC adsorbent, respectively. The contents of the flasks were stirred on a magnetic stirrer (Gallenkamp) at a speed of 700 rpm. For determining the concentration of viable cells in suspension using the method described in section 8.1.2, volumes of 5 mL were removed from the flasks at different intervals of time. The fines of Nyex®1000 were allowed to settle in each sample by giving 2 min settling time prior to their transfer to the respective dilution tubes for inoculation on the petri dishes followed by their incubation.

Adsorption Isotherm of *E. coli* cells onto GIC adsorbent

In order to estimate the capacity of Nyex®1000 for adsorbing *E. coli*, 100 mL samples of *E. coli* suspension with an initial concentration of 1.0×10^9 CFU mL^{-1} were added to various amounts of GIC adsorbent (0.5, 1, 2 and 8 g) in 250 mL volumetric flasks. Mixing was carried out using a magnetic stirrer (ER LAUDA, Germany) at 700 min^{-1} for 30 min (which was found to be the time required to achieve equilibrium). Afterwards, the samples were collected from each flask and were analysed for viable count. In this way the number of *E. coli* cells attached per gram of Nyex®1000 as a function of the suspension concentration at equilibrium was studied.

Batch adsorption and electrochemical regeneration studies using the mini-SBR

A specified volume of a known concentration of *E. coli* suspension was prepared in deionised water (unless otherwise stated) was mixed with a known quantity of GIC adsorbent in the mini-SBR (Figure 4.3) for 30 min using air from a compressor as described in chapter 4. After the completion of adsorption, the air supply was turned off and the adsorbent particles were allowed to settle for 2 min. A sample of the supernatant above the settled adsorbent was taken from the cell and analysed as described in section 8.1.2. In the cathode compartment, 0.3% (w/v) NaCl solution

acidified with 5 M HCl (to pH 1–2) (unless otherwise stated) was added as an electrolyte so that the catholyte was at the same level as the bed of settled adsorbent. Electrochemical regeneration of the settled GIC adsorbent was performed by applying a specified DC current for a fixed regeneration time so that the electrochemical regeneration of the adsorbent could take place. After the completion of regeneration, the current was turned off and a sample of water was again taken from the supernatant liquid for analysis (using the method described in section 8.1.2). Subsequently, the water present above the regenerated bed and the catholyte were siphoned off separately. Care was taken to minimise the removal of adsorbent during siphoning, and any adsorbent removed was allowed to settle out and returned to the cell. The water siphoned from the anode compartment was collected and sterilized before disposal. A measured volume of *E. coli* suspension of known concentration was added to the mini-SBR and re–adsorption was carried out under identical conditions to the initial adsorption stage. For adsorption and electrochemical regeneration over a number of cycles, the adsorption and regeneration procedure was repeated several times. The pH of the treated solution was also monitored during adsorption and regeneration cycles using a Cyber Scan pH 1500 meter (Eutech Instruments, Singapore). Samples of GIC adsorbent were collected during adsorption and electrochemical regeneration for SEM analysis.

A number of disinfection experiments were performed in the mini-SBR shown schematically in figure 4.3 (see chapter 4). However, in order to avoid the handling of large volumes of water contaminated with E. *coli* in the mini-SBR, another smaller unit was constructed with the same geometry as that shown in Figure 4.3. The area of each electrode in this smaller unit was 20 cm^2, with other dimensions as shown in figure 8.3.

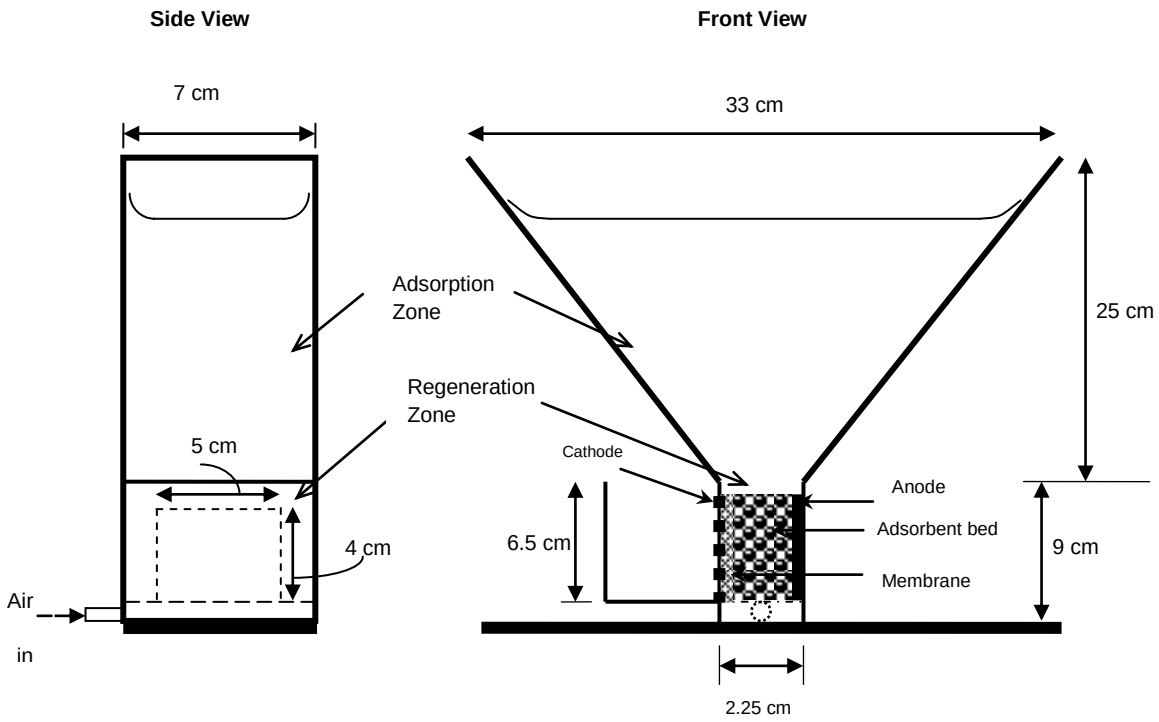

Figure 8.3: *Schematic diagram of the mini-sequential batch reactor with smaller dimensions to that of the mini-SBR shown in figure 4.3 (Chapter 4)*

8.1.4 Results and Discussion

Adsorption Kinetics

The results reveal that the adsorption of *E. coli* (MS101) at an initial concentration of 1.58×10^{9} CFU mL^{-1} onto GIC adsorbent with 100 g L^{-1} dose was surprisingly fast and almost 99.9% *E. coli* cells were removed from the solution after 10 min with a ca. 6.5-$\log_{10}$ reduction in the CFU concentration (Figure 8.4, a). However, these data do not show the precise kinetic behaviour or the equilibrium time because of the extremely fast removal of *E. coli*. Virtually all the *E. coli* cells were adsorbed onto the Nyex®1000 under the experimental conditions used for this study. After 10 minutes, no colony forming units were detected in the samples collected. In order to depict this zero *E. coli* concentration on a logarithmic plot, 1 CFU ml^{-1} was added to each measurement. To determine the equilibrium time, the dose of the GIC adsorbent was changed from 100 to 42 g L^{-1} so that there should be a measureable concentration of *E. coli* in solution after adsorption. The results from this experiment indicated that 30 min was required to attain equilibrium (Figure 8.4, b) with an

overall reduction of 0.2-$\log_{10}$ in bacterial suspension for an adsorbent dose of 42 g L^{-1}. Around 8-$\log_{10}$ reduction in *E. coli* concentration was observed for an adsorbent dose of 100 g L^{-1}. However, the actual reduction may be even greater than that calculated which was based on the detection limit (20 CFU mL^{-1}). Further trials are required to assess the adsorption kinetics in detail, but these experiments have shown that the rate of adsorption of microorganism is comparable with organic adsorption *(Brown et al. 2004a&b)*.

Rivera et al. (2001) studied the adsorption of *E. coli* K12 597 strain onto commercial activated carbons. The adsorption increased sharply up to 100% at around 4 hours. The authors had reported that it was due to the high mineral contents and hydrophobicity of the activated carbon. It is well known that surface hydrophobicity plays an important role in bacterial adsorption *(Stenstorm, 1988)*. On the other hand, the metallic oxides present in the mineral content also play an important role in the adhesion of bacteria on solid surfaces due to the formation of hydrogen bonds between surface hydroxyl groups and the bacterial surface polysaccharides *(Jucker et al. 1997)*. However, the elemental analysis of the GIC adsorbent shows that it is 98% carbon. The main constituents of its mineral content are Si, Cu, Cr, Mg, S, Mn, Fe and Pb as determined by Energy dispersive X-ray spectroscopy (EDS) (Figure 8.5). Silicon was found to be the main component of the quartz like species observed on the surface of the GIC adsorbent (Figure 8.6–8.7). Further investigation is needed to determine the influence of the mineral content of the GIC particles on the adsorption of E. *coli*.

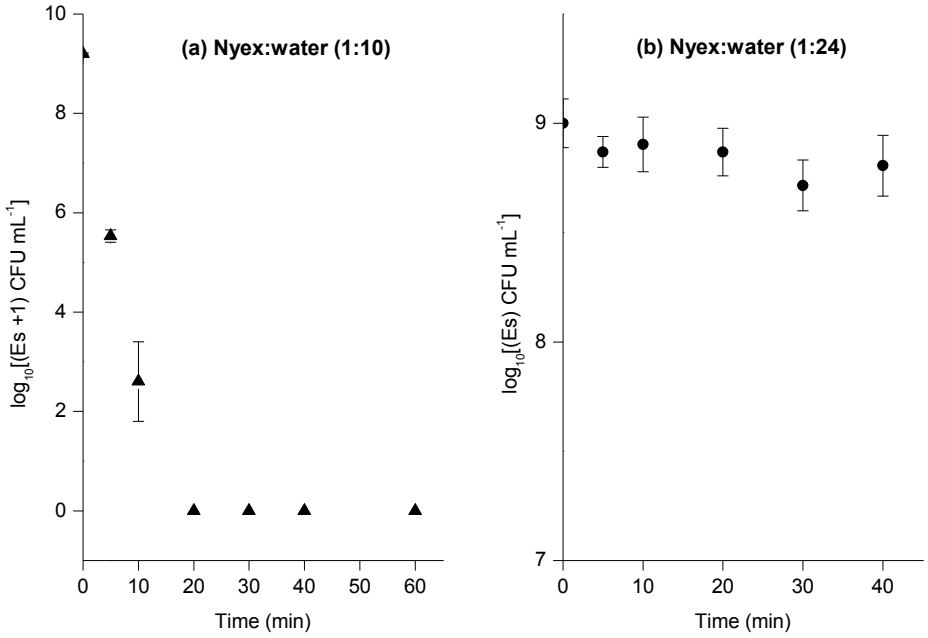

Figure 8.4: *Adsorption kinetics of E. coli* MS101 *onto GIC adsorbent at an initial concentration of (a): 1.58 × 10^9 CFU mL^{-1}, Nyex®1000 dose 100 g L^{-1} and (b): 1.0 × 10^9 CFU mL^{-1}, Nyex®1000 dose 42 g L^{-1}. Each data point represents the average of five samples and the error bars indicate standard errors calculated from the standard deviation. For (a) one was added to each data point so that the zero concentration appears on the logarithmic plot and Es denotes E. coli concentration.*

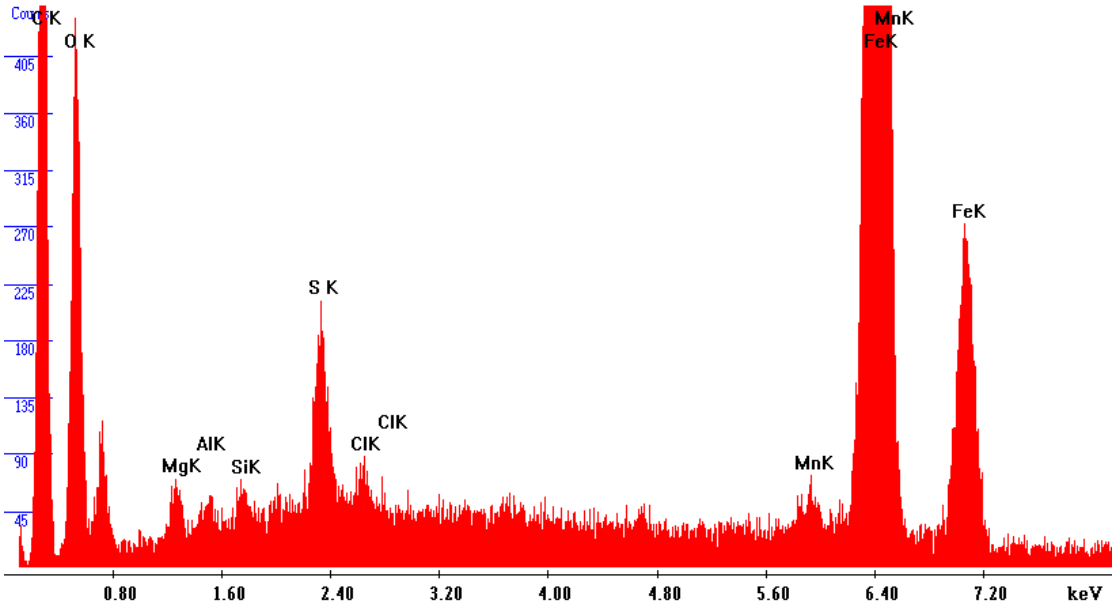

Figure 8.5: *EDS spectrum of Nyex®1000 particle showing the presence of Fe, S, Mn, Mg and Si*

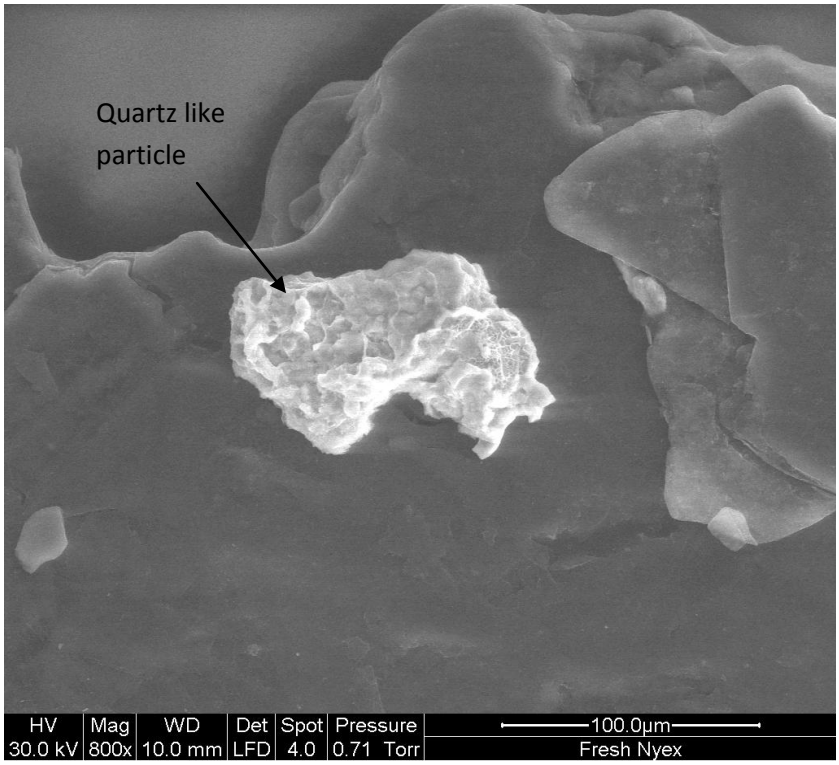

Figure 8.6: *Scanning electron micrograph of Nyex®1000 particle showing the presence of quartz like species at magnification 800x*

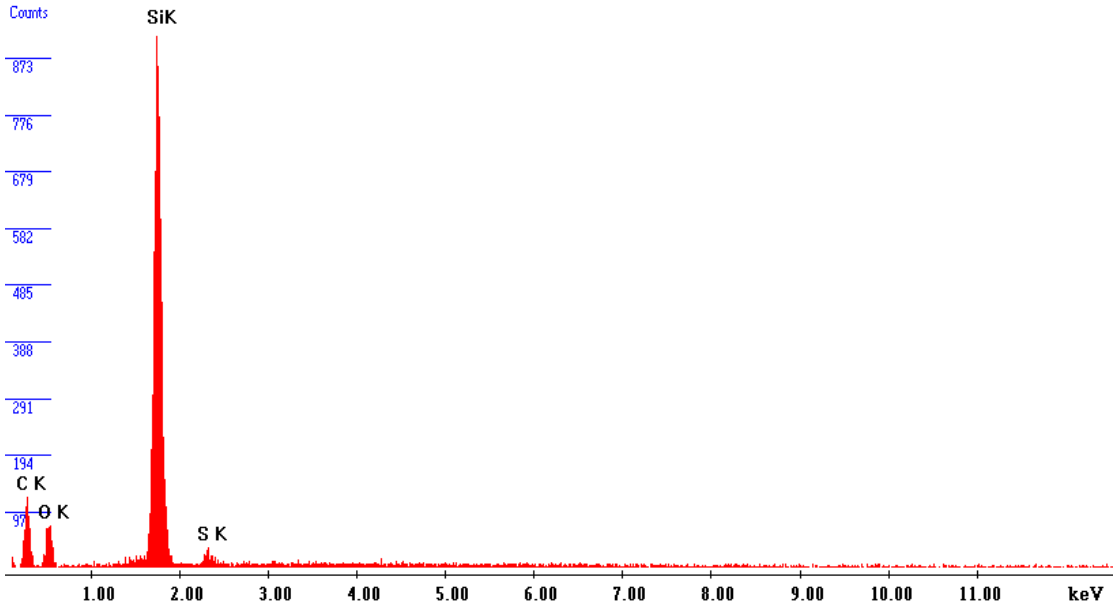

Figure 8.7: *EDS spectrum of quartz like particle on Nyex®1000 showing Si as the main component*

Adsorption Isotherm of *E. coli* cells onto GIC adsorbent

In an attempt to develop an isotherm for the adsorption of *E. coli* onto GIC adsorbent, various amounts of GIC adsorbent were mixed to the same initial concentration of *E. coli* in solution. For the range of concentrations studied, the amount of *E. coli* adsorbed per gram of GIC adsorbent increased sharply with an increase in the equilibrium concentration of *E. coli* in solution (Figure 8.8). The results show that the adsorptive capacity of GIC adsorbent for *E. coli* may be estimated at around 1.2×10^{10} CFU g^{-1} (Figure 8.8).

It is a well know fact that various adsorption isotherms can be applied to evaluate the adsorption of organic molecules on adsorbents. The Freundlich and the Langmuir isotherms were applied to the adsorption of phenol and its breakdown products on GIC adsorbent (see chapter 4). However, in the literature these isotherm models have also been applied to elucidate the mechanism of microorganism adsorption on carbon surfaces in a similar way to the adsorption of simple molecules on solid surfaces *(Drift et al. 1977; Soda et al. 1999; George and Davies, 1988)*. The removal of *E. coli* strain (V 2086) from wastewater by activated sludge flocs has been described to follow the Langmuir adsorption model *(Drift et al. 1977)*. *George and Davies, (1988)* has also shown the Langmuir isotherm for the adsorption of *E. coli* on activated carbon cloth. Evidence that the decrease in CFU mL^{-1} during the mixing of *E. coli* suspension with the GIC particles were due to adsorption was shown by scanning electron microscopy (Figure 8.9). Figure 8.9 shows *E. coli* cells adsorbed on the surface of the GIC adsorbent and the cell to cell interactions reveals that the adsorption was restricted to a mono-layer. However, complete surface coverage was not observed microscopically, suggesting some repulsion between E. coli cells on the surface. Similar results have been obtained by *George and Davies, (1988)* during the adsorption of *E. coli* (NCTC 10000) on activated carbon cloth. The isotherm appeared to be of Langmuir type.

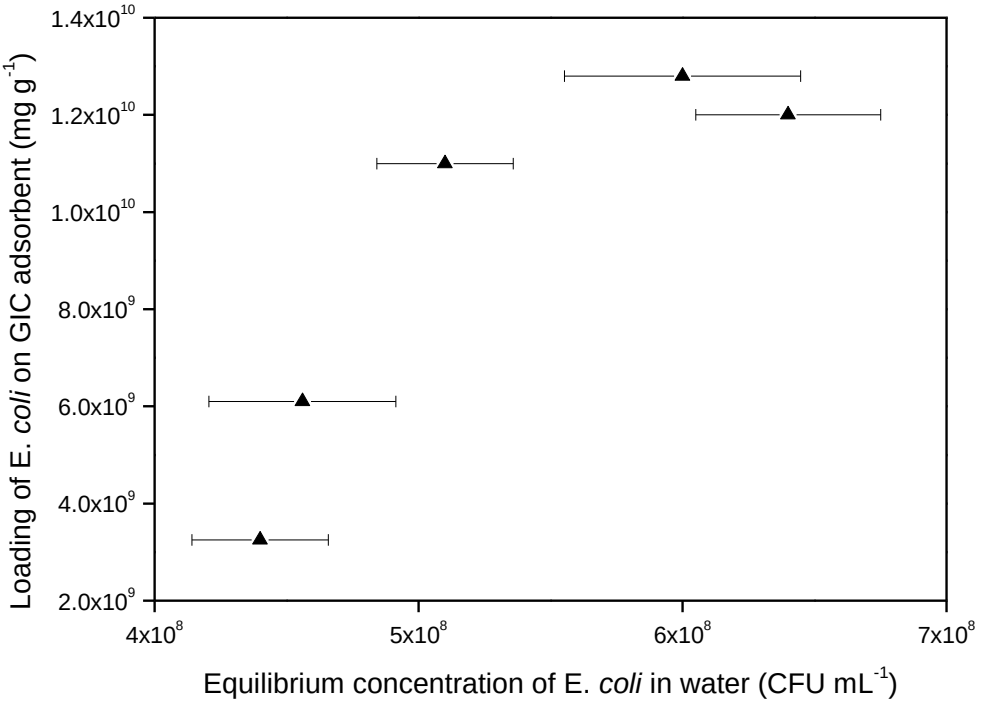

Figure 8.8: *Adsorption of E. coli on various amounts of GIC adsorbent in the range of 0.5–8 g with the same initial concentration of* E. coli*, 1.0 × 10^9 CFU mL^{-1}. Each data point on the abscissa shows the average of five samples and the error bars indicate standard errors calculated from the standard deviation.*

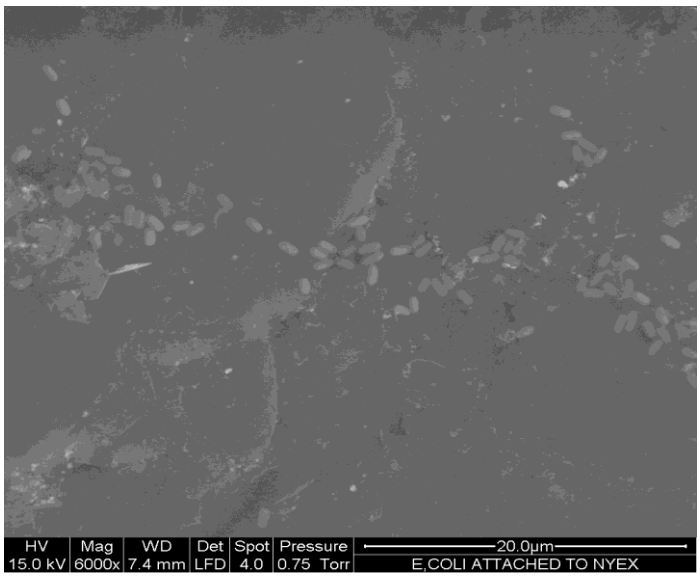

Figure 8.9: *Scanning electron micrograph of E. coli attached to a GIC particle at a magnification of 6000x*

Preliminary studies of adsorption and regeneration cycles with *E. coli* suspension

The effect of electrochemical regeneration was initially investigated using 400 mL of *E. coli* suspension (2.5×10^8 CFU mL^{-1}) prepared in a saline solution (0.9% NaCl solution in deionised water) over a number of adsorption and electrochemical regeneration cycles in the mini-SBR (Figure 4.3) using the procedure as described in section 8.1.3. This was the first attempt to investigate whether the adsorbed *E. coli* cells were destroyed during the electrochemical regeneration of the GIC adsorbent. In order to further validate the destruction of *E. coli*, a control run was conducted in such a way that all the experimental steps were exactly the same except that no current was passed during the regeneration cycles.

The results show that when current was applied during regeneration the adsorptive capacity of the GIC adsorbent did not diminish, giving a regeneration efficiency of 100%, with no colony forming unit being found after adsorption (Figure 8.10). An 8-$\log_{10}$ reduction of *E. coli* was achieved on each cycle. In contrast, the number of colony forming units began to increase after the first adsorption cycle for the control experiment where no current was applied during the regeneration cycles (Figure 8.10a). Consequently, the percentage regeneration efficiency fell to 56% for the 5^{th} adsorption cycle (Figure 8.10b). These results clearly show the gradual exhaustions of the adsorptive capacity of the GIC adsorbent during the course of adsorption cycles without current. Thus, it can be concluded that electrochemical regeneration has a significant effect in destroying *E. coli* adsorbed onto the surface of GIC adsorbent at a current density of 10 mA cm^{-2} for an *E. coli* suspension prepared in normal saline (0.9% NaCl w/v). However, when no current was passed an additional adsorption was observed giving apparent regeneration efficiency (Figure 8.10b). According to *Brown and Roberts (2007),* this apparent regeneration efficiency without electrochemical treatment can be explained by the second adsorption onto the loaded GIC adsorbent resulting in an increased liquid-phase equilibrium concentration. This is shown schematically in figure 8.11. During the initial loading of the GIC adsorbent, a liquid phase equilibrium concentration, C_{e1} is attained giving a corresponding solid phase equilibrium concentration, q_{e1}. If the adsorbent is used again under the same conditions without regeneration, then after the system has approached equilibrium, the liquid phase equilibrium concentration will be C_{e2}. This

gives an equivalent solid phase concentration, q_{e2}. Thus additional adsorbate is taken up by the adsorbent giving an apparent regeneration efficiency. In the case of bacterial adsorption on the GIC adsorbent, additional adsorption capacity without electrochemical regeneration could also be due to the formation of multiple bacterial layers. However, this needs further investigation.

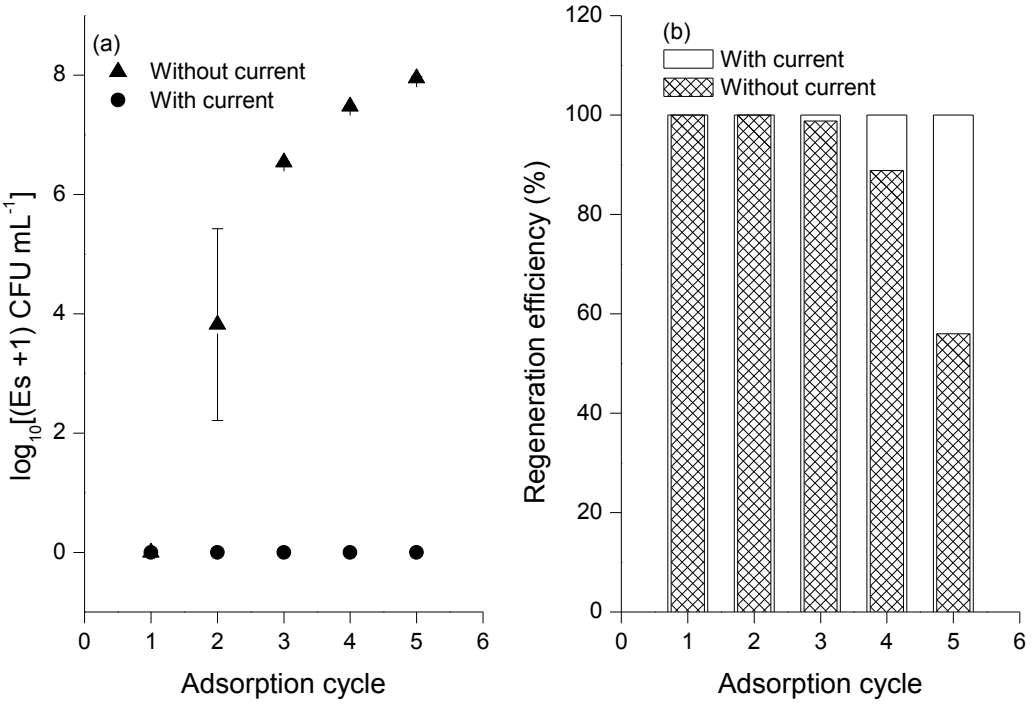

Figure 8.10: *Electrochemical regeneration of E. coli loaded GIC adsorbent in normal saline with an initial concentration of 2.5 × 10^8 CFU mL^{-1}, solution volume: 400 mL; adsorbent mass: 100 g; regeneration current: 0.5 A (corresponding to a current density of at 10 mA cm^{-2} based on the anode current feeder area of 50 cm^2), regeneration time: 20 min. (a) Adsorption cycles with and without current flow during regeneration; (b) Regeneration efficiency of GIC adsorbent with and without current. Cycle 1 corresponds to a fresh batch of adsorbent. Each data point in figure (a) represents the average of five samples and the error bars indicate standard errors calculated from the standard deviation. In order to show the zero point on the logarithmic plot 1 CFU mL^{-1} was added to each data point on the vertical axis where Es denotes the concentration of E. coli.*

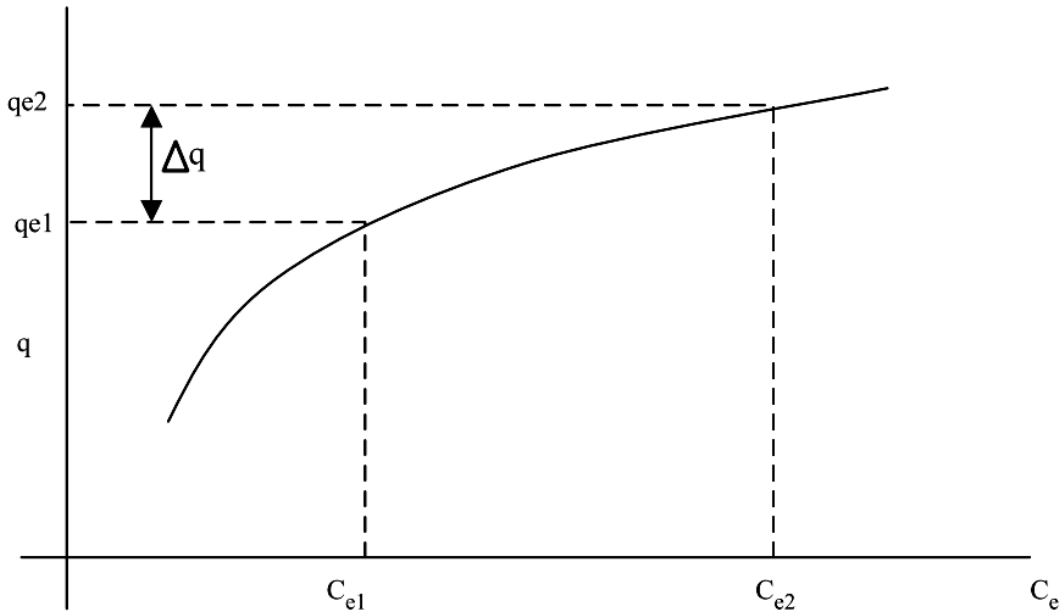

Figure 8.11: *Schematic diagram of loading onto fresh and loaded GIC adsorbent with no electrochemical regeneration. The curve gives the adsorption isotherm for fresh GIC adsorbent; Brown and Roberts, (2007)*

Three possible mechanisms were suggested that could achieve electrochemical disinfection in the process of adsorption with electrochemical regeneration using GIC adsorbents:

- Direct electrochemical disinfection: oxidation of the microorganisms causing cell deaths
- Electrochlorination: chloride in the water is oxidised to generate high concentrations of active chlorine at the surface of the adsorbent
- pH effects: anodic oxidation resulting in the formation of hydrogen ions at the anode surface decreasing the localized pH

A number of trials were carried out to evaluate these electrochemical disinfection mechanisms and these are discussed in the proceeding section.

Electro-chlorination and direct electrochemical disinfection

All the constituents of active chlorine such as molecular chlorine, hypochlorous acid and hypochlorite ions are strong oxidising agents and are therefore used for water disinfection. Molecular chlorine is normally considered a stronger disinfectant than hypochlorous acid and hypochlorite ions *(Rule et al. 2005).* Electrochlorination has been investigated thoroughly during electrochemical regeneration of GIC adsorbents (See chapter 4, section 4.3).

Trials in saline solution indicated strong electrochemical disinfection with regeneration efficiencies of 100%. The effect of electro-chlorination could be more significant when *E. coli* cells were suspended in saline solution. It has been shown in Chapter 4 that more free chlorine was produced in the presence of chloride ions along with GIC adsorbent in the anode compartment compared to the case when there was no chloride present with the anolyte, but with the same composition of catholyte (Figure 4.41, 4.48). Thus, to investigate the effect of electro-chlorination on disinfection, two trials were undertaken using a sample of *E. coli* suspension prepared in deionised water. In one trial, the catholyte was 0.3% NaCl solution acidified with HCl (to pH 1–2) and in the second trial, the catholyte was 0.3% Na_2SO_4 acidified with 5 M H_2SO_4 (to pH 1–2) giving a chloride free system. In all other respects the procedure was as described for batch adsorption and electrochemical regeneration in section 8.1.3.

The results show that without the use of normal saline with *E. coli* suspension the number of colony forming units was observed to increase during adsorption and regeneration cycles, even when 0.3% NaCl was used as the catholyte (figure 8.12a). This suggests that the high concentrations of free chlorine produced when normal saline was used in the anode compartment caused more disinfection. It was expected that in the absence of normal saline in the anode compartment, the GIC adsorbent would not be regenerated efficiently during the regeneration cycles owing to relatively low concentrations of free chlorine. However, the regeneration efficiency was fairly high and there was only a 9% drop in regeneration efficiency during the five regeneration cycles (Figure 8.12b). However the regeneration efficiency was higher than expected if the mechanism was only electrochlorination.

In addition, the figure 8.12 (a) indicated clearly that the number of colony forming units was significantly reduced during regeneration cycles from its initial values in the respective adsorption cycles leading to 8-$\log_{10}$ reduction during the first three cycles. This reduction is significantly higher than the reduction of bacteria due to adsorption (1.6-$\log_{10}$ reduction during the first adsorption). These results suggest that during electrochemical regeneration of the GIC adsorbent, very significant electrochemical disinfection of *E. coli* present in solution was also occurring. This phenomenon has also been observed during the electrochemical regeneration of GIC adsorbents loaded with phenol (See chapter 4, section 4.1.4). Thus, it can be concluded that the overall disinfection achieved in the process of adsorption with electrochemical regeneration using GIC adsorbents is a combination of electrochemical disinfection in the solution phase as well as disinfection on the surface of the adsorbent. This can be considered an additional benefit of the Arvia® process because electrochemical disinfection in solution was achieved without the use of any additional electrolyte.

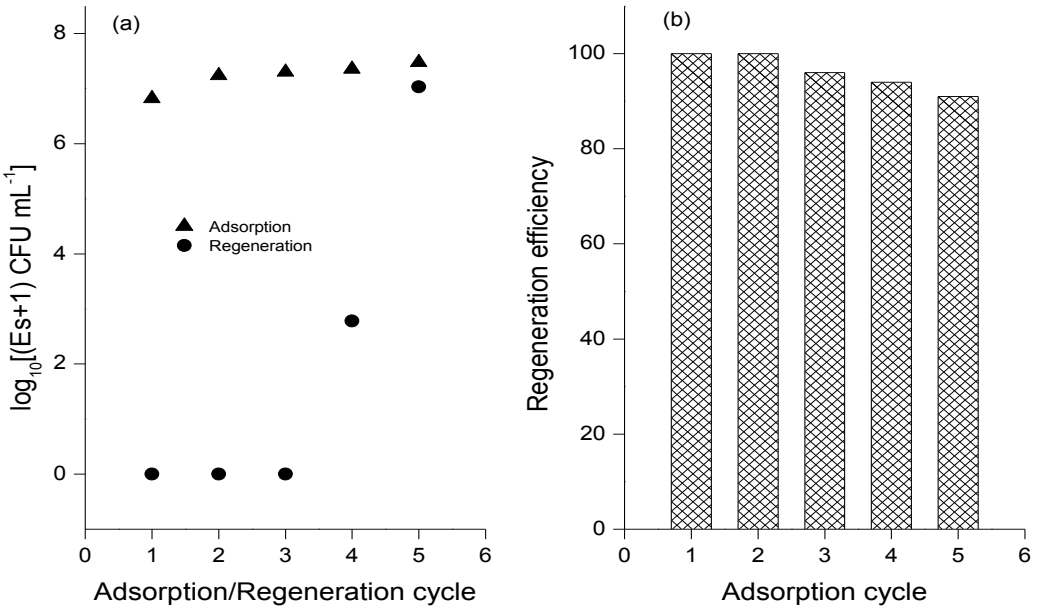

Figure 8.12: *Electrochemical regeneration of E. coli loaded GIC adsorbent in deionised water with an initial concentration of 2.72 × 10^8 CFU mL^{-1}; solution volume: 600 mL; adsorbent mass: 150 g; regeneration current: 0.5 A, corresponding to a current density of 10 mA cm^{-2} based on the anode current feeder area of 50 cm^2, regeneration time 20 min. (a) Adsorption and regeneration cycles; (b) Regeneration efficiency. Fresh adsorbent was used during the first cycle. In order to plot the zero concentration values on the logarithmic plot, 1 CFU mL^{-1} was added to each data point on the vertical axis where Es denotes the concentration of E. coli.*

In the second trial as described above, the possibility of the contribution of electro-chlorination during the regeneration of the GIC adsorbent was completely eliminated by replacing the acidified sodium chloride solution with a solution containing 0.3% Na_2SO_4 (w/v) and acidified with 5M H_2SO_4 (pH<1.5) as a catholyte. Several adsorption and regeneration cycles were performed in the mini-SBR after ensuring that there was no source of chloride ions. In this context, the *E. coli* pellets formed after centrifugation of broth were thoroughly washed with deionised water three times to remove any traces of NaCl present.

The results show that the percent regeneration efficiency was greater than 100% for all the regeneration cycles (Figure 8.13b). The increase in adsorptive capacity above the initial capacity could be due to the transfer of oxidising species from the electrochemical cell to the *E. coli* suspension in the solution trapped in the adsorbent bed, resulting in the removal of *E. coli* by chemical oxidation rather than adsorption. In addition, surface modification due to electrochemical treatment may induce additional adsorption sites so that the adsorption capacity may be increased. The effectiveness of the process was judged by the substantial decrease in the concentration of *E. coli* during adsorption and regeneration cycles as shown in figure 8.13a. Two possible explanations have been proposed for these results:

- When there is no competing reaction, more of the current is passed through the microorganisms resulting in a greater kill through direct electrochemical disruption of the cells
- In the absence of chloride ions, the electrochemical process is producing comparatively stronger disinfectants such as hydroxyl radicals. Free hydroxyl radicals play an important role in electrochemical disinfection due to their stronger oxidizing capability compared to chlorine *(Cong et al. 2008)*. The other disinfectants produced due to water discharge at anode have been discussed in Chapter 7 (see section 7.5.3).

The results also suggest that the electrochemical process employing Na_2SO_4 in the catholyte was effective for disinfection even without the generation of free chlorine. These results have important implications to address the issues associated with the formation of chlorinated disinfection by–products.

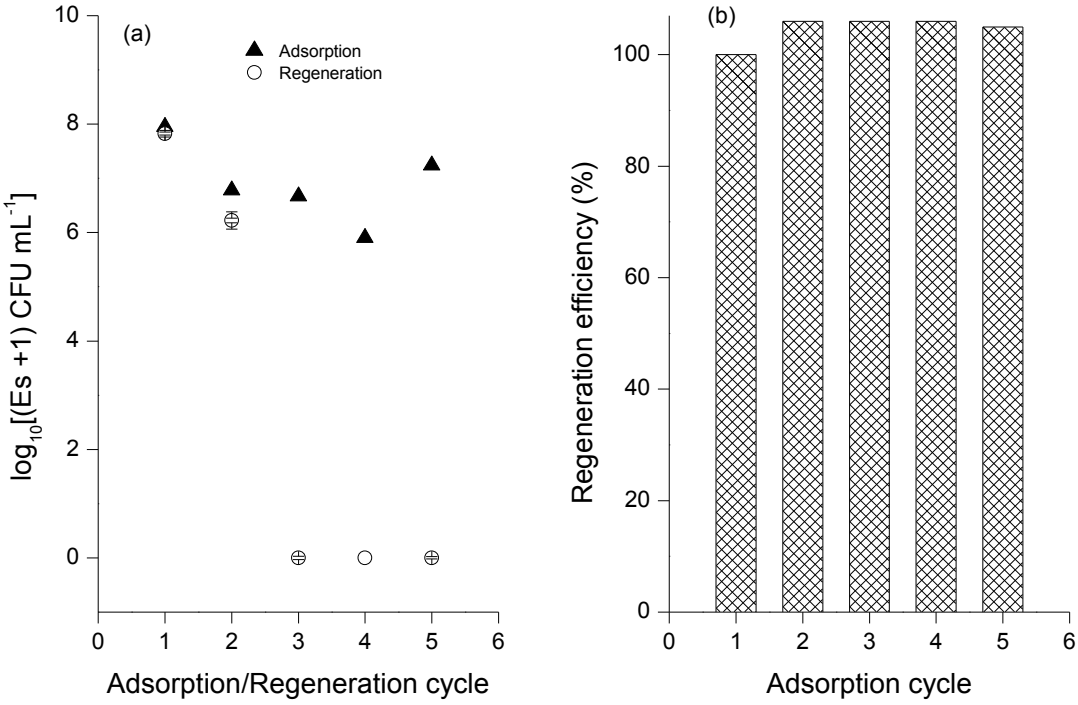

Figure 8.13: *Electrochemical regeneration of E. coli loaded GIC adsorbent in chloride free environment with initial concentration of 1.42 × 10^8 CFU mL^{-1}, solution volume: 600 mL; adsorbent mass: 150 g; regeneration current: 0.5 A, corresponding to a current density of 10 mA cm^{-2} based on the anode current feeder area of 50 cm^2, regeneration time 20 min. The catholyte was 0.3% Na_2SO_4 acidified with H_2SO_4. (a) Adsorption and regeneration cycles; (b) Regeneration efficiency. Fresh adsorbent was used at the start of the first cycle. Each data point in figure (a) indicates the average of five samples and the error bars indicate standard errors calculated from the standard deviation. In order to plot the zero concentration values on the logarithmic plot, 1 CFU mL^{-1} was added to each data point on the vertical axis where Es denotes the concentration of E. coli.*

Electrochemical disinfection of *E. coli* suspension without GIC adsorbent

The validation of the above mentioned findings was supported by performing electrochemical disinfection of E. *coli* suspension in the anodic compartment of the mini-SBR without the use of GIC adsorbent at three different experimental conditions as follows:

(a) *E. coli* cells were suspended in normal saline and aqueous NaCl acidified with HCl was used as the catholyte

(b) *E. coli* cells were suspended in sodium sulphate solution prepared in deionised water and aqueous Na_2SO_4 acidified with H_2SO_4 was used as the catholyte

(c) *E. coli* cells were suspended in sodium sulphate solution prepared in deionised water and aqueous NaCl acidified with HCl was used as the catholyte

In each case a current of 0.5 A was passed through the cell, corresponding to a current density of 10 mA cm^{-2}.

The results of these experiments show that electro-chlorination had a significant effect on the disinfection of *E. coli* in water. The presence of NaCl [i.e. with the experimental conditions described in (a) above] in the anode compartment led to 100% disinfection (8.3-$\log_{10}$ reduction) achieved after only 2 min of electrochemical treatment. In terms of rate, the highest disinfection was attained in this case. For the other two cases, complete disinfection was achieved after 20 min of electrochemical treatment, which corresponded to the time used to regenerate *E. coli* loaded GIC adsorbent at the same current density (10 mA cm^{-2}).

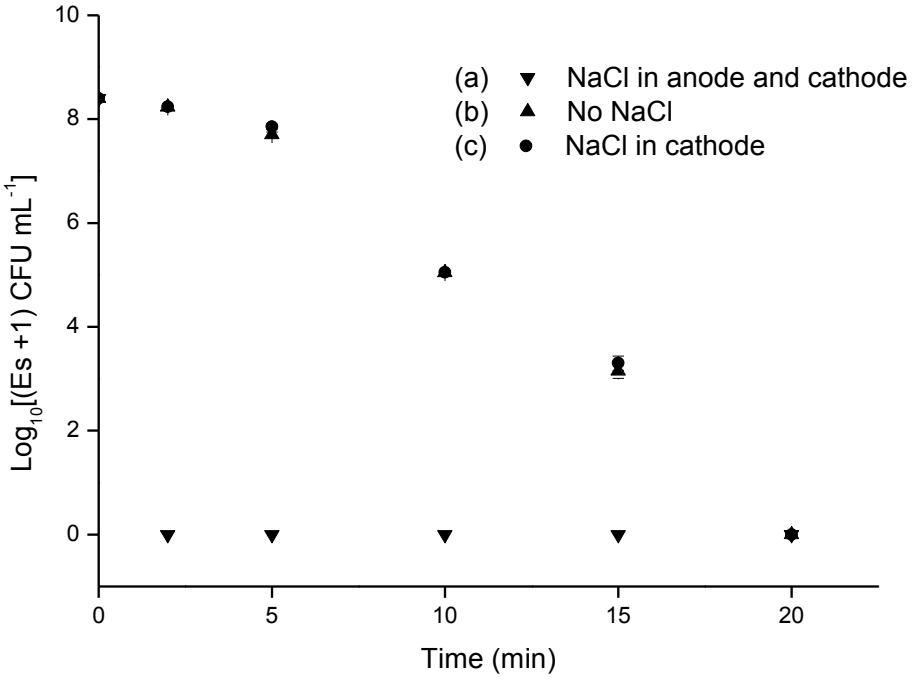

Figure 8.14: *Electrochemical disinfection of E. coli without GIC adsorbent at 0.5 A (10 mA cm^{-2}, anode current feeder area 50 cm^2) with different anolyte and catholyte conditions. Each data point represents the average of five samples and the error bars indicate standard errors calculated from the standard deviation. In order to plot the zero concentration values on the logarithmic plot, 1 CFU mL^{-1} was added to each data point on the vertical axis where Es denotes the concentration of E. coli.*

As mentioned earlier, when there was no NaCl added to the anolyte reactive hydroxyl radicals may provide more killing capacity than the electrochemically generated free chlorine, since similar disinfection performance was observed when NaCl and Na_2SO_4 were used as the catholyte. However, in the situation when NaCl was used as anolyte, the free chlorine produced rapidly disinfected the *E. coli* in a very short electrochemical treatment time (Figure 8.14). Similar observations have also been observed during electrochemical regeneration of *E. coli* loaded GIC adsorbent with the highest removal efficiency when NaCl was used in the anode compartment.

pH effects

In addition to the disinfection mechanisms discussed above, some other factor could also be responsible for disinfecting E. *coli* cells both on the surface of GIC adsorbent and in suspension. One possibility is that pH changes associated with the electrochemical regeneration of GIC particles could lead to disinfection. The pH changes associated with the electrochemical process for the above three mentioned situations are shown in figure 8.15. An abrupt drop in pH was observed within the first two minutes owing to the acidic conditions generated during the anodic oxidation of water. The pH change at the surface of the adsorbent may make a significant contribution to the disinfection of *E. coli* (Figure 8.16). Thus, the pH changes during regeneration process should be emphasized while discussing the mechanisms of electrochemical disinfection. During the adsorption of E. *coli* onto GIC particles the pH was always observed to decrease by 2.5 to 3 units from its initial value especially during the first adsorption. This was probably due to the presence of acidic groups on the surface of the GIC adsorbent (see chapter 6). Thus, pH changes occurring during both adsorption and electrochemical regeneration could also contribute to the disinfection of the bacteria.

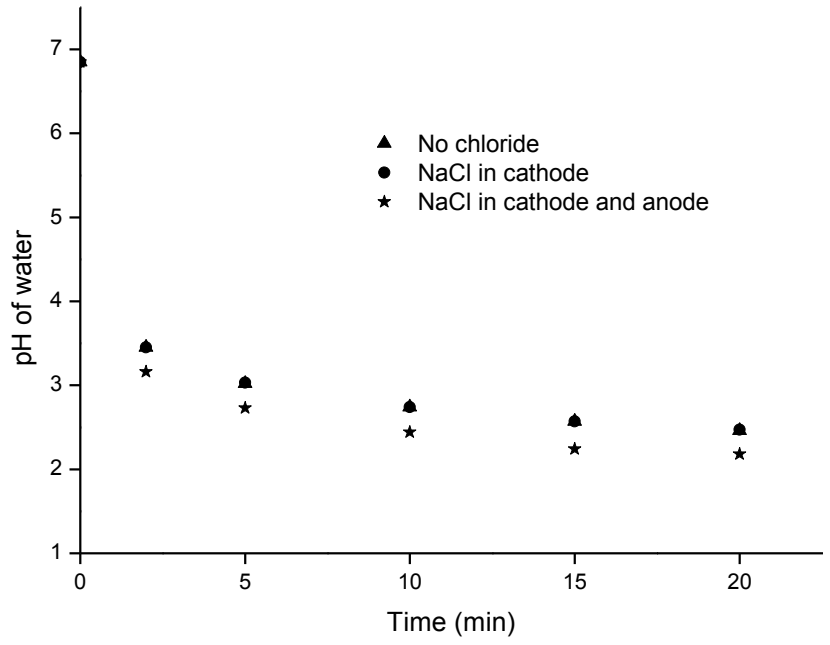

Figure 8.15: *Time dependence of pH during electrochemical disinfection of E. coli without GIC adsorbent at different anolyte and catholyte conditions, Current: 0.5 A; Current density: 10 mA cm^{-2}, anode current feeder: 50 cm^2*

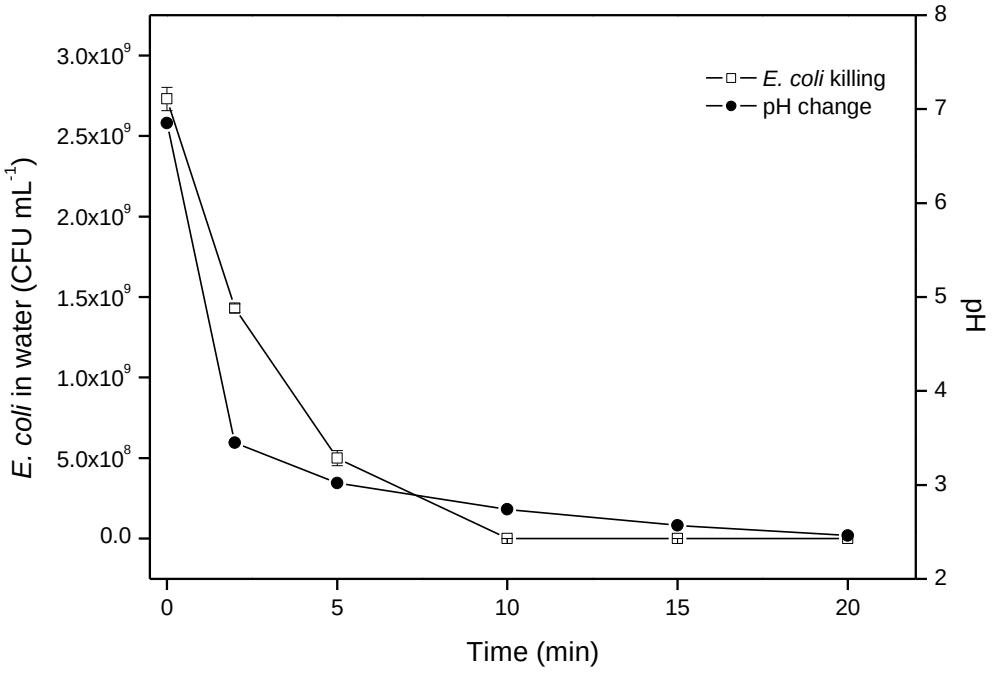

Figure 8.16: *Effect of pH on E. coli killing during electrochemical disinfection of E. coli without GIC adsorbent at 0.5 A, Current density: 10 mA cm^{-2}(anode current feeder: 50 cm^2), The anolyte was sodium sulphate solution in deionised water with E. coli cells and aqueous NaCl acidified with HCl was used as the catholyte. Each data point along the left hand side y-axis represents the average of five samples and the error bars indicate standard errors calculated from the standard deviation.*

In order to investigate the disinfecting effect of the pH changes, a phosphate buffered (pH 7.0) was added to the *E. coli* suspension and a series of adsorption and regeneration cycles were carried out. In all other respects the procedure was as described in section 8.1.3. The catholyte was composed of 0.3% (w/v) NaCl solution acidified with 5 M HCl (to pH 1–2) and *E. coli* cells were suspended in phosphate buffer solution.

The pH of the water was monitored during adsorption and regeneration, and it remained fairly constant throughout the duration of the experiment (See appendix D). The results show that the concentration of colony forming units after each cycle gradually increased over several adsorption and regeneration cycles (Figure 8.17a), indicating a decrease in the regeneration efficiency. These results suggest that the

GIC adsorbent was not regenerated effectively during the regeneration cycles when the pH was maintained at 7.0. The regeneration efficiency decreased to 27% after the fifth cycle (Figure 8.17b). These results indicate that the pH is an important factor in the electrochemical disinfecting process. However, removal of E. *coli* on the first adsorption at pH 7.0 was only around 60%, compared with close to 100% of the initial *E. coli* concentration in the first adsorption when no buffer was present. This suggested that pH also plays an important role in the adsorption of the microorganisms.

It was shown in chapter 4 that relatively low concentrations of free chlorine was generated at neutral pH, but free chlorine generation is greater at low pHs which would provide additional disinfecting potential at low pHs. Thus the amount of oxidants including chlorine was insufficient to disinfect *E. coli* at neutral pH. In addition, the charge passed was not influencing the disinfection process which could be due to the low current density used (10 mA cm^{-2}). Thus, it is desirable to evaluate the optimum regeneration conditions to effectively regenerate the *E. coli* loaded GIC adsorbent at neutral pH.

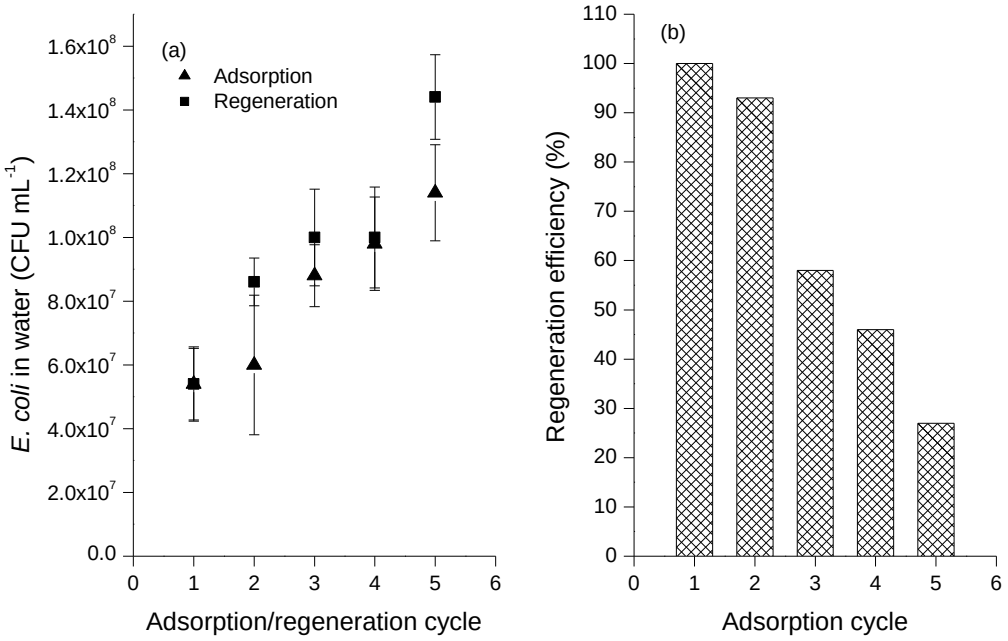

Figure 8.17: *Electrochemical regeneration of* E. coli *loaded GIC adsorbent in phosphate buffer (pH 7.0) with initial concentration of 1.36 × 10^8 CFU mL^{-1} without the presence of chloride in anolyte, solution volume: 600 mL; adsorbent mass: 150 g; regeneration current of 0.5 A (corresponding to 10 mA cm^{-2}); regeneration time 20 min. The catholyte was 0.3% NaCl acidified with HCl (a) Adsorption and regeneration cycles; (b) Regeneration efficiency. Fresh adsorbent was used for the first cycle. Each data point represents the average of five samples and the error bars indicate standard errors calculated from the standard deviation.*

Effect of current density on adsorption and regeneration cycles in the mini-SBR

The effect of current density on adsorption and regeneration was investigated in order to determine the optimum conditions for electrochemical regeneration of E. *coli* loaded GIC adsorbent in the mini-SBR at a pH of 7.0. As far as the process of adsorption with electrochemical regeneration using GIC adsorbents was concerned, the pH was not kept constant; however, during the continuous process the localized drop in pH in the regeneration chamber did not significantly affect the pH of the treated water (Figure 8.18). The aim of this study was to investigate the effect of current density on disinfection while keeping a constant regeneration time and neutral pH using phosphate buffer. The results showed that for current densities 10

and 30 mA cm^{-2}, there was observed almost a similar increase in the concentration of *E. coli* cells after the adsorption over several cycles (Figure 8.19a). The difference between these two current densities was more prominent after the regeneration cycles, with no *E. coli* cells detected for current densities of 30 and 50 mA cm^{-2}, suggesting that the rate of electrochemical disinfection in solution was greatly affected by the current density under these conditions (Figure 8.19b). Similar effects have been observed in solution during electrochemical regeneration of phenol loaded GIC adsorbent at a range of current densities (See chapter 4, section 4.1.4). Comparatively, a current density of 30 mA cm^{-2} gave improved regeneration efficiencies compared to 10 mA cm^{-2} (Figure 8.20). It is clear from figure 8.20 that 50 mA cm^{-2} was effective in achieving regeneration efficiencies above 100% and in producing complete disinfection of *E. coli* in solution during the regeneration cycles, suggesting that increasing the current density led to an increase in the production of oxidant species responsible for indirect oxidation. However, the voltage drop increases linearily with the current density, resulting in an increase of cell voltage and consequently higher energy consumption *(Brown, 2005)*. Hence a compromise has to be arrived at in selecting the current density. Based on the data obtained, 30 mA cm^{-2} was identified as a practical current density for disinfection of *E. coli* at neutral pH in the batch process of adsorption and electrochemical regeneration.

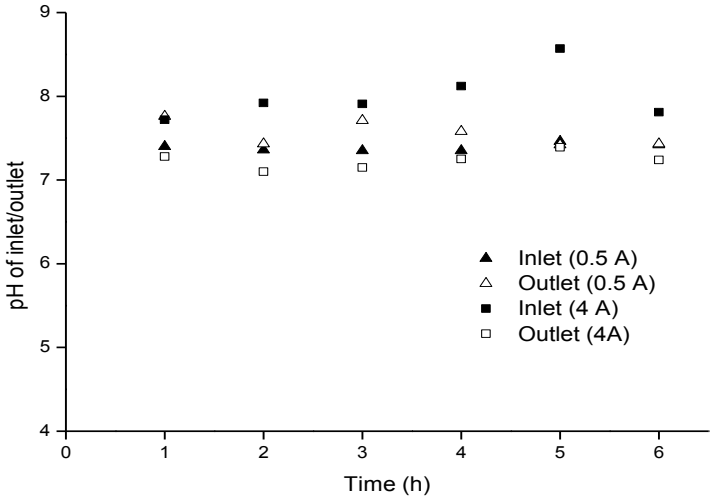

Figure 8.18: *Inlet and outlet pH during treatment of an effluent from the secondary clarifier of United Paper Mills (Shotton, UK) using a Gemini 100 unit (continuous Arvia® process) with regeneration currents of 0.5 & 4 A, and an effluent flow rate of 5 L h^{-1} (These data were collected by Arvia® personnel).*

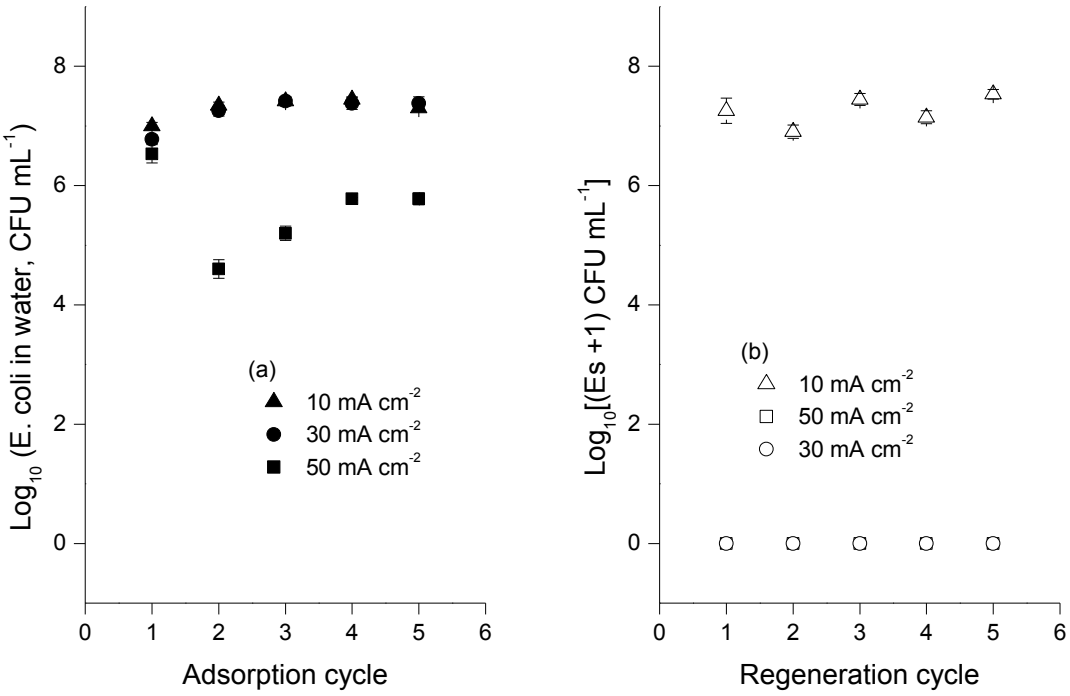

Figure 8.19: *Effect of current density on adsorption and regeneration cycles for* E. coli *suspension at pH 7.0, Nyex®1000 dose 60 g in 300 mL (200 g* L^{-1}*) with an E. coli concentration of* 1.30×10^{9}*,* 1.47×10^{9} *and* 1.10×10^{9} *CFU* mL^{-1} *for regeneration current densities of 10, 30 and 50 mA* cm^{-2} *respectively. Experiments were carried out in the small sized mini-SBR. Regeneration conditions: 0.2 to 1.0 A was applied to give current densities in the range 10 to 50 mA* cm^{-2} *for 20 min. The charge passed during each regeneration cycle was in the range of 4 to 20 C* g^{-1}*. Each data point represents the average of five samples and the error bars indicate standard errors calculated from the standard deviation. (b) In order to plot the zero concentration values on the logarithmic plot, 1 CFU* mL^{-1} *was added to each data point on the vertical axis where Es denotes the concentration of E. coli.*

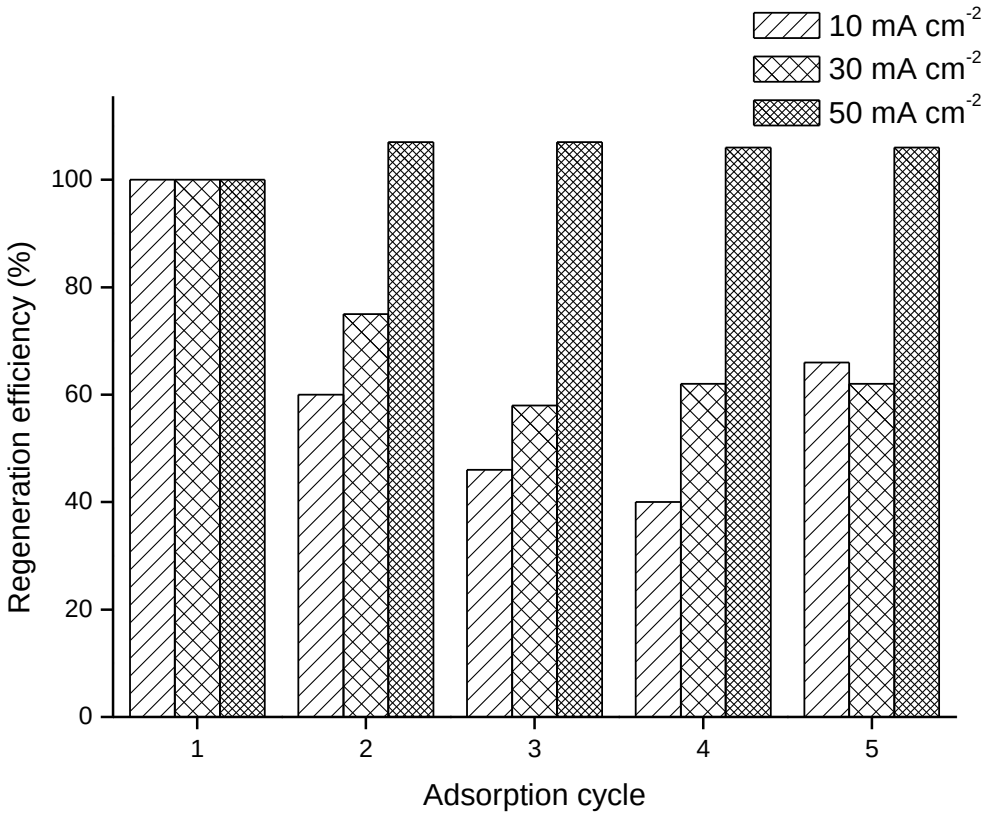

Figure 8.20: *Effect of current density on regeneration efficiency for GIC adsorbent loaded with E. coli, Regeneration current: 0.2, 0.6 and 1.0 A (corresponding to current densities of 10, 30 and 50 mA cm^{-2}), regeneration time 20 min and the charge passed was 4, 16 and 20 C g^{-1} respectively.*

Effect of regeneration time on adsorption and regeneration cycles in the mini-SBR

The effect of regeneration time on the electrochemical regeneration of the GIC adsorbent loaded with *E. coli* at pH 7.0 was investigated at a constant current density of 20 mA cm^{-2}. The concentration of *E. coli* after the adsorption cycles was observed to increase over several cycles, indicating that the adsorbent was not effectively regenerated with 20 min regeneration time. However, for 40 min regeneration time, the concentration of *E. coli* decreased with the number of cycles, leading to a conclusion that an increase in regeneration time has a direct effect on the regeneration of the GIC adsorbent loaded with *E. coli* (Figure 8.21a). The results also indicate that the regeneration efficiency increased from 50% or lower to over 100 % when the regeneration time was increased from 20 to 40 min at a current density of 20 mA cm^{-2} (Figure 8.21 b).

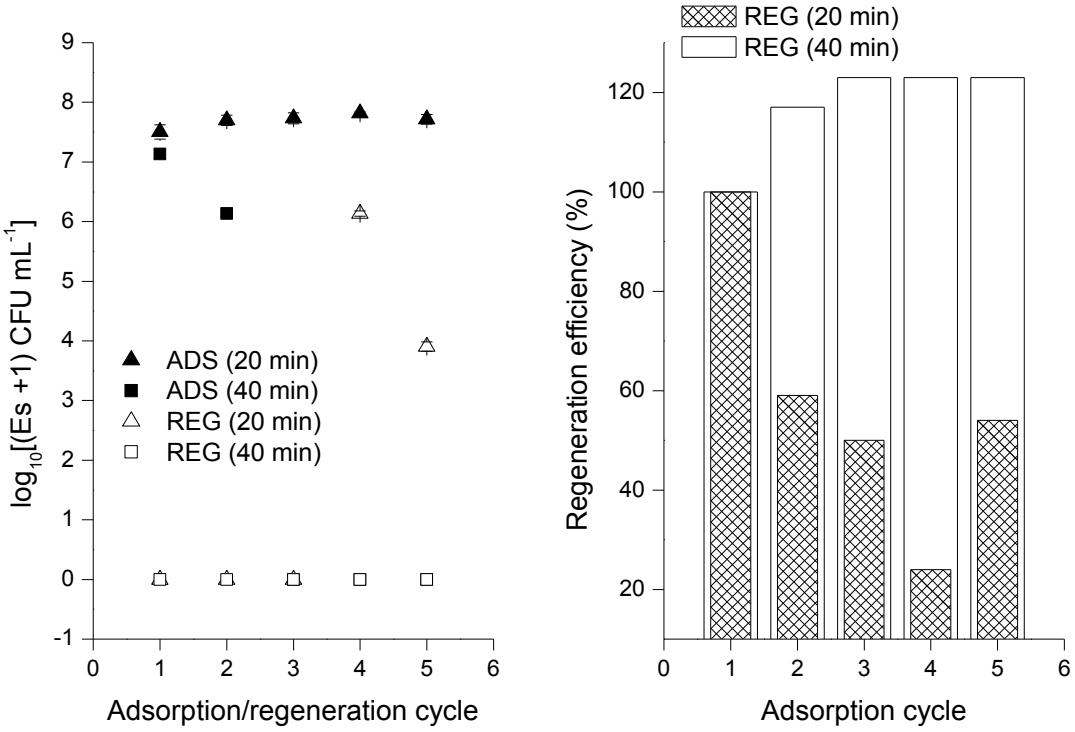

Figure 8.21: *Effect of regeneration time on adsorption and regeneration cycles for E. coli at pH 7.0, Nyex®1000 dose 60 g in 300 mL (i.e. 20 g L^{-1}) of E. coli suspension (7.6×10^7 and 3.34×10^7 CFU mL^{-1}) for regeneration times of 20 and 40 min respectively at 20 mA cm^{-2}, in the small sized mini-SBR (anode current feeder, 20 cm^2). Each data point for figure (a) represents the average of five samples and the error bars indicate standard errors calculated from the standard deviation. For the experimentally measurements where no E. coli were detected, 1 CFU mL^{-1} was added to each data point so that the logarithm could be plotted and Es denotes the concentration of E. coli.*

8.1.5 Conclusions

The process of adsorption with electrochemical regeneration using the GIC adsorbents has the capability of disinfecting a high population of *E. coli* in water. The GIC adsorbents have the potential to adsorb a large number of bacterial cells present in water with fast adsorption kinetics. In addition, mono-layer adsorption of *E. coli* onto GIC adsorbent with cell to cell interactions was observed. However, complete surface coverage was not observed. Disinfection of water was found to be a combination of two processes: the adsorption of microorganisms on GIC adsorbents followed by their deactivation on the surface; and electrochemical disinfection in solution due to indirect oxidation. Both of these processes occur simultaneously. The

rate of electrochemical disinfection in solution was found to be significantly higher than the disinfection achieved by adsorption with electrochemical regeneration. Possible mechanisms of disinfection by adsorption with electrochemical regeneration include electrochlorination, pH changes and deactivation by the direct oxidation of the *E. coli*. At the high concentrations used, about 50% of the *E. coli* were removed by adsorption which was subsequently disinfected during electrochemical regeneration of the GIC adsorbent. The overall process of disinfection was also found to be quite effective even when there was no source of chloride ions, suggesting that disinfection can take place without electrochlorination, which is one of the most important disinfection techniques for microorganisms in water. Current density and regeneration time were found to have a direct effect on the electrochemical regeneration of the GIC adsorbent loaded with *E. coli*.

8.2 Investigation of morphological changes of *E. coli* cells during adsorption and regeneration

To investigate the morphological changes of *E. coli* cells during adsorption and electrochemical regeneration, scanning electron microscopy (SEM) was used to examine the *E. coli* cells on the surface of the GIC adsorbents during these processes with the aim of exploring the changes in the structure of cells on the GIC surface. Samples of the GIC adsorbent were collected after adsorption and during electrochemical regeneration in the mini-SBR for the experiments as described in section 8.1.3. No special method was adopted to prepare the samples for SEM analysis; GIC samples were analysed as collected. No attempt was made to analyse the *E. coli* cells present in solution by SEM.

8.2.1 Adsorption and electrochemical regeneration in the mini-SBR without pH adjustment

Samples of GIC adsorbent were collected during adsorption and electrochemical regeneration of *E. coli* suspension prepared in deionised water. Electrochemical regeneration of adsorbent was performed at 0.5 A (10 mA cm^{-2}) for 20 min and the electrolyte in the cathode compartment was 0.3% NaCl solution (see section 8.1.3).

Figure 8.22 shows an SEM image of the *E. coli* cells on the surface of GIC particles. The *E. coli* cells were appeared to attach firmly to the surface by mono-layer formation. However, some of the cells were also observed to be gathered together as shown in figure 8.22. It was also interesting to note that the disinfection process was actually initiated during the adsorption of E. *coli* cells onto the GIC adsorbent even when there was no current passing. This was evident from the deformed shape of *E. coli* cells (Figure 8.23) during adsorption which otherwise should be rod like structure as shown in figure 8.1. In contrast, the colonization of bacteria on activated carbon is highly resistant to many disinfectants including chlorine *(Rivera et al. 2001). Lechevallier et al. (1984)* has demonstrated that bacteria attached to activated carbon show remarkable perseverance because they grow in cracks and crevices, and are coated by an extracellular slime layer. In addition, the bacteria cells are intertwined in the pores of the activated carbon. Consequently, bacterial cell in the cracks, crevices and pores of the carbon may never come into contact with disinfectants. However, GIC particles have smooth and flat surfaces (Figure 4.1) and therefore the adsorbed bacteria are directly in contact with the electrochemically generated disinfectants. A possible reason for the disinfection of bacteria during the adsorption process is the presence of acidic groups on the GIC surface (See chapter 6).

Two possible explanations have been proposed for this phenomenon to occur on the surface of the GIC adsorbent.

- The death of E. *coli* in solution due to low pH followed by the adsorption of dead cells onto the surface of GIC particles.
- Adsorption of E. *coli* cells onto the surface of GIC particles followed by their deformation due to the exposure of acidic conditions at the surface.

The role of pH on the survival of microorganisms is related to the ability of the organisms to maintain neutral pH in the cytoplasmic contents of the cell *(Mercado et al. 1996).* During electrochemical disinfection, there is an increase in cell permeability due to the formation of pores on the cell walls and the rate of transport of H^+ ions is also increased due to the osmotic imbalance around the cell. This in turn decreases the pH within the cell resulting in chemical modifications in the

fundamental constituents of the cell such as the DNA *(Mercado et al. 1996).* Consequently, due to the presence of higher concentrations of H^+ ions (low pH environment) the lysis of bacterial cells takes place.

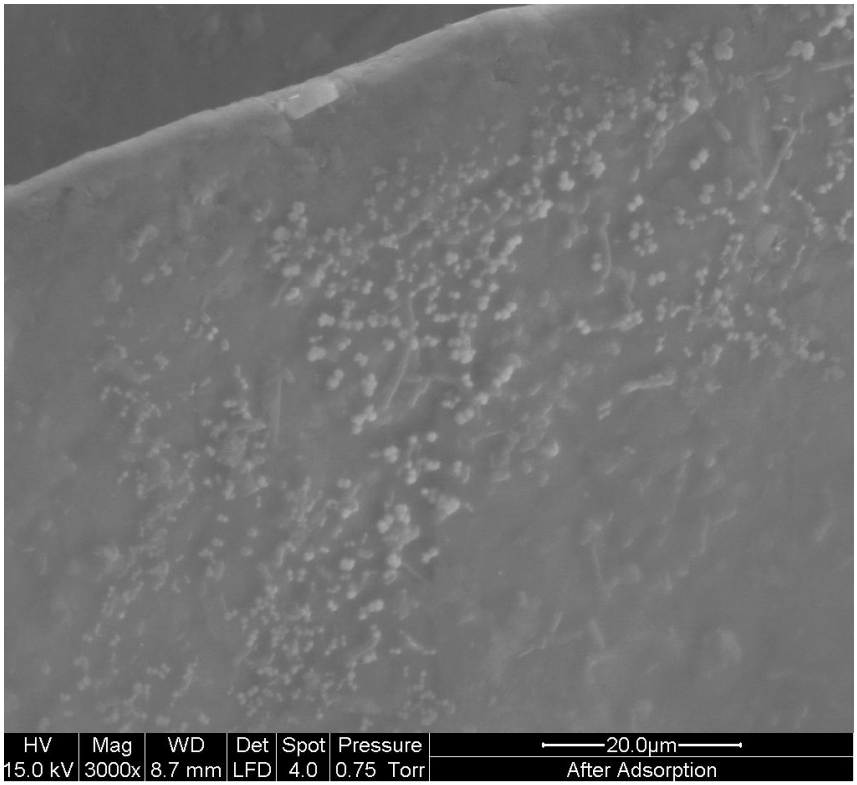

Figure 8.22: *Scanning electron micrograph showing E. coli adsorbed on the surface of a GIC particle at a magnification of 3000x*

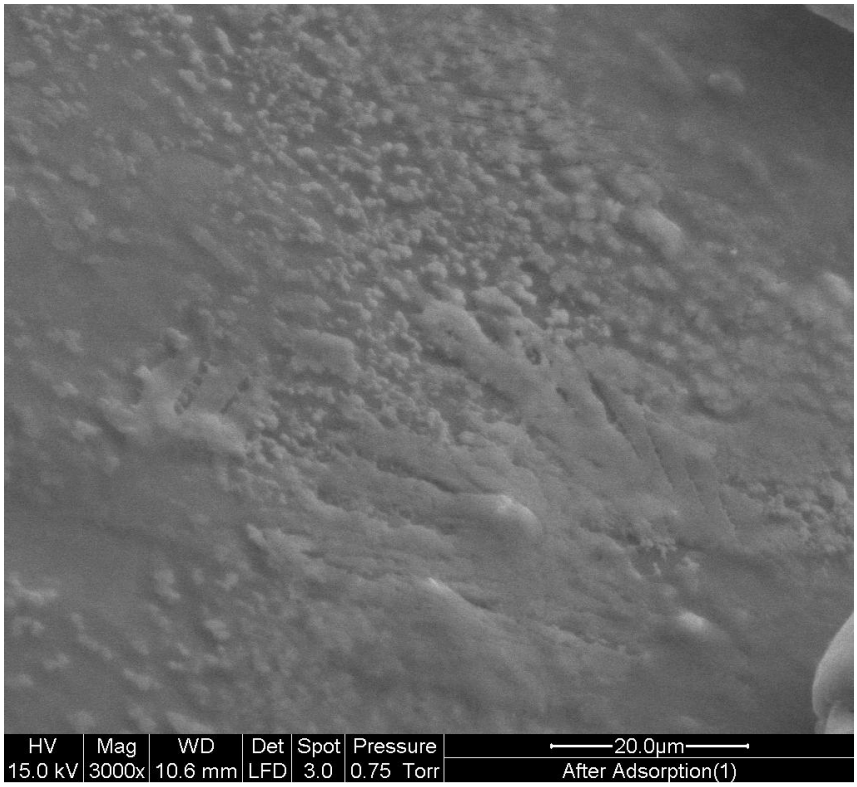

Figure 8.23: *Scanning electron micrograph showing deformations of attached E. coli (agglomeration of cells with release of extracellular slime) after adsorption on the surface of GIC adsorbent at 3000x magnification*

During the regeneration process, various changes in cell morphology were observed to take place simultaneously. Some of the *E. coli* cells were found in the form of long filaments (Figure 8.24). These filaments can be due to the formation of biofilms which will be discussed in the proceeding section. Most of the SEM images suggested that in the first instance the *E. coli* cells were shrunk into small elements during regeneration (Figure 8.25). These elements appeared to be converted into convex structures after their coagulation (Figures 8.26–8.27) with the development of roughness on the outer edges (Figure 8.28). The roughness might be due to the formation of perforations during the passage of current. The convex structures also showed that the thick material inside the deformed cells has either accumulated to one of its two corners or around the edges leaving a hollow portion inside these structures (Figure 8.28). Finally these small convex elements appeared to be completely destroyed. The order of occurrence of these phenomena regarding changes in cell morphology during regeneration cannot be ascertained with confidence. Some simultaneous changes in cell morphology during electrochemical

regeneration of GIC adsorbent were also observed (data not shown). The cell morphology observed during adsorption was somehow different from regeneration in such a way that several deformations appeared to take place at the surface of GIC adsorbent during the course of regeneration at 10 mA cm^{-2}. There was not a significant difference between the fresh and regenerated sample of GIC adsorbent as shown in Figures 8.29 and 8.30, suggesting that the dead masses were not accumulated on the adsorbent surface.

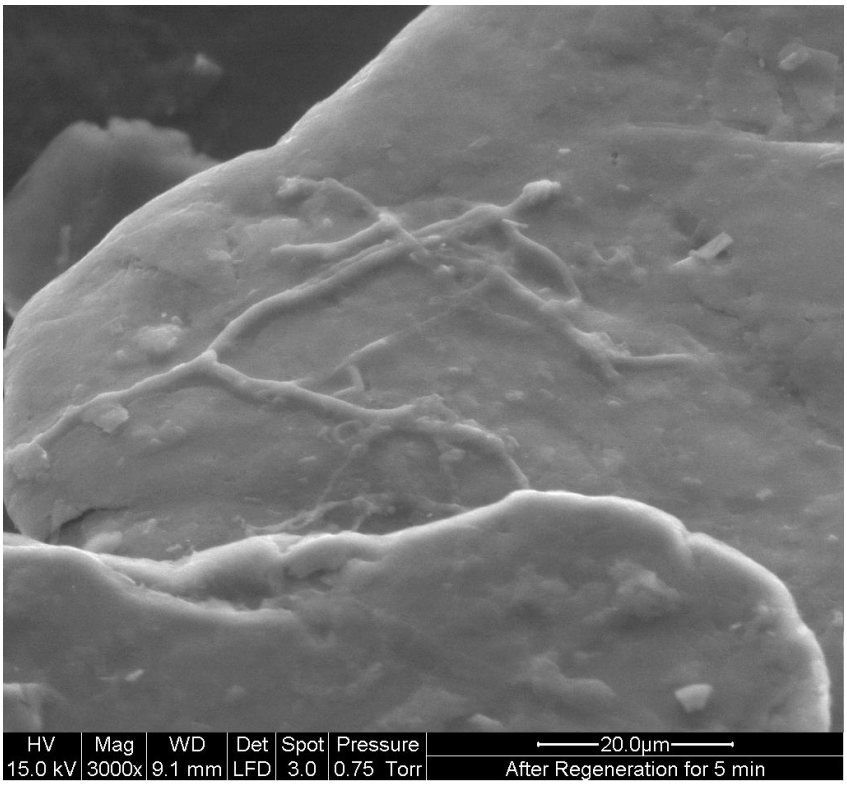

Figure 8.24: *Scanning electron micrograph showing long E. coli filaments after 5 min of electrochemical regeneration at magnification of 3000x*

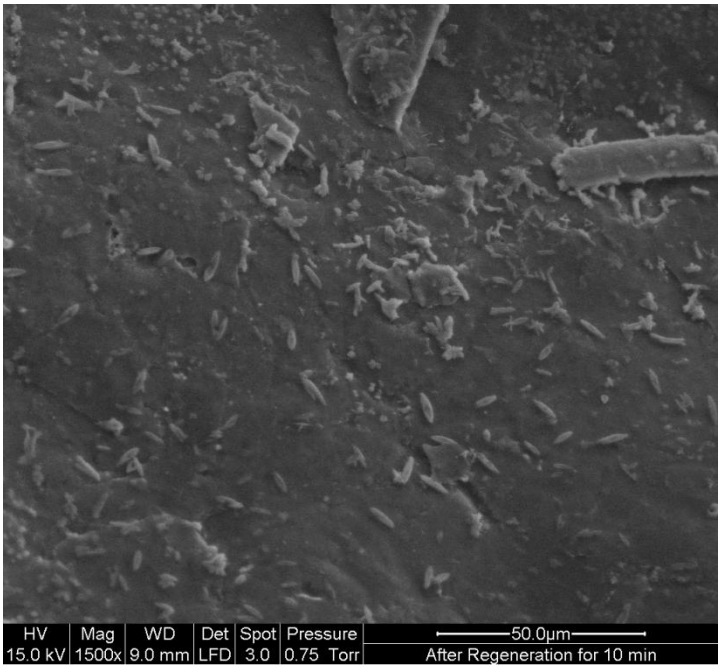

Figure 8.25: *Scanning electron micrograph showing the formation of convex structures during electrochemical regeneration of GIC adsorbent after 10 min at a magnification of 1500x*

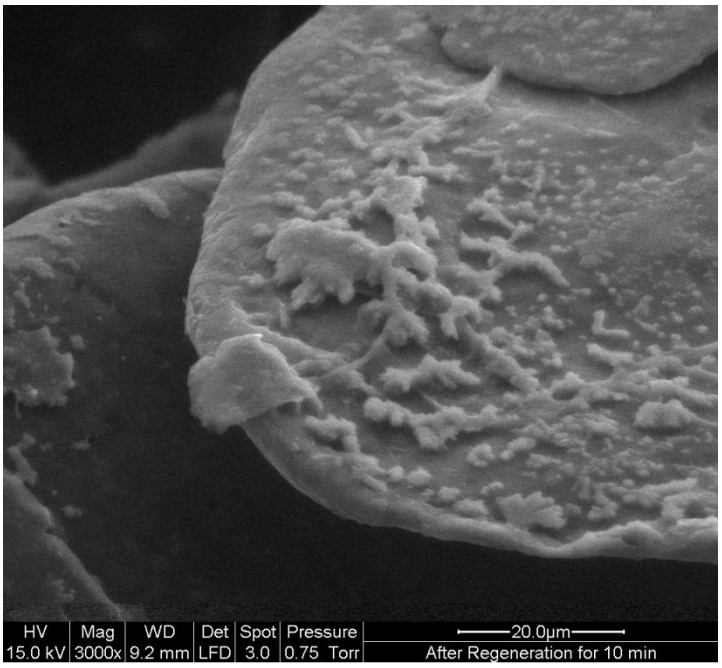

Figure 8.26: *Scanning electron micrograph showing the process of cluster formation during regeneration of GIC adsorbent after 10 min treatment*

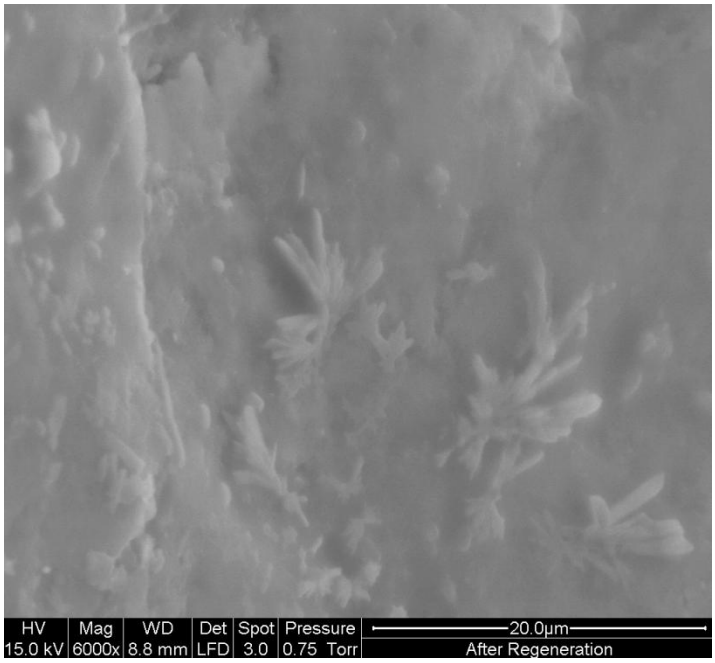

Figure 8.27: *High magnification scanning electron micrograph showing cluster formation during electrochemical regeneration of GIC adsorbent*

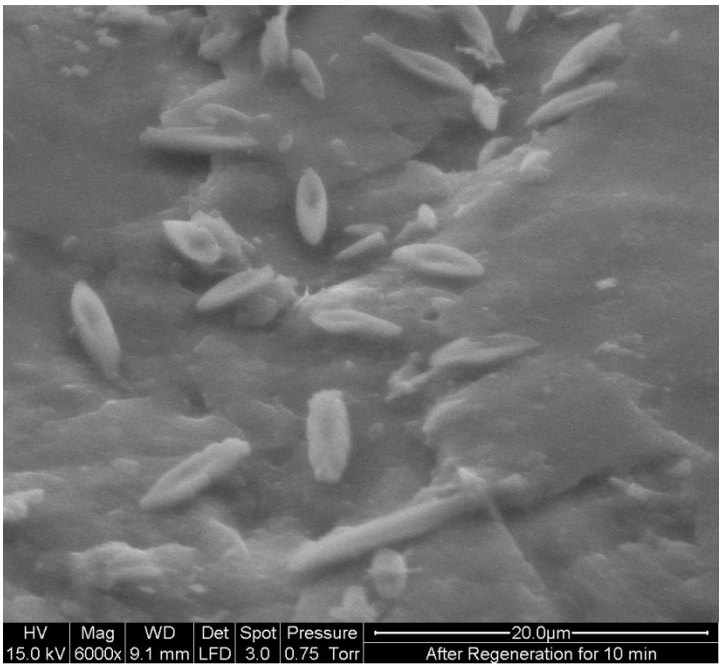

Figure 8.28: *High-magnification scanning electron micrograph showing formation of convex structures during regeneration of GIC adsorbent after 10 min treatment*

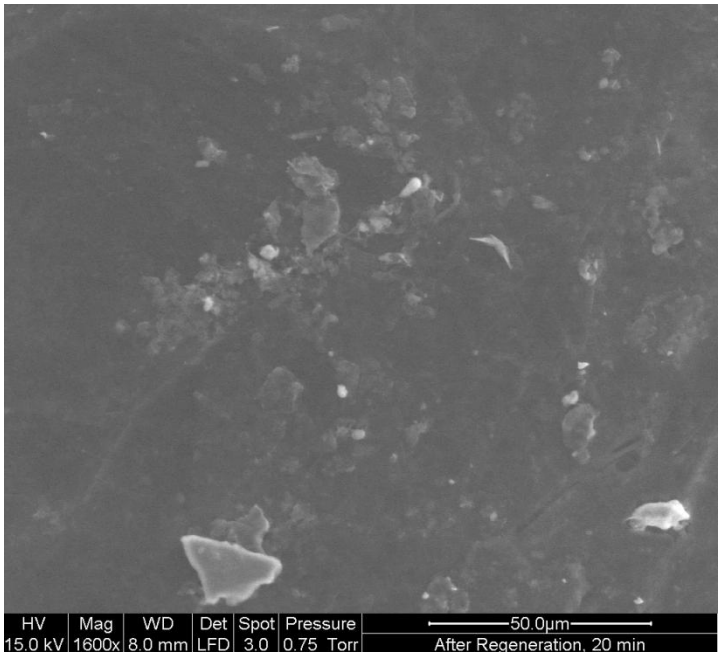

Figure 8.29: *Scanning electron micrograph of electrochemically regenerated GIC adsorbent after 20 min*

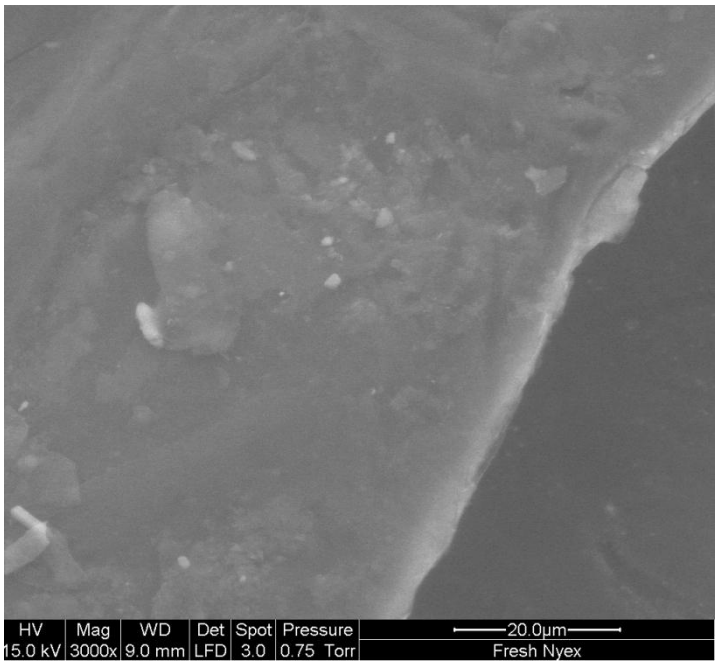

Figure 8.30: *Scanning electron micrograph of fresh GIC adsorbent at a magnification of 3000x*

8.2.2 Adsorption and electrochemical regeneration in the mini-SBR with neutral pH

During the investigation of the effect of current density on adsorption and electrochemical regeneration cycles as described in section 8.1.4, samples of GIC adsorbent were collected and analysed by SEM. No deformation of the cells was observed during the adsorption of *E. coli* on GIC adsorbent at neutral pH. The SEM images suggest that the whole surface of the adsorbent was blanketed by the *E. coli* suspension (Figure 8.31). The images indicate that the adsorption behaviour of *E. coli* on the GIC adsorbent was strongly dependent upon the pH of the cell suspension. Similarly, during the regeneration process the deactivation mechanism of the *E. coli* cells was not clear. The images show the formation of biofilms with the excretion of a thick material adhering to the surface of GIC adsorbent during the second adsorption after regeneration at 10 mA cm^{-2} for 20 min (Figures 8.32).

A biofilm is formed due to the accumulation of microorganisms on a solid surface with an extracellular polysaccharide matrix. They are more complex and have different characteristics compared to planktonic cells *(Donlan, 2002). Pimenov et al. (2001)* suggested the mechanism for the formation of these films on solid surfaces. They suggested that first the bacterial cells are transported to the surface of solids. This can occur due to the mobility of the bacteria and by convective flow of the fluid interacting with the surfaces. The next step is the initial attachment of bacteria to the solid surfaces which depends upon the attractive forces between the two surfaces including electrostatic interactions, van der Waal's forces, dipole interactions, chemical bonding and hydrophobic interactions. These forces in turn depend upon surface charges, hydrophobicity and pH of the liquid containing bacteria. Most bacteria and solid surfaces have a net negative charge *(McEldowney and Fletcher, 1986)*. Therefore, the adhesion depends upon the balance between opposing attractions and repulsive forces. It is well know that surface hydrophobicity correlates positively with adsorption of bacteria *(Rivera et al. 2001)*. The pH has a strong influence on the bacterial adsorption, which affects the surface charge of both bacteria and the solid surface, thereby affecting their electrostatic interactions. The pH suitable to increase adsorption is an intermediate value between pH values of the

point pf zero charge (pH_{pzc}) of the solid surface and the bacterium *(Rivera et al. 2001)*.

The attached bacteria excrete surface active compounds and forms polymeric surface-cell structures called fibrils due to which the attachment between the bacteria and surface is strengthened *(Weber, 1978)*. This is followed by surface colonization which is characterized by the division of attached cells and consequently micro-colonies are formed. Then large quantities of lipopolysaccharides are excreted from the bacteria which lead to the formation of a sticky and viscous biofilm on the solid surfaces.

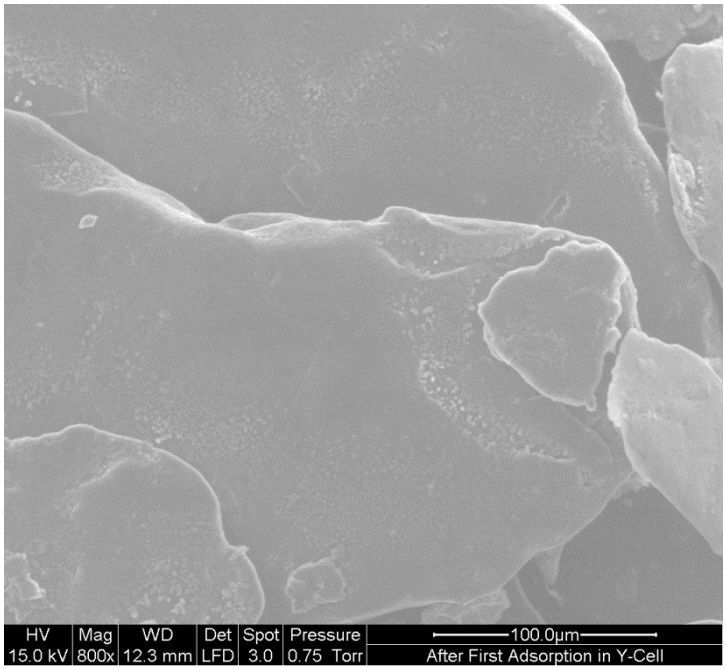

Figure 8.31: *Scanning electron micrograph of GIC adsorbent after first adsorption at neutral pH at 800x magnification*

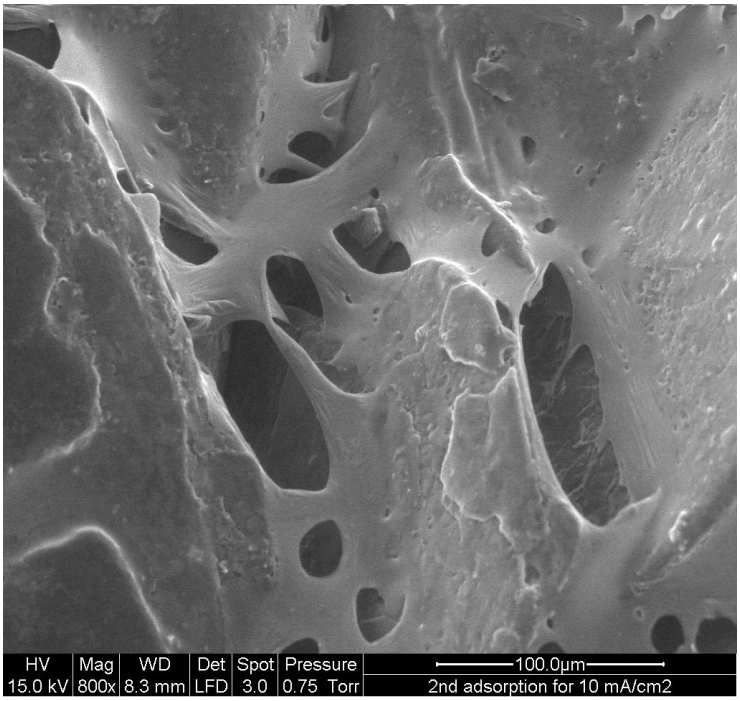

Figure 8.32: *Scanning electron micrograph of GIC adsorbent after the second adsorption showing the formation of a biofilm formed by the release of extracellular slime. Regeneration conditions: 10 mA cm^{-2} for 20 min.*

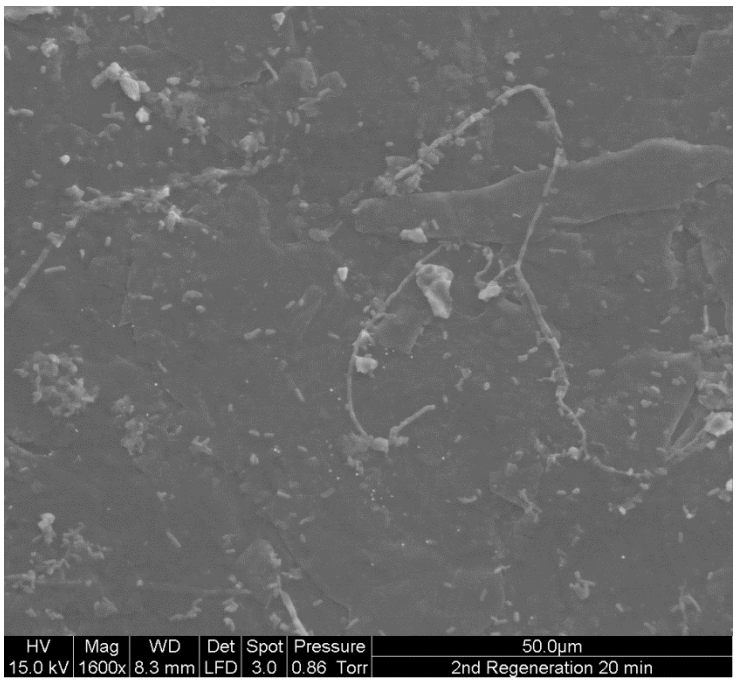

Figure 8.33: *Scanning electron micrograph of E. coli cells on GIC adsorbent along with the biofilm after second regeneration with a current density of 20 mA cm^{-2} and a regeneration time of 20 min.*

The SEM images taken after the second adsorption (Figure 8.32) suggest that the surface of GIC adsorbent had been exhausted because it was not effectively regenerated during the first regeneration at 10 mA cm^{-2} for 20 min. Similarly, an SEM image taken after the second regeneration (Figure 8.33) at 20 mA cm^{-2} for 20 min shows the presence of *E. coli* cells, indicating that the adsorbent was not effectively regenerated. These results also strongly support the previous findings about the lower values of regeneration efficiency obtained at low current densities (10 and 20 mA cm^{-2}) (see section 8.1.4).

On the other hand, figure 8.34 shows that the surface of the GIC adsorbent was partially regenerated during the first regeneration cycle at 30 mA cm^{-2} owing to the transfer of current at neutral pH. The images show that during electrochemical regeneration at 30 mA cm^{-2}, the GIC surface, which was covered with a blanket of *E. coli* biofilm (figure 8.31), fresh surface became available for the next adsorption cycle. It has been suggested that the electrical contact between adsorbed bacteria and the electrode may be disrupted by the formation of bacterial films (see chapter 7, section 7.5.3). However, for these biofilms the high electrical conductivity of the GIC adsorbents has overcome this problem, with the effective regeneration of the GIC particles achieved at 30 mA cm^{-2}. In addition, a constant voltage was observed during all the regeneration cycles at 30 mA cm^{-2} suggesting that a build up of microbial fouling of the GIC particles did not take place (See appendix D). However, a large number of adsorption and electrochemical regeneration cycles should be carried out to assess the microbial fouling of the GIC adsorbent particularly during continuous electrochemical disinfection.

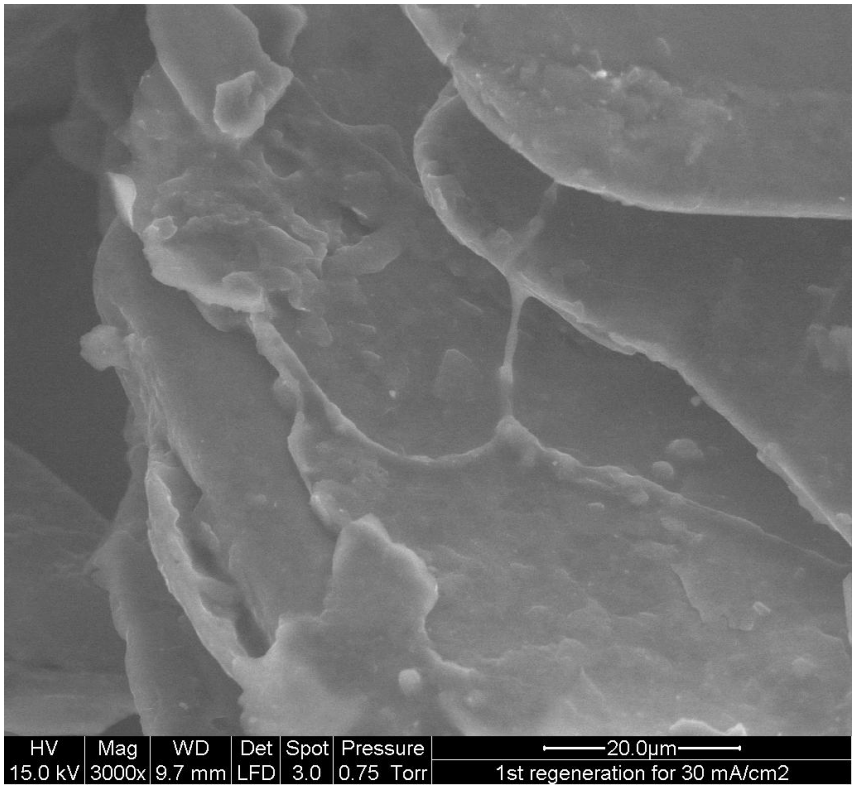

Figure 8.34: *Scanning electron micrograph of GIC adsorbent after the first regeneration cycle at 30 mA cm^{-2} for 20 min showing the effectiveness of the regeneration in releasing surface area for adsorption*

8.2.3 Conclusions

Scanning electron microscopy was found to be a useful method for investigating changes in the surface morphology of *E. coli* during adsorption and electrochemical regeneration. No special technique was required to prepare the samples for SEM investigation. Different mechanisms were observed to take place at the surface during adsorption and electrochemical regeneration when no attempt was made to adjust the pH of the water to be treated. During adsorption of high concentrations of *E. coli* at neutral pH biofilms were observed on the adsorbent surface with the release of an extracellular material. The biofilms of bacteria grown on the solid surfaces are resistant to chlorination but they appeared to be removed during electrochemical regeneration using the GIC adsorbents.

8.3 Simultaneous removal of organics and disinfection of water

The capability of the process of adsorption with electrochemical regeneration using the GIC adsorbents to degrade organic pollutants and disinfect microorganisms in water simultaneously can be illustrated by treating water in which both the organic impurities and microorganisms are present. A practical example of such a situation could be swimming pool water in which varieties of organic and inorganic impurities along with some microorganisms are present. The water in public swimming pools contains unwanted substances and microorganisms which come from the perspiration and urine of the swimmers. Microorganisms can enter into the water through faecal contamination. The other sources of pathogenic bacteria entering into water include human shedding from vomit, saliva or skin. A variety of microorganisms can contaminate the water including *E. coli*, *Staphylococcus aureus*, *Pseudomonas aeruginosa* and *Streptococcus faecalis (Singer, 1990)*. In this context, body fluid analogue (dose of body fluids from bathers) was chosen as a source of organic material. The composition of the body fluid analog was adapted from *Judd and Black, (2000)* and is given in table 8.2:

Table 8.2: *Composition of body fluid analogue (BFA), Judd and Black (2000)*

Constituent	**Concentration (mg L^{-1})**	**Carbon (mg L^{-1})**	**Nitrogen (mg L^{-1})**
Ammonium chloride	2000	–	520
Urea	14800	2960	6900
L-Histidine	1210	560	320
Hippuric acid	1710	1040	134
Citric acid	640	240	–
Sodium phosphate	4300	–	–
Creatinine	1800	770	67
Uric acid	490	180	160
Humic acid	390	–	–
Total	**5476**	**4980**	**7890**

8.3.1 Adsorption kinetics of BFA onto GIC adsorbent

The kinetic study of BFA was performed using the GIC adsorbent with initial concentrations of BFA (48 & 95 mg L^{-1}). The formulation given in table 8.2 was diluted accordingly. The kinetic experiments were conducted by mixing 50 g of GIC

adsorbent with 500 mL of BFA solution in a volumetric flask on a magnetic stirrer (Gallenkamp) operating at 700 rpm for 180 min. Samples of BFA were taken during the course of the kinetic study. These samples were analysed using a TOC analyser ($V_{CSH/CSN}$, Shimadzu Corporation) after their filtration through a 0.45 µm syringe filter (Phenomenex Ltd). The results suggest that adsorption of BFA onto GIC adsorbent was quite rapid (Figure 8.35). About 30% reduction in TOC (total organic carbon) was observed in the first two minutes for both the initial concentrations studied. After the initial rapid drop in TOC, there was a very gradual decrease in total organic carbon concentration observed after 30 min especially for 98 mg L^{-1} BFA. This could be due to attrition of the adsorbent leading to an increase in the surface area available for adsorption. Similar results have been obtained during the adsorption of phenol onto GIC adsorbent (See chapter 4, section 4.1.4). The time of equilibrium was approximated to 30 min.

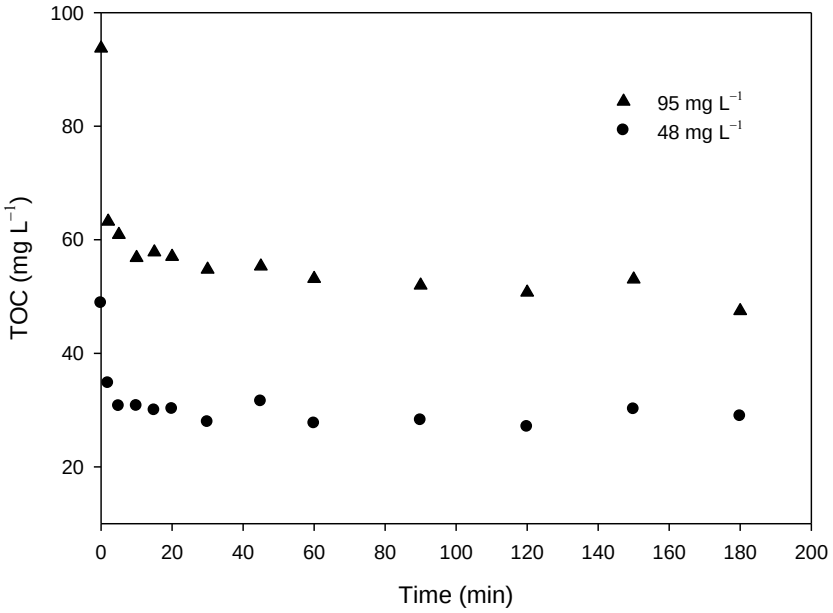

Figure 8.35: *Adsorption kinetics of BFA onto GIC adsorbent in volumetric flasks using 50 g of Nyex®1000 and 500 mL BFA solution with initial concentrations of 48 and 95 mg L^{-1}*

8.3.2 Batch adsorption and electrochemical regeneration in the mini-SBR with BFA and *E. coli*

In order to investigate whether BFA and *E. coli* in water collectively undergoes adsorption onto GIC adsorbent followed by electrochemical regeneration, a series of adsorptions and regenerations were carried out in the min-SBR. A total of 300 mL^{-1} of 86 mg L^{-1} BFA solution contaminated with 1.7×10^{7} CFU mL^{-1} *E. coli* was transferred to 60 g of GIC adsorbent in the mini-SBR (Figure 8.3). Adsorption and electrochemical regeneration were carried out using a fresh water stock suspension (containing both BFA and E. coli) on each cycle. In all other respects the procedure was as described in section 8.1.3 for batch adsorption and electrochemical regeneration. A sample of water was taken after each adsorption and electrochemical regeneration for determining total organic carbon and viable count for *E. coli* (see section 8.1.2).

The results show that there was about an average of 18% reduction in TOC during the adsorption cycles as shown in figure 8.36a. The TOC contents after the regeneration cycles were found similar to the corresponding adsorption cycles (Figure 8.36a). In studies with phenol (see section 4.1.4), it was found that indirect oxidation of phenol in solution led to undesirable breakdown products. The results with BFA (Figure 8.36a) appear to show that there was little or no indirect oxidation of the TOC content of the BFA in solution by electrochemically generated oxidants. This could be associated with the complex combination of components in the BFA as listed in table 8.2 and/or low current density used. In contrast, a 7-$\log_{10}$ reduction in the CFU mL^{-1} of *E. coli* was observed after the third adsorption cycle as shown in figure 8.36b. However, not even a single colony was observed during regeneration cycles suggesting that electrochemical disinfection in solution was significant under these conditions (Figure 8.36b). These results also indicate that the regeneration efficiencies were above 100% for both the BFA and *E. coli* as shown in figure 8.37.

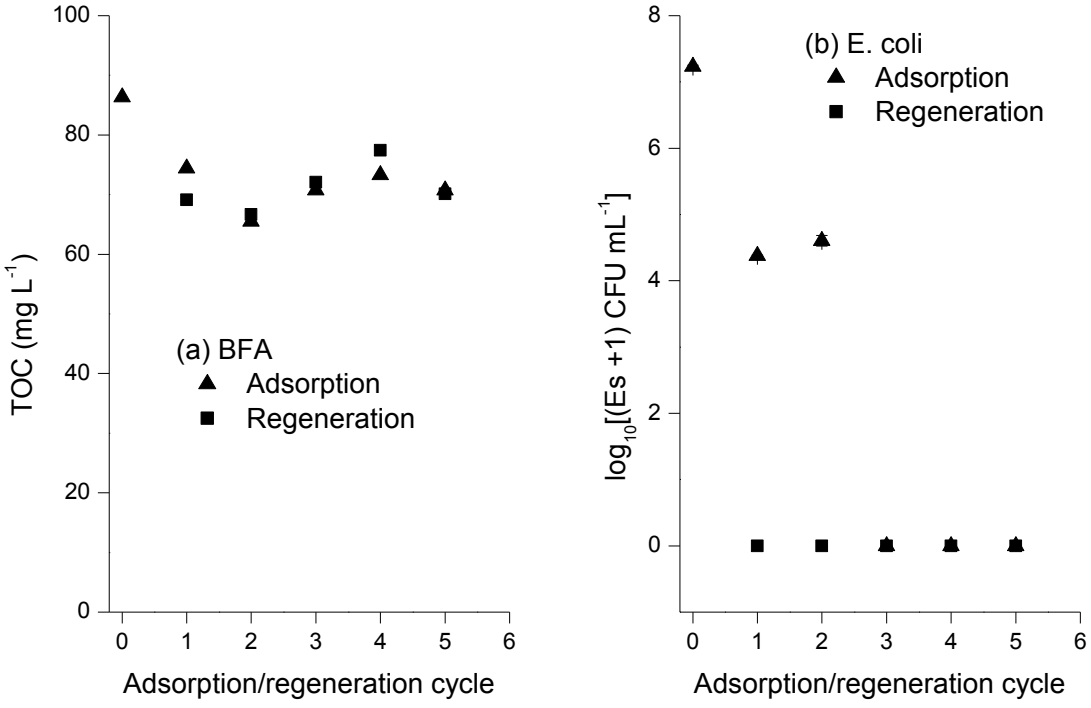

Figure 8.36: *Simultaneous removal of organics and disinfection of water in the mini-SBR at 20 mA cm^{-2} (0.4 A was applied for 20 min, anode current feeder: 20 cm^2), GIC dose 60 g in 300mL of water with initial TOC: 86 mg L^{-1} and E. coli: 1.7×10^7 CFU mL^{-1}.Catholyte used was 0.3% NaCl acidified with HCl (a) Adsorption and regeneration cycles showing TOC concentration after each operation; (b) Adsorption and regeneration cycles showing E. coli concentration, each data point represents the average of five samples and the error bars indicate standard errors calculated from the standard deviation. In order to show the zero point on the logarithmic plot 1 CFU mL^{-1} was added to each data point on the vertical axis where Es denotes the concentration of E. coli.*

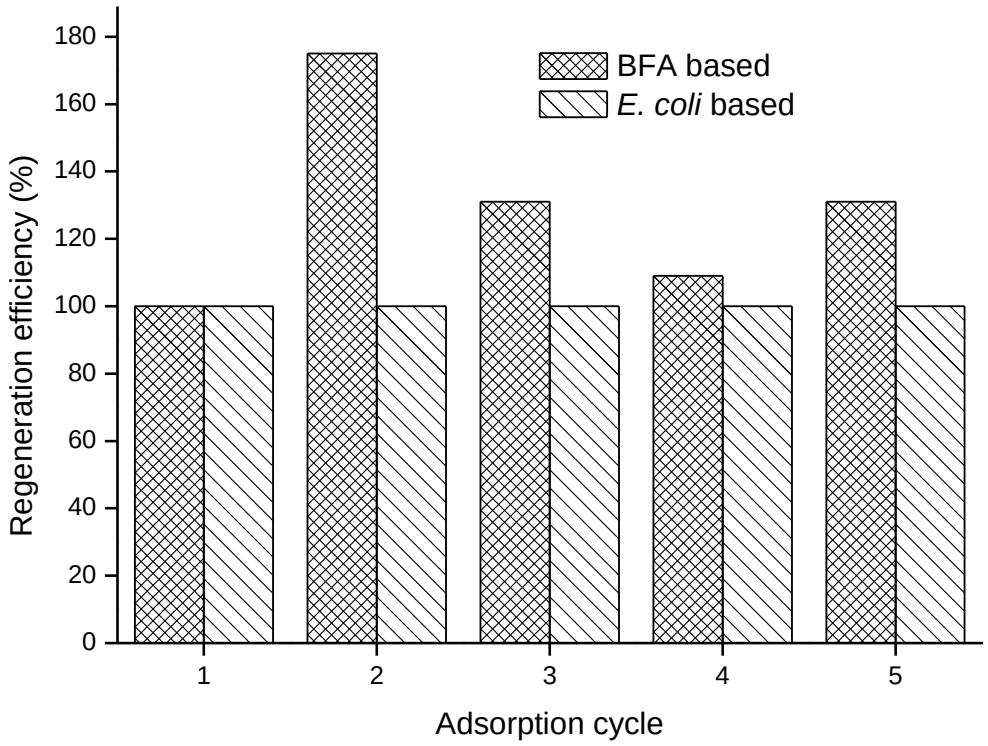

Figure 8.37: *Comparison of percent regeneration efficiency of GIC adsorbent based on BFA and E. coli, Regeneration conditions as in Figure 8.36.*

These results clearly show that for the conditions tested, the process of adsorption with electrochemical regeneration was fully capable of simultaneously treating the dissolved organics (i.e. the TOC associating with the BFA) and disinfecting a high concentration of *E. coli*. In order to further demonstrate the ability of the process to degrade organic pollutants and to disinfect water simultaneously at neutral pH, the same experiment was repeated with the only exception that BFA and *E. coli* feed was prepared by using phosphate buffers to adjust the pH at 7.0 and a current density of 30 mA cm^{-2} was used during regeneration (based on the previous work for neutral pH). The results show that on average 21% of the TOC in the water was removed during each adsorption and regeneration cycle (Figure 8.38a). The results also show that electrochemical disinfection of the BFA solution was not completely effective even at the relatively high current density used (30 mA cm^{-2}). However, the high regeneration efficiency obtained for BFA loaded GIC adsorbent suggests that BFA adsorbed after every adsorption was effectively oxidised during the subsequent regeneration (data not shown). On the other hand, approximately 6-$\log_{10}$ reduction in

E. coli concentration was observed after the third adsorption cycle as shown in figure 8.38b. These results clearly suggest that the Arvia® process has the potential to degrade both the organic impurities and the microorganisms present in water simultaneously at neutral pH.

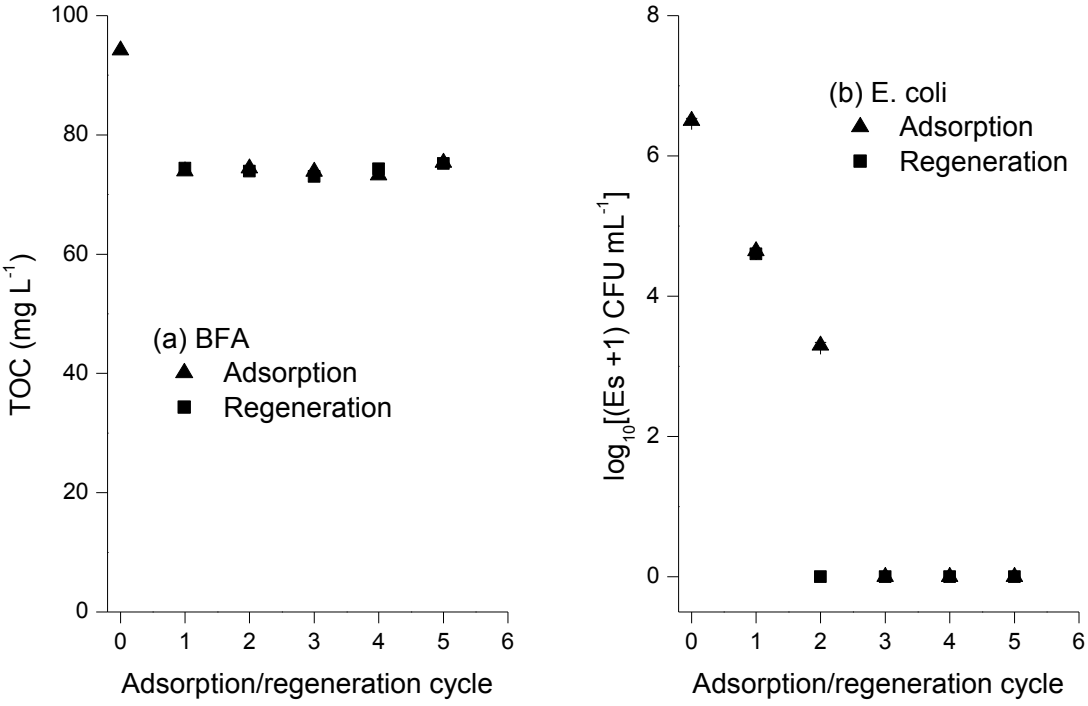

Figure 8.38: *Simultaneous removal of organics and disinfection of water in the mini-SBR at neutral pH and 30 mA cm^{-2} (0.6 A was applied for 20 min, anode current feeder area: 20 cm^2), Catholyte used was 0.3% NaCl (w/v) acidified with HCl, GIC dose 60 g in 300mL of water with initial TOC: 94 mg L^{-1} and E. coli: 3.2×10^6 CFU mL^{-1}. (a) Adsorption and regeneration cycles showing BFA; (b) Adsorption and regeneration cycles showing E. coli, each data point represents the average of five samples and the error bars indicate standard errors calculated from the standard deviation. (b) In order to show the zero point on the logarithmic plot 1 CFU mL^{-1} was added to each data point on the vertical axis where Es denotes the concentration of E. coli.*

8.3.3 Conclusions

The process of adsorption and electrochemical regeneration using the GIC adsorbents can simultaneously remove dissolved organics and disinfect bacteria present in water under controlled (neutral) and uncontrolled pH (acidic) conditions. However, the GIC adsorbent has a relatively low adsorption capacity for removing the BFA measured in terms of TOC. In addition, indirect oxidation was not observed to decrease the TOC of BFA in solution.

8.4 Different bacteria, fungus and yeasts

After evaluating the potential of adsorption and electrochemical regeneration using GIC materials to disinfect water using a model microorganism, *E. coli*, under various experimental conditions, a variety of other microorganisms including bacteria, fungus and yeasts have been tested with this process, including:

8.4.1 Bacteria

Pseudomonas aeruginosa

Pseudomonas aeruginosa (P. aeruginosa) is a gram-negative rod shaped free living bacterium that is ubiquitous in the environment *(Hardalo and Edberg, 1997)*. It has the ability to multiply in aqueous environments, food sources and may colonize biofilms on solid surfaces such as plumbing fixtures *(Hardalo and Ederg, 1997)*. It can also survive in distilled water and therefore it can be found in environments having low nutrient concentrations or high nutrient environments including sewages and the human body *(Mena and Gerba, 2009)*. *P. aeruginosa* can cause a variety of infections including endocarditis, osteomyelitis, pneumonia, urinary tract and gastrointestinal infections *(Mena and Gerba, 2009)*. *P. aeroginoas* is frequently found in natural waters including lakes and rivers. However, high concentrations of *P. aeruginosa* can also be found in swimming pools and hot tubs. This is due to the relatively high temperatures and aeration; both of these factors favour the growth *P. aeruginosa (Mena and Gerba, 2009)*. Epidemics have also been reported from exposure to *P. aeruginosa* in swimming pools and water slides *(Tate et al. 2003)*. In addition, it has resistance to many antibiotics and disinfectants *(Lambert, 2002)*.

A culture of *P. aeruginosa* (on nutrient agar plate) was available in the School of Chemical and Engineering and Analytical Science, University of Manchester, UK. However, its strain was not known. The suitability of the process was tested by performing a series of adsorption and electrochemical regenerations in the mini-SBR following the procedure described in section 8.1.3. The water contaminated with *P. aeruginosa* was prepared in phosphate buffer deionised water to keep the pH of the water at 7 throughout the course of the experiment according to the procedure described in section 8.1.3. The CFU mL^{-1} was determined using the viable count procedure described in section 8.1.2. During the adsorption of *P. aeruginosa* onto the GIC adsorbent, a mixing time of 30 min was applied. The suitable mixing time was determined from a kinetic study of *P. aeruginosa* onto GIC adsorbent according to the procedure described in section 8.1.3 (See appendix E). Regeneration of the GIC adsorbent loaded with *P. aeruginosa* was carried out at 30 mA cm^{-2} for 20 minutes in accordance with the conditions that were optimized for *E. coli* at neutral pH (see section 8.1.4).

The results indicate that a high removal of *P. aeruginosa* was achieved with the GIC adsorbent with ca. 3.0 $\log_{10}$ reduction during the first adsorption cycle and even higher in the subsequent adsorption cycles (Figure 8.39a). In addition, the GIC adsorbent was regenerated effectively with 100% regeneration on each adsorption cycle as shown in figure (8.39b). No *P. aeruginosa* was detected in the water after the regeneration cycles indicating that electrochemical disinfection of *P. aeruginosa* in solution was effective under the conditions used in this experiment (Figure 8.39a). Thus, it can be concluded that a high concentration of *P. aeruginosa* in water can be disinfected during adsorption and electrochemical regeneration using the GIC adsorbents.

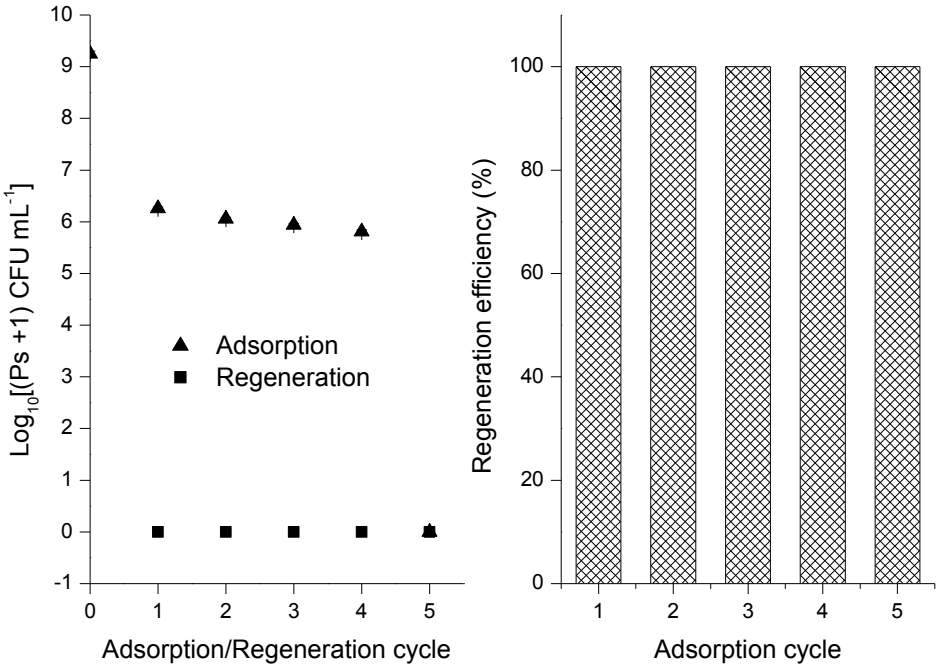

Figure 8.39: *Electrochemical regeneration of P. aeruginosa loaded GIC adsorbent in phosphate buffer (pH 7.0) with an initial concentration of 1.8 × 10^9 CFU mL^{-1}, solution volume: 300 mL; adsorbent mass: 60 g; regeneration current: 0.6 A corresponding to a current density of 30 mA cm^{-2}, regeneration time: 20 min at 30 mA cm^{-2}, anode current feeder (20 cm^2). The catholyte was 0.3% NaCl acidified with HCl (a) Adsorption and regeneration cycles; (b) Regeneration efficiency, where cycle 1 was carried out with fresh adsorbent. Each data point in figure (a) represents the average of five samples and the error bars indicate standard errors calculated from the standard deviation. In order to show the zero point on the logarithmic plot 1 CFU mL^{-1} was added to each data point on the vertical axis where Ps denotes the concentration of P. aeruginosa.*

Staphylococcus aureus

Staphylococcus aureus (S. aureus) is a gram positive bacterium usually arranged in grape like irregular clusters. Although it occurs widely in the environment it is found mainly on skin and the mucous membranes of animals. *S. aureus* can be released into environments including swimming pools, spa pools and other recreational waters by human contact. *S. aureus* is one of the main causes of pyogenic infections including boils, skin infections, abscesses, osteomyelities, septic arthritis, endocarditis, food poisoning and infection of clean surgical wounds *(Block, 2001)*. *S. aureus* has been found to be more resistant to chlorination than *E. coli* or *P. aeruginosa (Block, 2001)*.

A culture *of S. aureus* (on nutrient agar plate) was available in the School of Chemical and Engineering and Analytical Science, University of Manchester, UK. However, its strain was not known. Water contaminated with *S. aureus* was prepared in phosphate buffer deionised water to keep the pH of the water at 7 throughout the course of the experiment according to the procedure described in section 8.1.3. Normally, the treated water in the mini-SBR after each cycle of regeneration was replaced with a fresh bacterial suspension of same volume and concentration for the next adsorption cycle (see section 8.1.3). Keeping in view handling small volumes of pathogenic *S. aureus*, the behaviour when the same suspension of *S. aureus* was treated over several cycles was investigated by not siphoning off the treated water at the end of each regeneration. In all other respects the procedure was as described for batch adsorption and electrochemical regeneration in section 8.1.3. Thus, a number of adsorption and regeneration cycles were carried out even at relatively low current density (10 mA cm^{-2}) for *S. aureus* in water at pH 7.0. Prior to this experiment, studies of *S. aureus* adsorption onto the GIC adsorbent were carried out to evaluate the time required to achieve equilibrium and the adsorptive capacity according to a similar procedure to that described in section 8.13 for *E. coli*.

The kinetic study (See appendix E) indicated that the equilibrium time was around 30 min, and this adsorption time was used during the adsorption cycles in the mini-SBR. The results suggest that a high concentration of *S. aureus* was removed by adsorption and electrochemical regeneration with almost no detectable *S. aureus* after the second regeneration cycle in the mini-SBR as shown in figure 8.40. This also suggests that the process is quite effective in removing *S. aureus* present in water with a significantly higher reduction in the number of bacterial cells (ca. 9-$\log_{10}$ reduction) by treating a specific volume of water containing a high concentration of *S. aureus* over a number of cycles.

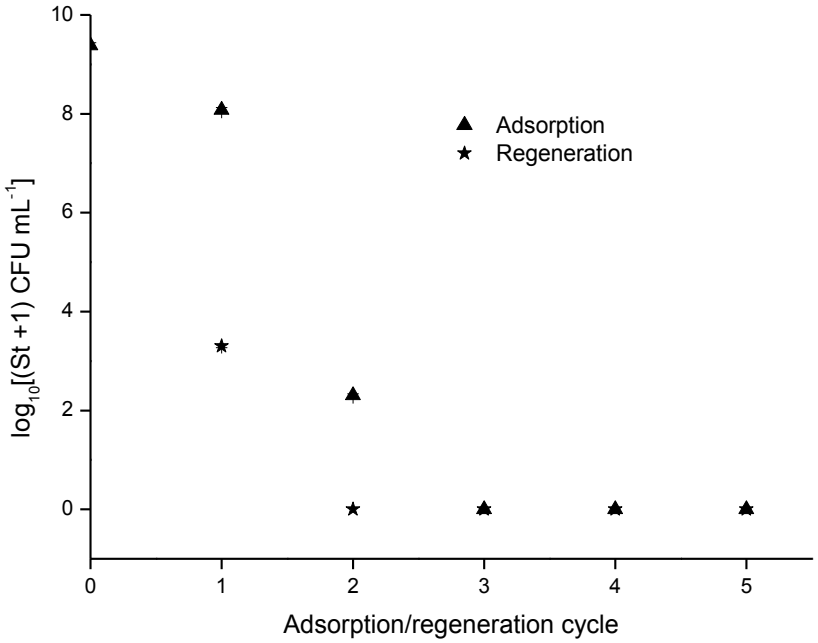

Figure 8.40: *Multiple adsorption and regeneration cycles with the same initial 1L of 2.4 × 10^9 CFU mL^{-1} S. aureus (prepared in phosphate buffer pH 7.0) with 150 g of GIC adsorbent in the mini-SBR at 10 mA cm^{-2}, regeneration current: 0.5 A applied for 20 minutes (anode current feeder, 50 cm^2). The catholyte was 0.3% NaCl acidified with HCl. Each data point represents the average of five samples and the error bars indicate standard errors calculated from the standard deviation. In order to show the zero point on the logarithmic plot 1 CFU mL^{-1} was added to each data point on the vertical axis where St denotes the concentration of S. aureus.*

Legionella pneumophila

Legionella pneumophila (L. pneumophila) is a gram negative rod shaped bacterium. It is one of the waterborne pathogens responsible for about 90% of all the cases of legionnaires, a fatal infectious disease *(Block, 2001)*. It occurs naturally in rivers and lakes. However, *L. pneumoplila* also live in cold storage tanks, cooling towers, fire-fighting equipment and spa baths. Stagnant warm water provides an ideal environment for the growth of this bacterium *(Delaedt et al. 2008)*. Inhalation of contaminated aerosols formed by showers, air conditioning systems and cooling towers can spread the disease *(Delaedt et al. 2008)*. Therefore, it is essential to eliminate *L. pneumophila* from water systems associated with public usage in order to prevent such outbreaks.

Test trials of adsorption and electrochemical regeneration using GIC adsorbents to disinfect *L. pneumophila* in water were carried out at University of Brighton in collaboration with the School of Pharmacy and Bimolecular Sciences. *L. pneumophila* strain ATCC 33152 serogroup 1 was obtained from Ian Cooper, School of Pharmacy and Bimolecular Sciences and used in these experiments. The bacteria were grown on buffered charcoal yeast extract (BCYE) agar plates at 37℃ for 2 days prior to carrying out these experiments.

Preparation of water containing L. pneumophila

A mass of 3 g of yeast extract was dissolved in 100 mL of deionised water and then sterilized in an autoclave at 121 ℃ for 15 min. A single colony of *L. pneumophila* was transferred gently from its culture on an agar plate into 100 mL of water containing yeast extract. It was then placed in an incubator at 37 ℃ for 24–48 hours. Afterwards, the contents of the flask were equally divided into four 50 mL centrifuge tubes with 25mL of broth in each tube and these were centrifuged at 5500 rpm for 10 min. Upon centrifugation, a small mass of *L. pneumophila* was collected at the base of each centrifuge tube. The supernatant from each tube was removed and the pellet was cleaned with deionised water three times. Finally, the clean bacterial pellets were suspended into 700 mL water to provide the contaminated feed for the experiment.

Preparation of agar plates for viable count

The agar plates used to inoculate water samples containing *L. pneumophila* were prepared by dissolving 12.5 g of charcoal yeast in 450 mL of deionised water. Buffered charcoal yeast extract (BCYE) was used as a supplement for the growth of *L. pneumophila* in charcoal yeast in such a way that one vial of BCYE (Oxoid) was added per 100 mL of the prepared agar. In all other respects, the procedure was as for the *E. coli* viable count described in section 8.1.2.

Staining of L. pneumophila after adsorption and electrochemical regeneration

A few drops of safranin were added to a mixture of GIC particles and water in a small test tube. The contents of the test tube were thoroughly shaken and then centrifuged at 10, 000 *g* for 10 seconds. Afterwards, the supernatant was removed from the test tube and a few drops of deionised water were added followed by

centrifugation with the same conditions. Finally, a few particles of GIC adsorbent were removed from the test tube and were placed on a glass side. These particles were then viewed through the microscope (Olympus, BH-2) at 100x magnification with the aim to investigate whether coloured species (*L. pneumophila*) were attached to the GIC particles.

Disinfection of water containing *L. pneumophila* by adsorption and electrochemical regeneration was carried out according to the procedure described above for *S. aureus*. A same batch of *L. pneumophila* was treated over several cycles of adsorptions and regenerations by not siphoning off the treated water at the end of each regeneration. It has already been seen that 30 min was required to achieve equilibrium during adsorption of *E. coli*, *P. aeruginosa* and *S. aureus* onto GIC adsorbent. Thus, the same time (30 min) was also applied for the adsorption of *L. pneumophila* onto GIC adsorbent in the mini-SBR. The electrochemical regeneration of *E. coli* loaded GIC adsorbent was effective at 10 mA cm^{-2} when no phosphate buffer was added into water to maintain a neutral pH (see section 8.1.4). However, electrochemical regeneration of GIC adsorbent loaded with *L. pneumophila* (when no phosphate buffer was added) was performed at 20 mA cm^{-2} because this bacterium has proved to be a refractory pathogen which is capable of resisting disinfection even after repeated cycles of chlorination *(Cooper and Hanlon, 2010).*

The results indicated that a high concentration (2.6×10^{7} CFU mL^{-1}) of *L. pneumophila* was removed by adsorption and electrochemical regeneration with no *L. pneumophila* cell detected in the water after the first regeneration cycle as shown in figure 8.41. About 95% of the *L. pneumophila* present in the water was removed during the first adsorption onto the GIC adsorbent which was effectively regenerated in the subsequent regeneration cycle (Figure 8.41). Thus, the process of adsorption and electrochemical regeneration of GIC adsorbents was found to be efficient in removing *L. pneumophila* present in water with a ca. 7.5-$\log_{10}$ reduction in the number of bacterial cells under these conditions. Further trials will be required to assess the regeneration of *L. pneumophila* loaded adsorbent over a number of adsorption and regeneration cycles when after every regeneration the treated water is replaced with a fresh bacterial suspension of same volume and concentration for the next adsorption cycle.

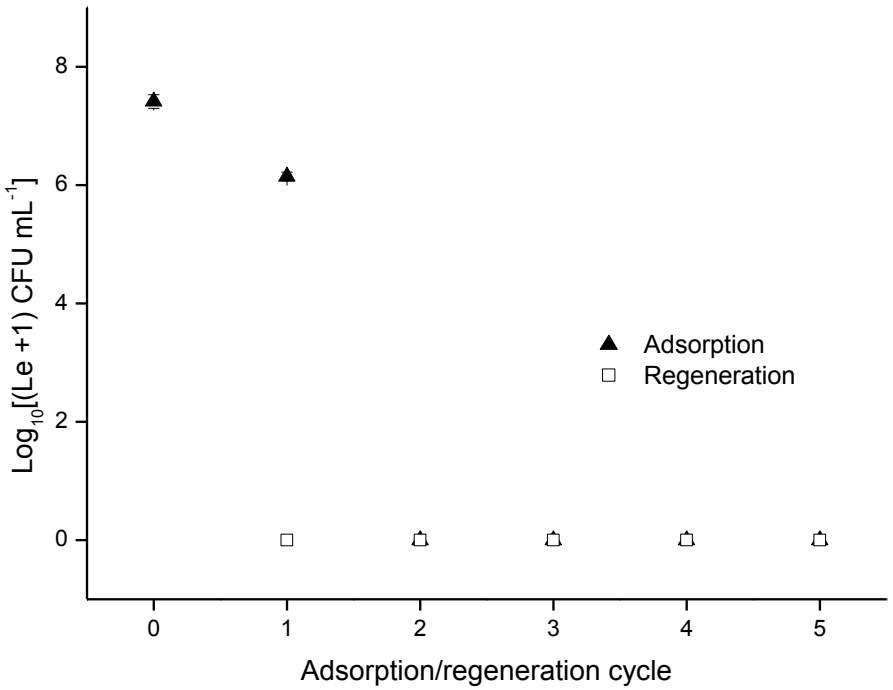

Figure 8.41: *Multiple adsorption and regeneration cycles with the same initial 1 L of 2.6 × 10^7 CFU mL^{-1} L. pneumophila with 150 g of GIC adsorbent in the mini-SBR at 20 mA cm^{-2}, regeneration current: 1.0 A applied for 20 minutes (anode current feeder, 50 cm^2). The catholyte was 0.3% NaCl acidified with HCl. Each data point represents the average of five samples and the error bars indicate standard errors calculated from the standard deviation. In order to show the zero point on the logarithmic plot 1 CFU mL^{-1} was added to each data point on the vertical axis where Le denotes the concentration of L. pneumophila.*

The adsorption of *L. pneumophila* on the GIC adsorbent was confirmed from the images of the GIC particles taken under a microscope (Olympus, BH-2) at 100x magnifications after staining with safranin according to the procedure as described above. Attachment of the stained bacteria on the GIC particle indicates the adsorption of *L. pneumophila* onto the adsorbent (Figure 8.42). In addition, the *L. pneumophila* were observed to be attached with the adsorbent particles in the form of clusters, particularly on the edges of the GIC particles. Some of the samples of the GIC adsorbent after electrochemical regeneration for 20 min at 20 mA cm^{-2} were also stained with safranin according to the procedure as described above. The images for the regenerated sample indicated that the coloured species initially adhering to the adsorbent particles had completely disappeared (Figure 8.42).

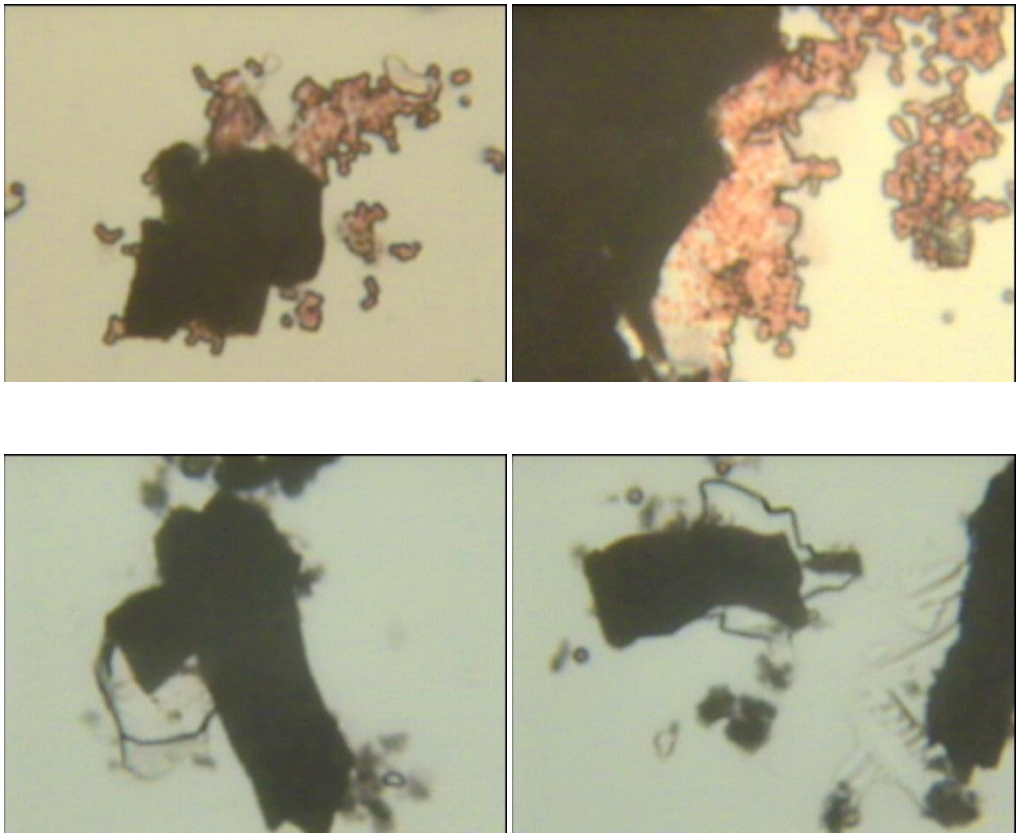

Figure 8.42: *Microscope images (at 100x magnification) of GIC particles after staining with safranin after adsorption (upper) and electrochemical regeneration (lower) in the mini-SBR, Regeneration conditions: 1.0 A was applied for 20 min (20 mA* cm^{-2}*)*

8.4.2 Fungi

Fungi are an important group of species for food and medical mycology, and biotechnology. They occupy a wide spectrum of habitats in animal and plant environments, and they are economically important both as harmful or useful microorganisms. They can contaminate foods and feeds at different stages including pre- and post-harvest, processing, and handling *(Abarca et al. 2004; Kozakiewicz, 1989; Samson et al. 2004)*. Food and fruits left exposed will typically be contaminated with *Aspergillus* or *Penicillum* species. By contrast, they are also frequently used in the fermentation industry for the production of organic acids, enzymes, vitamins, and antibiotics *(Samson and Pitt, 2000)*. Therefore water is not a primary route for acquiring human fungal infections. However, some fungi including *Fusarium* can produce toxic substance in water that are associated with a variety of

respiratory, neurological and other systemic symptoms *(Lonnen et al. 2005)*. Low concentrations of some of the fungi present in raw water supplies can pass through both sand filtration and disinfection and thus can occur in drinking water leading to potential health problems *(Niemi et al. 1982)*. In order to investigate whether adsorption using GIC adsorbents with electrochemical regeneration is effective in disinfecting fungal spores in water, *Aspergillus awamori (A. awamori)* was selected as a model species for water disinfection.

A strain of *Aspergillus awamori* (2B. 361 U2/1) classified by the Commonwealth Mycological Institute as in the *Aspergillus niger* complex, was available in the School of Chemical Engineering and Analytical Science, University of Manchester, UK. *A. Awamori* spores have a round shape with filamentous extensions (Figure 8.43). This strain was initially stored dry in the form of spores in sand at 4°C. Prior to experimental work, *A. awamori* spores were purified, sporulated, and stored on slopes at 4°C.

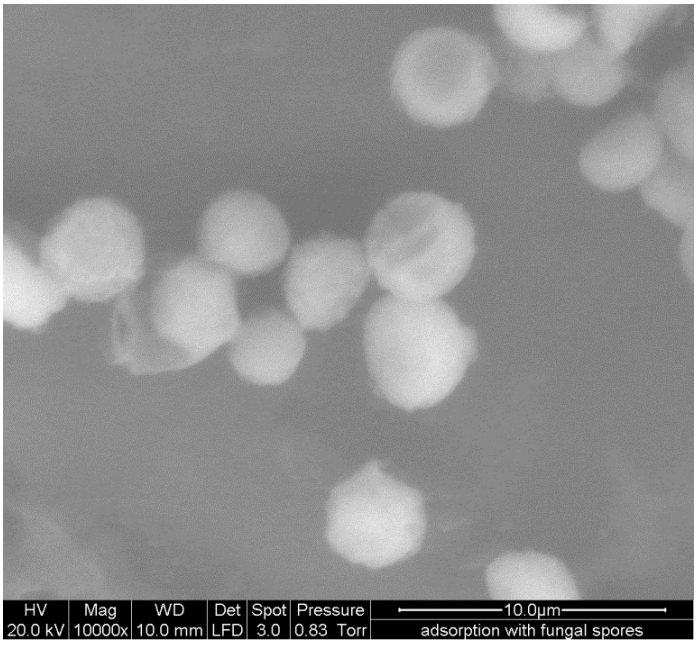

Figure 8.43: *SEM image of Aspergillus awamori showing round shape particles at 1000x magnification*

Cultures of *A. awamori* were sporulated on 100 mL solid medium, which consisted of 2% (w/v) whole wheat and 2 % (w/v) agar, in 500 mL flasks. The spores were suspended by adding 50 mL of sterilized saline water (0.9 % NaCl), with some drops of Tween 80 (0.01 % v/v) (Sigma-Aldrich®) to the flasks. The fungal spores were harvested by the manual shaking of the flasks with sterile glass beads. The transfer of spore suspension into 1 mL vials was achieved using a 1000 μL pipette with sterilized tips. Three vials of spore suspensions of a specific concentration were added to a model synthetic dilute wastewater with a composition given in Table 8.3 with the aim to give a realistic wastewater in which fungal spores could exist. In addition, sodium bicarbonate used in this composition will not allow a sudden drop in pH which could affect the viability of *A. awamori.* This low strength wastewater was similar to the one used by *Matsushige et al. (1990).* The spore concentration was measured using viable count technique.

Table 8.3: *Model wastewater used in the experiments for A. awamori*

Constituent	***Concentration (mg L^{-1})***
Glucose	*250*
Peptone	*200*
Urea	*10*
Meat extract	*140*
$CaCl_2.2H_2O$	*4*
$MgSO_4.7H_2O$	*2*
K_2HPO_4	*11*
NaCl	*7*
$NaHCO_3$	*300*

The kinetic study for the adsorption of *A. awamori* onto GIC adsorbent suggests that 30 min was required to achieve equilibrium (Figure 8.44a). These results are similar to the adsorption of bacteria including *E. coli*, *P. aeruginosa* and *S. aureus* investigated in this project. The results for sequential adsorption and electrochemical regeneration in the mini-SBR show the removal of fungal spores during these processes (Figure 8.44b) leading to regeneration efficiency above 96% for each

adsorption cycle. The data suggests that during the electrochemical process in the mini-SBR the fungal spores were removed completely from the solution due to indirect oxidation (Figure 8.44b). The adsorption of fungal spores onto the GIC adsorbent along with its electrochemical regeneration was further confirmed from the SEM images as shown in figure 8.45. The adsorption of fungal spores on the GIC adsorbent shows clustering of the spores on the surface, presumably due to spore to spore interactions of the spores on the surface. In addition, some of the spores were observed to adsorb one above the other (i.e. multilayer adsorption). A high population of spores was observed on the relatively rough surface of the GIC particle. The SEM image taken after regeneration confirms the complete destruction of the spores onto the GIC surfaces.

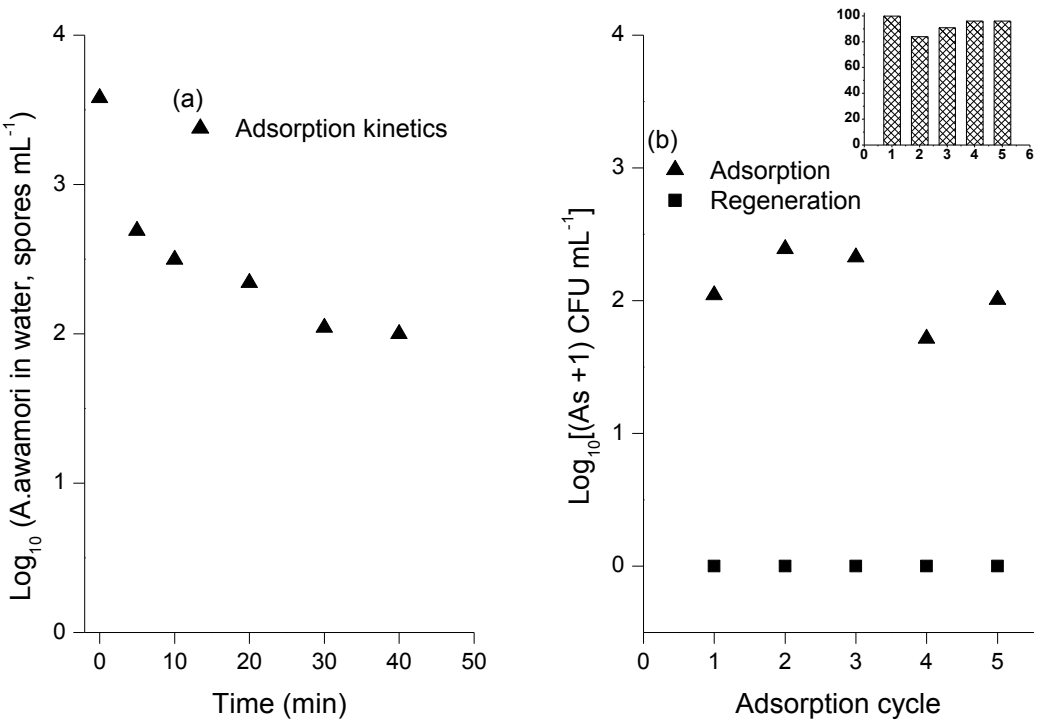

Figure 8.44: *Removal of A. awamori from water by adsorption and electrochemical regeneration using the GIC adsorbent, (a) adsorption kinetics: initial concentration 3800 spores mL^{-1}; GIC adsorbent dose 60g in 300 mL (b) sequential adsorption and electrochemical regeneration in the mini-SBR, regeneration was carried out at 0.4 A for 20 min (20 mA cm^{-2}, anode current feeder: 20 cm^2). In order to show the zero point on the logarithmic plot 1 CFU mL^{-1} was added to each data point on the vertical axis where As denotes the concentration of A. awamori.*

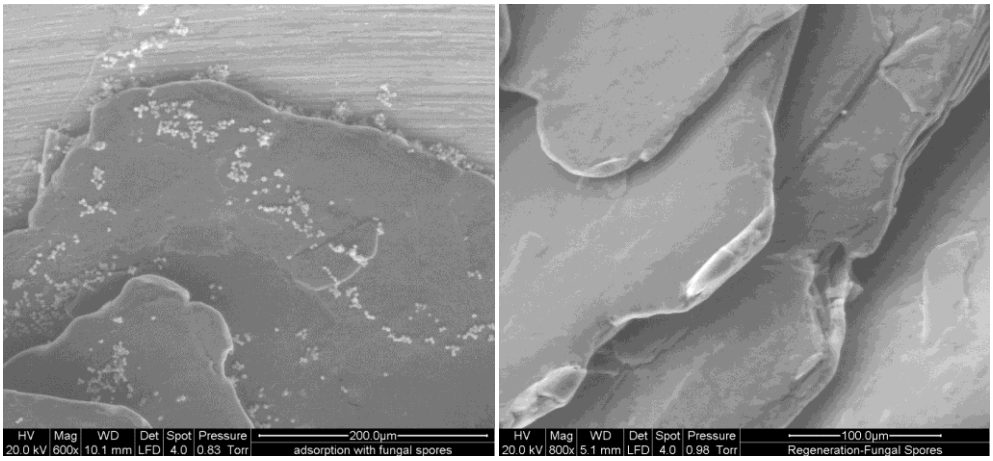

Figure 8.45: *Scanning electron micrographs of GIC adsorbent after adsorption of A. awamori (left) at 600x magnification and after electrochemical regeneration (right) at 800x magnificaition. Regeneration was carried out at 0.4 A for 20 min (20 mA* cm^{-2}*)*

8.4.3 Yeasts

Saccharomyces cerevisiae

In order to investigate the effectiveness of adsorption using GIC adsorbents with electrochemical regeneration to disinfect yeast in water, *Saccharomyces cerevisiae* (*S. cerevisiae*) was selected since this species has been intensively studied as a model eukaryotic organism in microbiology. The cells of *Saccharomyces cerevisiae* are spheroidal as shown in figure 8.46.

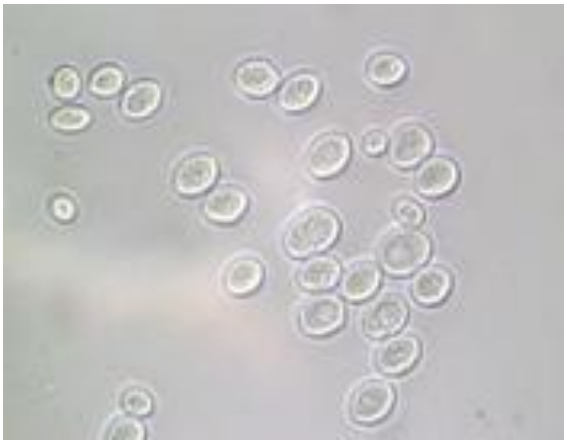

Figure 8.46: *Microscope image of S. cerevisiae in water at a magnification of 100x showing the spheroidal morphology of the yeast cells*

A culture *of S. cerevisiae* was available in the School of Chemical and Engineering and Analytical Science, University of Manchester, UK. The culture was grown in

100 mL of a broth medium composed of glucose, yeast extract, peptone and malt extract at concentrations of 20, 10, 6 and 6 g L^{-1}, respectively. Incubation was carried out at 30 ℃ for 48 h. Afterwards, a specific volume of this broth was added to the water to be treated in the mini-SBR in order to study the viability of *S. cerevisiae* in a general synthetic medium similar to a brewery effluent which contains glucose, yeast extract, peptone and malt extract.

A series of adsorption and electrochemical regeneration cycles were carried out according to the procedure as described in section 8.1.3. The results suggest the removal of S. cerevisiae from water by adsorption and its subsequent electrochemical regeneration in a way that reasonably high regeneration efficiency is achieved after each adsorption cycle (Figure 8.47). During the electrochemical regeneration of the GIC adsorbent, the oxidants produced were effective in disinfecting the *S. cerevisiae* in water leading to complete disinfection after each regeneration cycle, as shown in figure 8.47a.

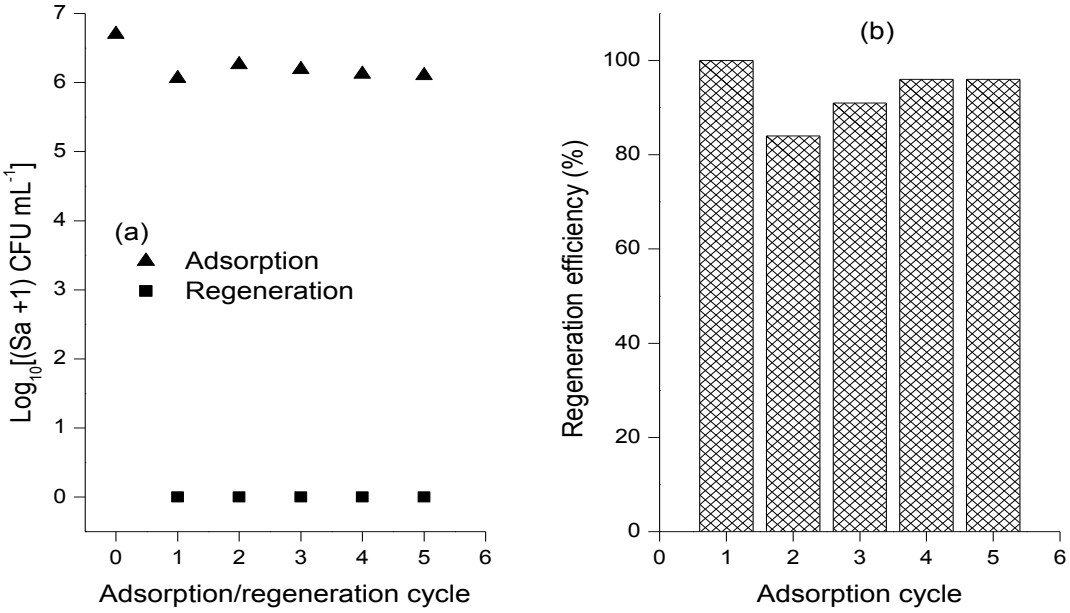

Figure 8.47: *Multiple adsorption and electrochemical regeneration cycles with S. cerevisiae in water in the mini-SBR, initial concentration: 5×10^6 CFU mL^{-1}, GIC adsorbent dose 60 g in 300 mL, regeneration was carried out at 0.4 A for 20 min (20 mA cm^{-2}). In order to show the zero point on the logarithmic plot 1 CFU mL^{-1} was added to each data point on the vertical axis where Sa denotes the concentration of S. cerevisiae.*

In addition to the removal of yeast from water, these findings may also have implications for the treatment of beer. In the beer industry, the clarification of beer is usually followed by pasteurisation so as to ensure the microbiological stability and the conservation of beer. Conventional heat treatment requires water loops to heat and cool the product and also induces an additional water and energetic consumption. Sterile filtration is another treatment but it is facing several challenges *(Fillaudea et al. 2006)*. One alternative to pasteurisation step could be the use of adsorption and electrochemical regeneration to sterilise the beer before conditioning. However, this application is beyond the scope of this project.

Rhodosporidium turoloides

Rhodosporidium turoloides (R. turoloides) Y4 is oil producing or oleaginous yeast *(Wu et al. 2011)*. Since these species contain intracellular valuable compounds such as lipids, therefore the disruption of this yeast would be interesting in order to release the lipids contained in vacoules within the yeast cell. Once the lipids are released biodiesel could be produced via a conventional transesterification process. Although the production of biodiesel through transesterification is not within the scope of this project, this could be an important implication after the successful removal of *R. turoloides* from water by adsorption with electrochemical regeneration using the GIC adsorbents. The present experiment aimed at investigating the capability of the Arvia® process to deactivate the cells and to assess the viability of the yeast in the mini-SBR. The other objective was to test yeast different from *S. cerevisiae* so that the results of the former can be confirmed.

A culture of *R. turoloids* was available in the School of Chemical and Engineering and Analytical Science, University of Manchester, UK. A series of adsorption and electrochemical regeneration cycles were performed according the procedure as described in section 8.1.3. The results indicated that ca. 96% of *R. turoloides* present in water were removed during the first adsorption and complete disinfection of the yeast was achieved during the subsequent regeneration. Regeneration efficiencies of above 100% were obtained for all the adsorption cycles (Figure 8.48). Comparison with the results for *S. cerevisiae* shows that after second adsorption in case of *R. turoloides* not even a single colony forming unit was detected. This suggests that

electrochemically generated oxidants entrapped within the adsorbent bed were more effective against *R. turoloides* than *S. cerevisiae*.

The adsorption of *R. turoloides* was further confirmed from the SEM image as shown in figure 8.49. Clusters of *R. turoloides* were observed to be adsorbed on the edges of the GIC particles, suggesting that there were more yeast cells on the edges than the planar surfaces.

Further work should be carried out to see if the yeast cells were disrupted during electrochemical regeneration of the GIC adsorbent loaded with *R. turoloides*.

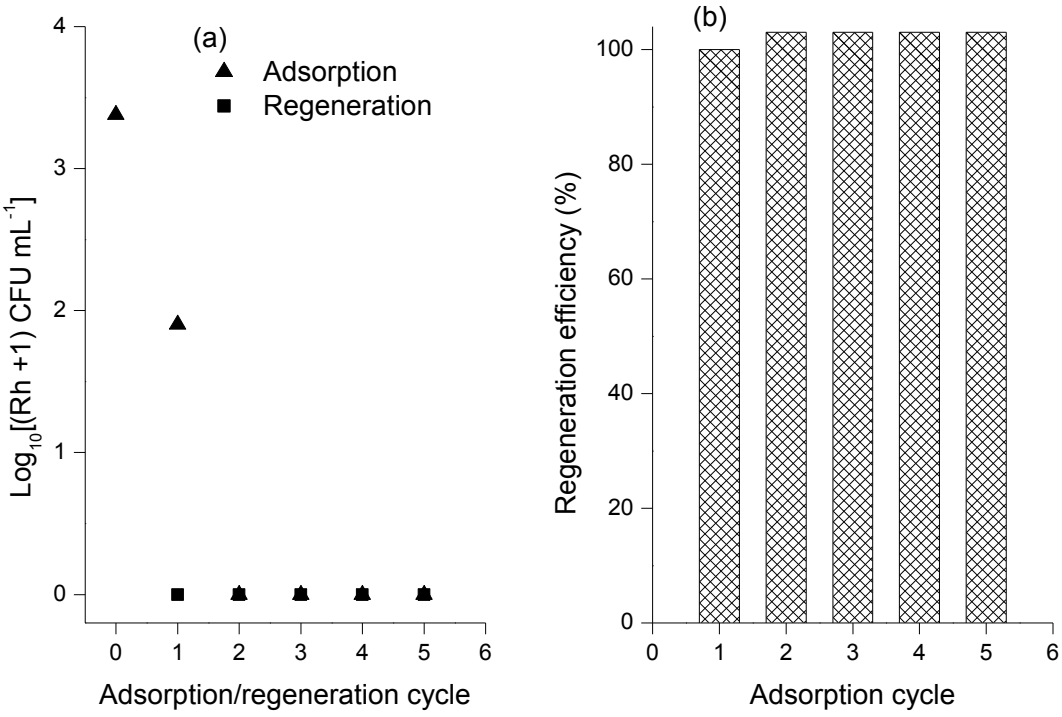

Figure 8.48: *Multiple adsorption and electrochemical regeneration cycles with R. turoloides in water in the mini-SBR, initial concentration: 2400 CFU mL^{-1}, GIC adsorbent dose 60 g in 300 mL, regeneration was carried out at 0.4 A for 20 min (20 mA cm^{-2}). In order to show the zero point on the logarithmic plot 1 CFU mL^{-1} was added to each data point on the vertical axis where Rh denotes the concentration of R. turoloides.*

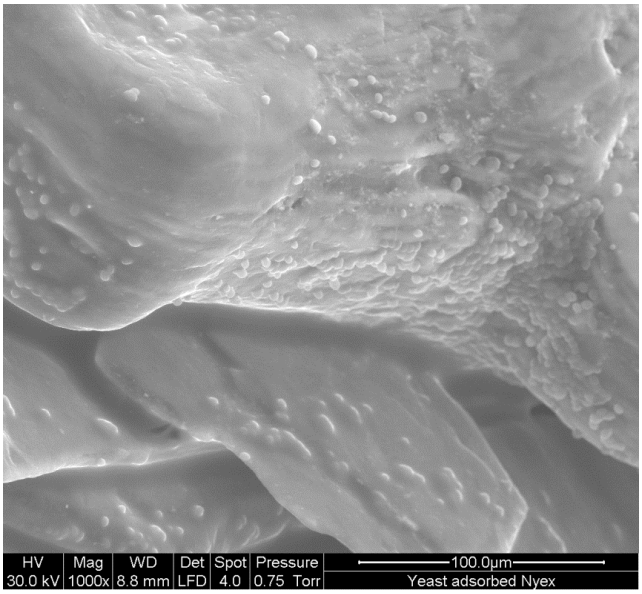

Figure 8.49: *Scanning electron micrograph of the GIC adsorbent with R. turoloides attached to its surface at a magnification of 1000x*

8.4.4 Protozoa

Free living protozoa are ubiquitous in natural water environments, but also proliferate in water treatment distribution systems *(Valster et al. 2009)*. The protozoans, *Cryptosporidium parvum*, *Cyclospora* and *Giardia lamblia* are of great concern because of their significant impact on human health. These protozoan species may cause symptoms including severe diarrhea, stomach cramps, nausea and vomiting lasting for longer periods *(Metcalf and Eddy, 2003)*. Waterborne cryptosporidiosis outbreaks occurred in Milwaukee, USA in 1993 in which 400,000 people were affected *(Metcalf and Eddy, 2003)*. The *Cryptosporidium parvum* and *Giardia lamblia* are the most resistant forms of protozoa and are found in almost all wastewaters *(Metcalf and Eddy, 2003)*. However, the conventional disinfection techniques including chlorination have not proved to be very effective in their inactivation.

Cryptosporidium parvum

In order to investigate whether adsorption with electrochemical regeneration using the GIC adsorbents can be applied to disinfect protozoan organisms effectively, *Cryptosporidium parvum* was selected as a model species. *Cryptosporidium parvum*

was obtained from EasySeed™ in the form of a kit (Z9ES-C100 EasySeed Cryptosporidium 100) which contained 10×10 vials, each containing 10 oocysts (eggs). One advantage of using this kit is that the cells were gamma irradiated. This means that they are already dead and therefore cannot cause disease, but the eggs are intact. Since they are morphologically stable, they will respond in the same way that living eggs would.

Four vials of *C. parvum* were added to 500 mL of deionised water. Prior to this, 2mL of 0.05% Tween (Sigma-Aldrich®) was added into each vial followed by their manual mixing. Afterwards, the water containing oocycts of *C. parvum* was transferred to the mini-SBR in which 100 g of GIC adsorbent was added. A series of adsorption and electrochemical regeneration cycles were carried out, treating the same batch of water on each cycle. In all other respects, the procedure was as described for batch adsorption and electrochemical regeneration in the mini-SBR (see section 8.1.3). Adsorption was carried out for 30 min and electrochemical regeneration was performed at 20 mA cm^{-2} for 20 min. After adsorption, and regeneration water samples with fines of GIC particles were collected. A small drop of a sample was placed on a microscope slide and viewed under a microscope which was connected to a camera and computer. Some of the samples were also stained using DAPI (Life Technologies™) on the microscope slide and viewed under the microscope.

C. parvum oocysts are spherical and of 4–6 μm in diameter with a characteristic shape and dark granules (Figure 8.50).

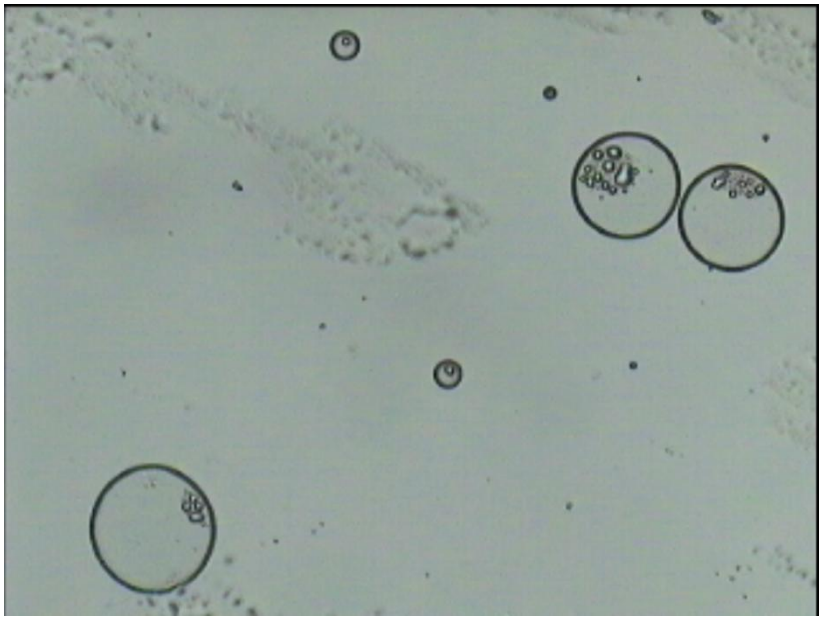

Figure 8.50: *Cryptosporidium parvum in water viewed under microscope at magnification 4.7 (BioMed, Leitz)*

During adsorption, some of the fines of GIC particles were observed to attach to the *C. parvum* cell as shown in figure 8.51. Based on SEM images (not shown), the *C. parvum* was not found to adsorb onto the large GIC flakes. The cells of C. parvum appeared to be covered with a thick cell wall (Figure 8.51). However, during electrochemical regeneration, some of the images taken under microscope indicated the destruction or thinning of the cell membrane as shown in figure 8.52. *C. parvum* is known to be a refractory organism resistant to chlorination and other disinfectants. In the cathode compartment, 0.3% NaCl aqueous solution was used as electrolyte and therefore due to the formation of free chlorine in the anode compartment containing the GIC adsorbent, electrochlorination is one of the most important factors responsible for disinfecting microorganisms in the mini-SBR (see section 8.1.4). As stated above, *C. parvum* are resistant to chlorination and therefore could not be disinfected. These were the preliminary trials that suggest that changing the catholyte to a chloride free solution and applying relatively high current densities may disinfect pathogenic *C. parvum*. In addition, a protocol for determining the number of *C. parvum* cells after adsorption and electrochemical regeneration needs to be developed. In this context, the GIC particles after adsorption and regeneration were stained with DAPI (4′,6-diamidino-2-phenylindole) to clearly visualize the change in morphology of the *C. parvum* during these processes but it was not

successful due to the formation of DAPI needles on the microscope slide as shown in figure 8.53. All of these issues will be the subject of future work.

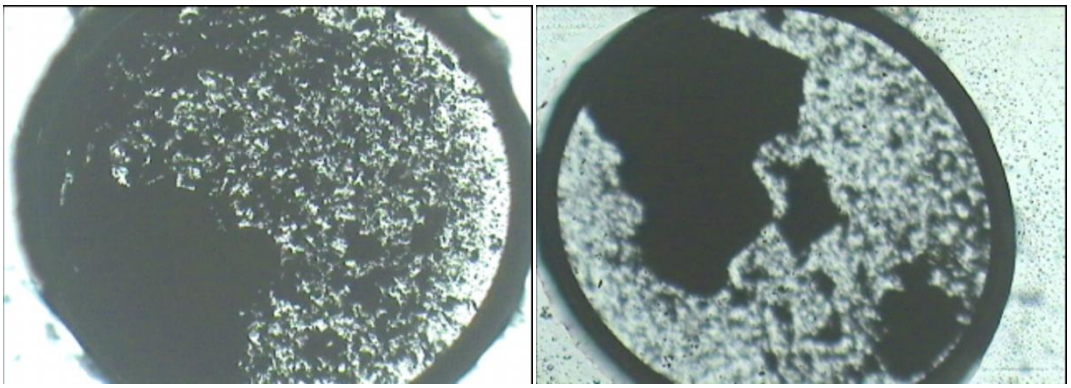

Figure 8.51: *Images showing fines of GIC adsorbent attached to a C. parvum cell when viewed under a microscope*

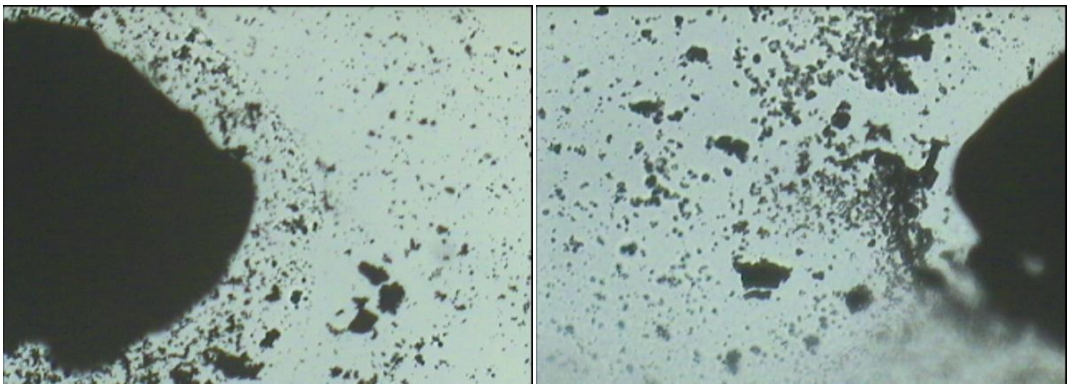

Figure 8.52: *Images taken during electrochemical regeneration of the GIC adsorbent for C. parvum under a microscope showing disintegration of the outer membrane of C. parvum*

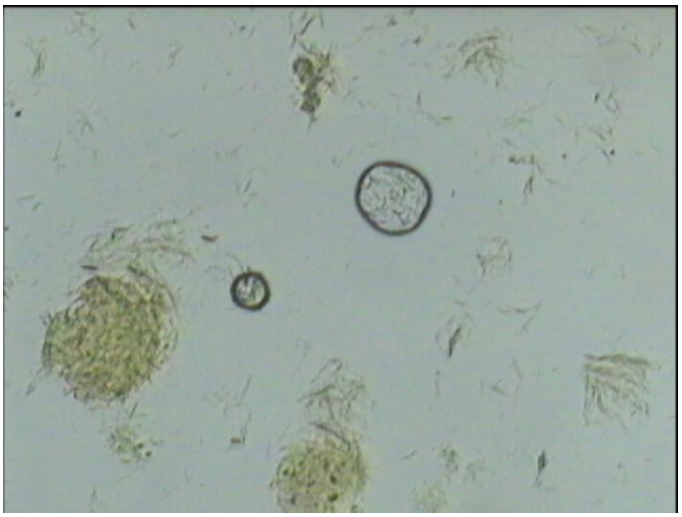

Figure 8.53: *Image of C. parvum in water stained with DAPI showing the presence of needle like contaminations*

8.4.5 Conclusions

The process of adsorption and electrochemical regeneration using the GIC adsorbents was found to be effective in removing a variety of bacteria, fungi and yeasts. The bacteria species studied were *P. aeruginosa*, *S. aureus* and *L. pneumophila*. The suitability of the process was also evaluated for the fungal species *A. awamori*. In addition, the Arvia® process was also found to be effective in disinfecting yeasts including *S. cerevisiae* and *R. turoloides*. Adsorption and electrochemical regeneration for some of these species were also confirmed from SEM images. On the other hand, disinfection of *C. parvum* by adsorption and electrochemical regeneration using the GIC adsorbent was not demonstrated successfully. However, a preliminary investigation regarding *C. parvum* suggests that using a chloride free solution in the cathode compartment and a relatively high current density might be effective.

8.5 Overall conclusions

This study has provided evidence that a process of adsorption and electrochemical regeneration using the GIC adsorbents can be employed for the disinfection of water. In particular it was found that adsorption of microorganisms on the GIC adsorbents is rapid and comparable to organics removal. Electrochemical disinfection is effective and appears to be achieved by a combination of direct electrochemical disinfection, electrochlorination and pH effects. It has also been demonstrated that the process can operate to simultaneously remove organics and to disinfect microorganisms. A variety of bacteria, fungi and yeasts were tested and evaluated by this process. However, the protozoan, *C. parvum* needs further investigation.

Whilst the results have demonstrated the potential of the process for water disinfection, it will be necessary to evaluate the process for continuous operation. Complete disinfection was generally achieved only after electrochemical regeneration, so continuous disinfection may require the treated water to flow through the regeneration zone, rather than a separate adsorption zone (as is the case in the existing Arvia process®). In addition, a number of areas have been highlighted which require further work.

Chapter 9
Conclusions and Recommendations

This chapter presents the key conclusions of the study carried out in this project. The work presented in this thesis is a preliminary investigation about the formation of breakdown products in liquid, gaseous and solid phases during the process of adsorption and electrochemical regeneration, and the application of the process to water disinfection. Therefore this chapter also discusses a number of areas for which further work is recommended.

9.1 Conclusions

9.1.1 Breakdown Products and Mechanism of Electrochemical Regeneration

This research has demonstrated that intermediate oxidation products are formed during the electrochemical regeneration of GIC adsorbents in the batch as well as continuous process of adsorption with electrochemical regeneration. Two mechanisms of organic oxidation which occur during electrochemical regeneration of the GIC adsorbents have been identified. The first is the complete oxidation of the adsorbed species on the surface of the adsorbent and the second involves the indirect electrochemical oxidation of organics in solution.

Investigation of the breakdown products has shown that these are formed largely due to the indirect electrochemical oxidation of organics in solution. The formation of non-chlorinated species was found to be dependant on current density and pH. However, the formation of these species can be minimised by applying higher current densities and treating solutions over several cycles of adsorption and regeneration.

The study of the formation of chlorinated breakdown products has shown that their concentrations depended upon a range of variables including current density, initial concentration, chloride contents and electrolyte type. In this context, the concentrations of chlorinated intermediates can be minimized by using low current

density, low initial concentrations, a chloride free environment and/or by treating the water over a number of adsorption and regeneration cycles.

The formation of free chlorine during batch electrochemical regeneration was investigated under a range of operating conditions including the initial concentration of chloride ions, current density and pH. The rate of formation of free chlorine was found to increase with an increase in chloride concentration and current density. A decrease in the rate of free chlorine formation was observed with an increase in pH. These findings have important implications in optimising the conditions for the formation of chlorinated oxidation products. In addition, the formation of free chlorine is useful for disinfection.

This work has also demonstrated that the continuous treatment of water by adsorption and electrochemical regeneration can be effective for the removal and oxidation of dissolved organic pollutants. The treatment process was able to remove 100% of the phenol from a feed solution containing up to 500 mg L^{-1} of phenol. In addition, 64% TOC removal was possible, which indicated that the process not only removes the contaminant but also destroys it by anodic oxidation. However, complete TOC removal was not obtained due the formation of breakdown products under the conditions studied. It was suggested that lower phenol concentrations and higher current density could be used to improve the percentage TOC removal.

It has also been shown that the GIC adsorbents have the capability of adsorbing a variety of intermediate oxidation products even at low concentrations. It can be anticipated that the development of GIC based adsorbents with increased adsorption capacity could further reduce the formation of breakdown products.

Among the gaseous breakdown products, CO_2 and CO were observed as the main components released in the gas phase. A gas measuring apparatus using a graduated cylinder enabled the measurement of the extremely small volumes of gases evolved during electrochemical regeneration of GIC adsorbents. The amount of evolved gases was found to increase with an increase in current density, as expected. Electrochemical regeneration at constant potential has shown that both the volume and concentration of these gases during regeneration of loaded adsorbent with phenol were higher than the corresponding values of these gases when no phenol was used, suggesting that the gases generated were associated with the oxidation of

adsorbed phenol. A preliminary mass balance has shown that about 60% of the adsorbed phenol was oxidised completely to CO_2. Further work is needed to determine the fate of the remaining phenol.

The fingerprints of the pollutant on the surface of GIC adsorbents during adsorption and electrochemical regeneration were investigated systematically using different surface techniques including FTIR, Raman spectroscopy, EDS and Boehm titration. No important spectral features were obtained with FTIR for GIC adsorbents with a range of techniques including ATR, DRIFTS and IR microscopy. Raman spectroscopy was successful in determining the graphite peaks but no surface groups were detected during adsorption and electrochemical regeneration. These disappointing results could be due to the inherent intractability in the GIC samples due to the nature of the graphite surface, the low concentrations of surface oxides and the low concentrations of adsorbates. Boehm titration was successful in showing that GIC adsorbent samples had phenolic, carboxylic and lactonic functional groups. The titration results also indicated that the concentrations of phenolic groups were higher on phenol loaded samples, confirming the adsorption of phenol on the adsorbent. These groups were also observed to decrease during electrochemical regeneration suggesting the oxidation of phenol at the surface of the adsorbent.

9.1.2 Disinfection of Water by Adsorption with Electrochemical Regeneration

This study has provided evidence that the process of adsorption and electrochemical regeneration using GIC adsorbents can be used for disinfection of water. It has also been demonstrated that the GIC adsorbents have the potential to adsorb a large number of microorganisms present in water with fast adsorption kinetics comparable to dissolved organics removal. Disinfection of water was found to be a combination of two processes: the adsorption of microorganisms followed by their deactivation on the surface; and electrochemical disinfection in solution due to indirect oxidation. The possible disinfection mechanisms involved in these processes include electrochlorination, pH changes and deactivation by direct oxidation of microorganisms. The process of disinfection was also found to be effective even when there was no source of chloride ions, suggesting that disinfection can take place without electrochlorination. Current density and regeneration time were found

to have a direct effect on the electrochemical regeneration of the GIC adsorbent loaded with microorganisms.

Scanning electron microscopy was found to be a useful tool for investigating changes in surface morphology of microorganisms during adsorption and electrochemical regeneration. With this technique, *E. coli* biofilms were observed on the adsorbent surface with the release of an extracellular material. Though the biofilms of bacteria grown on the solid surfaces were resistant to chlorination, the process of adsorption and electrochemical regeneration had the potential to deactivate these biofilms.

A variety of bacteria, fungi and yeasts were tested and evaluated by this process. However, disinfection of protozoa including *C. parvum* was not successfully demonstrated. A preliminary investigation suggested that using a chloride free solution in the cathode compartment and a relatively high current density might be effective. It has also been demonstrated that the process of adsorption with electrochemical regeneration using the GIC adsorbents can be used to simultaneously remove organics and to disinfect microorganisms.

9.2 Recommendations for Further Research

Whilst the conclusions from the work presented in this chapter are promising, there are a number of areas for which further research is recommended.

9.2.1 Investigation of the Formation of Polymeric Materials during Electrochemical Regeneration Using Phenol as Model Pollutant

As discussed in chapter 4, the process of treating water using GIC adsorbents with electrochemical regeneration involves low organic concentrations, low current densities, ambient temperature and slightly acidic conditions. Thus, it is most likely that under these conditions phenol was not converted into polymeric products. On the other hand, polymeric materials may have been produced and these could accumulate within the adsorbent bed. The deposition of polymeric films on the GIC surfaces may interfere in the supply of fresh pollutant from bulk solution during adsorption and in the removal of oxidation products during electrochemical

regeneration thus affecting the oxidation of adsorbed species. The GIC particles have a high surface area compared to the flat anode plate, and the coating coverage may be so small that a large number of regeneration cycles would be required to observe the formation of polymers on the GIC adsorbent. Therefore, further work should be carried out using techniques including gel permeation chromatography (GPC), X-ray photoelectron spectroscopy (XPS) and electrochemical quartz crystal microbalance (EQCM) to detect and analyse any polymeric material formed during electrochemical regeneration using phenol as a model pollutant.

EQCM is a useful technique that can be applied to monitor electrochemically induced mass changes at electrode surfaces during electrochemical processes *(Ferreira et al. 2006).* EQCM has been also used to investigate the processes accompanying electrooxidation of phenolic compounds *(Ferreira et al. 2006). Gattrel and Kirk, (1993a)* used GPC and XPS to evaluate the electrode passivation during phenol electrolysis at a platinum electrode. With GPC, the main polymeric products (with weight averaged molecular weights) formed during phenol oxidation can be determined. XPS could be used to evaluate the oxidation of these polymeric films. The XPS spectra of the polymeric films formed on platinum electrode showed that these films are reasonably homogenous in terms of their degree of oxidation. However, the spectra also showed significant amounts of hydroxyl groups as opposed to quinone functionalities, which indicates that the upper most regions of the film (56 to 84 $^{\circ}$A) can undergo further oxidation. Any unreactive material was confined to the innermost film (18 to 46 $^{\circ}$A). Thus, XPS analysis showed that the oxidation of these passivating polymeric films was incomplete, with many hydroxyl groups present *(Gattrel and Kirk, 1993a).*

In addition, other phenolic compounds including hydroquinone, alkylphenol, chlorophenol and amino phenol may be tested using the process of adsorption with electrochemical regeneration to evaluate the formation of polymeric materials either in solution or on the surface of GIC adsorbents.

9.2.2 Investigation of Mechanism of Electrochemical Regeneration Using High Capacity GIC Adsorbents

While extensive work has been undertaken in determining the breakdown products from the electrochemical regeneration of GIC adsorbents using phenol as a model

pollutant, a full understanding of the regeneration mechanism still needs further work. As mentioned in chapter 4, it is impossible to remove all the organics from the solution due to equilibrium between the concentration of organic in solution and on the surface of adsorbent. However, high capacity adsorbents may be suitable for achieving low discharge concentrations. In this context, GIC adsorbents with high adsorption capacity should be used to investigate the breakdown products, and the mechanism of electrochemical regeneration.

In addition, a number of other priority pollutants should be used to determine the breakdown products. This would be valuable in confirming the findings of the work carried out in this project and providing more information about the breakdown products. Special consideration would be given to the conditions that minimize the formation of toxic intermediates.

9.2.3 Surface Characterization of GIC Adsorbents during Adsorption and Electrochemical regeneration

Both FTIR and Raman spectroscopy were unable to provide useful data on the surface chemistry of GIC adsorbents during adsorption and electrochemical regeneration as discussed in chapter 6. Other techniques including photoacoustic spectroscopy (PAS) and temperature programmed desorption (TPD) should be used in order to further explore GIC samples after adsorption and electrochemical regeneration.

Photoacoustic spectroscopy (PAS) is an extension of IR spectroscopy and is a non-invasive reflectance technique with penetration depths in the range from micrometers down to several molecular monolayers *(Stuart, 2005)*. It is suitable for examining highly absorbing samples that are difficult to analyze by conventional IR techniques *(Settle, 1997; Stuart, 2005)*. PAS spectra can be obtained with minimal sample preparation and without physical alteration from a wide variety of samples including powders, polymer pellets, viscous glues, single crystals, and single fibers *(Settle, 1997)*. Typically, the modulated IR radiation is focused on a sample placed in a small cup located in an acoustically isolated chamber filled with an IR transparent gas such as helium or nitrogen. The sample absorbs photons of the IR radiation, which have the energy corresponding to the vibrational states of the molecules. The absorbed energy is released in the form of heat generated by the sample. This causes

temperature fluctuations and, subsequently, periodic acoustic waves. A sensitive microphone detects the resulting photoacoustic signal and then they are converted to an electrical signal. Fourier transformation of the resulting signal generates a characteristic IR spectrum *(Settle, 1997; Stuart, 2005).*

In temperature programmed desorption (TPD), the samples are heated in a vacuum or in a helium stream at a constant heating rate and the evolved gases (CO_2, CO, H_2O, H_2) are determined using a quadrupole mass spectrometer *(Boehm, 2002).* Surface oxygen groups decompose upon heating and consequently, CO_2 and CO are released depending upon the nature of the surface groups *(Figueiredo et al. 1999).* Generally, a CO_2 peak results from carboxylic groups at low temperatures, or lactones at high temperatures. Phenols, ethers, carbonyls and quinones generate a CO peak *(Figueiredo et al. 1999).* A number of different functional groups including carboxylic, lactonic, phenols, carbonyls, anhydride, ethers and quinone with their corresponding TPD characteristics can be found in the literature (see for example, *Figueiredo et al. 1999; Boehm, 2002*). With TPD, the adsorption of phenol on the GIC adsorbent could be monitored. In this context, the uptake and surface coverage may be determined. TPD can give the data on the strength of the adsorption bonding, the amount adsorbed and can identify the type of intermediates present on the surface of GIC adsorbents. In addition, high capacity GIC adsorbents should also be used to investigate the surface changes during adsorption and electrochemical regeneration.

9.2.4 Further Investigation of the CO_2 Produced From the Oxidation of Adsorbed Organics

As discussed in Chapter 5, it is difficult to detect and measure the amount of CO_2 produced from the oxidation of the adsorbed phenol. However, regeneration studies at constant potential have suggested that around 60% of the adsorbed phenol was oxidised completely to CO_2. This value is less than expected based on the regeneration efficiency of phenol loaded GIC adsorbent. However, phenol may also get oxidised to CO (see chapter 5) and other breakdown products including polymer (see chapter 4). Accurate determination of the amount of CO_2 and CO produced from the oxidation of adsorbed phenol is important to determine the fate of the contaminant. This information could be used to determine the extent to which

adsorbed organics are oxidised completely into CO_2 under a range of operating conditions. In addition, more useful data can be obtained by performing a mass balance study of the adsorbed organics. In this context, the amount of CO_2 and CO produced could be evaluated precisely using an isotope labelling technique.

Isotope labelling is a technique that can be used to trace the passage of a substance through a system *(Bahn et al. 2009)*. The substance is labelled with isotopes in its chemical composition. If these isotopes are detected in a certain part of the system, they must have been originated from the labelled substance. The idea is to label phenol before its adsorption onto the GIC adsorbent. During electrochemical regeneration, the identification of CO_2 with the isotope which was originally attached to phenol would indicate that this CO_2 was being produced due to the oxidation of the adsorbed phenol. The most obvious choice is a labelled carbon i.e 13C or 14C labelled phenol. Mass spectrometry (MS) and nuclear magnetic resonance (NMR) are used to detect isotopic differences. In addition, depending upon the nature of the isotope any other type of pollutant can be tested using the same idea. The actual methodology and the selection of a specific type of isotope will be the subject of future work.

9.2.5 Continuous Adsorption and Electrochemical Regeneration for Water Disinfection

As discussed in Chapter 8, the present work has investigated the application of adsorption and electrochemical regeneration using GIC adsorbents to disinfect a variety of microorganisms present in water. Further work would be useful to investigate the potential of the process to disinfect water in a continuous mode. This will be beneficial for large scale commercial applications of adsorption and electrochemical regeneration for water disinfection, such as the treatment of water at swimming pools. However, for complete disinfection the continuous process may require the treated water to flow through the regeneration zone rather than the adsorption zone as is the case in the existing continuous Avia® process *(Mohammad et al. 2011)*. Thus, the existing continuous operation may need to be modified for the complete disinfection of water.

9.2.6 Removal of Viruses from Water by Adsorption with Electrochemical Regeneration

Disinfection of a variety of bacteria, fungi and yeasts were evaluated successfully by adsorption with electrochemical regeneration using GIC adosrbents (See chapter 8). Viruses have been found to be more resistant to electrochemical inactivation than bacteria *(Drees et al. 2003)*. In addition, viruses are also often more resistant to chemical disinfectants including chlorine and ozone. Future work should be carried out to investigate the inactivation of viruses by adsorption and electrochemical regeneration using a model microorganism such as bacteriophage MS2 *(Drees et al. 2003)*.

REFERENCES

Abarca, M.L., Accensi, F., Cano, J., and Cabanes, F.J., (2004). Taxonomy and significance of black aspergilli. *International Journal of General and Molecular Microbiology*, 86, pp. 33–49.

Abdel-Aal, H.K., Sultan, S.M., and Hussein, I.A., (1993). Parametric study for saline water electrolysis part II: chlorine evolution, selectivity and determination. *Int. J. Hydrogen Energy*, 18 (7), pp. 545–551.

Adhoum, N., Monser, L., Bellakhal, N., and Belgaied, J., (2004). Treatment of electroplating wastewater containing Cu^{2+}, Zn^{2+} and Cr(VI) by electrocoagulation. *Journal of Hazardous Materials B112*, pp. 207–213.

Ahmaruzzaman, M., and Sharma, D.K., (2005). Adsorption of phenols from wastewater. *Journal of Colloid and Interface Science*, 287, pp. 14–24.

Aksu, Z., and Yener, J., (2001). A comparative adsorption/biosorption study of mono-chlorinated phenols on to various sorbents. *Waste Management*, 21, pp. 695–702.

Al-Degs, Y.S., El-Barghouthi, M.I., El-Sheikh, A.H., and Walker, G.M., (2008). Effect of solution pH, ionic strength, and temperature on adsorption behavior of reactive dyes on activated carbon. *Dyes and Pigments*, 77, pp. 16–23.

Ali, I., and Gupta, V.K., (2006). Advances in water treatment by adsorption technology. *Nature Protocols*, 1 (6), pp. 2661–2667.

Allen, S.J., and Koumanova, B., (2005). Decolourisation of water/wastewater using adsorption. *Journal of the University of Chemical Technology and Metallurgy*, 40 (3), pp. 175–192.

Allen, S.J., Gan, Q., Matthews, R., and Johnson, P.A., (2003). Comparison of optimised isotherm models for basic dye adsorption by kudzu. *Bioresource Technology*, 88, pp. 143–152.

Anderson, A.C., Reimers, R.S., and Dekernion, P., (1982). A brief review of the current status of alternatives to chlorine disinfection of water. *American Journal of Public Health*, 72, pp. 1290–1293.

Andreozzi, R., Caprio, V., Insola, A., and Marotta, R., (1999). Advanced oxidation processes for water purification and recovery. *Catalysis Today*, 53, 51–59.

Anglada, A., Ibanez, R., Urtiaga, A., and Ortiz, I., (2010). Electrochemical oxidation of saline industrial wastewaters using boron–doped diamond anodes. *Catalysis Today*, 151 (1–2), pp. 178–184.

Anglada, A., Urtiaga, A., and Ortiz, I., (2009). Contributions of electrochemical oxidation to waste-water treatment: fundamentals and review of applications. *J Chem Technol Biotechnol,* 84, pp. 1747–1755.

Anpilov, A.M., Barkhudarov, E.M., Christofi, N., Kopev, V.A., Kossyi, I.A., Taktakishvili, M.I., and Zadiraka, Y., (2002). Pulsed high voltage electric discharge disinfection of microbially contaminated liquids. *Letters in Applied Microbiology*, 35, pp. 90–94.

Arafat, H.A., Franz, M., and Pinto, N.G., (1999). Effect of salt on the mechanism of adsorption of aromatics on activated carbon. *Langmuir*, 15, pp. 5997–6003.

Arcand-Hoy, L.D., Nimrod, A.C., Benson, W.H., (1998). Endocrine-modulating substances in the environment: estrogenic effects of pharmaceutical products. *Int J Toxicoll*, 17, pp. 139–158.

Awad, Y.M., and Abuzaid, N.S., (1999). Electrochemical oxidation of phenol using graphite anodes. *Separation Science and Technology*, 34(4), pp. 699–708.

Bahn, M., Schmitt, M., Siegwolf, R., Richter, A., and Brüggemann, N., (2009). Does photosynthesis affect grassland soil-respired CO_2 and its carbon isotope composition on a diurnal timescale. *New Phytologist*, 182, pp. 451–460.

Balaji, S., Chung, S.J., Thiruvenkatachari, R., and Moon, S., (2007). Mediated electrochemical oxidation process: electro-oxidation of cerium (III) to cerium (IV) in nitric acid medium and study on phenol oxidation by cerium (IV) oxidant. *Chemical Engineering Journal*, 126, pp. 51−57.

Bande, R.M., Prasad, B., Mishra, I.M., and Wasewar, K.L., (2008). Oil field effluent water treatment for safe disposal by electroflotation. *Chemical Engineering Journal*, 137, pp. 503–509.

Bandoscz, T.J., (2006). *Activated carbon surfaces in environmental remediation*. UK: Elsevier.

Bandosz, T.J., and Ania, C.O., (2006). Surface chemistry of activated carbons and its characterization. *Interface Science and Technology*, 7, pp. 159–229.

Bansal, R.C., and Goyal, M., (2005). *Activated carbon adsorption*. Taylor and Francis group.

Bejankiwar, R.S., (2002). Electrochemical treatment of cigarette industry wastewater: feasibility study. *Water Research*, 36, pp. 4386–4390.

Berenguer, R., Marco-Lozar, J.P., Quijada, C., Cazorla-Amoro, D., and Morallon, E., (2009). Effect of electrochemical treatments on the surface chemistry of activated carbon. *Carbon*, 47, pp. 1018–1027.

Berenguer, R., Marco-Lozar, J.P., Quijada, C., Cazorla-Amoros, D., and Morallon, E., (2010). Comparison among chemical, thermal, and electrochemical regeneration of phenol-saturated activated carbon. *Energy Fuels,* 24, pp. 3366–3372.

Bergmann, H., Iourtchouk, T., Schöps, K., and Bouzek, K., (2002). New UV irradiation and direct electrolysis—promising methods for water disinfection. *Chemical Engineering Journal*, 85, pp. 111–117.

Berman, D., Rice, E.W., and Hoff, J.C., (1988). Inactivation of particle-associated coliforms by chlorine and monochloramine. *Appl. Environ. Microbiol*, 54, pp. 507–512.

Bertin, J., Kagan, H.B., Luche, J.L and Setton, R., (1974). Graphite electrolytic lamellar reagents in organic chemistry: esterifications in the presence of graphite bisulfate. *J. Am. Chem. Soc*, 96 (26), pp. 8113–8115.

Besenhard, J.O., and Fritz, H.P., (1983). The electrochemistry of black carbons. *Angew. Chem. Int. Ed. Engl*, 22, pp. 950–975.

Bhatnagar, A., and Jain, A.K., (2005). A comparative adsorption study with different industrial wastes as adsorbents for the removal of cationic dyes from water. *Journal of Colloid and Interface Science*, 281, pp. 49–55.

Biniak, S., Szymanski, G., Siedlewski, J., and Swiatkowski, A., (1997). The characterization of activated carbons with oxygen and nitrogen surface groups. *Carbon*, 35 (12), pp. 1799–1810.

Biswas, N., and Lazarescu, G., (1991). Removal of oil from emulsions using electrocoagulation. *Intern. J. Environmental Studies*, 38, pp. 65–75

Block, S.S., (2001). *Disinfection, sterilization and preservation*. 5th edition. USA: Lippincott Williams and Wilkins.

Boehm, H.P., (1994). Some aspects of the surface chemistry of carbon blacks and other carbons. *Carbon*, 32 (5), pp. 759–769.

Boehm, H.P., (2002). Surface oxides on carbon and their analysis: a critical assessment. *Carbon*, 40, pp. 145–149.

Boehm, H.P., Setton, R., and Stumpp, E., (1994). Nomenclature and terminology of graphite intercalation compounds. *Pure and Appl. Chem*, 66 (9), pp. 1893–1901.

Bolger, P.T., and Szlag, D.C., (2002). Reuse of nickel plating rinse waters, *Environmental Progress*, 21(3), pp. 203–208.

Bolyard, M., and Fair, P.S., (1992). Occurrence of chlorate in hypochlorite solutions used for drinking water disinfection. *Environ. Sci. Technol*, 26, pp. 1663–1665.

Bonfatti, F., Ferro, S., Lavezzo, F., Malacarne, M., Lodi, G., and Battisti, A.D., (2000). Electrochemical incineration of glucose as a model organic substrate ii. Role of active chlorine mediation. *Journal of The Electrochemical Society*, 147 (2), pp. 592–596.

Bonnett, R., Krysteva, M., Lalov, I.G., Artarsky, S.V., (2006). Water disinfection using photosensitizers immobilized on chitosan. *Water Research*, 40, pp. 1269–1275.

Boorman, G.A., Dellarco, V., Dunnick, J.K., Chapin, R.E., Hunter, S., Hauchman, F., Gardner, H., Cox, M., and Sills, R.C., (1999). Drinking water disinfection by-producs: review and approach to toxicity evaluation. *Environmental Health Perspectives*, 107 (1), pp. 207–217.

Boudenne, J.L., Cerclier, O., and Bianco, P., (1998). Voltammetric studies of the behavior of carbon black during phenol oxidation on Ti/Pt electrodes. *J. Electrochem. Soc*, 145 (8), pp. 2763–2767.

Boudenne, J.L., Cerclier, O., Galea, J., and Vlist, E.V.D., (1996). Electrochemical oxidation of aqueous phenol at a carbon black slurry electrode. *Applied Catalysis A: General*, 143, pp. 185–201.

Bradder, P., Ling, S.K., Wang, S., and Liu, S., (2011). Dye adsorption on layered graphite oxide. *J. Chem. Eng. Data*, 56, pp. 138–141.

Bratby, J., (2006). *Coagulation and flocculation in water and wastewater treatment*. 2nd edition. London: IWA Publishing.

Bringmann, J., Ebert, K., Galla, U., and Schmieder, H., (1995). Electrochemical mediators for total oxidation of chlorinated hydrocarbons: formation kinetics of Ag(II), Co(III) and Ce(IV). *Journal of Applied Electrochemistry*, 25, pp. 846–851.

Brown, N.W., (2005). Adsorption and electrochemical regeneration for wastewater treatment−development of a process, PhD thesis, University of Manchester.

Brown, N.W., (2009). A clear winner: Arvia Technology's novel electrochemical route to decontaminate wastewater recently won the Institution of Chemical Engineers Water Award. *Chemistry and Industry*, January 26.

Brown, N.W., and Roberts, E.P.L., (2007). Electrochemical pre-treatment of effluents containing chlorinated compounds using an adsorbent. *Journal of Applied Electrochemistry*, 37 (11), pp. 1329–1335.

Brown, N.W., Roberts, E.P.L., Chasiotis, A., Cherdron, T., and Sanghrajka, N., (2004b). Atrazine removal using adsorption and electrochemical regeneration. *Water Research*, 38 (13), pp. 3067–3074.

Brown, N.W., Roberts, E.P.L., Garforth, A.A., and Dryfe, R.A.W., (2004a). Electrochemical regeneration of a carbon-based adsorbent loaded with crystal violet dye. *Electrochimica Acta*, 49 (20), pp. 3269–3281.

Burgi, T., (2006). Attenuated total reflection infrared spectroscopy of solid catalysts functioning in the presence of liquid-phase reactants. *Adv. Catal*, 50, pp. 227–283.

Butterfield, I.M., Christensen, P.A., Curtis, T.P., and Gunlazuardi, J., (1997). Water disinfection using an immobilised titanium dioxide film in a photochemical reactor with electric field enhancement. *Water Research*, 31 (3), pp. 675–677.

Calvet, R., (1989). Adsorption of organic chemicals in soils. *Environmental Health Perspectives*, 83, pp. 145–177.

Camel, V., and Bermond, A., (1998). The use of ozone and associated oxidation processes in drinking water treatment. *Water Research*, 32 (11), pp. 3208–3222.

Campbell, A.T., Robertson, L.J., Snowball, M.R., Smith, H.V., (1995). Inactivation of oocysts of cryptosporidium parvum by ultraviolet irradiation. *Water Research*, 29 (11), pp. 2583–2586.

Canizares, P., Diaz, M., Dominguez, J. A., Garcia-Gomez, J., and Rodrigo, M. A., (2002). Electro-chemical oxidation of aqueous phenol wastes on synthetic diamond thin-film electrodes. *Ind. Eng. Chem. Res*, 41, pp. 4187–4194.

Canizares, P., Dominguez, J.A., Rodrigo, M.A., Villasenor, J., and Rodriguez, J., (1999). Effect of the current intensity in the electrochemical oxidation of aqueous phenol wastes at an activated carbon and steel anode. *Ind. Eng. Chem. Res*, 38, pp. 3779–3785.

Canizares, P., Gomez, J.G., Saez, C., and Rodrigo, M.A., (2003). Electrochemical oxidation of several chlorophenols on diamond electrodes: Part I. Reaction mechanism. *Journal of Applied Electrochemistry*, 33, pp. 917–927.

Canizares, P., Lobato, J., Gomez, J.G., and Rodrigo, M.A., (2004). Combined adsorption and electrochemical processes for the treatment of acidic aqueous phenol wastes. *Journal of Applied Electrochemistry,* 34, pp. 111–117.

Canizares, P., Martinez, F., Jimenez, C., Lobato, J., and Rodrigo, M.A., (2006). Coagulation and electrocoagulation of wastes polluted with dyes. *Environ. Sci. Technol*, 40, pp. 6418–6424.

Canizares, P., Paz, R., Saez, C., and Rodrigo, M.A., (2007). Electrochemical oxidation of wastewaters polluted with aromatics and heterocyclic compounds. *Journal of the Electrochemical Society*, 154 (11), pp. E165–171.

Canizares, P., Paz, R., Saez, C., and Rodrigo, M.A., (2008). Electrochemical oxidation of alcohols and carboxylic acids with diamond anodes: a comparison with other advanced oxidation processes. *Electrochimica Acta*, 53, pp. 2144–2153.

Chang, S.L., (1958). The use of active iodine as a water disinfectant. *Journal of the American Pharmaceutical Association*, 47 (6), pp. 417–423.

Charlier, A., Charlier, M.F., and Fristot, D., (1989). Binary Graphite Intercalation Compounds. *J. Phys. Chem. Solids*, 50 (10), pp. 987–996.

Chatzisymeon, E., Xekoukoulotakis, N.P., Coz, A., Kalogerakis, N., Mantzavinos, D., (2006). Electrochemical treatment of textile dyes and dyehouse effluents. *Journal of Hazardous Materials*, B137, pp. 998–1007.

Chatzisymeon, E., Fierro, S., Karafyllis, I., Mantzavinos, D., Kalogerakis and Katsousis, A., (2010). Anodic oxidation of phenol on Ti/IrO_2 electrode: experimental studies. *Catalysis Today*, 151, pp. 185–189.

Chen, G., (2004). Electrochemical technologies in wastewater treatment. *Separation and Purification Technology*, 38, pp. 11–41.

Chen, J.L., Chiou, G.C., and Wu, C.C., (2010). Electrochemical oxidation of 4–chlorophenol with granular graphite electrodes. *Desalination*, 264, pp. 92–96.

Chen, J-J., and Yeh, H-H., (2005). The mechanisms of potassium permanganate on algae removal. *Water Research*, 39, pp. 4420–4428.

Cheremisinoff, N.P., (2002). *Handbook of water and wastewater treatment technologies*. Butterworth-Heinemann

Cho, M., Chung, H., and Yoon, J., (2003). Disinfection of water containing natural organic matter by using ozone-initiated radical reactions. *Applied and Environmental Microbiology*, pp. 2284–2291.

Chung, D.D.L., (1987). Review: exfoliation of graphite. *Journal of Materials Science*, 22 (12), pp. 4190–4198.

Chung, D.D.L., (2000). Flexible graphite for gasketing, adsorption, electromagnetic interference shielding, vibration damping, electrochemical applications, and stress sensing. *Journal of Materials Engineering and Performance*, 9 (2), pp. 161–163.

Chung, D.D.L., (2002). Review Graphite. *Journal of Materials Science*, 37, pp.1475–1489.

Clesceri, L.S., Greenberg, A.E., and Eaton, A.D., (1998). *Standard methods for the examination of water and wastewater*. 20th edition. American Public Health Association.

Comninellis, C., (1994). Electrocatalysis in the electrochemical conversion/combustion of organic pollutants for wastewater treatment. *Electrochimica Acta*, 39 (11), pp. 1857–1862.

Comninellis, C., and Chen, G., (2010). *Electrochemistry for the environment*. London: Springer New York Dordrecht Heidelberg

Comninellis, C., and Nerini, A., (1995). Anodic oxidation of phenol in the presence of NaCl for wastewater treatment. *Journal of Applied Electrochemistry*, 25, pp. 23–28.

Comninellis, C., and Pulgarin, C., (1991). Anodic oxidation of phenol for wastewater treatment. *Journal of Applied Electrochemistry*, 21, pp. 703–708.

Comninellis, C., and Pulgarin, C., (1993). Electrochemical oxidation of phenol for wastewater treatment using SnO_2 anodes. *Journal of Applied Electrochemistry* , 23, pp. 108–112.

Cong, Y., Wu, Z., and Li, Y., (2008). Electrochemical inactivation of coliforms by in-situ generated hydroxyl radicals. *Korean J. Chem. Eng*, 25(4), pp.727–731.

Cooper, I.R., and Hanlon, G.W., (2010). Resistance of Legionella pneumophila serotype1biofilms to chlorine-based disinfection. *Journal of Hospital Infection*, 74, pp. 152–159.

Costa, C.R., Montilla, F., Morallon, E., and Olivi, P., (2010). Electrochemical oxidation of synthetic tannery wastewater in chloride–free aqueous media. *Journal of Hazardous Materials*, 180, pp. 429–435.

Costa, R.C., Botta, C.M.R., Espindola, E.L.G., and Olivi, P., (2008). Electrochemical treatment of tannery wastewater using DSA® electrodes. *Journal of Hazardous Materials*, 153, pp. 616–627.

Coughlin, R.W., and Ezra, F.S., (1968). Role of surface acidity in the adsorption of organic pollutants on the surface of carbon. *Environmental Science and Technology*, 2 (4), pp. 291–297.

Couillard, D., (1994). The use of peat in wastewater treatment. *Water Research*, 28(6), pp. 1261–1274.

Crittenden, J.C., Trussell, R.R., Hand, D.W., Howe, K.J., and Tchobanoglous, G., (2005). *Water treatment: principles and design*. 2nd edition. John Wiley and Sons, Inc.

Dabrowski, A., (1999). *Adsorption and its applications in industry and environmental protection*. Netherlands: Elsevier Science B.V.

Dabrowski, A., (2001). Adsorption: from theory to practice. *Advances in Colloid and Interface Science*, 93, pp. 135–224.

Dabrowski, A., Podkoscielny, P., Hubicki, Z., and Barczak, M., (2005). Adsorption of phenolic compounds by activated carbon: a critical review. *Chemosphere*, 58, pp. 1049–1070.

Dabrowski, A., Podkoscielny, P., Hubicki, Z., and Barczak, M., (2005). Adsorption of phenolic compounds by activated carbon—a critical review. *Chemosphere*, 58, pp. 1049–1070.

Dai, Q., Zhoh, M., and Lei, L., (2006). Wet electrolytic oxidation of cationic red X-GRL. *Journal of Hazardous Materials*, B137, pp. 1840–1874.

Daifullah, A.A.M., Girgis, B.S., and Gad, H.M.H., (2004). A study of the factors affecting the removal of humic acid by activated carbon prepared from biomass material. *Colloids and Surfaces A: Physicochem. Eng. Aspects*, 235, pp. 1–10.

Davidson, L., Quinn, Y., and Steele, D.E., (1998). Ruthenium-mediated electrochemical destruction of organic wastes. *Platinum Metals Rev*, 42 (3), pp. 90–98.

Deborde, M., and Gunten, U.V., (2008). Reactions of chlorine with inorganic and organic compounds during water treatment—Kinetics and mechanisms: a critical review. *Water Research*, 42, pp. 13–51.

Dedov, A.V., (2001). Sorption properties of thermally expanded graphite. *Chemistry and Technology of Fuels and Oils*, 37 (2), pp. 134–135.

Delaedt, Y., Daneels, A., Declerck, P., Behets, J., Ryckeboer, J., Peters, E., and Ollevier, F., (2008). The impact of electrochemical disinfection on Escherichia coli and Legionella pneumophila in tap water. *Microbiological Research*, 163, pp. 192–199.

Deng, Y., and Englehardt, J.D., (2007). Electrochemical oxidation for landfill leachate treatment. *Waste Management*, 27, pp. 380–388.

Diao, H.F., Li, X.Y., Gu, J.D., Shi, H.C., Xie, Z.M., (2004). Electron microscopic investigation of the bactericidal action of electrochemical disinfection in comparison with chlorination, ozonation and Fenton reaction. *Process Biochemistry*, 39, pp. 1421–1426.

Do, J.S., and Chen, M.L., (1994). Decolourization of dye-containing solutions by electrocoagulation. *Journal of Applied Electrochemistry*, 24, pp. 785–790.

Doelle, H.W., (1994). *Microbial process development*. World Scientific Co, Singapore.

Doniat, D., Corajoud, J.M., Mosetti, J., and Porta, A., (1980). Process for regenerating contaminated activated carbon. US Patent No. 4,217,191.

Donlan, R.M., (2002). Biofilms: microbial life on surfaces. *Emerging Infectious Diseases*, 8(9), pp. 881–890.

Doppalapudi R.B; Sorial, G.A., Asce M., and Maloney, S.W., (2003). Electrochemical reduction of 2,4-dinitrotoluene in a continuous flow laboratory scale reactor. *Journal of Environmental Engineering*, pp. 192–201.

Drees, K.P., Abbaszadegan, M., and Maier, R.M., (2003). Comparative electrochemical inactivation of bacteria and bacteriophage. *Water Research*, 37, pp. 2291–2300.

Dresselhaus, M.S., and Dresselhaus, G., (1981). Intercalation compounds of graphite. *Advances in Physics*, 30 (2), pp. 139–326.

Drift, C.V.D., Seggelen, E.V., Stumm, C., Hol, W., and Tuinte, J., (1977). Removal of Escherichia coli in wastewater by activated sludge. *Applied and Environmental Microbiology*, pp. 315–319.

Drogui, P., Elmaleh, S., Rumeau, M., Bernard, C., and Rambaud, A., (2001). Hydrogen peroxide production by water electrolysis: application to disinfection. *Journal of Applied Electrochemistry*, 31, pp. 877–822.

Ebert, L.B., (1976). Intercalation compounds of graphite. *Annu. Rev. Mater. Sci*, 6, pp. 181–211.

Eccleston, K.T., Brown, N.W., Roberts, E.P.L., and Richards, J.L., (2009). Adsorbents for treating contaminated liquids. US Patent 2009/0321361 A1.

Eccleston, K.T., Eccleston, A.J., Richards, J.L., Brown, N.W., and Roberts, E.P.L., (2010). Apparatus for the electrochemical regeneration of adsorbents. US Patent 7790024 B2.

Edeskuty, F.J., and Stewart, W.F., (1996). *Safety in the handling of cryogenic fluids*. New York: Premium Press.

Emeleus, H.J., and Sharpe, A.G., (1959). *Advances in inorganic chemistry and radiochemistry*. London: Academic Press Inc.

Ergun, E., Tor, A., Cengeloglu, Y., and Kocak, I., (2008). Electrolytic removal of fluoride from water: effects of process parameters and accompanying anions. *Separation and Purification Technology*, 64, pp. 147–153.

Fanning, P.E., and Vanice, M.A., (1993). A DRIFTS study of the formation of surface groups on carbon by oxidation. *Carbon*, 31 (5), pp. 721–730.

Ferrari, A.C., (2007). Raman spectroscopy of graphene and graphite: disorder, electron–phonon coupling, doping and nonadiabatic effects. *Solid State Communications*, 143, pp. 47–57.

Ferraro, J.R., and Nakamoto., (2003). *Introductory Raman spectroscopy*. 2nd edition: California. Academic press.

Ferreira, M., Varela, H., Torresi, R.M., and Tremiliosi-Filho, G., (2006). Electrode passivation caused by polymerization of different phenolic compounds. *Electrochimica Acta*, 52, pp. 434–442.

Figueiredo, J.L., Pereira, M.F.R., Freitas, M.M.A., and Orfao, J.J.M., (1999). Modification of the surface chemistry of activated carbons. *Carbon*, 37, pp. 1379–1389.

Filik, J., (2005). Raman spectroscopy: a simple, non-destructive way to characterise diamond and diamond-like materials. *Spectroscopy Europe*, 17 (5), pp. 10–17.

Fillaudeau, L., Blanpain-Avet, P., and Daufin, G., (2006). Water, wastewater and waste management in brewing industries. *Journal of Cleaner Production*, 14, pp. 463–471.

Fischer, J.E., (1980). Graphite intercalation compounds: electronic properties and their correlation with chemistry. *Physica B+C*, 99 (1–4), pp. 383–394.

Fortuny, A., Font, J., and Fabregat, A., (1998). Wet air oxidation of phenol using active carbon as catalyst. *Applied Catalysis B: Environmental*, 19, pp. 165–173.

Franz, M., Arafat, H.A., and Pinto, N.G., (2000). Effect of chemical surface heterogeneity on the adsorption mechanism of dissolved aromatics on activated carbon. *Carbon*, 38, pp. 1807–1819.

Freundlich, H., (1906). Uber die adsorption in losungen. *Z. Phys. Chem*, 57, pp. 385–470.

Friedel, R.A., and Carlson, G.L., (1971). Infrared spectra of ground graphite. *The Journal of Physical Chemistry*, 76(8), pp. 1149–1151.

Friedle, R.A., Queiser, J.A., and Carlson, G.L., (1971). Infrared and Raman spectra of intractable carbonaceous substances: reassignments in coal spectra. *Am. Chem. Soc., Div. Fuel Chem., Prep. Pap*., 15(1), pp. 123–136.

Fuente, E., Menendez, J.A., Diez, M.A., Suarez, D., and Montes-Moran, M.A., (2003). Infrared spectroscopy of carbon materials: a quantum chemical study of model compounds. *J. Phys. Chem. B*, 107, pp. 6350–6359.

Furdin, G., (1998). Exfoliation process and elaboration of new carbonaceous materials. *Fuel*, 77 (6), pp. 479–485.

Garcia-oton, M., Montilla, F., Lillo-Rodenas, M.A., Morallon, E., and Vaquez, J.L., (2005). Electrochemical regeneration of activated carbon saturated with toluene. *Journal of Applied Electrochemistry*, 35, pp. 319–325.

Gattrel, M., and Kirk, D.W., (1993a). A study of electrode passivation during aqueous phenol electrolysis. *J. Electrochem. Soc*, 140 (4), pp. 903–911.

Gattrell, M and Kirk, D.W., (1993b). A Study of the oxidation of phenol at platinum and preoxidized platinum surfaces. *J. Electrochem. Soc*, 140 (6), pp. 1534–1540.

Gattrell, M., and Kirk, D.W., (1990). The electrochemical oxidation of aqueous phenol at a glassy carbon electrode. *Can. J. Chem. Eng*, 68, pp. 997–1003.

George, N., and Davies, J.T., (1988). Parameters affecting adsorption of microorganisms on activated charcoal cloth. *J. Chem. Tech. Biotechnol*, 43, pp. 117–129.

Gherardini, L., Michaud, P.A., Panizza, M., Comninellis, C., and Vatistas, N., (2001). Electrochemical oxidation of 4-chlorophenol for wastewater treatment. *Journal of The Electrochemical Society*, 148 (6), pp. 78–82.

Giles, C.H., Macewan, T.H., Nakhwa, S.N., and Smith, D., (1960). Studies in adsorption. xi. a system of classification of solution adsorption isotherms, and its use in diagnosis of adsorption mechanisms and in measurement of specific surface areas of solids. *J. Chem. Soc*, pp. 3973–3993.

Gilroy, D.J., Kauffman, K.W., Hall, R.A., Huang, X., and Chu, F.S., (2000). Assessing potential health risks from microcystin toxins in blue-green algae dietary supplements. *Environmental Health Perspectives*, 108 (51), pp. 435–438.

Goertzen, S.L., Theriault, K.D., Oickle, A.M., Tarasuk, A.C.,and Andreas, H.A., (2010). Standardization of the Boehm titration. Part I. CO_2 expulsion and endpoint determination. *Carbon*, 48, pp. 1252–1261.

Gopal, K., Tripathy, S.S., Bersillon, J.L., and Dubey, S.P., (2007). Chlorination byproducts, their toxicodynamics and removal from drinking water. *Journal of Hazardous Materials*, 140, pp. 1–6.

Goshadrou, A., and Moheb, A., (2011). Continuous fixed bed adsorption of C.I. acid blue 92 by exfoliated graphite: an experimental and modelling study. *Desalination*, 269, pp. 170–176.

Guan, S., and Wang, S., (2007). Experimental studies on electrodeionization for the removal of copper ions from dilute solutions. *Separation Science and Technology*, 42, pp. 949–961.

Guillou, S., and Murr, N.I., (2002). Inactivation of Saccharomyces cerevisiae in solution by low-amperage electric treatment. *Journal of Applied Microbiology*, 92, pp. 860–865.

Guinea, E., Arias, C., Cabot, P.L., Garrido, J.A., Rodriguez, R.M., Centellas, F., and Brillas, E., (2008). Mineralization of salicylic acid in acidic aqueous medium by electrochemical advanced oxidation processes using platinum and boron-doped diamond as anode and cathodically generated hydrogen peroxide. *Water Research*, 42, pp. 499–511.

Gupta, V.K., Carrott, P.J.M., Carrott, M.M.L., and Suhas., (2009). Low-cost adsorbents: growing approach to wastewater treatment. *Critical Reviews in Environmental Science and Technology*, 39, pp. 783–842.

Haghseresht, F., Nouri, S., and Lu, G.Q., (2002). Effects of solute ionization on the adsorption of aromatic compounds from dilute aqueous solution by activated carbon. *Langmuir*, 18, pp. 1574–1579.

Halhouli, K.A., Darwish, N.A., and Al-Dhoon, N.M., (1995). Effects of pH and inorganic salts on the adsorption of phenol from aqueous systems on activated decolorizing charcoal. *Separation Science and Technology*, 30 (17), pp. 3313–3324.

Halling-Sorensen, B., Nielsen, S.N., Lanzky, P.F., Ingerslev, F., Lutzhoft, H.C.H., and Jorgensen, S.E., (1998). Occurrence, fate and effects of pharmaceutical substances in the environment–a review. *Chemosphere*, 36(2), pp. 357–393.

Hameed, B.H., and Rehman, A.A., (2008). Removal of phenol from aqueous solutions by adsorption onto activated carbon prepared from biomass material. *Journal of Hazardous Materials*, 160 (2–3), pp. 576–581.

Hammami, S., Bellakhal, N., Oturan, N., Oturan, M.A., Dachraoui, M., (2008). Degradation of acid Orange 7 by electrochemically generated $^{\bullet}$OH radicals in acidic aqueous medium using a boron-doped diamond or platinum anode: a mechanistic study. *Chemosphere*, 73, pp. 678–684.

Hamwi, A., and Marchand, V., (1996). Some chemical and electrochemical properties of graphite oxide. *J. Phys. Chem Solids*, 57 (6–8), pp. 867–872.

Han, Y., and Lu, Y., (2007). Preparation and characterization of graphite oxide/polypyrrole composites. *Carbon*, 45, pp. 2394–2399.

Hardalo, C., and Edberg, S.C., (1997). Pseudomonas aeruginosa: assessment of risk from drinking water. *Critical Reviews in Microbiology*, 23(1), pp. 47–75.

Hartonoa, T., Wanga, S., Mab, Q., and Zhu, Z., (2009). Layer structured graphite oxide as a novel adsorbent for humic acid removal from aqueous solution. *Journal of Colloid and Interface Science*, 333, pp. 114–119.

Hatfield, T.L., Kleven, T.L., and Pierce, D.T., (1996). Electrochemical remediation of metal-bearing wastewaters Part I: copper removal from simulated mine drainage waters. *Journal of Applied Electrochemistry*, 26, pp. 567–574.

Henschler, D., (1994). Toxicity of chlorinated organic compounds: effects of the introduction of chlorine in organic molecules. *Angew. Chem. Int. Ed. Engl*, 33, pp. 1920–1935.

Hernandez, J.E., and and Edyvean, R.G.J., (2011). Comparison between a two-stage and single-stage digesters when treating a synthetic wastewater contaminated with phenol. *Water SA*, 37 (1), pp. 27–32.

Hernandez, L., Hernandez, P., and Velasco, V., (2003). Carbon felt electrode design: application to phenol electrochemical determination by direct oxidation. *Anal Bioanal Chem*, 377, pp. 262–266.

Hernlem, B.J., (2005). Electrolytic destruction of urea in dilute chloride solution using DSA electrodes in a recycled batch cell. *Water Research*, 39, pp. 2245–2252.

Ho, C.C and Chan, C.Y., (1986). The application of lead-dioxide coated titanium anode in the electroflotation of palm oil mill effluent. *Water Research*, 20 (12), pp. 1523–1527.

Ho, Y.S., (2004). Selection of optimum sorption isotherm. *Letters to the Editor / Carbon*, 42, pp. 2113–2130.

Ho, Y.S., Porter, J.F., and Mckay, G., (2002). Equilibrium isotherm studies for the sorption of divalent metal ions onto peat: copper, nickel and lead single component systems. *Water, Air, and Soil Pollution*, 141, pp. 1–33.

Holloway, P.H., and Vaidyanathan, P.N., (2010). *Characterization of metals and alloys*. New York: Momentum Press®, LLC.

Hontoria-Lucas, C., Lopez-Peinado, A.J., Lopez-Gonzalez, J.D.D., Rojas-Cervantes, M.L., and Martin-Aranda, R.M., (1995). Study of oxygen-containing groups in a series of graphite oxides: physical and chemical characterization. *Carbon*, 33 (11), pp. 1585–1592.

Horan, N.J., (1990). *Biological wastewater treatment systems: theory and operation*. Chichester: John Wiley and Sons.

Hua, I., and Thompson, J.E., (2000). Inactivation of Escherichia coli by sonication at discrete ultrasonic frequencies. *Water Research*, 34 (15), pp. 3888–3893.

Huan, Z., Zhao.-hui, J., Lu, H., and Cheng.-hua, Q., (2006). Synthesis of nanoscale zero-valent iron supported on exfoliated graphite for removal of nitrate. *Trans. Nonferrous Met. Soc. China*, 16, pp. s345–s349.

Hutchinson, D.H., and Robinson, C.W., (1990). A microbial regeneration process for granular activated carbon–1. Process modelling, *Water Research*, 24(10), pp. 1209–1215.

Iglesias, M.J., Puente, G., Fuente, E., and Pis, J.J., (1998). Compositional and structural changes during aerial oxidation of coal and their relations with technological properties. *Vibrational Spectroscopy*, 17, pp. 41–52.

Inagaki, M., Konno, H., Toyoda, M., Moriya, K., and Kihara, T., (2000). Sorption and recovery of heavy oils by using exfoliated graphite Part II: recovery of heavy oil and recycling of exfoliated graphite. *Desalination*, 128, pp. 213–218.

Inagaki, M., Tashiro, R., Washino, Y., and Toyoda, M., (2004). Exfoliation process of graphite via intercalation compounds with sulfuric acid. *Journal of Physics and Chemistry of Solids*, 65, pp. 133–137.

Iniesta, J., Michaud, M.A., Panizza, M., Cerisola, G., Aldaz, A., and Comninellis, C., (2001). Electrochemical oxidation of phenol at boron-doped diamond electrode. *Electrochimica Acta*, 46, pp. 3573–3578.

Ion, A.C., Alpatova, A., Ion, I., and Culetu, A., (2011). Study on phenol adsorption from aqueous solutions on exfoliated graphitic nanoplatelets. *Materials Science and Engineering B*, 176 (7), pp. 588–595.

Ishizaki, C., and Marti, I., (1981). Surface oxide structures on a commercial activated carbon. *Carbon*, 19 (6), pp. 409–412.

Israilides, C.J., Vlyssides, A.G., Mourafeti, V.N., and Karvouni, G., (1997). Olive oil wastewater treatment with the use of an electrolysis system. *Bioresource Technology*, 61, pp. 163–170.

Jannakoudakis, A.D., Jannakoudakis, P.D., and Theodoridou, E., (1990). Electrochemical oxidation of carbon fibres in aqueous solutions and analysis of the surface oxides. *Journal of Applied Electrochemistry*, 20, pp. 619–624.

Janata, J., (2009). *Principles of chemical sensors*, 2nd edition, Springer Dordrecht Heidelberg London.

Jarvis, B., (1989). *Statistical aspects of the microbiological analysis of foods*. Netherlands: Academic Press.

Jarvis, B., (2008). *Statistical aspects of the microbiological examination of foods*. 2nd edition. Netherlands: Academic Press.

Jeong, J., Kim, J.Y., and Yoon, J., (2006). The role of reactive oxygen species in the electrochemical inactivation of microorganisms. *Environ. Sci. Technol*, 40, pp. 6117–6122.

Jiang, J.-Q., Wang, S., and Panagoulopoulos, A., (2006). The exploration of potassium ferrate (VI) as a disinfectant/coagulant in water and wastewater treatment. *Chemosphere*, 63, pp. 212–219.

Jiuhui, Q., (2008). Research progress of novel adsorption processes in water purification: a review. *Journal of Environmental Sciences*, 20, pp. 1–13.

Jucker, B.A., Harms, H., Hug, S.J., and Zehnder, A.J.B., (1997). Adsorption of bacterial surface polysaccharides on mineral oxides is mediated by hydrogen bonds. *Colloids and Surfaces B: Biointerfaces*, 9, pp. 331–343.

Judd, S., and Black, S., (2000). Disinfection by-product formation in swimming pool waters: a simple mass balance. *Water Research*, 34 (35), pp. 1611–1619.

Junli, H., Li, W., Nanqi, R., Fang, M and Juli., (1997). Disinfection effect of chlorine dioxide on bacteria in water. *Water Research*, 31 (3), pp. 607–613.

Juttner, K., Galla, U., and Schmieder, H., (2000). Electrochemical approaches to environmental problems in the process industry. *Electrochimica Acta*, 45, pp. 2575–2594.

Jyoti, K.K., and Pandit, A.B., (2001). Water disinfection by acoustic and hydrodynamic cavitation. *Biochemical Engineering Journal*, 7, pp. 201–212.

Karanfil, T., (1999). Role of granular activated carbon surface chemistry on the adsorption of organic compounds.1. Priority Pollutants. *Environ. Sci. Technol*, 33, pp. 3217–3224.

Karimi-Jashni, A., and Narbaitz, R.M., (2005). Electrochemical Reactivation of granular activated carbon: effect of electrolyte mixing. *Journal of Environmental Engineering*, 131 (3), pp. 443–449.

Kerwick, M.I., Reddy, S.M., Chamberlain, A.H.L., and Holt, D.M., (2005). Electrochemical disinfection, an environmentally acceptable method of drinking water disinfection. *Electrochimica Acta*, 50, pp. 5270–5277.

Kim, J., Cho, M., Byungtaek, O., Choi, S., and Yoon, J., (2004). Control of bacterial growth in water using synthesized inorganic disinfectant. *Chemosphere*, 55, pp. 775–780.

Kinnlburgh, D.G., (1986). General purpose adsorption isotherms. *Environ. Sci. Technol*, 20, pp. 895–904.

Kinoshita, K., (1988). *Carbon*, Wiley, New York, pp. 319.

Kitajima, Y., Shigematsu, A., Nakamura, N., and Matsunaga, T., (1988). Electrochemical sterilization using carbon fiber microelectrode. *Denki Kagaku*, 52, pp. 1082–1085.

Knettig, E., Thomson, B.M., and Hrudey, S.E., (1986). Competitive activated carbon adsorption of phenolic compounds. *Environmental Pollution Series B*, 12, pp. 281–299.

Kolaczkowski, S.T., Plucinski, P., Beltran, F.J., Rivas, F.J., and McLurgh, D.B., (1999). Wet air oxidation: a review of process technologies and aspects in reactor design. *Chemical Engineering Journal*, 73, pp. 143–160.

Korbahti, B.K., and Tanyolac, A., (2003). Continuous electrochemical treatment of phenolic wastewater in a tubular reactor. *Water Research*, 37, pp. 1505–1514.

Korbahti, B.K., Artut, K., Gecgel, C., and Ozer, A., (2011). Electrochemical decolorization of textile dyes and removal of metal ions from textile dye and metal ion binary mixtures. *Chemical Engineering Journal*, 173 (3), pp. 677–688.

Korbahti, B.K., Salih, B., and Tanyolac, A., (2001). Electrochemical conversion of phenolic wastewater on carbon electrodes in the presence of NaCl. *Journal of Chemical Technology and Biotechnology*, 77, pp. 70–76.

Korbahti, B.K., and Artut, K., (2010). Electrochemical oil/water demulsification and purification of bilge water using Pt/Ir electrodes. *Desalination*, 258, pp. 219–228.

Kozakiewicz, Z., (1989). Aspergillus species on stored products. *Mycology Papers*, 161, pp.1–188.

Kraft, A., (2008). Electrochemical water disinfection: a short review. *Platinum Metals Rev*, 52 (3), pp. 177–185.

Kraft, A., Stadelmann, M., and Blaschke, M., (2003). Anodic oxidation with doped diamond electrodes: a new advanced oxidation process. *Journal of Hazardous Materials*, B103, pp. 247–261.

Kraft, A., Stadelmann, M., Blaschke, M., Kreysig, D., Sandt, B., Schroder, F., and Rennau, J., (1999). Electrochemical water disinfection Part I: hypochlorite production from very dilute chloride solutions. *Journal of Applied Electrochemistry*, 29, pp. 861–868.

Kubitschek, H.E., (1990). Cell volume increase in Escherichia coli after shifts to richer media. *Journal of Bacteriology*, 172 (1), pp. 94–101.

Kumar, K.V., and Sivanesan, S., (2005). Comparison of linear and non-linear method in estimating the sorption isotherm parameters for safranin onto activated carbon. *Journal of Hazardous Materials*, B123, pp. 288–292.

Kummerer, K., (2004). Resistance in the environment. *Journal of Antimicrobial Chemotherapy*, 54, pp. 311–320.

Kuritz, T., and Wolk, C.P., (1995). Use of filamentous cyanobacteria for biodegradation of organic pollutants. *Applied and Environmental Microbiology*, pp. 234–238.

Lambert, P.A., (2002). Mechanisms of antibiotic resistance in Pseudomonas aeruginosa. *Journal of the Royal Society of Medicine*, 95 (41), pp. 22–24.

Langmuir, I., (1916). The constitution and fundamental properties of solids and liquids. *Journal of the American Chemical Society*, 38 (11), pp. 2221–2295.

Laszlo, K., and Szucs, A., (2001). Surface characterization of polyethyleneterephthalate (PET) based activated carbon and the effect of pH on its adsorption capacity from aqueous phenol and 2,3,4-trichlorophenol solutions. *Carbon*, 39, pp. 1945–1953.

LeChevallier, M.W., Hassenauer, T.S., Camper, A.K., and McFeters, G.A., (1984). Disinfection of bacteria attached to granular activated carbon. *Applied and Environmental Microbiology*, 48 (5), pp. 918–923.

Leng, C.C., and Pinto, N.G., (1997). Effects of surface properties of activated carbons on adsorption behaviour of selected aromatics. *Carbon*, 35 (9), pp. 1375–1385.

Leshin, V.S., Sorokina, N.E., and Avdeev, V.V., (2003). Graphite intercalation in H_2SO_4–CH_3COOH electrolytes. *Inorganic Materials*, 39 (8), pp. 826–832.

Levec, J., and Pintar, A., (1995). Catalytic oxidation of aqueous solutions of organics–an effective method for removal of toxic pollutants from waste waters. *Catalysis Today*, 24, pp. 51–58.

Li, J.-T., Li, M., Li, J.-H., Sun, H.-W., (2007). Decolorization of azo dye direct scarlet 4BS solution using exfoliated graphite under ultrasonic irradiation. *Ultrasonics Sonochemistry*, 14, pp. 241–245.

Li, J.-T., Song, Y.-L., Meng, X.-Y and Liu, C.-M., (2009). Decolourization of C.I direct blue 78 aqueous solution in presence of exfoliated graphite under ultrasound irradiation. *Indian Journal of Chemical Technology*, 16, pp. 411–416.

Li, L., Quinlivan, P.A., and Knappe, D.R.A., (2002). Effects of activated carbon surface chemistry and pore structure on the adsorption of organic contaminants from aqueous solution. *Carbon*, 40, pp. 2085–2100.

Li, M., Feng, C., Hu, W., Zhang, Z., and Sugiura, N., (2009a). Electrochemical degradation of phenol using electrodes of Ti/RuO_2 –Pt and Ti/IrO_2 –Pt. *Journal of Hazardous Materials*, 162, pp. 455–462.

Li, M., Feng, C., Zhang, Z., and Sugiura, N., (2009b). Efficient electrochemical reduction of nitrate to nitrogen using Ti/IrO_2 –Pt anode and different cathodes. *Electrochimica Acta*, 54, pp. 4600–4606.

Li, X.-y, Cui, Y.-h, Feng, Y.-j, Xie, Z.-m, and Gu, J.-D., (2005). Reaction pathways and mechanisms of the electrochemical degradation of phenol on different electrodes. *Water Research*, 39, pp. 1972–1981.

Li, X.Y., Diao, H.F., Fan, F.X.J., Gu, J.D., Ding, F., and Tong, A.S.F., (2004). Electrochemical wastewater disinfection: identification of its principal germicidal actions. *Journal of Environmental Engineering*, pp. 1217–1221.

Lim, J.L and Okada, M., (2005). Regeneration of granular activated carbon using ultrasound. *Ultrasonics Sonochemistry*, 12 (2005) 277–282.

Lin, S.H., and Hsu, F.M., (1995). Liquid-phase adsorption of organic compounds by granular activated carbon and activated carbon fibers. *Ind. Eng. Chem. Res*, 34, pp. 2110–2116.

Lin, S.H., Shyu, C.T., and Sun, M.C., (1998). Saline wastewater treatment by electrochemical method. *Water Research*, 32 (4), pp. 1059–1066.

Lonnen, J., Kilvington, S., Kehoe, S.C., Al-Touati, F., and McGuigan, K.G., (2005). Solar and photocatalytic disinfection of protozoan, fungal and bacterial microbes in drinking water. *Water Research*, 39, pp. 877–883.

Lugo-Lugo, V., Barrera-Diaz, C., Bilyeu, B., Balderas-Hernandez, P., Urena-Nunez, F., and Sanchez-Mendieta, V., (2010). Cr(VI) reduction in wastewater using a bimetallic galvanic reactor. *Journal of Hazardous Materials*, 176, pp. 418–425.

Madaeni, S.S., (1999). The application of membrane technology for water disinfection. *Water Research*, 33 (2), pp. 301–308.

Maksimova, N.V., Leshin, V.S., Mandrugin, A.A., Korobkov, V.I., Sorokina, N.E., Shornikova, N.O., and Avdeev, V.V., (2004). Radiotracer diagnostics of graphite intercalation compounds with sulfuric and acetic acids. *Inorganic Materials*, 40 (10), pp. 1035–1042.

Malik, P.K., (2004). Dye removal from wastewater using activated carbon developed from sawdust: adsorption equilibrium and kinetics. *Journal of Hazardous Materials*, B113, pp. 81–88.

Maluleke, M.A., and Linkov, V.M., (2003). Partial electrochemical oxidation of phenol on ceramic-based flat-sheet type electromembrane reactors. *Separation and Purification Technology*, 32, pp. 377–385.

Mangun, C.L., Benak, K.R., Daley, M.A and Economy, J., (1999). Oxidation of activated carbon fibers: effect on pore size, surface chemistry, and adsorption properties. *Chem. Mater*, 11, pp. 3476–3483.

Manisankar, P., Viswanathan, S., and Rani, C., (2003). Electrochemical treatment of distillery effluent using catalytic anodes, *Green Chemistry*, 2003, 5, pp. 270–274.

Mara, D., and Horan, N.J., (2003). *The handbook of water and wastewater microbiology*. UK: Academic Press, Elsevier.

Marder, L., Sulzbach, G.O., Bernardes, A.M., and Ferreira, J.Z., (2003). Removal of cadmium and cyanide from aqueous solutions through electrodialysis. *J. Braz. Chem. Soc*, 14 (4), pp. 610–615.

Marselli, B., Garcia-Gomez, J., Michaud, P.-A., Rodrigo, M.A., and Comninellis, C., (2003). Electrogeneration of hydroxyl radicals on boron-doped diamond electrodes. *Journal of The Electrochemical Society*, 150 (3), pp. 79–83.

Martinez-Huitle, C.A., and Brillas, E., (2008). Electrochemical alternatives for drinking water disinfection. *Angew. Chem*. 47 (11), pp. 1998–2005.

Martinez-Huitle, C.A., and Ferro, S., (2006). Electrochemical oxidation of organic pollutants for the wastewater treatment: direct and indirect processes, *Chem. Soc. Rev*, 35, pp. 1324–1340.

Maryasin, I., Sandbank, E., and Shelef, G., (1994). Removal of oil from water. US Patent. No. 5,282,975.

Matsunaga, T., Nakasono, S., and Masuda, S., (1992a). Electrochemical sterilization of bacteria adsorbed on granular activated carbon. *FEMS Microbiology Letters*, 93, pp. 255–260.

Matsunaga, T., Nakasono, S., Kitajima, Y., and Horiguchi, K., (1994). Electrochemical disinfection of bacteria in drinking water using activated carbon fibers. *Biotechnol Bioeng*, 43, pp. 429–433.

Matsunaga, T., Nakasono, S., Takamuku, T., Burgess, J.G., Nakamura, N., and Sode, K., (1992b). Disinfection of drinking water by using a novel electrochemical reactor employing carbon-cloth electrodes. *Applied and Environmental Microbiology*, pp. 686–689.

Matsunaga, T., Namba, Y., and Nakajima, T., (1985). Electrochemical sterilization of microbial cells. *Bioelectrochemistry and Bioenergetics,* 13, pp. 393–400.

Matsuo, Y., Higashika, S., Kimura, K., Miyamoto, Y., Fukutsuka, T., and Sugie, Y., (2002). Synthesis of polyaniline-intercalated layered materials via exchange reaction. *J. Mater. Chem*, 12, pp. 1592–1596.

Matsuo, Y., Watanabe, K., Fukutsuka, T., and Sugie, Y., (2003). Characterization of n-hexadecylalkylamine-intercalated graphite oxides as sorbents. *Carbon*, 41, pp. 1545–1550.

Matsushige, K., Inamori, Y., Mizuochi, M., Hosomi, M., and Sudo, R., (1990). The effects of temperature on anaerobic filter treatment for low strength organic wastewater. *Environmental Technology*, 11, pp. 899–910.

Mattson, J.S., Mark, H.B., Malbin, M.D., Weber, W.J., and Crittenden, J.C., (1969). Surface chemistry of active carbon: specific adsorption of phenols. *Journal of Colloid and Interface Science*, 31(1), pp. 116–130.

McEldowney, S., and Fletcher, M., (1986). Variability of the influence of physiochemical factors affecting bacterial adhesion to polystyrene substrata. *Applied and Environmental Microbiology*, 52 (3), pp. 460–465.

McKay, G., (1982). Adsorption of dyestuffs from aqueous solutions with activated carbon I: equilibrium and batch contact time studies. *J. Chem. Technol and Biotechnol*, 32, pp. 759–772.

Mckay, G., Geundi, M.E., and Nassar, M.M., (1987). Equilibrium studies during the removal of dyestuffs from aqueous solutions using bagasse pith. *Water Research*, 21 (12), pp. 1513–1520.

McKelvy, M.J., and Glaunsinger, W.S., (1990). Molecular Interaction Reactions in Lamellar Compounds. *Annu. Rev. Phys. Chem*, 41, pp. 497–523.

Mehta, M.P., and Flora, J.R.V., (1997). Effects of electrochemical treatment of granular activated carbon on surface acid groups and the adsorptive capacity for phenol. *Water Research*, 31 (9), pp. 2171–2176.

Meldrum, B.J., Orr, J.C and Rochester, C.H., (1985). Diffuse reflectance fourier-transform infrared spectroscopy: in situ surface oxidation of carbon. *J. Chem. Soc., Chem. Commun*, pp. 1176–1177.

Mena, K.D., and Gerba, C.P., (2009). Risk assessment of Pseudomonas aeruginosa in water. *Rev. Environ. Contam. Toxicol*, 201, pp. 71–115.

Mercado, V.H., Pothakamury, U.R., Chang, Fu-Jung., Barbosa-Canovas, G.V., and Swanson, B.G., (1996). Inactivation of Escherichia coli by combining pH, ionic strength and pulsed electric fields hurdles. *Food Research International*, 29(2), pp. 117–121.

Merzouk, B., Gourich, B., Sekki, A., Madani, K., and Chibane, M., (2009). Removal of turbidity and separation of heavy metals using electrocoagulation–electroflotation technique– a case study. *Journal of Hazardous Materials*, 164 pp. 215–222.

Metcalf and Eddy., (2003). *Wastewater Engineering, Treatment and Reuse*. 4th edition. New York: McGraw-Hill Companies, Inc.

Miguel, G.S., Lambert, S.D., and Graham, N.J.D., (2001). The regeneration of field-spent granular activated carbons. *Water Research*, 35(11), pp. 2740–2748.

Minghua, Z., Qizhou, D., Lecheng, L., and Dahui, W., (2005). Activated carbon adsorption- advanced electro-oxidative regeneration for the treatment of biorefractory organic pollutants. *Chinese Science Bulletin*, 50 (5), pp. 489–491.

Mirabella, F.M., (1998). *Modern techniques in applied molecular spectroscopy*. John Wiley and Sons, Inc.

Mishra, V.S., Mahajani, V.V., and Joshi, J.B., (1995). Wet air oxidation. *Ind. Eng. Chem. Res*,34, pp. 2–48.

Misra, A.K., Chandra, P., Shukla, J.B., (2006). Mathematical modeling and analysis of the depletion of dissolved oxygen in water bodies. *Nonlinear Analysis: Real World Applications*, 7, pp. 980–996.

Mohammed, F.M., Roberts, E.P.L., Hill, A., Campen, A.K and Brown, N.W., (2011). Continuous water treatment by adsorption and electrochemical regeneration. *Water Research*, 45, pp. 3065–3074.

Mollaha, M.Y.A., Morkovskyb, P., Gomesc, J.A.G., Kesmezc, M., Pargad, J., and Cockec, D.L., (2004). Fundamentals, present and future perspectives of electrocoagulation. *Journal of Hazardous Materials*, B114, pp. 199–210.

Montilla,F., Morallon, E., and Vazquez, J.L., (2005). Evaluation of the electrocatalytic activity of antimony-doped tin dioxide anodes toward the oxidation of phenol in aqueous solutions. *Journal of the Electrochemical Society*, 152 (10), pp. 421–427.

Monyakina, L.A., Maksimova, N.V., Nikolskaya, I.V., Avdeev, V.V., Ionov, S,G., (2004). The calorimetric investigation of the graphite–HNO_3 –R system (R=CH_3COOH, H_2 SO_4). *Journal of Physics and Chemistry of Solids*, 65, pp. 181–183.

Moore, R.M., Rouge, B., Whitton, C.M., Collinsville., Shepherd, L.H., and Rouge, B., (1992). Water treatment process. US Patent No. 5141652.

Moreno-Castilla, C., (2004). Adsorption of organic molecules from aqueous solutions on carbon materials. *Carbon*, 42, pp. 83–94.

Muranaka, C.T., Julcour, C., Wilhelm, A.-M., Delmas, H., and Nascimento, C.A.O., (2010). Regeneration of activated carbon by (photo)-fenton oxidation. *Ind. Eng. Chem. Res*, 49, pp. 989–995.

Murphy, O.J., Hitchens, J.D., Kaba, L., and Verostko, C.E., (1992). Direct electrochemical oxidation of organics for wastewater treatment. *Water Research*, 26 (4), pp. 443–451.

Murugananthan, M., Yoshihara, S., Rakuma, T., and Shirakashi, T., (2008). Mineralization of bisphenol A (BPA) by anodic oxidation with boron-doped diamond (BDD) electrode. *Journal of Hazardous Materials*, 154, pp. 213–220.

Narbaitz, R.M., and Cen, J., (1994). Electrochemical regeneration of granular activated carbon. *Water Research*, 28(8), pp. 1771–1778.

Narbaitz, R.M., and Karimi-Jashni, A., (2009). Electrochemical regeneration of granular activated carbons loaded with phenol and natural organic matter. *Environmental Technology*, 30 (1), pp. 27–36.

Narsetti, R., Curry, R.D., McDonald, K.F., Clevenger, T.E., and Nichols, L.M., (2006). Microbial inactivation in water using pulsed electric fields and magnetic pulse compressor technology. *IEEE Transactions on Plasma Science*, 34 (4), pp. 1386–1393.

Nevskaia, D.M., Santianes, A., Munoz, V., and Ruiz, A.G., (1999). Interaction of aqueous solutions of phenol with commercial activated carbons: an adsorption and kinetic study. *Carbon*, 37, pp. 1065–1074.

Ni, Z., Wang, Y., Yu, T., and Shen, Z., (2008). Raman spectroscopy and imaging of graphene. *Nano Res*, 1, pp. 273–291.

Niemi, R.M., Knuth, S., and Lundstrom, K., (1982). Actinomycetes and fungi in surface waters and in potable water. *Applied and Environmental Microbiology*, 43 (2), pp. 378–388.

Noel, M., and Santhanam, R., (1998). Electrochemistry of graphite intercalation compounds. *Journal of Power Sources*, 72, pp. 53–65.

Noyes, R., (1991). *Handbook of pollution control processes*. New Jersey: Noyes Publications.

Okachi, M., Lim, T.K, Nakamura, N., and Matsunaga, T., (1997). Electrochemical disinfection of drinking water using an activated carbon fiber reactor capable of monitoring its microbial fouling. *Appl Microbiol Biotechnol*, 47, pp. 18–22.

Okawa, K., Suzuki, K., Takeshita, T., and Nakano, K., (2007). Regeneration of granular activated carbon with adsorbed trichloroethylene using wet peroxide oxidation. *Water Research*, 41, pp. 1045–1051.

Oliveira, F.H., Osugi, M.E., Paschoal, F.M.M., Profeti, D., Olivi, P., and Zanoni, M.V.B., (2007). Electrochemical oxidation of an acid dye by active chlorine generated using $Ti/Sn_{(1-x)}Ir_xO_2$ electrodes. *J Appl Electrochem*, 37, pp. 583–592.

Oliveira, R.T.S., Salazar-Banda, G.R., Santos, M.C., Calegaro, M.L., Miwa, D.W., Machado, S.A.S., and Avaca, L.A., (2007). Electrochemical oxidation of benzene on boron-doped diamond electrodes. *Chemosphere*, 66, pp. 2152–2158.

Owen, G., Bandi, M., Howell, J.A., and Churchouse, S.J., (1995). Economic assessment of membrane processes for water and waste water treatment. *Journal of Membrane Science*, 102, pp. 77–91

Ozer, A., Ozer, D., and Ekiz, H.I., (1999). Application of Freundlich and Langmuir models to multistage purification process to remove heavy metal ions by using Schizomeris leibleinii. *Process Biochemistry*, 34, pp. 919–927.

Palaniswamy, D.K., Sorial, G.A., and Maloney, S.W., (2004). Electrochemical reduction of 2,4,6-trinitrotoluene. *Environmental Engineering*, 21(2), pp. 203–218.

Palma-Goyes, R.E., Guzman-Duque, F.L., Penuela, G., Gonzalez, I., Nava, J.L., and Torres-Palma, R.A., (2010). Electrochemical degradation of crystal violet with BDD electrodes: effect of electrochemical parameters and identification of organic by-products. *Chemosphere*, 81, pp. 26–32.

Palmas, S., Polcaro, A.M., Vacca, A., Mascia, M., and Ferrara, F., (2007). Influence of the operating conditions on the electrochemical disinfection process of natural waters at BDD electrodes. *J Appl Electrochem*, 37, pp. 1357–1365.

Pan, Q., Guo, K., Wang, L., and Fang, S., (2002). Novel modified graphite as anode material for lithium ion batteries. *J. Mater. Chem*, 12, pp. 1833–1838.

Pang, X.-y., (2010a). Adsorption capacity and mechanism of expanded graphite for polyethylene glycol and oils. *E-Journal of Chemistry*, 7 (4), 1258–1265.

Pang, X.-y., (2010b). Study on the discolored thermodynamics of dyes on expanded graphite loaded with titania. *International Journal of Chem Tech Research*, 2 (2), pp. 1281–1288.

Pang, X.-Y., and Gong, F., (2008). Study on the adsorption kinetics of acid red 3b on expanded graphite. *E-Journal of Chemistry*, 5 (4), 802–809.

Panizza, M., and Cerisola, G., (2003). Influence of anode material on the electrochemical oxidation of 2-naphthol. Part1. Cyclic voltammetry and potential step experiments. Electrochimica Acta, 48, pp. 3491–3497.

Panizza, M. and Cerisola, G. (2006). Electrochemical processes for the treatment of organic pollutants. In: D. V. Zinger (Eds.), *Advances in Chemistry Research*, Vol. 2. New York: Nova Science.

Panizza, M., Zolezzi, M., and Nicolella, C., (2006). Biological and electrochemical oxidation of naphthalenesulfonates. *Journal of Chemical Technology and Biotechnology*, 81, pp. 225–232.

Park, H., Vecitis, C.D., and Hoffmann, M.R., (2009). Electrochemical water splitting coupled with organic compound oxidation: the role of active chlorine species. *J. Phys. Chem. C*, 113, pp. 7935–7945.

Patakioutas, G., and Albanis, T.A., (2002). Adsorption–desorption studies of alachlor, metolachlor, EPTC, chlorothalonil and pirimiphos-methyl in contrasting soils. *Pest Management Science*, 58, pp. 352–362.

Patermarakis, G., and Fountoukidis, E., (1990). Disinfection of water by electrochemical treatment. *Water Research*, 24 (12), pp. 1491–1496.

Pelczar, M.J., Chan, E.C.S., and Krieg, N.R., (1993). *Microbiology*. 5th edition. India: Tata McGraw-Hill.

Pelletier, M.J., (1999). *Analytical applications of Raman spectroscopy*. Blackwell Science Ltd.

Pimenov, A.V., Mitilineos, A.G., Pendinen, G.I., Chernov, A.I.L., Shmidt, J.L., and Cheh, H.Y., (2001). The adsorption and deactivation of microorganisms by activated carbon fiber. *Separation Science and Technology*, 36(15), pp. 3385–3394.

Pimentel, M., Oturan, N., Dezotti, M., and Oturan, M.A., (2008). Phenol degradation by advanced electrochemical oxidation process electro-Fenton using a carbon felt cathode. *Applied Catalysis B: Environmental*, 83, pp. 140–149.

Pletcher, D., (2009). A first course in electrode processes, 2nd edition, RSC Publishing, UK.

Polcaro, A.M., Palmas,S., Renoldi, F., and Mascia, M., (2000). Three-dimensional electrodes for the electrochemical combustion of organic pollutants. *Electrochimica Acta*, 46, pp. 389–394.

Polcaro, A.M., Vacca, A., Mascia, M., Palmas, S., Pompei, R., and Laconi, S., (2007). Characterization of a stirred tank electrochemical cell for water disinfection processes. *Electrochimica Acta*, 52, pp. 2595–2602.

Porta, A., and Kulhanek, A., (1986). Process for the electrochemical decontamination of water polluted by pathogenic germs with peroxide formed in *situ.* U.S. Patent 4,619,745.

Prud'homme, R.K., Aksay, I.A., Adamson, D., and Abdala, A., (2009). Tire containing thermally exfoliated graphite oxide. US patent 2009/0054581 A1.

Pulgarin, C., Adler, N., Peringer, P., and Comninellis, C., (1994). Electrochemical detoxification of a 1,4-benzoquinone solution in wastewater treatment. *Water Research*, 28(4), pp. 887–893.

Pyo, M., and Moon, S., (2005). Indirect electrochemical oxidation of phenol by Ce^{4+}, controlling surface insulation of Au electrode. *Bull. Korean Chem. Soc*, 26(6), pp. 899–902.

Rajeshwar, K., and Ibanez, J.G., (1997). *Environmental electrochemistry: fundamentals and applications in pollution abatement*. Academic Press, Inc.

Rajkumar, D., Kim, J.G., Palanivelu, K., (2005). Indirect electrochemical oxidation of phenol in the presence of chloride for wastewater treatment. *Chem. Eng. Technol*, 28(1), pp. 98–105.

Rana, P., Mohan, N., and Rajagopal, C., (2004). Electrochemical removal of chromium from wastewater by using carbon aerogel electrodes. *Water Research*, 38, pp. 2811–2820.

Rao, N.N., Somasekhar, K.M., Kaul, S.N., and Szpyrkowicz, L., (2001). Electrochemical oxidation of tannery wastewater. *Journal of Chemical Technology and Biotechnology*, 76, pp. 1124–1131.

Rao, S.R., (2004). *Surface chemistry of froth flotation*. 2nd edition. NY: Klumer Academic/ Plenum Publishers.

Rastogi, K., Sahu, J.N., Meikap, B.C., and Biswas, M.N., (2008). Removal of methylene blue from wastewater using fly ash as an adsorbent by hydrocyclone. *Journal of Hazardous Materials*, 158, pp. 531–540.

Rege, S.U., and Yang, R.T., (1998). Desorption by ultrasound: phenol on activated carbon and polymeric resin. *AIChE Journal*, 44 (7), pp. 1519–1528.

Richardson, S.D., (2003). Disinfection by-products and other emerging contaminants in drinking water. *Trends in Analytical Chemistry*, 22(10), pp. 666–684.

Richardson, S.D., Thruston, A.D., Caughran, T.V., Chen, P.H., Collette, T.W., and Floyd, T.L., (1999). Identification of new drinking water disinfection byproducts formed in the presence of bromide. *Environ. Sci. Technol*, 33, pp. 3378–3383.

Rivera-Utrilla, J., Bautista-Toledo, I., Ferro-Garcia, M.A and Moreno-Castilla, C., (2001). Activated carbon surface modifications by adsorption of bacteria and their effect on aqueous lead adsorption. *Journal of Chemical Technology and Biotechnology*, 76, pp. 1209–1215.

Rodgers, J.D., Jedral, W., and Bunce, N.J., (1999). Electrochemical oxidation of chlorinated phenols, *Environ. Sci. Technol*, 33, pp. 1453–1457.

Rositani, F., Antonucci, P.L., Minutoli, M., and Giordano, N., (1987). Infrared analysis of carbon blacks. *Carbon*, 25 (3), pp. 325–332.

Rueffer, M., Bejan, D., and Bunce, N.J., (2011). Graphite: An active or an inactive anode. *Electrochimica Acta*, 56, pp. 2246–2253.

Rule, K.L., Ebbett, V.R., and Vikesland, P.J., (2005). Formation of chloroform and chlorinated organics by free chlorine mediated oxidation of triclosan. *Environ. Sci. Technol*, 39, pp. 3176–3185.

Rule, K.L., Ebbett, V.R., and Vikesland, P.J., (2005). Formation of chloroform and chlorinated organics by free chlorine mediated oxidation of triclosan. *Environ. Sci. Technol*, 39, pp. 3176–3185.

Ruthven, D.M., (1984). *Principles of adsorption and adsorption processes*. John Wiley and Sons, Inc.

Safavi, A., Maleki, N., and Tajabadi, F., (2007). Highly stable electrochemical oxidation of phenolic compounds at carbon ionic liquid electrode. *Analyst*, 132, pp. 54–58.

Samson, R.A., and Pitt, J.I., (2000). *In Integration of Modern Taxonomic Methods for Penicillium and Aspergillus Classification*. The Netherlands: Harwood Academic Publishers.

Samson, R.A., Houbraken, J.A.M.P., Kuijpers, A.F.A., Frank, J.M., and Frisvad, J.C., (2004). New ochratoxin or sclerotium producing species in Aspergillus section Nigri. *Studies in Mycology*, 50, pp. 45–61.

Schmalz, V., Dittmar, T., Haaken, D., and Worch, E., (2009). Electrochemical disinfection of biologically treated wastewater from small treatment systems by using boron-doped diamond (BDD) electrodes – contribution for direct reuse of domestic wastewater. *Water Research*, 43, pp. 5260–5266.

Schreiber, B., Brinkmann, T., Schmalz, V., and Worch, E., (2005). Adsorption of dissolved organic matter onto activated carbon—the influence of temperature, absorption wavelength, and molecular size. *Water Research*, 39, pp. 3449–3456.

Schueller, B.S and Yang, R.T., (2001). Ultrasound enhanced adsorption and desorption of phenol on activated carbon and polymeric resin. *Ind. Eng. Chem. Res*, 40, pp. 4912–4918.

Scialdone, O., Randazzo, S., Galia, A., and Silvestri, G., (2009). Electrochemical oxidation of organics in water: role of operative parameters in the absence and in the presence of NaCl. *Water Research*, 43, pp. 2260–2272.

Scott, J.L., Kraemer, D.G., and Keller, R.J., (2009). Occupational hazards of carbon dioxide exposure. *Journal of Chemical Health and Safety*, 16(2), pp. 18–22.

Semerjian, L., and Ayoub, G.M., 2003. High-pH-magnesium coagulation-flocculation in wastewater treatment. *Advances in Environmental Research*, 7, 389–403.

Serikawa, R.M, Isaka, M., Su, Q., Usui, T., Nishimura, T., Sato, H., and Hamada, S., (2000). Wet electrolytic oxidation of organic pollutants in wastewater treatment. *Journal of Applied Electrochemistry*, 30, pp. 875–883.

Settle, F.A., (1997). *Handbook of instrumental techniques for analytical chemistry*. Upper Saddle River, NJ: Prentice Hall PTR.

Shafeeyan, M.S., Daud, W.M.A.W., Houshmand, A., and Shamiri, A., (2010). A review on surface modification of activated carbon for carbon dioxide adsorption. *Journal of Analytical and Applied Pyrolysis*, 89, pp. 143–151.

Sharifian, H., and Kirk, D.W., (1986). Electrochemical oxidation of phenol. *J. Electrochem. Soc*, 133(5), pp. 921–924.

Shende, R.V., and Mahajani, V.V., (2002). Wet oxidative regeneration of activated carbon loaded with reactive dye. *Waste Management*, 22, pp. 73–83.

Shornikova, O.N., Sorokina, N.E., Maksimova, N.V., and Avdeev, V.V., (2005). Graphite intercalation in the graphite–H_2SO_4–R (R=H_2O, C_2H_5OH, C_2H_5OH, C_2H_5COOH) systems. *Inorganic Materials*, 41 (2), pp. 120–126.

Simond, O., and Comninellis, C., (1997). Anodic oxidation of organics on Ti/IrO_2 anodes using Nafion® as electrolyte. *Electrochimica Acta*, 42 (13–14), pp. 2013–2018

Singer, M., (1990). The role of antimicrobial agents in swimming pools. *International Biodeterioration*, 26, pp. 159–168.

Site, A.D., (2001). Factors affecting sorption of organic compounds in natural sorbent/ water systems and sorption coefficients for selected pollutants: a review. *J. Phys. Chem. Ref. Data*, 30 (1), pp. 187–439.

Smith, B.C., (2011). *Fundamentals of fourier transform infrared spectroscopy*. 2nd edition. Taylor and Francis group, CRC Press.

Smith, J.E., Renner, R.C., Hegg, B.A., and Bender, J.H., (1991). *Upgrading existing or designing new drinking water treatment facilities*. New Jersey: Noyes Data Corporation.

Smith, V., and Watkinson, A.P., (1981). Anodic oxidation of phenol for wastewater treatment. *The Canadian Journal of Chemical Engineering*, 59(1), pp. 52–59.

Soda, S., Ike, M., and Fujita, M., (1999). Adsorption of bacterial cells onto activated sludge floes. *Journal of Bioscience and Bioengineering*, 87 (4), pp. 513–518.

Soltani, B., and Moheb, A., (2010). Ultrasound irradiation facilitated adsorption of MTBE from aqueous solution using exfoliated graphite. *Chem. Eng. Technol*, 33 (7), pp. 1107–1111.

Son, H., Cho, M., Chung, H., Choi, S., and Yoon, J., (2004). Bactericidal activity of mixed oxidants: comparison with free chlorine. *J. Ind. Eng. Chem*, 10 (5), pp. 705–709.

Song, Y.-L., Li, J.-T., and Chen, H., (2008). Removal of acid brown 348 dye from aqueous solution by ultrasound irradiated exfoliated graphite. *Indian Journal of Chemical Technology*, 15, pp. 443–448.

Sorokina, N.E., Leshin, V.S., and Avdeev, V.V., (2004). Electrochemical intercalation in the graphite–H_2SO_4 –R(R=CH_3COOH, H_3PO_4) system. *Journal of Physics and Chemistry of Solids*, 65, pp. 185–190.

Steele, D.F., (1990). Electrochemical destruction of toxic organic industrial waste. *Platinum Metals Rev*, 34 (1), pp. 10–14.

Stehling, E.G., Campos, T.A., Brocchi, M., Azevedo, V.A.C., and Silveira, W.D., (2008). The expression of plasmid mediated afimbrial adhesion genes in an avian septicemic Escherichia coli strain. *Journal of Veterinary Science*, 9(1), pp. 75–83.

Stenstrom, T.A., (1989). Bacterial hydrophobicity: an overall parameter for the measurement of adhesion potential to soil particles. *Applied and Environmental Microbiology*, 55 (1), pp. 142–147.

Stoner, G. E., and Cahen, G. L., (1982). The mechanism of low frequency AC electrochemical disinfection. *Bioelectrochem.Bioenerg*, 9(3), pp. 229–243.

Strathmann, H., (1976). Membrane separation processes in advanced wastewater treatment. *Pure & Appl. Chem*, 46, pp. 213–220.

Streat, M., Patrick, J.W., and Perez, M.J.C., (1995). Sorption of phenol and para-chlorophenol from water using conventional and novel activated carbons. *Water Research*, 29 (2), pp. 467–472.

Stuart, B., (1997). *Biological applications of infrared spectroscopy*. UK: John Wiley and Sons.

Stuart, B., (2005). *Infrared Spectroscopy*. Kirk-Othmer Encyclopedia of Chemical Technology.

Suffet, I. H., (1980). An evaluation of activated carbon for drinking water treatment: a national academy report. *J. Am. Water Works Assoc*, 72, pp. 41–50.

Sutikno, T., and Himmeistein, K.J., (1983). Desorption of phenol from activated carbon by solvent regeneration. *Ind. Eng. Chem. Fundam*, 22 (4), pp. 420–425.

Szabo, T., Szeri, A., Dekany, I., (2005). Composite graphitic nanolayers prepared by self-assembly between finely dispersed graphite oxide and a cationic polymer. *Carbon*, 43, pp. 87–94.

Szpyrkowicz, L., Naumczyk, J., and Zilio-Grandi, F., (1996). Electrochemical treatment of tannery wastewater using Ti/Pt and Ti/Pt/Ir electrodes, *Water Research*, 29(2), pp. 517–524

Tahar, N.B., Abdelhedi, R., and Savall, A., (2009). Electrochemical polymerisation of phenol in aqueous solution on a Ta/PbO_2 anode. *J Appl Electrochem*, 39, pp. 663–669.

Tahar, N.B., and Savall, A., (1998). Mechanistic aspects of phenol electrochemical degradation by oxidation on a Ta/PbO_2 anode. *J. Electrochem. Soc*, 145(10), pp. 3427–3434.

Tan, T.C., and Teo, W.K., (1987). Combined effect of carbon dosage and initial adsorbate concentration on the adsorption isotherm of heavy metals on activated carbon. *Water Research*, 21 (10), pp. 1183–1188.

Tate, D., Mawer, S., and Newton, A., (2003). Outbreak of pseudomonas aeruginosa folliculitis associated with a swimming pool inflatable. *Epidemiology and Infection*, 130 (2), pp. 187–192.

Taylor and Butler, M., (1982). A comparison of the virucidal properties of chlorine, chlorine dioxide, bromine chloride and iodine. *J. Hyg., Camb*, 89, pp. 321–328.

Technology Review (2007). Membrane Technology: Removing contaminants in wastewater. *Filtration and Separation*, 44 (7), pp. 14–16.

Tennakoon, C.L.K, Bhardwaj, R.C., and Bockris, J.O., (1996). Electrochemical treatment of human wastes in a packed bed reactor. *Journal of Applied Electrochemistry*, 26, pp. 18–29.

Tessmer, C.H., Vidic, R.D., and Uranowski, L.J., (1997). Impact of oxygen-containing surface functional groups on activated carbon adsorption of phenols. *Environ. Sci. Technol*, 31, pp. 1872–1878.

Tiesler, E., (1985). Method and device for treatment of water, Deutsche Patent 3,527,733.

Toledo, L.C., Silva, A.C.B., Augusti, R., and Lago, R.M., (2003). Application of Fenton's reagent to regenerate activated carbon saturated with organochloro compounds. *Chemosphere*, 50, pp. 1049–1054.

Toyoda, M., Aizawa, J., and Inagaki, M., (1998). Sorption and recovery of heavy oil by using exfoliated graphite. *Desalination*, 115, pp. 199–201.

Toyoda, M., and Inagaki, M., (2000). Heavy oil sorption using exfoliated graphite: new application of exfoliated graphite to protect heavy oil pollution. *Carbon*, 38, pp. 199–210.

Toyoda, M., Nishib, Y., Iwashitab, N., and Inagaki, M., (2002). Sorption and recovery of heavy oils using exfoliated graphite. Part IV: Discussion of high oil sorption of exfoliated graphite. *Desalination*, 15, pp. 139–144.

Toyoda, M., Nishib, Y., Iwashitab, N., and Inagaki, M., (2002). Sorption and recovery of heavy oils using exfoliated graphite Part IV: discussion of high oil sorption of exfoliated graphite. *Desalination*, 151, pp. 139–144.

Troster, I., Fryda, M., Herrmann, D., Schafer, L., Hanni, W., Perret, A., Blaschke, M., Kraft, A., and Stadelmann, M., (2002). Electrochemical advanced oxidation process for water treatment using DiaChem® electrodes. *Diamond and Related Materials*, 11, pp. 640–645.

Tryba, B., Przepiorski, J., and Morawski, A.W., (2002). Influence of chemically prepared H_2SO_4-graphite intercalation compound (GIC) precursor on parameters of exfoliated graphite (EG) for oil sorption from water. *Letters to the editor/Carbon*, 41, pp. 2009 –2025.

Valster, R.M., Wullings, B.A., Bakker, G., Smidt, H., and Kooij, D.V.D., (2009). Free-living protozoa in two unchlorinated drinking water supplies identified by phylogenic analysis of 18S rRNA gene sequences. *Appl. Environ. Microbiol*, 75(14), pp. 4736–4746.

Vecitis, C.D., Schnoor, M.H., Rahaman, M.S., Schiffman, J.D., and Elimelech, M., (2011). Electrochemical multiwalled carbon nanotube filter for viral and bacterial removal and inactivation. *Environ. Sci. Technol*, 45, pp. 3672–3679.

Velegraki, T., Balayiannis, G., Diamadopoulos, E., Katsaounis, A., and Mantzavinos, D., (2010). Electrochemical oxidation of benzoic acid in water over boron-doped diamond electrodes: statistical analysis of key operating parameters, kinetic modeling, reaction by-products and ecotoxicity. *Chemical Engineering Journal*, 160, pp. 538–548.

Venczel, L.V., Arrowood, M., Hurd, M., and Sobsey, M.D., (1997). Inactivation of cryptosporidium parvum oocysts and clostridium perfringens spores by a mixed-oxidant disinfectant and by free chlorine. *Applied and Environmental Microbiology*, pp. 1598–1601.

Vlyssides, A., Barampouti, E.M., and Mai, S., (2004). Degradation of methylparathion in aqueous solution by electrochemical oxidation. *Environ. Sci. Technol*, 38, pp. 6125–6131.

Vlyssides, A.G., Karlis, P.K., and Zorpas, A.A., (1999). Electrochemical oxidation of noncyanide strippers wastes, *Environment International*, 25(5), pp. 663–670.

Walsh, F.C., (2001). Electrochemical technology for environmental treatment and clean energy conversion. *Pure Appl. Chem*, 73(12), pp. 1819–1837.

Wang, G., Sun, Q., Zhang, Y., Fan, J., Ma, L., (2010). Sorption and regeneration of magnetic exfoliated graphite as a new sorbent for oil pollution. *Desalination*, 263, pp. 183–188.

Wang, H.L., and Jiang, W.F., (2007). Adsorption of Dinitro Butyl Phenol (DNBP) from Aqueous Solutions by Fly Ash. *Ind. Eng. Chem. Res*, 46, 5405–5411.

Watts, R.J., Kong, S., Orr, M.P., Miller, G.C and Henry, B.E., (1995). Photocatalytic inactivation of coliform bacteria and viruses in secondary wastewater effluent. *Water Research*, 29 (1), pp. 95–100.

Weaver, J.C., and Chizmadzhev, Y.A., (1996). Theory of electroporation: a review. *Bioelectrochem Bioener*. 41 (2), pp. 135–160.

Weber, J.W., Jr., Pirbazari, M., and Melson, G.L., (1978). Biological growth on activated carbon: an investigation by scanning electron microscopy. *Environ. Sci. Technol*, 12 (7), pp. 817–819.

White, G.C., (2010). *White's handbook of chlorination and alternative disinfectants*. 5th edition. New Jersey: John Wiley & Sons, Inc.

WHO, (1992). *Our planet, our health. Report of WHO Commission on Health and Environment*. World Health Organization, Geneva

Wilcox, D.P., Chang, E., Dickson, K.L., and Johansson, K.R., (1983). Microbial growth associated with granular activated carbon in a pilot water treatment facility. *Appl. Environ. Microbiol*, 46 (2), pp. 406–416.

Wise, A.A and Kuske, C.R, (2000). Generation of novel bacterial regulatory proteins that detect priority pollutant phenols. *Applied and Environmental Microbiology*, pp. 163–169.

Wu, C., Liu, X., Wei, D., Fan, J., and Wang, L., (2001). Photosonochemical degradation of phenol in water. *Water Research*, 35 (16), pp. 3927–3933.

Wu, S., Zhao, X., Shen, H., Wang, Q., and Zhao, Z.K., (2011). Microbial lipid production by Rhodosporidium toruloides under sulfate-limited conditions. *Bioresource Technology*, 102, pp. 1803–1807.

Wu, Z., and Zhou, M., (2001). Partial degradation of phenol by advanced electrochemical oxidation process. *Environ. Sci. Technol*, 35, pp. 2698–2703.

Xiong, Y., He, C., An, T., Zhu, X., and Karlsson, H.T., (2003). *Water, Air, and Soil Pollution*, 144, pp. 67–79.

Yakovlev, A.V., Finaenov, A.I., Yakovleva, E.V., and Finaenova, E.V., (2004). Use of thermally expanded graphite in water-purification and water-treatment systems. *Russian Journal of Applied Chemistry*, 77 (11), pp. 1815–1817.

Yasuda, E., Inagaki, M., Kaneko, K., Oya, M.E.A., and Tanabe, Y., (2003). *Carbon alloys: novel concepts to develop carbon science and technology*. UK: Elsevier Science Ltd.

Yavuz, Y., and Koparal, A.S., (2006). Electrochemical oxidation of phenol in a parallel plate reactor using ruthenium mixed metal oxide electrode. *Journal of Hazardous Materials B136,* pp. 296–302.

Yeon, K.-H., Song, J.-H., and Moon, S.-H., (2004). A study on stack configuration of continuous electrodeionization for removal of heavy metal ions from the primary coolant of a nuclear power plant. *Water Research,* 38, pp. 1911–1921.

Yoon, J.-H., Yang, J.E., Shim, Y.-B., and Won, M.-S., (2007). Electrochemical degradation of benzoquinone in a flow through cell with carbon fibers. *Bull. Korean Chem. Soc*, 28(3), pp. 403–407.

Yue, X., Zhang, R., Wang, H., and Zhang, F., (2009). Sorption and decomposition of crude oil using exfoliated graphite/ZnO composites. *Journal of Physics and Chemistry of Solids,* 70, pp.1391–1394.

Zanoni, M.V.B., Sene, J.J., Selcuk, H., and Anderson, M.A., (2004). Photoelectrolytic production of active chlorine on nanocrystalline titanium dioxide thin film electrodes. *Environ. Sci. Technol*, 38, pp. 3203–3208.

Zareie, M.H., Korbahti, B.K., and Tanyolac, A., (2001). Non-passivating polymeric structures in electrochemical conversion of phenol in the presence of NaCl. *Journal of Hazardous Materials*, B87, pp. 199–212.

Zareie, M.H., Korbahti, B.K., Tanyolac, A., (2001). Non-passivating polymeric structures in electrochemical conversion of phenol in the presence of NaCl. *Journal of Hazardous Materials*, 87, pp. 199–212.

Zemann, A., and Volgger, D., (1997). Separation of priority pollutant phenols with coelectroosmotic capillary electrophoresis. *Anal. Chem*, 69, pp. 3243–3250.

Zhan, X.M., Wang, J.L., Weno, X.H., and Qian, Y., (2001). Indirect electrochemical treatment of saline dyestuff wastewater. *Environmental Technology*, 22, pp. 1105–1111.

Zhang, H., (2002). Regeneration of exhausted activated carbon by electrochemical method. *Chemical Engineering Journal*, 85, pp. 81–85.

Zhang, H., Ye, L., and Zhong, H., (2002). Regeneration of phenol-saturated activated carbon in an electrochemical reactor. *Journal of Chemical Technology and Biotechnology*, 77, pp. 1246–1250.

Zhang, K., Cheung, W.H., and Valix, M., (2005). Roles of physical and chemical properties of activated carbon in the adsorption of lead ions. *Chemosphere*, 60, pp. 1129–1140.

Zhao Z.G., and Gu, X. R., (1989). Adsorption of polyethylene glycols, polypropylene glycol and polyoxyethylene-polyoxypropylene block co-polymers on solid-liquid interfaces. *Acta Phys Chim Sci*, 5, pp. 185–189.

Zhao, M., and Liu, P., (2009). Adsorption of methylene blue from aqueous solutions by modified expanded graphite powder. *Desalination*, 249, pp. 331–336.

Zheng, Y.-P., Wang, H.-N., Kang, F.-Y., Wang, L.-N., Inagaki, M., (2004). Sorption capacity of exfoliated graphite for oils-sorption in and among worm-like particles. *Carbon*, 42, pp. 2603–2607.

Zhou, M., and Lei, L., (2006). The role of activated carbon on the removal of p-nitrophenol in an integrated three-phase electrochemical reactor. *Chemosphere*, 65, pp. 1197–1203.

Zhou, M., Dai, Q., Lei, L., Ma, C., and Wang, D., (2005). Long life modified lead dioxide anode for organic wastewater treatment: electrochemical characteristics and degradation mechanism. *Environ. Sci. Technol*, 39, pp. 363–370.

APPENDIX A

GC/MS spectra of phenol and its oxidation products

This appendix provides the GC/MS spectra of standard samples of phenol and its main oxidation products including p-benzoquinone, 4-chlorphenol, 2,4-dichlorphenol and 2,4,6-trichlorphenol. In addition, GC/MS spectra of some of the samples taken during electrochemical regeneration of phenol loaded GIC adsorbent are provided.

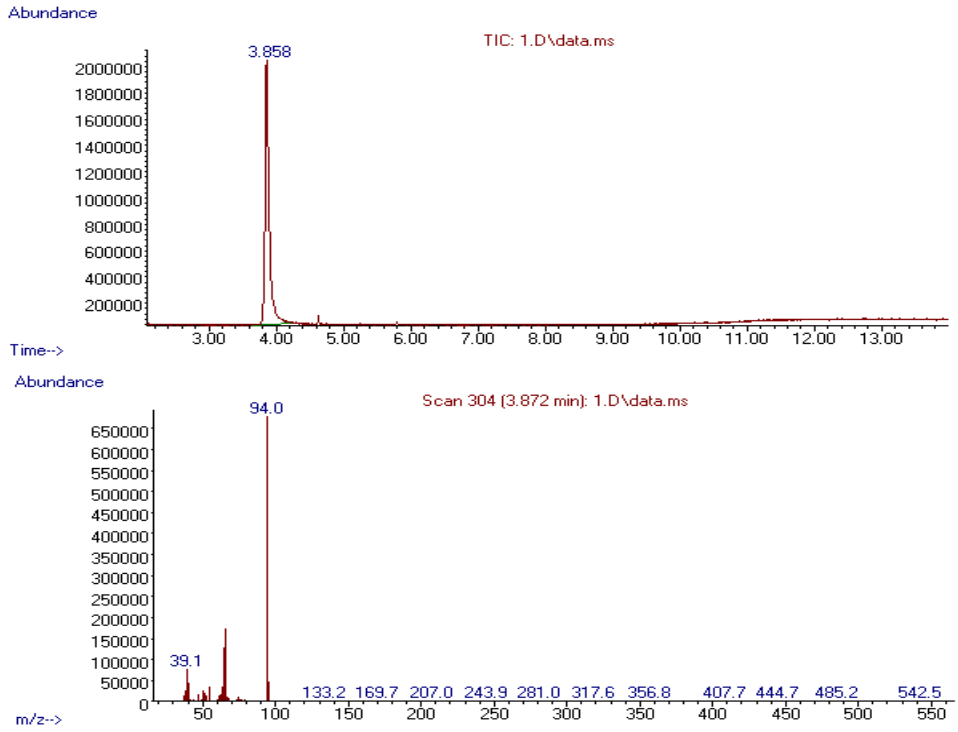

Figure A.1: *GC/MS spectrum of phenol*

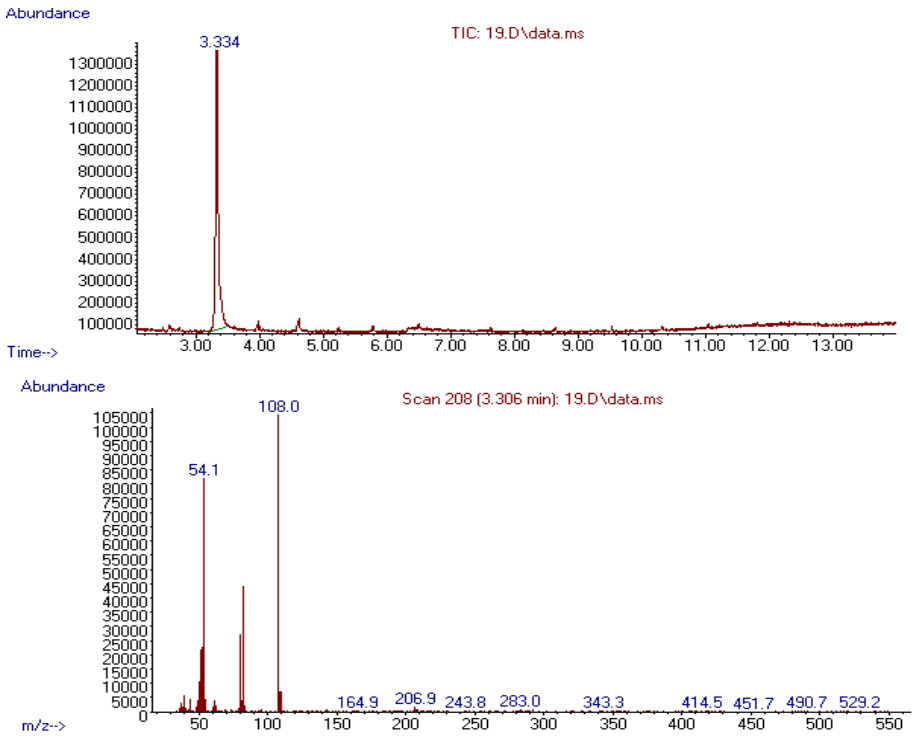

Figure A.2: *GC/MS spectra of p-benzoquinone*

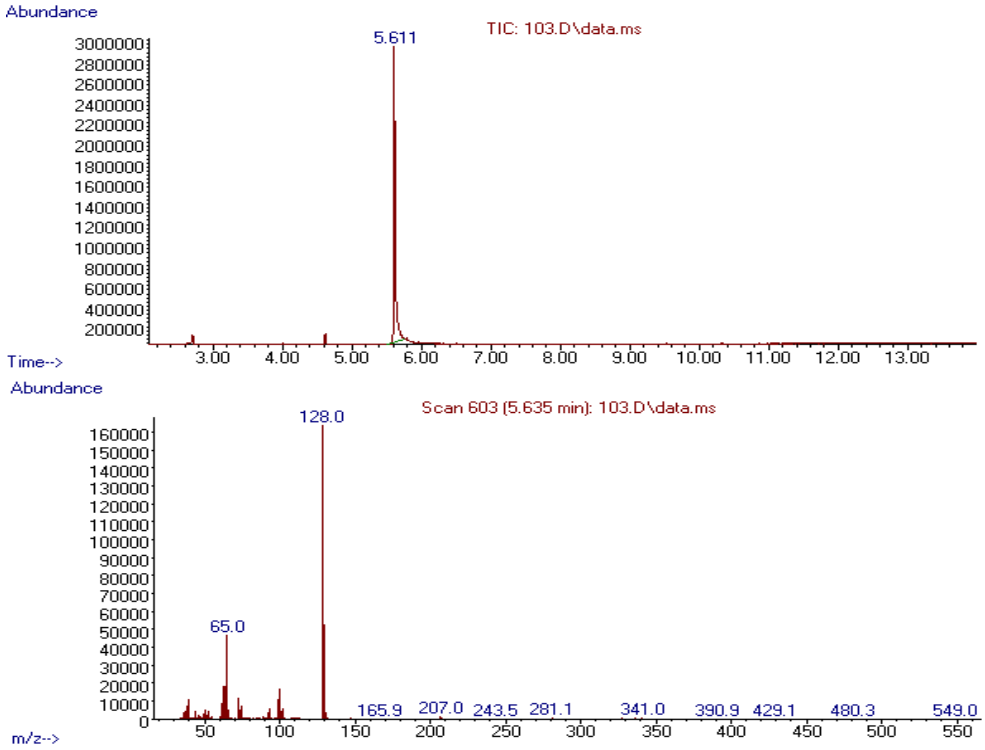

Figure A.3: *GC/MS spectra of 4-chlorophenol*

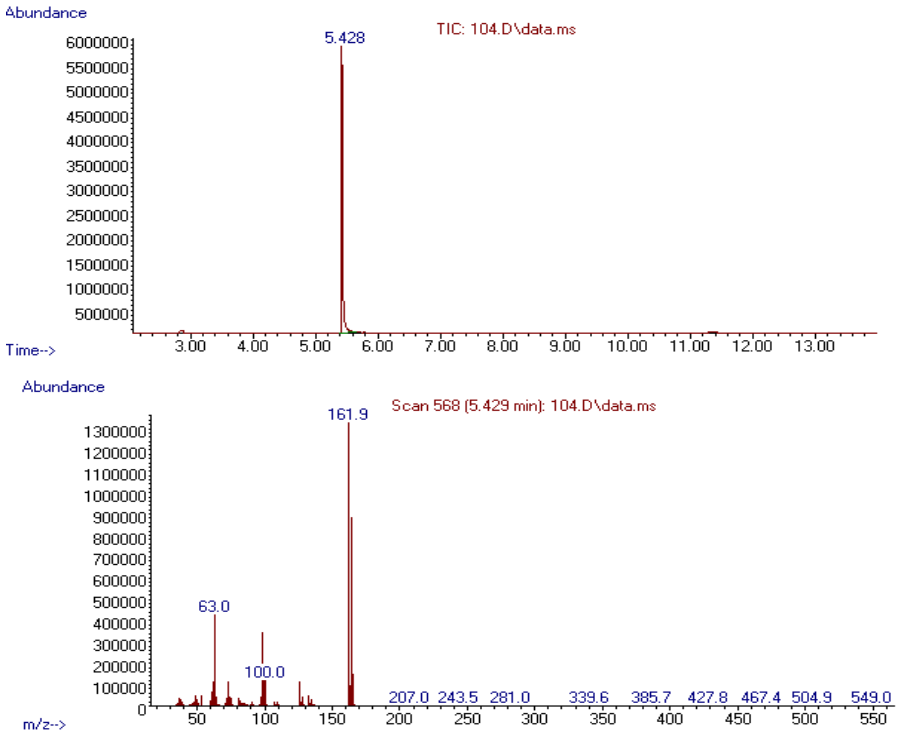

Figure A.4: *GC/MS spectra of 2,4-dichlorphenol*

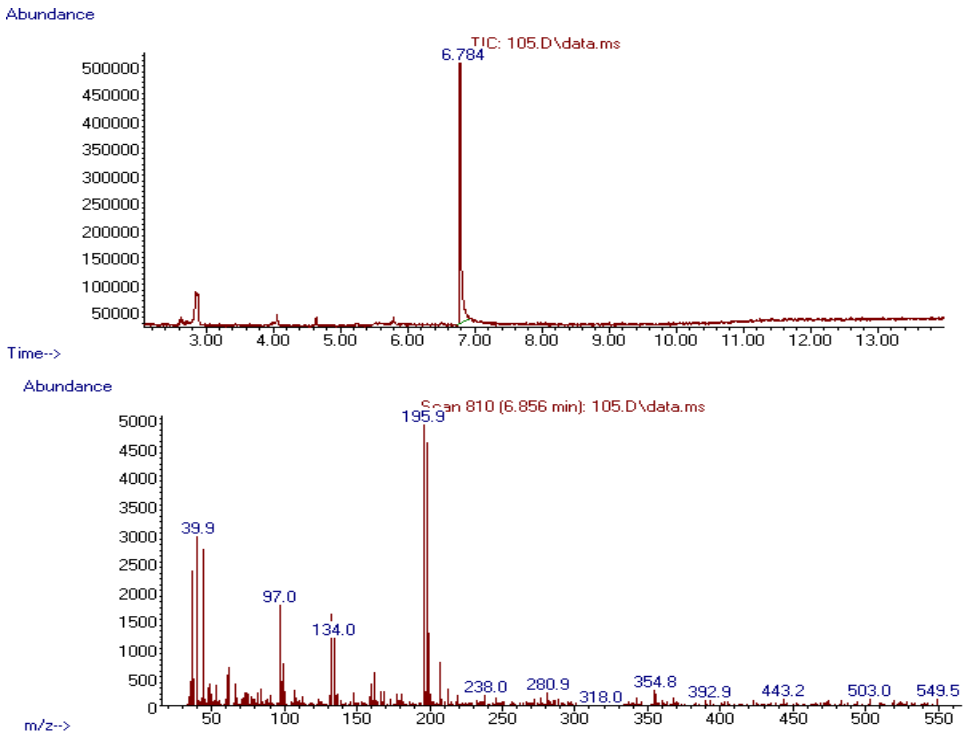

Figure A.5: *GC/MS spectra of 2,4,6-trichlorphenol*

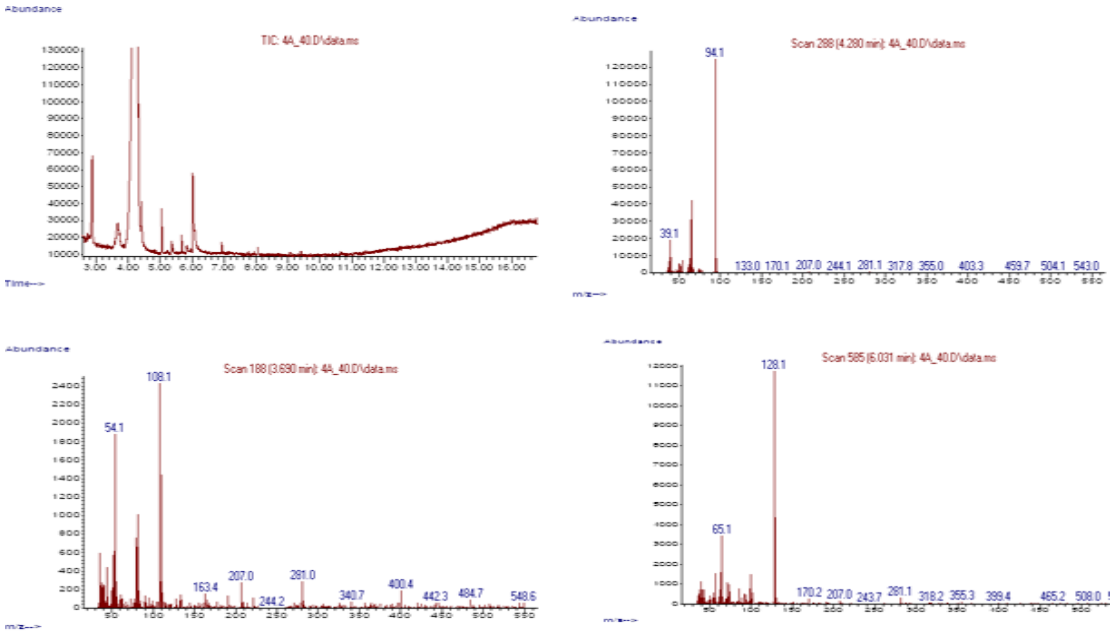

Figure A.6: *GC/MS spectra of solution obtained during electrochemical regeneration of phenol loaded GIC adsorbent in batch electrochemical cell at a current of 0.5 A (corresponding to current density of 20 mA cm^{-2}) for 20 min. Upper left (chromatogram); upper right (mass spectrum of phenol); lower left (mass spectrum of p-benzoquinone) and lower right (mass spectrum of 4-chlorophenol).*

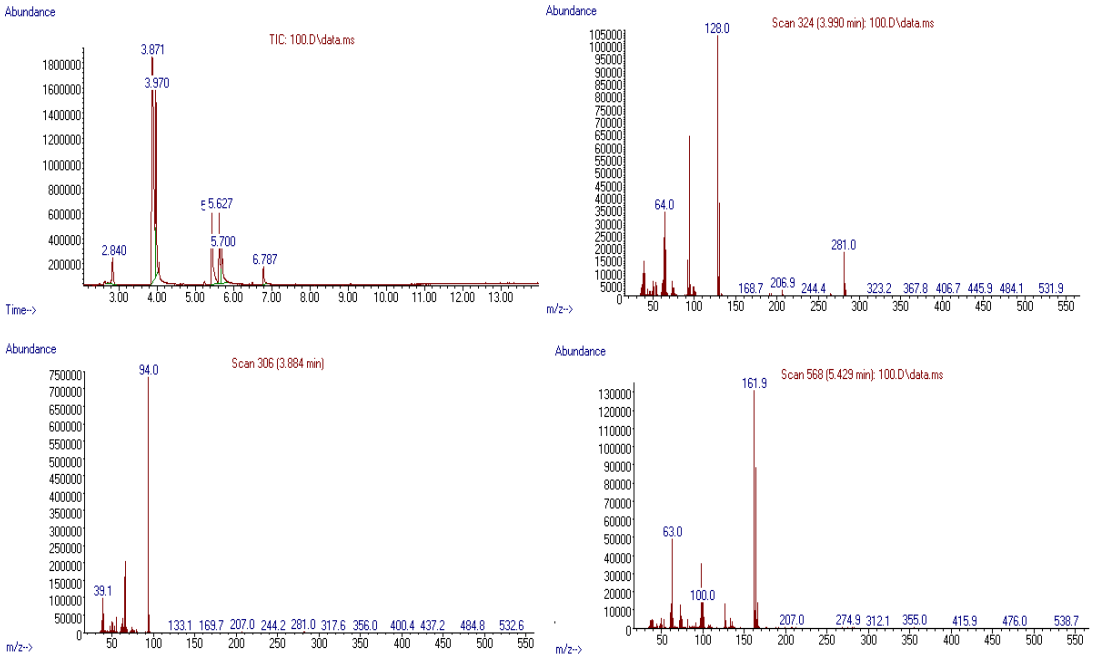

Figure A.7: *GC/MS obtained during electrochemical oxidation of phenol solution (100 mg L^{-1}) containing 0.5% Na_2SO_4 in batch electrochemical cell without GIC adsorbent at a current of 0.5 A (corresponding to current density of 20 mA cm^{-2}) for 20 min. The catholyte was 0.3% NaCl solution acidified with HCL. Upper left (chromatogram); upper right (mass spectrum of 2-chlorphenol); lower left (mass spectrum of phenol) and lower right (mass spectrum of 2,4-dichlorphenol).*

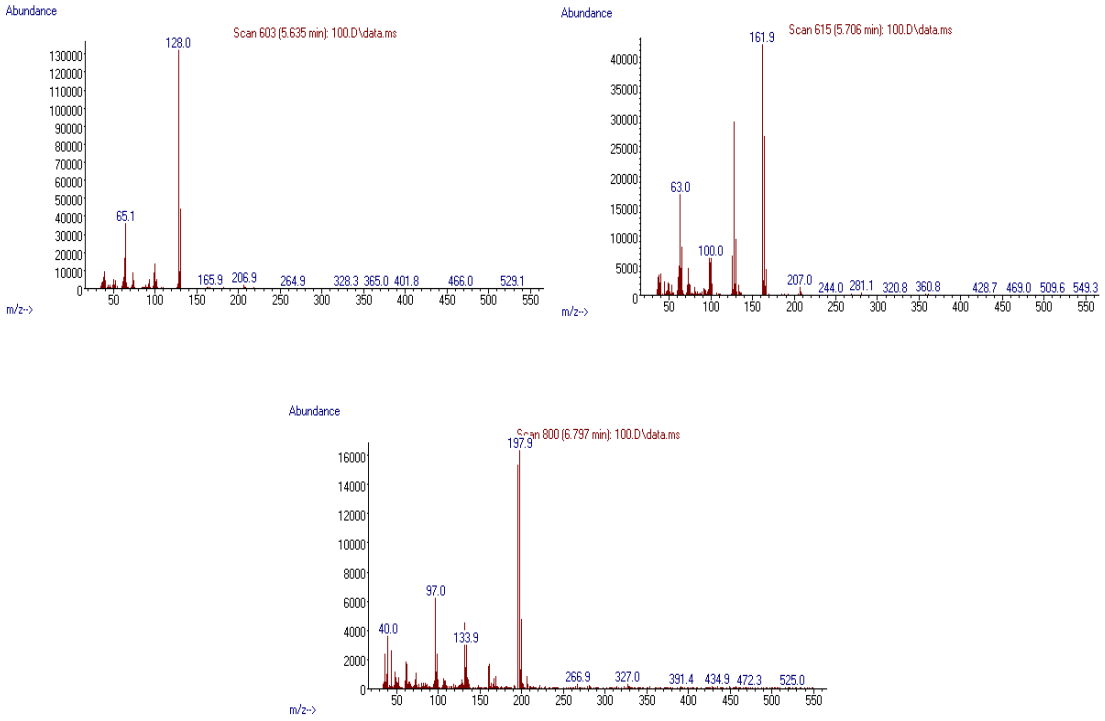

Figure A.8: *GC/MS obtained during electrochemical oxidation of phenol solution (100 mg L^{-1}) containing 0.5% Na_2SO_4 in batch electrochemical cell without GIC adsorbent at a current of 0.5 A (corresponding to current density of 20 mA cm^{-2}) for 20 min. The catholyte was 0.3% NaCl solution acidified with HCL. Upper left (4-chlorphenol); upper right (mass spectrum of 2,6-dichlorphenol); lower (mass spectrum of 2,4,6-trichlorphenol).*

Table A.1*: Elution time of phenol and its oxidation products during GC analysis using a HP-5MS column (Agilent Technologies)*

Compound	***Elute time (min)***
Phenol	3.89
p-benzoquinone	3.33
4-chlorphenol	5.61
2-chlorphenol	3.97
2,4-dichlorphenol	5.42
2,6-dichlorphenol	5.70
2,4,6-trichlorphenol	6.78

APPENDIX B

Surface Analysis Using Various FTIR Techniques

FTIR and ATR

In the literature, the spectra of adsorbates (for example phenol and nitophenol) on activated carbon have been reported using the ATR method *(Mattson et al. 1969).* Preliminary analysis of fresh GIC adsorbent (the material as supplied before it has been used for adsorption) was performed using FTIR-ATR but the spectrum had no features. In a second attempt to obtain a useful spectrum, a few particles of GIC adsorbent were placed onto the ATR crystal and the sample assembly was gently closed. The objective behind this trial was not to allow all of the radiation to be completely absorbed by the GIC particles and to have some refection of IR from the surface. However, this attempt was unsuccessful, and no useful spectral information was obtained from the data. Infrared investigations of carbonaceous materials including carbon blacks, coal chars, activated carbons and graphite have been remained difficult in the past because of intractability of these materials *(Friedle et al., 1971). Friedle and Carrlson, (1971)* were successful in getting two broad bands at 1587 and 1362 cm^{-1} during IR studies of the intensely ground graphite. Grinding of graphite can be difficult because of its lubricating characteristics. The authors succeeded in getting a good IR spectrum after 96 h of graphite grinding in a small reciprocating ball mill. Although the crystallinity of the graphite was lost because of the grinding, the carbon-carbon bonding remained intact. Since the present investigation was focused on evaluating the surface group changes during the electrochemical regeneration of the GIC adsorbent, it was not appropriate to grind the GIC particles at this stage as its surface characteristics could be affected.

The next trial was performed by using a KBr disc without grinding the samples according to the procedure as described in chapter 6 (section 6.3). The results show that there was still no formation of any useful peaks (Figure B1). There appears to be very little difference between the peaks on the spectra of fresh, adsorbed and

regenerated samples (Figure B1). In addition, the detected peaks in the spectra (2500–500 cm^{-1}) also appear to be of small intensities, and these were observed due to the presence of KBr in the samples (Figure B1). Two possible explanations have been proposed for the disappointing results obtained:

- Samples were not ground prior to analysis. The intensive grinding significantly reduces the graphite to minute particles on which infrared measurements were possible *(Friedle and Carrslon, 1971)*
- Very low concentrations of adsorbates were present on the GIC adsorbent surface

The lack of spectral information for the adsorbed and regenerated samples suggests that the concentration of adsorbate on the surface was too low to be detected. Based on the findings it can be concluded that FTIR with KBr disc and ATR are not suitable for studying adsorbed species on GIC adsorbents under the conditions employed for this investigation.

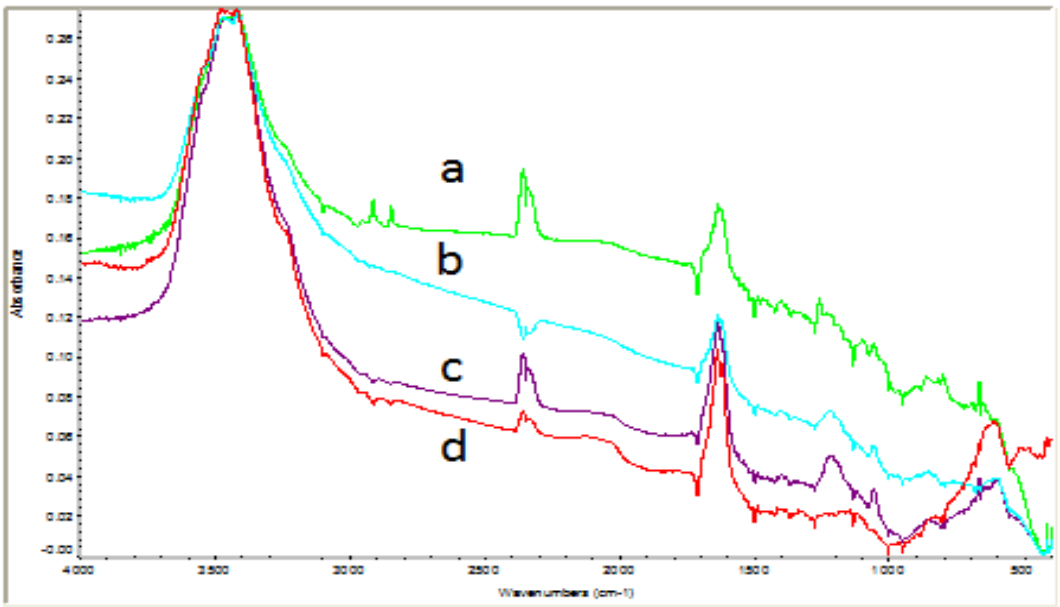

Figure B.1: *FTIR spectra of fresh (a) adsorbed (b) and regenerated GIC adsorbent (c), and KBr disc (d) in the range of 4000–400 cm^{-1} at a resolution of 4 cm^{-1}. Experimental conditions: 100 mg L^{-1} of 500 mL phenol solution was mixed with 130 g of GIC adsorbent for 30 min in the mini-SBR (giving a phenol loading on the adsorbent of around 0.1 mg g^{-1}); Regeneration of the settled adsorbent was carried out at 0.5 A (10 mA cm^{-2}) for 20 min.*

DRIFTS

The DRIFTS technique was applied to investigate the surface of GIC adsorbent during adsorption and electrochemical regeneration while accounting for the two probable causes for the disappointing results obtained from the FTIR studies discussed above.

Adsorption of phenol onto GIC adsorbent was carried out using comparatively high phenol concentrations (500 mg L^{-1}) so that a high adsorbent loading could be attained. The wet samples after adsorption and regeneration were air dried for 24 h. Afterwards, the samples were ground down to <300 μm in an agate mortar and mixed with KBr using the procedure as described in chapter 6 (section 6.3). The DRIFTS spectrum of phenol loaded adsorbent showed no bands as shown in figure B.2. This observation could be due to the dark GIC samples because DRIFTS works better with whiter samples *(Mirabella, 1998)*. However, these samples were diluted with KBr before their analysis using DRIFTS. For phenol, it is expected to have a peak for O–H stretch in between 3600–3100 cm^{-1} and in between 1300–1000 cm^{-1} for C–O stretch. Diffuse reflectance FTIR is preferable to avoid the problems caused by sample dilution *(Figueriredo et al. 1999)*. An important characteristic of diffuse reflectance of strongly absorbing species is that when a sample is diluted with a nonabsorbing matrix such as KBr the proportion of diffuse reflectance is increased in all the light reflected *(Settle, 1997)*. On the other hand, though relatively high phenol concentrations were used in these experiments, mixing of the adsorbent samples with KBr also dilutes an already small phenol or other organic compound signal. This also explains the low intensity of the spectra shown in figures B2–B4. Similar results were obtained with the regenerated adsorbent samples showing no detectable bands as shown in figures B3–B4. In addition, no band was observed for the fresh GIC adsorbent (data not shown). This could be because infrared spectroscopic methods are usually applied to highly oxidised carbons; otherwise the intensity of the absorption bands is not sufficient to detect *(Figueriredo et al. 1999)*.

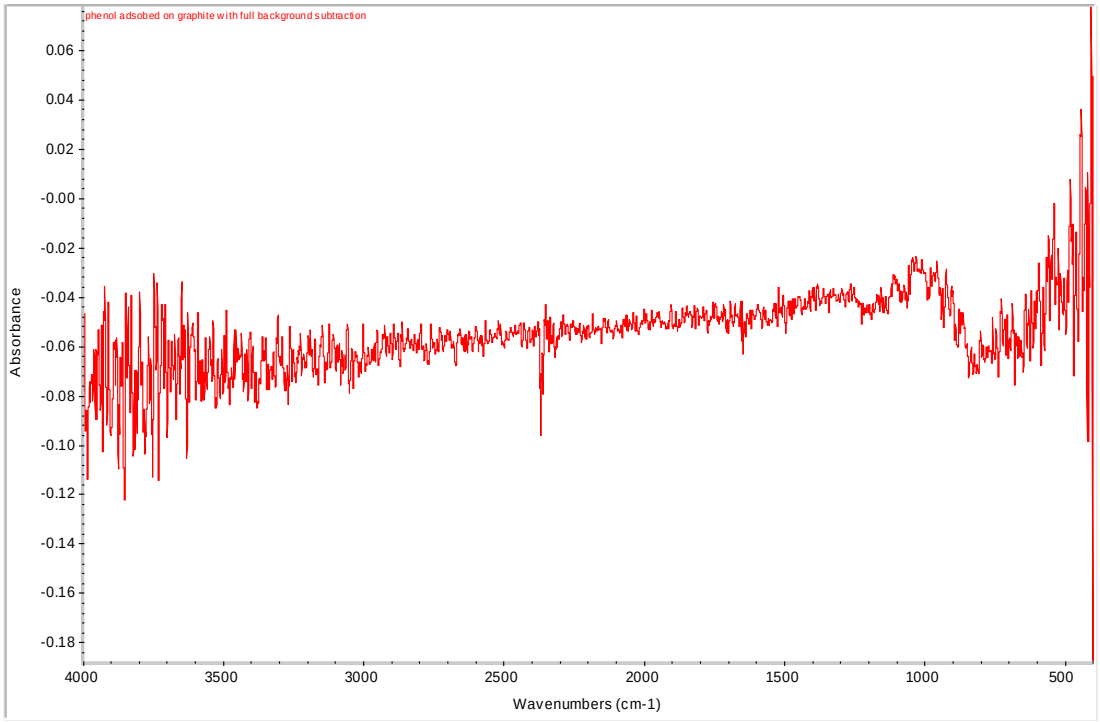

Figure B.2: *DRIFT spectrum of phenol loaded GIC adsorbent with subtraction of KBr and fresh GIC background. Adsorption conditions: 130 g of GIC adsorbent was mixed with 500 mL of 500 mg L^{-1} phenol solution for 30 min; giving an adsorbent loading around 0.28 mg g^{-1}.*

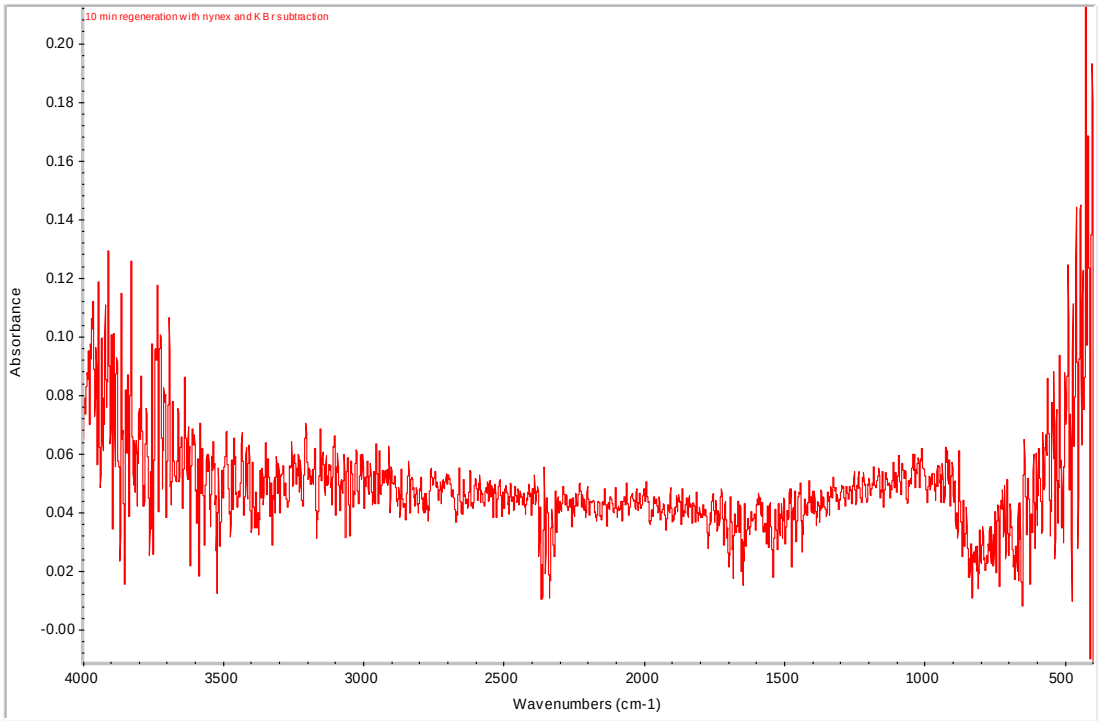

Figure B.3: *DRIFT spectrum of regenerated GIC adsorbent with subtraction of KBr and fresh GIC background. Regeneration conditions: A current of 0.5 A (10 mA cm^{-2}) was applied for 10 min in the mini-SBR.*

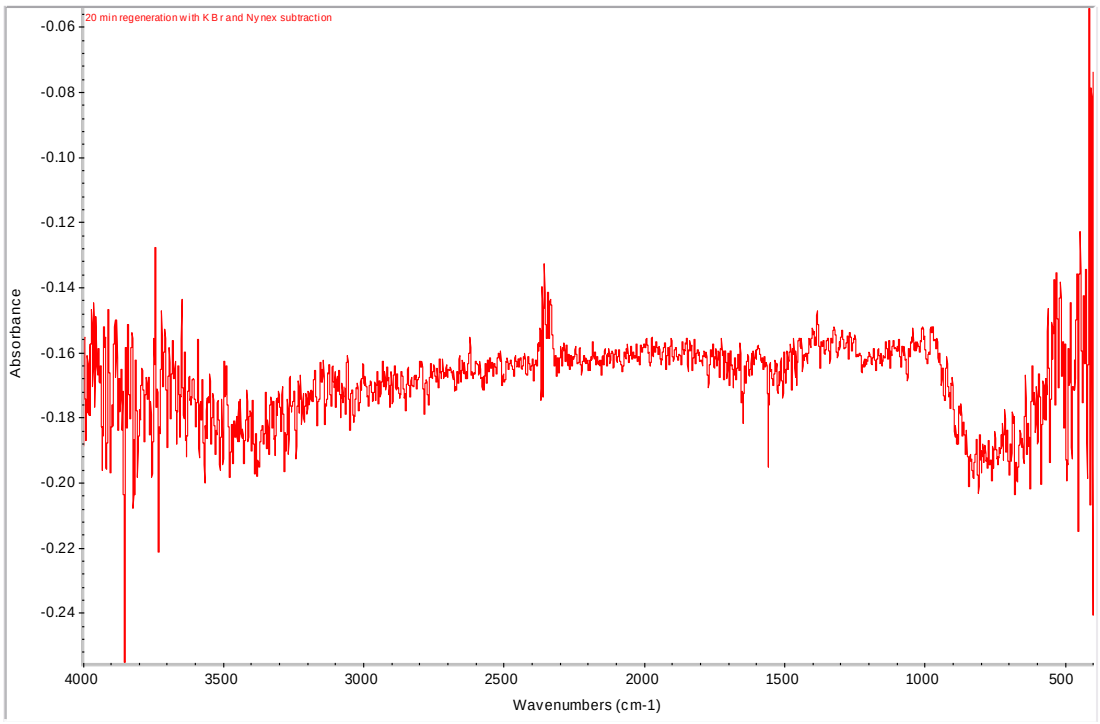

Figure B.4: *DRIFT spectrum of regenerated GIC adsorbent with subtraction of KBr and fresh GIC background. Regeneration conditions: A current of 0.5 A (10 mA cm^{-2}) was applied for 20 min in the mini-SBR.*

Infrared Microscope

Infrared microspectroscopy can be applied to take spectra of samples too small to be analysed by any other means. In addition, contaminant analysis is an important application of infrared microscope *(Smith, 2011)*. Thus, trials were made to analyse the GIC adsorbent samples using this technique.

Figures B5–B7 show the FTIR spectra of fresh, adsorbed and regenerated GIC adsorbent taken using the infrared microscope according to the procedure described in chapter 6 (section 6.3). The first spectrum is for fresh GIC adsorbent that was considered as background for all other samples. The spectrum was not able to detect the presence of any functional groups on the fresh GIC sample; only the usual weak water vapour and CO_2 bands (ca. 2300 cm^{-1} for CO_2; ca. 3800–3600 and ca. 1750–1400 cm^{-1} for water vapours) were observed (Figure B.5). The spectra of the phenol loaded GIC adsorbent and the electrochemically regenerated adsorbent were

very similar (B.6–B.7). The only bands of significance are in the range ca. 1200 and 800 cm^{-1} which suggest the presence of inorganic sulphate or silicate (Figure B.6). However, no such band was observed for fresh GIC adsorbent that could simply be that the signal was too weak to detect. There was no evidence of phenol or any other organic compound. However, two features are worth mentioning. The band at ca. 2300 cm^{-1} is due to atmospheric CO_2 (Figures B.6–B.7). The other feature is a sinusoidal ripple across the spectra. This usually occurs due to reflection from a sample with flat parallel sides. Thus, it can be concluded that infrared microscopy could not detect any surface groups present on GIC adsorbent during adsorption and electrochemical regeneration. This could be due to the small concentrations of adsorbates present on the GIC surface.

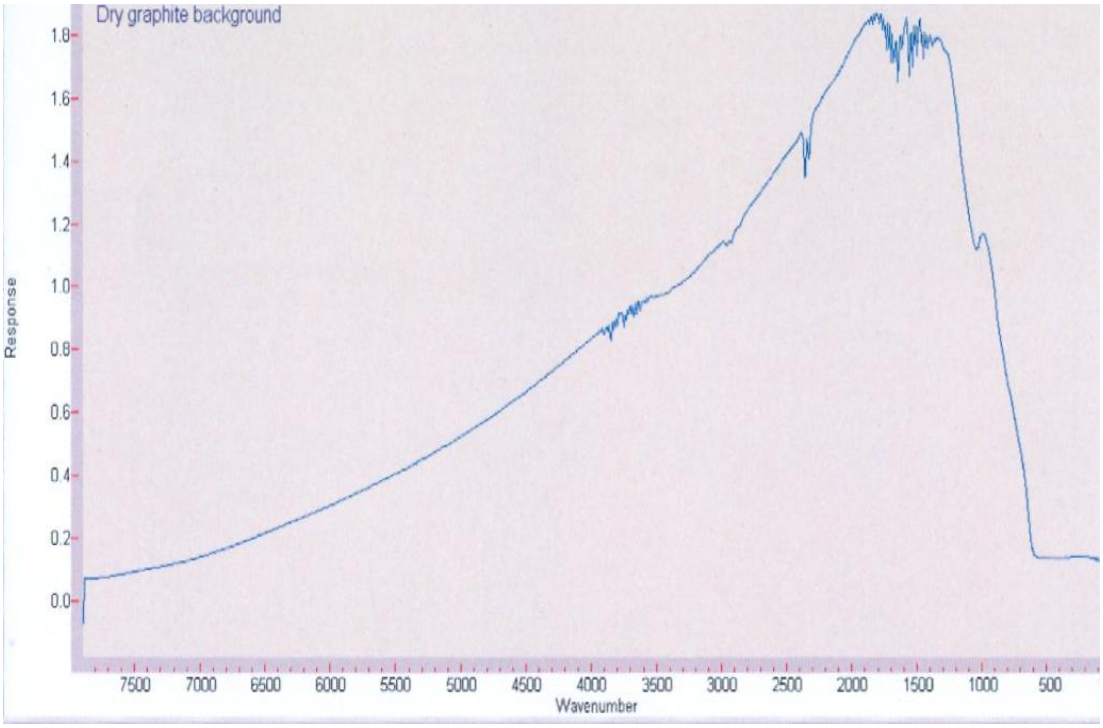

Figure B.5: *FTIR spectrum of fresh GIC adsorbent using infrared microscope in the range of 4000–400 cm^{-1} at a resolution of 4cm^{-1}.*

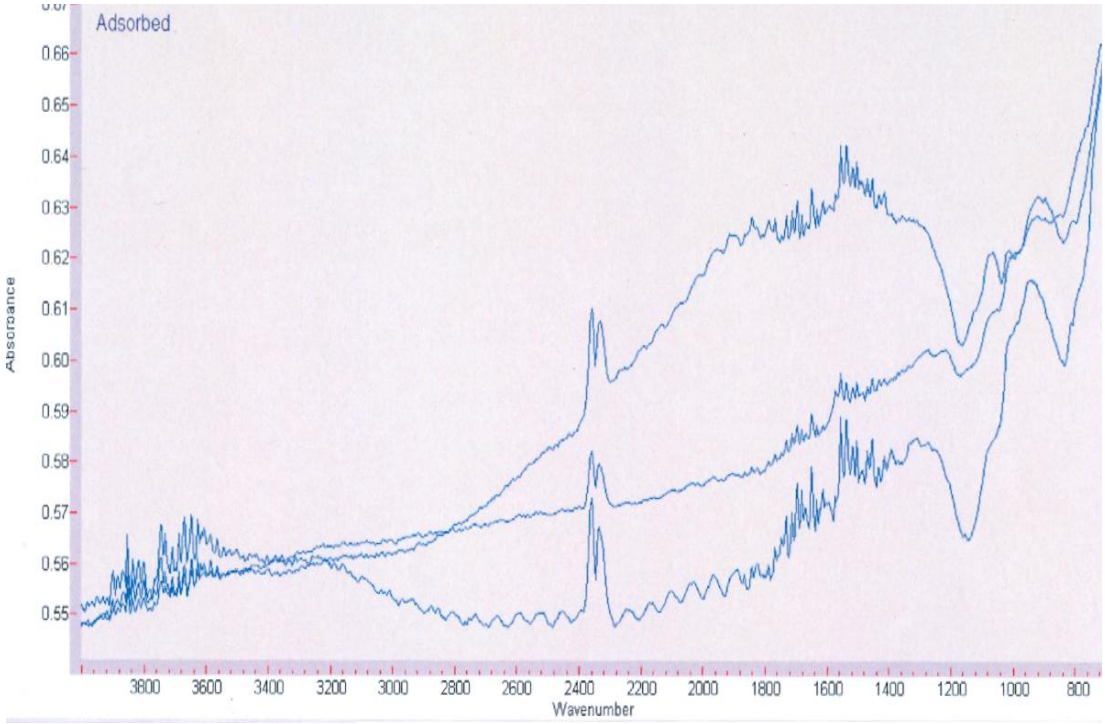

Figure B.6: *FTIR spectra of phenol loaded GIC adsorbent with subtraction of fresh GIC background using infrared microscope. Adsorption conditions: 130 g of GIC adsorbent was mixed with 500 mL of 500 mg L^{-1} phenol solution for 30 min, giving an adsorbent loading: of around 0.28 mg g^{-1}.*

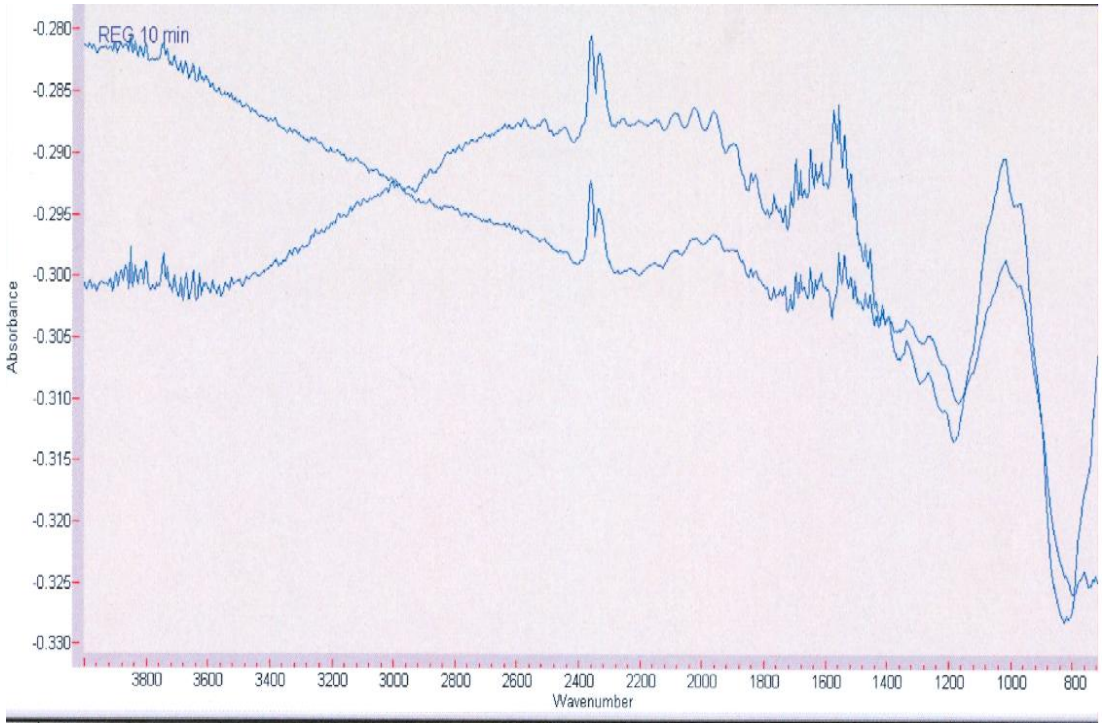

Figure B.7: *FTIR spectra of regenerated GIC adsorbent with subtraction of fresh GIC background using infrared microscope. Adsorption conditions as described in Figure B.6, regeneration current: 1.0 A (20 mA cm^{-2}) applied for 10 min in the mini-SBR.*

APPENDIX C
Application of Freundlich and Langmuir Isotherm Models to Chlorinated Oxidation Products of Phenol

This appendix provides a comparison of the Freundlich and the Langmuir isotherm models with the experimental adsorption data for the chlorinated oxidation products of phenol.

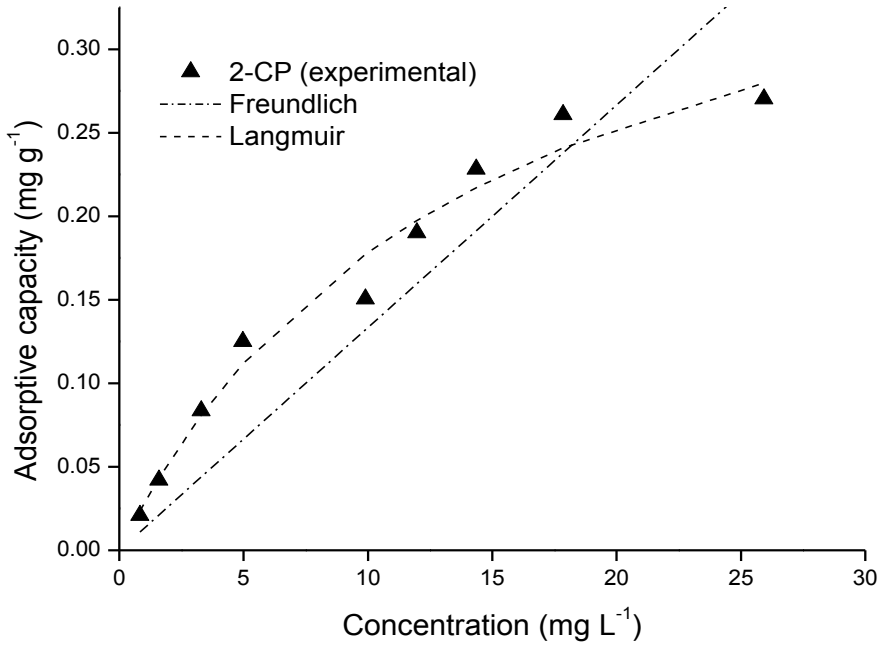

Figure C.1: *The Freundlich and Langmuir isotherm model obtained for the adsorption of 2-CP onto GIC adsorbent*

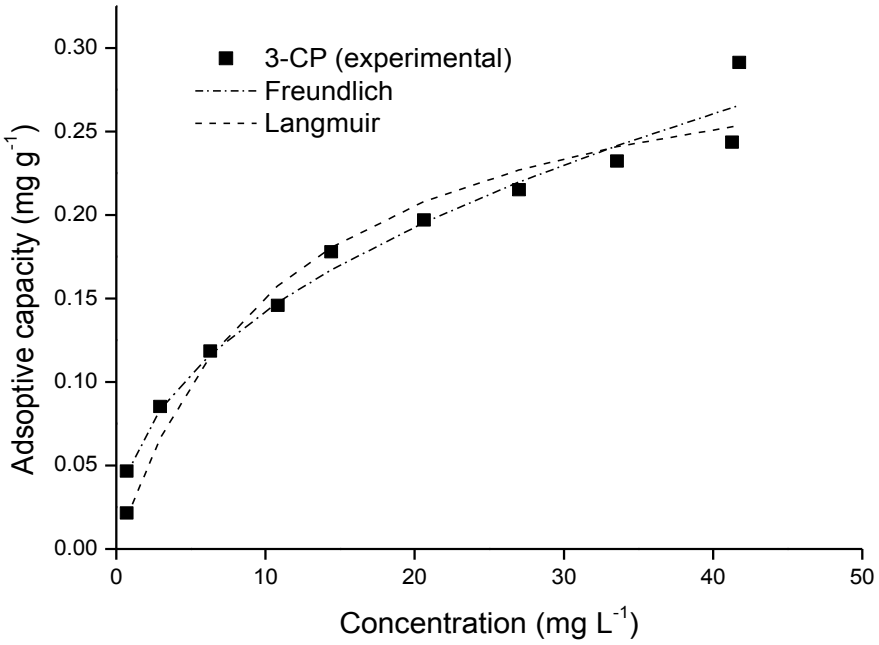

Figure C.2: *The Freundlich and Langmuir isotherm model obtained for the adsorption of 3-CP onto GIC adsorbent*

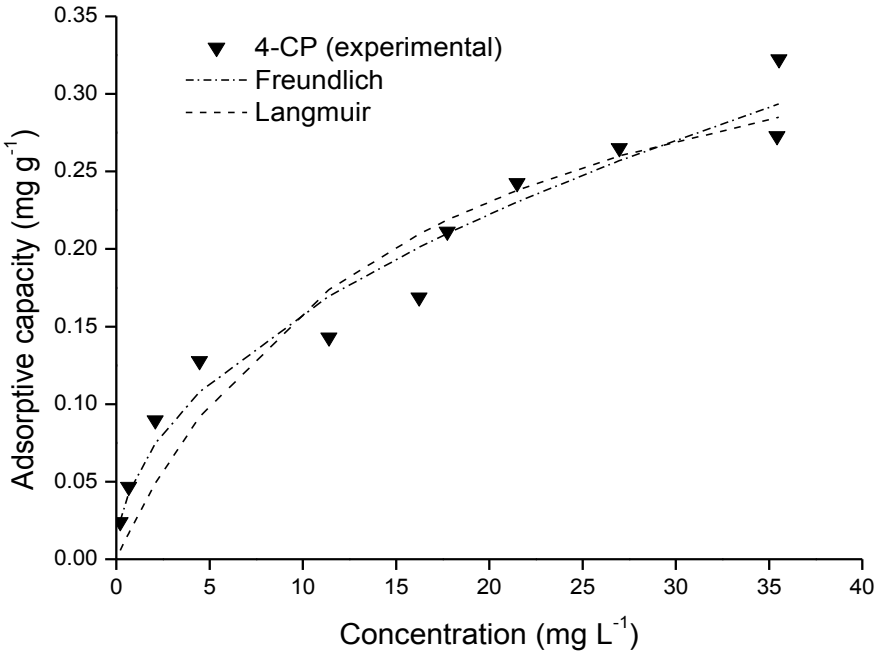

Figure C.3: *The Freundlich and Langmuir isotherm model obtained for the adsorption of 4-CP onto GIC adsorbent*

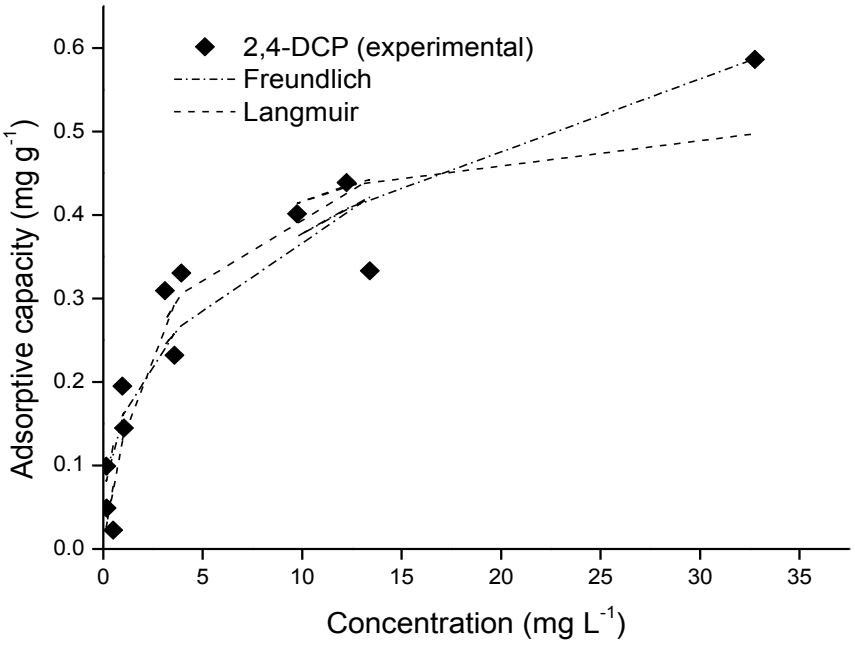

Figure C.4: *The Freundlich and Langmuir isotherm model obtained for the adsorption of 2,4-DCP onto GIC adsorbent*

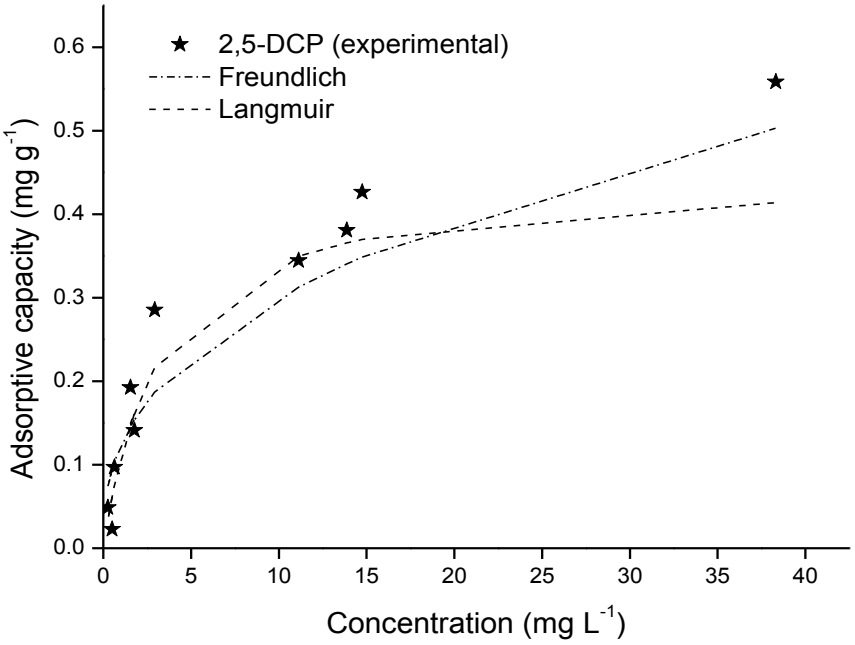

Figure C.5: *The Freundlich and Langmuir isotherm model obtained for the adsorption of 2,5-DCP onto GIC adsorbent*

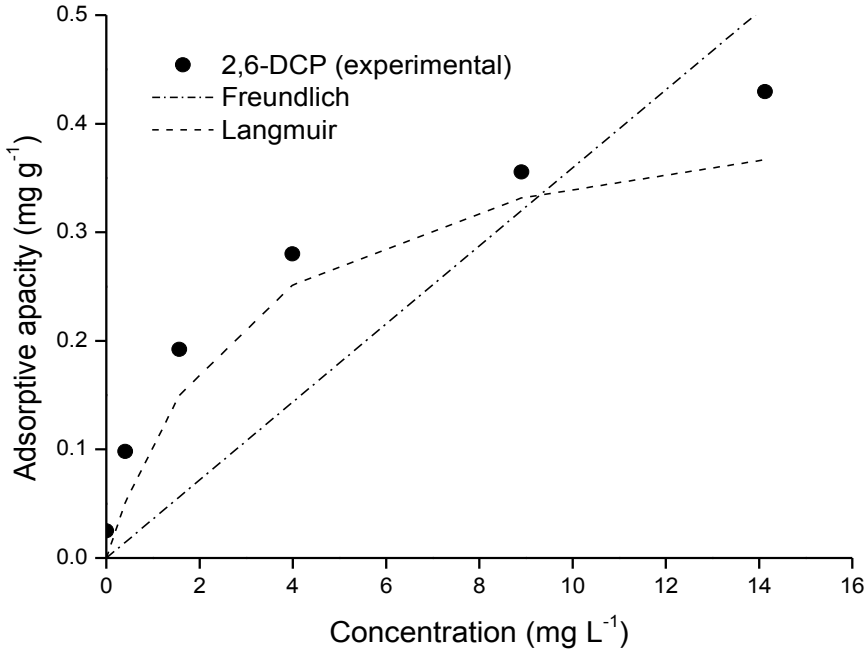

Figure C.6: *The Freundlich and Langmuir isotherm model obtained for the adsorption of 2,6-DCP onto GIC adsorbent*

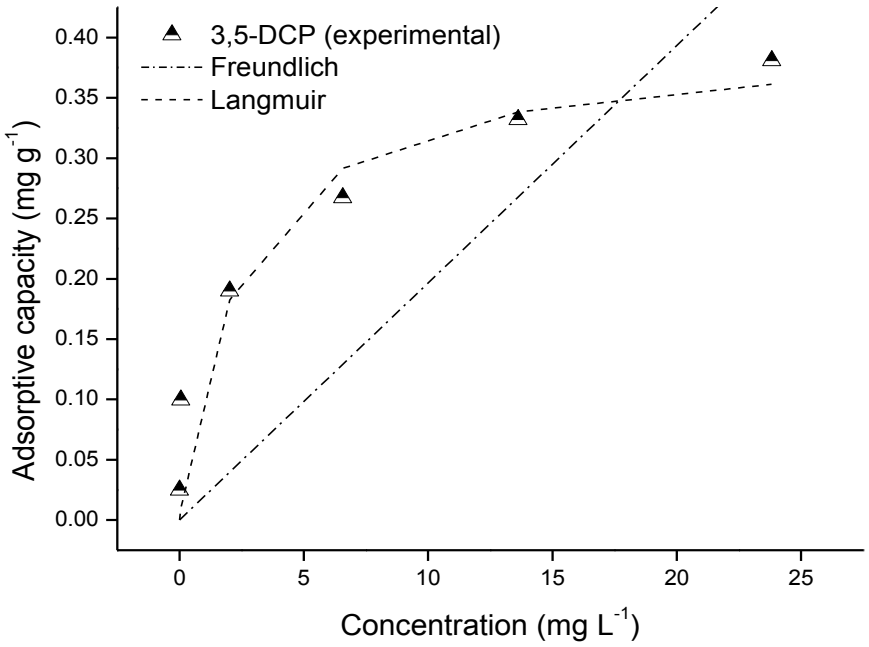

Figure C.7: *The Freundlich and Langmuir isotherm model obtained for the adsorption of 3,5-DCP onto GIC adsorbent*

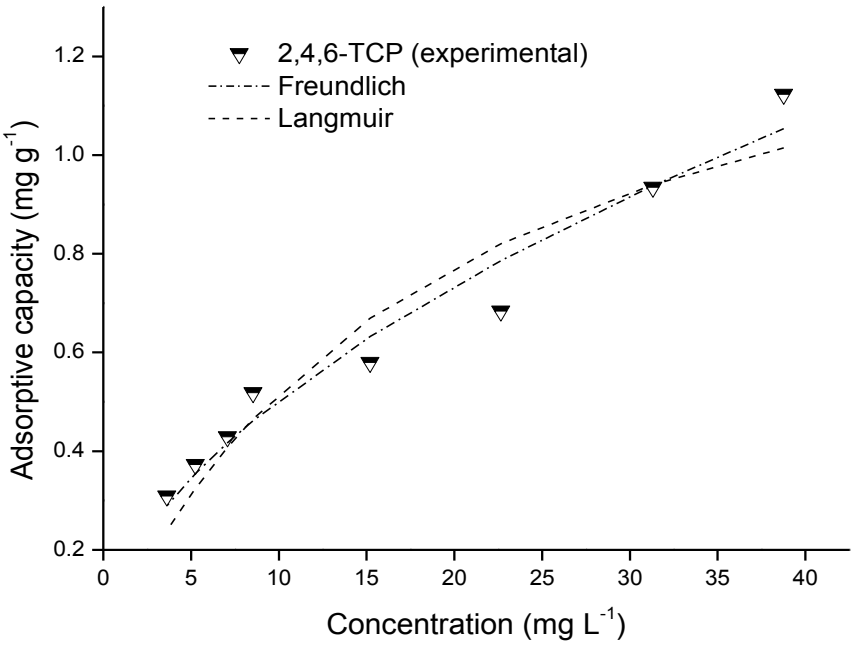

Figure C.8: *The Freundlich and Langmuir isotherm model obtained for the adsorption of 2,4,6-TCP onto GIC adsorbent*

Appendix D
Voltage and pH Data

Table D.1: *Voltage data at the end of the regeneration period over a number of cycles regenerating E. coli loaded GIC adsorbent in phosphate buffer (pH 7.0): Regeneration conditions: Regeneration current of 0.6 A (corresponding to 30 mA cm^{-2}) was applied for 20 min. The catholyte was 0.3% NaCl acidified with HCl.*

Regeneration Cycle	**Regeneration Time (min)**			
	5	**10**	**15**	**20**
	Voltage (V)			
1	15.99	15.45	15.54	15.10
2	15.10	14.20	15.25	15.29
3	15.04	15.27	16.01	15.14
4	14.35	14.61	15.51	15.48
5	14.59	14.46	15.13	14.69

Table D.2: *pH data at the end of the adsorption and regeneration period over a number of cycles for E. coli suspension in phosphate buffer (pH 7.0) with initial concentration of 1.36 × 10^{8} CFU mL^{-1} without the presence of chloride in anolyte, solution volume: 600 mL; adsorbent mass: 150 g; regeneration current of 0.5 A (corresponding to 10 mA cm^{-2}); regeneration time 20 min. The catholyte was 0.3% NaCl acidified with HCl.*

Cycle Number	**pH of the treated water**	
	Adsorption	**Regeneration**
1	7.10	6.70
2	7.03	6.58
3	6.99	6.43
4	6.99	6.62
5	7.01	6.74

Appendix E
Kinetic Data

This appendix provides the kinetic data for S. aureus and P. aeruginosa onto GIC adsorbent.

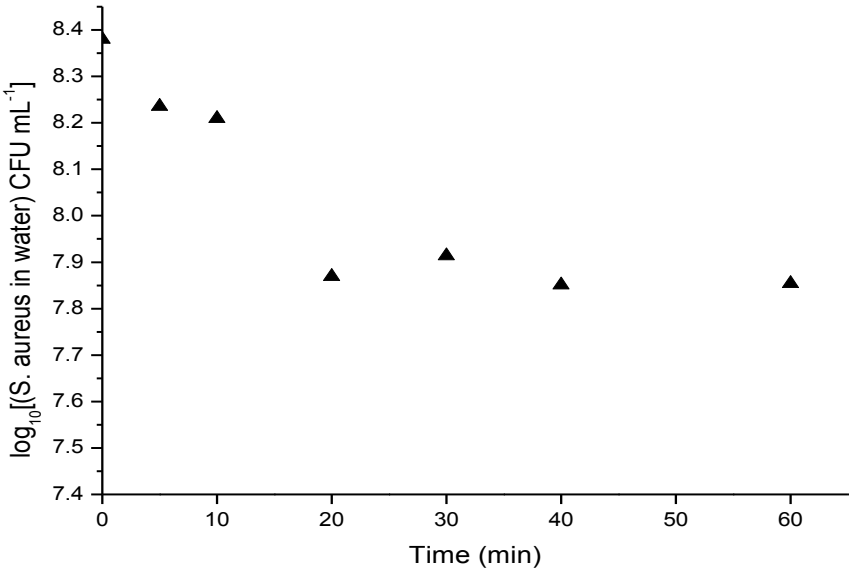

Figure E.1: *Adsorption kinetics of S. aureus onto GIC adsorbent at an initial concentration of 2.4 × 10^8 CFU mL^{-1}, Nyex®1000 dose 200 g L^{-1}*

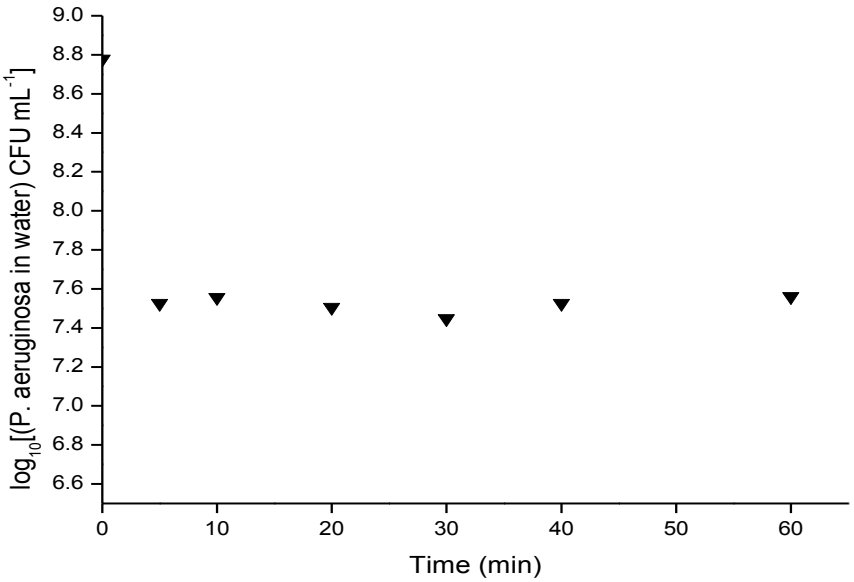

Figure E.2: *Adsorption kinetics of P. aeruginosa onto GIC adsorbent at an initial concentration of 6.0 × 10^8 CFU mL^{-1}, Nyex®1000 dose 100 g L^{-1}*

APPENDIX F
Calibration Curves

This appendix provides HPLC calibration curves for phenol and its oxidation products (chlorinated and non-chlorinated). A calibration curve for free chlorine determination is also provided.

F1. Calibration curves for phenol and aromatic oxidation products (non-chlorinated)

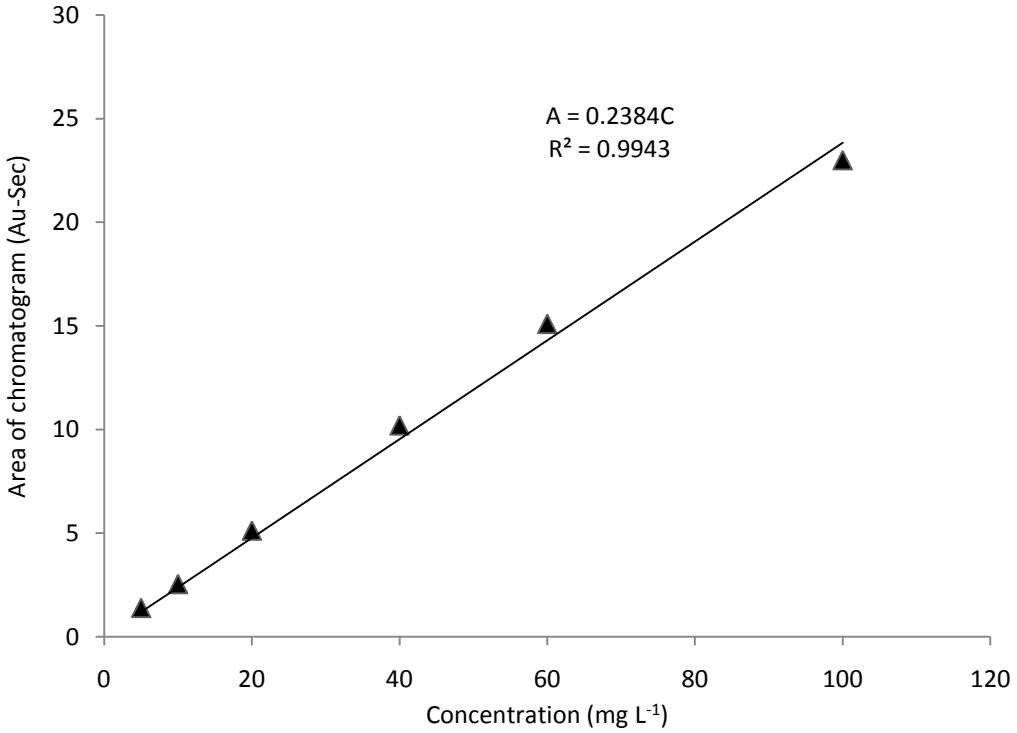

Figure F.1: *Calibration curve for phenol*

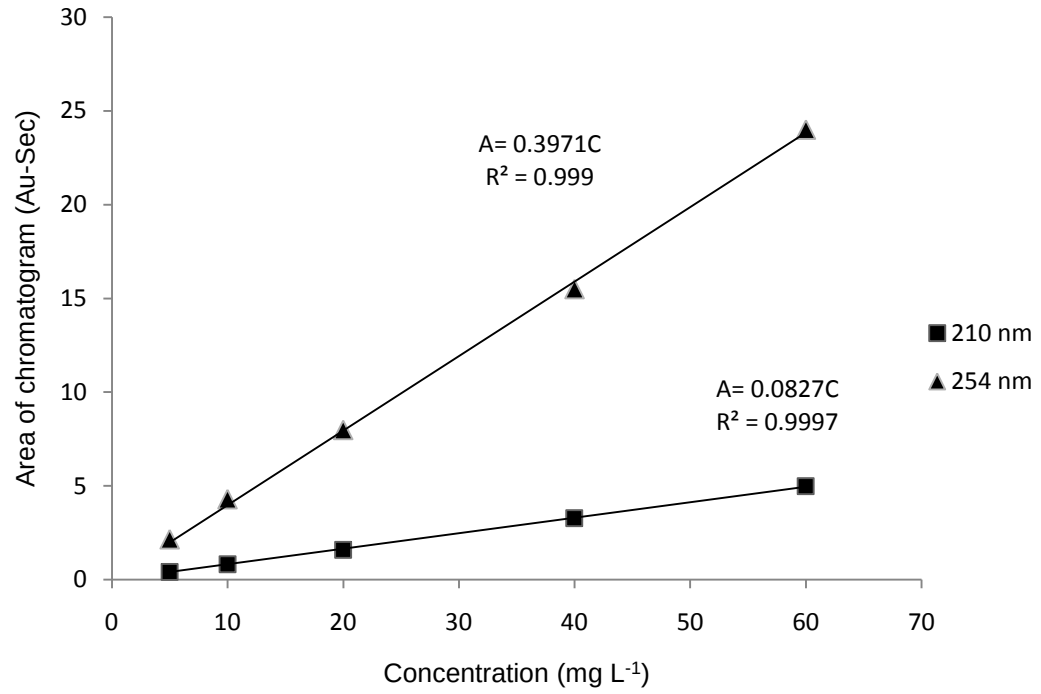

Figure F.2: *Calibration for p-benzoquinone*

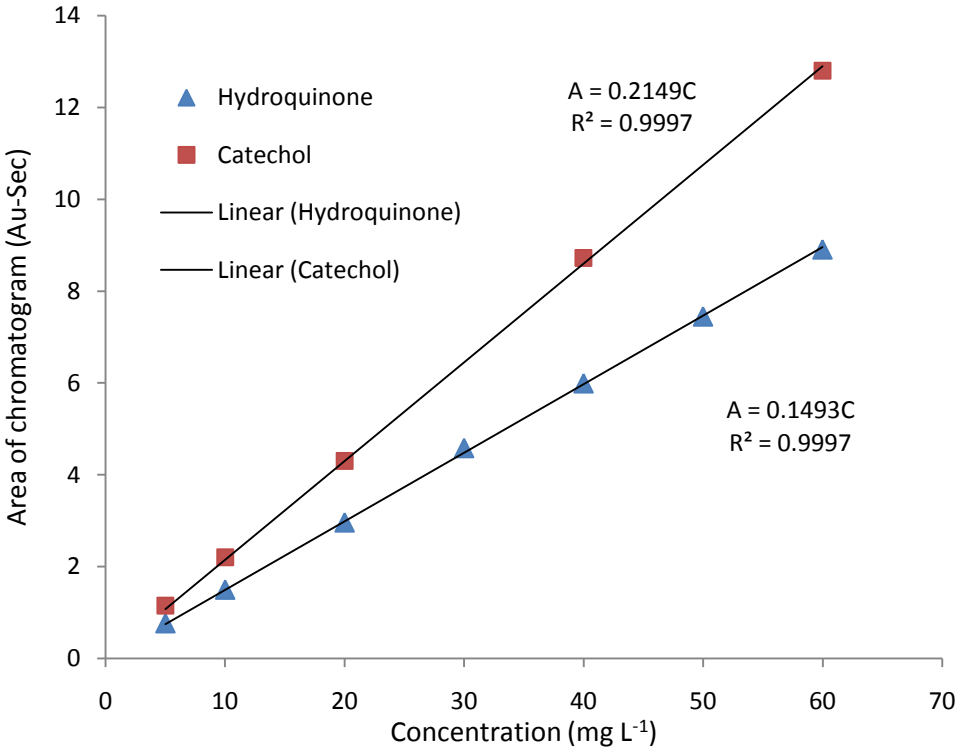

Figure F.3: *Calibration curves for hydroquinone and catechol*

F2. Calibration curves for aliphatic oxidation products of phenol (non-chlorinated)

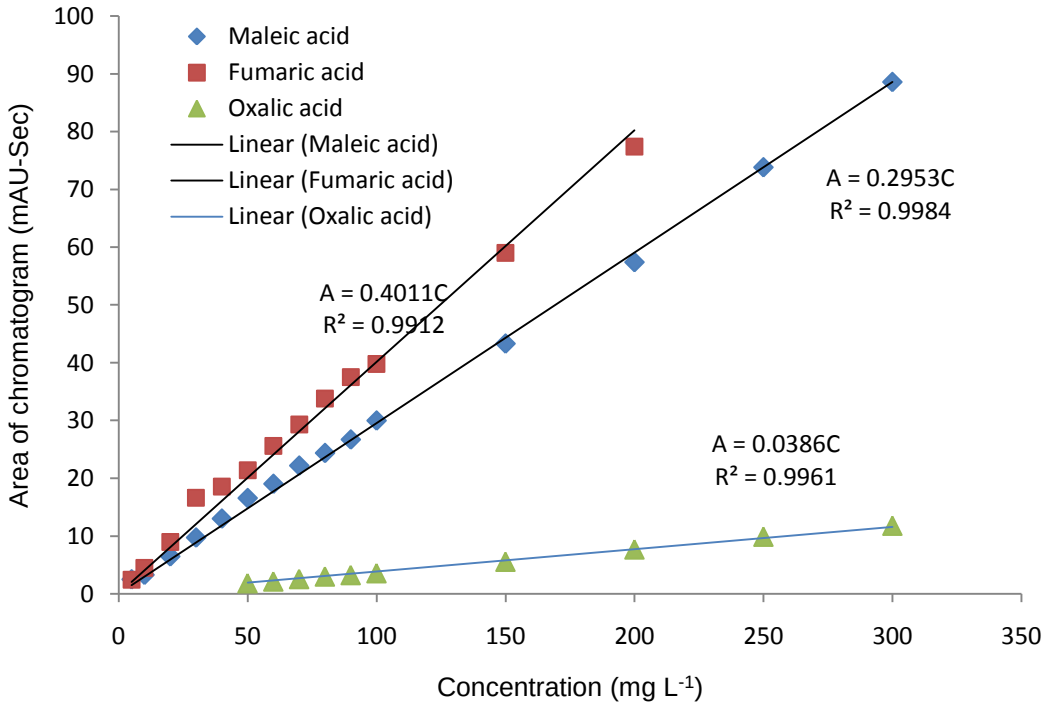

Figure F.4: *Calibration curves for maleic, fumaric and oxalic acids*

F3. Calibration curves for chlorinated oxidation products of phenol

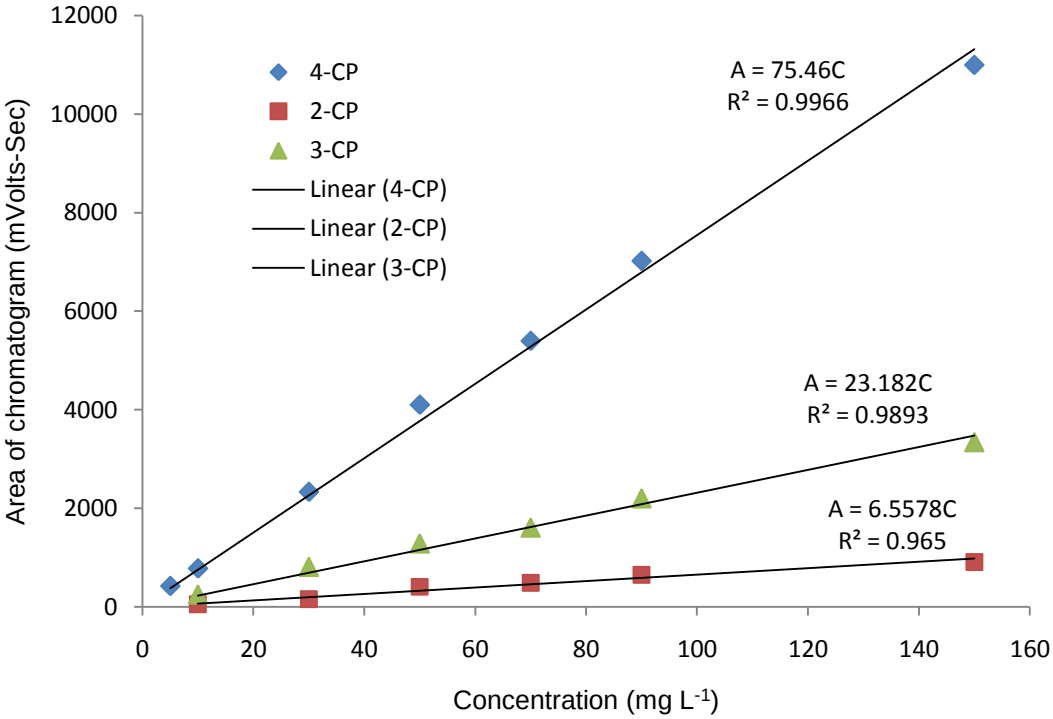

Figure F.5: *Calibration curves for 2-CP, 3-CP and 4-CP*

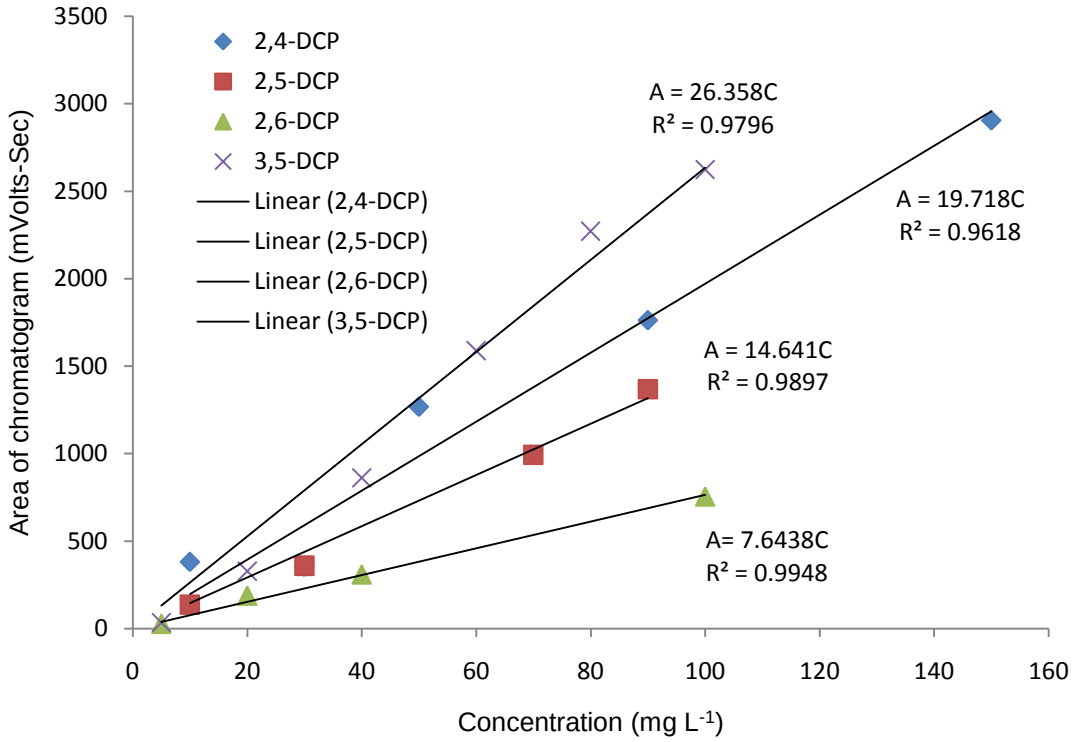

Figure F.6: *Calibration curves for 2,4-DCP; 2,5-DCP; 2,6-DCP and 3,5-DCP*

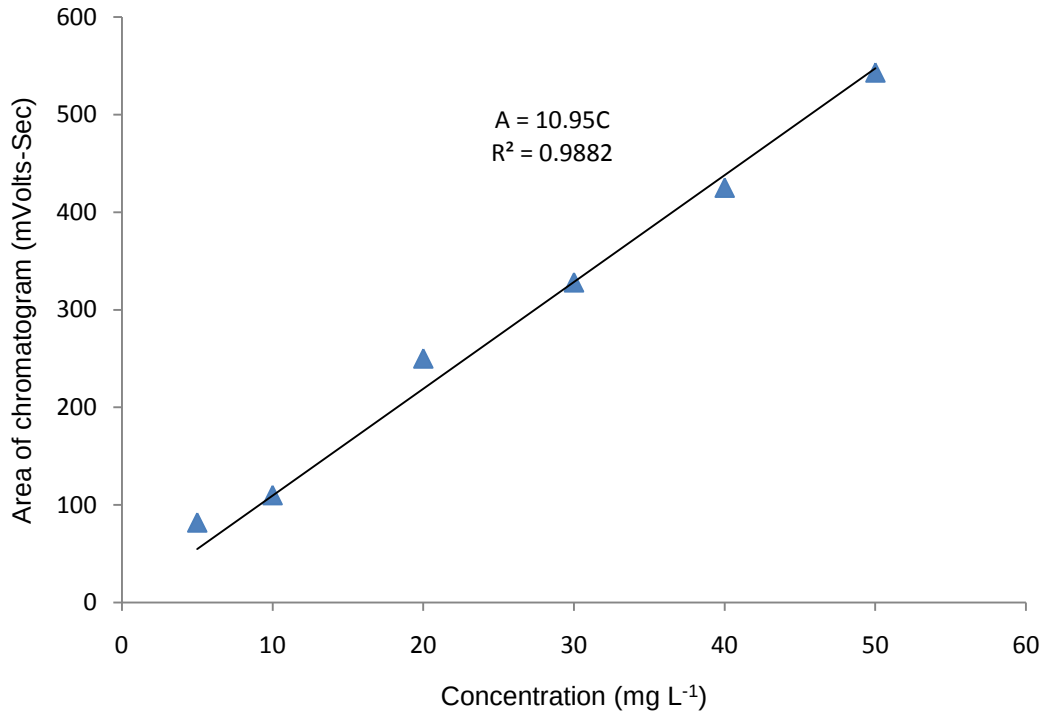

Figure F.7: *Calibration curve for 2,4,6-TCP*

F4. Calibration curve for free chlorine determination

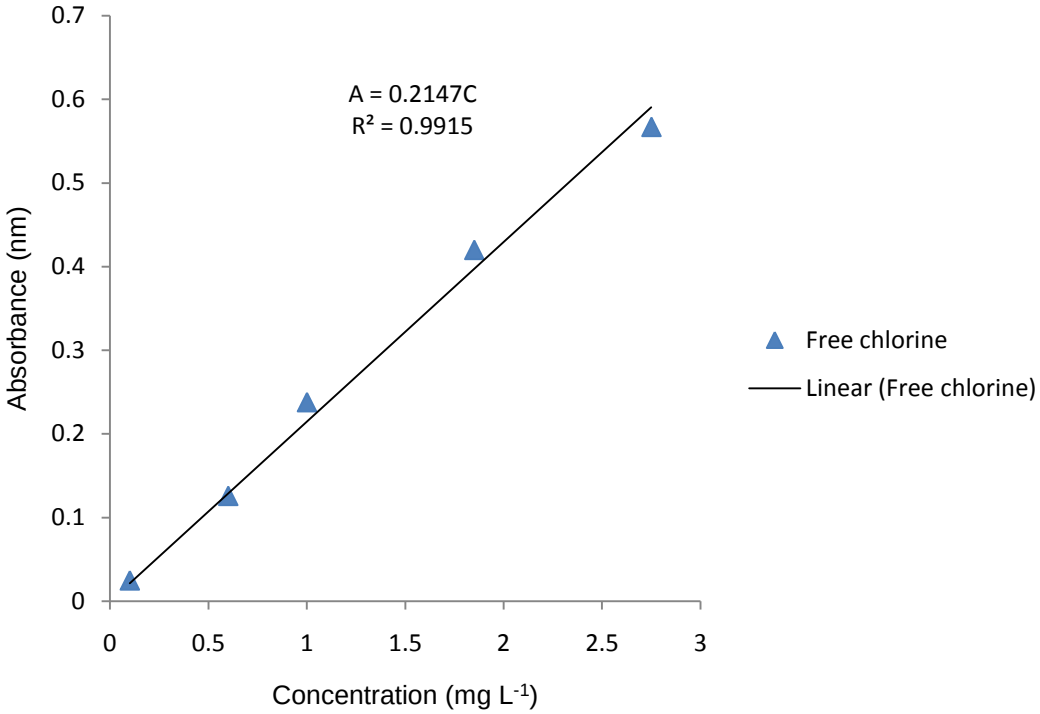

Figure F.8: *Calibration curve of free chlorine*

APPENDIX G
Standard Formation Potentials of Oxidants

Table G.1: *Standard formation potential of several oxidants, Troster et al. (2002)*

Oxidant		**Standard formation potential E^o (V)**
Hydroxyl radical	$H_2O/O^{\cdot}$	2.80
Ozone	O_2/O_3	2.07
Oxygen	H_2O/O_2	1.23
Chlorine	Cl^-/Cl_2	1.36
Hydrogen peroxide	H_2O/H_2O_2	1.77
Peroxodisulphate	$SO_4^{2-}/S_2O_8^{2-}$	2.01